PIERS 2005

Progress In Electromagnetics Research Symposium

Abstracts

August 22–26, 2005

Hangzhou, China

www.emacademy.org
www.piers.org

PIERS 2005 Abstracts

Published by

The Electromagnetics Academy
777 Concord Avenue, Suite 207
Cambridge, MA 02138
www.emacademy.org

Printed in Hangzhou, China

ISBN: 1-933077-06-9

Progress in Electromagnetics Research Symposium
August 22–26, 2005
Hangzhou, China

PIERS 2005 ORGANIZATION

PIERS Chair

J. A. Kong, MIT, USA

PIERS 2005 General Co-Chair

X. L. Yan, Zhejiang University, China

PIERS 2005 International Advisory Committee

D. Briggs, W. Chew, A. K. Fung, A. Gasiewski, T. M. Habashy, H. C. Huang, A. Ishimaru, S. G. Liu, K. K. Mei, P. Pampaloni, A. Priou, M. Raugi, K. Senne, M. Tateiba, W. Wiesbeck, J. Zehentner, W. X. Zhang

PIERS 2005 Technical Program Committee

W. Boerner, C. H. Chen, K. S. Chen, T. J. Cui, T. Grzegorczyk, Y. Hara, M. Hallikainen, S. He, W. Hong, K. Huang, K. Ito, K. Kobayashi, K. M. Luk, A. Massa, Z. P. Nie, J. Pribetich, C. Seo, X. Q. Sheng, L. Tsang, J. van Zyl, J. Vrba, T. X. Wu

PIERS 2005 Symposium Committee

H. S. Chen, K. S. Chen(Chair), Y. Du, J. T. Huangfu, Q. Jiang, L. Jylha, L. X. Ran, H. G. Wang, D. X. Yang, X. M. Zhang

PIERS 2005 Extended Papers Technical Committee

H. S. Chen, J. Chen, X. D. Chen, Y. Du, S. Famenini, T. M. Grzegorczyk(Chair), W. F. Herrington, B. A. Kemp, K. Li, J. Lu, L. X. Ran, L. F. Shen, Z. M. Thomas, H. G. Wang, W. Wong, B. I. Wu, B. Zach, X. M. Zhang

PIERS 2005 Administrative Committee

J. J. Bao, X. X. Cheng, J. T. Huangfu, Q. Jiang, Q. L. Jin, M. Lai, R. Lin, J. Lu, D. X. Wang, H. G. Wang, B. I. Wu, L. Y. Yu, B. Zhang, X. M. Zhang(Chair), H. F. Zhang, Y. Zhong

PIERS 2005 Local Arrangement Committee

H. S. Chen	J. Cong	Z. J. Dai	Y. Du(Co-Chair)
Y. M. Fang	G. W. Fu	S. Jiang	X. L. Kong
D. X. Li	L. Li	Z. Y. Li	R. P. Liu
P. M. Lou	Y. Luo	Y. L. Luo	L. Peng
Y. Qi	L. X. Ran(Co-Chair)	L. J. Shi	D. Wan
F. Wang	M. Y. Wang	Z. Y. Wang	S. Xi
X. L. Xu	Y. Yan	W. Z. Yan	Y. Yuan
D. P. Yue	J. J. Zhang	W. Zhao	Z. S. Zhou

PIERS 2005 SESSION ORGANIZERS

F. Ao	G. Berginc	D. J. Bergman	W. M. Boerner
L. Capineri	C. P. Chen	X. Chen	W. C. Chew
C. K. Chou	H. T. Chou	N. Engheta	M. A. Fiddy
V. Freilikher	A. K. Fung	Z. Gu	Y. Hao
S. He	R. B. Hwang	X. Huang	P. N. Jiao
R. Jin	H. Kikuchi	K. Kobayashi	A. V. Kudrin
G. Kyriacou	I. Lager	L. W. Li	Y. Luo
A. A. Maradudin	B. K. S. Nair	E. Njoku	Y. Okuno
Y. L. Pan	S. T. Peng	M. Piette	J. Pribetich
R. Ramer	J. Shen	K. Sheng	Y. Shestopalov
J. Shi	M. I. Stockman	V. Sudarshan	S. Tjuatja
K. F. Tong	D. P. Tsai	L. Tsang	G. Vandenbosch
K. J. Webb	C. G. Windsor	W. Wiscombe	J. Wu
R. B. Wu	G. Xie	T. Yamasaki	J. Yang
P. Yang	W. Y. Yin	S. Yueh	S. Zouhdi

PIERS 2005 SPONSORSHIP

- ☐ Zhejiang University
- ☐ The Electromagnetics Academy
- ☐ IEEE Geoscience and Remote Sensing Society
- ☐ K. C. WONG Education Foundation, Hong Kong
- ☐ Y. C. TANG Disciplinary Development Fund, Zhejiang University
- ☐ The Electromagnetics Academy at Zhejiang University
- ☐ MIT Center for Electromagnetic Theory and Application, Research Laboratory of Electronics

PIERS 2005 SESSIONS

Session 2A1
Advances in Microwave Remote Sensing

A Comparisons of Model Based and Image Based Surface Parameters Estimation from Polarimetric SAR

Hung-Wei Lee[1], **Jong-Sen Lee**[2]
Kun-Shan Chen[1], **J. C. Shi**[3]

[1]National Central University, Taiwan
[2]Naval Research Laboratory, USA
[3]University of California, USA

Surface can be characterized in terms of its material (dielectric) and geometric properties. The dielectric properties of surface are expressed primarily by its moisture content, and roughness described the geometric characteristics of surface. Various techniques for information retrieval from remotely sensed data have been proposed in a number of recent studies. Some of them are based on an empirical relationship between measured return signals and ground truth. Because of their development from a limited number of observations, these models are generally valid only for conditions under which those measured data were taken. These models also appear that no dependence on the roughness parameter, $l-$ correlation length. In this work, the potential of using the polarimetric SAR data over surface scatterers in order to invert surface parameters is investigated. The model-based and image-based inversion schemes are investigated and compared; the former is doing retrieval from a neural network trained with the AIEM model, while the later is schemed from a decomposition of coherency matrix. In model based approach, the only the surface scattering term of total return was used in order to remove the vegetation effects. The image based approach accounts for nonzero cross-polarzed, backscattering as well as depolarization by three polarimetric parameters, namely the scattering entropy(H), the scattering anisotropy(A), and the alpha angle(α). The features of these two schemes are discussed in terms of numerical aspects and physical implications of the surface parameters being inverted. Experimental data included E-SAR and AIRSAR polarimetric data sets. We also show the performances of inversion and discuss the advantages and drawbacks of both schemes.

Synthetic Aperture Radar Calibration and Field Experiment Setup

T. S. Lim, **Y. K. Chan**, **V. C. Koo**, **H. T. Ewe**, **H. T. Chuah**

Multimedia University, Malaysia

In 2002, the MASAR (Malaysian Airborne Synthetic Aperture Radar) project was initiated at Multimedia University (MMU), in collaboration with the Malaysian Centre for Remote Sensing (MACRES). The main objective of this project is to construct an instrument for earth resource monitoring in Malaysia. The proposed SAR system is a C-band, single polarization, linear frequency modulation radar. Before the flight campaign, preliminary testing and calibration were conducted to verify the functionality of the MASAR transmitter and receiver subsystems. The field experiment provides two-dimensional image resulting from range and cross range detection. Point target calibration technique is utilized for external calibration. In this paper, the field experiment setup, calibration of MASAR subsystems, radar hardware system as well as the Range-Doppler processing algorithm are presented. Both range detection and radar cross section (RCS) measurements capability are verified in the field experiments.

A Comparison of Autofocus Algorithms for SAR Imagery

V. C. Koo, **T. S. Lim**, **H. T. Chuah**
Multimedia University, Malaysia

A challenge in SAR system development involves compensation for nonlinear motion errors of the sensor platform. The uncompensated along-track motions can cause a severe loss of geometry accuracy and degrade SAR image quality. Autofocus techniques improve image focus by removing a large part of phase errors present after conventional motion compensation. It refers to the computer-automated error estimation and subsequent removal of the phase errors. Many autofocus algorithms have been proposed over the years, ranging from quantitative measurement of residual errors to qualitative visual comparison. However, due to the fact that different data sets and motion errors were employed, it is difficult to perform comparative studies on various algorithms. This paper compares and discusses some practical autofocus algorithms by using a common data set. A standard focal quality indicator based on image entropy is defined to measure how well an image is focused. Their implementation schemes and performance are evaluated in the presence of various phase errors, which include polynomial-like, high frequency sinusoidal, and random phase noise.

A Coherent Forest Synthetic Aperture Radar Calculation for PolInSAR Studies

Mark L. Williams
Defence Science and Technology Organisation, Australia

Shane R. Cloude
University of Adelaide, Australia

The use of the distorted-Born approximation for the coherent modeling of radar backscatter in remote sensing was pioneered in the 1980s. Since then the technique has been used extensively to predict microwave backscattering cross sections both of forests and other vegetation. New techniques in remote sensing, in particular PolInSAR, exploit the polarimetric and interferometric phase of multi-channel pixels in SAR imagery. It is desirable therefore to have in place a model capable of predicting these phases that may be used to explore the validity and limitations of these new techniques. Such a model is described here. The model has been constructed by combining a coherent, mean-field calculation, with the SAR image processing algorithm, and a high fidelity description of a forest. The calculation exploits the fact that a SAR image is formed by coherent integration of the received signal, modeled in the distorted-Born approximation. The effects of inhomogeneity in the forest canopy are accommodated in the calculation, which also incorporates the effects of ground surface roughness and understorey layer on direct and ground-volume returns. We present results of calculations for a forest of Scots Pine at L-Band for imaging parameters close to those of DLRs E-SAR sensor. We show that the properties of simulated imagery are close to expectation and observation, although the effects of multiple scattering within the canopy are not explicitly modeled. We perform multiple calculations designed to mimic fully polarimetric, interferometric SAR observations and use the simulated imagery to demonstrate PolInSAR techniques to recover tree height estimates and to enhance detection of concealed targets.

Microwave Sensing and Imaging of Buried Objects

Jonathan Bredow, **Saibun Tjuatja**
University of Texas at Arlington, USA

This paper reports on results of a study involving synthetic aperture (ISAR) imaging of buried objects. The purpose of the study is to further the understanding of how host loss tangent, homogeneity, and host/object contrast influence the resulting image. One goal of this work is to quantitatively establish dependency of image quality on each of these parameters for conventional ISAR imaging. Another goal is to provide a dataset that is sufficiently populated for quantitative performance comparisons of alternative imaging approaches.

The study uses carefully sieved soils and sand to control the homogeneity, and moisture content is varied from near 0 to about 15% by weight. Square, rectangular and round objects of foam, plastic and metal are used in the experiments. The setup consists of a large pot (1m high, by 1.2 diameter) that is rotated by a Scientific Atlanta azimuth-over-elevation positioner. Measurements are taken over 2 to 10 GHz using a step frequency approach. Transmit and receive antennas are fixed with 10° bistatic angle at 45° elevation with respect to the tank.

The findings to date support those of other experimenters for the case of dry sand. For example, with dry sand and object buried a few cm beneath the surface, using metal round and square objects, a ring corresponding to the edge of the round target and straight sides of the square target stand out clearly in the image. This also holds for foam objects of similar shape, although the image is "noisier" due to the lower contrast of the foam objects. For plastic objects, the image is not nearly so distinct since the contrast becomes very low. Imaging for this type of object appears to be enhanced by slightly moist conditions as a result of improved contrast. However, the improvement is not dramatic as a result of the increased penetration loss. Further increase in the moisture quickly degrades the image, as the penetration loss effect dominates over the contrast improvement effect. The study of effects of homogeneity has been done to this point for only homogeneous (sand) and strongly inhomogeneous cases (potting soil). Images for even high contrast cases are obscured in the latter case. Emphasis currently is on more careful examination of the effects of inhomogeneity with and without moisture.

The presentation is expected to comprehensively illustrate the effects of moisture, inhomogeneity and host/object contrast for conventional ISAR processing.

A Scattering Model for Inhomogeneous Medium with Vertical Structural Variation

Saibun Tjuatja, **A. K. Fung**, **Jonathan Bredow**
The University of Texas at Arlington, USA

A scattering model for inhomogeneous medium which accounts for the effects of vertical structural variation is developed based on the matrix doubling method. The medium with vertical structural variation is modeled as many sublayers with different physical characteristic determined by the vertical structural variation profile. Each sublayer is assumed to be statistically homogeneous. In addition to the effects of vertical structural variation, the scattering model also accounts for the effects of rough top and bottom layer boundaries. Model verification has been carried out using measurements from well characterized sea ice. Model analyses are carried out for saline and desalinated ice. In the saline ice case, better salinity profile sensitivity is observed at 5 GHz than at 10 GHz. On the desalinated ice case where the scatterers are air bubbles, the sublayer with larger scatterers dominates the back scattering level even though its thickness is less than 1/10 of the signal penetration depth. Applications of the developed model to microwave remote sensing of soil and other inhomogeneous media will be provided in the presentation.

A Theoretical and Measurement Study of Sea Ice and Ice Shelf in Antarctica as Electrically Dense Media

Mohan Dass Albert, **T. E. Tan**, **H. T. Ewe**, **H. T. Chuah**
Multimedia University, Malaysia

Due to Antarctica's remoteness and harsh weather condition, remote sensing technology has been an attractive tool in equipping Antarctica scientists with the monitoring information and the understanding of ice physical changes in Antarctica ecological system. Previous Antarctica researches on remote sensing of ice mainly utilize ice and snow scattering models based on independent scattering assumption. The needs of the consideration of coherent effects of the scatterers and the measurement of physical parameters affecting such effects are addressed in this study. Theoretical model based on radiative transfer theory with the incorporation of Dense Medium Phase and Amplitude Correction Theory (DM-PACT) [1] is developed. This concept of DM-PACT derived from antenna array theory requires an understanding of the distribution statistics of the scatterers in the homogeneous host medium. The ground truth measurement of multi-year period has been conducted at sea ice and ice shelf areas near Scott Base, Ross Island in Antarctica and a series of measurement of sea ice and snow physical parameters including distribution statistics of the air bubbles in sea ice are carried out. Theoretical study of the backscattering returns and scattering mechanisms in these electrically dense media is performed and analysis of important physical parameters affecting the radar returns is presented. Satellite measurements of the test areas from Radarsat have been acquired for comparison of model predictions and measurement data with promising results.

REFERENCES

1. Chuah, H. T., S. Tjuatja, A. K. Fung and J. W. Bredow, "A Phase Matrix for a Dense Discrete Random Medium: Evaluation of Volume Scattering Coefficient", *IEEE Transactions on Geoscience and Remote Sensing*, Vol. 34, No. 5, 1137, 1996.

Theoretical Modeling and Measurement Comparison of Season-long Rice Field Monitoring

J. Y. Koay, **C. P. Tan**, **H. T. Ewe**, **H. T. Chuah**
Multimedia University, Malaysia

Saiful Bahari
Malaysian Center for Remote Sensing, Malaysia

The development of a suitable scattering model for rice crops is essential for improving our understanding of remote sensing data in rice monitoring applications. In this study, the work of theoretical modeling and measurement comparison are applied on a season-long rice field monitoring to understand the scattering mechanisms involved in a rice growth period and to pursue the validation of the theoretical model with measurement data. The theoretical model is based on radiative transfer theory applied on layered rice crop discrete random medium. The dense medium phase and amplitude correction theory (DM-PACT) [1, 2] which considers the coherent effects of the scatterers is incorporated for the phase matrices of the scattereres of basic shapes modeled after rice crop physical geometry. For the collection of measurement data, C-Band scatterometer measurements and RADARSAT images will be obtained at regular intervals throughout an entire rice crop season. The study areas are the rice fields in Sungai Burung, Selangor, Malaysia. Ground truth measurements including canopy parameters such as plant geometry, plant density, plant moisture, and water depth are measured simultaneously. The theoretical study of the scattering mechanism for the rice crop medium throughout the season and the validation of the model simulation with measurement results are conducted. Sensitivity of physical parameters for the radar returns is investigated and analysis on the theoretical and measurement results for better understanding of the remote sensing of rice crop will be presented.

REFERENCES

1. Chuah, H. T., S. Tjuatja, A. K. Fung and J. W. Bredow, "A Phase Matrix for a Dense Discrete Random Medium: Evaluation of Volume Scattering Coefficient," *IEEE Transactions on Geoscience and Remote Sensing*, Vol. 34, No. 5, 1137, 1996.
2. Ewe, H. T. and H. T. Chuah, "Electromagnetic Scattering from an Electrically Dense Vegetation Medium," *IEEE Transactions on Geoscience and Remote Sensing*, Vol. 38, No. 5, 2093, 2000.

Backscattering from Multi-scale and Exponentially Correlated Surfaces

A. K. Fung, **N. C. Kuo**
The University of Texas at Arlington, U.S.A.

Most natural surfaces have been reported to have an exponential-like correlation function [Hayre and Moore, 1961; Oh et al., 1992] and generally contain more than one scale of roughness. In this paper we want to show that a multi-scale Gaussian-distributed, Gaussiancorrelated surface also possesses an exponential-like correlation function except for very small lag distances around the origin. As a result, angular backscattering from such a surface in the low frequency region behaves the same as if it is from an exponetially correlated surface. In the high frequency region, scattering from the two differently correlated surfaces are quite different as expected. Furthermore, we show that the correlation function for a multi-scale, Gaussian-distributed, Gaussian-correlated surface can be used to interpret backscattering from a known randomly rough surface that appears to possess an exponential correlation over a wide range of frequencies. These findings indicate that for natural surfaces the exponential correlation function may be a valid approximation to the real correlation in the low frequency region and it is not the correct function in the high frequency region. It also offers an explanation as to why many natural surfaces appear to be exponentially correlated.

A Generalization of 2D-Simulation to 3D for Isotropically Rough Surfaces

Nathan C. Kuo, **A. K. Fung**
The University of Texas at Arlington, USA

It is known that 3D simulation of scattering from randomly rough surfaces using the moment method leads to a very large matrix for a dielectric surface. Usually, a patch size of 10 wavelengths or more is needed and a minimum of 10 points per wavelength is required. This means a minimum of 200 unknowns for a dielectric surface in 2D and 200^2 unknowns in 3D, when the point matching method is used. The number of elements in the surface current matrix is 200^2 in 2D and 200^4 in 3D. It is clear that there is a huge difference between 2D and 3D calculations in both the number of unknowns and computational time. In this study we want to show that 2D simulation may be extended to 3D for isotropically rough surfaces through the ratio of the backscattering coefficients, based on modeling. More specifically, we show for two known surfaces reported by Oh et al. [1992] that the 2D simulated backscattering coefficients when converted to 3D by the stated ratio match the experimentally measured data as reported by Oh et al. [1992]. The ratio of the backscattering coefficients used here is based on the integral equation model evaluated with the same correlation functions and rms heights.

An Application of Sampling Theorem to Moment Method Simulation in Surface Scattering

E. Huang, **A. K. Fung**
The University of Texas at Arlington, USA

The method of moments (MoM) is a numerical procedure for solving the equation $Lf = g$, where L is a continuous linear operator, f is the unknown function to be determined and g is a known excitation. In essence, the procedure converts the linear equation into a matrix equation and determines the unknown function in the form of a set of samples of the function through matrix inversion. It is well known that the sampling theorem states that to completely represent a function, one requires a minimum of two samples per wavelength, when the basis function is the Sinc function. Thus, by choosing the Sinc function as the testing and basis functions in MoM implementation, we should have the smallest possible size for the matrix. To test the above stated approach, we calculate the scattering coefficient from a 2-D rough surface with a Gaussian distribution. The standard point matching approach is also used so that comparisons can be made between the two results. By comparing these numerical calculations with the IEM model, it is found that to achieve the same degree of accuracy, the number of unknowns used in the point matching method is an order of magnitude more than when the Sinc function is used as the basis function. This reduction in matrix size is specially significant in a three dimensional surface scattering problem, because we shall be able to reduce the matrix size by two orders of magnitude.

Session 2A2

Metamaterials in Antenna and Microwave Engineering

A Chiral Route to Negative Refraction

J. B. Pendry
Imperial College, UK

Veselago gave the original description for negative refraction [1]: when the electrical permittivity and magnetic permeability are both negative light bends the 'wrong way' at an interface. These properties are never simultaneously realised in nature so that it was only much later with the ability to construct artificial metamaterials that his vision could be realised [2-4]. Although Veselago referred to these materials as 'left handed' we stress that the sense in which Veselago used this term has nothing to do with chirality. We prefer to use the expression 'negatively refracting' to avoid confusion. Negative refraction never occurs in nature, and we rely on artificial materials, metamaterials, to realise the effect. Here we discuss the consequences of chirality and show that it offers an alternative route to negative refraction. We produce a practical design which is chiral, has many advantages, and exhibits novel properties.

If we describe the response of a chiral material as follows,

$$D = \mathcal{X}_{EE}E + \mathcal{X}_{EH}H$$

$$B = \mathcal{X}_{HE}E + \mathcal{X}_{HH}H$$

then,

$$k_{-\pm} = \pm\sqrt{\mathcal{X}_{EE}\mathcal{X}_{HH}} - i_{\mathcal{X}_{EH}},$$

where $\mathcal{X}_{EH}$ is assumed to be imaginary. If the material also has a resonant response then a typical dispersion is shown in figure 1. It is evident that if $\omega_0'' > \omega > \omega_0'$ one of the polarisations (dashed line) shows the negative dispersion characteristic of negative refraction. Further details can be found in [5].

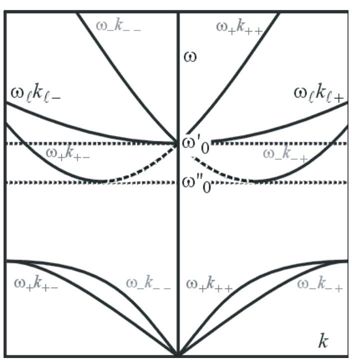

Figure 1 Dispersion of frequency, ω, versus wave vector, k, in an homogeneous and isotropic chiral medium showing the two polarisations as non degenerate. The subscripts on k refer first to the polarisation and second to the sign of the group velocity. In our convention, polarisation is positive if the projection of the photon spin on the z-axis is positive. It does not refer to the projection of spin onto the wave vector. Introducing the resonant dipoles into a chiral medium splits the resonant transverse bands and results in a range of frequencies below ω_0' in which negative refraction can be seen for one of the polarisations.

REFERENCES

1. Veselago, V. G., *Soviet Physics USPEKI*, Vol. 10, 509, 1968.
2. Pendry, J. B., A. J. Holden, W. J. Stewart, I. Youngs, *Phys. Rev. Lett.*, Vol. 76, 4773, 1996.
3. Pendry, J. B., A. J. Holden, D. J. Robbins and W. J. Stewart, *IEEE Trans. Micr. Theory and Techniques*, Vol. 47, 2075, 1999.
4. Smith, D. R., W. J. Padilla, D. C. Vier, S. C. Nemat-Nasser, S. Schultz, *Phys. Rev. Lett.*, Vol. 84, 4184, 2000.
5. Pendry, J. B., *Science*, Vol. 306, 1353, 2004.

Directive Beams from Small Apertures Loaded with Negative-Parameter Metamaterials

Andrea Alù[1,2], **Nader Engheta**[1]

[1]University of Pennsylvania, USA
[2]Università di Roma Tre, Italy

One of the basic concepts in the antenna theory states that the directivity of a given beam is directly related to the effective width of the aperture from which the beam itself is radiated. When uniformly illuminated, in fact, a wider aperture in general produces a more directive beam, and, by the same means, a sub-wavelength aperture is characterized by a very broad, almost uniform radiation. In this talk we discuss the possibility of overcoming this limitation in certain geometries by pairing together metamaterials with negative permittivity and/or permeability with conventional dielectrics.

As an example, a parallel-plate waveguide, when filled with pairs of slabs of double-positive and epsilonnegative materials, may support propagating modes even when its total size is sub-wavelength [1]. The modal field of such a structure is necessarily rapidly varying along the transverse cross section of the waveguide, in order to match the boundary conditions, and therefore if such a waveguide is ended with an aperture, with a proper design the radiation from this aperture may have a higher directivity than a uniformly illuminated aperture with the same size. Even though in principle this phenomenon may resemble the highly unstable solutions for superdirective arrays, in this case such a structure shows a relatively high robustness to changes in the design parameters, due to the inherent coupling between the slabs that is here exploited when establishing the resonant mode propagating in the waveguide containing metamaterials. This concept may be extended to other geometries, and in fact our preliminary analysis has shown that spherical and cylindrical sub-wavelength structures loaded with analogous pairings of metamaterials may be designed to support higher-order polariton modes while canceling the lower-order modes responsible for broaderbeam radiation. This in principle implies a higher directivity from a compact sub-wavelength structure. These concepts may be exploited both in the transmission scenario, i.e., building antennas radiating narrow beams from a small aperture, and in the reception case, i.e., designing receiving systems able to distinguish narrow changes in the angle of arrival of a given signal.

In this talk, first we discuss the physical background related to the synthesis of such directive subwavelength structures, and then we present our theoretical analysis and some of salient features of these concepts.

REFERENCES

1. Alù, A., N. Engheta, *IEEE Trans. Microwave Theory & Techniques.*, Vol. 52, 199, 2004.

Near-perfect Tunneling in a Waveguide Filled by a Metamaterial Due to the Amplification of Evanescent Waves

J. D. Baena[1], **L. Jelinek**[2], **R. Marqués**[1], **F. Medina**[1]

[1]Universidad de Sevilla, Spain
[2]Czech Technical University, Czech Republic

Amplification of evanescent electromagnetic waves in a left-handed slab is the physical phenomenon underlying the "perfect lens" effect recently described by Pendry [1], being still a controversial issue [2]. Metallic waveguides operating in cutoff provide a unique physical environment to produce and study these waves, since isolated evanescent modes can be excited in such environment. In this work, the tunneling of electromagnetic waves through a rectangular waveguide filled by a metamaterial is analyzed. Since fundamental modes TE_{01} in rectangular waveguides are the superposition of two symmetrical plane waves, the aforementioned results also show this amplification by a metamaterial slab in free space.

Enhanced tunneling across a waveguide filled with a metamaterial and sandwiched between two empty sections operating in cutoff has been demonstrated (Fig.1, solid line). The transmission is several orders of magnitude higher than the obtained when all waveguides are empty (Fig.1, dashed line). This effect has been explained by means of the effective medium metamaterial theory, according to which the decaying evanescent waves coming from the input are amplified in the metamaterial region and, conversely, the backward decaying waves coming from the output, are also amplified in the backward direction inside the metamaterial. The superposition of forward and backward modes allow for the transmission of energy, as it was noted in [3].

In particular, this effect has been experimentally verified when the metamaterial inside the waveguide is an uniaxial anisotropic magnetic medium with a negative effective permeability along x axis, consisting in an array of BC-SRR elements [4] (see Fig.2: lateral view (a), BC-SRR element (b), and top view (c)). The experimental results show a very good qualitative and quantitative agreement with the theoretical predictions of the metamaterial theory, thus being an additional support for the validity of such theory.

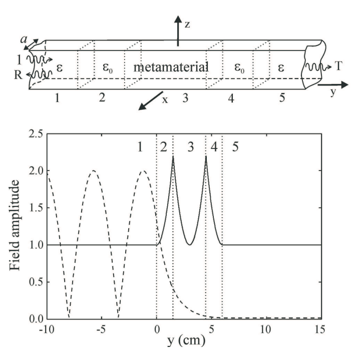

Figure 1

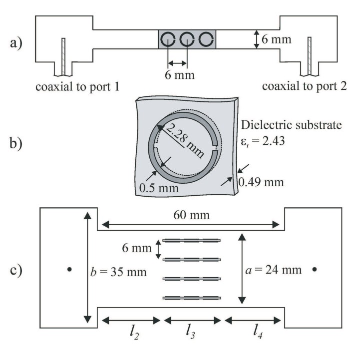

Figure 2

REFERENCES

1. Pendry, J., *Phys. Rev. Lett.*, Vol. 85, 3966, 2000.
2. N. García and M. Nieto-Vesperinas, *Phys. Rev. Lett.*, Vol. 88, 207403, 2002.
3. Pendry, J., *Phys. Rev. Lett.*, Vol. 87, 249704, 2001.
4. R. Marqués, F. Mesa, J. Martel and F. Medina, *IEEE Trans. on Antennas and Prop.*, Vol. 51, 2572, 2003.

Discussion on Negative Refraction and Perfect Lens

Long Gen Zheng
Naval University of Engineering, China

Wen-Xun Zhang
Southeast University, China

In Pendry's letter [1], the limitation of the conventional lens is addressed and an unconventional alternative is suggested. It is a lens made of negative refractive index medium. It can focus light even in the form of parallel-sided slab of this material. Furthermore, it focuses light in a double focusing manner. The new message delivered by Pendry in his letter is that this medium can cancel the decay of evanescent waves and thus can be used to fabricate perfect lens. A proof is thereafter given to show that the amplitude of an evanescent wave is recovered when it goes out of the slab. After careful study, we think that this message is problematic. In the letter, an evanescent wave is defined as a wave whose wave number is purely imaginary in one direction and real in other orthogonal directions. A surface wave is one example of this kind of evanescent wave. The key point is that an imaginary wave number in one direction does not mean the decay of the amplitude of a wave in that direction. The wave does not propagate in that direction at all. Instead, it propagates in other orthogonal directions with a non-homogeneous wave front. This evanescent wave may or may not turn into a propagational one, depending on the effective optical density of the material of the slab. When both permittivity and permeability are -1, the effective optical density of this material is the same as vacuum and thus it will never turn into a propagational one, either in or out of the slab. And there will be no reflection and transmission phenomena occurring in the vicinity of the slab. The proof, where a total transmission coefficient is concerned, becomes meaningless. In our opinion, a negative refractive index medium, if it exists, can never turn an evanescent wave into a non-evanescent one. In another word, negative refraction can not make a perfect lens.

REFERENCES

1. Pendry, J. B., "Negative Refraction Makes a Perfect Lens," *Physical Review Letters*, Vol. 85, No. 18, 3966, 2000.

Metamaterial Realisation and Its Applications to Antennas

Yang Hao[1], **S. Sudhakaran**[1], **D. Nyberg**[1,2]
C. Parini[1], **H. Cory**[1,3]

[1]University of London, UK
[2]Royal Institute of Technology, Sweden
[3]Technion, Israel

This paper aims to break traditional boundaries between material science and electromagnetics and bring together the recent advances in materials research that enables the manufacture of complex lattices with recently discovered unique microwave materials that are not found in nature. These so called metamaterials offer a variety of novel properties, which significantly impact on a wide range of application areas. Specifically, microwave metamaterials exhibit negative effective permittivity and/or permeability over a finite and controllable frequency range and provide novel control of electromagnetic wave propagation. They are formed from millimetre-scale periodic geometric structures, which modify the dispersion relation of microwave signals. Electromagnetic Band Gap (EBG) structures are a particular class of metamaterial that offer pass and stop bands to electromagnetic waves in the same way that semiconductors offer these properties to electrons. When the effective permittivity and permeability are simultaneously negative, metamaterials exhibit an anti-parallel nature in the electromagnetic wave propagation and associated Poynting vector. This class of metamaterial is termed $left - handed$ and contrasts with conventional materials that adhere to the so-called right-hand rule.

Unfortunately, to date, the harnessing of the LHMs novel properties to these applications remain only a theoretical possibility, as no practical technique for automated manufacture of three-dimensional LHMs exists. EBG have been manufactured but the structures are crude and mainly limited to two dimensions (using conventional printed circuit techniques) so resulting in limited performance or in 3D form is expensive and complex to manufacture. In this paper, we will explore novel applications of microwave metamaterials in antenna engineering by numerical modeling, rapid prototyping and experimental evaluation. Computer-controlled solid freeforming of periodic structures will be used for efficient fabrication of complex 3D structures.

Applications of microwave metamaterials will be also demonstrated. They include low SAR antennas for mobile, wearable devices and implanted body sensors; and shaped 2D and 3D metamaterials can offer directional gain from very compact antennas. In addition, layered metamaterials can be found in the design of zero phase delay lines, near-field phase shifter and lossless radome. Furthermore, conformal wire medium can be applied in antenna design with multiple beams. Numerical and experimental results will be presented at the conference.

Active Radome Using Controllable Metamaterial

Bae-Ian Wu[1], **Hongsheng Chen**[2], **Lixin Ran**[2], **Tomasz M. Grzegorczyk**[1], **J. A. Kong**[3]

[1]Massachusetts Institute of Technology, USA
[2]Zhejiang University, China
[3]The Electromagnetics Academy, USA

Recently, there have been growing interest in the study of passive left-handed metamaterials both theoretically and experimentally. Metamaterials are artificial materials synthesized by embedding specific inclusions, for example, periodic structures, in host media. Some of these materials demonstrate the property of either negative permittivity or permeability. If both happen at the same time, then the composite exhibits an effective negative index of refraction and is referred to as left-handed metamaterials.

The technology of such left-handed metamaterials also allows materials with custom designed constitutive parameters to be fabricated. With inclusion of electrically small lumped elements to to the structure, the properties of the metamaterial can be altered in a flexible manner. Furthermore, the included elements may be actively controlled such that each unit cell exhibits a specific amplitude and phase response upon the incidence of electromagnetic waves.

Using a commercially available software (CST Microwave Studio), simulations are done on a radome of metamaterial composed of a periodic collection of S rings loaded with capacitors. The S parameters of the metamaterial are analyzed and correlated with the loaded capacitance and the information is used as the basis to form an active radome. Far field radiation are calculated and examined for radomes with different phase change across the apertures. Beamsteering of the feasible active radome design is presented.

The authors would like to acknowledge discussions with Joe Pacheco, Robert Atkins, and Jeff Herd, and would like to thank Ken Senne for private communications on the topic.

Application of EBG Materials to Antennas and Absorbers

H. Nakano, **P. Huang**, **Y. Asano**, **K. Hitosugi**, **H. Mimaki**, **J. Yamauchi**
Hosei University, Japan

M. Miyata
Mitsumi Electric Co. Ltd, Japan

This paper presents three topics regarding EBG materials: realization of small antenna height using an EBG material, beam direction control for a low-profile antenna using an EBG material, and absorbing characteristics of an EBG material. The EBG material element in this paper has a mushroom-like structure.

(1) Low-profile Planar Antenna with EBG Material

The spiral antenna is one commonly used planar antenna; it is conventionally used with a conducting plate (a perfect electric conductor) to obtain a unidirectional beam. The antenna height above the conducting plate is chosen to be one-quarter wavelength at the design frequency. It is known that, as the antenna height decreases, the antenna characteristics deteriorate. To counteract this deterioration at a small antenna height (less than 0.04 wavelength at the lowest operating frequency), this paper proposes replacement of the conducting plate with an EBG material. The investigation shows that 1) deterioration in the axial ratio is decreased; 2) the input impedance becomes nearly constant over a wide frequency band.

(2) Reconfigurable Antenna with EBG Material

A wire inverted F antenna is composed of two vertical lines and one horizontal line above a conducting plate. Conventionally, the vertical line length (antenna height) is chosen to be approximately one-tenth of the operating wavelength. As the antenna height decreases, impedance matching to a 50-ohm line becomes difficult. This paper shows that replacing the conducting plate with an EBG material solves the impedance matching problem. In addition, if the dimensions of the EBG surface are properly chosen, a tilted radiation beam is obtained. It is also found that the direction of the tilted beam can be controlled by using switching circuits: one inserted into the original horizontal line (in the x-direction) and one inserted into each of two additional horizontal lines (in the $\pm$ y-direction).

(3) Absorbing Characteristics for Electromagnetic Waves

By adding dielectric loss to the substrate of an EBG, one can use it as an absorber. This EBG absorber can be made thinner than conventional absorbers, which are close to one-quarter guide wavelength in thickness. It is found that 1) the reflection coefficient is controlled by the loss in the dielectric substrate, and 2) the center frequency of an absorber can be controlled by the patch size. Note that the absorbing characteristics when the pins of the EBG are removed are also discussed in this paper.

Canalization of Sub-wavelength Images by Electromagnetic Crystals

P. A. Belov
Queen Mary University of London, UK

C. R. Simovski
St. Petersburg State University of Information, Technologies, Mechanics and Optics, Russia

The theoretical possibility of sub-wavelength imaging by a slab of left-handed medium (LHM) with $\varepsilon=\mu=-1$ was demonstrated by J. Pendry in his seminal work [1]. The focusing phenomenon in Pendry's perfect lens is based on two effects. The propagating modes of a source are focused in the LHM due to the negative refraction and the evanescent modes experience amplification inside the LHM slab. This allows to restore sub-wavelength details in the focal plane. It is an ambitious goal to obtain the sub-wavelength resolution without LHM in the optical frequency range. In this range the negative refraction phenomenon is observed in photonic crystals at frequencies close to the band gap edges. A flat *superlens* formed by a slab of photonic crystal was suggested by C. Luo et. al. in [2] and the sub-wavelength imaging was theoretically studied in [3]. The principle of Luo's superlens is similar to the principle of Pendry's perfect lens, but negative refraction is obtained due to a specific form of isofrequency contours (without backward waves inherent to LHM).

In the present paper we suggest to use the photonic crystal in a different regime than suggested by C. Luo et. al. in [2]. We do not involve negative refraction and amplification of evanescent modes, rather, we propose to transform the most part of the spatial spectrum of the source radiation into propagating eigenmodes of the crystal having practically the same group velocity (directed across the slab) and the same longitudinal components of the wave vector. The spatial harmonics produced by a source (propagating and evanescent) refract into the crystal eigenmodes at the front interface. These eigenmodes propagate normally to the interface and deliver the distribution of near-field electric field from the front interface to the back interface without disturbances. The incoming waves refract at the back interface and form an image. This way the incident field with sub-wavelength details is transported from one interface to the other one. We call the described regime as *canalization with sub-wavelength resolution*. This principle of operation is similar to that of the medium with zero refraction index [4]. The difference is that in our case the image is transmitted by waves which all vary identically with distance from the front interface, whereas in zero refraction index medium there is no such variation.

REFERENCES

1. Pendry J. B., "Negative Refraction Index Makes Perfect Lens", *Phys. Rev. Lett.*, Vol. 85, 3966, 2000.
2. Luo C., S. G. Johnson, J. D. Joannopoulos and J. B. Pendry, "All-angle Negative Refraction without Negative Effective Index", *Phys. Rev. B*, Vol. 65, 201104, 2002.
3. Luo C., S. G. Johnson, J. D. Joannopoulos and J. B. Pendry, "Subwavelength Imaging in Photonic Crystals", *Phys. Rev. B*, Vol. 68, 045115, 2003.
4. Ziolkowski R. W., "Propagation in and Scattering from a Matched Metamaterial Having a Zero Index of Refraction", *Phys. Rev. E*, Vol. 70, 046608, 2004.

Artificial Magnetic Conductor High Impedance Surface for Compact Directive Antennas

A. Ourir, **A. de Lustrac**
Université Pairs-Sud, France

Recent advances and applications of the High Impedance Surface (HIS) have proven that these structures present a solution to improve antenna performance [1]. This improvement occurs due to the stop bands and the high impedance presented by these periodic structures. A new Artificial Magnetic Conductor (AMC) based on microstrip technologyis proposed for the conception of HIS. This material presents a high impedance on a wide frequencyband.

We present in this paper numerical finite elements simulations and measurements characterizing the proposed AMC-HIS and its advantageous effect on microstrip antenna patterns. First,we make a quickdescription of the proposed AMC-HIS conception. Then, we present results showing the use of AMC-HIS to improve microstrip antenna performance in this band. Finallya Fabry-Perrot resonator formed bya PartiallyReflective Surface (PRS) disposed over the AMC-HIS, is studied. The last structure allows us to increase the gain and the directivity,and to enhance the compactness of microstrip antenna at the central frequencyof the AMC-HIS.

At first we surrounded patch antenna, designed to work at 10 GHz, by a AMC-HIS as it is showed in Figure 1(a). Then we compared its gain and directivity patterns to the lonely antenna patterns. Finally, we disposed a PRS over the antenna surrounded by the AMC-HIS to create a Fabry-Perrot Resonator as it is illustrated by Figure 1(b). Figure 1(c) presents the directivity patterns of the antenna compared to the AMC-HIS surrounded antenna and the Fabry-Perrot cavity. We obtain a directivity and a gain increase thanks to AMC-HIS. The resonator provides further enhancement. Moreover, the last structure is more compact ($L \sim \lambda/4$) than traditional Fabry-Perrot cavity($L \sim \lambda/2$) using metallic ground plane [1].

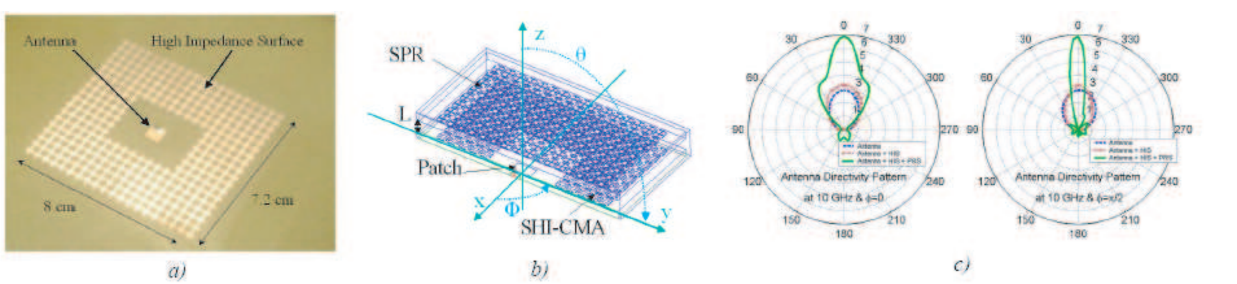

Figure 1: a) Patch antenna surrounded by AMC-HIS, b) Fabry-Perrot resonator, c) Directivity patterns of the different structures

REFERENCES

1. Feresidis, A. P., et al, "Low-profile High-gain Planar Antennas Based on Artificial Magnetic Conductor and Electromagnetic Band Gap Surfaces," *IEE. Proc.-Microw. Ant. Prop. 20.*, Vol. 148(6), 2001.

Optimization of a 500 GHz Receiver Using EBG Technology

I. Ederra, **R. Gonzalo**, **B. Martínez**, **C. Del Río**
Universidad Pública de Navarra, Spain

L. Azcona, **B. Alderman**, **P. G. Huggard**
Rutherford Appleton Laboratory, U.K.

B. P. de Hon, **M. C. van Beurden**
Eindhoven University of Technology, The Netherlands

A. Murk
University of Bern, Switzerland

L. Marchand, **P. de Maagt**
ESTEC, The Netherlands

The use of EBG crystals as substrates for planar antennas has been shown to offer great improvements in their radiation features. For imaging array applications the main advantages of configurations combining EBGs and planar antennas are the increase of directivity of each individual pixel and the reduction of mutual coupling between.

This paper presents some results concerning the design of each of the individual pixels which would constitute an imaging array at 500 GHz. Each of these pixels use a dipole antenna placed on top on of an EBG substrate as radiating element. Besides the dipole antenna, the detecting configuration consists of a Schotky diode and a RF filter, which was used to maximize the sensitivity. The silicon woodpile was the selected EBG structure due to its robustness and relatively straightforward machining.

An extensive study was made on the radiation and matching properties of the 8 symmetry positions of a dipole antenna on top of the woodpile structure. As a result, the perpendicular solid-solid symmetry position was selected, since it forms the best compromise between radiation pattern quality and impedance match. In this position the antenna feed lines run along a bar in the top layer and the dipole arms overlay a perpendicular bar in the layer immediately below.

The configurations were optimised in terms of sensitivity and radiation features. Different prototypes were manufactured and tested. The measured radiation patterns show increased directivity and reduced the back radiation. The sensitivity results are in good agreement with our predictions. The studied configurations show promising features which make them potential candidates to create imaging arrays.

Session 2A3

Microwave and Millimeter-wave Antennas

Probe Feed Stair Shaped Dielectric Resonator Antennas

R. Chair, **A. A. Kishk**, **K. F. Lee**
University of Mississippi, USA

Dielectric resonator antennas (DRAs) offer several advantages such as small size and high efficiency. At high frequencies, they have much less metallic loss than conventional patch antennas. DRAs can be made with a wide range of materials and can be fed with different excitation methods. However, traditional DRAs with simple geometries usually have narrow bandwidth, typically around than 10%.

In this paper, dielectric resonator antennas with stair shaped geometries and circular cross sections are shown to have wide impedance bandwidth. The stair shaped DRA with one or two steps are designed to resonate in the X-band (8 GHz - 12 GHz). The proposed DRAs are shown in Figure 1. The dielectric constant of the DRA is 10.2. Off center coaxial probe is used to excite the broadside mode radiation pattern. The wideband characteristics of one or two-steps DRAs are represented by two similar equivalent models. The one-step DRA is equivalent to having two resonant radiators containing a cylindrical disk and an annular ring while the two-steps DRA is equivalent to a cylindrical disk and two annular rings. These equivalent resonators have close resonant frequencies, but with different effective permittivities. The total lengths of both designs are less than 0.4 free space wavelengths at 10 GHz, which are good candidates for array applications. Simulation results obtained by the commercial software WIPL-D show that the impedance bandwidth of both geometries can achieve more than 30% with stable broadside radiation patterns. The computational results are verified experimentally.

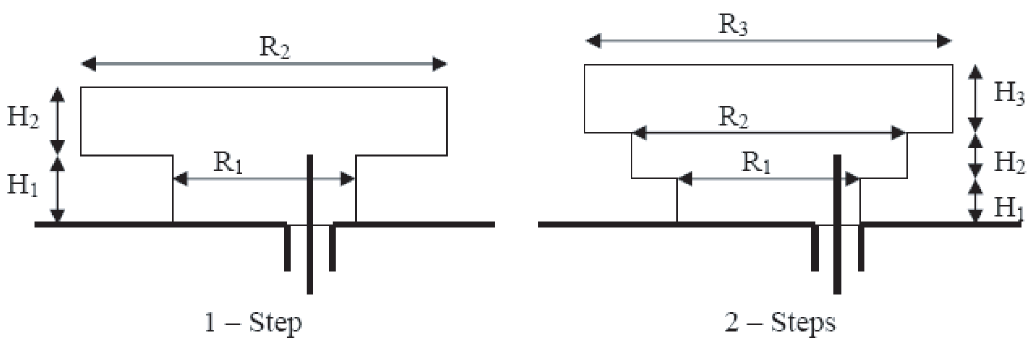

Figure 1: Geometries of the Stair Shaped DRAs

Wideband Aperture Coupled Rectangular Dielectric Resonator Antenna

Bin Li
City University of Hong Kong, China

Kwok Wa Leung
City University of Hong Kong, China

In recent years, tremendous efforts have been paid on investigating the linearly polarized (LP) wideband DRAs [1-2]. The strip-fed rectangular dielectric resonator antenna (DRA) has been studied theoretically and experimentally. It was found that, for some high-height rectangular DRA, the fundamental TE^y_{111} mode, together with the higher-order TE^y_{113} mode, can be excited to design a wideband LP DRA. The bandwidth of the dual-mode DRA of dielectric constant $\varepsilon_r = 10$ can be over 40%. However, this feeding method will add some conduction losses at high frequencies. In order to solve this problem, other feeding techniques such as the aperture coupled feed can be applied. In the strip-fed case, the TE^y_{111} and TE^y_{113} modes can be excited because they have similar field distributions near the ground plane. By introducing an effective quarter wavelength conducting strip, the two modes can be excited whereas the TE^y_{112} mode is suppressed. It is therefore believed that the same modes can be excited by an aperture coupled feeding structure, which can be used to design a wideband antenna. Apart from the above advantages of the aperture coupled feed over the strip-fed model, more dimensional parameters can be used for tuning. Preliminary results have demonstrated that a wideband antenna is obtainable.

REFERENCES

1. Kishk, A. A., "Wide-band Truncated Tetrahedron Dielectric Resonator Antenna Excited by a Coaxial Probe," *IEEE Trans. Antennas and Propagation*, Vol. 51, 2913, 2003.
2. Bit-Babik, G., C. Di Nallo and A. Faraone, "Multimode Dielectric Resonator Antenna of Very High Permittivity," *IEEE Antennas and Propagation Society International Symposium Digest, Monterey, California, USA*, Vol. 2, 1383, 2004.

A Circularly Polarized Low-Profile Loop Antenna with a Conducting Wall and Ring

H. Nakano, Y. Komine, J. Yamauchi
Hosei University, Japan

This paper presents a square loop antenna printed on a finite-sized dielectric substrate backed by a conducting plate (ground plate) of infinite extent. The antenna is designed to radiate a wide, circularly polarized (CP) beam at a frequency of 2.3 GHz (wavelength $\lambda_{2.3}$).

The square loop is defined by loop width w and outer side length s. The dielectric substrate is also square (with side length s), having relative permittivity ε_r and thickness B. The loop is excited at four points, each with a progressive 90-degree phase shift relative to their adjacent points, to obtain a CP wave. Analysis shows that this square loop has a radiation beam with a half-power beam width (HPBW) of 112 degrees.

To obtain a much wider HPBW, a conducting wall of height $H_{WL}(= B)$ surrounding the four sides of the dielectric substrate is added to the loop antenna, as shown in Fig.1. The wall (normal to the ground plate) has a conducting ring of width w_{ring}, which extends horizontally from the top of the wall. Analysis is performed to reveal the effects of w_{ring} on the HPBW. It is found that, as the ring width w_{ring} increases, the CP radiation beam becomes wider. When $w_{ring} = 0.11\lambda_{2.3}$, the HPBW is 180 degrees, and the gain between $\theta = 30$ degrees and 70 degrees is more than 2 dBi, where θ is the angle measured off the +z axis (normal to the antenna plane) toward the x-y plane (antenna plane). The frequency bandwidth for a VSWR = 2 criterion is calculated to be 2.3%.

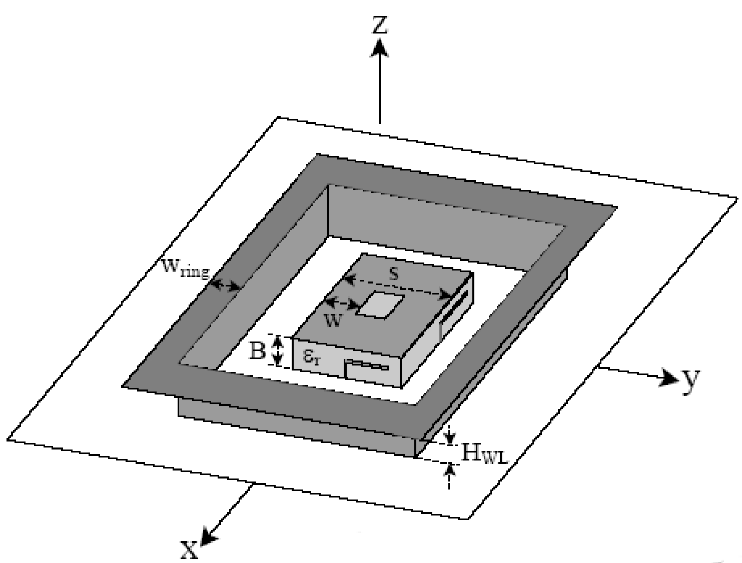

Figure 1: G.P. of infinite extent

An Unidirectional Magneto-electric Dipole Antenna

K. M. Luk
City University of Hong Kong, Hong Kong

Hang Wong
City University of Hong Kong, Hong Kong

Dipole antennas can be classified as electric or magnetic type. It is well established that an electric dipole antenna can be formed by exciting complementary currents in two thin wires; whereas, the magnetic dipole antenna can be constructed by a wire loop with current flowing in or by a radiating slot. Although the dipole antennas were developed long time ago, there are few antennas consisting of both electric and magnetic dipoles for performance enhancement. In this paper, a new antenna that incorporates both magnetic and electric dipoles characteristics simultaneously will be presented. The antenna has several attractive features such as wideband, low cross-polarization, low back radiation, stable radiation, high gain and unidirectional radiation pattern in both E and H-planes. It is highly attractive for modern mobile communication applications.

Internal Multi-band Antenna for Mobile Handset Applications

Soon-Ho Hwang, **Seong-Ook Park**
Information and Communications University, Korea

In the last decade, wireless communications have been dramatically developed with wireless devices. Simultaneously, mobile handsets design as well as its performance has been emphasized. So, since an internal antenna was introduced to the mobile phone in 1998, it has caused a lot of market interest. The reason is that internal antenna has several advantages such as comely design and less radiation power transmitted to human head compared to the conventional protruded monopole or helical type antenna. In addition, antenna market has required a small size, high radiation efficiency, and broad bandwidth for internal antenna.

This paper presents an internal multi-band antenna to satisfy with these requirements. This antenna covers four bands which are GPS(1575MHz), DCS(1710-1880MHz), PCS(1750-1870MHz), and UPCS(1850-1990MHz) for VSWR<2.0, respectively. Its bandwidth is approximately 600MHz. For designing this proposed antenna, it has 7mm height to optimize the radiation efficiency. The ground size of FR-4 PCB substrate has dimension of 36mm×72mm. And the radiating element is made of the rectangular shape of board. The board is composed of FR-4 with the length 15mm, the width 32mm, and the thickness 1mm. This board is used to achieve uniform performance under antenna mass production. The radiating parts are placed on top and bottom of the board. And the signal and ground lines from the board are connected to PCB. Also, this antenna is fed by coaxial cable as a feeding line. The radiating mechanism is similar to those of dipole antenna. Through the modification of dipole antenna such as variation of source and ground line, this proposed antenna can achieve a broad bandwidth. An asymmetric length of source and ground lines in dipole antenna caused different resonant frequencies. Consequently, two close resonant frequencies leaded to broad bandwidth in this antenna. In addition, a resonant frequency is changeable by varying the signal and ground line lengths. The measured return loss is smaller than -10dB in the desired frequency band. And there is good agreement with the measured and simulated results for the radiation patterns. Simulation was performed with Ansoft HFSS. The influence of antenna performance with plastic handsets, battery, and human head are presented.

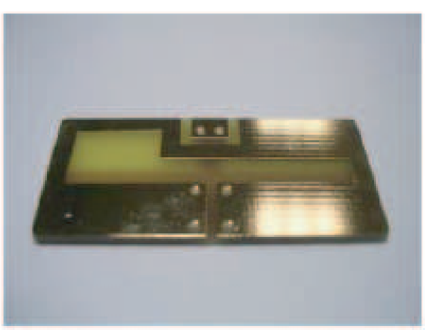

Figure 1: Radiating Element

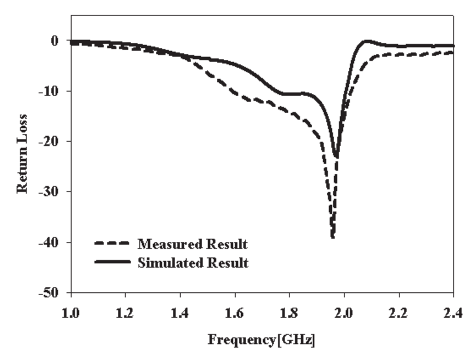

Figure 2: Return loss

Broadband Low Cross-Polarization Patch Antenna Using A Wideband Balun Feeding Network

Y. X. Guo[1], **L. C. Ong**[1], **K. M. Luk**[2]

[1]Institute for Infocomm Research, Singapore
[2]City University of HongKong, Hong Kong

The use of the L-probe as a proximity feed has proven to be an effective bandwidth widening technique for microstrip patch antennas with thick substrate. The capacitance introduced by the horizontal portion of the L-probe cancels out part of the inductance introduced by the vertical portion of the L-probe and this provides greater flexibility in enhancing the impedance matching of the antenna. For the L-probe proximity-fed rectangular patch antenna, a bandwidth of 35% and average gain of 7.5dBi has been achieved. Experimental studies have shown that the employment of a balanced feed for this antenna helps to substantially suppress the H-plane cross-polarization caused by the probe feed. However, the half-wavelength microstrip transmission line used in this scheme will produce a 180° phase difference only at the centre frequency. As a result, good H-plane cross-polarization suppression only takes place around the operating frequency and not across the entire passband.

In this paper, a novel broadband microstrip balun is proposed and employed for feeding the antenna to achieve consistently very low H-plane cross-polarization levels throughout the passband. The polarization performances, for the antenna using the proposed broadband balun feeding network and for the same antenna using a narrowband balun feeding network, are studied and compared. Two sets of feeding network, set A and set B, were simulated using IE3D. Set A refers to a commonly used narrowband microstrip balun, while set B refers to the proposed broadband microstrip balun. The maximum H-plane co-polarization levels and maximum H-plane cross-polarization levels for the two configurations are obtained and compared. It is observed that the antenna using set B yielded very low cross-polarization levels throughout the passband whereas the same antenna using set A delivered high cross-polarization except at frequency points around the operating frequency. It is also noteworthy that, compared to set A, the use of set B achieved equal or higher co-polarization levels and lower cross-polarization levels for every frequency points within the passband.

K Band X Type Slot Antenna Design on Silicon Substrate

Xiuping Li
Beijing University of Posts and Telecommunications, China

Hong Wang
Nanyang Technological University, Singapore

Junhui Zhao
Macao University of Science and Technology, Macao

A novel K-band Coplanar Waveguide (CPW) X type slot antenna is characterized on high-resistivity Si substrate (2000 ohm-cm). The X type slot antenna is fabricated on 500 μm Silicon substrate, with 2 μm Aluminum covered, and the layout is shown in Fig.1. The antenna is simulated by using Agilent Momentum, the simulated results show 1.2GHz bandwidth at VSWR<1.5, with center frequency 25.8 GHz and 2.5 dB gain is obtained. A coplanar transmission line with 100 μm GSG probe pitch is used for RF impedance matching, and the antenna is measured by using HP8510C Vector Network Analyzer. The measurement results in Fig.2 show that the antenna resonates around 27 GHz with a return loss greater than 21 dB, and around 1 GHz bandwidth is obtained. Fig.2 presents about 1 GHz frequency shift between the simulated and measured results, but the trends agree well.

Figure 1: X type slot antenna

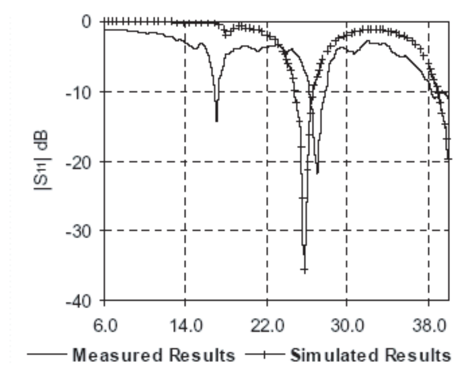

Figure 2: Measured and simulated return loss

Performance of Millimeter-wave Coplanar Patch Antennas on Low-k Materials

K. F. Tong
University College London, United Kingdom

K. Li, **T. Matsui**
National Institute of Information and Communications Technology, Japan

In this article, the simulation and experimental results of millimeter-wave Coplanar Patch Antennas (CPAs) using spin-on low-k dielectric substrate are presented. The antennas are designed for the direct integration of millimeter-wave / optical devices of coplanar waveguide (CPW) output terminals. Benzocyclobutene (BCB) with dielectric constant 2.7 is selected as the low-k dielectric substrate of the antennas. The measured resonant frequency and impedance bandwidth (S11 < -10dB) are 38.3GHz and 2.6% respectively. The maximum gain of the antenna is 4.2 dBi at 38.7GHz. Stable radiation patterns across the pass band are achieved. Good agreement between the simulation and measurement has been obtained.

A Bandwidth Enhancement Technique for Rectangular Microstrip Patch Antennas

Zaiyu Li
Chong Qing Three Gorges University, China

A bandwidth enhancement technique using parasitic elements for the microstrip patch antenna has been extended in this paper. This technique utilizes an additional rectangular ring surrounding radiating patch to improve bandwidth of the antenna while maintains the entire antenna size minimum. The proposed antenna was analyzed by the developed home code: finite-difference time domain(FDTD), and the dependence of the bandwidth on several design parameters, such as the width of gap and strip ring, is investigated. Especially, a structure operating at 27 GHz was purposed and optimized for applications in the LMDS (Local Mult-point Distribution System). The simulated results show that the bandwidth of the proposed antenna structure can be is up to 12.9%, which is larger than the that of a conventional rectangular patch antenna.

PBG Cells for the Harmonic Suppression of Microstrip Patch Antenna

Se-Hwan Choi, **Ho-Jun Lee**, **Jong-Kyu Kim**
Korea Electronics Technology Institute, Korea

Photonic Bandgap(PBG) structures usually mean periodic structures that exhibit band-stop and slow-wave characteristics. Generally, to make PBG structures in the microstrip line, specific patterns are periodically etched into ground plane. But such structures cause back radiation and gain reduction due to the presence of PBG holes. In the case of 1-D imensional PBG cell, these problems are not occurred because specific patterns are etched into transmission line itself. In this paper, we propose 1-D PBG cells which suppress the harmonic radiation from microstrip patch antenna.

PBG Cells with about 4mm length are fabricated on the RT/duroid 5880 substrate with the relative permittivity of 2.2 and the thickness of 20 mil. These cells produces the stop band characteristic of the transmission parameter at more than -10 dB from 19 to 35 GHz. To verify performance of PBG cells, two identical microstrip antennas are designed at 12 GHz. A rectangular patch has dimensions of 8.00mm $\times$ 7.98mm. Signal is fed to the antenna by the 50 ohm microstrip line with w = 1.59mm strip width and the impedance transformer with dimensions of 0.25mm $\times$ 4.7 mm. But one of these antennas has 50 ohm microstrip line with 1-D PBG cell for the comparison of the basic characteristics.

The return loss of these antennas was measured by the network analyser HP8510. The normal antenna resonates at frequencies of 12 GHz (fundamental), 24 and 28 GHz (corresponding to the second and the third harmonic frequencies). But PBG cell antenna does not have these harmonics.

In this paper, it is confirmed experimentally that the harmonic frequency of the microstrip patch antenna can be suppressed by inserting 1-D PBG cell in the feedline. 1-D PBG cell occupies very small area but can reduce harmonic radiations remarkably. Most planar antennas have harmonics that can disturb the other application. This 1-D PBG cell is very useful not only for the active antenna but also for whole planar antennas to suppress various harmonics.

Session 2A4

Microwave and Optical Devices

Antenna Analysis Using Wavelet Representations

Thomas Herzberg[1], **Rodica Ramer**[1], **Stuart Hay**[2]

[1]The University of New South Wales, Australia
[2]CSIRO ICT Centre, Australia

The aim of this work is to investigate the advantages of wavelet-type representations in electromagnetic analysis of antennas and related waveguide structures. A wavelet-type approach is described for the analysis of the modes of multi-conductor cylindrical waveguides where the conductors have polygonal cross-sectional shape. Such structures are of interest for example in the analysis of wideband array feeds for reflector antennas.

To find the modes and cut-off frequencies of the waveguides the method initially uses a Windowed Fourier Transform (WFT) representation of a potential function for the modes. This function is a linear combination of Gaussian elements, each consisting of a Gaussian window multiplied by a Fourier term defined in terms of a specified spatial frequency. The Gaussian windows and spatial frequencies are located on rectangular grids. For a given lowest spatial frequency, a sufficient condition for the maximum distance between the Gaussian windows is derived in order to maintain the frame property of the representation [1]. Frame bounds for various grid intervals have been estimated using an approach similar to [1] but for the two dimensional case.

To find the series coefficients of the potential function for TE, TM and TEM modes a general variational principle for the cut-off frequencies of the modes is applied. This results in a generalized linear matrix eigenvalue problem. The matrix elements consist of integrals over the cross-sectional area of the waveguide and the boundary of this region. For a subclass of cross-sections with orthogonal polygon edges, analytical solutions for these integrals are found in terms of the error function with complex argument.

Due to the good localization of the Gaussian windows the system matrices become sparse for large waveguide structures. This potentially allows solutions for large structures to be efficiently obtained by application of sparse-matrix eigenvalue solvers. Moreover, the accuracy of the solution can be increased by including more terms in the series. The analysis developed for this Gaussian WFT representation can easily be adapted to a wavelet representation using for example the Mexican-hat wavelet function.

REFERENCES

1. Daubechies, I., "Ten Lectures on Wavelets", *CBMS-NSF Conference Series in Applied Mathematics*, 1992.

Numerical Analysis of Wave Instability in Nonlinear Ferrite Structure Using Bifurcation Points of the Nonlinear Maxwell's Operator

G. S. Makeeva
Penza State University, Russia

O. A. Golovanov
Penza Military Institute of Artillery, Russia

M. Pardavi-Horvath
The George Washington University, USA

A new approach, based on the bifurcation theory, to develop mathematical models of nonlinear waves or oscillations in waveguiding or resonator structures (RS), containing bounded strongly nonlinear gyromagnetic medium, is proposed.

A numerical method for the analysis of the bifurcation points of the nonlinear Maxwell's operator was developed, using the reduction of nonlinear boundary problem to a system of ordinary differential equations together with the system of nonlinear functional equations. The Frechet's derivative was calculated to determine the eigenvalues of the linearized Maxwell's operator matrix.

The components of "weakly-nonlinear" waves were used to create the algorithm by the cross-sections method to solve the nonlinear diffraction boundary problem for a strip-slot RS with planar ferrite discontinuity.

The magnitudes of reflected signal waves, depending on the magnitude of the incident pumping wave, were determined using the numerical method of nonlinear autonomous blocs. Using our computational algorithm to determine the bifurcation points, the onset and the breakdown of self-oscillations, caused by the instability, were modeled. The transition regime from regenerative parametric amplification to parametric generation, depending on the magnitude of the pumping wave and resonator detuning was simulated infinitesimally close to the bifurcation points. This algorithm, based on the bifurcation analysis, is more complex that any other known ones, but the convergence and its stability for rounding errors is the best.

New results to model parametric excitations of magnetostatic or spin waves, solitons, and chaos in bounded strongly nonlinear ferrite, particularly in thin films and constrained geometries, will be described .

Mutual Coupling Effect on Thermal Noise in Multi-Element Antenna Systems

Snezana Krusevac[1], **Predrag Rapajic**[1], **Rodney Kennedy**[2]

[1] University of NSW, Australia
[2] ANU and NICTA, Australia

Multiple-input multiple output (MIMO) communication systems use antenna arrays to increase the communication capacity by exploiting the spatial properties of the multipath channel. Providing high capacity requires independence of the channel matrix coefficients, a condition generally achieved with wide antenna element spacings. For many subscriber units, such separations are unrealistic, and the resulting antenna mutual coupling can impact the communication system performance.

The prior studies have presented important findings concerning the effect of array mutual coupling on MIMO system performance, but they have neglected the influence of mutual coupling effect on thermal noise. The coupled antennae affect thermal noise power, a quantity that must be properly defined for closely spaced antennae in the multi-antenna system.

Thus, we shall present in this paper an network theory framework that enable including the mutual coupling effect on thermal noise in the analysis of MIMO systems. This framework includes a model for the thermal noise power calculation for the multi-antenna system in general case, including very small antenna spacings. Accurate analysis of thermal noise behaviour for coupled antennae in the multi-antenna system will be presented in this paper.

The application of the Generalized Nyquist's Thermal-noise Theorem enables extraction of the correlated part from the total thermal noise in closely spaced antenna elements in the multi-antenna system. The normalized correlated part by the total thermal noise power as a function of antenna spacings is estimated. The expectation that the higher correlation happens at smaller antenna spacing is confirmed by the simulation results. The analysis shows that thermal noise is partially correlated for antenna spacing from half of wavelength to zero.

Finally, we investigate signal-to-noise ratio (SNR) behavior in order to demonstrate the influence of mutual coupling effect on thermal noise on the communication performance of the multi-antenna system. We compare the SNR calculated using the classical method, which assume that only signal is affected by mutual coupling, and the presented method. We believe that the SNR in multiantenna system is underestimated if the effect of mutual coupling on thermal noise is not considered. Furthermore, theoretical consideration predicts that the underestimation grows when the number of antenna elements in the multi-antenna system increases. The predictions are confirmed by the simulation results.

Realization of Novel Dual-Mode Bandpass Filter

A. S. Shen[1], **G. M. Banciu**[2], **R. Ramer**[1], **A. Ioachim**[2], **R. Mansour**[3]

[1]University of New South Wales, Australia
[2]National Institute of Materials Physics, Romania
[3]University of Waterloo, Canada

A novel Dual-Mode Filter (DMF) is proposed and developed for mobile communication circuits. This new narrow band, low loss, dual-mode cross-slotted filter in a compact size is suitable for mobile and satellite communication.

The DMF layout presents two parts of slots, which are crossing a square patch. Furthermore, two additional fringe slots are introduced on each side of the square patch. The resonator is capacitively coupled to the external lines, which are placed at a right angle.

It is already known that, the conventional square patch dual-mode filters offer simple design, good power handling capability, etc. However, dual-mode patch filters usually require larger size than the dual-mode loop filters for the same frequency band. Moreover, an open microstrip patch is potentially a strong electromagnetic field radiator; therefore, the patch dual-mode resonators have high radiation losses and low unloaded quality factor. Even when shielded, the dual-mode patch resonators generate spurious couplings with the other circuit elements. The proposed DMF is smaller than a conventional patch dual-mode filter due to the presence of slots, which force the AC currents to flow along a longer path, avoiding the center of the square.

The filter was fabricated on a Rogers' Panel having a thickness of 0.635mm and a dielectric constant of 10.8. The use of a rather thinner panel provides a further reduction in the radiation losses and spurious couplings. Both lossless and lossy cases were considered. Initially, no perturbation in the filter symmetry was considered. The filter response presented a small resonance peak, indicating that the resonating modes are almost orthogonal and that only a weak coupling occurs, which is due to the asymmetric input/output couplings. In the presence of a perturbation, the coupling between the modes increases and the filter response improves. It is already known that a patch square mode filter does not present transmission zeros close to the pass-band. Although it was obtained by modifying a classical dual mode patch filter, DMF presents improved filter characteristics, with two transmission zeros on each side of the pass-band. The novelty of the proposed structure consists in the ability of controlling the resonant frequency and the bandwidth. It is found that the resonant frequency of the filter with 1% fractional bandwidth, could be shifted down to below 900 MHz.

REFERENCES

1. Zhu, L., P. M. Wecowski, and K. Wu, *IEEE Trans. on MTT*, Vol. 47, 650, 1999.
2. Casinese, A., A. Andreone, M. Barra, C. Granata, P. Orgiani, F. Palomba, G. Panariello, G. Pica and F. Schettino, "Dual Mode Superdonducting Planar Filters Based on Slotted Square Resonatoers," *IEEE Trans. on Applied Superconductivity*, Vol. 11, No. 1, 2001.
3. Cassinese, A., A. Andreone, M. Cirillo, F. Palomba, G. Panariello, G. Pica, R. Russo, F. Schettino, and R. Vaglio, *J. of Superconductivity*, Vol 14, No. 1, 2001.
4. Hsieh, L.-H., K Chang, "Dual-Mode Quasi-Elliptic-Function Bandpass Filters Using Ring Resonators With Enhanced-Coupling Tuning Stubs", *IEEE Trans. on MTT*, Vol. 50, 1340, 2004.
5. Banciu, M. G., G. Lojewski, A. Ioachim, L. Nedelcu, N. Militaru, A. Shen, R. Ramer, "New Planar Compact Dual Mode Filters for Mobile Communications", *CAS Proceedings to International Semiconductor Conf.*, 2004.

Designing Optical Switches Based on Silica Multimode Interference Devices

Zhe Jin, **Gangding Peng**
The University of New South Wales, Australia

Optimal design of optical switches based on silica multimode interference devices is discussed. The optimization includes two steps. First the sizes of multimode waveguides are adjusted to realize low loss and good uniformity multimode interference couplers. Then the shifted phases in the interferometer arms selected to achieve small cross talk according to reciprocal characteristics of the couplers. Thus the optimized devices turn out both low loss and small cross talk. The approach is verified by numerical simulations of the optical switches. We show that the approach could reduce the device loss and crosstalk by 1dB and 9dB.

Designing Weakly Guiding Multimode Interference Devices Using Self-imaging Theory

Zhe Jin, **Gangding Peng**
The University of New South Wales, Australia

Self-imaging theory that is developed for strongly guiding structures has been frequently used for designing multimode interference devices based on weakly guiding structure. In this paper we discuss how the self-imaging theory fits for the strongly guiding structure and study the validity of using self-imaging method in weakly guiding multimode interference structures, by investigating the dispersion relations of modes with regard to the width of a multimode waveguide. Through the establishment of the link between strongly guiding and weakly guiding in terms of the modal dispersion difference versus the width, we demonstrated how self-imaging method could be appropriately applied in weakly guiding structures.

Ytterbium-Codoping in Thulium Doped Silica Fiber

Jun Chang[1,2], **Gang-Ding Peng**[1], **Qing-Pu Wang**[2]

[1]Photonics The University of New South Wales, Australia
[2]Shandong University, China

Since the successful development of new all-wave optical fibres and the opening up of a new transmission window (S-band) in silica fiber, developing thulium doped fluoride or silica fiber for S-band optical amplification has been quite active. While thulium doped fluoride fiber has material related problems, thulium doping in silica fibre for S-band optical amplification has a fundamental problem that its relevant energy levels, i.e. $^3H_4$ and $^3H_4$ of Tm^{3+}, have very undesirable values of lifetimes and that this results in very low pump efficiency.

Here we propose a novel ytterbium-thulium codoping scheme. It is expected that ytterbium codoping could facilitate population inversion between the relevant energy levels, through a cross energy transfer process between Tm^{3+} and Yb^{3+}. Hence this scheme would mitigate the major deficiency of thulium-doped silica fiber. Moreover, ytterbium codoping could also help to reduce self-quenching effect in highly doped TDFAs. A set of nonlinear coupled ODEs, which govern the dynamics of optical amplification in the ytterbium-thulium codoped material system, was established based on the rate equations and propagation equations. In particular, we take into consideration of the energy transfer process between Tm^{3+} and Yb^{3+} in silica fiber host. We have also developed a novel computational strategy to solve the equations and studied various cases of ytterbium-thulium codoping under different parametrical conditions. We demonstrated that the gain characteristics and pump efficiency can be improved by ytterbium codoping and using an auxiliary pump at 980nm. We have also investigated the effects of the energy transfer parameters. It has been found that higher doping concentrations would produce higher gain improvements. This suggests that fabrication techniques for higher doping concentrations should be pursued in future.

RF Signal Distribution over Polymer Optical Fiber

Tao Jia[1], **Shilie Zheng**[1], **Xianmin Zhang**[1], **Xinyu Jin**[1], **Jian Xu**[2]

[1]Zhejiang University, China

[1]Institute of Chemistry, Chinese Academy of Sciences, China

As mobile services and wireless LANs proliferating into the office and residential environments, indoor or in-building wireless coverage will become more and more important in future. Radio over fiber (ROF) technology has been proposed as a solution for reducing overall system complexity. By this technology, the radio signals directly transmit over the fiber without processing at the antenna base station, and the complicated RF modem and signal processing functions are transferred from radio access points (RAUs) to a centralized control station. Therefore it reduces system-wide installation and maintenance costs, simplifies the remote antenna base station, and makes signal format transparent.

In ROF systems, the wiring needs to be easy to install, and easy to extend. Multimode optical fiber (MMF) provides a cost-reducing alternative for the commonly used single-mode fiber. Polymer optical fiber (POF) is emerging as an attractive alternative. Clear advantages offered by deploying POF are low installation and maintenance costs, large core diameter for easy coupling and splicing, and the ductility and flexibility for installation.

For transporting high bitrate signals, the limited bandwidth-length product of POF is a point of concern. In this paper, instead of using pure baseband (with respect to the modal bandwidth) transmission, it has been suggested that the frequency range beyond the 3-dB modal bandwidth point can be used to transmit data. The optical transmission characteristics of the radio over POF (RoPOF) link have been investigated. The possibility for passband transmission has been explored. In the experiments, the RF carried quadrature-phase-shift-keyed (QPSK) data, global system for mobile (GSM) signals and pacific digital cellular (PDC) signals over 20m and 50m POF are implemented. The eye diagrams and EVM of the signals are carried to evaluate the capability. The experimental results indicate that an improvement in the transmission performance of a SI-POF link could be achieved utilizing the passband channel, which situated above the 3-dB base bandwidth.

*This work is supported by Specialized Research Fund for the Doctoral Program of Higher Education (grant No.20010335037).

All-optical Microwave Mixers Using Stimulated Brillouin Scattering

Yichun Shen, **Guofeng Shen**, **Xianmin Zhang**
Zhejiang University, China

There is an increasing interest in radio over fiber systems (RoF) for the application of broadband wireless access networks in recent years. Traditionally, high frequency microwave generators, high frequency modulators and high speed photodetectors (PDs) are needed in base stations (BS) and center station (CS). This makes the systems complexity and expensive. In general, the band data is up converted by an external modulator and mixed down by another external modulator at the base station. It is limited by a significant amount of insertion loss and polarization sensitivity. Some techniques using nonlinearity of optoelectronic devices as the electric local oscillators (LOs) to mix with the photodetected microwave photonic signals have been reported. The drawback is that high frequency electrical LO signal sources are required. All-optical methods utilizing the nonlinear photodetection behavior of a high-speed PD and cross-gain modulation in a semiconductor optical amplifier have been tried to overcome this limitation.

In this paper, a novel and simple all-optical microwave mixer based on stimulated Brillouin scattering (SBS) is presented. The optic-link is simplified using a fiber Bragg grating to extract Stokes wave to mix with 11 GHz microwave photonic signal for up/down conversion. By stretching the fiber Bragg grating (FBG), the reflectivity at the Stokes wavelength can be adjusted. Then the power of the reflected Stokes wave can be precisely controlled by simply tuning the FBG. However, the more Stokes wave is reflected for mixing with the microwave photonic signal, and the less Stokes wave is transmitted for interacting with the modulated signal in the single mode fiber (SMF), which reduces the SBS effect. Therefore, it is clear that the reflectivity of FBG needs to be tuned to the optimum value for attaining the largest forward Stokes wave power. The microwave mixer based on the 2nd order Stokes wave for 22 GHz microwave photonic signal down conversion is also presented. The long fiber ring is used to produce the 2nd order Stokes wave for mixing with 22GHz microwave photonic signal for down conversion. The power of down conversion signal can be controlled by tuning the power of the input 22GHz microwave photonic signal before long fiber ring. The conversion of 11GHz and 22GHz microwave photonic signal is experimentally realized. The phase noise of conversion signal is also measured.

Photonic Microwave Filter Synthesis Using Tabu Algorithm

Jinyue Lu, **Hao Chi**, **Xianmin Zhang**
Zhejiang University, China

Transversal photonic microwave filters (PMFs) are important parts in fiber-optic microwave\millimeter wave processing systems. In this paper, the problem of synthesis of FIR photonic microwave filter with linear phase response is addressed and a novel method employing tabu algorithm is proposed. As an illustration of the proposed method in the application of filter design, the optimization of fiber Bragg grating (FBG)-based photonic microwave filter is demonstrated. Due to the incoherent interference property of most PMFs, only positive taps are available in the filtering response, which makes the conventional digital filter design method can not be applied readily. Some methods have been proposed to design photonic microwave filters, such as that based on genetic algorithm and that based on simulated annealing) algorithm. However, in previous works, the linear phase response characteristic of filters have not been considered carefully, while which are important to communication systems for suppressing phase distortion. In this work, we present a novel design method based on Tabu Search algorithm and discuss the issue regarding linear phase response of PMFs in detail. Tabu algorithm is a meta-heuristic search developed by Glover for large combinational optimization tasks and is characterized by its ability to escape local optima by introducing a FIFO queue called tabu list into the hill-climbing method. In the proposed design method, FBGs are used as the tapping and weighting elements of PMF. The tapping coefficients of PMF are optimized by Tabu algorithm. In the optimization process, the linear phase response of PMF as a constraint condition is carefully considered. As a comparison, the designs of PMF with and without linear phase response are both demonstrated. Numerical results confirm the effectiveness of the proposed method and also show that the proposed method can be effectively applied to design different filtering systems with different constraints.

*This work was supported by the National Natural Science Foundation of China (Grant No. 60407011 and 60271010) and Zhejiang Provincial Natural Science Foundation of China (Grant No. Y104073 and 602064).

Session 2A5

Compuational Electromagnetics–Recent Advances

Advanced Numerical Techniques for Large PEC Cavity Modeling

C. F. Wang, **Y. Xu**, **F. G. Hu**, **Yeow Beng Gan**
National University of Singapore, Singapore

The air intake structure greatly affects the overall electromagnetic scattering response of real airborne targets. This has motivated the development of accurate and efficient methods to model the electromagnetic scattering of such structure. This presentation summarizes the work done on several newly developed numerical techniques in Temasek Laboratories @ NUS, for electromagnetic scattering from large PEC cavity, as follows:

I. Equivalent Models and Integral Equations

Two sets of coupled integral equations have been formulated using two different equivalent current models for indented screens or open-ended cavity, respectively. Numerical verifications, accuracy, and well-posedness of the coupled integral equations will be discussed to facilitate understanding on how integral equations can be applied to the study of cavity problems. Further development on these integral equations with fast algorithms results in robust solvers for modeling of large cavity structures.

II. Development and Extensions of the Field Iterative Method (FIM)

Three distinct phenomena are observed from the interior scattering of cavity: 1) induction of an aperture field by sources in the exterior region; 2) propagation of electromagnetic fields down the duct, "guided" by the walls; and 3) reflection at the termination end. Upon reflection, the fields propagate back towards the aperture, which are integrated to obtain scattered field. This basic understanding of interior scattering from large PEC cavity gave rise to the original field iterative method (FIM) proposed by Reuster and Thiele. We have improved the original FIM through the use of an accurate equivalent model and fast algorithm, namely FAFFA-FIM, for modeling of large 2D and 3D PEC cavities.

III. Non-Overlapping Domain Decomposition Method (DDM)

A non-overlapping domain decomposition method is applied to solve surface integral equations for electromagnetic scattering from cavities. This scheme allows the cavity to be divided into sub-domains and modeled on sub-domains sequentially or in parallel. Thus, the memory requirement and CPU time for modeling of large cavity structures can be dramatically reduced. Moreover, interior resonances are eliminated from this scheme, in contrast to that in the Generalized Network Formulation.

IV. Development of Fast Higher-Order FE-BI Code

The higher-order FE-BI method proposed by Jin and Liu et al is suitable for computation of the echo area of inhomogeneously-filled and arbitrarily-shaped cavity. Through using the frontal solver, higher-order FE-BI method can efficiently handle electromagnetic scattering from large and deep cavities. Typical numerical results and findings for cavity modeling will be shown at the conference.

Broad-Band MLFMA and Plane-wave Expansions of the Green's Function

H. Wallén, **J. Sarvas**
Helsinki University of Technology, Finland

Efficient multilevel fast multipole algorithms (MLFMA) are based on plane-wave expansions of the Green's function $G(\mathbf{r})$. The traditional MLFMA is based on the following plane-wave expansion given by the Rokhlin translation formula,

$$G(\mathbf{D}+\mathbf{d}) = \frac{e^{ik|\mathbf{D}+\mathbf{d}|}}{4\pi|\mathbf{D}+\mathbf{d}|} \approx \frac{ik}{(4\pi)^2} \int_{-\pi}^{\pi} \int_{0}^{\pi} T_L(\theta,\varphi) e^{i\mathbf{k}(\theta,\varphi)\cdot\mathbf{d}} \sin\theta \mathrm{d}\theta \mathrm{d}\varphi, \quad \mathrm{D} > \mathrm{d}, \tag{1}$$

with an explicit expression for the translation function T_L. This presentation, however, suffers from the well-known *low-frequency breakdown*, which occurs if the side length of the division cube is essentially smaller than the wave-length. To overcome this problem and to achieve a *broad-band* MLFMA one has to resort to other representations of the Green's function. Several recent proposals for broad-band MFLMA, including (L. J. Jiang and W. C. Chew, Microwave Opt. Tech. Lett., 40, 117-122, 2004) and (E. Darve and P. Havé, Phil. Trans. A, 362, 603-628, 2004), have been based on the following *spectral presentation*, also called *inhomogeneous plane-wave expansion*, of the Green's function,

$$G(\mathbf{r}) = \frac{e^{ikr}}{4\pi r} = \frac{ik}{8\pi^2} \int_{-\pi}^{\pi} \int_{\Gamma} e^{i\mathbf{k}(\theta,\varphi)\cdot\mathbf{r}} \sin\theta \mathrm{d}\theta \mathrm{d}\varphi, \quad \hat{\mathrm{z}}\cdot\mathbf{r} > 0. \tag{2}$$

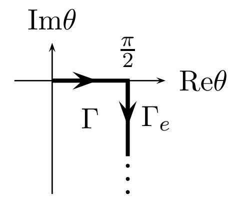

Another recent proposal (L. Xuan, A. Zhu, R. J. Adams, and S. D. Gedney, AP-S/URSI Symposium, Monterey, CA, 119-1198, 2004), called the uniform MFLMA (UMLFMA), is based on a modification of the Rokhlin translation formula so that the θ-integration is over horizontal lines from $-\pi - i\alpha$ to $\pi - i\alpha$, $\alpha > 0$ depending on the division level, and the translation function is found numerically. In our presentation we propose an efficient broad-band MLFMA based on the spectral representation of the Green's function and designed to combine the best features of the above approaches. For the propagating part (real θ), we use an entirely FFT-based direction independent approach. For the direction dependent evanescent part we use highly efficient generalized Gaussian quadrature for the complex θ integral. A novel feature is the use of efficient interpolation and anterpolation matrices in θ-direction based on a simple least squares procedure. For small division cubes the outer-to-inner translations in both cases can also be carried out efficiently by direction dependent precomputed translation functions, which are found by a simple least squares procedure. We also present numerical examples which show that our method is error controllable. UMLFMA is direction independant, and therefore, it has a lower computational cost than our method but, as the examples demonstrate, in our method the error controllability is much better.

Scattering and Radiation Modeling Using Hybrid Integral Equation Approach and Mixed Mesh Element Discretization

Cai-Cheng Lu, **Zhiyong Zeng**
University of Kentucky, USA

A mixed mesh algorithm is developed for the integral equation modeling of scattering by three dimensional complex radar targets that consist of conducting surfaces and radar absorbing materials. The integral equation combines the surface integral equation (for conducting surfaces) and the volume integral equation (for dielectric material regions). Because both surface and volume domains are to be modeled, and because of the constraints of good connectivity in a mesh, it is sometimes very difficult to model a complex scatterer using only one type of mesh element. The mixed mesh element scheme is proposed to overcome this difficulty. In this scheme, the surface is modeled by a set of triangles and quadrangles, and the dielectric volume is modeled by a set of tetrahedrons, prisms of triangle base, and prism of quadrangle base (the hexahedron). Including the mixed mesh elements in target discretization makes it possible for flexible meshing and for improving mesh quality. It is known that better mesh quality is essential to solution accuracy as well as to the solution efficiency. Most previous modeling programs adopt only one type of mesh element such as triangle only or quadrangle only. The combination of different types of mesh elements provides flexibility when complex targets are considered. For example, for a simple three-dimensional ogive shaped target, the sharp tip can be easily modeled by triangles, and the relatively smooth part can be more efficiently modeled by quadrangles. Similar conclusion applies to the combination of tetrahedron and hexahedron elements. In the discretization of the hybrid integral equations, the Rao-Wilton-Gllison basis functions are selected for the triangle and tetrahedron elements, and the roof-top basis function is used for the quadrangle and hexahedron mesh elements. The discretized matrix equation is solved using conjugate gradient method and the matrix-vector product in the iteration is accelerated by the multilevel fast multipole algorithm. Our simulation shows that as long as the average edge length remains the same, the results from single element mesh and combined element mesh are of the same order, but the later uses less number of unknowns, and sometimes less iteration numbers. The presentation will show how the continuity conditions are retained across the mixed mesh elements, and numerical examples will also be provided to demonstrate the validation and application of the mixed mesh algorithm.

Simulating Antennas on Complex Platforms

W. C. Chew[1], I. T. Chiang[1], M. K. Li[1], G. Sorenson[1]
A. Hesford[1], Y. Liu[1], Z. G. Qian[1], M. S. Tong[1]
L. J. Jiang[2], H. Y. Chao[3], Y. H. Chu[4], S. Ohnuki[5]
V. Bodrov[6], H. P. Hsu[7], J. Song[7]

[1]University of Illinois, USA
[2]IBM, USA
[3]NCTU, Taiwan
[4]Agilent, USA
[5]Nihon University, Japan
[6]GM, USA
[7]HRL, USA

This talk will review our work on simulating automobile antennas on a complex platform. The complex platform here is a car. The antenna can operate in the GHz range, and therefore, the whole car can be many wavelengths long. Moreover, the antennas and the car body consist of a mix of materials that are metal and dielectric, as well as absorbing materials. We will discuss how these complex geometries and complex materials can be modeled using integral equation method.

This problem is mainly solved by integral equation method. The integral equation is first derived from Maxwell's equations using the Green's function method. Then the integral equation can be converted to a matrix equation either using the method of moments (MOM), or the Nystrom method. The material part can be modeled by volume integral equation, while the wire part can be modeled by wire basis functions. Thin dielectric sheets can be modeled by the thin dielectric sheet approximation. For absorptive or reactive surfaces, they can also be modeled by the impedance boundary condition.

When the antenna together with the whole car is simulated, huge computational resource is needed when conventional methods are used to solve the problem. By the use of fast methods, and good preconditioning methods, the memory and CPU resources can be reduced. We will discuss the use of the multilevel fast multipole algorithm (MLFMA) to accelerate the solution of integral equations. When iterative solvers are used to solve the resultant matrix equation, the iteration counts often become unpredictable. We will discuss the use of various preconditioners to reduce the iteration numbers needed to solve the radiation problem.

The most difficult part of this problem is that the geometry needed to model the antennas and the platform has mixed lengthscales, viz., the antenna has fine details, and may need to be modeled by very fine meshes, while the car body has generally smooth surfaces, and it can be modeled with relatively coarse meshes. Therefore, ill-conditioning from disparate grid sizes comes about, and way to overcome this ill-conditioning problem has to be overcome. Due to the mixture of fine and coarse meshes, hierachical tree structure needs to be used to for the tree-based fast solvers. Moreover, block diagonal preconditioning generally can be used to accelerate the convergence of these problems.

Modified C-PMCHW Formulation for Scattering from Dielectric Coated PEC Bodies

Jian Feng Zhang, **T. J. Cui**
Southeast University, China

The electromagnetic (EM) scattering from arbitrarily shaped three-dimensional dielectric-coated PEC bodies is a very interesting topic and has been studied by many investigators. In this work, an accurate model has been established based on the equivalence principle for the EM scattering by a PEC object coated with multiple dielectric layers, which can be solved using the method of moments (MoM). Several surface integral equations (SIE) are derived from the equivalence sub-problems, and the original problem can be described by the equivalent electric current J and the equivalent magnetic current M. On each dielectric-dielectric (D-D) interface, a set of four SIE are derived from the interior and exterior equivalence. A set of two SIE exist on the dielectric-PEC (D-P) interface. By applying the boundary conditions on the D-D interfaces, the PMCHW formulation is obtained. On the D-P interface, in order to overcome the interior resonance, a modified combined-field integral equation (CFIE) written as $\alpha \mathrm{E}|\tan + (1-\alpha)\eta_0 H|\tan = 0$ has been adopted to yield accurate and stable solutions, instead of using its original form: $\alpha \mathrm{E}|\tan + \hat{n} \times [(1-\alpha)\eta_0 H] = 0$. Then, the traditional MoM is applied to solve the coupled integral equations by expanding the unknown currents J and M with RWG basis functions followed by the Galerkin's procedure. The reason why to use the modified CFIE will be explained below.

Because the PEC target is coated with dielectric layers, the magnetic field integral equation (MFIE) on the D-P interface includes the contribution from the magnetic current on the interior D-D interface close to the PEC object through $\hat{n} \times (i\omega F - \nabla\Phi)$. If we use the original CFIE, an extra calculation of a line integral arising from $\langle f_i, \hat{n} \times \nabla\Phi \rangle$ is required. Using the modified CFIE, however, such an extra calculation is not needed. We remark that the modified CFIE cannot be reduced to MFIE ($\alpha = 0$), because the principle value of $\langle f_i, i\omega A f_j \rangle$ is zero when the field and source points are in the same triangle patch, which yields a worse-conditioned impedance matrix. Fortunately, MFIE is not usually used due to the resonant problem. In the modified CFIE, however, the impedance matrix becomes well conditioned because of the contribution of the electric field integral equation. Numerical results have verified the above conclusion, i.e., the modified CFIE can give stable and accurate simulations without computing the additional line integrals.

*This work was supported in part by the National Science Foundation of China for Distinguished Young Scholars under grant 60225001, and in part by the National Science Foundation of China under grant 60496317.

The Time-domain Finite Element Method for Electromagnetic Analysis

J.-M. Jin, **D. Jiao**, **Z. Lou**, **R. Petersson**
University of Illinois at Urbana-Champaign, USA

Because of their potential to simulate transient phenomena, perform broadband characterization, and model nonlinear devices, numerical methods that can predict electromagnetic fields directly in the time domain have received much attention in recent years. The best-known technique is the finite-difference time-domain (FDTD) method. Progress has also been made on the time-domain method of moments (MoM) that solves integral equations. As far as the finite element method is concerned, a variety of time-domain approaches have been proposed during the past few years. One class of approaches solves Maxwell's equations directly. This usually can result in an explicit scheme, which does not require a matrix solution in each time step. However, these approaches generally work in a leapfrog fashion similar to the FDTD method. As a result, the well-developed frequency-domain finite element method cannot be adapted easily to the time domain. Another class of approaches to formulating the time-domain finite element method is to solve the second-order vector wave equation, or the curl-curl equation, obtained from Maxwell's equations in a similar manner used in the frequency domain. The major disadvantage of these approaches is the need to solve a matrix equation in each time step.

In this talk, we review our recent progresses in the development of the finite element analysis in the time domain using the second approach. These include the implementation of perfectly matched layers (PML) and boundary integral equations (BIE) for the mesh truncation, the development of an accurate waveguide port condition, the application to general scattering and antenna problems, and a novel formulation for the analysis of periodic structures. Numerical examples will be shown to demonstrate the accuracy and capability of the method.

A Domain Decomposition Symmetric FEM-BEM Formulation, Free of Internal Resonances, for Solving Electromagnetic Problems

Seung Mo Seo, **Kezhong Zhao**, **Marinos N. Vouvakis**, **Jin-Fa Lee**
The Ohio State University, USA

The hybrid FEM-BEM is one of the most appealing methods for the analysis of unbounded electromagnetic problems. The final matrix resulting from the coupling of the two methods traditionally ends up with a non-symmetric system [1]. The drawback of the conventional FEM-BEM was tackled in reference [2]. To circumvent the straightforward solution technique, a single-level IE-QR [3] was adopted for the BEM computation.

This paper is the extension of the previous symmetric FEM-BEM work. The key ingredient of the proposed method is considering FEM and BEM as two separate domains. Therefore, the resulting matrix solution is sought through iteration process between FEM and BEM domains. The process translates to non-conformal meshes between FEM and BEM. This unique feature enables us to the efficient computation of the FEM-BEM. For two domains, existing algorithms for FEM and BEM meshes are directly applied. For example, we can employ a p-type MUltiplicative Schwarz (pMUS) preconditioner [4] to solve FEM matrix effectively. Moreover, the current approach uses a Direct Boundary Integral Equation (BIE) formulation [5], which is coercive and free of internal resonance problem. Also, due to the coupling to the FEM, the final BEM matrix is dominated by a positive-definite matrix, thus is well conditioned. The IE-FFT algorithm [6] further speeds up the computation of the BEM matrix. The IE-FFT is grid- or FFT-based algorithm and integral kernel is interpolated on a regular grid. Details of the formulations and numerical examples will be shown in the presentation.

REFERENCES

1. Liu, J. and J.-M. Jin, *IEEE Trans. Antennas Propagat.*, 1212, 2002.
2. Vouvakis, M. N., S.-C. Lee, K. Zhao and J.-F. Lee, *IEEE Trans. Antennas Propagat.*, 3060, 2004.
3. Seo, S. M. and J.-F. Lee, *IEEE Trans. Antennas Propagat.*, 2141, 2004.
4. Lee, J.-F. and D. K. Sun, *IEEE Trans. MTT*, 864, 2004.
5. Buffa, A. and R. Hiptmai, *Topics in Computational Wave Propagation Direct and Inverse Problems*, 83, 2000.
6. Seo, S. M., M. V. Vouvakis, C.-F. Wang and J.-F. Lee, *IEEE Trans. Antennas Propagat.*, submitted for publication.

Preconditioned Iterative Solution of the Combined-field Integral Equation with the MLFMA

Levent Gürel, **Özgür Ergül**, **Tahir Malas**
Bilkent University, Turkey

Iterative solution of large problems of computational electromagnetics, which are obtained from mathematical formulations of real-life electromagnetic problems, is considered. In particular, our work on the fast multipole method (FMM) and the multi-level fast multipole algorithm (MLFMA), iterative solvers, preconditioners, and integral-equation formulations will be emphasized. Our efforts to reduce the number of iterations will be presented within the context of electric-field integral equation (EFIE), magnetic-field integral equation (MFIE), and combined-field integral equation (CFIE). The effects of various iterative solvers and preconditioners on the iteration counts will also be addressed.

Combining the EFIE with the MFIE to obtain the CFIE can also be interpreted as a mode of preconditioning. In this context, we consider the simultaneous solution of the EFIE and MFIE in the least-squares (LS) sense, instead of adding them into a single equation. Simultaneous solution of the square EFIE matrix equation and the square MFIE matrix equation requires the solution of a rectangular CFIE matrix equation. For this purpose, the MLFMA is employed within the framework of a stable LSQR algorithm by carefully implementing the matrix-vector products involving the Hermitian system, in addition to the regular matrix-vector products, to preserve the $O(N \log N)$ complexity.

In addition, explicit preconditioning schemes will be reported. Both exact and approximate inverses of sparse matrices containing electromagnetic near-field interactions of various strengths are used as preconditioners. Thresholding and reordering of the sparse near-field matrix are considered. Comparisons with some other popular preconditioners will be given. Spectra, convergence rates, and other relevant metrics of preconditioned linear systems derived from computational electromagnetics will be studied.

Numerical Solutions of Random Rough Surface Scattering Problems Using the UV/SMCG Method

Peng Xu
City University of Hong Kong, China

Leung Tsang
University of Washington, USA

Rough Surface scattering effects are important problems in microwave remote sensing of soil and snow. In remote sensing of soils from 1.5 Ghz to 19 Ghz, the rms heights can vary from a fraction of a wavelength to 1 to 2 wavelengths. In active and passive microwave remote sensing of snow from 5 Ghz to 37Ghz, the rms height of the rough interface between snow and ground can vary from a fraction of a wavelength to several wavelengths. To use a single physical model over such a wide frequency range with a single set of physical parameters of rms height and correlation function, we have used Numerical Maxwell Model based on 3-D simulations of Maxwell equations (NMM3D). Fast numerical algorithms have been developed to accelerate Method of Moment solutions of Maxwell equations. The common methods include sparse-matrix canonical grid method (SMCG), and the multilevel fast multipole method (ML-FMM). Recently we have also used the multi-level UV method. When the rms height of the rough surface increases, the applicability of the SMCG method depends on the memory storage or the efficiency of computing the near interactions and the accuracy of the Taylor series expansion of the far interactions. Therefore, the SMCG method is only suitable for surfaces up to a moderate roughness.

In the multilevel UV method, we have used fast coarse-coarse sampling to search rank of each block, and construct matrix U and V to compress each block based on interpolation technique. The accuracy of the UV method is controllable by varying the threshold, which is corresponding to blocks' ranks. The rank will increase with increase of level number in 3-D problems. Then the memory requirement at higher levels becomes larger in spite of considerable compression.

In this paper a procedure is developed for combining the multilevel UV method with the SMCG method in the computation of 3-D wave scattering from rough surface. It handles near and intermediate field interactions in the multilevel UV method and far field interactions in the SMCG method. This hybrid UV/SMCG method removes large memory requirement of both the UV method in far field and the SMCG method in near field. The computational complexity for the UV/SMCG method is still $O(N \log N)$. The tradeoff between UV part and SMCG part is controlled by selecting a neighborhood distance r_d. By choosing a larger neighborhood distance, only a small number of Taylor's expansion terms is required in the far field SMCG part. This means that a large surface area problem with a large rms height can be solved by the hybrid UV/SMCG method.

We demonstrate the UV/SMCG technique in 3-D scattering problem of Gaussian random rough surface with exponential correlation function and with Gaussian correlation function. The frequency dependences of scattering using a single set of physical parameters are illustrated in the simulations. The numerical simulation results are compared with the small perturbation method (SPM) and the Kirchhoff approximation (KA). We have also implemented the UV/SMCG method on parallel computation.

A Strategy for Parallel Implementation of the FDTD Algorithm Using the Grid-enabled MPI

Juan Du, **Shouzheng Zhu**

East China Normal University, China

The Finite-Difference Time-Domain method (FDTD) remains one of the most widely used numerical time-domain techniques in electromagnetism. In order to reduce the computational time and the computer storage demand, the strategy of domain decomposition provides an easy way of parallelizing FDTD. In terms of parallelism technique, the Message-Passing Interface (MPI) is becoming the new international standard for parallel programming. In this paper, a parallel implementation of the FDTD algorithm based on parallel sockets communication is proposed. The optimized MPI program could easily run on a grid-enabled MPI (MPICH-G2), which is a complete implementation of the MPI-1 standard using Globus Toolkit services to support efficient and transparent execution in heterogeneous Grid environments. The results show that more efficient communication can be achieved, and this kind of grid parallel computing environment proved to be low-cost, more practical and more efficient.

Computation was carried out on two HP2.4GHz PCs, each with 512 Mbytes of memory and representing one process equipped with MPICH-G2. The PCs are interconnected with a 100Mbps Ethernet, the compiler is gcc3.4, and the operational system is RedHat Linux9.0. Once the computation begins, MPICH-G2 selects the most efficient communication method possible between the two processes. In this optimized algorithm, the Globus communication (Globus IO) with the option of utilizing parallel sockets via Globus' GridFTP has been introduced. Consequently, a set of parallel sockets between a pair of designated processes can be applied for better use of the available bandwidth over a high-bandwidth network.

A numerical simulation of an X-waveband waveguide has been realized using one-dimensional Cartesian topology. The optimal socket pairs and different computational scales have been explored in this paper. The memory requirement, computational time of the processors and the speedup are also given in detail. Numerical results show that the optimized algorithm based on parallel sockets can provide more efficient communication in a grid-enabled MPI environment, when compared with the serial and the original MPI parallel implementation of the conventional FDTD algorithm. Meanwhile, the grid parallel computing is promising method in the field of high performance computing.

Scattering of Electromagnetic Waves from Vibrating Perfect Surfaces: Simulation Using Relativistic Boundary Conditions

Mingtsu Ho
WuFeng Institute of Technology, Taiwan

One-dimensional numerical simulation of electromagnetic waves scattered from vibrating perfect conductor is reported in this paper. The computational results are generated by the method of characteristics with the application of the relativistic and characteristic variable boundary conditions. The perfect conductor may oscillate either in zigzag or sinusoidally. For easy observation of oscillatory effects on the reflected electromagnetic waves, objects are set to vibrate at a very high frequency with constant amplitude such that the extreme instantaneous velocity is about one tenth of the speed of light. The numerical calculations show that the reflected electric fields bear the oscillatory characteristics of the vibrating perfect conductor and that the change in magnitude are in agreement with the theoretical Doppler shift values.

The governing equations for electromagnetic problems in source-free region are the Maxwell's equations. The boundary conditions employed in the present simulation are the combination of the relativistic boundary conditions and the characteristic variable (CV) boundary conditions. The change in the field magnitude due to the relative motion between electromagnetic wave and perfect conductor is predictable by the multiplying factor $(1+\beta_{Max})/(1-\beta_{Max})$ where β_{Max} is the ratio of the maximum PEC instantaneous velocity to the speed of light and ranges from − 0.1 to + 0.1, respectively corresponding to the approaching and receding cases.

The reflected electric fields are shown in Figure 1 where the vibration frequency (f_v) of conductor is either identical with or twice as high as that of the incident wave (f_i). The Doppler shift values in the reflected electric field magnitude are also computed and compared with the theoretical values as listed in Table 1. Given in Figure 2 are the phase differences for various cases in which they are calculated on the basis of the stationary case.

Table 2A5 .2: Comparison of the calculated with the theoretical values: magnitude and frequency of the reflected electric fields.

Vibration	Extreme	Maximum Magnitude		Minimum Magnitude		Frequency (GHz)	
Type	Velocity(C)	Theoretical	Calculated	Theoretical	Calculated	Theoretical	Calculated
Sinusoidal	±0.1000	1.2222	1.2248	0.8182	0.8154	1.0000	1.0000
Sinusoidal	±0.1000	1.2222	1.2248	0.8182	0.8154	2.0000	2.0000
Zigzag	±0.1000	1.1361	1.1457	0.8802	0.8675	1.0000	1.0000
Zigzag	±0.1000	1.1361	1.1457	0.8802	0.8675	2.0000	2.0000

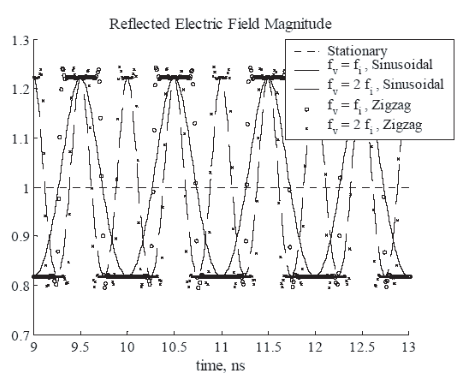

Figure 1: Reflected electric field magnitudes ($f_i = 1$ GHz).

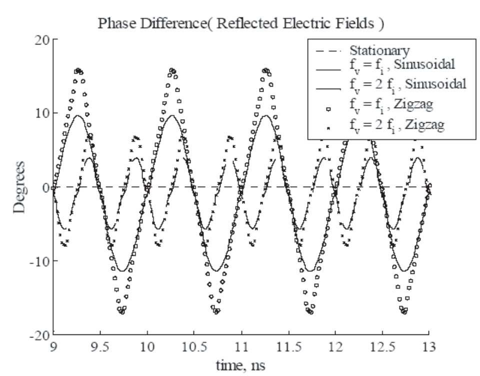

Figure 2: Phase difference in the reflected electric fields ($f_i = 1$ GHz).

Session 2A6

Electromagnetic Modeling and Inversion (Faraday)

New Global and Local Electromagnetic Field Modeling and Inversion

Ganquan Xie, **Jianhua Li**, **Feng Xie**
GL Geophysical Laboratory, USA

In this paper, we present a new Global and Local electromagnetic field modeling and inversion method (GL), which combines Global analytic electromagnetic (EM) fields and Local EM fields. Therefore, the new method is called the Global and Local EM field method. We derived new differential-integral equations and integral-differential equations for the EM field. Based on the new equations, we construct the GL EM forward modeling and inversion. The finite inhomogeneous domain is imbedded into the infinite whole or layered background domain. The incident background EM field is called an initial global field. The global EM fields are improved by local scattering EM fields in sub domains locally and successively. The total GL EM field is obtained when the global field is passing through the inhomogeneous domain. We have proved that the finite GL iterations can be used to obtain exact discrete EM field which satisfies the discrete integral equation. The GL EM field converges to the exact MAXWELL EM field when the mesh step is going to zero with $O(h^2)$ convergent rate.

Super convergent rate $O(h^4)$ is obtained when the Gaussian integral points are used. The GL method is difference from FEM method and FD method. The GL method overcomes the difficulties in FD method and FEM method. There is no any artificial boundary and absorption condition and no any boundary error in the GL method. There is only 3 by 3 matrices are needed to solve in the GL method. The GL method is different from Born approximation and its modified Born like versions. The GL Method can obtain exact EM field in the all frequency and high contrast inhomogeneous parameters. The GL EM method has overcome Born like method's difficulties on the high frequency and high contrasts of the material properties. Also the GL method is different from GILD EM modeling and inversion. Many simulations show that the GL EM field is fast convergent to exact EM field for high frequency and contrast, while FEM method fails to simulate EM wave field in the high frequency. The GL method will have very widely applications in the electromagnetic sciences and engineering, geophysical exploration, antenna designs, microwave astronomers, weather radar imaging, GPR, nondestructive testing, the mechanical problems, the heat diffusion, seismic wave propagation, quantum mechanics and quantum electromagnetic field in nanometer sciences. The Parallel GL method is high parallel performance. The 3D GL acoustic, 3D GL EM field and 3D GL elastic wave modeling software are developed.

REFERENCES

1. Xie, Ganquan, Jianhua Li, Feng Xie, "New Global and Local Electromagnetic Field Modeling And Inversion", *GLGEO Report GLP04008, GLGEO Copyright*, 2004.

New Topography Inversion Using EM Field

Baiyao Ruan, **Youxue Wang**
Guilin University of Technology, China

The topography will distort the electromagnetic signal seriously in an electromagnetic investigation, especially in an area with strong relief where the topography response must be considered, so it is necessary to calculate the topography effect by numerical modeling method. In Magnetotelluric (MT) survey, because the source used is a plane wave, numerical modeling and correction is relatively simple, and the topography effect basically has been conquered. For electromagnetic modeling in frequency domain with an artificial source and 3D topography, however, because the source and topography both are three dimensional and the electromagnetic variation near source is very strong, there are a lot of obstacles in the numerical modeling.

One numerical method, using boundary element to model the electromagnetic filed induced by artificial source in frequency domain with 3D topography, is put forward in this paper. In this method, firstly, by using vector integral theory and boundary conditions of electromagnetic filed, the boundary problem of two electromagnetic fields in the upper half space (air) and lower half space (earth medium) was transform into two vector integral equations just related to the topography, one magnetic equation for computing magnetic field and another electrical equation for computing electrical field. And then, the topography integral was decomposed into a series of integrals in a triangle element. For the integral in triangle element, we suppose that the electromagnetic filed in the triangle element is the stack of the electromagnetic field in the unlimited air space and the earth medium response which is a constant, so the computing becomes simple and convenient with a high accuracy. By the decomposition and computation, each vector integral equation can be calculated by solving three linear equations which are related to three Cartesian directions respectively. The matrix of these linear equations is of diagonally dominant, and can be solved by SSOR method. The topography response of vertical magnetic field induced by a vertical magnetic dipole source is shown in this paper.

REFERENCES

1. Xu S. and H Zhou, "Modeling the 2D Terrain Effect on MT by the Boundary Element Method", *Geophysical Prospecting*, Vol. 45, 931, 1977.
2. Zhdanov M. S., P.E.Wannamaker, "Methods of Geochemisty and Geophysics, 35: Three-Dimensional Electromagnetics", *Proceeding of the Second International Symposium, Elsevier*, 2002.
3. Elena Y. Fomanko, "MT and Control Source Modeling Algorithms for 3D Media with Topography and Large Resistivity Contrasts", *Proceeding of the Second International Symposium*, 1999.
4. Endo M., K.Noguchi, "Three Dimensional Models Considering the Topography for the Case of Time Domain Electromagnetic Method", *Proceeding of the Second International Symposium*, 1999.
5. Xie G., J. Li, E. Majer et al., "3-D Electromagnetic Modeling and Inversion", vol. 65, no 3, 2000.
6. Xie G., C. Lin, F. Xie et al., "GILD EM Modeling In Geophysics And Nanometer MaterialsUsing A Magnetic Field Integral Equation", *ASEG book, 3DEM*, 2003.

A Laser Gauge Blocks Using GL Electromagnetic Filed

Kuoyi Chang[1], **Jianhua Li**[2]

[1]National Huwei University Of Sciences & Technology, Taiwan
[2]GL Geophysical Laboratory, USA

The gauge blocks technology is very important in the industrial standard in the world. Authors have been studying gauge blocks performance and measurement for ten more years. Recent, we study a new advanced Laser Gauge Blocks technology by using GL Electromagnetic field [1,2]. We use a special laser ray to make calibration of gauge blocks and obtained extremely high accurate. The performance and measurement of the calibration of gauge blocks are simulated in PC first. Once accurate of the performance and measurement of the calibration is caught to high standard, then the performance and measurement of the calibration of gauge blocks are actually processing automatically by a novel sensor. The real time simulation is a key in the new laser gauge blocks technology. The analytic electromagnetic filed is the global field. In the short time of the laser electromagnetic radiation met the block, the simulation controls the sensor to obtained calibration gains and accurate measurement.

REFERENCES

1. Xie, Ganquan and Jianhua Li, "New 3D global an local electromagnetic modeling". *GLGEO technology report*, GLGEO03001, 2003.
2. Xie, G., C. Lin, F. Xie, J. Li, and C. Chen, "GILD EM Modeling In Geophysics And Nanometer Materials Using A Magnetic Field Integral Equation", *Three Dimensional Electromanetics*, 2003.

The Manufacturing and Analysis for the Calibration System of the Precision Square

Kuoyi Chang
National Huwei University of Sciences & Technology, Taiwan

This project is mainly intended to design, to develop and to manufacture a new Calibration system to measure the precision square and the correct squareness. The system is involved with the base of the Calibration system of the Precision levels and the Z axis of granite. The Z axis consists of a length electrical gauges, a linear encoder, an automatically controller unit and a precision guide way. The squareness error is the difference of the electrical reading over measuring length in precision rotary guide way. In order to acquire the quality a laser interferometer and a laser autocollimator alignment are adopted in to the system. We use a new electrical detective instrument to control the precision. The electromagnetic field modeling is used to simulate Laser field in the dynamic measurement. The calibration system has been approved to reach the resolution of 0.1 μm and the application range of 1200 μm/m.

Simulation of the Grounding Grid by Coupling the Unidemensional Finite Element Method(FEM) and the Three-dimensional FEM

Yan Gan, **Jiang Jun Ruan**
Wuhan University, China

A novel method, which is based on electromagnetic field theory, to analysis the property of the grounding grid is forwarded in this paper. Considering the difficulties of the three-dimensional FEM in analyzing of the grounding grid, we propose an innovation method—-coupling of the unidimensional and three-dimensional FEM. No matter what kind of conductor we use in making the grounding grid, the equivalent radium of the conductor is much smaller comparing with the dimension of the surrounding soil which will be taken into account during calculation. Therefore, it is reasonable to use unidimensional units in modeling the grounding grids and three-dimensional units in modeling soil surrounded it. The coupling mechanism of the unidimensional units and the three-dimensional units is carefully discussed. Suppose there are n nodes after meshing, whatever kind of units we use, we will obtain set of equations which can be expressed in matrix form $[K][\phi] = [f]$ where $[K]$ is $n \times n$ coefficient matrix; $[b]$ is $n \times 1$ nodal voltage matrix; $[f]$ is $n \times 1$ excitation matrix. By combining the coefficients of unidimensional units and three-dimensional units in matrix $[K]$ we can couple these two kinds of units together. Besides, a reasonable good solution can only be obtained by strictly controlled mesh. Cuboid element is used as three-dimensional units in calculation owning to its superior property. In order to mesh the whole region into cuboids, the overall model must be carefully designed and the meshing must be carefully controlled as well. Some useful meshing skills were also presented in this paper. To testify the accuracy and efficiency of this method, we use both of the three dimensional FEM and that coupled with unidimensional FEM in a same model respectively. The calculation results show that with the proposed method, the number of the dissected units is reduced and the calculation speed is obviously fastened meanwhile the calculation accuracy is adequately ensured.

REFERENCES

1. Cardoso, Jose Roberto, "FEM modeling of grounded systems with ungounded approach", *IEEE transactions on magnetics,* Vol. 30. No. 5, 1994,
2. Yuan, Jiansheng, "Simulation of substation grounding grids with unequal-potential", *IEEE transactions on magnetics,* Vol. 36. No. 4, 2000,
3. Wu, Wen, "Transient analysis of grounding system under lightning stroke using 3D FEM method", *International conference on Power System Technology*, 2002.

A New Novel Means of Transducing Tensile Stresses

Wei-Chih Wang[1], **Chi-Ting Ho**[3], **Yi-Ru Lian**[2], **Ching-Kong Chao**[2]
Ruey-Fang Shyu[3], **Wei-Ching Chuang**[3]

[1]University of Washington at Seattle, USA
[2]National Taiwan University of Science and Technology, Taiwan
[3]National Formosa University, Taiwan

A novel means of transducing tensile stress using a diffractive Bragg grating based polymeric sensor is presented. The diffraction gratings are successfully fabricated on a polydimethylsiloxane (PDMS) polymer using the holographic interference and micromolding technique. The micro MTS tensile test incorporated with the Raman experiment showed that a relationship between the load and the observed diffraction pattern shift could be obtained. The results show an excellent correlation between the optical measurement and load with a tensile sensitivity of 0.05N. However, this value would be much lower if a better optical and mechanical setup were used.

A New Method to Fabricate Polymer Waveguides

Wei-Ching Chuang, **Chi-Ting Ho**, **Ruey Fang Shyu**
National Formosa University, Taiwan

Polymer waveguides were successfully fabricated by a new method, which was incorporated with a micro-molding process. The refractive index of the UV polymer used in these experiments was changed by an extremely low electric field. The experiment of the near field measurement with end fire coupling has shown that the light had been totally restricted to inside the core layer of the waveguide. This process is easy and simple for mass production of any shape of polymer waveguides.

Hard Magnetic Material for Perpendicular Magnetic Anisotropic Field in Electromagnetic Actuator Fabrication

Ruey Fang Shyu[1], **H. Yang**[2], **C.-T. Pan**[3], **Peter Tsai**[4]

[1]National Formosa University, Taiwan
[2]National Chung Hsing University, Taiwan
[3]National Sun Yat-Sen University, Taiwan
[4]IDEC Taiwan Corporation, Taiwan

This paper describes a high power electromagnetic microactuator fabrication method that combines the hard magnetic Fe/Pt process, Ni/Fe permalloy magnetic circuit design, bulk micromachining, and excimer laser ablation. The hard magnetic material Fe/Pt is deposited under low temperature less than 300°C by sputter onto a suspension diaphragm to produce a perpendicular magnetic anisotropic field. The magnetic circuit with closed loop design is applied to concentrate the magnetic flux and increase the magnetic force. The magnetic field induced by the planar coil and Ni/Fe permalloy enhances the interaction with Fe/Pt to induce attractive and repulsive displacement, provide a large output force, and operate at high frequency. This high power electromagnetic microactuator is demonstrated with minimum dimensions with a magnetic force two times greater than conventional magnetic micro-actuators.

The magnetic and structural properties of Fe/Pt equiatomic alloy thin films elicit great scientific and application interest. These films have potential for high-density recording media and high-energy permanent magnets because of their exceptional magnetic properties. With the growing interest in the MEMS field, we present the perpendicular hard magnetic field concept and apply it to microactuators traditionally used in recorder hard drives. Soft magnetic material is usually used in microactuators to facilitate diaphragm actuation. In this study, a perpendicular hard magnet is applied to microactuator to enhance the vibration angle and displacement. A planar coil is placed at the bottom to provide electrical induction to the magnet. The essential feature is that the Fe/Pt thin film can undergo a phase transition from a disordered face centered cubic structure into an ordered face centered tetragonal structure after post-deposition annealing, or when deposited at an elevated substrate temperature. The long range ordering has critical effects on the magnetic properties of the films. It is well known that the ordered Fe/Pt alloy has a very high anisotropy constant K1 of 7×10^7 erg/cc. Fe/Pt thin film deposited using magnetron sputtering tends to grow with a (111) texture. In this research, the Fe/Pt thin film was deposited onto a NiO buffer layer of nanometer size. Fe/Pt can grow onto the NiO layer within the normal film direction and produce perpendicular magnetic anisotropy.

The Fe/Pt multilayers were deposited onto NiO buffer substrates by sputtering. The Fe/Pt layer thickness was about 1500 nm. The base pressure of the sputtering chamber was 2×10^{-6} Torr at high purity. Ar ions were used for deposition at a pressure of 1 mTorr. Two targets were used, Fe target (99.95% in purity) and Pt target (99.995% in purity). The Fe/Pt composition was adjusted using the sputter-gun power. The research provides a new method for integrating the Ni/Fe permalloy, high aspect ratio (more than 5) microelectroplating, closed loop magnetic circuit, hard magnetic material Fe/Pt anisotropy, bulk micromachining and excimer laser ablation processes. This design method concentrates the magnetic flux and increases the magnetic force. This microactuator can provide 2 times greater output force larger than the conventional method. The result shows that the deflection angle approaches to 82° under a magnetic force of 4840 A/m.

Optimal Design of Matched Load by Immune Micro Genetic Algorithm

Yubo Tian[1], **Jian Qian**[2], **Fei Meng**[1]

[1]Jiangsu University of Science and Technology, China
[2]Nanjing University, China

Optimal design of terminal matched load of rectangular waveguide is a traditional problem in electromagnetic field. All we know that the simplest method is to put a gradual change dielectric absorbing slice that act as an impedance convertor in rectangular waveguide. Because the varying of the slice thickness is continuous, this kind of matched load is long in size, and it doesn't satisfy some specific demands. For example, to a plane antenna array system, we hope that its terminal matched load has some characteristics, such as small size, light weight, good absorbing effect and broad band. For the sake of lighting the weight of matched load and improving the absorbing performance, H-plane T-kind matched load is adopted in our design.

In the optimal process of the matched load, genetic algorithm (GA) is adopted. It is well known that for conventional GA, sizing the population is problem-specific and a strong function of the length and cardinality of the chromosome. For most optimal problems, the length of the chromosomes is a function of the number of parameters to be optimized, the individual parameter range, and the step size to be implemented. Hence, for a multidimensional search space, a large population base and several generations are required to achieve optimal or near optimal results, and this places a considerable burden on the CPU time and computer resource. One possible approach to solve this problem is to employ micro genetic algorithm (MGA). Simultaneously, combines MGA with niche and shuffle technique to improve the efficiency. Simply speaking, the MGA starts with a random and small population (generally 5-50), which evolves in a conventional GA fashion and convergences after a few generations. At this point, keeping the best individual from the previously converged generations (elitist strategy), a new random population is chosen and the evolution process restarts. Although the sizing of initial population is small, it can avoid premature convergence. In the process of MGA, immune operator is also added to speed up the evolution process, and abbreviate immune MGA to IMGA. Immune operator is a kind of intelligence algorithm that simulates the immune function of natural system. It can achieve the dynamic balance between the convergence of population and diversity of individual, and accelerate the optimal process under the certain precision condition.

Comparing with simple genetic algorithm (SGA), the operating time of IMGA is cut down and the calculation efficiency is improved dramatically. For obtaining the optimal result, the running time of SGA is 1970.62 CPU second and the reflect coefficient is -32.838 dB, whereas the running time of IMGA is 25.75 CPU second and the reflect coefficient is -35.778 dB. The final optimal result is that the material parameters are $\mu_r = 4.031 - j0.0355$, $\varepsilon_r = 1.167 - j0.353$, and the width and thickness of upper and nether layer are 9.64mm, 1.45mm and 10.53mm, 2.49mm, the reflect coefficient is lower than -30 dB within 600 MHz band width (from 9.4 GHz to 10 GHz). It has good agreement with the computing result of Ansoft HFSS.

Advanced GILD EM Modeling And Inversion

Ganquan Xie, **Jianhua Li**, **Feng Xie**
GL Geophysical Laboratory, U.S.A.

In this paper, we propose a new advanced Global Integral and Local Differential (GILD) Electromagnetic (EM) modeling and inversion (AGILD). We drove a new EM differential integral strip equation. We used it on the boundary strip and MAXWELL differential equation in the internal domain to construct the AGILD. A new 9 cells local weak regularizing inversion scheme is presented. The new AGILD is fast modeling and reasonable stable inversion. AGILD preserved GILD's merits and is simpler than the GILD. Recently, we developed a novel and powerful GL modeling and inversion. The GL and AGILD can be joint working in the geophysics, GPR and weather radar imaging, optical electric, nondestructive testing, material sciences and engineering.

REFERENCES

1. Xie, Ganquan and Jianhua Li, "New Parallel SGILD Modeling and Inversion", *Physics D*, Vol. 133, 477, 1999.

Manufacturing of Micro Tungsten Carbide Electrode Using Supersonic Aided Electrolysis

Feng-Tsai Weng
National Huwei University of Science and Technology, Taiwan

A practical micromachining technology was developed for the fabrication of micro electrode using a nontraditional machining process in this paper. High-aspect-ratio of micro tungsten carbide rod can be easily obtained by described machining process. Tungsten carbide rods were selected as masters. Original diameter of tungsten carbide rods were 3mm which were processed to 50m using precision grinding process in first step, then the master can be machined to final desired diameter on the anode in supersonic aided electrolysis. Surface roughness was investigated of supersonic aided agitation compared with no agitation in electrolysis. Machined surface of the master piece is even, ionized particles of anode can be removed by supersonic aided agitation during electrolysis. Microelectrode with a tip of about 1m can be achieved by proposed process. Machined micro tungsten carbide rods are of high aspect ratio which can be used for the application micro EDM machining, micro tool and for the machining of micro filter with array micro holes. Proposed machining technology is of high potential in nano-scaled machining for microelectrode.

Session 2A7

Microwave Dielectric Measurements

Anisotropic Vortex Dynamics Related to Screening Currents and Microwave Currents under Magnetic Fields on High Tc Superconductors

Tamio Endo[1,2], **Hong Zhu**[1], **Takahisa Sakurada**[1], **Ajay K. Sarkar**[1], **Masanori Okada**[1]
Hirofumi Yamasaki[2], **Kazuhiro Endo**[2], **M. Shahabuddin**[3]

[1]Mie University, Japan
[2]National Institute of AIST, Japan
[3]University of Jamia Millia Islamia, India

Reentrant phase (RP) was proposed by Fisher and Nelson for strong two dimensional high Tc superconductors. Due to less interaction between 2D pancake vortices at low fields, there is Liquid-RP just above Meissner phase under Solid mixed phase. It is very difficult to detect this RP experimentally because it is quite narrow. The vortex phase is concerning to mobility of vortex, then we tried to detect this RP employing "modulated microwave absorption (MA) technique" utilizing induced vortex dynamics due to high-frequency modulation field. The MA vs field (H) spectrum for H//c shows only a sharp first peak: **P1** arising from **Meissner** state at low field at well low temperatures (T). At some higher T, it shows a **Dip** just above P1 and following Broad peak: **Pb**. The Dip and Pb arise from the **Liquid-RP** and **Solid phase**, respectively. At much higher T, the Dip and Pb disappear because it approaches to critical temperature. From these results of MA vs T, we can obtain RP experimentally. It exhibits a narrow entrance of RP which is strictly similar to the theoretically proposed RP.

Microewave power (Pm) dependence of MA was obtained for H//c at low T. The Dip and Pb appear at higher Pm and they shift to low field with increasing Pm. Their sharp drops in rather low Pm region are explained by sample temperature rise. However, their gradual drops in much higher Pm region is interpreted by vortex interaction between Abrikosov Votex induced by the applied field (AVa) and Josephson Vortex induced by microwave magnetic field (JVw). AVa is pinned by JVw at the higher Pm then the upper Solid phase boundary extends to higher field.

MA spectra were measured for Crossing field configuration (H//45°). With increasing Pm, the Dip is extremely enhanced and Pb is shifted to higher fields. JVw decouples 2D pancake vortices then melting is promoted at the low field. While at the higher fields, AVa is pinned by the applied field-induced Josephson vortices (JVa) and JVw, then the upper Solid-Liquid boundary is shifted up.

Effect of Particle Size on the Microwave Dielectric & Mechanical Properties of PTFE-ceramic Based Compsite Substrates

R. Ratheesh[1], **S. N. Potty**[1], **K. P. Murali**[1]
V. Priyadarshini[1], **P. Mohanan**[2]

[1]Government of India, India
[2]Cochin University of Science & Technology, India

Composite materials having tailored dielectric properties are needed in electronic industry for transmission of electrical signals at microwave frequencies as a means to enable the miniaturization of the circuits. Ceramic-filled polymers such as epoxy, PTFE, and various types of thermoset hydrocarbons show their suitability for wireless applications. Among them, PTFE composites have excellent electrical properties, high temperature resistance, and outstanding solvent resistance. How ever, to obtain PTFE composite systems having excellent dielectric properties and dimensional stability, homogeneity of the filler loading and interface between the matrix and the filler play an important role. Dielectric properties of the composite system depend on the volume fraction, size and shape of the filler materials. In the present work, an attempt has been made to systematically evaluate the effect of filler size on the dielectric as well as mechanical properties of composite substrates. Ceramic particles having average particle size ranging from 100 nm to 5 micron has been used as particulate fillers. The nanosized particles used for the present study is derived through sol-gel route. Silane coating has been employed to preclude moisture absorption on filler materials. Theoretical modeling has been employed to arrive at composite system with specific dielectric properties. The PTFE/ceramic composite system has been fabricated through compression moulding technique. The uniformity of the filler in the PTFE matrix is ensured through shear mixing. The mechanical properties such as Ultimate Tensile Strength (UTS), Youngs Modulus etc have been studied using Universal Testing Machine. SEM studies have been employed to evaluate the matrix filler interface. The void content and pore size distribution of the laminated substrate have been ascertained using Mercury Porosimetry studies. Microwave dielectric properties of the composite substrates have been studied in the X-band region using waveguide cavity perturbation techniques. It is found that particle size and shape have profound influence on the mechanical properties of the PTFE/ceramic composites.

Novel Low Loss Temperature Stable Ca5-xZnx Nb2TiO12 Dielectrics

P. V. Bijumon, **M. T. Sebastian**
Regional Research Laboratory, India

Sreedevi K Menon, **P. Mohanan**
Cochin University of Science & Technology, India

Dielectric materials play a vital role in the microwave telecommunication technology. These materials are key components in the realization of low-loss, temperature-stable resonators, filters, antennas and multilayer circuit modules for satellite and broadcasting equipments and in many other microwave devices. Dielectric resonator (DR) materials are critical for miniaturization and better performance of wireless systems, both for the terminals and base-stations as well as for handsets. Recently Bijumon et al. reported the microwave dielectric properties of Ca5Nb2TiO12 [Ca(Ca1/4Nb2/4Ti1/4)O3 in complex perovskite form] ceramics with εr= 48, Qu x f $>$ 26 000 at 4 GHz and τf=+40 ppm/oC, when the samples were sintered at 1550oC/4h. More recently, this material is reported to be suited for the bandwidth enhancement of DR loaded microstrip patch antennas and for the fabrication of wide band dielectric resonator antennas. High dielectric constant along with relatively high quality factor makes these ceramics competent enough to use as DRs. But the relatively high f value precludes their use in practical circuits. Solid solution phase formation between compounds with positive and negative f values is reported as an effective method to tailor the dielectric properties of polycrystalline ceramics. With this point of view, effort has been made to synthesize and characterize Ca5-xZnxNb2TiO12 $(0 \leq x \leq 1)$ ceramics with improved microwave dielectric properties. In this study the dielectric properties of Ca5-xZnxNb2TiO12 ceramics at microwave frequencies were investigated as a function of Zn2+ content for x varying from 0 to 1, to tune the f values near to zero. The structure was analyzed by X-ray diffraction techniques and microstructure was studied by scanning electron microscopic methods. The τf and εr decreased with increase in mole fraction of Zn substitution, whereas Qu was found to be increasing with increase in x. The composition with x = 0.64 in Ca5-xZnxNb2TiO12 was found to have stable resonant frequency with temperature. Ca4.36Zn0.64Nb2TiO12 has εr= 43, Qu x f = 29 000 at 4 GHz and τf= 0. Since this low loss material has the desired characteristics for microwave resonators, it can emerge as a potential candidate for use in base station filtering equipments in the S and C band and as dielectric resonator antennas in wireless communication devices.

Microwave Heating and Quasi-simultaneous Measurement of Temperature Dependent Dielectric Parameters

S. B. Kumar, **G. M. B. Parkes**, **P. A. Barnes**, **M. J. N. Sibley**
University of Huddersfield, U.K.

G. Bond
University of Central Lancashire, U.K.

Microwave heating relies on the ability of an applied electric field to polarise the charges in a dielectric material and the inability of the polarisation to keep pace with the varying electric field. The efficiency of the material being heated by microwaves is determined by the dielectric properties of the material. Although the dielectric properties of many materials are known at room temperature, the lack of knowledge of their variation with temperature makes the current work highly relevant. In addition, possible 'microwave effects' [1] observed when materials are heated using microwaves can also be investigated.

The equipment uses a single mode cavity for heating, and microwave power (maximum of 1kW) is fed into the cavity depending on the required heating rate. After a pre-set interval of the heating cycle, the heating power is turned off and dielectric measurements are carried out. The heating power is then turned on and this cycle continues until the set temperature is reached. A custom-designed four port waveguide permits both in-situ heating and dielectric measurement but these activities cannot be carried out truly simultaneously because the high power heating microwaves could leak to the measurement port which would destroy the sensitive dielectric measuring equipment. The dielectric properties are determined using the cavity perturbation method [2] and the resonant parameters are measured using an HP 8720ET Network Analyser (NWA). In addition to controlling the heating and measuring modes, the computer also controls the NWA, temperature sensor and the sequencing of heating/measuring cycle.

We show that physical and chemical changes in materials such as solid-solid phase changes, dehydration, melting etc. under microwave heating can be identified from the sample's permittivity-temperature profile. The following materials, silicon carbide (SiC), potassium nitrate (KNO_3), silver iodide (AgI), zinc acetate ($Zn(CH_3COO)_2{\cdot}2H_2O$) and copper sulphate pentahydrate ($CuSO_4{\cdot}5H_2O$) were used in this study. The dielectric constant-temperature profile of SiC showed that its dielectric constant remained essentially constant over the temperature range used while those of AgI and KNO_3 showed considerable changes at their corresponding solid-solid phase change temperatures. For copper sulphate and zinc acetate, the profiles clearly revealed dehydration peaks around their corresponding dehydration temperatures. The technique described is therefore a new form of thermal analysis which supplements existing, conventional TA techniques. The additional information on dielectric properties obtained using this microwave thermal analysis makes the technique quite promising. The technique is shown to be an efficient tool for distinguishing physical processes. Furthermore, even chemical reactions can be monitored via permittivity-temperature profiles. We demonstrate the potential to adopt the technique for online permittivity measurement in industrial applications for monitoring chemical processes rather than using time consuming ex-situ sample analysis.

REFERENCES

1. Robb, G R, A Harrison and A G Whittaker, "Temperature-resolved, $in-situ$ X-ray diffraction of silver iodide under microwave heating", *Phys Chem Comm*, Vol. 5, 135, 2002.
2. Mathew K T and U Raveendranath, *Sensors update'(Wiley-VCH, Germany, 1999)*, Vol. 7, 185, 1999.

A Novel Technique for Localizing the Scatterer in Inverse Profiling of Two Dimensional Circularly Symmetric Dielectric Scatterers Using Degree of Symmetry and Neural Networks

Vinu Thomas, **C. Gopakumar**, **Jaimon Yohannan**, **Anil Lonappan**
G. Bindu, **A. V. Praveen Kumar**, **V. Hamsakutty**, **K. T. Mathew**
Cochin University of Science and Technology, India

Inverse profiling with microwaves employ low power microwave radiation to illuminate an object placed in an imaging region. The resulting scattered field measurements at points on a measurement domain outside the imaging region are inverted to get tomographic reconstructions of the object's complex permittivity. The inverse problem of microwave imaging is ill posed in the Hadamard sense. Generally speaking the ill posedness of the inverse problem is due to the limited amount of data that can be collected. The inverse problem is also highly nonlinear, because of multiple scattering and hence the solution is prone to be trapped in local minima. One way to minimize the risk of local minima is to use a priori knowledge about the scatterer, so that the nonlinear problem is linearized about a different background. Such a priori knowledge includes, but is not limited to, the upper and lower bounds of the complex permittivity of the scatterer and knowledge of a part of the scatterer. In this paper a novel strategy for minimizing the unknowns in inverse profiling of a two dimensional circularly symmetric dielectric scatterer is presented. A custom defined degree of symmetry vector of the measured scattered field, computed as a function of the difference between the first half and the spatially reflected second half of the measured scattered field vector, is employed for the purpose of localizing the scatterer. The degree of symmetry vector is seen to exhibit unique features for the location, radius and bounds of complex permittivity of the unknown scatterer. A Neural Network based approach is employed for the classification of the degree of symmetry into different classes, each unique with respect to the position, radius and dielectric contrast of the scatterer. Thus the degrees of freedom in the inversion for the unknown object can be reduced. This aids the global convergence of the solution and also accelerating the convergence. The computation time is considerably reduced. The technique has been tested on synthetic exact and noisy data and the results are promising.

Synthesis of Dielectric Resonator for Microwave Filter Designing

Jaimon Yohannan, **A. V. Praveen Kumar**
V. Hamsakutty, **Vinu Thomas**, **K. T. Mathew**
Cochin University of Science and Technology, India

Microwave resonators made with high performance ceramic dielectric materials are very useful as compact frequency standards, filter elements, and distributed inductive or capacitive circuit elements. The high Q obtained in the UHF and microwave frequency range makes these resonators ideal for many applications. When cost, size, and stability are important, these resonators are the best choice. The resonant frequencies and the Q factors of various modes in isolated dielectric resonators can be accurately computed by using the surface integral equation formulation for bodies of revolution.

In this paper, ceramic resonators of cylindrical shape made of rutile are presented. The dielectric constant and Q of these materials are measured from the $TE_{01\delta}$ resonant mode. Cylindrical discs of different aspect ratio (height/diameter) are studied. The temperature coefficient of dielectric constant and resonant frequency are studied by Hakki-Coleman method.

The design of a dielectric resonator filter depends on its natural resonant frequencies. Since exact solutions of dielectric resonators having shapes other than a sphere or a doughnut cannot be rigorously computed, approximate techniques must be adopted to solve the problem. Two types of resonant modes can be excited in a dielectric resonator, namely, the H-mode and the E-mode. The H-mode is defined as the mode, which has a large normal component of magnetic field at the boundary surfaces; and the E-mode is the mode with no predominant normal component of magnetic field at the surfaces.

The band pass filter layout is generated, simulated and optimized position of perfect coupling is obtained by filter design software, which is then used for the design of a practical band pass filter.

The Determination of Scattering Parameters of Microwave Networks with Nonstandard Connectors and Its Applications

Ping Chen, **Wenfeng Guo**, **Ruixin Wu**, **Jian Qian**
Nanjing University, China

Microwave vector network analyzers (VNA) are widely used in the scattering [S] parameters measurement of microwave networks. Usually the ports of VNAs are coaxial ports. However the ports of object devices in actual measurement are various, so connectors are needed. For the purpose of accurate measurement, the influence of these connectors can't be neglected, and it can be corrected by calibration process if the connectors are standard. But if the object devices are nonstandard, the influence of the connector can't be removed with standard calibration process. To solve this problem, a modified calibration method was introduced by R. A. Speciale [1], which treats the connector as an equivalent two-port reciprocal network and determines its [S] parameters employing three reference measurements [2][3]. Measured results at the reference plane, where the standard calibration carried out , can be calibrated by the [S] parameters of the equivalent network to obtain the true parameters at the measure plane. In our work, the [S] parameters of the nonstandard connector are determined by measuring three shorting stubs with different electric lengths. Using this method, the reflection coefficient of a nonstandard small match load with the size of $19mm \times 5mm$ is accurately measured at X-band.

This method is also successfully used in the measurement of absorbing performance of pyramidal absorbers at radio frequencies. For the measurement, a tapered square coaxial line is used. Since the operating frequencies are very low, the size of the measure system is very large, which is twenty meters high. The square coaxial line and its adapter can be treated as the nonstandard connector. Different with the measurement of small load, the [S] parameters of the connector are determined by an adjusted short terminal instead of the shorting stubs with fixed lengths. The measurement results calibrated by this method are quite closed to the results measured by time domain measurement method.

REFERENCES

1. Speciale, R. A., "A Generalization of the TSD Network-analyzer Calibration Procedure, Covering n-port Scattering-parameter Measurement, Affected by Leakage Errors", *IEEE Trans. Microwave Theory. Tech.*, Vol. 25, No. 12, 1100, 1977.
2. Silva, E. F. da and M. K. Mcphun, "Calibration Techniques for One Port Measurement", *Microwave J.*, 97, 1978.
3. Chang, C. W., K. M. Chen and J. Qian, "Nondestructive Determination of Electromagnetic Parameters of Dielectric Materials at X-band Frequencies Using a Waveguide Probe System", *IEEE Trans. Instrum. Meas.*, Vol. 46, No. 5, 1084, 1997.

Electrical Properties of Biological Materials at Microwave Frequencies

S. B. Kumar
University of Huddersfield, U. K

J. Jacob
Newman College, India

K. T. Mathew
Cochin University of Science and Technology, India

Electrical properties of biological tissues and their interaction with electromagnetic waves have attracted the attention of researchers working in the field of medicine and electromagnetics. Extensive research had already been done in these fields and is still going on since its results have direct impact on human life. In this modern world where microwaves are extensively utilized for communication, the study of the dielectric properties of tissues at these frequencies are of special interest. In order to understand the interaction of electromagnetic field with tissue, it is important to know its complex permittivity accurately [1]. Recently, microwave imaging [2] has emerged as another field of great potentiality. The knowledge of the dielectric properties of various biological tissues at these frequencies is of much significance in deriving useful information in this kind of imaging.

In this paper, dielectric studies of some body fluids like bile, gastric juice, pancreatic juice, saliva and sweat in the microwave region have been carried out. The work is also extended to solid biological materials like pancreatic stone and bile stone. As many of the body fluids are available only in small quantities the cavity perturbation method is employed for its characterization. This method is well-accepted as it provides best results and requires only small amount of sample.

Dielectric properties such as conductivity, loss tangent, absorption coefficient and penetration depth are determined from the measured complex permittivity values. This information finds application in numerical simulation of cells, microwave imaging, Specific Absorption Rate (SAR) determination and medical applications.

REFERENCES

1. Staebell, Katie F., Devendra Misra, "An Experimental Technique for In Vivo Permittivity Measurement of Materials at Microwave Frequencies", *IEEE Trans. on Microwave Theory and Techniques*, Vol. 38, No. 3, 337, 1990.
2. Larsen, Lawrence E., John H. Jacobi, "Medical Applications of Microwave Imaging", *IEEE Press, The Institute of Electrical and Electronics Engineers, Inc., New York*, 1985.

Electromagnetic Characterization of Concrete over 1 GHz for Subsurface Radar Applications

M. Adous[1,2], P. Queffelec[1], X. Derobert[2], J. L. Mattei[1]
L. Laguerre[2], V. Baltazart[2]

[1]LEST-UMR CNRS 6165, France
[2]LCPC de Nantes, France

One of the more popular non destructive technique used in civil engineering infrastructures is Ground Penetrating Radar (GPR). For the last decade, it has gained considerable popularity for the evaluation of reinforced concrete structures pathologies [1,2]. However, accurate interpretation of data collected is not possible without the knowledge of the electromagnetic properties of the investigated medium. Previous research work has been directed toward the measurements of electromagnetic properties of hardened concrete specimens at limited frequency range above 1 GHz [3]. In the recent years, GPR systems have been able to be used in a high-frequency range (3.5-13 GHz) in order to improve the spatial resolution. In consequence, it is necessary to knowledge the electromagnetic properities of specimen conrete in this frequence range.

In the centimeter wave range, the electromagnetic modeling of concrete is very complex. Indeed, in this frequency range, the wavelength is comparable to the length of the aggregates of the concrete. The phenomenon of the diffusion is added to dielectric polarization and makes difficult the electromagnetic modeling of such material. The previous researches studying the mixing laws of heterogeneous materials consider that the length of the heterogeneities is much smaller compared with the wavelength. These mixing laws cannot be used to describe the effective permittivity of concrete at high frequencies. In this context, the database for the electromagnetic properties of concrete is needed in the centimeter wave range.

The aim of this paper is to present an electromagnetic analysis of an open-ended rectangular waveguide probe by a mode matching technique in order to measure the dielectric properties of concrete over a wide frequency range corresponding to 3.5 GHz-13 GHz. The choice of this method satisfies different criterions linked to the frequency range and the *Representative Elementary Volume* (REV) for the test sample. This method has been chosen among different cells (coaxial probe, rectangular waveguide probe, etc.) using numerical simulations obtained by *HFSS* software (Finite Element Method-3D). The electromagnetic analysis takes into account all the evanescent modes generated by the heterogeneities of the concrete or excited at the discontinuity aperture/concrete. Different numerical simulations and measured results will be presented in order to validate our analysis [4].

REFERENCES

1. Bükyüköztürk, O., "Imaging of Concrete Structures", *NDT* & *E*, Vol. 31, 233, 1998.
2. Bungey, J. H., "Sub-surface Radar Testing of Concrete: a Review", *Const.* & *Build. Mat.*, Vol. 18, 1, 2004
3. Robert, A., "Dielectric Permittivity of Concrete Between 50 MHz and 1 GHz and GPR Measurements for Building Materials Evaluation", *Journ. Appl. Geophys.*, Vol. 40, 89, 1998.
4. Adous, M., et al., "Caractérisation électromagnétique des Matériaux de génie Civil Dans une Large Bande de Fréquence", *Journ. Caract. Micro. Mat. , France Avril*, 2004.

Session 2P1a

Synergy in Passive and Active Electromagnetic Sensing

Polarimetric Microwave Remote Sensing of Ocean Surface Vector Winds

Simon Yueh[1], **William J. Wilson**[1], **S. Vincent Hsiao**[2]

[1]California Institute of Technology, USA
[2]Jet Propulsion Laboratory, California Institute of Technology, USA

The near surface ocean wind, generating the momentum flux affecting ocean circulation and mixing, is a key driving force in air-sea interaction processes. Global mapping of near surface ocean wind vectors is crucial for many oceanographic and atmospheric studies. To obtain this key measurement, scientific satellite scatterometers, including the NASA scatterometer (NSCAT), the SeaWinds scatterometer on the QuikSCAT spacecraft and the SeaWinds scatterometer on the Japanese Advanced Earth Observation System satellite, were launched to acquire a time-series of global ocean surface winds.

As a potential alternate technique to active microwave radar, the passive microwave polarimetry for surface wind vector measurements has been investigated in the range of wind speed from 3 to 15 m/s by many aircraft field campaigns. Based on these experimental observations, the US Navy together with the National Polar Orbiting Environmental Satellite System (NPOESS) launched the Windsat with multi-frequency polarimetric radiometers in January 2003 to demonstrate the passive polarimetry for large spatial coverage of ocean surface wind vector measurements from space.

In this paper, we presented the analysis of 6 months of Windsat data with results in the form of a geophysical model function, relating the polarimetric observations to wind speed and direction. The polarimetric third and fourth Stokes parameter observations from the Windsat 10, 18 and 37 GHz channels were collocated with the ocean surface winds from the Global Data Assimilation System (GDAS) operated by the National Center for Environmental Prediction (NCEP). The collocated data were binned as a function of wind speed and wind direction, and were expanded by sinusoidal series of the relative azimuth angles between wind and observation directions. The coefficients of the sinusoidal series, corrected for atmospheric attenuation, have been used to develop an empirical geophysical model function.

The empirical geophysical model function compares very well with the airborne observations acquired by the Jet Propulsion Laboratory polarimetric wind radiometers. We also compared the model function with the analysis from a two-scale ocean scattering model. The ocean surface spectrum used by the two-scale model was tuned with the NASA QuikSCAT scatterometer model function. There is very good agreement between the empirical and theoretical models, indicating the consistency of theoretical basis for active and passive microwave remote sensing of ocean surfaces.

We have applied the empirical geophysical model function for retrieving ocean surface wind vectors from the WINDSAT radiometer data. The retrieved winds are compared with the GDAS winds to estimate the Windsat retrieval accuracies. The standard deviation of GDAS and Windsat wind speed differences is about 1 m/s for less than 10 m/s wind speed and increases to about 2 m/s for 20 m/s wind speed. The standard deviation of wind direction differences, reducing with increasing wind speed, is below 20 degrees for wind speed above about 6 m/s.

A Comparison of Radar and Radiometer Responses to Soil Moisture at L-band Using Simulations and Experimental Data

Eni G. Njoku, **Tsz K. Chan**
California Institute of Technology, USA

The Hydros mission, planned for launch at the end of this decade, is designed to measure soil moisture and freeze/thaw state from space using combined radar and radiometer multi-polarization L-band sensing. The wide-swath Hydros measurements, made at a constant 40° incidence angle, will provide complete global mapping every 2-3 days at a radar spatial resolution of 3 km and a radiometer spatial resolution of 40 km. Optimal estimation of soil moisture from these measurements in regions with significant vegetation cover requires knowledge of the multi-polarization L-band signatures of heterogeneous land surfaces at varying spatial scales. A model simulation study has been carried out to simulate the effects of noise and spatial resolution on soil moisture retrievals in vegetated regions. L-band radar and radiometer airborne data have also been acquired in the SMEX02 field experiment conducted over agricultural fields in Iowa. The simulations and experimental data are being used to develop and evaluate combined algorithms for improved estimation of soil moisture. Results from radiometer and radar retrieval algorithms are presented in this paper, including the sensitivity of the results to uncertainties in measurement and model errors. The AIRSAR and PALS data from SMEX02 demonstrate the sensitivity of L-band radar and radiometer measurements to soil moisture in agricultural fields with vegetation water contents up to 5 kg/m^2. The sensitivity is shown at varying scales from 10 m to 1600 m in the presence of vegetation and soil moisture heterogeneity within fields ($< 800m$) and between fields ($> 800m$). The soil moisture retrieval results using the radar and radiometer algorithms are consistent with parallel simulation study results and with the stated Hydros accuracy goals of 4% volumetric soil moisture for vegetation water content up to ~ 5 kg/m^2. However, the robustness of retrievals in more varied terrain, and optimization of the resolution and accuracy trade-offs between radar and radiometer, need further development.

A Combined Radar and Radiometer Concept for a Next-Generation Surface-to-Depth Soil Moisture Mission

M. Moghaddam
University of Michigan, USA

Y. Rahmat-Samii
University of California, USA

Eni Njoku, **E. Rodriguez**
Jet Propulsion Laboratory, USA

D. Entekhabi
Massachusetts Institute of Technology, USA

Soil moisture is a key state variable in the hydrologic cycle over the land surface. Simultaneous estimation of deep (order 0.1 to 5 m) and shallow (order 0.01 to 0.1 m) soil moisture at spatial resolutions on the order of 1 km could provide a major breakthrough for estimation of vertical flow in the soil column linking surface hydrologic processes with that in the subsurface. In this paper, a combined radar and radiometer large-aperture antenna system concept, spanning the frequency decade 0.14-1.4 GHZ, for a nextgeneration soil moisture mission, which allows the estimation of surface and subsurface soil moisture below canopies with densities that make them opaque in higher microwave frequencies. Currently, spaceborne L-band (21 cm wavelength) radiometer and radar measurement systems are being considered which could enable surface soil moisture retrievals over surfaces with up to 4-5 kg/m^2 of vegetation water content, representing about 65% of land surface excluding permanent ice and snow-covered areas, leaving the remaining 35% unaddressed. While this is the best that could be achieved with the available technology today, the system concept discussed here will enable surface and deep soil moisture estimates for areas covered with substantially more vegetation (20 kg/m^2 and more). The uniqueness and impact of this system is that it can simultaneously provide soil moisture at multiple columns starting from surface to depths of several meters, under substantial vegetation canopies of exceeding 20 kg/m^2 water content, and at 3-day intervals. The spatial resolution will be 1km for the synthetic aperture radar (SAR) instruments operating at 137 MHz and 435 MHz, and 20 km for the radiometer operating at 1414 MHz. The enabling technology proposed here is a single 50-m deployable, lightweight, low package volume mesh reflector with multiple feeds that subilluminate the reflector to (1) synthesize a long aperture on the reflector for the radar instrument, and (2) provide multiple radiometer footprints to achieve a high-resolution and large contiguous swath on the ground. The overall system concept, antenna design, and simultaneous operation of radar and radiometer systems will be discussed.

A Simple Method for Spatial Disaggregation of Radiometer Derived Soil Moisture Using Higher Resolution Radar Observations

Ujjwal Narayan, **Venkat Lakshmi**
University of South Carolina, U.S.A.

This paper presents a technique for estimation of soil moisture by combining radiometric brightness temperatures in the LH band with horizontally co polarized L band radar backscattering coefficients. The approach is to use radiometric estimates of soil moisture at a lower resolution to compute the sensitivity of radar to soil moisture at the lower resolution. This estimate of sensitivity is then disaggregated using vegetation water content, vegetation type and soil texture information, which are the parameters on which radar sensitivity to soil moisture depends and are generally available at a scale of radar observation. The method discussed in this paper has potential applicability in soil moisture retrieval from proposed passive/active L band satellite instruments. The HYDROS instrument is proposed to have an L band radiometer and L band radar onboard. The passive instrument will have spatial resolution of the order of tens of kilometers and will operate along with the active instrument that will take observations at a resolution of tens of meters. The present study applies the methods presented to a limited data set obtained from the SMEX02 campaign held in June - July 02 in Iowa during which an airborne L band radiometer (PALS) and an L band synthetic aperture radar (AIRSAR) were used to coincidentally acquire data over the same region on 3 days and 400 m and 30 m resolutions respectively. In situ sampling of soil and vegetation parameters was also done. To demonstrate the applicability and limitation of the technique over a period of weeks, a simulated experiment was performed, the results of which have been presented and discussed in this study.

Session 2P1b

Techniques in Microwave Remote Sensing of Snow and Soil Moisture

A Simplified Soil Moisture Inversion Model Based on IEM over Bare Soil from ERS Wind Scattermeter Data

Jianming Wang[1], **J. Shi**[2], **Wei Liu**[2]

[1]Institute of Remote Sensing Applications, CAS, China
[2]University of California, USA

The ERS-1/2 wind scatterometer(WSC) has a resolution cell of about 50km but provides a high repetition rate (less than four days) and makes measurements at multiple incidence angles. In order to estimate effective surface reflectivity (related to soil moisture content) over bare soil using this instrument, an original methodology based on the integral equation model(IEM) is presented that takes advantage of multiple view angular observations which means two independent observations at the same resolution cell simultaneously. This method includes two steps. First, a simplified two parameter surface scattering model is calibrated by IEM simulated database over a wide parameter space as: $\sigma_{vv}^0 = A(\theta, SR)(\Gamma^0)^{B(\theta)}$ the surface roughness SR is represented by the parameter A which depends on the incident angle. The parameter B depends only on the incident angle. Second, regression analyses are carried out using the simulated database for the relation of two A of different incident angles from two antenna observation. From the model simulated database, our technique works quite well in estimation of Γ^0. The possibility of applying the model to retrieve soil moisture is investigated using a set of data collected from the Intensive Observation Period(IOP'98) field campaign in 1998 of the Global Energy and Water Experiment(GEWEX) Asian Monsoon Experiment Tibet(GAME/Tibet). The retrieved values obtained for the bare surface are consistent with ground measurements collected in these areas.

REFERENCES

1. Wagner, W., K. Scipal, "Large-scale Moisture Mapping in Western Africa Using the ERS Scatterometer", *IEEE Transactions on Geoscience and Remote Sensing*, Vol. 38, 1777, 2000
2. Grippa, M., I. H. Woodhouse, "Retrieval of Bare Soil and Vegetaiton Parameters from Wind Scatterometer Measurements over Three Different Climatic Regions", *Remote Sensing of Environment*, Vol. 84, 16, 2002.
3. Ulaby, F. T., R. K. Moore and A. K. Fung, "Microwave Remote Sensing: Active and Passive", *Norwood, MA, Artech House*, Vol. 2-3, 1986.
4. Frison, P. L., E. Mougin, P. Hiernaux, "Observation and Interpretationof Seasonal ERS-1 Wind Scatterometer Data over Northern Sahel (Mali)", *Remote Sensing of Environment*, Vol. 63, 233, 1998.
5. Fung, A. K., Z. Li and K. S. Chen, "Backscattering from a Randomly Rough Dielectric Surface", *IEEE Trans. Geosci. Remote Sensing*, Vol. 30, 356, 1992.
6. Wu, T. D., K. S. Chen, "A Reappraisal of the Validity of the IEM Model for Backscattering From Rough Surfaces", *IEEE Trans. Geosci. Remote Sensing*, Vol. 42, 743, 2004.
7. Dobson, M. C., F. T. Ulaby, M. T.Hallikainen, M. A. El-Raynes, "Microwave Dielectric Behavior of Wet Soil: Part II. Dielectric Mixing Models", *IEEE Transactions on Geoscience and Remote Sensing*, Vol. GE-23, 35, 1985.

Monitoring of Seasonal Snow in Finland with Passive and Active Microwave Sensors

Martti Hallikainen, **Panu Lahtinen**, **Matias Takala**, **Jouni Pulliainen**
Helsinki University of Technology, Finland

Information on seasonal snow cover is vital for several applications ranging from management of water resources, including hydropower operations and flood prediction, to global studies involving the water and energy flux at the Earth's surface, the hydrological cycle of snow-covered areas, and the global change. Since seasonal snow mostly appears at high latitudes, microwave radiometer and radar, due to their nearly all-weather capability and independence of lighting conditions, are suitable for monitoring seasonal snow on various scales. Microwave response to snow depends substantially on several snow parameters and, additionally, on soil properties, vegetation (forest) characteristics and surface geometry.

We report results on using satellite data from passive and active microwave sensors for monitoring of seasonal snow cover in Finland. Radiometer data are from the SSM/I sensor on the DMSP satellite and scatterometer data are from the SeaWinds sensor on the QuikScat satellite. We concentrate on using 19.35 and 37.0 GHz data (V and H polarization) from the SSM/I instrument and 13.4 GHz data (VV and HH polarization) from the QuikScat sensor. The data cover a total of five winters: 1999-2000 through 2003-2004. By the summer of 2005 we add 18.7 and 36.5 GHz data (V and H polarization) from the AMSR-E instrument on the Aqua satellite to our analysis.

Feasibility of these satellite data for monitoring the following snow characteristics and events are analyzed: Extent of snow-covered area, snow water equivalent, snow depth, onset of snow melt, and end of snow melt. A total of 19 test sites are used in Finland with ancillary ground truth data on snow water equivalent, snow depth, precipitation, and air temperature (minimum and maximum). Results for progress in snowmelt in Finland are compared against MODIS-derived snow-cover maps.

Dense Media Scattering, Absorption and Emission in Snow Based on Numerical Maxwell Model of 3 Dimensional Simulations (NMM3D)

Kaki Tse[1], **Zhongxi Li**[1], **Yunhua Tan**[1], **Leung Tsang**[2], **C. H. Chan**[1]

[1]City University of Hong Kong, Hong Kong
[2]University of Washington, USA

In a dense medium, the particles are densely packed. An important application is in microwave remote sensing of snow because the ice grains in snow are densely packed together. The classical approach of independent scattering is not valid. There are 3 physical features in the classical results. (1) In the classical theory, when the particles are small compared with wavelength, scattering is proportional to frequency of the 4th power. Also the classical theory uses a Rayleigh phase matrix. (2) The phase matrix has a mean cosine equal to zero. (3) Also the Rayleigh phase matrix zero cross polarization in the plane of incidence.

In the past, we have used a dense media radiativfe transfer theory (DMRT) based on quasicrystalline approximation (QCA) and using sticky particles as a model. The DMRT/QCA model predicts a weaker frequency dependence than the classical model. It also predicts a nonzero mean cosine of scattering.

In this paper, we solve Maxwell equations in 3D numerically (NMM3D) for a medium containing densely packed spheres. The scattering properties of the dense medium, which include bistatic scattering coefficients, backscattering coefficients and emissivities, are important for in microwave . remote sensing. The spheres are randomly positioned in a box. The spheres can attach together to form aggregates. Maxwell equations are cast in the form of Foldy Lax multiple scattering equations. SMCG is used to solve the unknown coefficients and the scattered field is calculated by the solved coefficients. The results of the scattered field are averaged over realizations and numerical result for the phase matrices are calculated. We compare the simulated results with the classical theory and addressed the departures of the results from the classical theory. The departures are shown in all 3 classical physical features. We also compare the phase matrix with that based on QCA/DMRT. A distinct feature of the NMM3D is the large cross polarization that is exhibited due to near field coherent interactions that exist for spherical particles.

The simulated phase matrices are used in dense media radiative transfer theory. Using that we compute the backscattering coefficients and brightness temperatures in microwave remote sensing.

Study of Snow Water Equivalence Inversion Technique with Experimental Data

Lingmei Jiang[1,2], **Jiancheng Shi**[1]

[1]University of California, USA
[2]Beijing Normal University, China

Remote sensing of snow cover is important for climate change studies and successful water resource management. So our ability to monitor snow cover and volumetric storage water has great impact on assessing global climate changes and improving management of water supply. And estimating techniques of snow water equivalence (SWE) are common inputs to water resource management and flood forecasting. In this paper simulating emission database is established based on the dense medium radiative transfer theory (DMRT), covering the most possible natural snow properties - a range of snow densities and grain sizes and underground dielectric and roughness properties - frozen/nonfrozen, a range of soil moisture, and roughness properties.

We used first-order scattering radiative transfer model as our basic inversion model. We characterize the relationship of the underground surface emission signals at the different frequencies and polarizations under AMSR-E sensor considerations to reduce the number of unkowns to describe the underground surface emission signals in the inversion model. The surface emission signals are highly correlated at different frequencies as long as the sensor looks at the same surface (same soil moisture, texture, and roughness properties). And we expect that snow characters such as extinction coefficient, volume albedo are also correlated at different frequencies and polarization. From these relationships we can obtain snow depth at the homogeneity snow pixel. To test the inversion approach, PSR Multiband Polarimetric Imaging during CLPX 2002 with the corresponding snow pits measurements was used. The accuracies showed that this inversion technique estimated snow depth very well in this area. In future this technique will be improved and implemented with AMSR-E data. And we still need to study mixed pixel problem to improve current snow depth retrieval accuracy.

Snow Water Equivalence Retrieval Using Dual-Frequency and Polarization Ku-Band Radar

Jiancheng Shi
University of California, Santa Barbara, USA

The study of snow has become an important area of research in the natural sciences, particularly in hydrology and climatology. Snow water equivalence is the most important parameter. Active microwave sensors are highly sensitive to the most snowpack parameters interested by hydrologists. However, the studies have found, in general, that the sensitivities of radar measurements to dry snow water equivalence are very weak at C-band. The higher-frequency radar is needed to provide the reliable measurements for quantitative retrieval of snow water equivalence.

In this study, we evaluated the feasibility of using the dual frequency (13.4 GHz and 17GHz Ku-band) and dual polarization (VV and VH) radar to estimate snow water equivalence. The components in this study include:

1. Using Model to Establish a Database for Algorithm Development: The simulation model is a second-order radiative transfer model where 1) the surface scattering components s are simulated by IEM model for the co-polarized signals and the semi-empirical model of VH/VV for the cross-polarization signals, 2) the volume scattering component are calculated by the dense medium model with ellipsoid grain shape in order to simulate the cross-polarization signals, and 3) the bi-static IEM model is used for the boundary condition so that the interaction components between snow volume scattering and the surface scatterings can be correctly simulated.

2. Decomposition Technique: We found that the depolarization factor VH/VV is proportional to the volume scattering and surface-volume scattering contributions and inversely relates the surface scattering contribution. Using this phenomenon, we developed a technique the estimate the snow volume and the ground surface scattering components.

3. Estimation of SWE Using the Volume Scattering Components: We found that the ratio of the volume scattering components from two frequencies can be written as a function of snow optical thickness at corresponding frequencies. In this way, the effects of snow volume scattering albedo can be minimized so that the optical thickness of snow pack at each frequency can be estimated. Then, the albedo and SWE can be estimated.

4. Estimation of the Snowpack Optical Thickness Using the Ground Surface Scattering Components: It is found that the surface scattering components of VV polarization at two Ku-band can be also used to estimate the snowpack optical thickness. This is due to the surface backscattering at snow-ground interface is almost identical since the surface is rough at 13.4 and 17 GHz. The difference in the surface scattering components (after passing snowpack) results from the difference in optical thickness of snowpack at these two frequencies. However, the other snow extinction properties are still required for estimation of SWE.

It is found that the both the volume and surface scattering components are required for SWE estimation in order to cover a wide range snow properties.

Estimation of Snow Wetness Using Multi-polarized SAR Data in C Band

Qin Yu
Institute of Remote Sensing Applications, CAS, China

Jiancheng Shi
California Institute of Technology, USA

Snow wetness is important for hydrological and climate investigation for it identifies the immediate contribution to local runoff. Previous work has shown the potential of SAR data to retrieve snow wetness.

This paper presents 1) the simulation of snow backscattering and its validation with CLPX data; 2) an algorithm for snow wetness retrieval. For first order polarimetric model, there are two major scattering sources- volume scattering from snow pack and air-snow surface scattering component taken into consideration. First order Advance IEM has been employed for surface scattering simulation and Dense Media Radiative Transfer theory with ellipsoid ice grain shape for snow volume scattering. To calculate HV polarized surface scattering of snow we utilized a semi-empirical model developed by Oh et. al. Validation of the simulation has been conducted. Using the simulated snow backscattering data base in C band, which covers the most possible wet snow physical properties and surface roughness conditions, an algorithm to retrieve snow wetness has been introduced in this paper. The main idea is that depending upon which scattering component is dominant and then controls the response to snow wetness, then with the decomposed the surface and volume scattering signals, snow wetness is to be estimated using each scattering component.

The Development of Geometry-optics Method for Vegetation Single Scattering Albedo

Zhongjun Zhang, **Min Chen**
Beijing Normal University, China

In passive microwave remote sensing, single scattering albedo of vegetation is important in retrieve vegetation-covered soil moisture if the zero-order model is used. Vegetation is usually assumed to consist of discrete scatters of dielectric spheres, discs and cylinders with specific size and distributions. As frequency goes higher, Geometry-Optics (GO model) is used to calculate the transmissivity and absorptivity of disc currently, which require the normal of discs lie in the incident plate. In this paper, this GO approach is further developed to obtain single scattering albedo of randomly distributed discs by polarimetric decomposition when the normal of disc varies, so that more realistic and accurate vegetation scattering parameters can be obtained.

Multifrequency Microwave Radiometry of the Snow Melting Cycle and the Retrieval of Snow Water Equivalent

P. Pampaloni, **M. Brogioni**, **G. Macelloni**, **S. Paloscia**
IFAC-CNR, Italy

R. Ranzi
University of Brescia, Italy

The monitoring of the melting cycle of snow is very important for the management of water resources, as well as for flood and avalanche forecasting. During the melting process, typical grains of dry snow are transformed into large rounded grains. During the night-refreezing phase, which mainly involves the upper layer of snow cover, the crystals aggregate in polycrystalline grains, and may form surface crusts. This transformation impacts on the emission and scattering properties of snow, which change in accordance with the daily melting and refreezing cycles.

A study of the melting cycle of snow was carried out by combining microwave passive measurements with meteorological data and snow modelling. The experiment took place in the eastern Italian Alps from early February to late May 2003 in the framework of the European project ENVISNOW. Brightness temperature at C-, Ku- and Ka- bands (vertical and horizontal polarizations) and backscattering coefficient at Ku-band (VV), were continuously measured (24h/day) with ground based sensors. Remote sensing observations were supported by meteorological data (wind speed and direction, air temperature and relative humidity, incoming and reflected solar radiation, net radiative flux in the snowpack and heat flux in the ground), and snow measurements (depth, density, water equivalent, liquid water, hardness, grain size and shape).

A continuous simulation of the snow temperature, depth, and liquid water content was performed for the entire monitoring period by means of a physically based distributed snowmelt model (PDSM). In this model, the melting rate was estimated on the basis of the energy balance equation and the meltwater flux within the snowpack was computed through a two-layer model, un upper layer 10 cm deep, and a lower layer representing the remaining of snowpack. A radiative transfer model based on the Strong Fluctuation Theory (SFT) implemented for interpreting microwave emission and backscattering was also based on this two-layer scheme. Each snow layer was considered as a collection of spherical ice particles, surrounded by a thin film of water, embedded in air. The permittivity of these particles was computed by using the Maxwell-Garnett mixing formula. Both hydrological and remote sensing approaches gave useful and coherent results in describing the snow melting and refreezing cycles. Microwave active and passive data were consistent each other. During the melting cycle, the presence of liquid water caused an increase of absorption with a consequent increase of the brightness. The electromagnetic model was found to be able to reproduce microwave measurements once driven with appropriate input data, which, in this case, were obtained either from ground surveys or from outputs of the snowpack model. An inversion of the electromagnetic model based on a neural network provided the retrieval of snow parameters.

Session 2P2

Selected Topics in Metamaterials and Plasmonic Media

Nano-Concentration of Optical Energy in Graded Nanoplasmonic Waveguides

Mark I. Stockman
Georgia State University, USA

We predict that propagation of surface plasmon polaritons (SPPs) toward a sharp edge of smoothly (adiabatically) graded metallic layer causes their slowing down and asymptotic stopping. This is accompanied by a concentration of electromagnetic energy and enhancement of local optical fields.

As such a nano-concentration effect, we consider the adiabatic energy concentration in a conic nanoplasmonic waveguide [1]. In this case, SPPs are created in the $m = 0$ plasmonic state at the wide (microscopic) edge of the system and propagate toward the tip of the conic waveguide. As local radius R of the cone waveguide decreases, both the phase and group velocity tend to zero $\propto R$. This asymptotic stopping leads to the accumulation of SPPs at the tip and their adiabatic transformation to the standing surface plasmons, which causes highly enhanced local fields This process is only limited by the minimum local radius of the cone tip $R \sim 2$ nm below which the spatial dispersion of dielectric responses and Landau damping become important [2].

For silver, it is possible to have local optical intensity at the tip increased by three orders of magnitude. An example of local optical fields in the cross section of a conic plasmonic waveguide are shown in Fig.1. This allows one to clearly see the shortening the SPP wavelength toward the tip related to their slowing down and the corresponding enhancement of the local fields.

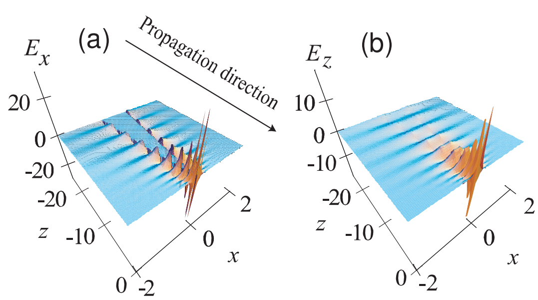

Figure 1: Snapshot of instantaneous fields (at some arbitrary moment): Normal component E_x (a) and longitudinal component E_z (b) of the local optical electric field are shown in the longitudinal cross section (xz) plane of the system. The fields are in the units of the far-zone (excitation) field. Adopted from Ref. [1].

We also present results for two-dimensional focusing nanoplasmonic waveguides. In conclusion, we will discuss the many prospective application of this effect.

REFERENCES

1. Stockman M. I., "Nanofocusing of Optical Energy in Tapered Plasmonic Waveguides", *Phys. Rev. Lett. 93*, 137404-1-4, 2004.
2. Larkin I. A., M. I. Stockman, M. Achermann, and V. I. Klimov, "Dipolar Emitters at Nanoscale Proximity of Metal Surfaces: Giant Enhancement of Relaxation in Microscopic Theory", *Phys. Rev. B 69*, 121403(R)-1-4, 2004.

Sub Wavelength Focussing Using Silver Nanolayers

J. B. Pendry
Imperial College London, UK

The resolution that can be achieved in an image is limited by the largest Fourier component that can reach the image. Consider a wave of the form $\exp(ik_x x + ik_z z - i\omega t)$ where z is the axis of the imaging system: resolution in the x direction is determined by the largest value of k_x that can reach the image. In vacuo we have,

$$k_z = \sqrt{\omega^2 c^{-2} - k_x^2}$$

where c is the velocity of light, and there is a cut-off at $k_x = \omega/c$ which limits the resolution to of the order of the wavelength, $\Delta \approx 2\pi/k_{x\,max} = \lambda$. On the other hand in anisotropic media [1],

$$\frac{k_x^2}{\varepsilon_z} + \frac{k_z^2}{\varepsilon_x} = \frac{\omega^2}{c^2}$$

and if it happens that $\varepsilon_x > 0$, $\varepsilon_z < 0$, then,

$$k_z = \sqrt{|\varepsilon_x|}\sqrt{\omega^2 c^{-2} + k_x^2/\sqrt{|\varepsilon_z|}}$$

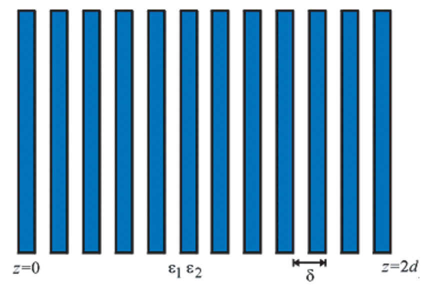

Figure 1: Alternating layers of silver ($\varepsilon_1 < 0$) and dielectric ($\varepsilon_2 < 0$) with a spacing very much shorter than the wavelength, $\delta \ll \lambda$, generate an effective anisotropic medium with $\varepsilon_{x\,eff} > 0$, $\varepsilon_{z\,eff} < 0$. There are strict requirements of smoothness at the interfaces which make the manufacture a considerable challenge.

and there is no cut off for k_x. Balmain et al have also investigated the properties of these asymmetric systems experimentally [2] in the microwave region of the spectrum. In principle all Fourier components of the image can be transported through the system and used to form a perfect image.

It is proposed that a structure comprising alternating thin layers of dielectric and silver [3] could be used to make a metamaterial that achieves the desired properties at optical frequencies; see figure 1. Averaging electric fields applied along first the x- axis and then along the z- axis gives,

$$\varepsilon_{x\,eff} = \frac{1}{2}(\varepsilon_1 + \varepsilon_2), \qquad \varepsilon_{z\,eff} = \frac{1}{2}(\varepsilon_1^{-1} + \varepsilon_2^{-1})$$

where for simplicity we have assumed the silver layer ($\varepsilon_1 < 0$) and the dielectric layer ($\varepsilon_2 > 0$) of equal thickness. Evidently if one average is positive the other must be negative and hence we achieve the desired anisotropy, $\varepsilon_{x\,eff} > 0$, $\varepsilon_{z\,eff} < 0$.

The possibilities of this unusual structure for sub wavelength imaging will be investigated.

REFERENCES

1. Smith, D. R. and D. Schurig, *Phys. Rev Lett.*, Vol. 90, 077405, 2003.
2. Balmain, K. G., A. A. E. Luttgen and P. C. Kremer, *IEEE Antennas Wireless Propag. Lett.*, Vol. 1, 146, 2002.
3. Ramakrishna, S. A. and J. B. Pendry, *Phys. Rev.*, Vol. B67, 201101, 2003.

Series and Parallel Arrangements of Optical Nanocircuit Elements

Nader Engheta[1], **Alessandro Salandrino**[1,2], **Andrea Alù**[1,2]

[1]University of Pennsylvania, U.S.A.
[2]Università di Roma Tre, Italy

It is well known that in certain noble metals such as Ag, Au, the plasma frequency is in the visible or ultraviolet (UV) regimes, and thus these metals behave as plasmonic materials in the optical frequencies, i.e., their permittivity has a negative real part [1]. These metallic (and non-metallic) nanoparticles may be tailored to function as nanocircuit "lumped" elements, i.e., nano-inductors, nanocapacitors and nano-resistors operating at the optical wavelength [2]. The conventional circuits in the lower frequency domains (such as in the RF and lower frequency range) indeed involve elements that are much smaller than the wavelength of operation, and it is known that the circuit theory may be regarded as the "approximation" to the Maxwell equations in the limit of such small size. We have explored how these circuit concepts and elements may be extended to the optical frequencies when dealing with plasmonic and non-plasmonic nanoparticles. In order to form parallel and series arrangements of such optical nanocircuit elements, one would need to juxtapose two (or more) of them very closely

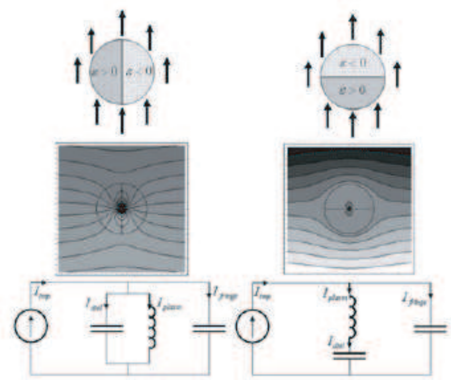

Figure 1: Amplitude contours of the E-filed intensity

with specific orientations with respect to the illuminating electric field. (See Figure below as an example). The potential distribution around this fused (cylindrical) structure, when illuminated with an electric field, provides useful information about its behavior as combined circuit elements. The figure presents the potential distribution and equipotential surfaces for the two cases of electric field being parallel (left column) and perpendicular (right column) to the plane interface between the two cylindrical halves with permittivities ε and -ε. The equivalent circuit for each scenario is also shown in the figure. In this talk, first we will discuss the concepts and issues for synthesizing nanocircuit lumped elements in the optical regime, and then we will present the analysis and salient features of such fused nanostructures that behave as parallel and series nanocircuit elements at optical frequencies.

REFERENCES

1. Bohren, C. F. and D. R. Huffman, *Absorption and Scattering of Light by Small Particles, Wiley, New York*, 1983.
2. Engheta, N. , A. Salandrino, and A. Alù, *http://arxiv.org/abs/cond-mat/0411463*

Homogenization of 3D Structured Composites of Complex Shaped Inclusions

O. Ouchetto, **S. Zouhdi**, **A. Bossavit**
Laboratoire de Génie Electrique de Paris LGEP-Supélec, France

G. Griso
Université Pierre et Marie Curie, France

B. Miara
ESIEE, Laboratoire de Modélisation et Simulation Numérique, France

The study of electromagnetic fields in artificial structured materials is becoming a vibrant area of technological research in very wide frequency range from optical regime to microwaves with great promise for societal benefits.

Artificial materials consist of a mixture of metallic or dielectric particles in a host medium. The interest for these materials comes from the fact that a composite has, in general, better characteristics than those of its components (typical example are metamaterials and photonic crystals). It has been shown that artificial materials may significantly improve the performance of antennas, microwave filters and other devices for applications in radio, millimeter wave, and photonic engineering. The characterization and study of these "engineered" materials is thus of increasing relevance.

In this paper a new technique is presented for the accurate computation of the effective constitutive parameters of lattices containing particles with complicated shape. This technique is based on the periodic unfolding method. The method is based on the decomposition of the fields in a main part without micro-oscillations, and a remainder part taking them into account. The idea of this decomposition is inspired by the method of Finite Element approximations. Verification data is presented for lattices of dielectric cubes obtained with the Maxwell-Garnett method. Corrector results are also studied as a function of frequency.

Homogenization Methods for Negative Index Media

Vasundara V. Varadan
University of Arkansas, USA

Both theorists and experimentalists use homogenization methods to extract the frequency dependent effective material properties of a collection of resonant structures such as split rings, wires, helices and Omega shapes. The terminology negative index materials or negative index media may be a misnomer since it implies a continuous medium of infinite extent. To date only finite samples of structures that exhibit negative refraction at MW and THz frequencies have been realized. Effective material properties were extracted by making reflection transmission measurements using a free space focused plane wave illumination with TRL calibration, assuming the thickness of a planar sample of the effective medium to be the distance between the phase calibration planes. The calibration planes were chosen to coincide with the front and back surface of the actual physical sample. Thus the homogenization volume for the inverse problem was the volume of the physical structure. Theorists using homogenization methods assume an arbitrary volume whose dimensions are 'large' compared to 'wavelength'. In this paper, samples of different thicknesses and hence different homogenization volumes will be prepared and effective properties will be extracted from S-parameter measurements. The samples to be considered are periodic and randomly dispersed Omega shapes, helices and wire/split ring resonator samples. In previous papers, negative properties have been extracted for such samples at MW frequencies. The results of samples of the same 'material' of different thicknesses will be compared to study if we have truly realized effective properties and if the negative properties persist for all samples.

Free-Space Electromagnetic Characterization of Materials for Microwave and Radar Applications

Habiba Hafdallah Ouslimani, **Redha Abdeddaim**, **Alain Priou**
University Paris X, Ville d'Avray, France

Characterization of the electrical material properties ε_r, μ_r and tanδ is of prime importance for all microwave and antenna design applications. Experimental "S" parameters in wide frequency band are used. Problem related to the calibration elements, calibration references planes and the thickness samples (d) are reported. Problem of calibration can be avoided by using noncontact free space electromagnetic characterization based on the measurement of the insertion transfer function. This method allows spatial correction of the experimental set-up. Problem of the sample thickness (d) is essentially due to the existence of multiple solutions when solving the set of basis equations with S_{21}, S_{11}, ε_r and μ_r . This is the principal reason why some algorithms give spurious solutions or didnt converge. In this work, we developed a method combining several solutions suggested otherwise based on:

- Free-space electromagnetic characterization associated with an adapted wave-guide LRL ("line-reflect-line") calibration method in the 8-12GHz X band range,
- Insertion mode to correct spatial dependence of the transfer function (S_{21}),
- An electrical E-wall to correct the phase of the reflection parameter (S_{11}).
- A supplementary criterion on loss material is used to obtain a unique solution.

We have experimentally characterized a 50mm thick dielectric material and extracted its relative permittivity in the X band. The obtained results are in excellent agreement with the known value.

DNG-NRD Directional Couplers

António L. Topa, **Carlos R. Paiva**, **Afonso M. Barbosa**
Instituto Superior Técnico, Portugal

Left-handed (LH) materials, in which both permittivity and permeability assume negative real values, exhibit unusual properties due to the fact that the Poynting vector of a plane wave is anti-parallel with its phase velocity, i.e., the waves propagating in these media, are backward waves. This property has suggested that the refraction index should be assumed negative [1].

Recently, Shelby et al. [2], inspired by the work of Pendry et al. [3], constructed a composite medium, exhibiting this anomalous behavior in the microwave regime, by arranging arrays of small metallic wires and split ring resonators, and they demonstrated the anomalous refraction for this medium. The possibility to built composite materials with simultaneously arbitrarily negative real values of ε and μ, more recently termed double-negative (DNG) materials [4], [5], has prompted a renewed interest in these phenomena. The application of these media to the design of new devices is a topic of great importance.

The non-radiative dielectric (NRD) waveguide is a very used technology in the millimetre-wave integrated circuit regime [6]. This paper addresses the problem of electromagnetic wave propagation in NRD waveguiding structures where the common double-positive dielectric media are replaced by DNG dielectric media. In this work, we assume lossless, homogeneous, and isotropic DNG materials.

The full-wave analysis, for the propagating modes of a DNG-NRD directional coupler, is presented. New propagation characteristics, such as anomalous dispersion, super-slow waves, and contra-directional coupling are reported. These unusual features may provide physical insight into other waveguide geometries, with potential applications in the design of new devices and components.

REFERENCES

1. Veselago, V. G., "The Electrodynamics of Substances with Simultaneously Negative Values of ε and μ," *Sov. Phys.Usp.*, Vol. 10, No. 4, 509, 1968, *Russ. Usp. Fiz. Nauk*, 517, Vol. 92, 1967.
2. Smith, D. R., W. J. Padilla, D. C. Vier, S. C. Nemat-Nasser and S. Schultz, "Composite Medium with Simultaneously Negative Permeability and Permittivity," *Phys. Rev. Lett.*, Vol. 84, No. 18, 4184, 2000.
3. Pendry, J. B., A. J. Holden, D. J. Robbins, and W. J. Stewart, "Magnetism from Conductors and Enhanced Nonlinear Phenomena," *IEEE Trans. Microwave Theory Tech.*, Vol. 47, 2075, 1999.
4. Ziolkowski, R. W. and E. Heyman, "Wave Propagation in Media Having Negative Permittivity and Permeability," *Phys. Rev. E*, Vol. 64, No. 5, 056625, 2001.
5. Engheta, N., "Ideas for Potential Applications of Metamaterials with Negative Permittivity and Permeability," *Advances in Electromagnetics of Complex Media and Metamaterials*, ser. NATO Sci., S. Zouhdi, A. H. Sihvola, and M. Arsalane, Eds. Norwell, MA: Kluwer, 19, 2002.
6. Yoneyama, T. and S. Nishida, "Nonradiative Dielectric Waveguide for Millimeter-Wave Integrated Circuits," *IEEE Trans. Microwave Theory Tech.*, Vol. MTT-29, 1188, 1981.

The Surface Wave Modes Coupling on the Boundary of Metamaterial

G. Granet[1], **A. Poyedinchuk**[2], **N. Yashina**[2]

[1]Universite Blaise Pascal, France
[2]IRE NAS of Ukraine, Ukraine

The spectral problems for eigen waves and mode (natural oscillations) of the wavy periodic boundaries of the media with negative permittivity or/and permeability are considered. By means of C-method [1,2] the homogeneous boundary value problems are reduced to the problems for characteristic values of operator-functions in which the spectral parameter occurs in non linear way [3-5].

The numerical algorithms and corresponding codes have been constructed and implemented for computation of complex frequencies of eigen modes (oscillations) and propagation constants of surface waves.

The numerical experiments oriented to the study of regularities and peculiarities in the spectral characteristics (eigen complex frequencies, propagation constants of eigen modes and waves, corresponding electromagnetic field patterns, etc) behavior with geometrical and electromagnetic parameters of periodic boundary varying have been carried out within rather wide range of parameters.

Special attention has been focused on the study of the phenomenon of eigen modes (oscillations) and eigen waves coupling. Earlier this phenomenon had been studied for unclosed screens [4], perfectly conducting gratings [2] and waveguide open resonators [5]. It has been shown the following: there is certain totality of values of geometrical parameters such that even weak variation of this totality results in abrupt and pronounced changes in the behavior of eigen frequencies, depending on these parameters; in the appearing of hybrid configurations of the electromagnetic field pattern of eigen oscillations.

On the base of the theory of critical points (Morse's critical points) of analytical functions of several variables [6,7] the mathematical model of the inter mode coupling phenomenon, arising on the wavy periodic boundary of material with single or/and double negative parameters has been developed.

REFERENCES

1. Chandezon, J., A. Ye. Poyedinchuk, Y. A. Tuchkin and N. P. Yashina, "Mathematical Modeling of Electromagnetic Wave Scattering by Wavy Periodic Boundary between Two Media", *PIERS*, Vol. 38, 130, 2002.
2. Chandezon, J., G. Granet, A. Ye. Poyedinchuk, N. P. Yashina, "Rigorous Model for the Materials With Negative Permittivity and Permeability Electromagnetic Study", *PIERS, 2004, Pisa, Italy*, Vol. 28, 2004.
3. Shestopalov, V. P. and Yu. K. Sirenko, "Dynamic Theory of Gratings", *Kiyev, Naukova Dumka, 1989, In Russian*, 1989.
4. Poyedinchuk, A. Ye., Yu. A. Tuchkin and V. P. Shestopalov, "Regularization of Spectral Problems of Wave Scattering on Unclosed Screens", *Soviet Physics Doclady*, Vol. 32, 1987.
5. Pochanina, I. E., N. P. Yashina, "Electromagnetic Properties of Open Waveguide Resonators", *Electromagnetics*, Vol. 13, 325, 1993.
6. Gilmore, R., "Applied Theory of Catastrophes", *Mir, Moscow*, 1984.
7. Melezhik, P., V. Koshparenok, A. Poyedinchuk and V. Shestopalov, "On Analytical Nature of the Phenomenon of Intertype Interaction of Eigenoscillations", *Doklady AN SSSR.*, 300, 1988.

Higher-order Resonant Modes of a Metasolenoid

Liisi Jylhä, **Stanislav Maslovski**, **Sergei Tretyakov**
Helsinki University of Technology, Finland

Microwave magnetic materials are designed as artificial media formed by metal or dielectric inclusions, because naturally available magnetic materials loose their magnetic properties at microwave and millimeter-wave frequencies. A new magnetic particle called "metasolenoid" was introduced in[1,2], see Figure1. It consists of a stack made from several single split-ring resonators (SRR) packed close one to another.

The higher-order resonant modes of the metasolenoid are characterized and the dependency of the resonant frequencies on the dimensions of the metasolenoid are studied both numerically and analytically. Both these approaches are in a reasonable agreement. Higher-order resonant modes can be characterized based on the magnetic field pattern inside the metasolenoid or based on the direction of the current in each loop.

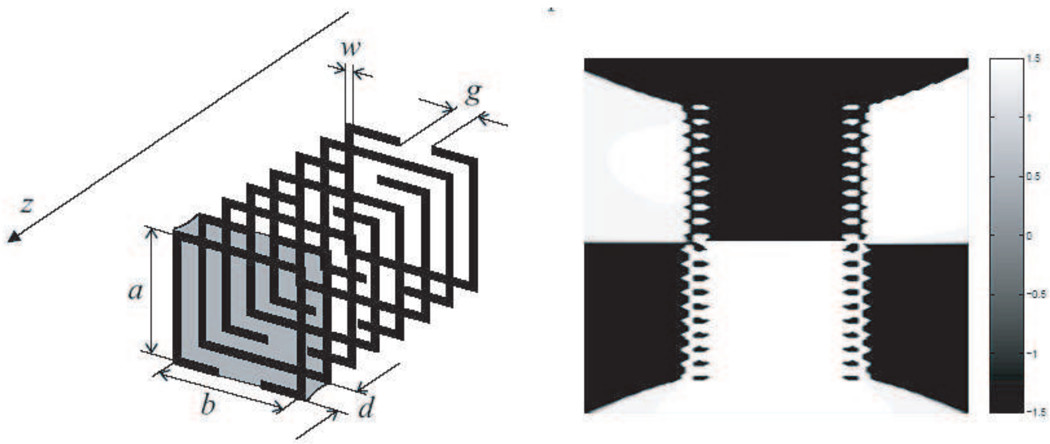

Figure 1: Geometry of the metasolenoid and phase of the longitudinal magnetic eld in one of the eigenmodes

This study suggests that the metasolenoid can be used not only as a magnetic inclusion (at its fundamental resonance), but also as a waveguiding structure supporting waves with small wavenumbers and as a high quality resonator with characteristic spatial field distributions. Such structures can find applications in the design of delay lines, filters, and sensors.

REFERENCES

1. Ikonen, P., S. Maslovski, S. Tretyakov, I. Kolmakov, "New Artificial High-Permeability Material for Microwave Applications", *Progress in Electromagnetics Research Symposium, PIERS 2004, Pisa, Italy*, 485, March 28-31, 2004.
2. Maslovski, S., P. Ikonen, I. Kolmakov, S. Tretyakov, and M. Kaunisto, "Artificial Magnetic Materials Based on the New Magnetic Particle: Metasolenoid", to appear in *Journal of Electromagnetic Waves and Applications*.

THz Spectroscopy and Ellipsometry of Magnetic Metamaterials

W. J. Padilla[1], **Ta Jen Yen**[2], **N. Fang**[2], **D. C. Vier**[3]
David R. Smith[4], **J. B. Pendry**[5], **X. Zhang**[2], **D. N. Basov**[3]

[1]Los Alamos National Laboratory, USA
[2]University of California at Los Angeles, USA
[3]University of California San Diego, USA
[4]Department of Electrical & Computer Engineering, UK
[5]Imperial College, UK

We present S and P polarized measurements of artificial bianisotropic magnetic metamaterials with resonant behavior at infrared frequencies. These metamaterials consist of an array of micron sized copper rings fabricated upon a quartz substrate. Simulation of the reflectance is obtained through a combination of electromagnetic Eigenmode simulation and Jones matrix analysis, and we find excellent agreement with the experimental data. It is shown that although the artificial magnetic materials do indeed exhibit a magnetic response, care must be taken to avoid an undesirable electric dipole resonance, due to lack of reflection symmetry in one orientation. The effects of bianisotropy on negative index are detailed and shown to be beneficial for certain configurations of the material parameters.

Perfect Electromagnetic Conductor (PEMC) in Electromagnetics

Ismo V. Lindell, **A. Sihvola**
Helsinki University of Technology, Finland

Perfect electric conductor (PEC) and perfect magnetic conductor (PMC) can be generalized to perfect electromagnetic conductor (PEMC), a medium where certain linear combinations of electromagnetic fields are required to vanish. In differential-form representation the corresponding medium is characterized as being the simplest possible medium. PEMC medium is defined through one scalar parameter, the PEMC admittance, whose zero and infinite limits give the PMC and PEC media, respectively. In the present paper a duality transformation is defined which has the property of transforming PEMC medium to PEC medium and an isotropic medium ('air') to itself. Thus, problems involving PEMC objects in air can be transformed to problems with PEC objects in air which can be solved through traditional techniques and then transformed back. Several simple examples are treated to demonstrate the principle, including reflection from a PEMC plane, propagation of modes in a PEMC waveguide, scattering from a PEMC object and image theory for the PEMC plane. Because of its nonreciprocity, PEMC material has the property of giving cross-polarized component to a wave reflected from its surface. Thus, it has the potential of offering applications to antenna engineering.

REFERENCES

1. Lindell, I.V., *Differential Forms in Electromagnetics, New York: Wiley*, 2004.
2. Lindell, I.V. and A. Sihvola, "Perfect Electromagnetic Conductor", *J. Electromag. Waves Appl.*, to appear.

Scattering Properties of PEMC (Perfect Electromagnetic Conducting) Materials

A. Sihvola, **I. V. Lindell**, **P. Yla-Oijala**
Helsinki University of Technology, Finland

The PEMC medium is a special type of metamaterial which is a generalization of the well-known concepts of PEC (perfect electric conducting) and PMC (perfect magnetic conducting) media. Perfect electromagnetic medium is characterized by an admittance-type parameter $M = \cot\vartheta$, and the choices of $\vartheta = 0$ and $\vartheta = \pi/2$ give the PEC and PMC cases, respectively. For the basic properties of PEMC media [1].

The PEMC medium belongs to the class of bi-isotropic media. Its magnetoelectric parameters are nonzero. It is also non-reciprocal, which means that electromagnetic reflection problems involving boundaries of PEMC materials lead to cross-polarized effects. This fact suggests possibilities of applying such media in designs that require transformation of the polarization state of the wave, for example in connection with reflector antennas.

Even if the constitutive material parameters have infinite amplitudes for PEMC medium, the composite involving particles or scatterers with such a character are well-behaved, just like the more "ordinary" metal-dielectric composites. This presentation will focus on the homogenization of composites including PEMC particles and discuss the macroscopic properties of such media. The interesting phenomena that are encountered in connection with scattering from plasmonic spheres (i.e., single-negative material parameter values) will be compared with the special effects that are encountered with PEMC spheres. In addition, we will discuss the effects of the size of a spherical PEMC particle on the bistatic scattering diagrams and polarization transformation effects of this scatterer. These calculations have been performed with a versatile MoM scattering code where the boundary condition on the totally reflecting particle has been modified to conform with the special boundary condition of PEMC medium [2].

REFERENCES

1. Lindell and Sihvola, "Perfect Electromagnetic Conductor", *Journal of Electromagnetic Waves and Applications*, to appear, 2005.
2. Yla-Oijala, Taskinen, Sarvas, "Surface Integral Equation Method for General Composite Metallic and Dielectric Structures with Junctions", *Progress in Electromagnetic Research*, to appear.

Negative Refraction of Magnetic Metamaterial

Yanyan Liu, **Xiaokai Zhang**, **Michael Border**, **Rong Cao**, **John Q. Xiao**
University of Delaware, USA

Recent theoretical and experimental results have proven the existence of a novel type of metamaterials that exhibit negative index of refraction[1]−[2], a property that does not exist in any known nature occurring materials. Those metamaterials are referred as "left-handed" material (LHM) or negative index of refraction material (NIM). Although scientists only use non-magnetic materials to realize LHMs based on arrays of split resonant rings (SRRs) and wires, it is possible to realize the magnetic LHM (m-LHM) in microwave range by using nanocomposites consisting of metallic magnetic entities of nanometer size embedded in an insulating dielectric matrix[3]. In those nanocomposites, the permittivity ε of metal is always negative below the plasma frequency, while the permeability μ could also be negative for some magnetic materials in the vicinity of the ferromagnetic resonance frequency (FMR). In this paper, we developed a new technique to measure the index of refraction by detecting peak shift of the resonance in coaxial airline contains m-LHM on a normal dielectric substrate. With this technique, the refraction properties of our magnetic metamaterials have studied. We have observed the resonance peak shifted to higher frequency in $Fe-SiO_2$ nanocomposites magnetic above 12.5GHz, which indicates the index of reflection n of the sample goes to negative. Also, the thickness dependent peak shift indicated the sample has negative refraction index in similar frequency range. This new type of m-LHM is easy to make in a large quantity. In addition, its anisotropic physical properties may also be tuned by controlling the magnetic anisotropy.

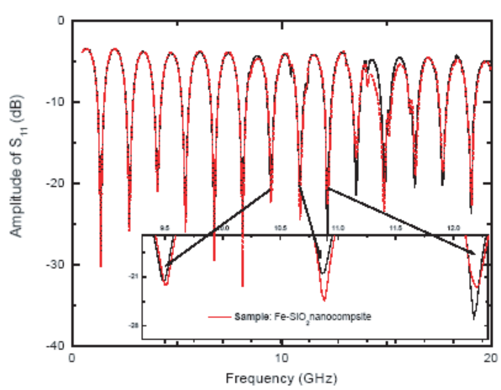

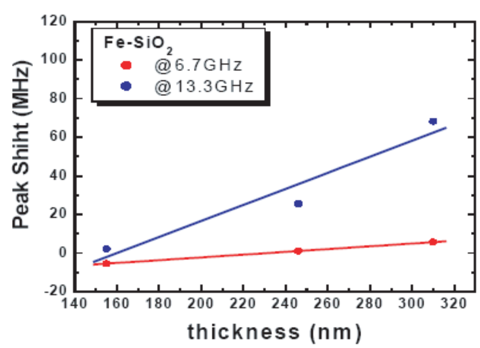

REFERENCES

1. Veselago, V. G., *Sov.Phys.USPEKHI*, Vol. 10, 509, 1968.
2. Shelby, R. A., D. R. Smith, and S. Schultz, *Science*, Vol. 292, 77, 2001.
3. Chui, S. T., Liangbin Hu, *Phys.Rev.B.*, Vol. 65, 144407, 2002.

Conception, Simulation and Characterization of a Controllable Left-handed Material

A. Djermoun
Université Paris X, France

A. de Lustrac, **F. Gadot**, **E. Akmansoy**
Université Paris-Sud, France

In this study, we present the conception, the simulation and the characterisation of a controllable left-handed material operating between 7 and 16 GHz. This material, composed from discontinous metallic wires including PIN diodes and Split Ring Resonators (SRR) is optimized to have a controllable permittivity and fixed permeability. The sign of the permittivity is controlled by the electrical state of the PIN diodes. For the two electrical states of the diodes, ON (passing) and OFF (blocked), we have calculated and measured the transmission of the material with a finite element software (HFSS from Ansoft) and an scalar network analyser Marconi 6400, demonstrating the switching of the electromagnetic state of the material between a left handed state and a reflective state, and the negative refraction index of the material.

An Analysis of Dispersion Relations for Left Hand Media Exhibiting Backward Wave Propagation

J. F. Woodley, **M. Mojahedi**
University of Toronto, Canada

Recently, left handed media (LHM) have attracted much attention due to their unusual electromagnetic properties. Because the index of refraction is negative in such media the phase velocity is also negative. On the other hand, in the pass-band the group velocity is necessarily positive so that, as a result, a wave propagating in such a medium will exhibit anti-parallel phase and group velocities. This behavior, which has been dubbed backwards wave behavior, is characteristic of the LHM. Therefore, a study of backwards wave behavior and the conditions necessary for achieving it could produce valuable insight into the problem of producing a negative index of refraction. From a three dimensional wave propagation point of view we perform a study which determines the form of the index of refraction required to produce this backwards wave behavior. This is done starting with the assumption that the group and phase velocities are perfectly anti-parallel (the angle between the vectors is 180°). Using this assumption the group velocity can be set equal to the negative of the phase velocity (multiplied by an arbitrary positive constant) resulting in a non-linear differential equation in three dimensions which can be solved for the index of refraction. This index of refraction will be such that it exhibits backwards wave propagation at all frequencies. The results of this analysis show that, in this case, the index must have a simple parabolic form and that, for the simple case of one dimensional propagation, the resulting dispersion relation agrees with that derived for a distributed system of series capacitances and shunt inductor (i.e. the dual of the simple transmission line model). The study is then repeated for the situation where the perfect anti-parallel condition between phase and group velocity vectors is relaxed. In this case the backward behavior only requires that a component of the group and phase velocity vectors be anti-parallel (the angle between the vectors is between 90° and 270°). In addition, the nature of dispersion in LHM is analyzed. It is found that the LHM dispersive behavior is subject to a hard limit in the pass-band due to the condition that the group velocity must be positive in this band. Further analysis of this dispersive behavior based on the Kramers-Kronig relations will also be considered.

Session 2P3a

Array Antennas

Large Finite Array Performance Prediction from Small Array Results

A. A. Kishk
University of Mississippi, USA

Large finite arrays are usually analyzed based on the analysis of infinite arrays, which is based on Floquet mode analysis. However, the finite array includes elements around the edges that differ from the rest of the array performance. Therefore, special treatment has to be considered to include the edge elements effects on the antenna performance. These analyses are computationally very complicated. The analysis based on Floquet modes depends on the scanning angle. Therefore, the analysis has to be repeated for each scanning angle.

Here the performance of the large finite array can be predicted using a simpler and more efficient technique. The technique is based on the knowledge of the mutual impedances between the elements of a smaller array of a lattice similar to the required large finite array. Such mutual impedances can be provided based on computational techniques or measurements. Once the mutual impedance matrix of the small array is provided, the large finite array mutual impedance matrix can be constructed. The construction of the new mutual impedance takes into consideration the effect of the edge elements. From the mutual impedance matrix the effective (active) impedance of the array elements can be computed. Also, with the same mutual impedance the active array elements impedance are predicted for any scanning angle. Also, the effective excitation current to each element is accurately computed from which an array factor is computed with the effect of the mutual coupling into consideration. The new array factor can be used to compute the radiation patterns of the antenna array using the pattern multiplication method.

The technique is tested and verified usng an array of rectangular microstrip patches. A study is performed to find the appropriate small array size that provides better prediction for the large finite size array. The predicted effective impedance using this technique is compared with the actual effective impedance for the large finite array.

A New Hybrid Method for the Analysis of Radome Enclosed Slot Antenna/Arrays

Xiao-Chun Nie, **Yeow Beng Gan**, **Ning-Yuan**, **Le-Wei Li**
National University of Singapore, Singapore

Layered dielectric radomes are often used to house airborne scanning radar antennas to protect the antennas from environmental and aerodynamical effects. However, the presence of the radome will affect the radiation performance of the enclosed antennas significantly, due to interactions between the antenna and radome. An efficient analysis of the antenna-radome system is thus very important to the antenna/radome designer.

So far, a variety of approaches have been employed to investigate the changes to the radiation pattern of an antenna covered by a radome. These approaches can be broadly grouped into three categories: 1) high-frequency (HF) methods; 2) low-frequency (LF) methods; and 3) analytical methods which are only applicable to radomes of special shapes. High frequency (HF) methods are unable to account for the interactions between the antenna and radome, and therefore cannot predict the changes to the current distribution on the antenna. Low frequency (LF) methods, although providing accurate solution to the problem, are limited by the extensive computational requirements to handling radomes of small electrical sizes. Fast algorithms can be used to reduce the computational requirement of the LF methods to some extents, thereby increasing the size of radome that can be analyzed. However, as practical radomes are typically of several tens of wavelengths in size, the computational requirement remains prohibitive.

To cope with such an electrically large and complex problem, a hybrid method that combines the integral equation (IE) method and Physical Optics (PO) is proposed. Consider a slot antenna-radome system, the integral equation is established at the aperture of the slot antenna by enforcing continuity of the tangential components of the magnetic fields. Equivalent PO currents are assumed on the walls of the radome, induced by the radiated field from the antenna. The reflected fields due to the PO currents on the radome are coupled back into the integral equation to take into account the effects of the radome on the antenna. By solving the resultant integral equation, the magnetic current distribution on the antenna can be obtained and thus the radiation pattern and input impedance of the antenna can be evaluated. This method leads to significant reduction in memory requirement and computational complexity since PO is applied to the electrically large radome, with unknown currents defined only on the aperture of the slot antenna. The accuracy of the method is further improved by using integral equation method for the region surrounding the tip of the radome.

A significant advantage of the present method over existing hybrid methods is that it includes the coupling between the antenna and radome. Since the current distribution on the antenna in the presence of the radome is accurately evaluated, both the radiation pattern and input impedance of the antenna can be predicted accurately. Numerical examples will be presented to validate the method and demonstrate its efficiency.

Scattering from Waveguide-Fed Planar Slot Arrays

Sembiam R. Rengarajan
California State University, USA

Waveguide-fed planar slot arrays are employed in a number of ground and space based communications and radar systems. A number of papers in the literature discuss the analysis and design of slot array antennas. The scattering from such antennas has not received much attention in the literature. Josefsson studied the scattering from a single slot in an infinite ground plane with a waveguide loading at the back [1]. Fan and Jin presented numerical results computed for the scattering from a slotted waveguide array [2]. A hybrid moment method and high frequency technique has been used in that work. The array consists of stacked waveguides and each waveguide is assumed to be end-fed in the antenna transmit mode.

In this work we consider two types of feeding in the antenna transmit mode. The first one is similar to Fan and Jins array in which longitudinal offset radiating slots are cut in the broad wall of each radiating waveguide. Each radiating waveguide is end-fed by a TE10 mode wave with appropriate amplitude and phase. The second configuration consists of a feed waveguide transverse to the radiating waveguides with centered-inclined coupling slots providing the excitation of each radiating waveguide. The feed waveguide is again end-fed by a TE10 mode source. The planar slot array consisting of a number of sub-arrays is also considered.

In the scattering problem the source of excitation is a plane wave. The scattering from the slots is determined from the equivalent magnetic currents. There is an additional component of scattered wave that is obtained by the physical optics technique when the plane wave illuminates a flat ground plane (with the slots being shorted). The slot scattering is determined by first formulating coupled integral equations for the equivalent magnetic currents and then by solving them by the method of moments.

In the symposium we will discuss all the details of the analysis and computation. Results will be presented for different parameters such as the angle of plane wave incidence, polarization, and for a few slot arrays with different aperture distributions.

REFERENCES

1. *IEEE Antennas and Propagation Society International Symposium*, 942, 1990;
2. *Electromagnetics*, Vol. 19, No. 1, 109, 1999.

Sparsity Analysis of Two-Dimensional Ultra-Wideband Focused Array

Ayman Al-Zayed, Malek G. M. Hussain
Kuwait University, Kuwait

Array beamforming based on ultra-wideband (UWB) electromagnetic waveforms have found numerous applications in ground-probing radar (GPR), wireless communications, localization systems, and medical diagnosis and imaging, especially for early detection of breast cancer. In a recent paper (PIER 2004, vol.49, pp.143-159, 2004), the principle of two dimensional focused array (TDFA) beamforming was introduced to generate ultra-wideband (UWB) electromagnetic missiles with localized energy. The decaying behavior of the radiation energy of the electromagnetic missile is not governed by the classical inverse distance-square law. The focused energy pattern allows for a trade-off between the focusing distance, frequency bandwidth, and array size for improved depth-of-focus and resolution. Such a trade-off is desirable in practice to account for possible restrictions that might be imposed on certain design parameters. In this paper, the performance of the TDFA is analyzed in terms of array sparsity; a situation that occurs when a random number of array elements become faulty and inactive; their life time expires. The focused-energy pattern of the UWB electromagnetic missile is expressed in terms of a two-dimensional matrix, referred to as sparsity matrix, whose elements are assigned the values {1}, and {0}; {1} indicating an active element while {0} indicating inactive array element. Computer plots of focused energy patterns of the TDFA are derived for sparsity matrices of different patterns of element distributions. The depth of focus, or the focusing bandwidth of the energy patterns, changes as a function of the distribution pattern of the elements of the sparsity matrix. The depth of focus, like the half-power beamwidth of a typical antenna pattern, is an effective measure of the performance of the TDFA. A degradation in the focusing power of the TDFA can affect the accuracy of ranging as well as image quality of a radar system. It will be shown that the degradation in focusing power due to array sparsity can be minimized by proper design of the UWB signal and antenna array structures.

Experimental System of a Wideband Optically Controlled Phased Array Antenna

Mou-Ping Jin, **Wei Guan**, **Mei-Qing Qi**, **Jun Guo**
East China Research Institute of Electronic Engineering, China

Optical beamforming for phase-array antennas have been intensely studied during the last decade. It offers many advantages such as small size, low weight, no susceptibility to electro-magnetic interference, wide instantaneous bandwidth or squint-free array steering. A experimental system of a wideband optically controlled phased array antenna is presented.

The array antenna is shown in Fig.1. The two dimensional array consists of 96 wideband elements grouped into 24 columns. Each column is steered by a 5-bit electronic phase shifter. Every three columns are combined to form one subarray, which is controlled by one 5-bit fiber optic time delay, so each column is controlled by 10 bits of time shift in total.

The 5-bit photonics true-time-delay is based on RF switch. It provides the coarse delay steps ranging from 0.25ns to 7.75ns for the subarrays, while the electronic phased shifters provide fine differential delay ranging from 0.01ns to 0.32ns. The key components inside the photonics true-time-delay unit are 1:8 RF switch, eight semiconductor laser, one 4×8 fiber coupler, four detectors, 1:4 RF switch and post AMP, as shown in Fig.2.

The radiation patterns are tested in an indoor far-field measurement system. The test array patterns at 0 and ±45 degrees are shown in Figure 3. Note that no beam squint in beam direction over 2.5 to 3.5GHz range by using true-time-delay beamforming network. A conventional array with phase shifters could not have achieved this performance.

Figure 1: 96-element phased array antenna controlled by photonics

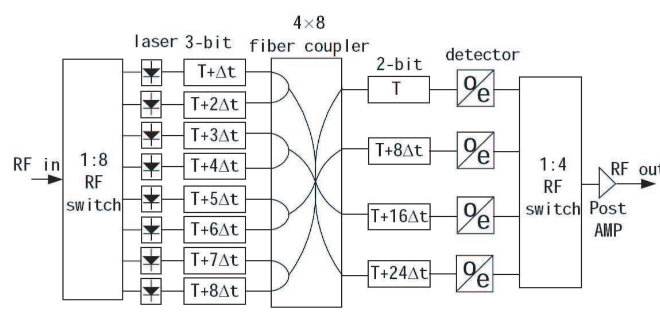

Figure 2: 5-bit photonics true-time-delay unit

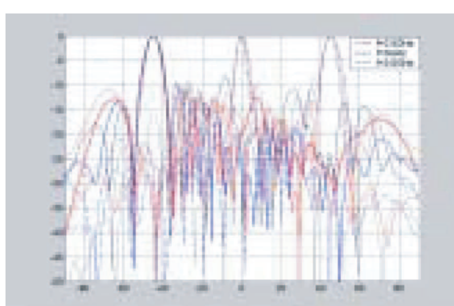

Figure 3: Radiation patterns for 0° and ±45° at 2.5, 3 and 3.5GHz

Switched Parasitic Yagi-uda Diversity Antenna for MIMO Base Station

Yan Cheng, **Xi-Yu Zhang**, **Zaiping Nie**, **Wei-Hong Xiao**
University of Electronic Science and Technology of China, China

Multiple-input multiple-output (MIMO) is one of the most competitive technologies in the next generation mobile communications. It can greatly increase channel capacity and spectrum efficiency by employing multiple transmit antennas and multiple receive antennas simultaneously. A key feature of MIMO systems is the ability to turn multi-path propagation, fading of wireless channel, into a benefit. And this cannot be achieved without multiple antenna systems.

In this paper, a new structure design for MIMO base station antenna is presented and its characteristics are evaluated. The central operating frequency of this base station diversity antenna is 2.14GHz. Since the space limitation of the antennas for base stations is not so cruel as that of antennas for mobile terminals, this antenna configuration can make full use of base station to achieve array gain as well as diversity gain.

There are four diversity branches in this multi-antenna structure, each of them is a linear yagi-uda antenna array with folded-dipole as active element. Each linear yagi-uda antenna array, called a diversity branch(as shown in figure 1), contains four switchable yagi-uda antennas which are arranged vertically along the z-axis with a distance of λ between each other. And the array gain can be obtained along the θ-direction. The radiation pattern of the four-element yagi-uda antennas used in this antenna system can be changed by switching their reflector and directors elements via RF switches. When these switches are turned on, the antenna is a folded-dipole yagi-uda antenna; when these switches are turned off, the reflector and directors of yagi-uda antenna are no longer reflector and directors, and the antenna works as a folded-dipole with several cylinder scatters. There is a top reflector above the four branches to expand the DOA of the electromagnetic waves. And the pattern diversity will be obtained along the ϕ-direction. Fundamental characteristics of this base station diversity antenna are examined through both simulation and experiment in this paper.

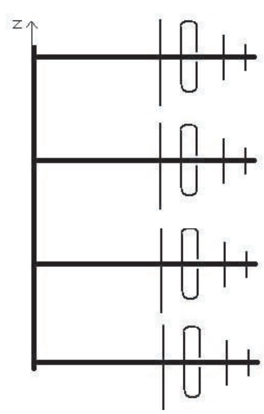

Figure 1: A diversity branch

Session 2P3b

Dielectric Waveguides and Antennas

A New Design for Terahertz Photonic Crystal Fiber Using the Finite-Difference Time-domain Method

Liang Wang, **Dongxiao Yang**, **Qing Chang**
Zhejiang University, China

With unsplit anisotropic perfectly matched layer (APML) for the boundary treatment, a new design for terahertz photonic crystal fiber (PCF) by using the finite-difference time-domain (FDTD) method is present. Electromagnetic fields of guided mode and transmission spectrum in PCFs are computed.

Study of Broadband Dielectric Resonator Antennas

Qinjiang Rao
University of Quebec, Canada

Tayeb A. Denidni
University of Quebec, Canada

Over last decade, dielectric resonator antennas (DRAs) have attracted abroad attention due to their many attractive features in terms of high radiation efficiency due to free from metallic and surface wave losses, light weight, small size and low profile. Moreover, DRAs can accommodate a variety of feed structures, such as a coaxial probe, microstrip feed line coupled to a narrow slot, aperture coupled and CPW feed. However, one bottleneck in the development of dielectric resonator antennas is the considerable narrow bandwidth, as compared to that of ordinary microwave antennas. For this reason, broadband operation is highly desirable in most applications for DRAs.

This paper reviews recent progress in broadband designs for DRAs. The attention mainly focuses on the DRA broadband operation mechanism and the development of novel configurations, including DR radiation elements and feed structures. These DRAs can be approximately classified into three categories: 1) a single dielectric resonator, 2) two or multi- dielectric resonators, 3) hybrid dielectric resonators with other resonators.

Design of A DGPS Beacon Active Receiving Antenna

Da-Fang Yi
Southwest China Institute of Electronics Technology, China

Tianxin Xiong, **Kemin Sheng**
Southwest Jiaotong University, China

GPS (Global Positioning System) techniques are now widely used in industries such as navigation and positioning. DGPS (Differential GPS) is introduced for further improving the positioning precision. One way of DGPS implementation is the beacon technique in which the existent marine radio navigation beacon stations are utilized. A MSK (Minimum frequency Shift Keying) data modulated sub-carrier is added to the transmitted beacon signal for transmitting modified DGPS data, so that 1 meter level of high positioning precision for ships or vehicles can be obtained. Up to now, most of the countries and regions all over the world have established DGPS beacon stations. A universal frequency band (283.5 - 325 kHz) and a channel band (500 Hz) are also specified. However, in the general environment of mobile communications, the most used traditional whip antennas or loop antennas are not suitable for this application. The low profile and non-directional receiving antenna characteristic is very practical. Based on this consideration for the requirement of mobile DGPS receiving antennas, this paper presents a highly effective and practical design technique for a DGPS active beacon receiving antenna.

A ferrite magnetism antenna design scheme is used for the antenna. This type of antenna has the good qualities not only in small dimensions, high Q value, and easily matching with the amplifier stage, but also in its anti-interference behavior, for most of interferences are generated from electrical utilities like engines and spark plugs on ships and vehicles, and it has been demonstrated by experiments that they have less influences on this antenna.

The designed antenna is composed of 2 parts. One is the RF signal receiving unit that is made up of 4 square arranged ferrite magnetism rods on which the coils are circum-columnar. The other is RF circuits including impedance matcher, signal amplifier, phase shifter, and a combiner. When the RF signal is received by the 4 ferrite magnetism coils, they are separated into 2 branches with certain amplitude. One is called parallel branch and the other is orthogonal. Then the phase of the orthogonal signal is 90 degree shifted. Since the signals of the 2 branches are orthogonal in space and in phase with each other, they form a circular polarization wave when they are combined, and they are independent of direction of the incident plane wave. After the signal passes through a proper amplifier with sufficient gain, it is output to the DGPS receiver.

REFERENCES

1. Bixby, Jim, "DGPS Receiver Hardware Description," November, 1998.
2. Betke, Klaus, "Transmission Characteristics of Marine Differential GPS(DGPS) Stations[S]". http://www.nensch.de/.

The High-Mode-Merging Technique for Dielectric Waveguides

Jinsheng Tang, **Kemin Sheng**, **Jun Gao**
Southwest Jiaotong University, China

The mode-matching method and transverse Technique for dielectric waveguides was developed in 60s-70s last century[1].After that, there are only few attentions were paid. But it may be a effective method. Now a derived method -highmode-merging method is approached.

As we've known that lots of high modes are caused as some EM wave meets a non-uniform part of material say, a dielectric discontinuous structure. The electric and magnetic waves of each mode can be represented as the voltage and current on a transmission line respectively. Then a dielectric step discontinuity can be seen as a building block of a network which connects with all these transmission lines. This network can be described by a matrix.. Then, the guidance and leakage properties of it can be got by the transverse resonance technique of mode-matching method. This method is rigorous , but rather complicated. Lots of computer work are needed and only can be used for further application of symmetric structure.

In the highmode-merging technique only the transmission line of dominant mode remained and all ones of high modes are cancelled, but their influences still remains numerically. They are merged into dominant mode. Then the problem can be treated as a two-port network, which is a little bit different from one for which only dominant mode is considered[2]. In this way, the expressions of impedance matrix elements are obtained. And it can be carried by a simple circuit equivalently. Some numerical examples are given with results got by equivalent- dielectric-constant method (EDC-method) for comparison. Present method can be used for asymmetric dielectric structures and even periodic structures, because for two-port network, it is easy to treat the cascade of matrixes. More further works will be done later.

*This work is supported by foundation of Southwest Jiaotong University, grant no.2004b05.

REFERENCES

1. Peng, S. T. and A. A. Oliner, "Guidance and Leakage Properties of a Class of Open Dielectric Waveguides: Part I-Mathematical Formulations", *IEEE on Trans MTT*, Vol. MTT-29, No. 3, 785, 1981.
2. Sheng, Kemin and Ziyuan Shen, "An Equivalent Network and an Equivalent Circuit for a Dielectric Step Structure", *Journal of Southwest Jiaotong University*, No. 2, 83, 1995.

Properties of Focused Flat-topped Multi-Gaussian Laser Beam by a Lens with Spherical Aberration

Xiqing Wang, **Qingfeng Wang**, **Qing Huang**
Southwest Jiaotong University, China

Starting from the generalized Huygens-Fresnel diffraction integral formula, the properties of focused flat-topped multi-Gaussian laser beams by a lens with spherical aberration(SA) have been discussed. The expressions for the axial light intensity of flat-topped multi-Gaussian laser beams focused by a lens with spherical aberration have been derived. Based on these expressions, the influence of the Fresnel number of fundamental Gaussian beams on the axial intensity distribution also has been discussed numerical calculations for the axial intensity distribution, as well as the best focal position and the maximum intensity on the axial of the focused beam were performed and the results were analyzed. The numerical calculations showed that when the flat-topped multi-Gaussian laser beams with a fixed beam order N, he changing of SA would affect the best focal position greatly. For the lens with a fixed SA, the changing of N would also affect the best focal position. When a lens without SA, the best focal position was not at the geometrical focus. With the number of N increasing, the best focal position shifted towards the geometrical focus. It is shown also that when the Fresnel number of Gaussian beams was small, the best focal positions corresponding with the positive and negative spherical aberration were at the left of that of aberration-free. When the Fresnel number of Gaussian beams was large, the best focal positions corresponding with the positive and negative spherical aberration were at the both side of that of aberration-free. For the lens with positive spherical aberration, no focal shift even the positive focal shift could be achieved by changing the value of Fresnel number of Gaussian beams.

Propagation Characteristics of Confocal Elliptical Coaxial Lines Filled with Multilayered Media

Tianxin Xiong[1,2], **Rugui Yang**[1]

[1]Southwest Jiaotong University, China
[2]Sichuan Normal University, China

The elliptical waveguides has a wide area of applications, such as radar feed line, multiplex communicationelectron accelerator, microwave heater and dual-mode filter. In 1938, Chu first created the theory of the transmission theory of the electromagnetic waves in elliptical waveguide. From then on, more attentions was paid to the elliptical waveguide. In resent years, some researchers have investigated the confocal elliptical coaxial line filled with one kind of media. Although lots of investigations about the elliptical waveguide or the confocal elliptical coaxial line have been done, the propagation characteristics about the confocal elliptical coaxial line filled with multilayered media are not discussed yet.

In this paper, by using the method of separation of variables in the elliptical coordinate system, a recursive formula for the electromagnetic fields in a confocal elliptical coaxial line filled with multilayered homogeneous isotropic media is derived, and the eigenequationf fort odd and even modes, is presented. When the confocal elliptical coaxial line is filled with two layers of media, the propagating modes are hybrid modes($HEM_{mn}^{e,o}$). In order to demonstrate propagation characteristics due to the influence of the refractive index of media and the eccentricity, the variation of the normalized propagation constant of some modes vs the normalized frequency are shown in Fig.1-2. These results show that the propagation characteristic is less influenced by the eccentricity, and the propagation characteristic of the lower order modes is less influenced by the refractive index of the filled media also. Calculations show that the eigenequation of the circular coaxial line can be gotten from the eigenequation of the elliptical coaxial line using the asymptotic formulae of Mathieu and the modified Mathieu functions.

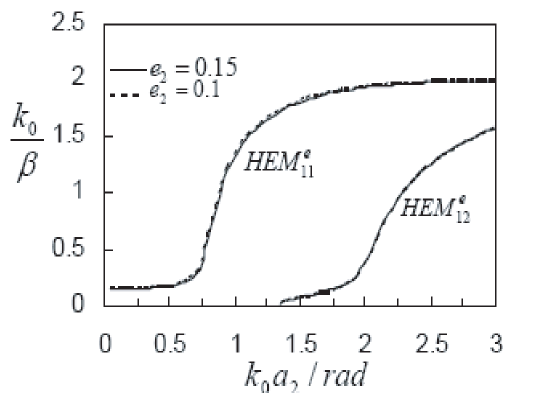

Figure 1: Nomalized propagation constant (β/k_0) versus normalized frequency (k_0a_2) on an elliptical coaxial line filled with two layers of dielectrics as the eccentricity of coaxial wall is different ($m = 1$, $\mu_1 = \mu_2$, $n_1 = 2.0$, $n_2 = 2.2$, $e_0 = 2e_1$, $e_1 = 2e_2$)

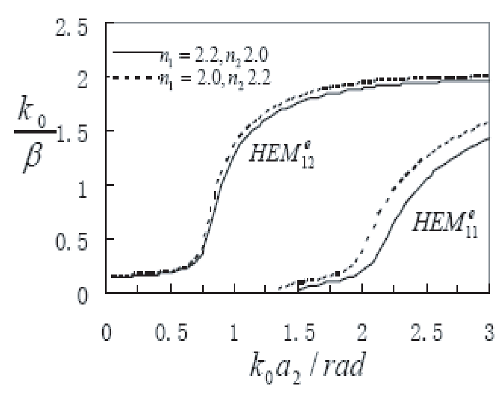

Figure 2: Nomalized propagation constant (β/k_0) versus normalized frequency (k_0a_2) on an elliptical coaxial line filled with two layers of dielectrics as the same eccentricity of coaxial wall ($m = 1$, $\mu_1 = \mu_2$, $e_0 = 2e_1$, $e_1 = 2e_2$, $e_2 = 0.1$)

Propagation Characteristics of Elliptical Waveguide Filled with Multilayered Confocal Chiral Mediums

Tianxin Xiong[1,2], **Rugui Yang**[1], **Kemin Sheng**[1]

[1]Southwest Jiaotong University, China
[2]Sichuan Normal University, China

Guiding properties of chirowaveguide have been investigated since 1990s due to its potential applications. Circular chirowaveguide from filling with one kind of chiral medium to filling with multilayered chiral mediums has been investigated, and its capability of mode conversion has been reported. Mode bifurcation in circular chirowaveguide has also been discussed. In addition, the propagation characteristics of the circular waveguide filled with multilayered chiral mediums has also been studied.

In this paper, we will investigate the propagation characteristics of elliptical waveguides filled with multilayered confocal chiral mediums. Suppose the permittivity, permeability and chiral parameter of the i-th layer of the reciprocal chiral medium are ε_i, μ_i and χ_i. The major semiaxis and minor semiaxis of the i-th layer are a_i and b_i, respectively, where i=1,2,...,N. The wall of the elliptical waveguide is perfectly electric conductor. The constitutive relations are showed as follows:

$$\vec{D}_i = \varepsilon_0\varepsilon_{ri}\vec{E}_i - j\chi_i\sqrt{\varepsilon_0\mu_0}\vec{H}_i \qquad \vec{B}_i = \mu_0\mu_{ri}\vec{H}_i - j\chi_i\sqrt{\varepsilon_0\mu_0}\vec{E}_i$$

It is assumed that time-harmonic electromagnetic waves propagate in the positive z direction. Employing the method of separation of variables in the elliptical coordinate system, the electric and magnetic fields for even modes in the z direction can be gotten. From Maxwell's equations, the relations between the transverse and the longitudinal electromagnetic fields can be gotten and the transverse electromagnetic fields $(E_{\xi i}, H_{\xi i}, E_{\eta i}, H_{\eta i})$ can also be found. Using the continual conditions of E_{zi}, H_{zi}, $E_{\eta i}$ and $H_{\eta i}$ on $\xi = \xi_i$, where ξ is radial coordinate and $\xi \in [0, \xi_N)$, η is angular coordinate and $\eta \in [0, 2\pi)$, we can find the recursive formula of electromagnetic fields between the i-th layer and the i+1-th layer and the mode eigenequation can also be gotten. Finally, some numerical examples are presented to analyze the propagation characteristics influenced by the permittivity, permeability, chiral parameters and the eccentricity of the elliptical waveguide.

Propagation Properties of Flat-topped Multi-gaussian Laser Beams Passing through ABCD Optical System

Li Wang, **Qingfeng Wang**, **Xiqing Wang**
Southwest Jiaotong University, China

The propagation formula of flat-topped multi-Gaussian laser beams (FMGB) passing through a first order ABCD optical system is derived by using the general Huygens-Fresnel diffraction integral. Based on the second-order and high-order moment, the closed-form expressions for beam width, M^2 factor and Kurtosis parameter K of flat-topped multi-Gaussian laser beams are also derived. Numerical calculations for beam waist width are performed and the results are analyzed. Compared the beam waist width that obtained in this paper with the approximate equation given by Tovar, where the beam waist width of FMGB is defined to be the distance from the most distant Gaussian beam at which the amplitude is reduced to $1/e$ its maximum value, there is a discrepancy between two equations. With the increase of beam order N the discrepancy becomes lager. Numerical calculations show that the M^2 factor of FMGB increases with increasing beam order N , but the K parameter for the beam waist plane of FMGB decreases with increasing N. When $N = 0$, M^2 factor has the minimum value 1 and K has the maximum value 3. When beam order N is lager than 10, the kurtosis of beam waist plane is approaching constant 1.80. The lens system is taken as an example, the analytical expressions of the waist width and waist positions of FMGB are given. It is showed that the waist position of FMGB is a function of Fressnel number of Gaussian beams N_w, system parameter s/f and the order of FMGB. The expression and numerical results show that the best focal point depends strongly on the system parameter s/f. When $s/f < 1$, the waist and the best focal point are at the left of geometric focal plane. When $s/f = 1$, the waist and the best focal point are coincide with geometric focal plane. When $s/f > 1$, the waist and the best focal point are at the right of geometric focal plane.

Session 2P4

Scattering and Radiative Transfer: Basic Research and Applications 1

Landmarks in the Development of the 3D Cloud Radiation Field since 1970

Warren Wiscombe
NASA Goddard Space Flight Center, USA

This talk will attempt to identify the high points in the development of the 3D cloud radiation field. My own career interleaved with much of this history, including the strong move away from just using computers and toward field programs, and also the effort to fit the new knowledge into climate models. Thus, this talk will bring the perspective of a participant in much of the history that will be described. The 3D cloud radiation field began in the 1970s, but attracted few adherents because of severe limitations on computer time and memory, and also because of ignorance of cloud structure (beyond the qualitative classifications of Luke Howard which had ruled for 170 years). The earliest landmarks were Monte Carlo calcuations for cubic clouds, whose main point was the drastic errors incurred by ignoring cloud 3D-ness. This line of development ramified until the early 1990s, leading finally to randomly placed cubes with sizes drawn from a probability distribution. A parallel line of development began with the landmark paper of Lovejoy in 1982, which showed that cloud geometric structure was fractal and not at all like Euclidean solids. Further research showed that cloud liquid water structure was also most naturally described by fractals – but multifractals, not the monofractals of Mandelbrot's famous book or Lovejoy's early work. By the mid-1990s, the multifractal picture was dominant. Meanwhile, the growth in computer power made possible Monte Carlo calculations that could only be dreamed about even in the 1980s, in turn making it possible to calculate many realizations of a cloud field and get statistically significant results for the first time. After several false starts and blind alleys, analytical-numerical radiative transfer methods finally reached a plateau of perfection in the form of SHDOM, the now widely-used model of Evans. The field is now sufficiently mature that its first book has just been published, edited by Marshak and Davis. The talk will end with some Hilbert-like challenges for future generations of cloud-radiation scientists.

Effects of Multiple Scattering on Lidar Signals and Influences of Particle Characteristics

David M Winker
NASA Langely Research center, Virginia

Lidar retrievals are most often based on a solution of the classic lidar equation, which is a single-scatter approximation that ignores higher order (multiple) scattering. Multiple scattering can alter the apparent extinction or transmittance of the medium, can produce depolarization of the return signal, and can produce stretching of the return pulse. For most lidar systems the magnitude of the multiply-scattered signal is so small these effects are insignificant and can usually be ignored without introducing significant errors. Effects of multiple scattering on the lidar return signals must be considered in certain cases, however, and lidar systems have also been designed which measure and based retrievals on multiple scattering.

Satellite lidars are one class of systems where multiple scattering effects must be taken into consideration. Because a satellite system is necessarily far from the atmosphere, the footprints are much larger than typical ground-based or airborne systems. Because of this, an algorithm intended to retrieve extinction from satellite lidar data must explicitly account for multiple scattering effects on the return signal. This issue was first encountered by the Lidar In-space Technology Experiment (LITE), which flew on the Space Shuttle in 1994, and has been an issue for all subsequent satellite lidars, including the CALIPSO lidar, scheduled for launch in 2005, will be used as an example.

For lidars, the nature of the effects of multiple scattering is fundamentally dependent on the scattering phase function of the scattering particles and on the sensing geometry of the lidar. The magnitude of the volume extinction coefficient and homogeneity of the scattering medium also play a role. When the scattering medium becomes highly turbid and the scattering approaches the diffusion regime, multiple scattering overwhelms the single-scattered component of the return signal and pulse stretching becomes significant. To fully understand the multiple scattering issue for space lidars, it is necessary to examine the multiply-scattered lidar return signal for a variety of particle types and a variety of scenarios.

This paper will discuss the lidar multiple scattering problem, primarily in the context of satellite lidars: the effects on lidar signals, impacts on retrievals, and the dependence on particle characteristics.

Towards Generalized Boundary Conditions in DISORT

I. Laszlo
National Oceanic and Atmospheric Administration, USA

W. J. Wiscombe, **S-C. Tsay**
National Aeronautics and Space Administration, USA

K. Stamnes
Stevens Institute of Technology, USA

We describe a considerably generalized treatment of boundary conditions in the Discrete Ordinate Radiative Transfer Code (DISORT). The non-Lambertian surface reflection option in previous versions has been replaced by a more general and realistic bidirectional reflectance distribution function (BRDF). This formulation of the lower boundary now allows for a BRDF that depends on the incident polar angle, reflected polar angle, and azimuth angle between the incident and reflected directions. This enables us to separate the Fourier components, needed in DISORT, by expanding the bidirectional reflectivity in a Fourier cosine series. To maintain high accuracy the coefficients of the Fourier expansion are calculated from the defining equation by Gaussian quadrature. Because the integrand of this equation contains the cosine function whose frequency increase as the number of streams used in the intensity calculations increases, the integrand becomes a highly oscillating function for large number of streams. This requires a high-order Gaussian quadrature in the integral, which combined with the need to evaluate the Fourier coefficients separately at a large number of incident and reflected directions, makes the process computationally expensive. Alternative ways of calculating the coefficients, that included discrete fast Fourier Transforms, have been explored, and the relationship between computational accuracy and speed has been established. In previous versions of DISORT, the top boundary condition is restricted to be a constant, with the idea that this may usefully approximate a thermally emitting upper boundary, or a highly scattering one such as a cloud. This restriction has now been relaxed using a treatment similar to that applied for the surface. This allows for an input of a radiation field at the top that is a function of the incident polar angle. This feature is useful, for example, in the long-wavelength part of the spectrum in a cloudy atmosphere, where the radiation incident at the top of the cloud can be computed outside of DISORT using a computationally less expensive model.

Evaluation of an Improved Parameterization of Radiative Properties of Clouds Using Cloud Model Simulations and Earth Observing System Satellite Observations

Kuan-Man Xu[1], **Yali Luo**[2], **Ping Yang**[3]

[1]NASA Langley Research Center, USA
[2]National Institute of Aerospace, USA
[3]Texas A & M University, USA

Radiative properties of clouds, particularly the radiative properties of ice clouds or cirrus clouds, are far from being well understood and being properly represented in numerical models of atmosphere. To make progress toward a better representation of radiative properties of clouds, we need to develop a reliable parameterization of radiative properties of both water and ice clouds for use in numerical models of atmosphere and to evaluate the improvement of new parameterizations using direct satellite observations of radiative fluxes and cloud properties. In this study, a numerical cloud model with different parameterizations of radiative properties is used to perform simulations of a large ensemble of tropical deep convective systems observed by Earth Observing System (EOS) satellite and quantitatively compare the differences resulted from different parameterizations of radiative properties of clouds.

The cloud model employs the Fu-Liou radiative transfer scheme . The Fu-Liou radiative transfer model has 6 and 12 bands selected for solar and thermal IR regions, respectively. The standard formulation of radiative properties of clouds is largely dependent on the generalized diameter for ice and the equivalent radius for liquid. A new parameterization will be provided by Dr. Ping Yang and implemented in the same cloud model. Dr. Yang computed the scattering and absorption properties of ice crystals using a combination of the finite-difference time-domain technique, the T-matrix method, and an improved geometric optics method [6] and parameterized the bulk single-scattering properties of clouds as functions of cloud physical properties such as effective size (D_e), liquid water content (LWC) or ice water content (IWC). For example, the extinction and absorption efficiencies and the asymmetry factor can be parameterized as the function of effective particle size at each wavelength as follows:

$$< Q_e >= \frac{2+\eta_1 D_e^{-1}}{1+\eta_2 D_e^{-1}+\eta_3^{-2}},\ < Q_a >= \frac{\xi_0+\xi_1 D_e^{-1}}{1+\xi_2 D_e^{-1}+\xi_3 D_e^{-2}},\ < g >= \frac{\zeta_0+\zeta_1 D_e^{-1}}{1+\zeta_2 D_e^{-1}+\zeta_3 D_e^{-2}}$$

where η_i, ξ_i, and ζ_i (i=0, 1, 2, or 3) are fitting coefficients that are functions of wavelength λ. This parameterization scheme has some advantages, compared with the conventional parameterization scheme based on polynomials. For example, when D_e is large, the parameterized extinction efficiency approaches to 2, the asymptotic value for large particles, whereas it approaches to zero for small particles. With the parameterization results, the basic optical properties required as the inputs for a radiative transfer scheme such as the optical thickness, extinction efficiency, and single-scattering albedo can be determined in a straightforward manner.

The EOS satellite observations include top-of-the-atmosphere (TOA) albedo, TOA reflected solar radiation, outgoing longwave radiation, cloud optical depth, ice/liquid water path and cloud height, temperature and pressure information. Statistical properties of these properties will be compared with those of simulations using different parameterizations of radiative properties of clouds. The improvement will be measured by the statistical significance level of the difference of histograms between two sets of simulations or between simulations and observations. A bootstrap method will be used to obtain the statistical significance level.

Small-scale Drop Size Variability: Empirical Models for Drop-size-dependent Clustering and Its Impact on Estimation of Cloud Optical Properties

Alexander Marshak[1], **Yuri Knyazikhin**[2], **Michael Larsen**[3], **Warren Wiscombe**[1]

[1]NASA/GSFC, Climate and Radiation Branch, USA
[2]Boston University, USA
[3]Michigan Technological University, USA

Most cloud radiation models assume that the mean number of drops of a given radius is proportional to volume. The analysis of aircraft measurements of individual drop sizes shows that, for sufficiently small volumes, this proportionality breaks down; the number of cloud drops of a given radius is instead proportional to the volume raised to a drop-size-dependent non-unit power. The coefficient of proportionality, a generalized drop concentration, is a function of the drop size. For abundant small drops the power is unity as assumed in the conventional approach. However, for rarer large drops, it falls increasingly below unity. This empirical fact leads to drop clustering, with the larger drops exhibiting a greater degree of clustering. The generalized drop concentration shows the mean number of drops per cluster, while the power characterizes the occurrence frequency of clusters.

We will show striking examples of the spatial distribution of large cloud drops using models that simulate the observed power laws. In contrast to currently used models that assume homogeneity and a Poisson distribution of cloud drops, these models illustrate strong drop clustering, the more so the larger the drops. The strong clustering of large drops arises naturally from the observed power-law statistics. The data analysis suggests that clustered drops likely have a stronger radiative impact compared to their unclustered counterpart; ignoring it results in underestimation of the contribution from large drops to cloud horizontal optical path. The clustering phenomenon also helps explain why remotely sensed cloud drop size is generally larger than measured in situ.

Effects of Aerosol Size Distribution and Vertical Profile on the Polarization Spectra in the Oxygen A-band

Qilong Min, **Minzheng Daun**
State University of New York at Albany, USA

A successive order of scattering vector radiative transfer model was used to simulate the high-resolution polarization spectra in the oxygen A-band. The effects of aerosol size distribution and vertical profile on the radiance and polarization at the top and bottom of the atmosphere were analyzed. The impacts of instrument specification on information content are also investigated. The deeper in the absorption line (stronger absorption) the higher altitude scattering events are occurred, and the less contribution comes from the surface reflection. Spectral polarization is very sensitive to the aerosol size distribution and refractive index. Polarized radiances are dominated (>95%) by the first and second orders of scattering. The polarization due to higher orders of scattering can be simply parameterized. These insights provide a methodology for developing a fast forward model of vector radiative transfer and for retrieval algorithms to derive information of aerosol size distribution and vertical profile from high-resolution oxygen A-band measurements.

Approximation of Single-Scattering Properties of Ice and Snow Particles for High Microwave Frequencies

Guosheng Liu
Florida State University, USA

As satellite high-frequency passive microwave data have recently become available, there is an increasing demand for an accurate and computationally efficient method to calculate the single-scattering properties of nonspherical ice particles, so that it may be used in radiative transfer models for physical retrievals of ice water path and snowfall rate. In this study, we present two such approximations for calculating the single-scattering properties of three types of large ice particles: bullet rosettes, sector snowflakes and dendrite snowflakes, for the frequency range of 85 to 220 GHz, based on results of discrete-dipole approximation (DDA) modeling. By analyzing the DDA modeling results, it is noted that, for nonspherical ice particles, the scattering and absorption cross sections and the asymmetry parameter have a magnitude between those of the two imaginary equal-mass spheres. One is a solid-sphere, and the other is an ice-air mixed soft-sphere whose diameter equals the particle's maximum dimension. Therefore, the first approximation involves substituting the single-scattering properties of a nonspherical ice particle with those of an equal-mass sphere, which can be calculated by Lorenz-Mie theory, with an effective dielectric constant derived by mixing ice and air using the Maxwell-Garnett formula. The diameter of such an equal-mass sphere, D, is bigger than the diameter of the solid-sphere, D_0, but smaller than the particle's maximum dimension, D_{max}. Defining a softness parameter, $SP = (D - D_0)/(D_{max} - D_0)$, it is found that the best-fit equal-mass sphere has a SP value of 0.2∼0.5 for calculating the volume scattering coefficient, depending on frequency and particle shape. At 150 GHz, the best-fit softness parameter is found to be ∼1/3 when averaging over all particle shapes. For calculating the asymmetry parameter, the DDA model results show that the best-fit softness parameter is close to 0 (i.e., the same as the solid-sphere) for frequencies higher than 150 GHz while it is about 0.3 for 85.5 GHz. The second approximation presented is a polynomial fit to the scattering and absorption cross sections and the asymmetry parameter using the particle size parameter as an independent variable. For the scattering cross section, three fitting curves are derived for, respectively, rosettes, sector snowflakes and dendrite snowflakes. For the absorption cross section, a single curve is used to fit all particle shapes. For the asymmetry parameter, two curves are derived, one for rosettes and one for snowflakes. The best-fit softness parameter for three particular frequencies (85.5, 150, and 220 GHz) and for three particle shapes in the first approximation, as well as the coefficients of the polynomial fit in the second approximation, are presented. After implementing these approximations in a radiative transfer model, radiative transfer simulations are carried out for a snowfall and an ice cloud case. The simulated brightness temperatures based on the two approximations agree with each other within 3 K, but are significantly different from those based on the solid- and the soft-sphere approximations.

Accounting for Unresolved Clouds in a 1D Solar Radiative Transfer Model

Jiangnan Li
University of Victoria, Canada

New methods for the treatment of solar radiative transfer through overlapping and inhomogeneous clouds are presented. First, a new approach to cloud overlap is shown. For the adjacent cloud blocks, the traditional maximum overlap can be relaxed to a mixture of maximum and random overlap treatments for layers that are adjacent but not fully correlated. Second, a new radiative transfer algorithm has been developed to deal with these various cloud overlap circumstances that is simple enough for implementation in a general circulation model (GCM). When compared to appropriate benchmark calculations, we find that this new method can produce accurate results in heating rates and fluxes with relative errors generally less than 8%. Third, a new and very simple approach to treating radiative transfer through a cloud with horizontal subgrid-scale inhomogeneities is developed. This approach uses an optical depth scaling technique to represent the subgrid-scale inhomogeneity. Finally, by combining all of the above elements, we provide a new algorithm for the combined treatment of cloud overlap and inhomogeneity and we show that it yields very reasonable accuracies for heating rates and fluxes. Through benchmark comparisons, we show that this new algorithm provides significant improvement over existing schemes in GCMs.

The Radiative Characteristics of Ice-over-water Cloud Systems

J. Huang[1], **B. Lin**[2], **P. Minnis**[2], **Y. Yi**[3], **T. F. Fan**[4], **R. Arduini**[4]

[1]Lanzhou University, China
[2]NASA Langley Research Center, USA
[3]Analytical Service & Material Inc., USA
[4]SAIC, One Enterprise Parkway, USA

A two-layer cloud model is used to simulate multi-layered cloud radiative characteristics at spectra of visible (VIS), near infrared (NIR), thermal infrared (IR) and microwave (MW) wavelengths. The upper and lower layers consist of ice particles and water droplets, respectively. The scattering and absorption processes for this simple two-layer cloud radiative transfer model are simulated at particular solar zenith, viewing zenith, and relative azimuth using 11 ice cloud models and 7 water cloud models. The lookup tables of top-of-atmosphere (TOA) radiances at these wavelengths for the multilayer cloud systems are developed. For a ice-over-water cloud system, microwave satellite measurements are used to estimate cloud liquid water path and cloud water temperature of the lower level water cloud. The cloud properties of the upper-layer ice cloud are then derived using these lookup tables. The preliminary results from multiple sensor TRMM Aqua, and ARM data suggest that the new method may significantly improve the accuracy of ice cloud properties of multilayer cloud systems and reduce the overestimation of optical depth.

A Monte Carlo Simulation Study of the Polarimetric Signature of Stochastic Media

Yongxiang Hu
NASA Langely Research Center, USA

A full Stokes vector Monte Carlo model has been developed to the radiative properties of three-dimensional stochastic cloud imbedded in a layer of aerosols. The semi-analytic Monte Carlo model is tailored at fast calculations of the Stokes vectors at selected viewing geometry. The theoretical model results of uniformed clear sky and water cloud targets are compared with the NASA Langley Hyper-spectral Polarimeter (HySPAR) cloud/aerosol measurements for instrument calibration purposes. The polarimetric and anisotropic information from the along-track multi-angle HySPAR measurements will help reveal the stochastic properties of the boundary layer cloud systems.

On the Scattering and Absorption Properties of Nonspherical Ice Crystals in the Earth's Atmosphere

Ping Yang[1], **K. N. Liou**[2], **Bryan A. Baum**[3], **Yongxiang Hu**[3]

[1]Texas A & M University, U.S.A.
[2]University of California, U.S.A.
[3]NASA Langley Research Center, U.S.A.

In this talk, we review the progress in the theoretical and numerical studies of the scattering and absorption properties of ubiquitous nonspherical ice crystals in the Earth's atmosphere. The majority of ice crystals in the atmosphere occur in cirrus clouds, which normally reside in the upper troposphere in midlatitudes. In the tropics, these clouds can extend to the lower stratosphere associated with deep cumulus convection. Ice particles are also frequently observed in the polar regions due to cold temperatures. The global cirrus cover has been estimated to be about 20 to 25%, but recent analysis using the satellite infrared channels at the 15 mm CO2 band has shown that their frequency occurrence is more than 70% in the tropics. It is also noted that many thin and subvisual cirrus have not been detected from the present radiometers and spectrometers on board satellites. Because of their high location in the atmosphere and the ice particles' size spectrum (from a few micron to thousand of micron) and shape (spanning from plate, solid and hollow columns, bullet rosette, aggregate, to more irregular shape and surface structure), the radiative properties of cirrus clouds differ significantly from low and middle clouds, which reflect a substantial portion of incoming sunlight, referred to as the solar albedo effect. However, cirrus clouds can also trap a large amount of the thermal infrared radiation emitted from the surface and lower atmospheres, referred to as the infrared greenhouse effect. The radiative properties of cirrus clouds, which contain a variety of ice crystal sizes and shapes, determine the competition between the solar albedo and infrared greenhouse effects, essential to the discussion of the Earth's climate and climate change. Moreover, to achieve precision and accuracy in the satellite remote sensing of cirrus and mixed-phase clouds the correct scattering properties of nonspherical ice particles must be utilized. Recognizing the importance of cirrus clouds in remote sensing and climate research, substantial efforts have been carried out in the last two decades to understand and determine the fundamental scattering and absorption propertied of ice crystals. We will review these efforts from the perspectives of theoretical and computational approaches. In particular, we will highlight the method of geometric optics and its improvements based on which ray tracing can be performed for large ice crystals with complex geometries and the finite-difference time domain numerical method that can be used for the solution of light scattering by small nonspherical and inhomogeneous ice crystals. Additionally, we will show the band-averaged bulk scattering property results including single scattering albedo, asymmetry factor, and phase function, which are obtained from a particle-size dependent mixture of various ice crystal habits.

A New Approach to Solve Correlated k-Distribution Function

Hua Zhang[1,2], **Guangyu Shi**[2]

[1] National Climate Center
[2] Institute of Atmospheric Physics (IAP), China

The resorting profile of absorption coefficient is fitted with Voigt function by employing the similarity between it and a single mixed broadened Voigt line type. In this way, simple mathematical fitting formulae are obtained to solve k-distribution function at any pressures and temperatures. Thus, a new correlated k-distribution method is proposed on the basis of it. Finally, taking mid-latitude summer atmosphere as an example, longwave cooling rates are calculated for three major gases by the new method, and then compared with the corresponding results by line-by-line integration.

Application of a Vector Radiative Transfer Model in Satellite Remote Sensing of Aerosol Optical Properties over Land

Xuehua Fan, Hongbin Chen
Institute of Atmospheric Physics, CAS, China

Zhigang Han
Beijing Institute of Applied Meteorology, China

Philippe Goloub
University of Sciences and Technology of Lille, France

The retrieval of aerosol optical properties over land from satellite measurements is difficult because the radiance from the surface and that from the aerosols are ambiguously mixed. The POLDERPolarization and Directionality of the Earth's Reflectancesinstrument, which flew on ADEOS (ADvanced Earth Observation Satellite), provides polarized reflectance measurements that can be used to distinguish atmospheric and ground contributions to reflectance. Thus, polarized reflectance measurements can be used for aerosol retrievals over land surfaces. In this paper a vector radiative transfer (VRT), named the RT3 model, is used for sensitivity study. This RT3 model developed by Evans (1996) has been modified and improved by Han (2000), which solves the plane parallel case of polarized monochromatic radiative transfer for isotropic media with doubling and adding technique. The geometry observation conditions are input in the modified RT3 model to simulate POLDER polarized measurements. It is assumed that the aerosol particles are spherical so that the Mie theory is applicable. The normalized reflectance and the normalized polarized reflectance of top of atmosphere are calculated at three POLDER polarized channels 443nm, 670nm and 865nm. Sensitivity of polarized reflectance is analyzed to surface albedo, the complex index of refraction, the aerosol size distribution and aerosol optical depth. The appropriate channels and aerosol models are evaluated from the sensitivity study for satellite retrieval of aerosol optical properties over land with POLDER instrument.

Session 2P5a

Inverse Scattering Methods for Imaging and Structure Synthesis

Minimum Phase and Inverse Scattering

Mike A. Fiddy
University of North Carolina, USA

We describe a method that allows one to calculate strongly scattering permittivity distributions from scattered field measurements or designed/desired scattered field patterns. The inverse scattering problem can be formulated in terms of a Fourier relation between scattered field data and a secondary source, the product of the scattering function and the total field $\Psi(\mathrm{r})$ in the domain of the scatterer $\mathrm{V}(\mathrm{r})$, i.e. we can estimate from measured or pre-specified scattered field data, only a function of $\mathrm{V}\Psi$. In the weakly scattering case, e.g. the first Born approximation, can one assume that the total field is well approximated by the incident field, allowing one to recover an estimate of the scattering distribution. While extended or iterative Born approximation methods have been developed, imaging of strongly scattering objects remains a difficult problem to solve in practice. Our previous work has adopted a different approach to attack this problem based on a nonlinear filtering method designed to numerically separate the scattering potential function from the unwanted total field $\Psi(\mathrm{r})$. This kind of filtering, cepstral or homomorphic filtering, involves taking the logarithm of the inverted scattered field data, followed by Fourier transformation and linear filtering. It rarely succeeds because $\log\mathrm{V}\Psi$ is not usually a well-behaved function and hence its Fourier transform is hard to interpret and filter. Preprocessing $\log\mathrm{V}\Psi$ to ensure it is a continuous function requires that $\mathrm{V}\Psi$ has no real zeros which is unlikely since V by definition is the fluctuation of, say, the permittivity about the background mean permittivity and Ψ represents an oscillating field. A condition which remedies this problem is when V is a minimum phase function; i.e. if the phase of $\mathrm{V}\Psi$ is continuous and lies between $\pm\pi$. Under these circumstances, the real and imaginary parts of $\log\mathrm{V}\Psi$ are related by a Hilbert transform and it follows that the Fourier transform of $\log\mathrm{V}\Psi$ must be causal from Titchmarsh's theorem. The Fourier transform of $\log\mathrm{V}\Psi$ is also known as the cepstrum of $\mathrm{V}\Psi$. We discuss a post-data measurement method which allow one to enforce the minimum phase condition on an estimated $\mathrm{V}\Psi$ by exploiting the conditions of Rouche's theorem. There is an equivalence between enforcing the minimum phase condition in this way and adding a reference wave to a scattered field in order to form a hologram. In either case, we have imposed a condition for which the amplitude of $\mathrm{V}\Psi$ encodes the phase. The significance of this relationship and the ability to then calculate an estimate of the strongly scattering function $\mathrm{V}(\mathrm{r})$ by nonlinear filtering is described. We illustrate the effectiveness of this approach using the IPSWICH microwave data set provided by AFRL and we also show the use of the method in structure synthesis applications, i.e. when a prescribed scattered field is to be generated from a strongly scattering structure one can fabricate.

Synthetic Spectra from Rough Surface Scattering

A. A. Maradudin, **T. A. Leskova**
University of California, USA

W. Zierau
Westfaelische Wilhelms-Universitaet Muenster, Germany

In recent years interest has arisen in the design of diffractive optical elements for spectral functions, in particular in the design of one-dimensional rough surfaces that synthesize the infrared spectra of real compounds [1,2,3]. Such surfaces can be used in correlation spectroscopy, in which the degree of correlation between the transmission of light through, or its reflection from, an unknown sample and that of a reference cell containing a known compound is determined over a fixed spectral range, as a means of identifying the unknown sample [4]. In the case that the known compound in the reference cell is toxic and/or corrosive, it is useful to have a diffractive optical element that synthesizes the infrared spectrum of that compound for use in a correlation spectrometer. In contrast to the deterministic approach to the design of one-dimensional rough surfaces that synthesize experimental infrared spectra adopted in [1,2,3], we propose an alternative, probabilistic approach to the solution of this problem. It is based on the assumption that the surface profile function of the surface defined by $x_3 = \zeta(x_1)$ has the form

$$\zeta(x_1) = bd_n, \quad n_b < x_1 < (n+1)b, \quad n = -N, -N+1, \ldots, N-1, \tag{1}$$

where $\{d_n\}$ are independent, identically distributed, random deviates, and b is a characteristic length. Therefore, the probability density function of d_n, $f(\gamma) = \langle\delta(\gamma - d_n)\rangle$, where the angle brackets denote an average over an ensemble of realizations of the $\{d_n\}$, is independent of n. The problem of determining $f(\gamma)$ reduces to the problem of reconstructing a function from a knowledge of the modulus of its Fourier transform, where the latter function is expressed in terms of the spectrum we wish to reproduce. The solution of this problem is obtained by the use of a modified Gerchberg-Saxton algorithm [5]. A sequence of $\{d_n\}$ is obtained from $f(\gamma)$ by means of the rejection method, and a realization of the surface profile determined by the use of Eq. (1). Our approach is validated by means of scattering calculations based on the Kirchhoff approximation.

REFERENCES

1. Sinclair, M. B., M. A. Butler, A. J. Ricco and S. D. Senturia, *Appl. Opt.*, Vol. 36, 3342, 1997.
2. Sinclair, M. B., M. A. Butler, S. H. Kravitz, W. J. Zubrzycki and A. Ricco, *Opt. Lett.*, Vol. 22, 1036, 1997.
3. Zhou, G., F. E. H. Tay and F. S. Chau, *Opt. Express*, Vol. 11, 1291, 2003.
4. Goody, R., *J. Opt. Soc. Am.*, Vol. 58, 900, 1968.
5. Gerchberg, R. W. and W. O. Saxton, *Optik*, Vol. 35, 237, 1972.

A Modified Perturbation Method for Three-Dimensional Time Harmonic Impedance Tomography

D. G. Drogoudis, **G. C. Trichopoulos**, **G. A. Kyriacou**
Democritus University of Thrace, Greece

J. N. Sahalos
Aristotle University of Thessaloniki, Greece

A reconstruction algorithm for three dimensional time harmonic impedance imaging based on the Modified Perturbation Method (MPM), [1], is proposed. Both the object conductivity (σ) and permittivity (ε) are reconstructed. The realization that both conductivity and the dielectric constant (ε_r) are strongly depended on the frequency of the injected current, has led to new research areas called Impedance Spectroscopy and Time Harmonic EIT, e.g. [2], [3]. Our previous work, [1], has modified the classical perturbation technique by substituting the sensitivity matrix with the most accurate Jacobian matrix, which was calculated from closed form expressions deduced from the electrical circuits compensation theorem. In our next step we have expanded our algorithm for time harmonic EIT using a quasi static approximation, ignoring magnetic field effects in Maxwell equations. This is widely accepted to be valid for frequencies up to about 100MHz. In this manner a Laplace equation for a complex voltage and a complex dielectric constant is obtained as:

$$\overline{\nabla} \cdot \varepsilon_r * \overline{\nabla} V = 0 \qquad where \qquad \varepsilon_r^* = \varepsilon_r \varepsilon_0 - j(\sigma/\omega) \tag{1}$$

We applied this method for two dimensional imaging (cross section of an object) and encouraging results was obtained. Now our aim is the application of this method for three dimensional imaging of the object conductivity (σ) and permittivity (ε). For the application of the algorithm, the whole object to be imaged was simulated and the measurements sequence was mimicked, solving the complex Laplace equation. The solution domain is now infinitely extended, since the air surrounding the object is characterized by $\sigma = 0$ and $\varepsilon_r = 1$. The Finite Element Method is used for the solution of (1) in conjunction with 1st order absorbing boundary conditions (ABCs).

A lot of successful reconstructions are carried out and the algorithm is found to converge fast as the original MPM. Some of these results will be presented at the conference along with a number of new subjects that need investigation.

REFERENCES

1. Kyriacou, G. A., C. S. Koukourlis, J. N. Sahalos, “A Reconstruction Algorithm of Electrical Impedance Tomography with Optimal Configuration of the Driven Electrodes”, *EEE Trans. on Medical Imaging*, Vol. 12, 430, 1993.
2. Otto, G. P. and W. C. Chew, “Time-Harmonic Impedance Tomography Using the T-Matrix Method”, *EEE Trans. on Medical Imaging*, Vol. MI-13, 508, 1994.
3. Polydorides, N., “Image Reconstruction Algorithms for Soft Field Tomography”, *PhD thesis, Univ. of Manchester*, 2002.

Session 2P5b

FDTD

On the Essential Reason of Numerical Reflection from the PML

Yong Zhang, **K. R. Shao**, **X. W. Hu**
Huazhong University of Science and Technology, China

J. D. Lavers
University of Toronto, Canada

The Perfectly Matched Layer (PML) introduced by Berenger is widely accepted as an efficient numerical absorber used in time-domain electromagnetic solvers. Many other modifications and extensions of the PML absorbing boundary condition have been published in the literature. Theoretically, all the PMLs can absorb outgoing waves without reflection from the vacuum-PML interfaces and PML-PML interfaces. However, in actual computation with discrete method such as Finite-Difference Time-Domain (FDTD), amount of numerical reflection always occurs. There has also been much effort analyzed numerical reflection in the PML in order to optimize wave absorption. But in fact, numerical reflection with closed-form expression is difficult to obtain, even this closed-form expression itself bases on the continuity propagation of waves. In FDTD, only spatial and temporal samples in disretized points are investigated, this is the reason that PML loses its perfectly matched characteristic in the discretized space-time domain.

This paper analyzes two problems to indicate the contradictions of the PML when it is used in FDTD as an absorbing boundary condition (ABC). Vector iterative mode method, which is established in this paper and two kinds of numerical reflection are investigated by it, indicates that it is the iterative mode of FDTD itself induces numerical reflection from the PML. PML, the widely accepted efficient ABC and developed from continuous space-time, has no truly matched characteristic in a discretized space-time of FDTD.

*This work was supported by National Natural Science Foundation of China (NSFC) under Grant No.50477045 and Specialized Research Funds for the Doctoral Program of High Education (SRFDP) under Grant 20030478063.

The Real-world Performance of Staircased and Conformal ADI-FDTD

H. Songoro[1], **S. Benkler**[2], **N. Chavannes**[2], **P. Futter**[1]

[1]Schmid & Partner Engineering AG, Switzerland
[2]Foundation for Research on Information Technologies in Society, Switzerland

Background

The alternating direction implicit finite difference time domain method for Maxwell's equations (ADI-FDTD) is an approximation of the Crank-Nichoslon time integration scheme (CN) applied to a staircased/conformal discretization on the Yee grid. The ADI-FDTD factorization retains the unconditional stability and the global 2^{nd} order of accuracy of CN while leading to a lower computational cost, making it attractive. However, the additional error term introduced by the approximation of CN can become a dominant term of the truncation error for large time-steps or at material interfaces. Existing studies about the accuracy of ADI-FDTD have been limited to the simplest applications, and that has led many to question the practical interest of ADI-FDTD for EM real-world simulations.

We have therefore assessed the performance of staircased/conformal ADI-FDTD for complex 3D models and for a wide range of applications.

Study

We have integrated into SEMCAD X, a 3D CAD FDTD simulation platform, an ADI-FDTD solver supporting modern modeling features such as conformal discretization, U-PML for conductive media, plane wave excitation, voltage sources, lumped elements. That has enabled us to simulate complex setups for which ADI-FDTD provides a performance advantage compared to staircased/conformal FDTD. This is the case for electrically overdiscretized models, for instance due to the presence of very fine geometrical features or because of the need to operate at frequencies relatively low for the overall spatial discretization.

We have considered industry driven applications, such as the simulation of commercially available mobile phones in the proximity of highly detailed and heterogenous phantoms or such as the calibration of E-field probes at low frequencies. One of the key issues when using ADI-FDTD is the choice of the time-step, which is not driven by a stability criteria but by the research of a compromise between an acceptable truncature error and a competitive calculation time compared to the staircased/conformal FDTD. We have therefore evaluated different approaches to determine an optimal ADI time-step.

Discussions

We provide an assessment of the accuracy of ADI-FDTD with respect to the time-step through comparison with reference results obtained from staircased/conformal FDTD or from measurement when the FDTD simulation could not be performed due to an exceedingly large number of iterations.

Finally, we discuss and define the domain of applicability of ADI-FDTD and its possible use within industrial R&D environments.

Transient Propagation in Media with a Negative Refractive Index Simulated by ADI-FDTD Method

Hong-Xing Zheng, **Dao-Yin Yu**
Tianjin University, China

To simulate the electromagnetic (EM) wave in media with a negative refractive index efficiently, an algorithm combining finite-difference time-domain (FDTD) method with an alternating-direction implicit (ADI) scheme is developed in this paper. At the time before, a general formulation for the EM wave interaction with stratified media was developed by Kong [1]. Then it was simulated by using FDTD method [2] that the EM wave undergoes negative refraction at the interface between a positive and negative refractive index material. However, this FDTD technique needs more computation resources because of restriction of Courant stability condition.

The ADI-FDTD updating equations are constructed on the basis of equations in [1]. Use the implicit algorithm to simultaneously compute the fields, the restriction of Courant stability condition is avoided. Numerical experiments are given to substantiate the proposed algorithm. The numerical stability and dispersion relation have been discussed. Results based on our formulation, which are verified for both copolarization and cross-polarization of the reflected and transmitted waves from a photonic crystal slab, are performed excellent agreement with those based on analytical formulas [1].

By properly choosing photonic crystal, which is essentially inherently lossless, the numerical calculations are performed on a well understood realistic system. The dielectric constant is modulated in space. Although the permittivity ε and permeability μ are locally positive, both the ε_{eff} and the μ_{eff} are negative with negligible imaginary parts in a certain frequency region for a global crystal. In this region, the refractive index n is confirmed to be unambiguously negative. Simulation pattern shows the detailed time-dependent sequence trapped at the interface, gradually reorganizes itself, and finally propagates along the negative angle direction. This phenomenon provides an explanation for the occurrence of negative refraction. It clarifies some of the controversial issues, especially the negative refraction considered as violating causality and the speed of light [3].

REFERENCES

1. Kong, J. A., "Electromagnetic Wave Interaction with Stratified Negative Isotropic Media", *Progress In Electromagnetics Research, PIER 35*, 1, 2002.
2. Foteinopoulou, S., E. N. Economou and C.M. Soukoulis, "Refraction in Media with a Negative Refractive Index", *Phys. Rev. Lett.*, Vol. 90, No. 10, 107402, 2003.
3. Valanju, P. M., R. M. Walser and A. P. Valanju et al., "Wave Refraction in Negative-Index Media: Always Positive and Very Inhomogeneous", *Phys. Rev. Lett.*, Vol. 88, No. 18, 187401, 2002.

Modeling and Simulation of Optical Planar Chirality by ADI-FDTD Algorithm

Hong-Xing Zheng
Tianjin University, China

It is reported that the chiral structures affect the polarization state of light [1] recently. This structure was made up of artificial metal-on-silicon chiral planar gratings of wallpaper group symmetry. In order to determining the optical behavior of this structure, the finite-difference time-domain (FDTD) method is used. The electromagnetic wave propagation in the chiral or bi-isotropic media has been modeled by the FDTD technique, one model with Drude-Born-Fedorov (DBF) constitutive relations was studied in [2] and the other with a set of α-β constitutive relations was developed in [3]. These techniques took more computation effort because of restriction of Courant stability condition.

A new FDTD method with the alternating-direction implicit (ADI) scheme is proposed for a characteristic optical planar chirality. The Maxwell's curl equations are discretized by central difference approximation. Based on the DBF relations, the ADI-FDTD updating equations are constructed. Use an implicit algorithm to simultaneously compute the fields, the restriction of Courant stability condition is avoided. The developed formulation is shown to provide good results for multiple frequencies for both dielectric and chiral objects. Numerical results for one and three dimensional electromagnetic scattering problems are performed excellent agreement with those based on experiment.

To reduce the numerical dispersion in the ADI-FDTD method, artificial anisotropic parameters are added into the ADI-FDTD formulas. Therefore, we can control the error of the numerical phase velocity, causing the numerical dispersion to decrease significantly. The numerical stability and dispersion relation are discussed. Numerical experiments are given to substantiate the proposed algorithm. Results based on this formulation are verified for both copolarization and cross-polarization of the reflected and transmitted waves from a chiral slab due to normal and oblique incident plane wave. Validation is performed by comparing the ADI-FDTD results with those based on the experimental results reported in [1].

REFERENCES

1. Papakostas, A., A. Potts, D. M. Bagnall, S. L. Prosvirnin, H. J. Coles and N. I. Zheludev, "Optical Manifestations of Planar Chirality", *Phys. Rev. Lett.*, Vol. 90, No.10, 107402, 2003.
2. Ji, F., E. K. N. Yung and X. Q. Sheng, "Three-Dimensional FDTD Analysis of Chiral Discontinuities in the Waveguide", *Int. J. Infrared Millimeter Waves*, Vol. 23, No. 10, 1521, 2002.
3. Zheng, H.-X., X.-Q. Sheng and E. K.-N. Yung, "Computation of Scattering From Conducting Bodies Coated with Chiral Materials Using Conformal FDTD", *J. Electromagn. Waves Appl.*, Vol. 18, No. 11, 1471, 2004.

High Frequency Crosstalk Analysis of PCB Layouts Using FDTD Method

C. N. Pai
National Cheng Kung University, Taiwan

J. H. Chou
National Cheng Kung University, Taiwan

With the advances in semiconductor manufacturing technology, especially in reducing feature sizes and increasing IC integration levels, the processing speeds of future CPUs enter the regime of GHz. To accommodate this development trend, the circuit density and operating speed of current and future printed circuit board (PCB) have to increase accordingly. Thus, electromagnetic compatibility of PCB becomes one of the dominant factors affecting PCB developments. In this study, emphasis is focused onto the crosstalk, trace to trace coupling between PCB lands for different layouts including micorstrips and coplanar strips. A finite difference time domain (FDTD) numerical method is adopted to explore the phenomena using the full Maxwell equations together with the perfectly matched layers as the boundary conditions. The keys results are as follows. For microstrips, the crosstalk electric fields decrease as the trace width and the trace spacing increase. For coplanar strips, the crosstalk electric fields also decrease as the trace width increases. However, they will increase when the trace spacing increases due to the increase of loop area. In addition, the crosstalks of both layouts are more serious as the source frequency increases. On the other hand, the crosstalk electric fields can be reduced either by proper grounding, symmetric layouts or different mode velocities in different traces. In other words, grounding plays an essential role in the reduction of crosstalk of PCB layouts.

The Iterative Multi-Region Technique Based on the FDFD Method for Electromagnetic Scattering from Multiple Three Dimensional Objects

Mohamed H. Al Sharka, **Veysel Demir**, **Atef Z. Elsherbeni**
University of Mississippi, USA

It is not easy to numerically analyze a large-scale electromagnetic problem that requires large computer memory and long computation time, thus several approaches have been suggested to deal with this problem. One of the approaches to overcome this problem is to divide the computational domain into smaller sub-domains and then to combine the sub-domain solutions after introducing the effect of interactions between these sub-domains. Among the available techniques that tackle one class of these large-scale problems is the domain decomposition method (DDM), which in general requires either common boundaries or overlapping regions between the sub-domains.

In this study, we present a new technique based on the finite difference frequency domain (FDFD) method and an iterative procedure between the sub-domains to calculate the scattering from multiple objects. The problem is decomposed into separated sub-domains, each sub-domain containing a scatterer or a group of scatterers. In each sub-domain, the scattered electromagnetic near fields are calculated due to the incidence of a time-harmonic wave, using the FDFD method. Then fictitious electric and magnetic currents on imaginary surfaces surrounding the objects in these sub-domains are calculated, using the equivalence principle. Radiated fields by these currents are then considered as incident fields on the opposing sub-domains. The same procedure of calculating the sub-domain field components, the fictitious currents and the radiated fields on the opposing domains is repeated iteratively until a convergence criterion is achieved.

The procedure presented here, referred to as Iterative Multi-Region (IMR) technique, requires solution of fields in the sub-domains a number of times instead of one solution of the complete domain. This technique effectively reduces the size of the required memory, especially for practical and three-dimensional problems. Furthermore, the CPU time reduction can be achieved if the separation between the sub-domains is large and/or coarser grids are used in some of the sub-domains, which may not be possible to use if only one domain is used for the solution of the problem. This IMR technique has been used successfully to calculate scattered fields from multiple two and three-dimensional scatterers.

Automated and Robust Conformal Mesher for Complex Conformal FDTD Applications

S. Benkler, **H. Songoro**, **N. Chavannes**, **N. Kuster**
Foundation for Research on Information Technologies in Society, Switzerland

Introduction and Objectives

The Finite-Difference Time-Domain (FDTD) method originally presented by Yee has become one of the most successfully used technique in electromagnetic (EM) computations. However, a well known shortcoming is that the staircasing meshing can lead to inaccuracies in the geometrical discrezation of complex models. This shortcoming can be overcome by using conformal meshing in which modifications in the original Yee scheme need only to be applied to cells in the immediate vicinity of the structure's material interfaces. However, key issues such as the robustness of the conformal mesher and stability of the modified Yee scheme need to be addressed in order to allow application of the schemes within, e.g., commercial EM simulation environments and general R&D purposes.

The objectives of this study thus were (1) the development and implementation of novel and robust 3-D CAD analysis algorithms for the fully automated generation of locally conformal FDTD meshes from arbitrarily complex geometries and (2) their application to different conformal Yee schemes and their comparison, as well as providing guidelines on their specific applicability.

Methods

All implementations and simulations were conducted using the simulation platform SEMCAD X which provides a 3-D ACIS based solid modeling environment and a full featured EM ADI/FDTD solver, both of which allow processing of complicated structures.

The surface triangle mesh of the CAD object is discretized with computer graphics methods (scan conversion algorithm). The result is a description of the environment to simulate in which each voxel knows its material and its possible cut-planes of the material transitions.

With the knowledge of these geometrical details the common FDTD update algorithm can be improved with respect to accuracy while maintaining the grid in its original spatial resolution. Incorporating the novel conformal mesher to subsequently assess the performance of various schemes, different averaging functions (arithmetic, harmonic, others) and weights (line, area, volume) are compared to each other for dielectric material transitions. For PEC surfaces contour path based subcell models were validated and compared to each other (stability, complexity, accuracy).

Results and Discussion

The developed and implemented techniques were applied and validated to different largely inhomogeneous, complex 3-D configurations, e.g., CAD models of cars and mobile phones, each consisting of several hundred distinguished sub-parts. The conformal mesher has proven to be suitable not only for simple benchmark structures but for the generation of arbitrarily shaped locally conformal 3-D FDTD grids including real-world geometries without any limitations to complexity.

Although a number of existing publications address the comparison of conformal FDTD methods used for simple benchmark cases, this study provides a thorough investigation of such schemes applied to real-world problems. Therefore, the suitability and limitations of various subcell models was addressed regarding dielectric and PEC transitions. Special attention was drawn to the stability issue and thus to the proposed reduction of the CFL bounded timestep.

All methods outlining good performance were finally implemented incorporating the novel mesher and applied to a level of modeling complexity demonstrating their eligibility for real-world applications.

An Upwind Leapfrog Scheme for Computational Electromagnetics: CL-FDTD

Yong Zhang, **K. R. Shao**, **X. W. Hu**
Huazhong University of Science and Technology, China

J. D. Lavers
University of Toronto, Canada

The upwind leapfrog method, originally developed from computational aeroacoustics and elastodynamics, has a more compact stencil compared with a classical leapfrog method such as Finite-Difference Time-Domain (FDTD) method. This approach preserves the time-reversibility of the leapfrog algorithm, which results in no dissipation, and it permits more flexibility by the ability to adopt a characteristic based method. Moreover, it leads to a more natural treatment of outer boundaries and material boundaries.

This paper introduces upwind-leapfrog scheme into computational electromagnetics, and develops a novel characteristic-line finite-difference time-domain (CL-FDTD) method by combining the PDE features of electromagnetics. In illustrating 1D and 2D problems, this paper set the implementation of discretation and iteration of CL-FDTD algorithm, and points out the merits of the proposed method. By compared with FDTD algorithm, CL-FDTD has less numerical dispersion, it has no requirement to deal with outer boundary conditions, and can precisely simulate accident signals that difficult to FDTD algorithm.

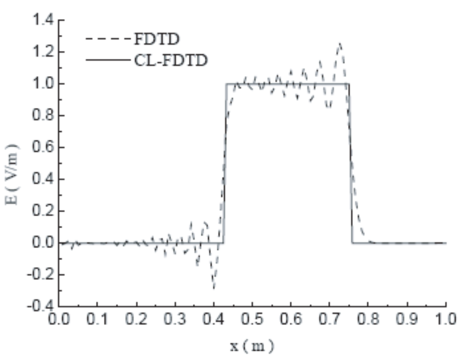

Figure 1: Comparison between CL-FDTD and FDTD on simulating accident signals

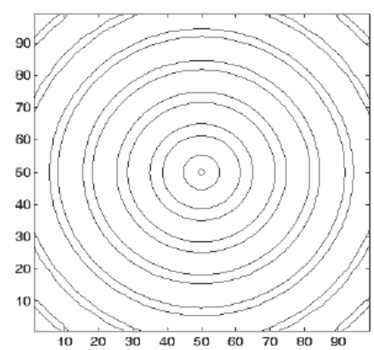

Figure 2: Contour lines of point source radiation simulated by CL-FDTD

*This work was supported by National Natural Science Foundation of China (NSFC) under Grant No.50477045 and Specialized Research Funds for the Doctoral Program of High Education (SRFDP) under Grant 20030478063.

Session 2P6

Electromagnetic Modeling and Inversion (Maxwell)

Simultaneous Inversion of Formation Resistivity and Geometric Boundary Location from Phase Induction Logging Data

Xiaobo Deng, **Zaiping Nie**, **Yanwen Zhao**, **Feng Yang**
University of Electronic Science and Technology of China, China

The phase induction log consists of one transmitter coil and two receiver coils, and measure phase difference of two receiver coils to obtain information of formation conductivity in an oil well. In this paper, inversion equation is obtained by applying the variation principal in a two-dimensional axisymmetrical inhomogeneous medium, which is solved by using the conjugate gradient (CG) method, the formation resistivity and boundary location per bed are simultaneously reconstructed from the phase induction logging data. An efficient numerical mode matching (NMM) method is used as a forward solver. The inversion result of synthetic data shows the validity of this inversion method.

Transmission and Reflection in a Periodic Superconductor/Dielectric Film Multilayer Structure

Chien-Jang Wu
National University of Kaohsiung, Taiwan

Microwave transmission and reflection in a periodic superconductor/dielectric film multilayer structure in the mixed state are theoretically calculated. It is based on the model of vortex dynamics of a type-II superconductor in the mixed state as well as the transfer matrix method in a stratified medium. We have made some numerical analyses in the microwave transmission and reflection as functions of temperature, dielectric thickness, and number of periodicity as well. The results indicate that the temperature-dependent reflection can be enhanced by increasing the number of periodicity. In addition, both microwave reflection and transmission will be reduced if the thickness of dielectric film is increased.

Efficient Analysis of Multilayered Planar Periodic Structures Using the MOL-FFT and GSM

D. X. Wang, **E. K. N. Yung**
City University of Hong Kong, Hong Kong

R. S. Chen
Nanjing University of Science and Technology, China

An efficient technique is proposed for the analysis of planar periodic structures illuminated by an arbitrary incidence wave. The technique is based on a combination of the Fast Fourier Transformation (FFT) and the method of lines (MOL). Through the use of an iteration procedure, the FFT is directly accommodated into the MOL for efficiently and rapidly obtaining the general scattering matrix (GSM) of a single-layer periodic structure. The technique has been used to analyze arbitrarily shaped structures in the spatial domain but compute the GSM in the spectral domain via an inverse FFT. For a multilayered periodic structure, the general scattering matrix is calculated by cascading the GSM of each interface with the substrate considered as a building block. Numerical experiments have been made for multilayered structures with arbitrary shape and the results are in good agreement with those published in previous contributions.

Space Electromagnetism: Modeling Magnetic Levitation of Superconducting Saturn Rings

Vladimir V. Tchernyi, **Andrew Yu. Pospelov**
Russian Academy of Sciences, Russia

Hypothesis of possible superconductivity of the iced matter of the rings of Saturn (based on the data of Voyager and Pioneer space missions) allow us to explain many phenomena which have not been adequately understood earlier. By introducing into planetary physics the force of magnetic levitation of the superconducting iced particle of the rings, which interact with magnetosphere of the planet, it becomes possible to explain origin, evolution, and dynamics of the rings; to show how the consequent precipitation of the rings matter upon the planet was concluded; how the rings began their rotation; how they were compressed by the magnetic field into the thin disc, and how this disc was fractured into hundreds of thousands of separated rings; why in the ring B do exist pokes? why magnetic field lines have distortion near by ring F; why there is a variable azimuth brightness of the ring A; why the rings reflected radio waves so efficiently; why there exists strong electromagnetic radiation of the rings in the 20.4 kHz-40.2 MHz range and Saturnian kilometric radiation; why there is anomalous reflection of circularly polarized microwaves; why there are spectral anomalies of the thermal radiation of the rings; why the matter of the various rings does not mix but preserves its small-scale color differences; why there is an atmosphere of unknown origin nearby the rings of Saturn; why there are waves of density and bending waves within Saturns rings; why planetary rings in the solar system appear only after the Belt of Asteroids (and may be the Belt of Asteroids itself is a ring for the Sun); why our planet Earth has no rings of its own.

New AGILD EMS Electromagnetic Field Modeling

Ganquan Xie[1], **Jing Li**[2], **Jianhua Li**[1]

[1] GL Geophysical Laboratory, U.S.A
[2] Yue Yang Ke Mei Da Mechanics Company, China

The Electromagnetic Stirring (EMS) technology has widely application in the metal continuous casting. Stirring is exciting a variable magnetic field in metal liquid. The magnetic field generate induction current. The induction current in the metal flow interacts with magnetic field to generate EM force, which makes perfect motion to improve casting. The EM force strength is proportional with square of the magnetic field strength. The key of the optimized control of EMS is to adjust several parameters for best EM force and deep magnetic penetration. In this paper, we present a new GL EMS modeling. The govern magnetic field equation in EMS is

$$\Delta^2 H = i\omega\mu\sigma H$$

A new magnetic field integral equation[1] is

$$H(r) = H_b(r) + i\omega\mu \int\limits_{\Omega} (\sigma - \sigma_b) G_b(r', r) H(r') dr'$$

where H is the magnetic field, the H0 is incident magnetic field with 1-10 Hz, (1-8 HZ in most industrial EMS). $G_b(r', r)$ is background Green function. According to new GL EM modeling and inversion [2], we developed 3D GL EMS modeling. Our GL EMS modeling needs not to solve large matrix and no complex boundary condition. Therefore, our new GL EMS Modeling is fast and accurate without any boundary error. The simulation shows that the AGILD EMS modeling is a very powerful tool for the design of excellent MES systems in Billent/Bloom and metal continuous casting systems. The simulation is performed by using GLGEO's software GL EMS modeling.

REFERENCES

1. Xie, Ganquan and J. Li, "New Parallel SGILD Modeling and Inversion", *Physics D*, Vol. 133, 477, 1999.
2. Xie, Ganquan, Jianhua Li, Feng Xiem, "New Global and Local Electromagnetic Field Modeling and Inversion", *PIERS 2005 in Hangzhou, China*, 2005.

Electromagnetic Stirring Using GL Electromagnetic Field

Jing Li[1], **Ganquan Xie**[2], **Zhiqiang Liao**[1]

[1]Yue Yang Ke Mei Da Mechanical Company, China
[2]GL Geophysical Laboratory, USA

The Electromagnetic Stirring (EMS) technology is very useful in the continuous casting. Use optimize control system to supply a optimization electromagnetic force and magnetic penetration is key technology in the continuous casting. Using new GL modeling and inversion{1}{2}, we develop a fast electromagnetic fielding in the continuous casting, in particular, in mod EMS for Billet/Bloom casters. Our system has widely applications in many metal continuous casting and can be used for obtaining the high qualify products.

REFERENCES

1. Xie, Ganquan, Jianhua Li, Feng Xiem, "New Global and Local Electromagnetic Field Modeling and Inversion", *PIERS 2005 in Hangzhou, China*, 2005.

Applications and Advantages of the KMD_EMS System

Zhiqiang Liao[1], **Jing Li**[1], **Ganquan Xie**[2]

[1]Yue Yang Ke Mei Da Mechanical Company, China
[2]GL Geophysical Laboratory, USA

The electromagnetic stirrer (EMS) has widely applications in the sciences and industrial engineering. In particular, the EMS is important tool in the metal continuous casting. The KMD_EMS is new electromagnetic stirrer sequence products of the Yue Yang Kemeida Mechanics Company. There are MEMS, SEMS, and FEMS in the KMD_EMS. We developed new real time control system and new electric power system in the KMD_EMS. The adapter from AC to DC is in market. Our senior engineering developed a new AC-DC-AC power source transform system which can stable transform the frequency of the current to the 1-10 low frequency current. Our AC-DC-AC power source system is very stable and self protected. We developed 1-8 HZ KMD_EMS systems and installed them in the many steel and metal continuous casting systems. Our KMD_EMS control system consists of the new control technology and EM modeling and PC. The real time controlling system is of stable and high anti-jamming ability, and high power rate. The system has many subsystems that can independent control each flow. Some new magnetic force and flow pressure and pore sensors are used. In the near future, we will use new GL EMS modeling to improve my real time control system and increase the efficiency of our KMD_EMS. The GL EMS modeling is new novel Global and Local electromagnetic stirring software mode and patented by GL GEOPHYSICAL Laboratory[1,2]. The GL EMS challenges to FEM, FD and Born like EM modeling. The GL EMS has many advantages over FEM, FD, and Born like modeling.

REFERENCES

1. Xie, Ganquan, Jianhua Li, Feng Xie, "New Global and Local Electromagnetic Field Modeling and Inversion", *PIERS 2005 in Hongzuo*, 2005.
2. Xie, Ganquan, Jianhua Li, Feng Xie, "New Global and Local Electromagnetic Field Modeling And Inversion", *PIERS 2005; GLGEO Report GLP04008, GLGEO Copyright, 2004*, 2005.

On the Solution of the Inverse Problems in Non Destructive Electromagnetics Measurements

S. Calcagno, **F. C. Morabito**, **M. Versaci**
University Mediterranea, Italy

Non destructive evaluation and quality measurement can be considered a strategic activity in industrial concerns, mostly in electronics, aeronautics and telecommunication applications. The relevant methodologies and techniques justify a deep interest in ensuring safety in industrial equipments, in the field of the production of energy and in biomedical environment, therefore involving several scientific disciplinary fields. In the light of the previous considerations, the basic assumption is that in the industry, whereas one must deal with high cost maintenance of research and/or technologic plants, the invasivity of inspection procedures must be reduced as much as possible. On the basis of these observations, decisions must be taken often turning critical enough to jeopardize the operation of the system itself, or even worse the safety of the sta17involved in particular actions. The development of aordable, reproducible and quick methodologies is then considered a matter of primary importance, in order to infer conclusions on the state of the system starting from the acquired signals without compromising the integrity and the operation as well. The international research is very active in the field of quality evaluation but a great dierentiation exists between the groups specifically expert in Non Destructive Testing, in terms of inspection methodologies and signal acquisition, and those active in the field of extracting meaningful information from measurements. Our scientific-disciplinary sector and research distinguished itself in developing systematic methodologies to solve these problems, in terms of electric and magnetic characterization of materials, modelling of the direct problem, numeric simulation, formulation and solution of the inverse problem. Up-to-date applications in structural design try to get performances as close as possible to the limit behavior from the materials traditionally used in buildings. This fact made of great relevance itself well known and settled issues, which is the control of in-service structures, in civil as well as in industrial fields. More, new innovative approaches in studying mechanics of materials led to the formulation of models close to the actual behavior but without turning out too heavy under the analytical and then, in the final analysis, computational point of view. The so-posed problem can be seen as an inverse one: starting from measurements, for instance along the border of the system, configuration of interest take place, which likely produce the pattern of measurement. Measurements can be acquired by means of dierent kind of sensors, whereas the processing takes the rule to mix data to increase the content of information with respect to the readings from each sensor. Neural network and fuzzy systems allow to solve the above-mentioned problems by the building of a settled model of the inverse problem at the same time improving the conditioning of the numeric problem. The use of wavelet transforms allows pre-processing of raw data also in order to speed up learning procedures. Learning techniques without supervisor have in addition been employed when patterns libraries werent available. We have obtained interesting results about soft computing techniques for the solution of the inverse electromagnetic problem. In addition, Fuzzy theory and Entropy was exploited to measure how far is a given defect from a well-known depth. A sort of classification based on the depth of a defect has been performed in this way.

REFERENCES

1. Calcagno, S., Morabito F. C., Versaci M., "A Novel Approach for Detecting and Classifying Defects in Metallic Plates," IEEE Trans. on Magnetics., vol. 39, pp.1531-1534, 2003.

Absence of Poles in Integrand of Green's Function for a Three-layer Medium

Evgeny G. Saltykov
Moscow State University, Russia

The Green's function $u(z, x)$ satisfies the Helmholtz equation with the ingomogeneous term of δ-function type

$$\frac{\partial^2 u}{\partial z^2} + \frac{\partial^2 u}{\partial x^2} + k^2(z)u = -2\delta(z - z')\delta(x - x')$$

and the radiation condition at infinity $u \to 0$ when $r = \sqrt{z^2 + x^2} \to \infty$.

The function u has the logarithmic singularity in the source point $M'(z', x')$. The equation is considered when $z, z', x, x' \in R$. We suppose that the coefficient $k^2(z)$ depends on one variable z and takes three values $k_l^2 = \varepsilon + j\sigma_l$, $\varepsilon_l \in R, \sigma_l > 0$, $l = 0, 1, 2$, j is the imaginary unit. $\sigma_0 < \sigma_1 < \sigma_2$. The function u satisfies the conjuction condition in the points of the coefficient continuity jump.

We obtain the problem solution expanding the function u as the function of the variable x in the Fourier integral.

The integrant of the Green's function represents the fraction with the denominator which is the Wronskian of linear independent depending on the variable z solutions of the ordinary equation . The Wronskian $w(\alpha)$ contains the factor $1 + q$ which could be equal to zero.

$$q = \rho^2\rho^0 e^{-2\eta^1 H},$$

$$\rho^2 = \frac{\eta^1 - \eta^2}{\eta^1 + \eta^2}, \quad \rho^0 = \frac{\eta^1 - \eta^0}{\eta^1 + \eta^0},$$

$$\eta^l = \sqrt{\alpha^2 - k_l^2}, \quad l = 0, 1, 2, \ Re\,\eta^l \geq 0,$$

H is the thickness of the middle layer, α is a spectral parameter of the Fourier expansion.

We prove that the integrant of Green's function has no poles in the comlex plane of the spectral parameter α of the Fourier transform.

For that purpose we consider the function $w(\alpha)$ in the upper half-plane of a complex plane of a spectral parameter $\alpha = \alpha_1 + j\alpha_2$. We divide the upper half-plane by the hyperbolae $\alpha_2 = \sigma_i/2\alpha_1, i = 0, 2$ into three parts.

Taking into account that $Im\,\eta^l < 0$, $l = 0, 1, 2$ in the domain on the left of the hyperbolae $\alpha_2 = \sigma_i/2\alpha_1, i = 0, 2$ and $Im\,\eta^l > 0$ on the right of them we prove that $1 >\mid q \mid$ outside the hyperbolae.

We prove also that the inequality $1 >\mid q \mid$ holds on the boundary of the internal domain. Taking into account the Rouché theorem we obtain that $w(\alpha) \neq 0$ in the internal domain and therefore in the whole complex plane α.

In [1] the case was considered when the conductivity of the middle layer σ_1 is equal to the arithmetic mean of the conductivities of the upper σ_0 and the lowerσ_2 layers.

REFERENCES

1. Dmitriev, V. I., Saltykov E. G., "Absence of Poles in Integrand of the Green's Function for Special Model of Three Layers Medium. International Conference", *"Differential Equations and Related Topics" dedicated to the Centenary Anniversary of Ivan G. Petrovskii. Moscow*, 111, 2001.

A New Method for the Inverse Electromagnetic Scattering Problems

C. J. Jiang, **Lianlin Li**, **Fang Li**
Institute of Electronics, Chinese Academy of Science, China

A novel method for the computation of the inverse electromagnetic scattering fields is presented which makes the scattering and inverse scattering problems related.

An integral

$$A = \int\limits_{v'} J \frac{e^{-jkR}}{4\pi R} dr'$$

by using the transform

$$\frac{e^{-jkR}}{R} = \frac{e^{-j\pi}}{\sqrt{\pi}} \int_0^\infty e^{j(k^2/X^2 + R^2X^2/4)} dX$$

can be written as:

$$A(r) = \frac{e^{-j\pi}}{\sqrt{\pi}} \int J(r') \int_0^\infty e^{j(k^2/x^2 + R^2x^2/4)} dx dr'$$

The singularity of the integral is avoided. This equation can be unfolded to

$$A(r) = \frac{2e^{-j\pi}}{\sqrt{\pi}} \int e^{jX^2r^2/4} e^{jk^2/X^2} X^2 \int j(r') e^{j(r'X^2/2)^2)} \frac{1}{X^2} e^{-j(X^2/2)r'r} d(r'X^2/2) dX$$

After some transforms

$$A(r, h(r)) = \frac{e^{-j\pi}}{\sqrt{\pi}} \int G(r, n) e^{jhn} dn$$

where G is related with the scattering sources. It shows that the scattering problem and the inverse scattering problem is of a Fourier transform relationship.

This new method can be easily employed to solve the inverse scattering problems just by doing some inverse Fourier transform. For scattering field this new method can be employed also for avoiding singularity of the integral equation. Due to the FFT and IFFT arithmetic is so mature and fast, this new method can be used to settle the equations by computer easily and efficiently. Some beautiful examples are given in this presentation.

Nondestructive Testing Using a New GL Electromagnetic Inversion

Tieqi Wang
Hunan Electric Power Test Research Institute, China

Ganquan Xie
GL Geophysical Laboratory, USA

In this paper, we present a nondestructive testing using a new 2.5D GL and stochastic GL electromagnetic (EM) modeling and inversion. An impulse or harmonic source excites the electromagnetic wave to propagate in the material with crack. We measure the scattering EM wave in the some places near the material or the boundary of materials. From the measured EM data, we recover the crack sample, location, and electric properties. The new nondestructive testing method can be useful for evaluating health of the metal and non metal material with several size and complex geometry and high contrast variable properties. Our GL EM and GL acoustic inversion can joint to use for coupled electromagnetic and acoustic non destructive testing.

REFERENCES

1. Xie, Ganquan, Jianhua Li and Feng Xie, "New Global and Local Electromagnetic Field Modeling And Inversion", *GLGEO Report GLP04008, GLGEO Copyright.*

New Two Dimensional MT Inversion

Chein-Chang Lin
National Formosa University, Taiwan

Ganquan Xie
GL Geophysical Laboratory, USA

How-Wei Chen
National Chung Cheng University, Taiwan

C. S. Chen
National Center University, Taiwan

In this article, we propose a new two dimension MT inversion. We derive TE and TM Garlerkin Frechet integral equation. The Garlerkin Frechet integral equation for TM inversion is as follows

$$\oint\limits_{\partial\Omega} \frac{1}{\Omega}\frac{\partial\delta H_y}{\partial n} H_y^* ds = -\int\limits_{\Omega} \frac{\delta\sigma}{\sigma^2}[\frac{\partial H_y}{\partial x}\frac{\partial H_y^*}{\partial x} + \frac{\partial H_y}{\partial z}\frac{\partial H_y^*}{\partial z}]d\Omega$$

By hoosing the test electromagnetic field in three continuative vertical line, we construct a three adjoin vertical layers scheme for TE and TM nonlinear inversion. Our TE and TM inversion schemes are sparse and fast. Many synthetic and field data inversions show that our TE and TM schemes are stable and high resolution..

Our MT inversion is useful for geophysical and earthquake exploration, geothermal, material sciences, and environmental sciences and engineering. First, we describe the TM inversion. Second, we describe the TE Inversion. Third, we describe the TEM joint inversion.

REFERENCES

1. Xie, Ganquan, Jianhua Li, Ernest Majer, Daxin Zuo, and Michael Oristaglio, “3-D Electromagnetic Modeling and Nonlinear Inversion: Geophysics”, *SCI*, Vol. 65, No.3, 804, 2000.

New GL And GILD Superconductor Electromagnetic Modeling

Ganquan Xie, **Feng Xie**, **Jianhua Li**
GL Geophysical Laboratory, U.S.A.

The electromagnetic (EM) field distribution in the superconductor is an important topic. In this paper, we present a new GILD and GL modeling for the magnetic field in the superconductors. We use the magnetic integral equation globally and second order London–Maxwell magnetic Garlerkin equation locally to construct GILD superconductor EM modeling. We derived a new magnetic integral equation to construct GL superconductor EM modeling The GILD and GL superconductor modeling can be widely used for the complex inhomogeneous vortex state superconductor media in the applications.

Comparisons between the Vector Finite Element Method and Staggered-grid Finite Difference Method for MT forward Modeling

Xueming Shi[1], **Jiaying Wang**[1], **Hisashi Utada**[2], **Wenli Wu**[3]

[1]China University of Geosciences, China
[2]University of Tokyo, Japan
[2]Institute of Geophysical & Geochemical Exploration, China

Many three-dimensional (3D) magnetotelluric (MT) surveys have been carried out in the complex geological structure mountain areas because of the improvements in electromagnetic (EM) instrument and the progress of 3D forward modeling techniques and inversion schemes. The three commonly used modeling mythologies are the integral equation, finite difference, and finite element. The staggered-grid finite difference method (SFD) combined with divergence corrections have been widely studied and developed for computing the responses for 3d geological structures. However, the finite element methods are still not widely used in 3D MT modeling.

We developed an algorithm for computing MT responses of 3D models using vector finite element (VFE) combined with divergence corrections recently. The system of equation for VFE is based on the second order differential Maxwell's equations for either electric field or magnetic field form. The divergence corrections are enforced by the scalar potentials based on the conservation equations for electric current or magnetic flux when the solution of the fields are non-divergence free.

In this paper, we firstly compare the formulae between the VFE and SFD algorithm in detail, then we compare the results of two commonly used 3D models (3D-1 and 3D-2) model of COMMEMI projects by Zhdanov. The speed and accuracy of these two algorithms are discussed. The results imply that the vector finite element combined with divergence corrections be another powerful tool to numerical modeling of 3-D inhomogeneous conductivity structures and can be applied for 3-D MT inverse problems of field data.

Session 2P7

On-Chip EMC/EMI Problems in RFIC/MMIC/RFMEMS

The Enhancement of Q-factor for Patterned Ground Shield (PGS) Inductors at High Temperatures

Jinglin Shi
Institute of Microelectronics, Singapore

Wen-Yan Yin
National University of Singapore, Singapore

In the past few years, various methods have been explored to improve the performance of on-chip spiral inductors for silicon-based RFIC's. Among these, the method of introducing a patterned ground shield (PGS) between metal coil and silicon substrate is quite worth mentioning. The ground shields can be designed in different patterns, and are easily realized in standard silicon technologies without additional cost. However, there are still some uncertainties in choosing a PGS to effectively enhance the performance of on-chip spiral inductors, transformers and other passive devices.

In this paper, comparative studies on the enhancement in Q-factor of patterned ground shield (PGS) inductors at high temperatures are performed. The PGS inductors are fabricated using both $0.18\mu m$ and $0.35\mu m$ CMOS processes, and the two-port S-parameters are measured at temperatures T = 298, 318, 338, 358, and 378K, respectively. With respect to the same geometry of on-chip spiral non-PGS inductors, the degradation of its Q-factor, due to the increase in temperature, can be effectively compensated by using PGSs. However, the separation between PGS and top metal coil should be chosen appropriately so as to achieve desired shielding effectiveness at high temperatures.

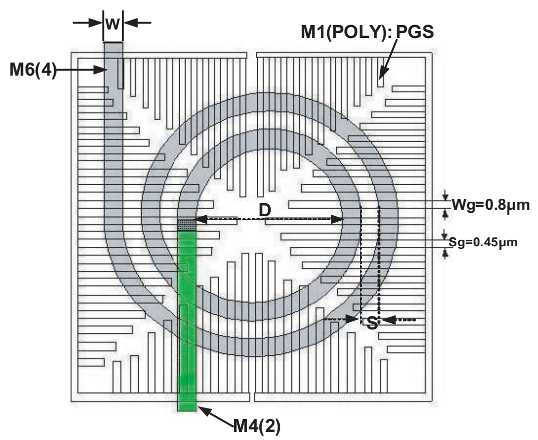

Figure 1: Top view of an on-chip spiral PGS inductor with $N = 2$.

Transfer Functions of On-chip Global Interconnects Based on Distributed RLCG Models

Kai Kang, **Wen-Yan Yin**, **Le-Wei Li**
National University of Singapore, Singapore

For high speed digital ICs, local interconnects, the majority of on-chip interconnects, can be safely treated as a lumped element, because its length is negligible compared to wavelength. However, for global interconnects, whose lengths are always up to a chip-edge in length, their overall electromagnetic characteristics need to be treated appropriately. In this paper, a compact transfer function for a RLCG interconnect with an arbitrary source impedance and an unmatched terminal load, as given by Eq. (1), is rigorously derived with on-chip global interconnect boundary conditions. A single distributed RLCG interconnect with an arbitrary source impedance is either terminated by an open-end circuit or loaded by a capacitive termination, can be used to accurately model different types of on-chip and off-chip high-speed global wires. The simplified expressions of the transfer function for single on-chip interconnect derived here can provide physical insight into and accurate estimation of transient response, time delay, and overshoot for high-speed global interconnects with the inclusion of conductance. Some compact expressions that describe the transient response of high-speed distributed RLCG coupled interconnects are also derived here, and their simplified forms enable us to accurately estimate peak crosstalk voltage between two and three distributed RLCG interconnects.

$$\begin{aligned} V_{fin}(x=L,s) = 2V_{inf}(L,t) + \frac{bZ_0 e^{-\sigma t}}{Z_0+R_{tr}} \sum_{n=1}^{q}\sum_{i=0}^{n}\sum_{j=0}^{\infty} \frac{n(n-1+j)!}{i!j!(n-i)!}(-1)^i \Gamma^{n-i+j} \\ \times \left\{ \left[\frac{t-(2n+1)L\sqrt{lc}}{t+(2n+1)L\sqrt{lc}}\right]^{\frac{i+j-1}{2}} I_{i+j-1}\left[b\sqrt{t^2-((2n+1)L\sqrt{lc})^2}\right] + \right. \\ (1+\Gamma)\left[\frac{t-(2n+1)L\sqrt{lc}}{t+(2n+1)L\sqrt{lc}}\right]^{\frac{i+j}{2}} I_{i+j}\left[b\sqrt{t^2-((2n+1)L\sqrt{lc})^2}\right] + \\ \frac{1}{\Gamma}\left[\frac{t-(2n+1)L\sqrt{lc}}{t+(2n+1)L\sqrt{lc}}\right]^{\frac{i+j+1}{2}} I_{i+j+1}\left[b\sqrt{t^2-((2n+1)L\sqrt{lc})^2}\right] + \\ (1+\Gamma)^2(\Gamma-1)\sum_{k=1}^{\infty}\Gamma^{k-2}\left[\frac{t-(2n+1)L\sqrt{lc}}{t+(2n+1)L\sqrt{lc}}\right]^{\frac{k+i+j}{2}} \\ \left. \cdot I_{k+i+j}\left[b\sqrt{t^2-((2n+1)L\sqrt{lc})^2}\right]\right\} \times U_0(t-(2n+1)L\sqrt{lc}) \qquad (1) \end{aligned}$$

where $U_0(t)$ is a unit step function, $I_v(-)$ is a v th-order modified Bessel function, r, l, c and g are distributed resistance, inductance, capacitance and conductance respectively.

Electromagnetic-thermal Investigation of On-chip Multi-layer and Multiple Coupled (A)Symmetrical Interconnects

Wen-Yan Yin, **X. T. Dong**, **Yeow Beng Gan**
National University of Singapore, Singapore

Based on a large number of theoretical work, some analytical equations have been proposed in the past decades for fast calculation of per-unit-length series impedance and shunt admittance, slow-wave factor, attenuation constant and characteristic impedance of single silicon-based interconnect. Concurrently, much work has also been done on the modeling of coupled interconnects. For example, using complex image method, Weisshaar et al [1] proposed some analytical equations for the self-impedance, self-admittance, and mutual impedance of coupled interconnects. To accurately describe wideband electromagnetic -thermal characteristics of coupled interconnects, the effect of each geometric or physical parameter, such as metal line thickness, electrical conductivity and operating temperature, must be treated appropriately. The rise in temperature due to Joule heating or self-heating of all on-chip metal lines can degrade interconnect characteristics, such as signal waveform distortion, electromigration, power handling capability and thermal breakdown of the interconnect. In a high-power RF circuit, thermal effects on the interconnect performance are serious design constraints. In this paper, a parametric study on the global modeling of on-chip multi-layer and multiple coupled (a)symmetrical interconnects has been performed. In particular, their wideband frequency-dependent distributed parameters, pulse waveform distortion, crosstalk (Fig.1) and average power handling capability (APHC) are studied.

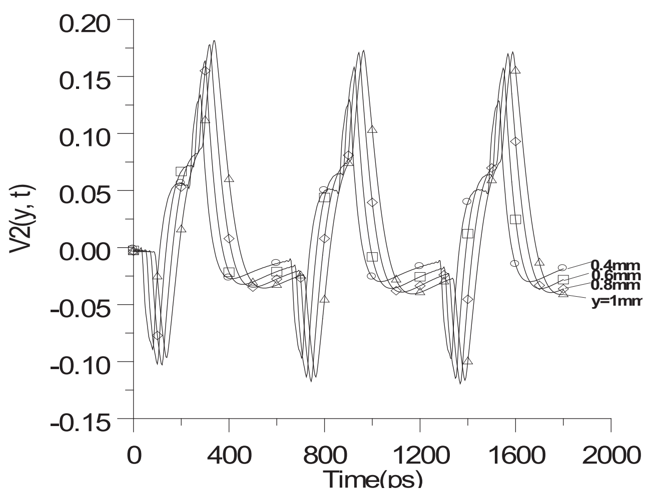

Figure 1: Crosstalk of a periodic square pulse propagating in a set of coupled interconnects.

REFERENCES

1. Weisshaar, A., H. Lan and A. Luoh, "Accurate Closed-Form Expressions for the Frequency-Dependent Line Parameters of On-Chip Interconnects on Lossy Silicon Substrate", *IEEE Trans. Advanced Packaging*, Vol. APK-25, 288, 2002.

Distributed Parameter Extraction of High-Density 3D Interconnects in High-speed Circuits Using Finite Element Method

Jianfen Xu
Shanghai Jiaotong University, China

Jun-Fa Mao
Shanghai Jiaotong University, China

As the interconnect effects are increasingly becoming important in high-speed circuits due to rapid increase in device density and operating frequency, parasitic parameter extraction of resistance, capacitance, inductance and conductance turns to be a key factor and needs to be investigated thoroughly. Thus, various numerical methodologies have been proposed with some accelerating progress in the past decades. In all these algorithms, there exists a trade-off between computational time and accuracy of the result.

To accurately extract distributed capacitance and inductance of three-dimensional interconnects including multiple conductors and multilayered dielectrics (Fig.1), finite element method (FEM) has been implemented in this paper. Compared to boundary element method (BEM) which is based on integral equations, FEM is more powerful to treat complex structures in geometric configuration or in physical properties of the media. Our developed program can be used to capture the relation between parasitic parameters and geometric parameters of the interconnects. Also, the matrix in computation is a large sparse one, which can be easily convergent with shorter computational time. By adopting automatic adaptive meshing method and a well defined post process arithmetic, some extracted distributed parameters are obtained with higher accuracy.

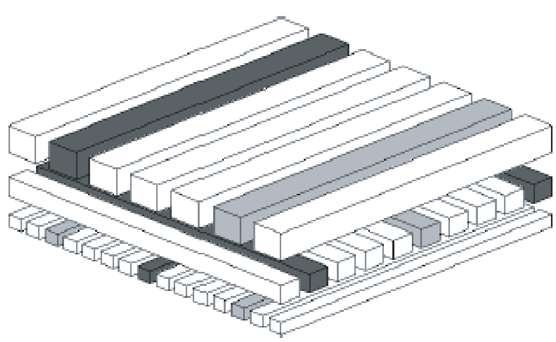

Figure 1: Three-dimensional interconnect structure.

Study on the Scattering Properties of the Chamfered 90° Bent Microstrip Line

Ke Wei Wang[1,2], **Jun Hong Wang**[1,2]

[1]Beijing Jiaotong University, China
[2]Ministry of Education, China

As we know, the discontinuities of the microstrip transmission line have important effect on the whole property of the circuit, especially in the high frequency band. A lot of works regarding this subject have been done, many of them were carried out by the numerical method, or the integrated commercial software. In theory, the microstrip lines connected to the discontinuity must be extended to infinite, then we can get the S-parameters at reference ports near the discontinuity. However, in the simulation method, the semi-infinite transmission lines are simulated by transmission lines with finite length terminated with matching loads. This approximation is accurate enough for many cases, but for small scattering problem, such as the chamfered micorstrip bend, the minor mismatching of the load may introduce significant errors to the calculation results of the S-parameters of the bend. In our study, the structures with and without discontinuity were simulated simultaneously, then the reflection and transmission parameters due to the discontinuity were extracted by taking the effect of the mismatching of terminal load away from the total effect, therefore the reflection and transmission properties of the discontinuity can be studied individually. The above method was used to analyze the reflection and transmission characteristics of the chamfered 90°-bent microstrip line. It is found that the chamfered size of the bend can be optimized to get overall optimum reflection coefficient. The results show that if dielectric constant is fixed, the optimum chamfered size increases with the characteristic impedance of the transmission line. Usually, for different structure parameters, the optimum chamfered size is different, though the characteristic impedance of the transmission lines may be the same.

A Semi-discrete Method for Transient Analysis of High-speed Interconnects with Frequency-dependent Parameters

Min Tang, **Jun-Fa Mao**, **Xiao-Chun Li**
Shanghai Jiao Tong University, China

With the continuing trend in the very large scale integration (VLSI) industry toward higher operating speeds, faster rise times, and smaller devices, frequency-independent models fail to model the interconnects accurately and the frequency dependence of R-, L-, C- and G- parameters has to be taken into account. In parallel to these developments, research efforts continue toward accurate and robust transmission line models for interconnects with frequency-dependent parameters. However, it is often the case that specific assumptions are made about the frequency -dependent property which is inaccurate for Gigascale integration(GSI).

In the recent past, a systematic methodology was proposed for the development of interconnects with frequency-dependent losses. The model makes no assumption about the frequency-dependent parameters and is compatible with a wide class of SPICE-based transient circuit simulators. Nevertheless, the finite difference time domain(FDTD) algorithm is restricted by Courant limit to insure its stability. Thus, both spatial and temporal segments must be small enough to achieve satisfying accuracy, which leads to time-consuming calculation.

In this paper, an effective method for the transient analysis of high-speed interconnects with frequency-dependent parameters is presented. This method starts from frequency-domain telegrapher's equations. A robust vector-fitting algorism is used to generate rational function approximations to the elements of the impedance and admittance matrixes of interconnects. Then, the time-domain equations including convolutions are obtained by inverse Laplace transform. By the discretization of the spatial variation of the voltages and currents along the transmission lines while remaining the temporal derivatives unchanged, the telegrapher's equations are approximately transformed into a set of first-order ordinary differential equations. To provide second-order accuracy of discretization, the voltage points and current points are interlaced. These equations can be solved with the precise integration method. Traditional numerical convolution is replaced by recursion algorithm in the computation of inhomogeneous items in the ordinary differential equations, so that the computational efficiency rises greatly. This method can solve the time response of interconnects with arbitrary terminal networks. It need not decouple the telegraphers equations for multiconductor transmission lines, and is also suitable to nonuniform coupled transmission lines. To demonstrate the accuracy and stability of the proposed method, several numerical examples are presented and the response waveforms are in good agreement with SPICE simulation results.

Optimization of Spiral Inductors on Silicon Based on Annealing Accuracy Penalty Function with Genetic Algorithms(GA)

Haili Lin
Shanghai Jiaotong University, China

Jun-Fa Mao
Shanghai Jiaotong University, China

Using the physical model of CMOS RF planar spiral inductors and GA optimization method, it is not necessary to select the optimal parameters with the contour plots of the Q-factor, since the conventional equivalent Q-factor method changes with the art and process. However, to apply GA for the optimization of a spiral inductor, all geometrical and physical parameters must be included and treated appropriately.

In this paper, we set the optimization object function to be:

$$Q = \frac{\omega L_s}{R_s} \cdot \frac{R_p}{R_p + [(\omega L_s/R_s)^2 + 1] \cdot R_s} \cdot \left[1 - (C_s + C_p) \cdot (\frac{R_s^2}{L_s} + \omega^2 L_s)\right] \tag{1}$$

Thus, Eq. (1) is simplified to be:

$$Q = f(x_1, x_2, \cdots x_m, x_{m+1} \cdots, x_n) \tag{2}$$

where $x_1, x_2, \cdots, x_m$: the landscape orientation parameters of inductor landscape orientation (geometrical parameters of inductors); and $x_{m+1}, x_{m+2} \cdots, x_n$: the longitudinal parameters (art and process).

Under the restriction $L(x_1, x_2, \cdots x_m) = constant$, according to different optimization parameters, we can add others restrictions integrated with the optimization object function given by Eq.(1).

Then, we can obtain the detail optimization object function as below:

$$\begin{cases} Max \qquad Q = f(x_1, x_2, \cdots x_m, x_{m+1} \cdots, x_n) \\ St \qquad L(x_1, x_2, \cdots x_m) = constant \\ \qquad g_i(x) \geq 0 \\ \qquad h_j(x) \leq 0 \end{cases} \tag{3}$$

Now, we refer the method of annealing accuracy penalty function with Genetic Algorithms to construct the GA optimization object function:

$$F(\sigma_k, x) = Q(x) + Sign \cdot P(\sigma_k, x) \tag{4}$$

and

$$P(\sigma_k, x) == \sigma_k \cdot [|L(x) - constant| + \sum |g_i(x)| + \sum |h_j(x)|] \tag{5}$$

It will be shown that this method is very flexible with high calculation efficiency.

Frequency Selective Broadband Stabilization of pHEMT Transistor

Lingyun Li, **Jun-Fa Mao**
Shanghai Jiao Tong University, China

It is known that amplifier's stability is one of the key specifications in the design of a circuit. The transistors used can be potentially unstable over some impedances and frequencies. Designer can take the risk of instability to implement a potentially unstable transistor by selecting proper source and load impedance carefully. While for better reliability, unconditional stable transistor is required, thus the amplifier is stable whatever port impedance is loaded. However, if the transistor is stabilized only in the interested band, it's hard to avoid band oscillation. So-called full-band unconditional stable transistors are the best candidates in the design of an amplifier. To the best of our knowledge, some stabilization techniques have been proposed by some researchers, but they are only effective over narrow frequency band. If they are implemented in broadband, the transistor will be deteriorated, which cannot provide acceptable gain.

In this paper, a new feedback stabilization method was introduced, which omitted the dc-block capacitor in the feedback path. Hence, the transistor can be unconditional stable over a wide frequency range. Since current leakage between the drain and gain may be significant especially in power amplifier. An optimized lossy network will be also introduced, which stabilizes the amplifier by frequency selectively providing lossy resistive loading to the transistor. Under such conditions, the transistor can be unconditional stable over all frequency range and provides its power gain as much as desired.

A Fully Integrated CMOS High-Speed Amplifier

Fuhua Li
Suzhou University, China

Zhengfan Li, **Jun-Fa Mao**
Shanghai JiaoTong University, China

Jixiang Zhao
China Jiliang University, China

The high-speed optical communication systems have become increasingly important because of the urgent demands for multimedia communication. In these systems, there is a strong demand for low-cost, wide-band, high-speed limiting amplifier. Traditionally, the wide-band and high-speed amplifier had been implemented in GaAs process. To lower the cost, several types of fully integrated CMOS ultra broadband amplifier have been investigated in recent years, which can be used as limiting amplifier.

In this paper, a novel limiting amplifier topology with a low-pass network is proposed for ultra broadband amplification in CMOS technology and a transmission line model is employed in our novel low-pass network. The low-pass network, gain and bandwidth of the amplifier are discussed. To demonstrate the practical viability of the limiting amplifier with low-pass network, a single-end input and single-end output two-stage amplifier has been fabricated in standard 1.8-V 0.18-μm digital CMOS process in Semiconductor Manufacturing International Corporation (SMIC). Such a test amplifier has achieved a bandwidth of 6 GHz, a gain of 15 dB and it consumes 70 mW from 1.8-V supply.

High-speed Clock Tree Simulation Method Based on Moment Matching

Xiao-Chun Li, **Jun-Fa Mao**, **Min Tang**
Shanghai Jiao Tong University, China

One of the most challenging tasks involved in high-speed VLSI design is to fast simulate clock trees accurately and effectively. In deep submicronmeter era, transmission line effect must be treated appropriately for the analysis of high-speed clock trees. To the best of our knowledge, most of the existing techniques for clock tree simulations are based on lumped RC trees, distributed RLC trees or lumped RLC trees. For example, Elmore delay is the most popular delay model for lumped RC trees. In order to improve the delay of clock trees, buffer insertion technique as well as interconnect width-sizing technique has been widely used in clock tree design. Hence, simulation methodologies for clock trees with buffer insertion need to be further explored.

Clock trees in VLSI are usually designed as symmetric H-tree for zero skew. In this paper, an effective and accurate method is proposed for simulation of symmetric clock trees with buffer insertion and without buffer insertion. In this method, transmission line effect, based on moment matching technique, has been treated appropriately. Our simulation process has three steps:

(1) The clock tree structure is simplified as a chain structure for its symmetric characteristics by using Y matrixes of transmission lines and buffers. For clock trees without buffer insertion, the clock tree structure is modeled as a chain of interconnects with different width and length. For clock trees with buffer insertion, the clock tree structure is simply modeled as a chain of interconnects with different width and length, and buffers with different size.

(2) The transfer function of clock trees is iteratively calculated from the leaf nodes to the root node based on the ABCD matrixes of transmission lines and buffers.

(3) Time domain responses and 50% delay are derived based on moment matching technique.

On the other hand, our methodology can be also used in fast simulation and high-level synthesis of zero-skew clock trees.

Session 3A1

Rough Surface Scattering

Discrimination of Metallic and Colored Surface States by Optical Pattern Projection Method

T. Inari, N. Aoki
Kinki University, Japan

In the optical pattern projection method called by the authors for surface roughness measurement, the roughness is detected from the qualities of the output image, such as contrast, formed by an imaging system including a target surface. We will report the relation between the roughness and contrasts for metallic surfaces and the colored plastics in the range of Ra of about 0.1 m and below, using a video camera. For the colored plastic surfaces, the authors explain that the sensitivity for gloss depends on the contrast of the formed image under additional illumination by other light sources.

Young's Interference Pattern Formed with Symmetrical Partially Coherent Sources

Zu-Han Gu
Surface Optics Corporation, USA

It has been shown not long ago by Emil Wolf [1], the Young's interference pattern is formed by partially coherent light. The coherent properties of interfering beams from two pinholes after they passed through a moving diffuser are determined by the correlation function of the heights of the diffuser surface and speed with which the diffuse is moving.

We report the recent experimental results displaying the Young's interference of light produced by a pair of symmetric partially coherent sources. The experimental results are compared with the results of rigorous computer simulations.

REFERENCES

1. Wolf, Emil, "Coherence of Two Interfering Beams Modulated by a Uniformly Moving Diffuser", *Journal of Modern Optics*, Vol. 47, No. 9, 1569, 2000.

The Interference of Two Collett-Wolf Beams

Zu-Han Gu
Surface Optics Corporation, USA

E. R. Méndez
CICESE, Mexico

M. Ciftan
Army Research Office, USA

T. A. Leskova, **A. A. Maradudin**
University of California, Irvine, USA

We consider a monochromatic beam in free space that is a superposition of two beams produced by Collett-Wolf sources characterized by identical cross-spectral density functions of the form $W^{(0)}(\mathbf{x}_\parallel, \mathbf{x}'_\parallel|\omega) = \langle U(\mathbf{x}_\parallel, 0|\omega)\, U^*(\mathbf{x}'_\parallel, 0|\omega)\rangle = A^2(\omega)\exp[-x_\parallel^2/4\sigma_s^2]\exp[-(\mathbf{x}_\parallel - \mathbf{x}'_\parallel)^2/2\sigma_s^2]\exp[-\mathbf{x}'^2_\parallel/4\sigma_s^2]$, where $\mathbf{x}_\parallel$ and $\mathbf{x}'_\parallel$ are two dimensional position vectors in the plane $x_3 = 0$, $U(\mathbf{x}_\parallel, 0|\omega)$ is a component of the radiated field in the plane of the source ($x_3 = 0$) at the frequency ω, and the angle brackets denote an average over the ensemble or realizations of the functions $\{U(\mathbf{x}, 0|\omega)\}$. In the limits $\sigma_s \gg \sigma_g$, a beam described by this cross-spectral density function is called a Collett-Wolf beam. In the present case $U(\mathbf{x}_\parallel, x_3|\omega) = U_1(\mathbf{x}_\parallel, x_3|\omega) + U_2(\mathbf{x}_\parallel, x_3(\omega)$, where the spatial distributions of the fields are assumed to be symmetric or antisymmetric with respect to the x_1x_3 plane, $U_2(x_1, x_2, x_3|\omega) = \pm U_1(x_1, -x_2, x_3|\omega)$. The mean intensity of the resulting beam at a distance x_3 from the source is $\langle I(\mathbf{x}_\parallel, x_3|\omega)_\pm\rangle = 4\sigma_s^2/\sigma_{\mathit{eff}}^2(x_3)\exp[-x_\parallel^2/\sigma_{\mathit{eff}}^2(x_3)]\{1 \pm \exp[-x_2^2/\sigma_2^2(x_3)\}$, where $\sigma_{\mathit{eff}}^2(x_3) = 2\sigma_s^2 + x_3^2(c/\omega)^2(1/2\sigma_s^2 + 2/\sigma_g^2)$ and $\sigma_2^2(x_3) = 4(\sigma_g^2/\sigma_s^2)\sigma_{\mathit{eff}}^2(x_3)$. The upper sign gives the result when the two beams are symmetric with respect to the x_1x_3 plane; the lower sign gives the result when the two beams are antisymmetric with respect to this plane. In the former case the output radiation in the far field is a beam with an intensity distribution that displays a narrow bright line at its center that diverges with the distance from the source plane much more slowly than the beam itself. In the latter case the radiated beam has an intensity distribution with a narrow dark line at its center. These results suggest that the interference of two symmetric Collett-Wolf beams can be used to produce a pseudo-nondiffracting beam. The results of the theoretical calculations are confirmed by the results of experimental measurements of the interference of a pair of Collett-Wolf beams created by a Michelson interferometer.

Surface Scattering in Dispersive Media

F. Bass, **V. Freilikher**, **D. Mykhaylova**
Bar-Ilan University, Israel

Time and spatial dispersions mean that the permittivity and the permeability of a medium contain time and spatial derivatives respectively or, in other words, that the electric displacement and the magnetic flux density are non-local functions of time and coordinates. As a consequence, in dispersive media there exist several types of waves (modes) that have different dispersion relations, and therefore different phase and group velocities. As an electromagnetic wave of a certain type propagates in the dispersive medium, the presence of any inhomogeneity, (for example, of an interface) results not only in the reflection or scattering, but also in the transformation into other modes. In this presentation we consider the scattering of electromagnetic waves from a random, smoothly rough surface bounding a semi-infinite dispersive medium. The statistical moments of the reflected wave and of modes generated by scattering have been calculated in the Kirchhoff approximation. The coherent (average) field is described by a matrix R_{ij} where the diagonal elements present the reflection coefficients of the incident modes, and the off-diagonal terms correspond to the transformation coefficients, i.e. to the amplitudes of the generated waves. It is shown that while the angle of reflection of the incident wave is equal to the angle of incidence, the Snell's low for the coherent component of the reflected radiation that is transformed into other modes is violated. In the general case the ratio of the sines of the angles of incidence and reflection for the cross-modes differs from unit, and depends on the frequency of the signal. Angular distribution of the incoherently scattered intensity (scattering diagram) is calculated. It is shown in particular that in dispersive media the intensity of the scattered field depends on the frequency even in the geometrical optics approximation.

Scattering and Transmission of Light by a Thin Metal Film with Corrugated Surfaces

E. R. Méndez[1], **T. A. Leskova**[2], **A. A. Maradudin**[2]

[1]Centro de Investigación Científica y de Educación Superior de Ensenada, México
[2]University of California, Irvine, USA

We calculate the reflectivity and transmissivity of $p-$ and $s-$polarized light in a system that consists of a dielectric material characterized by a real positive dielectric constant ϵ_1 in the region $x_3 > \zeta_1(x_1)$, a metal film characterized by a complex frequency–dependent dielectric function $\epsilon_2(\omega)$ in the region $-H+\zeta_2(x_1) < x_3 < \zeta_1(x_1)$, and a dielectric material characterized by a real positive dielectric constant ϵ_3 in the region $x_3 < -H + \zeta_2(x_1)$. The surface profile functions $\zeta_{1,2}(x_1)$ are assumed to be single–valued deterministic functions of x_1 that are at least twice differentiable. The light in the form of a plane wave of wavelength λ is incident on the metal film from the region $x_3 > \zeta_1(x_1)$, and its plane of incidence, and of scattering, is the x_1x_3 plane. The angle of incidence is arbitrary, but we focus on the case of normal incidence. We consider first the case where $\zeta_1(x_1) = -H\cos(2\pi x_1/a)$, while $\zeta_2(x_1) \equiv 0$. The amplitudes of the reflected and transmitted Bragg beams are calculated as functions of λ by a rigorous numerical solution of the equations of scattering theory [1], or by the numerical solution of the corresponding reduced Rayleigh equations [2]. As a second example we consider the case where $\zeta_1(x_1) = -(H/2)\cos(2\pi x_1/a)$, while $\zeta_2(x_1) = -\zeta_1(x_1) = (H/2)\cos(2\pi x_1/a)$. The last example we consider is one in which the surface profile functions $\zeta_1(x_1)$ and $\zeta_2(x_1)$ are single realizations of random functions of x_1 defined by $\zeta_1(x_1) = -(H/2)\sum_{n=-\infty}^{\infty} c_n s(x_1 - nb)$, and $\zeta_2(x_1) = -\zeta_1(x_1)$, where c_n is a random deviate such that $c_n = 1$ with probability p and $c_n = 0$ with probability $1-p$, while the function $s(x_1)$ is assumed to have a Gaussian form, $s(x_1) = \exp(-x_1^2/a^2)$, with $a \cong b/5$. The results of these calculations shed light on the roles of periodicity and surface plasmon polaritons in producing the enhanced transmission through thin metal films pierced by subwavelength holes measured, e.g. in [3].

REFERENCES

1. Simonsen, T. A. Leskova, A. A. Maradudin, and O. Hunderi, "Wavelength Dependence of the Light Scattered from a Dielectric Film Deposited on a Metal Substrate", *SPIE*, Vol. 4100, 65, 2000.
2. Leskova, T. A. and A. A. Maradudin, *unpublished work*.
3. Ebbesen, T. W., H. J. Lezec, H. F. Ghaemi, T. Thio, and P. A. Wolff, "Extraordinary Optical Transmission through Subwavelength Hole Arrays", *Nature, London*, Vol. 391, 667, 1998.

Scattering from Randomly Rough Surfaces with Very High Slopes Using the Kirchhoff Approximation

Neil C. Bruce
Universidad Nacional Autónoma de México, Mexico

One of the most popular and useful methods for calculating the scattering of light from rough surfaces is the Kirchhoff approximation. This method has been developed to include shadowing and multiple scatter effects. However, the Kirchhoff approximation, even with multiple scattering included, has been limited to low-sloped surfaces because of the way that the surface is sampled in the calculation. A modification of the Kirchhoff approximation is presented to calculate the scattering of electromagnetic radiation from rough surfaces with very high, or even infinite, slopes in the 1D case. The modification involves a simple change in the way the surface normal is described which allows the diffraction integral to be written as the sum of two contributions, one for the contribution along the surface and the other for the contribution due to the changes in height. Here, if the slope is infinite, the first contribution is zero, but the second correctly includes the effect of the part of the surface of interest. The single and double scatter contributions to the total scattered intensity are calculated numerically with this new formulation with shadowing included explicitly. Results obtained with the proposed method are compared to the traditional formulation of the Kirchhoff approximation for scattering of light from Gaussian random rough surfaces, and to results of an integral equation numerical technique for surfaces with rectangular shaped grooves (with infinite slope). Results of calculation with the method for the case of rectangular obstacles of random heights and widths in contact with a flat plane will be presented.

Scattering of Surface Plasmon Polaritons by Surface Structures

T. A. Leskova, **Alexei A. Maradudin**
University of California, Irvine, USA

J. A. Sanchez-Gil
Instituto de Estractura de la Materia, C.S.I.C., Spain

When a surface plasmon polariton propagating on an otherwise planar metal surface in contact with vacuum impinges on a surface defect, a portion of it is converted into a reflected surface plasmon polariton, and a portion is converted into volume electromagnetic waves in the vacuum that propagate away from the surface. Such scattering processes have been studied theoretically for one-dimensional surface defects [1] and for two-dimensional surface defects [2]. The defects assumed in these investigations were spatially localized in the direction of propagation of the surface plasmon polariton [1], or localized in a finite area of the plane of which the surface wave propagates [2]. In contrast, we consider in the present work the scattering of surface plasmon polaritons from two extended surface structures. The first is a groove or ridge on which the surface plasmon polariton impinges at oblique incidence. On the assumption that the incident surface plasmon polariton is propagating in the x_1 direction, the surface is defined by the equation $x_3 = \zeta(x_1, x_2)$, where $\zeta(x_1, x_2) = A \exp[-(x_1, \cos\theta + x_2 \sin\theta)^2/R^2]$ where the amplitude A can be either positive (ridge) or negative (groove), and θ is the angle the ridge or groove makes with the x_2 axis. The second structure we consider is a layer of thickness d of the same metal as the substrate, with a parabolic boundary, for which $\zeta(x_1, x_2) = \theta(x_1 - a x_2^2)\theta(x_1)$, where $\theta(z)$ is the Heaviside unit step function. The reduced Rayleigh equation for the interaction of a surface plasmon polariton with a two-dimensional rough surface [3] is solved numerically for the amplitude of the p- and s-polarized components of the scattered field. From these solutions the cross sections for the scattering of the incident surface plasmon polariton into other surface plasmon polaritons or into volume electromagnetic waves are determined.

REFERENCES

1. Sánchez-Gil, J. A., *Appl. Phys. Lett.*, Vol. 73, 3509, 1998.
2. Shchegrov, A. V., I. V. Novikov, and A. A. Maradudin, *Phys. Rev. Lett.*, Vol. 78, 4269, 1997.
3. Maradudin, A. A. and W. M. Visscher, *Z. Phys. B*, Vol. 60, 215, 1985.

Symmetries and Backscattering Effects in the Second-harmonic Generation by Random Systems of Two-dimensional Particles

E. R. Méndez
Física Aplicada - CICESE, México

C. I. Valencia
CCMC - UNAM, México

We consider the scattering and generation of second harmonic radiation by systems of metallic particles in random positions. The particles are assumed to be invariant in the direction perpendicular to the plane of incidence (two-dimensional particles). Of particular interest is the angular distribution of the scattered light generated by this kind of system at both, the fundamental and harmonic frequencies.

Assuming that the medium that generates the second harmonic radiation is homogeneous and isotropic, we employ a numerical technique [1] that permits the study of systems that present multiple scattering. First, we present scattering calculations for the fundamental frequency and discuss the coherent effects that give rise to the phenomenon of enhanced backscattering. Then, we consider the generation of second-harmonic light by such systems, discusing the possibility of observing coherent backscattering effects. The strongest second-harmonic signal is obtained when the system is illuminated with p-polarized light and, thus, only this case is considered; with the assumed geometry, the second harmonic field is also p-polarized. The consequences of the symmetry of the scattering systems on the second harmonic radiation patterns and on the backscattering effects will also be discussed.

REFERENCES

1. Valencia, C. I., E. R. M'endez, and B. S. Mendoza, "Second harmonic generation in the scattering of light by two-dimensional particles," *J. Opt. Soc. Am B*, Vol. 20, 2150, 2003.

A Statistical Kirchhoff Model for EM Scattering from Gaussian Rough Surface

Yang Du[1], **Tao Xu**[1], **Yingliang Luo**[1], **J. A. Kong**[2]

[1] Zhejiang University, China
[2] Massachusetts Institute of Technology, U.S.A.

In this paper we propose a statistical Kirchhoff model (SKM) for shadow-corrected EM scattering from a rough surface. It treats the local coordinates and Fresnel reflection coefficients statistically over the orientation distribution of surface unit norm as characterized by the joint probability distribution function of its two directional slopes. In calculating the incoherent scattered power, for a Gaussian rough surface, the joint probability distribution function of surface unit norms at two different surface points is shown to follow a joint Gaussian distribution with zero mean and covariance matrix of special form. Decomposition of such covariance matrix into uncorrelated term and fully correlated terms of different types not only assists a better understanding of the interaction between any pair of points on the surface, but also enables the simplification of calculation of the expectation of the product of Kirchhoff term at one point and the conjugate Kirchhoff term at another point. The validity of SKM is demonstrated through the good agreements between model predictions and method of moment (MM) simulations for statistically known surfaces. Moreover, from such comparisons it appears that the validity region of SKM can be extended to that of SPM where conventional Kirchhoff model fails.

Session 3A2

Meta-materials and Structures with Negative Refraction 1

Negative Index Materials: New Designs and Results

C. M. Soukoulis[1,2]

[1]Iowa State University, USA
[2]Research Center of Crete, Greece

Negative refraction, a phenomenon first hypothesized by Victor Veselago in 1968 to occur in materials whose permittivity and permeability are simultaneously negative, has now been confirmed in several independent studies. These experiments demonstrate that it is indeed possible to design and fabricate an artificial material, now known as *metamaterials*, having an index-of-refraction that is negative over some finite band of frequencies. Some of the more striking or exotic wave propagation behavior predicted to occur in negative index materials, such as reflectionless compact lenses, near-field refocusing, *perfect* lensing, phase compensation and novel wave-guiding phenomena-place challenging demands on the material parameters.

We will present transfer matrix calculations of metallic wires, split ring resonators (SRR) and left-handed materials (LHM). Our results show that the transfer matrix method can capture all the details characteristics of the metamaterials. In particular the dependence of the resonance frequency and its width on the structural parameters of the SRR and the size of the unit cell are studied. Also the dependence of the imaginary part of effective permittivity of arrays of metallic wires is studied in detail. It is found that the imaginary part of effective permittivity has small values even for wires as small as 20 micron in diameter. The transfer matrix is very useful in calculating both the amplitude and the phase of the transmission and reflection coefficient. These numerical data were used in the determination of the effective parameters of the metamaterials. It was indeed found that the refractive index was unambiguously negative in the frequency region where both ε and μ were negative. Finally, we will show that SRR have a strong electric response, equivalent to that of cut wires, which dominates the response of LHM. A new criterion is introduced to clearly identify if an experimental peak is left- or right-handed.

Finite difference time domain (FDTD) simulations will be presented for the transmission of the EM wave through the interface of the positive and negative refraction index. It is found that the wave is trapped temporarily at the interface and after a long time the wave front moves eventually in the direction of negative refraction. The differences between negative refraction in photonic crystals and left-handed materials will be also discussed.

Another way to obtain negative refraction and left-handed behavior is to use photonic crystals, where the negative refractive index is the analog of the negative electron mass in semiconductors. Experimental and theoretical results for negative refraction and subwavelength resolution in 2D photonic crystals will be presented. Scanning transmission measurement technique is used to measure the spatial power distribution of the focused electromagnetic waves that radiate from a point source. Full width at half maximum of the focused beam is measured to be $0.21/\lambda$, which is in good agreement with the finite difference time domain method simulations. We also achieve a sub-wavelength resolution for the image of two incoherent point sources, which are separated by a distance of $\lambda/3$.

New experimental results on metallic SRRs reveal that a magnetic resonance response at 100 THz exists. This negative magnetic permeability can be coupled with a negative permittivity to give materials with a negative index of refraction at almost optical wavelengths. Possible extensions of the magnetic resonance response of metallic SRRs at 1.5 microns will be also discussed.

Finally, demonstrating the disadvantages of the currently used SRR designs due to the lack of symmetry, we will introduce more symmetric, multi-gap SRRs, which are very promising components for future 2d and 3d isotropic left-handed structures.

Subwavelength Focusing Properties and Mechanisms of a Photonic Crystal Slab with Negative Refraction

Sailing He
Zhejiang University, China

Through the mechanism of amplification of evanescent waves, a slab of left-handed material (with simultaneously negative permittivity and permeability) can focus the field of a point light source at the image side (in the far field region) with a spot size of subwavelength (i.e., overcome the diffraction limit). Subwavelength focusing by a slab of special photonic crystal with negative refraction is also possible theoretically. However, its experimental realization at an optical frequency requires much effort both theoretically and technologically. Properties and mechanisms of subwavelength focusing are studied for some distinct types of photonic crystals, and some recent results will be presented.

On the Character of Negative Parameter Values in Homogenized Metamaterials

A. Sihvola
Helsinki University of Technology, Finland

J. C. Doe
Physics Department MIT, USA

What are called as metamaterials in the recent electromagnetics discussion form a very broad class of materials. Of these media, very many types are characterized by negative values for various parameters. What is the reason of negativity in these media?

One obvious expression of negative index of refraction is the fact that the wave entering such a medium is bent to the "wrong" direction, as predicted by Snell's law if indeed the index is less than zero. And since the refractive index is the square root of the product of the permittivity and permeability, one may feel confident with the idea that then both the permittivity and permeability have to be negative (although this is not such a straightforward conclusion when one thinks of the choice of the square roots [1]).

Then permittivity and permeability have to be negative. But this is counter-intuitive because we are used to thinking of permittivity (and permeability) as a measure of electric (magnetic) energy density. The commonly given explanation to defend the possibility of such a behavior is that resonating elements can cause it in a limited frequency band—this negativity is of course a high-frequency phenomenon—through the plasma-type characteristics.

This is certainly valid thinking. However, collecting all kinds of more and less strange polarizable effects under the same integrated parameter may bring the danger of inflating these constitutive terms like permittivity and permeability. Warnings into this direction have been heard from physicists [2] as it comes to "ordinary" matter. It is even more important to be aware of the technical definition of permittivity and permeability when dealing with "metamaterials".

This is an essential question that cannot be bypassed when one is trying to homogenize metamaterials. In the presentation, the meaning, limitations, restrictions, and degrees of freedom of these constitutive parameters of homogenized metamaterials will be discussed.

REFERENCES

1. McCall, M. W., A. Lakhtakia, W. S. Weiglhofer, "The Negative Index of Refraction Demystified", *European Journal of Physics*, Vol. 23, 353, 2002.
2. *The Feynman Lectures on Physics, II, Chapter 10.*

Mechanisms for High Electromagnetic Wave Transmissions

Lei Zhou
Fudan University, China

Weijia Wen, **C. T. Chan**, **Ping Sheng**
Hong Kong University of Science and Technology, China

We present here two mechanisms for high electromagnetic wave transmissions. We first rigorously demonstrate that electromagnetic (EM) waves transmit perfectly through a slab of negative-permittivity media sandwiched between two identical slabs with appropriate permittivity, although each single slab is nearly opaque. Distinct from other mechanisms, this transparency is accompanied by extraordinary high magnetic field, and is robust against incidence angles. Microwave experiments, in excellent agreement with finite-difference-time-domain simulations, are performed to successfully realize this idea. Numerical calculations with realistic material parameters are conducted to design a structure to realize the transparency for a solid Silver film in near infra-red frequency regime. Next, we show by both theory and experiment that EM waves can totally transmit through a metal plate with disjoint slit patterns, at wavelengths much larger than the lateral dimension of each pattern. The transmission is independent on the incidence angles, thickness of the metal plate and the periodicity of the pattern arrays. We show the physics to be governed by the resonance inside the silt patterns, which establishes a $k = 0$ tunneling mode.

Left-Handed Spin Waves

Daniel D. Stancil
Carnegie Mellon University, USA

In 1964 Veselago [1] considered the properties of electromagnetic media with both negative permittivity and negative permeability. The recent demonstration of a "double-negative" medium [2] has stimulated significant interest in this topic, including ways of creating artificially structured media with improved properties. Such media have a number of interesting properties, including a negative Doppler effect, a negative Cerenkov effect, and negative refraction.

Veselago pointed out that double-negative media would also exhibit a negative group velocity-in fact he treated the terms as synonymous. He also pointed out that gyromagnetic ferromagnetic metals could potentially exhibit negative group velocity, though only over a small cone of angles near the direction of an applied magnetic field.

It is interesting to consider the spin-wave modes of a magnetized thin film in this context. First analyzed by Damon and Eshbach in 1961 [3, 4], a tangentially-magnetized film is known to exhibit backward wave behavior within a range of angles around the direction of the bias field. Consequently, such a film supports left-handed spin wave modes, and is a medium of interest for exploring many properties of left-handed media.

Such a magnetized medium exhibits a tensor permeability in which two of the diagonal elements become negative over the band of spin wave propagation. However, the permittivity is not negative over this range. Instead, the left-handed behavior is the result of anisotropic spin wave propagation characteristics along with the thin-film boundary conditions.

Careful consideration of the electromagnetic fields of the left-handed mode show that the fringing fields external to the film are right-handed, while the fields inside the film are left-handed. The mode exhibits a net left-handed behavior since [5]

$$k \cdot \int_{-\infty}^{\infty} e \times h^* \, dy < 0.$$

Experiments are proposed that would enable left-handed media characteristics such as negative Doppler shifts to be observed.

REFERENCES

1. Veselago, V. G., "The electrodynamics of substances with simultaneously negative values of ε and μ", *Usp. Fiz. Nauk*, Vol. 92, 517, 1964.
2. Smith, D. R., W. J. Padilla, D. C. Vier, S. C. Nemat-Nasser and S. Schultz, "Composite Medium with simultaneously Negative Permeability and Permittivity", *Phys. Rev. Lett.*, Vol. 84, No. 18, 4184, 2000.
3. Damon, R. W. and J. R. Eshbach, "Magnetostatic modes of a ferromagnet slab", *J. Phys. Chem.. Solids*, Vol. 19, 308, 1961.
4. Stancil, D. D., *Theory of Magnetostatic Waves, (Springer-Verlag, New York)*, 1993.
5. Gupta, S. S., "Power flow and energy distribution of magnetostatic bulk and surface waves in dielectric layered structure", *IEEE Trans. Magn.*, Vol. MAG-18, 1639, 1982.

Negative Refraction and Anomalous Reflection in Anisotropic Metamaterial: an Analogical Study on Anisotropic L-C Transmission-line Network

Yijun Feng, **Xiaohua Ten**, **Yan Chen**, **Tian Jiang**
Nanjing University, China

Artificial electromagnetic metamaterials have significantly broadened the range of electromagnetic wave propagation phenomena available. In recent years, both theoretical and experimental works on isotropic metamaterials with simultaneously negative permittivity and permeability have indicated the negative refraction of electromagnetic wave [1]. Such metamaterial could be realized through isotropic 2-dimensional L-C loaded transmission-line network structure, which has been used to experimentally demonstrate backward-wave radiation, negative refraction and sub-wavelength focusing at microwave frequencies [2]. Anisotropic metamaterials for which some elements of the permittivity and permeability tensors have negative value have also been studied theoretically, which demonstrated that negative refraction can be realized in such media under some different combinations of its medium parameters [3-5].

In the presented work, we will report our recent studies on anomalous electromagnetic wave refraction and reflection that occurs at the interface between vacuum and an anisotropic medium for which some elements of the permittivity and permeability tensors have negative value. Such an anisotropic medium has been successfully realized and analogically studied by a 2-dimensional periodic L-C network. Two types of anisotropic network called "Never-cutoff" and "Anti-cutoff" have been constructed with different properties of the transverse component of the wave vector. The dispersion relation has been obtained through circuit network analysis by applying Bloch boundary conditions, which exhibits hyperbolic dispersion surface in phase space. Positive refraction of wave vector while negative refraction of energy has been demonstrated in the microwave frequency band. Anomalous reflection has also been studied at the interface between vacuum and $Anti-cutoff$ anisotropic medium. We also show that partial focusing of electromagnetic wave can be obtained by a slab of the anisotropic medium.

REFERENCES

1. Shelby, R., D. R. Smith, S. Schultz, *Science 292*, 77, 2001.
2. Grbic, G. V. Eleftheriades, *Phys. Rev. Lett.*, Vol. 92, 117403, 2004.
3. Lindell, V., S. A. Tretyakov, K. I. Nikoskinen and S. Ilvonen, *Microwave Opt. Technol. Lett.*, Vol. 31, 129, 2001.
4. Smith, D. R. and D. Schurig, *Phys. Rev. Lett.*, Vol. 90, 077405, 2003.
5. Zhou, Lei, C. T. Chan, and P. Sheng, *Phys. Rev. B 68*, 115424, 2003.

Calculation of the Index of Refraction of Meta-materials

Qiang Sui[1,2], **Cixiang Liu**[1], **Chao Li**[1], **Fang Li**[1]

[1]Institute of Electronics, Chinese Academy of Sciences, China
[2]Communication University of China, China

This paper focuses on the relationship of the index of refraction versus the frequency. The index of refraction was calculated by three dimensional Finite Difference Time Domain (FDTD). The structure under study is the well-known periodic arrangement of rods and split-ring resonators. The index can be calculated by phase measurement of the wave in a slab of meta-material and by refraction angle of wave through a prism made of meta-material. A plane wave for FDTD can be obtained by using 2-direction periodic boundary condition. The prism is constructed by one-direction periodic boundary condition, that it is infinite long. The negative phase propagation can be observed in the simulation results. The calculation results of the two ways are in good agreement.

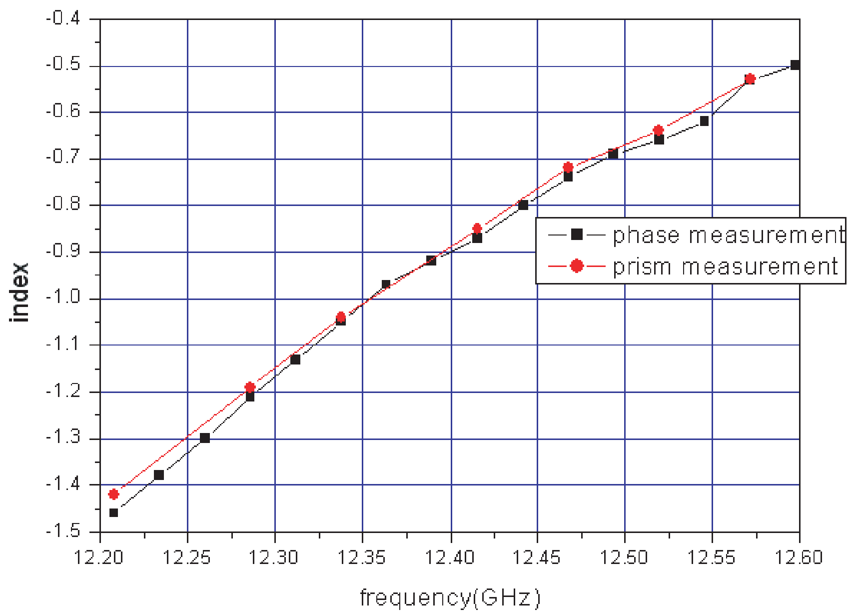

Negative Refraction in the Polariton Regime

David W. Ward, **Keith A. Nelson**
Massachusetts Institute of Technology, USA

K. J. Webb
Purdue University, USA

Negative refraction has been realized at microwave frequencies [1], but the search for terahertz negative refractive materials is just getting underway. We consider the role that polaritons in ferroelectric crystals may play in extending negative refraction into the terahertz frequency range.

Phonon-polaritons are an admixture of far infrared light waves and lattice vibrations which can be generated through impulsive stimulated Raman scattering (ISRS) and dierence frequency mixing (DFM) in a ferroelectric crystal [2]. Characteristic to the polariton regime is polariton dispersion, in which an avoided crossing between electromagnetic and vibrational degrees of freedom result in two branches for the dispersion relation separated by a bandgap, in which polariton propagation is forbidden. Through finite-difference-time-domain (FDTD) simulations, we illustrate a third branch of dispersion that appears when a negative magnetic permeability is introduced that overlaps with a ferroelectric resonance (Figure 1). Recent developments in terahertz magnetic metamaterials [3] and multiferroic nanostructures [4] offer viable routes to achieving the negative polaritonic materials discussed here. Among other functionalities of negative index polaritonic materials, we demonstrate reverse Cerenkov terahertz radiation generated through ISRS and DFM (Figure 2).

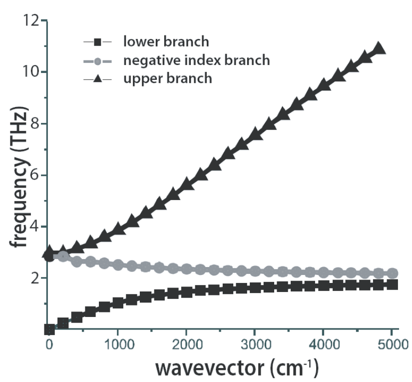

Figure 1: Dispersion curve illustrating regular polariton dispersion and negative index polariton dispersion.

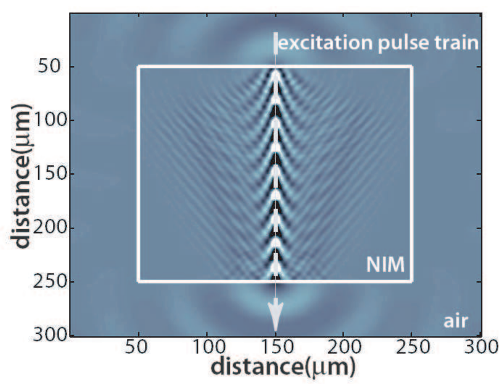

Figure 2: Reverse Cerenkov cone generated through ISRS with an optical excitation pulse train (travelling downward in figure) in a negative index polaritonic material (NIM).

REFERENCES

1. Shelby, R. A., D. R. Smith and S. Schultz, "Experimental verification of a negative index of refraction", *Science*, Vol. 292, 77, 2001.
2. Dougherty, T. P., G. P. Wiederecht and K. A. Nelson, "Impulsive stimulated Raman scattering experiments in the polariton regime", *J. Opt. Soc. Am. B*, Vol. 9, 2179, 1992.
3. Yen, T. J. , W. J. Padilla, N. Fang, D. C. Vier, D. R. Smith, J. B. Pendry, D. N. Basov and X. Zhang, "Terahertz Magnetic Response from Articial Materials", *Science*, Vol. 303, 1494, 2004.
4. Zheng, H. et al., "Multiferroic $BaTiO_3$-$CoFe_2O_4$ Nanostructures", *Science*, Vol. 303, 661, 2004.

Polarimetric Scattering from a Layer of Spatially-Oriented Metamaterial Small Spheroids

Hongxia Ye, **Ya-Qiu Jin**
Fudan University, China

The complex scattering amplitude functions of a small metamaterial spheroid are derived under the Rayleigh approximation. The scattering density of metamaterial spheroid is much stronger than dielectric spheroid, and the scattering patterns of metamaterial spheroid are symmetric along the spheroid axis, different from the dielectric spheroid, which are symmetric along the incident direction.

The Mueller matrix solution for polarimetric scattering from a layer of random metamaterial small spheroids is constructed. Bistatic scattering of horizontally and vertically aligned metamaterial and dielectric spheroids are numerically calculated. The co-polarized bistatic scattering coefficients of metamaterial spheroids are apparently stronger than dielectric spheroids. In the case of horizontal orientationscattering from metamaterial spheroids layer is much stronger at $\theta_s > 0$ than at $\theta_s < 0$, while dielectric spheroids is symmetric. The co-polarized backscattering coefficients σ_{hh} , σ_{vv} and σ_{hh}-σ_{vv} of metamaterial and dispersive dielectric spheroids are presented to show the dependence upon frequency. The σ_{hh}-σ_{vv} of metamaterial spheroids varies remarkably with frequency and takes a peak value around $f = 7.1GHz$, which happens to be the resonance frequency of inclusions of metamaterial. The σ_{hh}-σ_{vv} of dielectric spheroids varies slightly, although it is dispersive with frequency.

The co-polarized and cross-polarized backscattering coefficients and polarizability degree of a layer of non-uniformly oriented metamaterial spheroids under illumination of an elliptic polarized plane wave are numerically simulated. Effects of metamaterial parameters on scattering pattern and scattering mechanism are interpreted. Numerical results indicate that scattering of metamaterial particles is enhanced largely and demonstrates asymmetric directivity. Meanwhile, polarized difference of σ_{hh}-σ_{vv} strongly varies with frequency due to constitutive dispersion of $\varepsilon(\omega)$ and $\mu(\omega)$.

Research on the Negative Permittivity Effect of the Thin Wires Array in Matematerial by Transmission Line Theory

Qun Wu[1], **Fan-Yi Meng**[1], **Ming-Feng Wu**[1], **Jian Wu**[2], **Le-Wei Li**[1,3]

[1]Harbin Institute of Technology, China
[2]National Key Laboratory of Electromagnetic Environment, China
[3]National University of Singapore, Singapore

Matematerial is also called negative refractive index material, which represents a dielectric medium that exhibits negative refractive index phenomenon and has simultaneously negative permittivity and negative permeability [1-4]. In 1998, Pendry et al derived the effective permittivity model of a symmetric thin wire array and stated that the negative permittivity effect can be exhibited by the array. It is then considered a classic work, because it resolved a key problem for fabrication of the matematerial. Soon after this, in 1999, the negative permeability effect of the periodic SRR's (Split Rings Resonators) array was found, and in 2000 the metamaterial is firstly fabricated through reasonably arranging the thin wires and SRR's. Worth noting is that the Pendry's permittivity model was derived through making use of the plasmon theory and leading the concept of the effective density and mass of electrons, so it is difficult to understand the model from the angle of macrophysics.

From this point, we propose, in this paper, the utilization of the transmission line theory to derive the effective permittivity model of the thin wire array. Firstly, the equivalent transmission line structure of the array, where a plane wave is propagating, is presented according to the response of the array to the incident electromagnetic wave. Secondly, an effective permittivity model applicable for the array is derived using the transmission line theory. The validity of the model derived has been proven by numerical simulations. The description of theoretical derivation exhibits clear physical concepts and provides a new approach to understand the negative permittivity effect of the thin wire array from the macrophysics.

To author's acknowledge, this is a novel concept for application of the transmission line theory to derive the effective permittivity model of an asymmetric thin wire array. The discussions will be given in detail during the presentation.

REFERENCES

1. Veselago V. G., "The electrodynamics of Substances with Simultaneously Negative Values of ϵ and μ", *Soviet Physics Uspekhi*, Vol. 10(4), 509, 1968.
2. Shelby R. A., D. R. Smith, et al, "Microwave Transmission through a Two-Dimensional, Isotropic, Left-Handed Metamaterial", *Appl. Phys. Lett.*, Vol. 78(4), 489, 2001.
3. Pendry J. B., "Negative Refraction Makes a Perfect Lens", *Phys. Rev. Lett.*, Vol. 85, 3966, 2000.
4. Smith D. R., S. Schultz, et al, "Determination of Effective Permittivity and Permeability of Metamaterials from Reflection and Transmission Coefficients", *Phys. Rev. B*, Vol. 65, 195104-1, 2002.

Session 3A3

Nanoscopic Electromagnetics

Surface-enhanced Raman Scattering in Small Noble-metal Nanoparticles

V. N. Pustovit
Jackson State University, USA

T. V. Shahbazyan
Jackson State University, USA

Surface-enhanced Raman scattering (SERS) from molecules adsorbed on small metal particles has attracted increasing interest during past two decades. The main SERS mechanism has electromagnetic (EM) origin and is due to the strong surface plasmon (SP) local field near the metal surface [1]. Recent observations of enormous (up to 10^{15}) enhancement of single-molecule Raman scattering [2] as well as emerging possibilities of nanoparticle-based Raman sensors have prompted a new interest in single particle SERS and, in particular, in finite-size effects in small nanoparticles. Although classical EM enhancement is size-independent, quantum corrections due to the discreteness of the electron spectrum result a weaker enhancement in small nanoparticles.

Here we address the role of quantum confinement in SERS in small nanoparticles. In noble-metal nanoparticles, the confining potential has different effect on s-band and d-band electrons. Namely, the spillout of delocalized s-electrons beyond the classical nanoparticle boundary results in an incomplete embedding of s-electron distribution in the background of localized d-electrons whose density profile follows more closely the classical shape. In the absence of d-electron population in the nanoparticle surface layer, the effective dielectric constant is reduced relative to the bulk, giving rise to a blue shift of the SP resonance in Ag nanoparticles [3].

Specifically, we performed calculations of the local field and Raman enhancement factor, based on time-dependent local-density approximation, in small Ag nanoparticles. We found that, the effect of underscreening of s-electrons by d-electrons in the surface layer leads to a stronger SP local field acting on a molecule located in a close proximity to the metal surface. This results in an additional enhancement of the Raman signal. Importantly, such an enhancement becomes more pronounced for small nanoparticles due to the larger volume of surface layer.

*Supported by NSF under grants DMR-0305557 and NUE-0407108, by NIH under grant 5 SO6 GM008047-31, and by ARL under grant DAAD19-01-2-0014.

REFERENCES

1. Schatz, G. C. and R. P. Van Duyne, J. J. Chalmers, P. R. Griffiths, eds., *Handbook of Vibrational Spectroscopy, Wiley*, 2002.
2. Nie, S. and S. R. Emory, *Science*, Vol. 275, 1102, 1997.
3. Liebsch, A., *Phys. Rev.*, Vol. 48, 11317, 1993.

Lifetimes of Quasi-Static Eigenstates of a Nano-Cluster

David J. Bergman[1], **Uri Evra**[1], **Xiangting Li**[1,2]

[1]Tel Aviv University, Israel
[2]Shanghai Jiaotong University, China

The strongly localized quasi-static eigenstates (also known as surface-plasmon resonances) which are found in a small nanometric cluster of spherical inclusions can form the basis for some interesting potential applications such as SPASER [1] and nanolens [2]. In a SPASER, a strong coherent electric field, oscillating at a frequency ω in the visible or infra-red spectral range, can be excited in a spatial region whose linear dimensions are much smaller than the wavelength appropriate to that frequency. In a nanolens an incident electromagnetic field, oscillating at such a frequency, can be focused to a spot whose size is much less than the relevant wavelength.

An important property of such resonances is their finite radiative lifetime, which is infinite in the strict quasi-static limit. One needs to solve the full Maxwell's Equations in order to find the radiative decay rate, and consequently the lifetime, of such an eigenstate.

We report on calculations of such lifetimes for a certain set of small clusters of closely spaced spherical inclusions. We also discuss how symmetry properties of such a cluster can be exploited to ensure that certain eigenstates have especially long radiative lifetimes.

REFERENCES

1. Bergman, D. J. and M. I. Stockman, "Surface plasmon amplification by stimulated emission of radiation: Quantum generation of coherent surface plasmons in Nanosystems", *Phys. Rev. Letters*, Vol. 90, 027402-1, 2003.
2. Li, K., M. I. Stockman, and D. J. Bergman, "Self-similar chain of metal nanospheres as an efficient nanolens", *Phys. Rev. Letters*, Vol. 91, 227402-1, 2003.

Electromagnetic Properties of Aggregated Metal Nanospheres Revisited

Vadim A. Markel
University of Pennsylvania, USA

Optical, and more generally, electromagnetic properties of aggregated nanospheres attracted significant attention in the past two decades. Two physical objects have been of particular importance: colloid metal clusters and carbonaceous soot aggregates. However, even in the quasistatic limit, accurate numerical solution to the Laplace equation for these objects requires formidable computational power which was not commonly available until recently. This is especially true in the spectral range when strong resonance interaction is present, typically in the optical and near-IR range for metals. On the other hand, interest in aggregated nanoparticles, including ordered systems, has been reinvigorated by the recent dramatic advances of nanofabrication capabilities. In my talk I will discuss some new results concerning electromagnetic responses of aggregated nanospheres, both ordered and disordered, and, in particular, the results of simulations which have become computationally feasible only in the past few years.

New Method to Calculate Electrical Forces Acting on a Sphere in an Electrorheological Fluid

David G. Stroud, **Kwangmoo Kim**
Ohio State University, USA

Xiangting Li, **David J. Bergman**
Tel Aviv University, Israel

We describe a new method to calculate the electrical force acting on a sphere in a suspension of dielectric spheres in a host with a different dielectric constant, under the assumption that a uniform electric field is applied. The method uses a spectral representation for the total electrostatic energy of the composite. The force is expressed as a certain gradient of this energy, which can be expressed in closed analytical form rather than evaluated as a numerical derivative. The method is applicable even when both the spheres and the host have frequency-dependent dielectric functions and non-zero conductivities, provided that the system is in the quasistatic regime. In principle, it includes all multipolar contributions to the force,and it can be used to calculate multi-body as well as pairwise forces. We also will present several numerical examples, including forces involving fluids with finite conductivities. The force between two spheres approaches the dipole-dipole limit, as expected, at large separations, but departs drastically from that limit when the spheres are nearly in contact. The force may also change sign as a function of frequency when the host is a slightly conducting fluid. Finally, the force in a system of three spheres does not always decompose into a sum of two-body forces. This last result indicates the importance of angle-dependent forces in this geometry.

Electromagnetic Interactions of Solid State Nanocrystals with Their Nanoenvironment

Thomas A. Klar
Ludwig-Maximilians-Universität München, Germany

Metal- as well as semiconductor nanocrystals show electromagnetic responses that are decisively determined by their nanoscopic dimensions. In the case of II-IV semiconductor nanocrystals the absorption and fluorescence spectra can be tuned by the size of the nanoparticles due to the quantum confinement effect. Differently, the absorption and scattering spectra of noble metal nanoparticles are dominated by the nanoparticle plasmon resonance which is a collective oscillation of the conduction band electrons. Hybrid systems comprising these solid state nanocrystals as well as chromophores or biomolecules show interesting spectroscopic features due to mutual electrodynamic interactions on a nanoscopic length scale.

For example, noble metal nanoparticles absorb energy from surface bound fluorescent molecu-les but also change their radiative lifetime. Both effects lead to a very efficient quenching of fluorescence that can be used in biophysical applications. [1,2] Furthermore, a change of the refractive index in the metal particles' nanoenvironment shifts the scattering spectrum of the nanoparticles. This opens the way to use single gold nanoparticles as a sensitive assay for the detection of proteins. [3,4]

Semiconductor nanoparticles of several different sizes can be used to construct an energy gap gradient normal to multiple layers of nanocrystals applying the layer-by-layer technique. The diameters of the nanocrystals are monotonically increased or decreased in subsequent layers. In such devices we observe a highly efficient funnelling of excitation energy from layers comprising smaller nanocrystals towards the layer with the largest nanocrystals. Most important, not only excitations in radiative states are transferred but also excitations from trapped states, usually lost for luminescence, can be effectively recycled, hence increasing the overall luminescence yield. [5,6]

REFERENCES

1. Dulkeith, E. et al., *Phys. Rev. Lett.*, Vol. 89, 203002, 2002.
2. Dulkeith, E. et al., *Nano Letters, accepted*.
3. Raschke, G. et al., *Nano Letters*, 3935, 2003.
4. Raschke, G. et al., *Nano Letters*, 41853, 2004.
5. Franzl, T. et al., *Appl. Phys. Lett.*, Vol. 84, 2904, 2004.
6. Franzl, T. et al., *Nano Letters*, Vol. 4, 1599, 2004.

Broken Symmetry and the Optical Responses of Metal Nanostructures

Martti Kauranen, **Brian K. Canfield**, **Sami Kujala**
Tampere University of Technology, Finland

Konstantins Jefimovs, **Tuomas Vallius**, **Jari Turunen**
University of Joensuu, Finland

The optical properties of metal nanoparticles are dominated by plasmon resonances that depend on the size, shape, and dielectric environment of the particles. We use electron-beam lithography to prepare two-dimensional arrays of noncentrosymmetric L-shaped gold nanoparticles and investigate their linear and second-order nonlinear optical properties.

Our samples consist of a glass substrate, a 2-nm chromium adhesion layer, 20 nm layer of gold, and a 20 nm protective glass layer. The nominal linewidth of the particles is 100 nm and the length of the arms 200 nm. The particles are arranged in a square lattice with 400 nm period. For ideal particles with equal arm lengths, the bisector of the arms is a reflection axis, which defines a proper coordinate system of the samples. In practice, however, the reflection symmetry may be broken by unequal arm lengths, overall shape deviations, and small-scale defects.

Polarized transmission through the samples was measured at normal incidence at the wavelengths of 820 nm and 1060 nm. In both cases, the principal directions for transmission were found to be shifted from the expected directions by more than the measured differences in the arm lengths suggest. The shifts at the two wavelengths were 11.5° and 7.6°, respectively. Such strong dispersion of the axes is associated with the low symmetry of the samples, which also implies that the samples are chiral, i.e., they should exhibit optical activity. To verify this, we measured the polarization azimuth rotation of the transmitted light. The influence of the anisotropy was removed by averaging the results for all orientations of the linear input polarization. No azimuth rotation was measured at 1060 nm. However, the rotation at 820 nm was 0.3°, showing that the samples do exhibit optical activity.

The reflection symmetry of the ideal samples also leads to strong polarization selection rules for the second-order response. The second-order response was measured at normal incidence using 1060 nm as the fundamental wavelength and detecting second-harmonic light at 530 nm. All combinations of the fundamental and second-harmonic polarizations along the assumed axes of the ideal sample were used. The signals forbidden by symmetry were found to be at most one order of magnitude weaker than the allowed signals. The nonlinear measurements thus provide additional evidence of the broken symmetry of the samples.

Coherent, Nonlinear, and Active Nanoplasmonics

Mark I. Stockman
Georgia State University, USA

David J. Bergman
Tel Aviv University, Israel

We discuss the dramatic development in the theory of nanoplasmonic systems that have taken place recently. The basis of the nanoplasmonic phenomena are eigenmodes [surface plasmons (SP's)] that have nontrivial localization-delocalization properties on the nanoscale [1]. In particular, they are singular on the nanoscale, which causes the depolarization of the second harmonic generation (SHG) on nanosystems [2] observed experimentally [3]; at the same time, SP's cannot be Anderson localized, which causes dephasing of the SHG [2, 3].

One of the most important theoretical predictions has been the possibility to coherently control the distribution of the local optical field energy at the nanoscale. Using the phase modulation of the excitation ultrashort pulse, it is possible to concentrate this energy in space and time [4]. For nonlinear photoprocesses, such as two-photon excitation or SHG, it is possible to coherently control the integral response at any given point of the system [5]. This prediction has directly been confirmed recently for two-photon excitation of electron photoemission from nano-rough metal surfaces measured by means of electron microscopy [6, 7].

Principally different development has been a step toward quantum or active nanoplasmonics. This has been an introduction of Surface Plasmon Amplification by Stimulated Emission of Radiation (SPASER). A spaser is a resonant metal nanosystem embedded in a solid of semiconductor quantum dots (QD's). These QD's are excited by a femtosecond UV pulse making them a gain medium. In the nano-proximity of the metal nanosystems, the QD's undergo radiativeless transitions exciting SP's in this nanosystems. The stimulated emission leads to accumulation of a macroscopic number of coherent SP's in a single mode causing generation of an ultrashort pulse of nanolocalized optical fields, which will have numerous prospective applications.

REFERENCES

1. M. I. Stockman, S. V. Faleev, and D. J. Bergman, "Localization Versus Delocalization of Surface Plasmons in Nanosystems: Can One State Have Both Characteristics?", *Phys. Rev. Lett.*, Vol. 87, 167401-1, 2001.
2. Stockman, M. I., D. J. Bergman, C. Anceau, S. Brasselet, and J. Zyss, "Enhanced Second-Harmonic Generation by Metal Surfaces with Nanoscale Roughness: Nanoscale Dephasing, Depolarization, and Correlations", *Phys. Rev. Lett.*, Vol. 92, 057402-1, 2004.
3. Anceau, C., S. Brasselet, J. Zyss, and P. Gadenne, "Local Second-Harmonic Generation Enhancement on Gold Nanostructures Probed by Two-Photon Microscopy", *Opt. Lett.*, Vol. 28, 713, 2003.
4. Stockman, M. I., S. V. Faleev, and D. J. Bergman, "Coherent Control of Femtosecond Energy Localization in Nanosystems", *Phys. Rev. Lett.*, Vol. 88, 67402-1, 2002.
5. Stockman, M. I., D. J. Bergman, and T. Kobayashi, "Coherent Control of Nanoscale Localization of Ultrafast Optical Excitation in Nanosystems", *Phys. Rev. B*, Vol. 69, 054202-10, 2004.
6. Kubo, A., K. Onda, H. Petek, Z. Sun, Y. S. Jung, and H. K. Kim, *in The 2004 Ultrafast Phenomena Conference, Niigata, Japan*, 2004.
7. Kubo, A., K. Onda, H. Petek, Z. Sun, Y.-S. Jung, and H.-K. Kim, "Attosecond Kinematic Micrography of Surface Plasmon Dynamics", *Nature (2004 (submitted))*, 2004.

Polarization Conversion and "Focusing" of Light Propagating through a Small Chiral Hole in a Metallic Screen, Geometrical Chirality and the Reyleigh-wien Paradox

A. V. Krasavin, **A. S. Schwanecke**, **N. I. Zheludev**
University of Southampton, UK

M. Reichelt, **T. Stroucken**, **S. W. Koch**
Philipps University, Germany

Metallic films structured on the nanoscale show a range of unusual properties such as extraordinarily high transmission of light through metallic films perforated with round holes and strong linear birefringence for arrays of asymmetrical openings. Metallic films with arrays of chiral (twisted) holes, i.e. holes that are not their mirror images over any line in the plane of the film show polarization effects in diffraction that depend on whether the structural elements of the array are twisted clockwise or anticlockwise, while their microscope images in polarized light display unusual symmetries.

Here we show for the first time that propagation of light through a metallic screen containing a hole of twisted shape is sensitive to whether the incident wave is left or right circularly polarized. The transmitted light accrues a component with handedness opposite to the incident wave intensity of which peaks at a wavelength close to the hole overall size. We also observed a strong concentration of the transmitted field at the center of the chiral hole when the handedness of the chiral hole and the waves polarization state are the same. We investigate the relation of this new nanoptical effect with the magnitude of the geometrical chirality of the hole and discuss the effect in the context of the Reyleigh-Wien paradox.

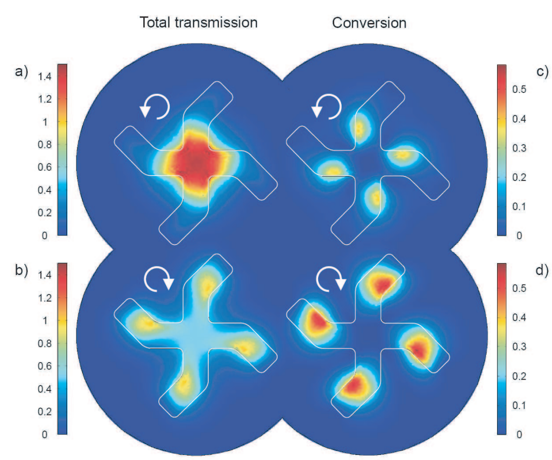

Figure 1: On the left: intensity maps of transmitted radiation for (a) clockwise and (b) counterclockwise polarizations of the incident wave. On the right: intensity maps of the circular converted component of the transmitted radiation for (c) clockwise and (d) counterclockwise polarizations of the incident wave.

Optical Negative-Refraction Metamaterials, Nano-Layers and Nano-Transmission Lines

Nader Engheta[1], **Andrea Alù**[1,2], **Alessandro Salandrino**[1,2]

[1]University of Pennsylvania, U.S.A.
[2]Università di Roma Tre, Italy

In the past few years, investigating various properties of left-handed (LH) or double-negative (DNG) media, in which both permittivity and permeability possess negative real parts in a certain frequency range, has become the subject of interest for many research groups worldwide. The first experimental demonstration of anomalous negative refraction in these engineered media was conducted in the microwave regime [1]. In the near-infrared (IR) and visible regimes, however, constructing such negative-index materials encounters some challenges, mainly due to the fact that in these frequency regimes the magnetic permeability due to the molecular currents in a material approaches to that of the free space, and therefore the simple scaling of the metallic split-ring resonator SRR (which was used in the microwave regime) down to the optical wavelength may face some related issues. Several ideas have been suggested by others to overcome some of these challenges [2-5].

Here we present another approach to design sub-wavelength inclusions that exhibit magnetic dipolar resonant response, and thus provide the possibility of having negative effective magnetic dipole moment and negative effective permeability at optical frequencies. The idea is based on the collective resonance of an array of plasmonic nanospheres arranged in a circular pattern to form a single sub-wavelength "loop" of plasmonic nanospheres. In this loop, it is not the conventional conduction current (as in the SRR at microwaves) that produces the magnetic dipole moment, but instead it is the plasmonic resonant feature of every nanosphere that induces a circulating "displacement" current around this loop. Unlike the case of the conventional metallic loops or SRRs at the microwave frequencies, here the size of this loop does not directly influence the resonant frequency of the induced magnetic dipole moment, but rather the plasmonic resonant frequency of the nano-particle is the main determining factor for this resonance to happen. Embedding many of these loops in a host medium may lead to a bulk medium with negative effective permeability at certain band of optical frequencies.

In addition, we show how by properly arranging plasmonic and non-plasmonic nano-elements as nano-inductors and nano-capacitors, optical nano-transmission lines can be formed. If the arrangement involves series plasmonic elements and shunt non-plasmonic elements, this will provide positive-index transmission lines in the optical frequency. However, if the shunt plasmonic and series non-plasmonic elements are used, we may synthesize negative-index (or left-handed (LH)) transmission lines in the optical domain. As the nanostructures gets closer, in the limit, plasmonic and non-plasmonic nano-layers may be formed as layered structures with negative index or positive index properties. This may lead to interesting sub-wavelength focusing effects in the optical layered structures, together with a road map for development of negative-refractive-index (or left-handed) materials in the IR and visible regimes.

REFERENCES

1. Shelby, R. A. et al., *Science*, Vol. 292, No. 5514, 77, 2001.
2. Podolskiy, V. A. et al., *J. Nonlin, Opt. Phys. Mat.*, Vol. 11, 65, 2002.
3. O'Brien S. et al., *Phys. Rev. B*, Vol. 69, 241101, 2004.
4. Shvets, G. and Y. A. Urzhumov., *Phys. Rev. Lett*, Vol. 93, 243902, 2004;
5. Povinelli M. L. et al., *Appl. Phys. Lett*, Vol. 82, 1069, 2003

Session 3A4

Scattering and Radiative Transfer: Basic Research and Applications 2

Iterative Approach to Scattering from the Targets above a Rough Surface

Hongxia Ye, **Ya-Qiu Jin**
Fudan University, China

Multiple scattering from the object above a randomly rough surface, especially for electromagnetic (EM) wave incidence at low grazing angle (LGA), has become of interest in many important applications. The tapered wave incidence is usually adopted. To take account interactions of the object with the underlying rough surface, the width of tapered wave, g , should be large to ensure the incident EM wave density enough on both the object and surface. It has been studied (Ye and Jin 2005, TAP in press) that the width g is related to incident angle θ_i and object height h. Too large g makes scattering computation much more difficult.

This paper develops a new approach to numerical iteration of scattering from the object (or multi-objects) above randomly rough surface. It based on the idea that most significant contribution from rough surface to the object is in the specular direction. The object and rough surface are alternatively analyzed. The object is illuminated by the plane wave, and rough surface is illuminated by the tapered wave. Note that the phases of plane wave and tapered wave are uniform. Interactions between the object and rough surface are considered iteratively by updating the right side excitation of MoM matrix equation. On each iteration, the excitations of the object and rough surface are represented as the original incident field plus the scattered field from each other. The iterations are terminated when the induced surface currents on the object and rough surface are converged.

In this method the value of g is only related to incident angle θ_i, not to the object height h, and an expression of g value to ensure computation accuracy is also derived. Some numerical examples of bistatic scattering from a 2-D object and rough surface are presented and discussed. The results show that in our new iterative approach small g can yield accurate and efficient computation. Our approach can be extended to fast and efficient computation for bistatic scattering from multi-objects above randomly rough surface, especially at LGA.

Radiation-Transfer Calculations for the Diffuse Reflectance from Pigmented Coatings

Fernando Curiel[1], **Rubén G. Barrera**[2], **Eduardo Nahmad-Achar**[1]

[1]Centro de Investigación en Polímeros, Grupo Comex, México
[2]Universidad Nacional Autónoma de México, México

We use a numerical solution of radiation transfer equations to calculate the diffuse reflectance of a pigmented film composed by a transparent pigment embedded in a latex resin. We introduce in the calculation experimentally determined values for the optical absorption of the resin as well as for the particle size distribution of the pigment, and analyze the sensitivity of the diffuse reflectance to the different parameters of the model.

Light Scattering Statistics of Particle Aggregates

F. Moreno, **F. González**, **J. M. Saiz**, **O. Merchiers**
Universidad de Cantabria, Spain

Light scattering by particle aggregates has been the focus of attention of many researchers during the last few years [1]. This is not only for its interest in the basic field of light-matter interaction but also for its implications in practical fields like atmospheric remote sensing (the aggregate components are in the microscopic scale) [1] and biosensing (the aggregate components are in the nanoscopic scale) [2]. In general, in these applications, information about the scattering system has been obtained through the measurement of the electromagnetic properties (intensity and polarization) of the scattered radiation, and, more precisely, observing its evolution as a function of the parameters that characterize both the incident radiation and the scattering geometry. Also, the study of statistical properties of the scattered radiation has provided with new tools for the analysis of particle scattering systems [3,4]. Based on previous research [5,6], a study of the statistics of the fluctuations of the scattered intensity by models of particle aggregates constituted by a low number of components (non-gaussian regime) will be presented in this contribution. One of the objectives of this study is to analyze the influence of multiple scattering between the components of the aggregate. To do this, basic aggregate geometries formed by a few particles, under the dipole approximation will be analyzed by conventional numerical simulation techniques and the Coupled Dipole Method. Different combinations of optical properties of the components and geometrical parameters of the aggregate will be envisaged. The behavior of several statistical indicators, like the probability density function of the intensity fluctuations, the second order factorial moment, or the probability of obtaining zeros in the cross-polarized component, will be analyzed.

REFERENCES

1. Mishchenko, M. I., J. W. Hovenier and L. D. Travis, "Light scattering by nonspherical particles. Theory, Measurements and Application.", Eds. *Academic Press. San Diego*, 2000.
2. Khlebtsov, N. G., A. G. Melnikov, L. A. Dykman, V. A. Bogatyrev, "Optical properties and biomedical applications of nanostructures based on gold and silver bioconjugates" in "Photopolarimetry in remote sensing", G. Videen, Y. Yatskiv and M. Mishchenko, eds. *NATO Science Series*, vol. 161, 265, 2004.
3. Pitter, M. C., K. I. Hopcraft, E. Jakeman, J. G. Walker, "Structure of polarization fluctuations and their relation to particle shape", *J. Quant. Spect. Rad. Transfer*, vol. 63, 433, 1999.
4. Videen, G., D. R. Prabhu, M. Davies, F. González, F. Moreno, "Light scattering fluctuations of a soft spherical particle containing an inclusion", *Appl. Opt.*, vol. 40, 4054, 2001.
5. Merchiers, O., J. M. Saiz, F. González, F. Moreno, "A two particle model to study fluctuations of the scattered radiation. Multiple scattering effects", *J. Opt. Soc. Am A (to be published)*, 2004
6. González, F., F. Moreno, J.M. Saiz, J.L. de la Peña, "Intensity and polarization fluctuation statistics of light scattered by systems of particles" in "Photopolarimetry in remote sensing", G. Videen, Y. Yatskiv and M. Mishchenko, eds. *NATO Science Series*, vol. 161, 175, 2004.

The Computations of the Scattering and Absorption Properties of Nonspherical Ice Crystals at the Infrared Wavelength

Heli Wei[1], **Ping Yang**[2], **Hung-Lung Huang**[3]
Bryan A. Baum[3,4], **Yong X. Hu**[4]

[1]Anhui Institute of Optics & Fine Mechanics, Chinese Academy of Sciences, China
[2]Texas A & M University, USA
[3]University of Wisconsin-Madison, USA
[4]NASA Langley Research Center, USA

Ice clouds have been identified as one of the most uncertain components in atmospheric research. Various particle morphologies including complex bullet rosettes and aggregates have been observed frequently in cirrus clouds. The research of radiative properties of ice clouds and remote sensing requires the basic single-scattering properties of various ice crystals (nonspherical particles) within the clouds.

This study reports on the development of a comprehensive set of the scattering and absorption properties for seven nonspherical ice crystal habits in the near- through far-infrared spectral region from 3 to 100 m. The specific ice particle shapes, or habits, include hexagonal plates, hexagonal solid and hollow columns, aggregates, 3D bullet rosettes, spheroids, and droxtals. The calculations are carried out for particle maximum dimensions ranging from 2 m to 10000 m. The single-scattering properties of the aforementioned ice particles are computed from a composite method based on the finite-difference time-domain (FDTD) technique, an improved geometric optics method (IGOM), and the equivalent-spherical solution. For the single-scattering properties of spheroids, we use the rigorous T-matrix code developed by Mishchenko and Travis for small and moderate size parameters. Detailed light scattering computations are performed at those wavelengths where sharp variation gradients of the refractive index occur. The computed results at these wavelengths form the database. In turn, the scattering parameters can be developed at a higher spectral resolution through interpolation if required.

The spectral variations of the single-scattering properties are discussed, as well as their dependence on the particle maximum dimension and effective particle size. Furthermore, a parameterization of the bulk optical properties is developed for midlatitude cirrus clouds based on a set of particle size distributions obtained from various field campaigns.

A Geometric Optical Model and Its Combination with 1-D Vegetation Radiative Transfer Model

Qing He, **Daren Lu**
Institute of Atmospheric Physics, Chinese Academy of Science, China

A geometric optical model is developed in this paper, and its combination with 1-D vegetation radiative transfer model is analyzed. The geometric optical model is developed based on the geometric optical model with mutual shadowing (GOMS) of Li and Strahler [2]. Compared with the GOMS model, three major modifications are made in our model. (1) Using poisson crown projection distribution instead of the poisson crown distribution ued in GOMS model to avoid the overestimate the background area when observation direction near nadir. (2) For uniform tree height case, the position calculation of crown self shadowing and mutual shadowing are added in our model. The sunlit and viewed canopy areal proportion and shaded and viewed canopy areal proportion are calculated based both on the area and the positions of these shadowings. (3) In our model, the crown is a semitransparent object instead of the opaque one in GOMS model, and the shaded crown and shaded background are treated as the partly sunlit ones. Set the sunlit part as unit "sunlit degree", the "sunlit degree" of shaded crown and shaded background are determined by the proportion of direct radiation that could pass though the crown and reach the shaded part without been intercepted by the vegetation tissue. Compared with homogeneous canopy, the sphere crown shape can cause different cumulated leaf area and gap proportion variation with solar and viewing angles. So Leaf Area Index (LAI) adjusting coefficient and gap proportion adjusting coefficient are used in our model to account for the sphere crown shape caused LAI and gap proportion variation. Then, combine the areal proportions calculated by the geometric optical model, the two adjusting coefficients, and the uncollided scattering, first collided scattering, and multiply scattering calculated by the 1-D radiative transfer model, the reflectance of heterogeneous canopy can been got. Combined with 1/2 Discrete model [1], our model agrees well with the Monte-Carlo models in Three-Dimensional Heterogeneous Scene experiment in first phase of Radiation Transfer Model Intercomparison (RAMI) exercise [3]. Model results also showed good agreement with observation over boreal broadleaf forest (old aspen). For conifer forest (old jack pine and old black spruce), needles are grouped tightly in shoots, so the sphere shaped shoots are treated as the basic foliage units for radiation modeling, which is quite different from foliage's slice shape assumption used in most radiative transfer models. When the decrease of leaf reflectance and transmittance caused by shoot's sphere shape is counted, the model is able to reproduce with great accuracy the bidirectional reflectance of conifer forest.

REFERENCES

1. Gobron, N., B. Pinty, M. M. Verstraete and Y. Govaerts, "A semidiscrete model for the scattering of light by vegetation", *J. Geophys. Res.*, Vol. 102, 9431, 1997.
2. Li, X. and A. H. Strahler, "Geometric-optical bidirectional reflectance modeling of mutual shadowing effect of crowns in a forest canopy", *IEEE Transactions on Geoscience and Remote Sensing*, Vol. 30, 276, 1992.
3. Pinty, B., et al., "The Radiation Transfer Model Intercomparison (RAMI) exercise", *J. Geophys. Res.*, Vol. 106, 11937, 2001.

Interaction between a Couple of Spherical Particles: Analogy with Circular Young Slits

S. Lecler, **Y. Takakura**, **P. Meyrueis**
Louis Pasteur University of Strasbourg, France

We study electromagnetic coupling of light by a couple of particles in order to have a better understanding of the elementary physical phenomena that can be observed when multiple scattering occurs. This comprehension has a great interest when light scattering is used to find the statistical description of media containing a large amount of particles which have the same order of size than the wavelength. It is particularly true for new applications where the studied media can be made of very dense and closed non-spherical particles (powders for instance). In this case the methods based on the Mie theory and which consider that each particle only scatters the incident light, can no more be used. In these materials multiple and dependent scattering occurs. New algorithms was developed to study multiple scattering, but also to take into account of the shape of particles and of the statistical behavior of the medium. Unfortunately, because of the high complexity of interactions between particles, it is often difficult to identify the elementary physical phenomena that happen. With the systematic study of electromagnetic coupling of light within two spherical dielectric spheres, we point out these elementary physical phenomena. The results are compared with the basic case where each particle of the couple scatters only the incident light. The scattering response is described in term of polarization, scattering diagram and normalized cross section. These parameters are studied for various geometrical configurations. Resonance effects are observed and the criterium between simple and multiple scattering is discussed. All our calculations have been made with a T-matrix algorithm. Principles, advantages and limitations of this algorithm will be described. This study makes possible a better understanding of multiple scattering effects.

A Fast Radiation Code for Data Processing of FY-4/Atmospheric Infrared Sounder

Xuan Feng, **Fengsheng Zhao**
National Satellite Meteorological Center, China

FY-4 is the second generation of the China Geostationary Meteorological Satellite which will be launched in 2012. An atmospheric infrared sounder onboard FY-4 is a 373-channel high resolution spectrometer with a spectral resolution of 2cm^{-1}. The retrieval of atmospheric temperature and humidity profiles needs a fast accurate forward-model to calculate the radiance received by each channel of the instrument. In this connection, we have developped a radiative transfer code aiming at FY-4/atmospheric infrared sounder. It is shown that the code has a reasonable accuracy by comparing with the most detailed radiation models(line-by-line models).

Parameterization for Longwave Scattering of Ice Cloud for Use in Atmospheric Model

Joon-Bum Jee[1,2], **K.-T. Lee**[1,2], **P. Yang**[1,2], **W.-H. Lee**[1,2]

[1]University of Kangnung, Republic of Korea
[2]Texas A&M University, USA

A parameterization for the scattering of longwave radiation by ice clouds have been developed based on spectral property calculations with shapes and sizes of ice crystal. For this parameterization, the size distribution data by Fu [1] and Michell and Arnott [2] are used. And the considered shape of ice crystal are plate, solid column, hollow column, bullet-rosette, droxtal, aggregate, and spheroid [3].

The properties of longwave scattering by ice crystal are presented as a function of the extinction coefficient, single-scattering albedo, and asymmetry factor. The heating rate and flux by radiative parameterization model [4] are calculated for wide range of ice crystal size, shape, and optical thickness, the their calculation results are compared with the calculation results by using a six-stream discrete ordinate scattering algorithm.

REFERENCES

1. Fu, Q., "An accurate parameterization of the solar radiative properties of cirrus clouds for climate models", *J. Climate*, Vol. 9, 2058, 1996.
2. Michell, D. L. and W. P. Arnott, "Amodel predicting the evolution of particle size spectra and radiative properties", *J. Atmos. Sci.*, Vol. 53, 2967, 1994.
3. Yang, P., M. G. Mlynczak, H. L. Wei, D. P. Kratz, B. A. Baum, Y. X. Hu, W. J. Wiscombe, A. Heidinger and M. I. Mishchenko, "Spectral signature of cirrus clouds in the far-infrared region: single-scattering calculation and radiative sensitivity study", *J. Geophys. Res.*, Vol. 108(D18), 4569, 2003.
4. Chou, M.-D., K.-T. Lee and P. Yang, "Parameterization of shortwave cloud optical properties for a mixture of ice particle habits for use in atmospheric models", *J. Geophys. Res.*, Vol. 107(D21), 4600, 2002.

The Study on Fast Radiative Transfer Model under Cloudy Condition

Jianguo Niu[1], **Ping Yang**[1], **Heli Wei**[2]

[1]Texas A & M University, USA
[2]Anhui Institute of Optics & Fine Mechanics, Chinese Academy of Sciences, China

For the purpose of cloudy radiance assimilation in the hyperspectral satellite remote sensing, a flexible fast forward model under cloudy condition (LY2) has been developed. The fast model combines any line-by-line forward radiative transfer calculation with pre-calculated cloud properties to provide a fast estimation of upwelling radiation of satellite measurements under (1) cloud free, (2) a single layer ice cloud, (3) a single layer water cloud, or (4) two layer cloud conditions.

A lookup-table of reflectance and transmittance of both ice cloud and water cloud has been generated using DISORT for various cloud optical thicknesses, effective sizes, satellite viewing angles, and wave numbers based on the computations of single scattering properties of cloud particles. By coupling the reflectance and transmittance of cloud with clear sky atmospheric optical thickness, the upwelling radiance at the top of the atmosphere can be fast derived.

A comparison for simulation conducted by LY2 and by DISORT has been made for the following three conditions of single layer ice cloud, single layer water cloud, and one layer ice cloud over water cloud. It shows promising consistency between two models. The accuracy of the brightness temperature for single layer ice/or water cloud simulated by LY2 is better than 0.5 kelvin degree in the LW region (600 $\sim$ 1200 cm-1); for two layer (one layer ice cloud over one layer water cloud) cloud is better than 1 kelvin degree in LW region.

Session 3A5

Poster Session 1

SAR Imagery Classification Using Multi-Class Support Vector Machines

G. Angiulli, **V. Barrile**, **M. Cacciola**
University Mediterranea, Italy

Classification of earth regions from SAR imagery represents an important developing application of microwave remote sensing. Nowadays, SAR radars allow to make remote surveys with better performances than optical or infrared applications; moreover, SAR radars can be even employed in remote sensing application with prohibitive meteorological situations. On this context, it is inserted the problem of a good recognizing of punctual zones inner a SAR image, according to the specific civil or military application in which remote sensing is applied. Therefore, it is very important in land cover classification using remotely-sensed data that a human visual analisys is supported by an automatic metodology analysis of the same SAR imagery. In our article, we try to solve the problem of pattern identification in a SAR image by using an automatic algorithm based on Support Vector Machines (SVMs) , or better on Multi-class Support Vector Machines (M-SVMs) [1], because there are more than two classes of elements inner test image of our proposed algorithm. Moreover the classes have not clear outlines, with a presence of transition regions among classes. We have chosen to work with Support Vector Machines because their formulation embodies the Structural Risk Minimisation (SRM) principle, which has been shown to be superior to traditional Empirical Risk Minimisation (ERM) principle ,employed by Neural Networks [2]. SRM minimises an upper bound on the expected risk, as opposed to ERM that minimises the error on the training data. It is this difference which equips SVM with a greater ability to generalise, which is the goal in statistical learning. After the description of theorical principles of SVMs and MSVMs, Finally, we illustrate the conclusions of our work, with a comparison among our M-SVM classifiers, a Multi- Layer Perceptron Neural Networks (MLP), a Probabilistic Neural Network (PNN; it is a variant of Radial Basis Network used for classification problems), and a Fuzzy C-means system (FCM). All of them are created and trained on the same SAR image. Our proposed algorithm returns interesting results, with a reliability factor around to 94%, against the 89% given by MLP (the best performances among the non-SVM-based classifiers).

REFERENCES

1. Hsu, C. W., Lin C.-J., “A comparison of methods for Multi-class Support Vector Machines,” *IEEE Trans. on Neural Network*, Vol. 13, 415, 2002.
2. Gunn, S.R., Brown M., Bossley K.M, “Network performance assessment for neurofuzzy data modelling,” *Intelligent Data Analysis*, Vol. 1208 of Lecture Notes in Computer Science, 313, 1997.

Intrinsic Optical Anisotropy in Zinc-blende Semiconductor Quantum Wells

Chun-Nan Chen, **Wei-Chih Chien**, **Kao-Feng Yarn**
Sheng-Hsiung Chang, **Meei-Ling Hung**
Far-East College, Taiwan

An analytical oriented k p method is developed in this paper and applied to calculate the optical transition strength of zinc-blende semiconductor quantum wells. The optical matrix elements and the hole effective masses in the quantum wells are presented in analytical forms. Calculations are performed for quantum wells oriented in arbitrary growth directions. The in-plane polarization angle is adopted as a key parameter in the calculations performed to explore the variation of the optical transition strength in the well plane.

General oriented planes provide a further crucial degree of freedom, which gives device designers a greater flexibility when tailoring the band structure of the semiconductor heterostructures used in advanced optical devices. However, low-symmetry planes will result in optical anisotropy on the growth surface. These non-(001)-oriented planes yield an alteration of the crystal symmetry in the different growth directions and cause a modification of the valence band structure. Many of the optoelectronic devices used in modern optical telecommunication systems require a polarization-independent operation. However, laser diodes are designed in such a way that operation in the polarization direction reduces the threshold current. Therefore, detailed studies of the in-plane optical anisotropy phenomenon are required.

In the theoretical derivation of semiconductors and their heterostructures, the k p approach tends to be the most widely adopted since its calculations and application are relatively straightforward. As an alternative to the conventional k p method, an analytic expression for the k p Hamiltonian can be obtained by expanding the Hamiltonian of the bond orbital model (BOM) in a Taylor series with respect to the wave vector k and then truncating the series to the second order in k. This analytical k p method is more straightforward and computationally efficient than the conventional k p method and can be used to study many optical and electrical problems relating to the semiconductor heterostructures grown on substrates of various orientations.

Finally, the efficient methods presented in this study are beneficial to the design of optical devices fabricated on any substrate orientation. Furthermore, the current investigation provides valuable guidelines for the design of polarization stabilization devices, which require polarization control or selectivity.

Existence of Electromagnetic Radiation in Humans in ELF Band

Jolana Lipkova, **Jaroslav Cechak**
University of Defence, Czech republic

Every living organism on this planet is surrounded by energy in the form of a signal environment. This energy is produced by humans themselves, which results from the substance of living and survival, then it occurs in the form of natural and artificial signals of terrestrial origin and also signals of extraterrestrial origin, signals of both near and distant space. If human beings had the possibility, the gift to see in a far wider spectrum, if they were not only limited to the visible region of spectrum, they would certainly be surprised how dense the signal environment on our planet is. The magic word 'energy', which is the cause of everything, the word that is used in any form and is connected with all living and nonliving, plays an important role.

There are no doubts that humans themselves radiate energy. On the other hand, it must be realized how weak this field is. One component of this energy is formed by signals emitted by the brain. They are signals in extremely low frequencies (ELF) and it is very interesting to understand them and to learn how to control them. The signals emitted by the nature itself are not less interesting. An overwhelming majority of these signals affect almost all audible range and by detecting them we are able to understand many natural processes.

The presented contribution is aimed at the area of possibility to detect signals in the ELF band. It presents a designed and used aerial system suitable for the reception of ELF signals. The contribution includes a separate chapter on Schumann resonance which explains many processes in human mind.

It presents designed methods and procedures of digital processing of recorded signals in the ELF band. The following chapter deals with an analysis and filtration of signals radiated by human body and their interpretation on the background of Schumann resonance including their harmonic multiples.

The results of digital processing of ELF signals are presented in the contribution in a graphical form, as well as in the form of photographs taken during the recording of signals.

The conclusion of the contribution deals with the possibilities of using the analysis of ELF signals for the detection of persons, for example, stuck under an avalanche, caved in a mine, etc.

TFBAR Size Effects on the Impedance Characteristics in Out-of-band Rejection

Yong-Dae Kim[1], **Sung-Hoon Choa**[2], **In-Sang Song**[2], **Jong-Gwan Yook**[1]

[1]Yonsei University, Korea

[2]Samsung Advanced Institute of Technology, Korea

Recently, TFBAR filter has been developed to use in miniaturized wireless communication system instead of ceramic or SAW filters because TFBAR filters are much smaller than the above types of filters. The performance of TFBAR filter is determined by a unit resonator. Moreover, the electrical impedance of TFBAR is one of the very important characteristics in addition to insertion and return losses. to investigate the impedance characteristics in stop-band regions, the various shape TFBARs are fabricated, having different the areas of resonators. Fabricated air-gap type TFBAR is shown in Fig.1. in this work, aluminum nitride is sandwiched between the top and bottom electrodes as a piezoelectric material, and a very thin air-gap is placed under the membrane to avoid the over-mode phenomenon due to the silicon substrate loading. The series and parallel resonant frequencies of TFBAR are 1.920 GHz and 1.961 GHz. As the area of unit TFBAR increases, it is shown that the electrical impedance in out-of-band is significantly decreasing, while the frequency spacing between the series and parallel resonant frequency remains unchanged. The reason is that as the area of resonator increases, the electrical and mechanical capacitance of resonator changes and affects the resonant frequencies. In this paper, it is investigated on how the size of TFBAR affects the electrical impedance characteristics in stop-band region.

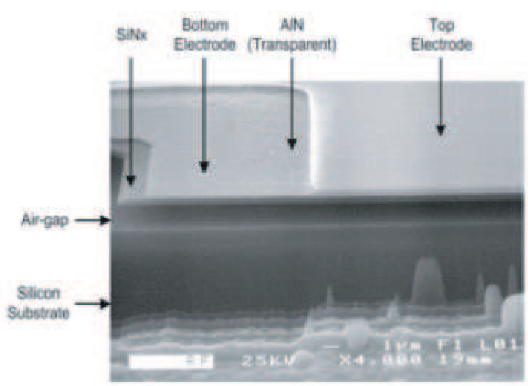

Figure 1: Cross-section of fabricated TFBAR

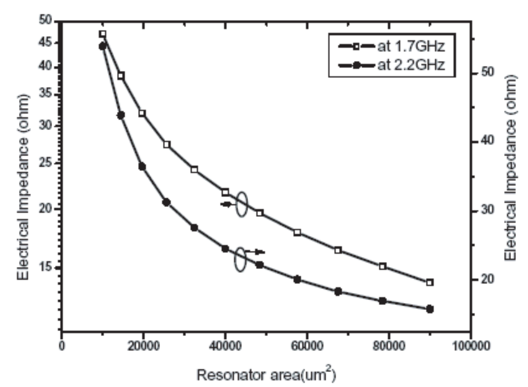

Figure 2: Impedance graph due to various size

The Optimal Design Method of Completely Open Architecture Permanent Magnet for Magnetic Resonance Imaging

Yingying Yao, **Youtong Fang**, **Guangzheng Ni**
Zhejiang University, China

Chang Seop Koh
Chungbuk National University, Korea

A lot of efforts to enlarge the “open” degree of traditional MRI equipments have been done in order to provide convenient access to the imaging region and a better imaging quality. However, existing open architecture designs include double iron pole pieces with intervening support members so that they all can hardly be utilized for interventional diagnostic or surgical procedures. In this paper, a completely open architecture magnet is proposed. Its imaging region, where a patient to be imaged is supposed to be located, exists on one side of a planar, or many-sided surface. The imaging region is completely open, and satisfies the requirement of a MRI system for obtaining images during the surgical procedure. A new flexible design method is proposed to facilitate the construction of a completely open MRI magnet by combining the magnetic dipole pair model and optimization algorithm. Based on the magnetic dipole pair model and saddle point rule [1], the initial structure of the magnet is constructed by several pairs of permanent magnet blocks which are magnetized in different directions. Some compensative parts and iron shell are placed in proper positions to get a higher magnetic field strength at the imaging region. To get a magnetic field with higher homogeneity and field strength at the imaging region, the magnetic flux density within the imaging region is calculated using finite element analysis and is expanded by using spherical harmonics of Legendre polynomials. The least square fit method is used to determine the magnitudes of each term. Then genetic algorithm is used to design the dimensions and orientations (directions of the magnetization) of each permanent magnet block and minimize the summation of harmonics within the imaging region. A numerical implementation shows that the new design provides a main magnetic field having sufficient homogeneity and strength at the imaging region, which is defined outside of the magnet structure, and minimizes the cost of this MRI equipment.

Loss of Information in Random Electromagnetic Field as a Quality Coefficient

Konrad Skowronek, **Jerzy Frąckowiak**, **Piotr Szymkowiak**, **Grzegorz Trzmiel**
Piotr Walczak, **Artur Woéniak**
Poznan University of Technology, Poland

The typical methods of research (measurement) of magnetic and electric field distribution are a method of deterministic analysis. In most cases useful results are given. Application of more advanced optimization (for example: reliability calculations) may lead to wrong results. The method of description of random fields with outcome set is a very profitable way of solving linear and nonlinear fields problems, because it reduces the problem to a set of deterministic outcome.

The evaluation of loss of information in system of random magnetic and electric field was presented in the paper. The set of field parameters in a specified points of the space is obtained from electromagnetic field measurement. The subsets of parameters values may be treated as the subsets of outcomes of random variables witch defines field parameter in a specified point (for some assumptions). The numerical analysis of that subset gives probabilistic parameters of the field. The calculation of loss of information was introduced as an example as well as the set of simplifying assumptions in the system model. The application of presented analysis was also mentioned. The significance of the presented analysis is, that it offers an analytical solutions to the statistical estimation of maximum expected values as well as probabilistic parameters of examining systems. At present, one could try forecasting, or even controlling reliability of this (or similar) equipment during long-lasting application of the equipment under many-years' operation in random conditions.

General Analysis on Nonmatched Characteristics of the PML and a Novel Parameter Optimization Method

Yong Zhang, **K. R. Shao**, **X. W. Hu**
Huazhong University of Science and Technology, China

J. D. Lavers
University of Toronto, Canada

Perfectly matched layer (PML) is a layer especially designed by Berenger to simulate free space at the boundaries of a Finite-Difference Time-Domain (FDTD) computational domain. Theoretically, all the PMLs can absorb outgoing waves without any reflection from the vacuum-PML interfaces and PML-PML interfaces, and this is the matched characteristic of the PMLs. However, in actual computation with discrete method such as FDTD, no truly matched characteristic existed in the PMLs, thus amount of numerical reflection inevitably occurs.

This paper firstly analyzes the nonmatched characteristics of the PMLs in FDTD, and then proves that it is the iterative parameters make the PMLs get wideband absorption quality, and these parameters are independent of the simulative frequency. A novel parameter optimization method is also presented in this paper to optimize a conductivity serial.

Fig.1 and Fig.2 show the relationship between theoretical and actual reflections determined by above four profiles. Their large deviations indicate the inherent contradiction of the PML Theory in FDTD.

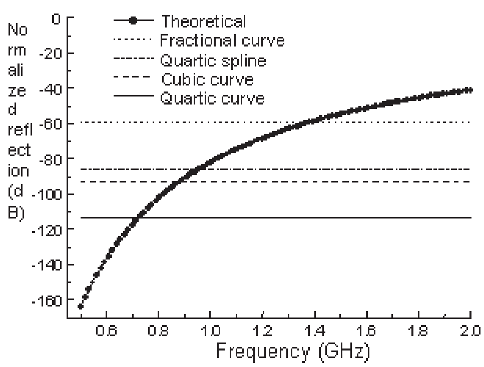

Figure 1: Reflection coefficients as a function of frequency

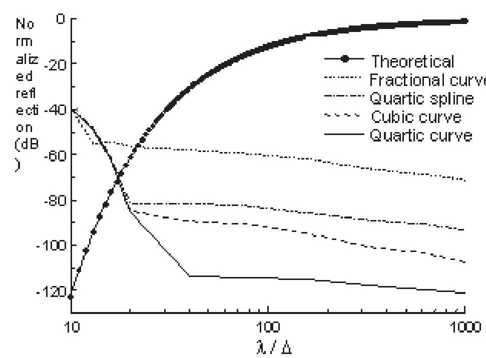

Figure 2: Reflection coefficients as a function of λ/Δ

*This work was supported by National Natural Science Foundation of China (NSFC) under Grant No.50477045 and Specialized Research Funds for the Doctoral Program of High Education (SRFDP) under Grant 20030478063.

Modified Wilkinson Power Divider with EBG

Ban Leong Ooi, **Daoxian Xu**, **Guang Zhao**
National University of Singapore, Singapore

The Wilkinson power divider and combiner have been widely used for microwave power amplifiers [1], and [2]-[3]. They have same structure, which consists of two $\lambda/4$ branches of transmission line and a termination resistor, where λ is the wavelength of the transmission line.

In the basic structure of a Wilkinson power divider [1], and [4]-[5], the two transmission lines and the termination resistor R match all input and output ports simultaneously and provide a good isolation between the input ports of the power combiner and between the output ports of the power divider. Also, they can handle arbitrary power levels from input to output ports. If the harmonics are suppressed in the power divider or combiner structure, we can eliminate separate harmonic rejection filters from the circuit and design an area-effective power amplifier (as reported in [3]).

The use of photonics materials has been driving the relative theory to the propagation of optical waves [6]. The theory of photonic band-gap (PBG) or electromagnetic band-gap (EBG) was developed initially for optical frequencies and can easily be applied to millimeters waves and microwaves [6]. Generally, EBG can diminish the propagation constant causing the wave to move slowly [7]. Then in this paper, we utilize the spiral EBG into the power divider design and attempt to achieve better divider performances.

The measured insertion loss of the modified power divider is better than -3.5dB from 1.2GHz to 2.2GHz and the bandwidth is 58.8% centered at 1.7GHz. The measured return losses of the divider are less than -10dB from 0.4GHz to 2.6GHz for the input port and from 0.2GHz to 2.15GHz for the two output ports.

REFERENCES

1. Wilkinson, E., "An N-way hybrid power divider", *IRE Trans. Microwave Theory Tech.*, Vol. MTT-8, 116, 1960.
2. Pozar, D. M., *Microwave Eng.: Addison-Wesley*, 395, 1990.
3. Yi, K. H. and B. Kang, "Modified Wilkinson power divider for nth harmonic suppression", *IEEE Microwave and Wireless Components Letters*, Vol. 13, No. 5, 178, 2003.
4. Nishikawa, K., T. Tokumitsa and I. Toyoda, "Miniaturized Wilkinson power divider using three-dimensional MMIC techonology", *IEEE Microwave and Guided Wave Letters*, Vol. 6, No. 10, 372, 1996.
5. Ogawa, H., T. Hirota and M. Aikawa, "New MIC power dividers using coupled microstrip-slot lines: Two-sided MIC power dividers", *IEEE Trans. Microwave Theory Tech.*, Vol. MTT-33, 1155, 1985.
6. Rocha, A. R. B. and H. C. C. Fernandes, "Dynamic method for antennas with PBG", *Twenty Seventh International Conference on Infrared and Millimeter Waves*, 89, 2002.
7. Kretly, L. C. and A. Tavora. A. S., "A PBG-photonic band gap-static phase-shifter for steerable antenna array", *Microwave and Optoelectronics Conference*, Vol. 1, 211, 2003.

A Global Optimization Algorithm Based on Constructing a Surrogate Objective Function with Design Sensitivity Analysis

Yingying Yao, **Guangzheng Ni**, **Shiyou Yang**
Zhejiang University, China

Chang Seop Koh
Chungbuk National University, Korea

The deterministic method, such as the gradient method incorporated with the design sensitivity analysis, is preferred to the engineering design, especially for the 3D shape optimal design, since it requires much less computation of the objective function. However, its optimum value depends on the choice of starting point and sometimes falls into local minima. The stochastic optimization methods, such as genetic algorithm, give the global optimum solution in most cases. However, when combined with finite element analysis for an engineering application, they are computationally time-consuming because they require a lot of computations of the objective function. In this paper, a new surrogate objective function is suggested for the global optimization of electromagnetic devices. The surrogate objective function is constructed using gradient radial basis function. At each sampling point, the objective function value and its gradient are computed by combining the Design Sensitivity Analysis with Finite Element Method. The surrogate objective function is obtained by using Least Square Method through matching the design sensitivity (the gradient vector) as well as the objective function value itself in the design variable space. After the surrogate objective function is constructed, the global optimum point is found by using Genetic Algorithm. Applications to benchmark problems and the optimum design of a permanent magnet system show the effectiveness of the proposed algorithm.

Coaxial Antenna for Microwave Hyperthermia

A. Rhattoy, **S. Bri**
Université Moulay Ismail Meknes, Morocco

M. Audhuy-Peudecederf
ENSEEIHT-INPT, Toulouse, France

During the last decades, many studies are interested in the study of the electromagnetic waves like source of energy; the latter are used not only in industry, but also in the scientific and medical applications. The quasi-totality of the work relating to the antennas concern the radiation to the infinite one, which cannot be the case of the applicators microwaves.

Our contribution consists of the study of cylindrical antennas structure of various geometrical configurations, making it possible to model the distribution of the power in material according to the treatment wants.

We present in this paper a coaxial applicator in which the radiating source is a circular slot realised by exterior conductor interruption of a coaxial guide. The guide is immersed in a strong dissipated medium. A dielectric material girdle without losses or an air layer is inserted among the radiating slot and the load. In these papers, we study a single slot radiation. We analyse the radiating field distributions in the load, the approaching field influences and the role of dielectric girdle on the dissipated power distribution in the load.

For calculates the power and the SAR distribution around applicator, we have use the modal decomposition method, and finites elements method and to validate the method of calculation we have compared the theoretical with the experimental results.

Analysis of Circular Patch Microstrip Antennas on Anisotropic Substrates Using Hertz Potential Method

Giordano Miranda Feitoza[1], **Sandro Gonçalves da Silva**[1]
José de Ribamar Silva Oliveira[2], **Adaildo Gomes d'Assunção**[1]

[1]Federal University of Rio Grande do Norte, Brazil
[2]Centro Federal de Educação Tecnológica do Rio Grande do Norte, Brazil

Microstrip structures are suitable for microwave applications because of their characteristics such as small volume, low weight, and low cost. Usually, they are developed on isotropic substrates. Nevertheless, in last years, several papers were devoted to the characterization of microstrip structures, such as resonators, patch antennas and frequency selective surfaces, on anisotropic layers, because dielectric materials are in fact anisotropic ones.

The analysis is developed for the suspended microstrip circular patch antenna, where the conducting patch is printed on a dielectric uniaxial anisotropic layer, that is separated from the ground plane by a second layer filled with air. The dielectric layer above the conducting patch is filled with air. The analysis uses a combination of the Hertz vector potential technique and the method of moments, in the Hankel domain.

Firstly, the Hertz vector potentials are defined in each dielectric layer and then used to determine, by imposing the boundary conditions, the dyadic Green's function for the circular patch microstrip antenna. In the anisotropic layer, the Hertz vector potentials are oriented along the optical axis, that is perpendicular to the microstrip ground plane. Secondly, the Green's function and the method of moments are used to get numerical results for the circular patch antenna resonant frequency, bandwidth, and quality factor.

Results are obtained for circular patch antennas on boron nitride and sapphire substrates. Note that the height of the air-filled layer can be varied to adjust the antenna characteristics.

Figure 1 shows the geometry of a circular patch microstrip antenna on a uniaxial anisotropic layer. This is a particular case of the analysis developed in this work. The numerical results obtained for this antenna are in agreement with the results published recently in the literature. A good agreement was also observed for the particular case of circular patch antennas on isotropic substrates.

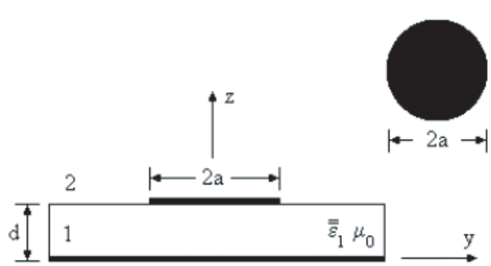

Figure 1: Geometry of a circular patch microstrip antenna on uniaxial anisotropic substrate.

A Quick Capacitance Extraction Tool for IC Interconnections

Jintao Xue, **Gaofeng Wang**, **Yong Feng**, **Yang Yang**, **Qing Xu**
Wuhan University, China

A system capable of automatic interconnect capacitance extraction is described. With a GDSII layout format file and an interconnect technology description file as input, the system displays the layout in 2-D/3-D modes, and extracts interconnect parasitic capacitance automatically for the selected critical nets or entire layout. Employing a multipole accelerated GMRES based fast three-dimensional (3-D) field solver, the system exacts parasitic capacitance very quickly and accurately for arbitrary interconnects embedded in piece-wise constant dielectrics. The system represents a significant performance leap in 3-D interconnect capacitance extraction, making it well suited for high-accuracy interconnect characterization of packaging, critical nets, block IP, standard and custom cell designs. A quick 2-D capacitance extraction solver is also integrated into this system. Examples show that compared with a 3-D solver, a 2-D solver exhibits accurate and very quick capacitance extraction for long parallel interconnects, but introduce large errors for non-parallel or short parallel conductors. A multi-solver manager which selects a 2-D or 3-D solver automatically according to the 2-D/3-D characterization of an interconnect geometry to maintain an accurate yet quick extraction is suggested. The system architecture and numerical techniques of capacitance extraction solvers are discussed in this paper. The good capacitance extraction accuracy of 2-D/3-D solvers is verified for some structures in comparison with published data. In the end, the speedup of the adaptive, hierarchical multipole accelerated GMRES based 3-D solver is proved for $k \times k$ crossing bus structures. For a 8×8 crossing bus structure, the multipole accelerated GMRES based 3-D solver exhibits more 44 times speedup than a direct matrix-vector product based 3-D solver.

A Circuit Model for Cylindrical Plasma Waveguide

Bin Yuan, **Fang Cheng**, **Wei Xu**, **He Zhou**, **Lei Zhao**
Shanghai JiaoTong University, China

I. Introduction

In this paper the circuit model of cylindrical plasma waveguide is studied. It will prompt the progress of plasma microwave devices effectively. The plasma devices have been used successfully in steering antenna, microwave mirror, Traveling-Wave-Tube (TWT) and plasma filters. Some related basic theories, such as dispersion relationships of waves in plasma, attenuation theory, and single-mode propagation theory of microwaves in plasma have been studied. But, a circuit model of cylindrical plasma waveguide, one of the basic theories of plasma filter and TWT, has not been investigated. After adopting quantum and hydromagnetic theory, considering the flexibility of plasma, the model special for cylindrical, magnetized, cold plasma waveguide in VHF/UHF band is presented. This model is not only the result of theoretical analysis but also proved by numerical analysis and experiment. The method adopted here can also be applied to develop other circuit models in HF, X and millimeter bands.

II. Circuit Model for the Waveguide

In the circuit model, the total capacitance and inductance are caused by two facts, one is the effect of quantum and the other is the hydromagnetic function.

The hydromagnetic function results in the electrostatic capacitance and the magnetic inductance. This function is introduced into and represented by the anisotropic dielectric tensor e and the permittivity tensor m . Thus, the formulas of the capacitance and the inductance are formulated from Maxwell equations consequently.

A lossless circuit model is founded after taking the effect of quantum into account. Extending this model, a lossy circuit model including collision frequency loss of the electrons and ions is established.

III. Numerical Analysis and Experimental Results

The numerical analysis consists of two parts, field analysis and circuit simulation. For the first part, CST software is adopted and the distribution of field is got to evaluate the formula of theory. The circuit simulation is realized by ADS software and the S parameters of the model are got, which will be compared with the experimental data.

As about the experiment, several pieces of tubes and coupling devices are fabricated. The results of experiment are presented in three tables.

IV. Conclusion

The circuit model in VHF/UHF band has been presented. The formulas of parameters based on the effect of quantum and the hydromagnetic function are formulated. Based on these formulas, the effects of static magnetic field on the propagation of plasma waveguide in VHF/UHF band can be derived directly, which proves the model in another aspect too.

The work is supported in part by the National Natural Science Foundation of China under Grant 60371022.

Feature Enhanced of Stripmap SAR Images Based a Conjugate Gradient Method

Cheng-Yen Chiang[1], **Kun-Shan Chen**[1]
Tzong-Dar Wu[2], **Chi-Huei Tseng**[1], **Yu-Chang Tzeng**[3]

[1]National Central University, Taiwan
[2]National Taiwan Ocean University, Taiwan
[3]National United University, Taiwan

Target identification and recognition of SAR images require good feature selection and enhancement. Due to the coherent process, it is difficult to discriminate the SAR target feature properties simply using the shape, shadow, tone, color and texture, to name a few. The scattering center is one of the important properties for extracting the SAR feature. This involves working on raw data (amplitude and phase) as part of image formation. In this paper, we modified an algorithm based a conjugate gradient (CG) optimum method originally proposed for spot mode SAR images, in order to enhance the stripmap mode SAR targets. The SAR image reconstruction method for spotlight mode uses the range profile data that displays on spatial frequency domain in polar form. By the conventional method it is resampled to be in rectangular form, followed by using inverse Fourier transform with properly weighted window. In [1] the recompiling method is done by introducing a projection operator kernel. Directly applying CG method, one has to change the data format to range profile of polar form but suffer from information loss in this recompiling processing. To avoid this information degradation, it has been suggested to replace SAR projection operator kernel by Fourier transform kernel, and let it have suitability for stripmap mode data.

To validate the effectiveness and efficiency of the modified method, a series of RADARSAT SAR images at fine mode were tested with ground truth available overpass the image acquisition. We also compared the performance with MV (Minimum Variance) and MUSIC (Multiple Signal Classification) methods. Performance indices include target to clutter ratio, 3 dB mainlobe width and CPU time. It was demonstrated that modified method provides the best performance among the three methods.

REFERENCES

1. Müjdat Çetin and William Clem Karl, "Feature-Enhanced Synthetic Aperture Radar Image Formation Based on Nonquadratic Regularization", *IEEE Trans. Image Processing*, Vol. 10, No.4, 623, 2001.

A Modification to the Rytov and Born Approximation

Y. L. Liu, **Lianlin Li**, **Fang Li**
Institute of Electronics, Chinese Academy of Science, China

Wave propagation and scattering in the random media have been an important topic for many years. The Born and Rytov approximation are used to solve the wave equation and analyzing the correlative problem in most cases. However this approximation can be used for weak fluctuation only. For the cases of strong fluctuation, Some methods such as parabolic equation approximation, ray approximation, Huygens methods, path integral method and multi-phase screen etc were proposed. All these methods are complex. In this paper, the reasons why the Born and Rytov approximation cannot been used for strong fluctuation are analyzed. A modification method is proposed. The Green function in finite space is used instead of that in free space. The result show that this modification method can extend into case of strong fluctuation well.

A New Algorithm for the Electromagnetic Computation

Lianlin Li, **C. J. Jiang**, **Fang Li**
Institute of Electronics, Chinese Academy of Science, China

This report describes a method for computation of the electromagnetic problems by the Laguerre polynomial expansion in time domain.

$$\vec{E}(\vec{r},t)=\sum_{n=0}^{N_t}\vec{e}_n(r)f_n(st) \tag{1}$$

$$\vec{H}(\vec{r},t)=\sum_{n=0}^{N_t}\vec{h}_m(r)f_n(st) \tag{2}$$

where $f_n(st)=e^{-0.5st}L_n(st)$ and $L_n(\cdot)$ is Laguerre function. According the orthonormal of Laguerre function the Maxwell equations in time domain, boundary value problem combined with initial value, are changed into only boundary value problem

$$\nabla\times\vec{e}_m(\vec{r})=s\mu(\vec{r})[0.5\vec{h}_m(\vec{r})+\sum_{n=0}^{N_t}(\vec{h}_n(\vec{r})\sum_{i=0}^{n-1}\delta_{i,m})]-\sigma_m(\vec{r})\vec{h}_m(\vec{r})-s\int_0^{\infty}J_m(\vec{r},t)f_m(\vec{r},st)dt \tag{3}$$

$$\nabla\times\vec{h}_m(\vec{r})=-s\varepsilon(\vec{r})[0.5\vec{e}_m(\vec{r})+\sum_{n=0}^{N_t}(\vec{e}_n(\vec{r})\sum_{i=0}^{n-1}\delta_{i,m})]+\sigma_m(\vec{r})\vec{e}_m(\vec{r})+s\int_0^{\infty}J(\vec{r},t)f_m(\vec{r},st)dt \tag{4}$$

It can be operated by finite difference methodfinite element method and method of moment etc. In this case any complex electromagnetic problems can be solved involving inhomogeneous and anisotropic bodies with arbitrary shape. Additionally, unlike the finite difference in time domain and the moment techniques in time domain, there is no later time error caused by the accumulative numerical error.

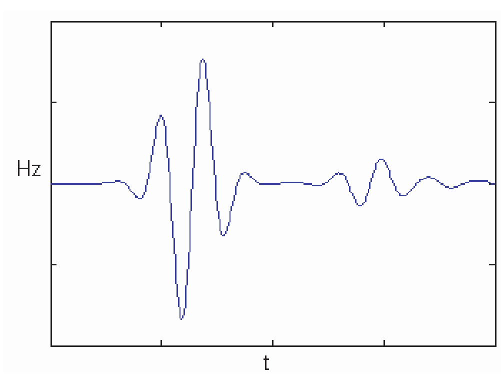

Numerical results validate the method and show its capabilities. The problem of a cylindrical eliminated by sine-Gauss wave as an example is shown in Figure 1.

Ionospheric Radio Tomography Using ARMA

Lianlin Li, **C. J. Jiang**, **Y. L. Liu**, **Fang Li**
Institute of Electronics, Chinese Academy of Science, China

Ionospheric tomography can be viewed as an inverse problem. The potential of imagine large ionospheric structures by applying tomography techniques has been received interest and increasing attention in ionospheric research. Unlike other tomography techniques, such as in medical field etc, here the data is available only from some finite discrete position and from a finite angular sector. Furthermore, the data can be easily corrupted by noise. How do reconstruct deteriorated image under this condition? In this paper a technique using ARMA (Auto Regressive Moving Average) is proposed. By ARMA the original data automatically extrapolated. The total electron content $TEC = \int\limits_{path} N(x,y)ds$, where N(s) the electron density at point (x, y) is extrapolated as

$$N(x,y) = \frac{a_0x^0 + a_1x^1 + a_2x^2 + a_3x^3 + \cdots + a_mx^m}{b_0x^0 + b_1x^1 + b_2x^2 + b_3x^3 + \cdots + b_nx^n} \equiv N(m,n,x,y)$$

where coefficient are determined by TEC of the region where at least two rays are passed (Fig. 1).

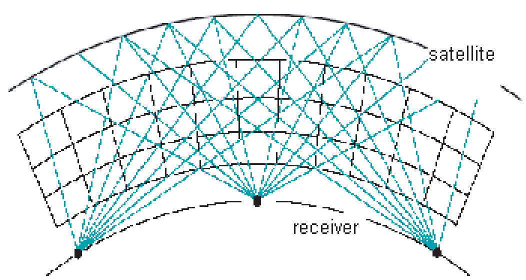

Figure 1: Scheme showing the geometry involved in a Ionospheric tomography

An example of simulation is given in Fig. 2.

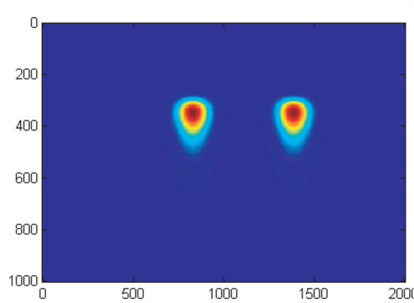

Figure 2.1: the image of electron density of the ionosphere

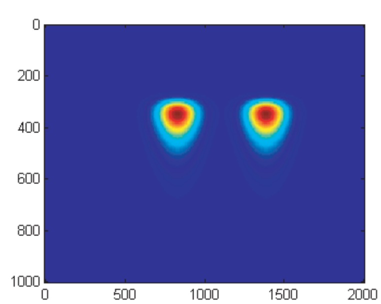

Figure 2. 2: the image of electron density of the ionosphere by ARMA

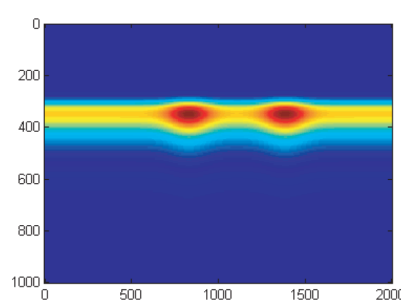

Figure 2.3: the image of electron density of the ionosphere by Yeh's method

Rigorous Nonlinear Analysis of Propagating Waves in the Strip-slot Waveguiding Structure with a Strongly Nonlinear Semiconductor Discontunity

Galina. S. Makeeva
Penza State University, Russia

Oleg. A. Golovanov
Penza Military Institute of Artillery, Russia

Martha. Pardavi-Horvath
The George Washington University, USA

The goal is the investigation into the nonlinear interactions of electromagnetic waves with bounded strongly nonlinear semiconductor medium in waveguiding structures (WGS). The mathematical simulation is based on the solution of diffraction boundary problems for nonlinear Maxwell's equations, complemented by the equation of the motion of charge-carriers in semiconductors.

The computational algorithm for solving of nonlinear diffraction boundary problem was developed using cross-sections method. The Cauchy's problems for a system of ordinary differential equations were solved using Runge-Kutta's numerical method; the system of nonlinear functional equations were solved using Newton's numerical method.

Using this algorithm the accurate electromagnetic modeling of the diffraction and nonlinear interactions of waves on the semiconductor discontinuity with planar geometry in strip-slot WGS was carried out. The magnitudes of reflected (in local coordinate system on output cross-sections of semiconductor insertion) modes on combination frequencies were determined, if the magnitudes of incident (on input cross-section) fundamental and higher modes were known.

Using the numerical method of nonlinear autonomous blocs, the magnitudes of reflected modes at four multiple time harmonics depending on the magnitude of incident fundamental mode were calculated taking into account variable geometry sizes of semiconductor insertion; the optimum length for the efficiency of frequency multiplication was determined.

Using our computational algorithm to analyze the bifurcation points of the nonlinear Maxwell's operator the onset of self-excited oscillations in the distributed Gunn diode with planar geometry included in strip-slot WGS depending on the value of biasing electric field were simulated infinitesimally close to the bifurcation points.

DDWS Radar Signal Generator

Heng Qi, **Lixin Ran**
Zhejiang University, China

In this paper, a realization of radar signal generator (RSG) using the technique of DDWS (Direct Digital Waveform Synthesize) is introduced. The system is composed of high-speed programmable ASIC device, Synchronized Dynamic RAM, and high-resolution 14-bit, 300MHz DA convertors. Many kinds of radar signals can be generated using such single scheme, one of which is the chirp signal with a bandwidth more than 80MHz. The system noise is usually one of the key problems in RSG design. A digital pre-distortion technology has been utilized to solve the noise. The pre-distortion module stores the waveforms and compensates their amplitudes and phases which have been disturbed by the system. This process allows the output signal obtaining good noise performance.

Figure 1 shows the spectrum and the waveform of a chirp signal generated by the DDWS generator, which has a bandwidth more than 40MHz and a signal-noise ratio exceeding 45dB.

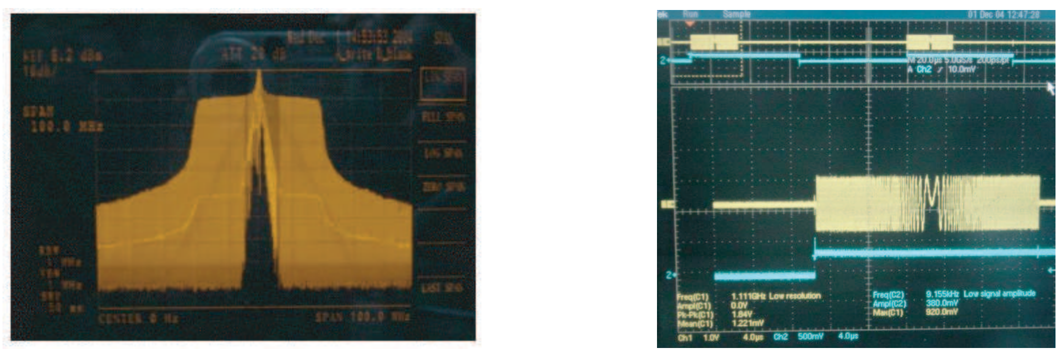

Figure 1: Chirp signal generated by the DDWS generator

Analysis of Strip Gratings Placed Close to DNG Slabs

Masamitsu Asai[1], **Jiro Yamakita**[2]

[1]Kinki Univ., Japan
[2]Okayama Pref. Univ., Japan

Metamaterials possessing negative real parts of permittivity and permeability at some frequencies named double negative (DNG) materials have been of increasing interest in the community of physics, radio science etc [1]. Vectors of electric and magnetic fields and wave vectors of EM waves in this kind of materials from left-handed (LH) systems 1ems corresponding to the negative indices of refraction (NRI) which V.G. Veselago first theorized in 1967 [2]. Potential applications and concepts have been reported especially since perfect lens concept was suggested [3] and the NRI was experimentally verified by constructing an artificial LH material [4]. Analyses of scattering from plane gratings on the other hand have been fundamental research themes [5] and propagating and evanescent fields influenced by the reversal of Snell's law and lens properties etc. based on NRI are things to be studied. This paper presents a matrix-based analysis to simulate scattered waves from an infinitely thin metallic strip grating which is placed close to a slab of DNG medium. The grating is assumed to have periodicity Λ and width of each strip W and to be placed on DPS and DNG slabs with thickness d_P and d_N respectively. This structure infinitely extends to y and z directions and is placed between semi-infinite air regions. An incident wave with propagation vector parallel to xz plane is assumed to illuminate. When the thickness of the DPS region d_P becomes small, not only the propagation fields but also the evanescent ones from the grating enter the DNG region and the diffraction characteristics, not just on the reveal of the direction, could be influenced by the negative index of refraction. The quantitiative effects are numerically investigated.

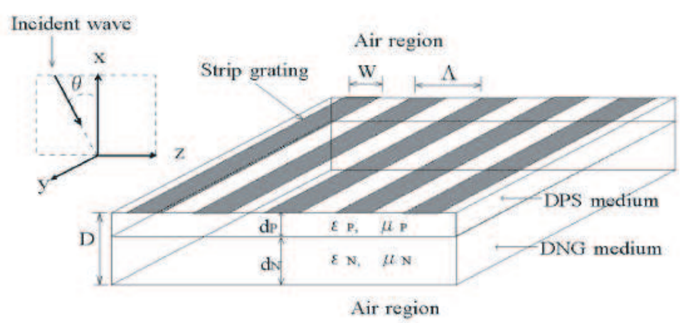

Figure 1: A Strip Grating and DNG Slab

REFERENCES

1. *IEEE Trans. Antennas Propag., Specical Issue on Metamaterials*, Vol. 51, No. 10, 2003.
2. Veselago, V. G., *Soviet Physics Uspekhi, 1968 English translation, 1967 Russian*, Vol. 10, No. 4, 509.
3. Pendry, J. B., *phys. Rev. Lett.*, Vol. 85, 3966, 2000.
4. Shelby, R. A., D. R. Smiath and S. Schults, *Science*, Vol. 292, 77, 2001.
5. Asai, M. and J. Yamakita, H. Wakabayashi, *Proc. APMC 2002*, Vol. 3, 1533, 2002.

Magnetic Fields Computation and Optimal Design of High Temperature Superconducting YBCO Flywheel Models

Guo Qiang Zhang
The Institute of Electrical Engineering, Chinese Academy of Sciences, China

Archie M. Campbell, **Amit Rastogi**, **Tim Coombs**
Cambridge University, UK

Thanks to the adoption of the superconducting bearing, flywheel electric energy storage systems achieved low loss and high energy density. Meanwhile, with the applications of bulk high Tc superconductors (HTS), the maximum magnetic energy of the combined system between HTS and permanent magnets exceeds the limitation by pure permanent magnet systems.

The fundamental feature of the YBCO superconductors is the tendency to partially exclude magnetic flux from their interiors by developing a shielding current that flows near the surface. If the external field is lowered, the shielding current is induced only on the surface of the HTS and the original applied field is trapped in the center of HTS. However, if the change in the applied field is large enough, the shielding current flows in the whole volume of the HTS.

Previously, the calculations of magnetic field in YBCO superconductors have been treated in ways similar to ferromagnetic materials. The critical-state models, such as Bean model or Kim model, have been successfully used to describe the hysteretic behavior of HTS and to predict the current distribution inside HTS bulks. However, finite element software to include ferromagnetic and superconducting materials is not readily available.

A new calculation procedure, which can be called the Trapped Field Magnet (TFM) method, is proposed in this paper to predict the magnetic flux distributions and the stiffness of a flywheel model.

The experimental results in field-cooled condition show that the proposed procedure can be used to get a reasonable field distribution when the displacement of the rotor is less than a few millimeters. The calculated stiffness in zero field-cooled condition is also presented.

Multiuser Adaptive Modulation for MIMO-OFDM System

Ling-Yun Cai, **Chun-Ling Zhang**, **You-Yu Xu**
Hai-Bin Zhang, **Wen-Tao Song**
Institute of Wireless Communications Technology, China

Orthogonal Frequency Division Multiplexing (OFDM) is a powerful technique employed in wireless communications systems suffering from frequency selectivity. Combined with multiple antennas at the transmitter and receiver as well as adaptive modulation, OFDM proves to be robust against channel delay spread. In the existing algorithm, the power, subcarrier and bit allocation in multiuser for single antenna and antenna diversity systems are proposed to show that the adaptive power and bit allocation can improve the system performance.

In this paper, assuming knowledge of the instantaneous channel gains for all users, we propose the novel power and bit allocation scheme, in which the lowest transmission rate requirements of the different users are considered, in which the multi-antenna is considered as the different channel. The algorithm includes: (1) the power and subcarrier allocation due to the lowest transmission rate requirement; (2) the bit allocation; (3) the power and bit allocation revision. During the power allocation the users have the different degree power remain, which is often wasted in the existing scheme. However, in this paper we collect these remain power and reallocate it to other users and shown in algorithm step (3), so as to improve the transmission rate.

Finally, the simulation results show that our proposed algorithm outperforms multiuser MIMOOFDM systems with static time-division multiple access (TDMA) or frequency division multiple access (FDMA) techniques, which employ fixed and predetermined time-slot or subcarrier allocation schemes. We have also quantified the improvement in terms of the overall required transmit power, the bit-error rate (BER). In addition, the MQAM technique is only employed in the paper due to the practical application of a variable-rate variable-power.

Bipolar Optical Correlation Implemented by Incoherent Spectral Amplitude/Polarization Coding on Differential Photo-detectors

Yao-Tang Chang, **Jen-Fa Huang**
National Cheng Kung University, Taiwan

As for conventional spectral amplitude coding (SAC) scheme in local area network, it exists crucial limitation that the number of simultaneous active users is increased. The codeword length is naturally increased in order to achieve the same performance [1]. In incoherent OCDMA system, conventional SAC scheme is mostly concerned that the multiple access interference (MAI) can be eliminated [2]. Furthermore, phase induced intensity noise (PIIN) is increased such that the numbers of simultaneous active users are limited [3]. In order to implement bipolar spectral system, Dennis et al. [4] configured an approach by representing a bipolar codeword as two serial unipolar sequences. However, the approach make a result that bit-error-rate (BER) is severely degraded due to occupying double spectrum (optical bandwidth) on non-flat spectrum of incoherent source.

In the proposed bipolar SAC/SPC scheme, two orthogonal polarization states (e.g., vertical and horizontal states) of lightwave carrier are utilized to transmit signal pulse in single mode fiber. The SAC/SPC chip words are assigned from Walsh-Hadamard matrix with the two orthogonal polarization states. In the bipolar chip words, positive value (+1) is referred as the vertical state of polarization (SOP), and negative value (-1) is referred as the horizontal SOP. SAC/SPC encoder/decoder structured with fiber Bragg gratings (FBGs) and polarization beam splitters (PBS) are verified suitable for bipolar spectral system. That is, all the bipolar code, which have successfully been applied in radio frequency (RF) domain, such as maximal sequence and Walsh-Hadamard codes can be directly adopted as signature codeword.

Since the proposed scheme is achieved double spectral efficiency compared to previous done work [4], it implies that the number of simultaneous active users can be dramatically increased under the same optical bandwidth. Applying the same PIIN analysis modular derived by E.D.J. Smith et al. [3], the evaluation result shows that MAI is completely eliminated in theoretical. Moreover, BER versus simultaneous active users can be upgraded 195% for given error probability of 10^{-9} under PIIN is only considered.

Recently, technologies on compensation of polarization mode dispersion (PMD) have reached significant achievement in wavelength division multiple access (WDMA) system [5]. With such advanced PMD compensation, the proposed scheme thus becomes more probably feasible on implementing in long-haul network.

REFERENCES

1. Salehi, J. A., "Code division multiple-access techniques in optical fiber network-Part I: Fundamental principles," *IEEE Trans. on Commun*, Vol. 37, No. 8, 824, 1989.
2. Huang, J. F. and C. C. Yang, "Reductions of Multiple-Access Interference in Fiber-Grating- Based Optical CDMA Network," *IEEE Trans. on Commun.*, Vol. 50, No. 10, 1680, 2002.
3. Smith, E. D. J., R. J. Baikie, and D. P. Taylor, "Performance enhancement of spectralamplitude-coding optical CDMA using pulse-position modulation," *IEEE Trans. on Commun*, Vol. 46, No. 9, 1176, 1998.
4. Dennis T. and J. F. Young, "Optical implementation of bipolar codes," *IEEE J. Lightwave Technol.*, Vol. 28, No. 3, 287, 1999.
5. Khosravni, R., S. A. Havstad, Y. W. Song, P. Ebrahimi, and A.E. Willner, "Polarization- mode dispersion compensation in WDM systems," *IEEE Photon. Technol. Letter*, Vol. 13, No. 12, 1370, 2001.

The High Dimension of Chaotic Attractors in Gyrotron with Non-Fixed Field Structure

E. V. Blokhina, A. G. Rozhnev
Saratov State University, Russia

S. P. Kuznetsov
Institute of Radio-Engineering and Electronics of RAS, Russia

We investigate some features of complex behavior, particularly the dynamics at chaos transition in distributed system, describing the non-fixed field structure gyrotron dynamics. Nonstationary behavior in gyrotron was investigated on the base of numerical solutions of the electromagnetic field excitation and electron motion equations set with appropriate initial and boundary conditions. In studied system control parameters are frequency mismatch (Δ) and beam current (I_0).

We carried out the investigation of complex dynamics on and chaos regimes at region of Δ values $\Delta \approx 0.0$ and $\Delta > 0.6$ (at these values the transitions from periodic automodulation to chaotic oscillations are possible). Analysis of nonstationary regimes was carried out on base of phase portraits, power spectra of output field and the estimation of the set of Lyapunov exponents.

At $\Delta \approx 0.0$ the chaotic oscillations are realized after period doubling bifurcation sequence. This chaotic regime is "not developed"; it is characterized by single positive Lyapunov exponent. At $\Delta > 0.6$ chaotic regimes arise after the quasiperiodic motion destruction as a result of mode competition. Such kind of chaotic oscillations is called "hyperchaos" and these oscillations are "developed" in terms of the presence of two positive Lyapunov exponents.

The special feature of dynamics regimes, observing in our system, is the presence of attractors with high dimension. On the one hand, the attractor dimension D can be estimated with the help of the Lyapunov exponents values set Λ_i, using formula $D = m + \sum\limits_{i=1}^{m} \Lambda_i/|\Lambda_{m+1}|$, where m is defined in such way, that $S_m = \sum\limits_{i=1}^{m} \Lambda_i > 0$, but $S_{m+1} = \sum\limits_{i=1}^{m+1} \Lambda_i < 0$. On the other hand, in the under study system large number of high-Q eigenmodes are present, and, although these modes correspond with electromagnetic field oscillations in gyrotron cavity, interacting weakly with electron beam, the presence of modes leads to appearance of corresponding number of negative Lyapunov exponents with small absolute values. As a result the attractor dimension, defined on Lyapunov exponents values, is found to be essentially greater, then dimension of attractors, obtained in investigated earlier microwave system, like backward wave oscillator, in which self Q-factor of electrodynamic system is low.

The Hybrid Method for Arbitrary Weak Guidance Optical Waveguides Simulation

Maxim V. Eliseev, **A. G. Rozhnev**
Saratov State University, Russia

Alexander B. Manenko
Russian Academy of Sciences, Russia

Open inhomogeneous dielectric waveguides with complex transverse section are the large class of waveguides including optical and microwave devices, such as dielectric antennas, optical fibers and sensors, integral optics structures, Bragg fibers, photonic bandgap fibers and microstructured fibers. The usage of traditional numerical methods for calculation of guided mode properties nearby the cutoff frequencies and of the leaky modes leads to difficulties due to specific features of the problem. As an effective and accurate solution of this problem, the hybrid finite element - integral equation method has been suggested.

The non-local integral boundary conditions on the auxiliary contour have been employed to eliminate the far fields from consideration. Thus, the open space problem has been transformed to the problem with the bounded region. The algebraical equations obtained have been solved by the Arnoldi algorithm, which allows efficiently to treat the complex matrices of large orders. The results showed that the method is universal and accurate.

The cutoff frequencies and the dispersion characteristics of scalar guided modes have been calculated for practically important types of dielectric waveguides with complex core shape (elliptical, rectangular, 8-like) for core aspect ratio from 1.0 to 100.0.

The transformation of the dispersion characteristics of elongated dielectric waveguides (core aspect ratio from 1.0 to 100.0) nearby cutoff frequency has been investigated. The boundary value of frequency dividing areas of 2D and 3D behaviour was found. The boundary value depends on the aspect ratio of the waveguide core. Even if the aspect ratio is large, the planar approximation cannot be used on the frequencies below this boundary value.

The cutoff frequencies of higher guided scalar modes of elongated waveguides has been investigated. For LP_{m1} modes the planar approximation is not applicable on the cutoff frequency for aspect ratio of waveguide core below 50.0. For LP_{m2} modes, the planar approximation can be used on the cutoff if the aspect ratio is higher than 10.20 (depending on the mode number).

The dispersion, the radiation losses, the field power distribution are calculated for scalar leaky modes in the multiplayer waveguides (Bragg fibers) including elliptical Bragg fiber (aspect ratio 1.1-5.0), Bragg fiber with excentrical layers and coupled Bragg fibers. The effects of the guide cross section perturbations were studied.

The method could be also applied to the systems with dielectric losses or active medium and analysis of the vector modes (including the case of anisotropic systems).

An Efficient Time Synchronization for Radio Spectrum Monitoring and Wireless Sensor Networking

Cheung-Ching Wang
National Changhua University of Education, Taiwan

Yih-Chuan Lin
National Formosa University, Taiwan

This paper addresses the problem of time synchronization among a set of distributed autonomous nodes that work collaboratively for dealing with timing-related tasks in various remote sensing or telemetry situations, such as wireless sensor network [1] and radio spectrum monitoring [2-3]. There are many different methods of distributed time synchronization existed in common use today. For example, systems such as the Global Positioning System (GPS) [4] provides with earth wide references to the U.S. time information standard to a time server that performs the Network Time Protocol (NTP) [5] for distributing time received from GPS to network-connected nodes. For most consumer-based usage, the nodes with GPS receiver can directly synchronize to a long-lifetime time standard with a relative high precision. However, in the case of sensor networks, the GPS's properties of high-power consumption, large size, and expensive cost make the GPS approach not adequate for the environment of small sensor nodes. In this paper, we propose to adopt the notion of radio clock [6] with the time synchronization of distributed sensor network. The reason of incorporating the radio time services lies in the simple architecture, small-size, and low-power characteristics of radio clock receivers. A simple prototype receiver of radio time services is implemented and used to illustrate its feasibility for telemetry applications. Furthermore, we investigate the problem of radio spectrum monitoring, which is an important task for spectrum regulation, to show the wide applicability of the low frequency radio time services.

REFERENCES

1. Elson, J. and D. Estrin, "Time Synchronization for Wireless Sensor Networks," *In Proceedings of International Parallel and Distributed Processing Symposium, San Francisco, CA, USA, April 2001*, 2001.
2. Clarricoats, P. J. B., Y. Rahmat-Samii and J. R. Wait, "Radio Direction Finding and Super resolution", *IEE Electromagnetic series 33, Peter Peregrinus Ltd., London, United Kingdom*, 1991.
3. ITU, "Spectrum monitoring handbook", 2002.
4. McNeff, J. G., "The Global Positioning System," *IEEE Trans. on Microwave Theory and Techniques*, Vol. 50, No. 3, 645, 2002.
5. Mills, D. L., "Internet Time Synchronization: The Network Time Protocols." In Z. Yang and T. A. Marsland, editors, *Global States and Time in Distributed Systems. IEEE Computer Society Press*, 1994.
6. Lombardi, M. A., "Radio Controlled Clocks," *In Proceedings of 2003 NCSL International Workshop and Symposium.*

Space-time Block Codes with Optimal Coupling Antenna Selection

Ling-yun Cai, **Haibin Zhang**, **You-yu Xu**, **Wentao Song**
Institute of Wireless Communications Technology, China

The performance of multiple-input multiple-output (MIMO) systems can be improved by employing a larger number of antennas than actually used and selecting the optimal subset based on the channel state information. The existing selection algorithm includes: optimum selection based on capacity maximization, gradual elimination based on matrix simplifying and a simple selection based on maximum Frobenius norm. Space-time block codes (STBC) provide maximal diversity advantage over a fading channel. Coupling antenna selection with the Almouti scheme can further increase the diversity order. In the existing scheme, the coupling antenna selection utilizes the criteria just like the MIMO antenna selection selecting the best subset to couple. However, all the schemes give up other antennas, whose channel states are not good and lead to capacity decreasing.

In this paper, we propose a novel technique that provides additional diversity gain by coupling antenna selection with STBC. Such a scheme is based on maximum Frobenius norm for every transmitter antenna, and then the optimal coupling antenna selection can be applied according to the Frobenius norm value. Specifically, we do not give up any antennas in transmitter and receiver. We present the optimal coupling antenna selection rule and quantify the improved performance in terms of gain in bit error rate (BER) and the improvement in outage capacity.

Satellite Interference Detection by Source Signal Processing

Cheung-Ching Wang[1], **Yih-Chuan Lin**[2]

[1]National Changhua University of Education, Taiwan
[2]National Formosa University, Taiwan

Nowadays, even a minimally experienced technician with off-the-shelf equipment can disrupt the satellite transmissions. Since the interference signal from earth station is transmitted upward to the satellite and if the unknown transmitter is always a motion station such as SNG (Satellite News Gathering), it is very difficult to detect the geographic location of the illegal station. In particular, the duration of interfered signal is also short and intermittent; this increases the difficulty of detection. To solve this, Smith and Steffes [1, 2] proposed a satellite interference location system by the different time and phase measurement techniques. They have used two methods to estimate the position of the unknown transmitter. One method involves measuring differential time delays of a single uplink signal observed through two adjacent spacecrafts. Another one uses a short baseline interferometer composed of the two cross-polarized and spatially separated antenna feeds aboard an affected satellite. The unique location is obtained by employing an appropriate combination of the two methods. According to TDOA (Time Difference of Arrival) and FDOA (Frequency Difference of Arrival), the position can be determined. Although they are good at the development of geographic location algorithm. However, they do not mention how to detect whether the program content is an authentic or a counterfeit one. In the duration of interfered signal, the wrong information will unlimitedly broadcast to the public users who located in the coverage of the affected satellite. To avoid this, we propose a monitoring method that can provide an immediate detection of the unauthorized program transmitted through satellite transponder and a limitation of the interfered signal broadcasting. Simultaneously, the location of illegal satellite station proceeds to determine the bearing information.

The proposed mechanism mainly includes three functions: detection, prevention and location. In detection component, to provide the video sequence authentication, the authorized code including timestamp, copyright number and secret code are used as watermark to be embedded into the video sequence of MPEG-2 streams. Then the watermarked signals are transmitted through the transponder of satellite and relayed to the receiver of monitoring station. Thus, the monitoring station can detect the watermark signal from watermarked signals to authenticate the video contents. If the watermarked signal has no authorized right, its illegal use will be easily detected by the watermarking algorithm, and thus the SMS (Satellite Monitoring System) can send a control signal to suspend the transponder operation for limiting the illegal content to broadcast for the public broadcasting network. Meanwhile, the geolocater will be driven to locate the source of interference signal. The bearing information of the terrestrial satellite, therefore, can be determined using the positioning technique. Consequently, the proposed system can provide better defense against intentional interference for the satellite broadcast.

REFERENCES

1. Smith, William Whitfield and Jr. Paul G. Steffes, "A satellite interference locating system using differential time and phase measurement techniques", *IEEE Aerospace and Electronics Systems Magazine*, Vol. 6, Issue 3, 3, 1991.
2. Smith, W.W., Jr., Steffes, P.G., "Time delay techniques for satellite interference location system", *IEEE Transactions on Aerospace and Electronic Systems*, Vol. 25, Issue 2, 224, 1989.
3. Wernek, S.B., "A Satellite Monitoring System", *Tenth International Conference on Digital Satellite Communications*, Vol. 2, 661, 1995.

Synthesize of Multilayer Passive Structures Using Genetic Algorithms

Ricardo Cardoso de Souza, **Glauco Fontgalland**, **Marcos A. Barbosa de Melo**
Federal University of Campina Grande, Brazil

In this paper Genetic Algorithms (GA's) were used in order to synthesize dielectric multilayer passive filters. Symmetric structures with plane or corrugated interfaces and TEM waves with normal or oblique incidence in relation to incidence plane were considered. The genetic algorithm optimization objective is to obtain each layer thickness to get the best frequency response related to scattering parameters. To do this the designer need to specify the number of layers, each material refraction index, the frequency range operation, the interface declivity angle and the genetic operations to be used. Beside this, GA randomly generates incidence angles to simulate a multipath environment or the designer can specify one to simulate, for example, a antenna test in a controlled environment. These data are processed by routines created in Matlab® or genetic algorithm implementation. Some kind of genetic operations were implemented resulting in different algorithm performances.

A two port waveguide junction in a cascaded configuration, as the structure analyzed here, is a common device used in many electromagnetic circuits. This can be represented by a cascade of transfer functions, each one representing an impedance of the discontinuity in structures like line transmissions, corrugated surfaces, impedance transformers or filters. A broad class of cascaded structures for many applications can be implemented without cumbersome changes in the algorithm codes.

Some project considerations were done. The materials are non-magnetic and dispersion free. Conductive losses were neglected and all the reflections are specular, i.e., without scattering losses. The algorithm is guided towards the optimal design through the formulation of a proper objective or cost function. Considering a low-pass filter synthesis for a example, given a set of frequencies f_m+ $(m = 1, \ldots, N+)$ at which the scattering parameter S12 needs to be maximized and a set of frequencies f_m- $(m = 1, \ldots, N-)$ at which the scattering parameter S_{11} to be maximized, a cost function F suited for the present problem is formulated as shown in Eq. 1.

$$F = \sum_{1,N^-} \omega_t (1 - |\Gamma(f_m{}^+)|^2)^\alpha + \sum_{1,N^+} \omega_r |\Gamma(f_m{}^-)|^{2\alpha} \tag{1}$$

The coefficients α, ω_t and ω_r weight the relative importance of the filter performance for the different frequency ranges. These coefficients can shape the frequency response and as result of trade-offs between transmission, transition and rejection bands. We can choose the kind of filter response, like low-pass or high pass, by maximizing or minimizing reflectance or transmittance terms in Eq. 1. Typical coefficients value ranges were determinate empirically using many simulation tests for normal incidence in a plane interface. Curve blue colored shown a better filter performance for a 0.7 cutoff frequency and curve yellow colored considered all coefficients equal to one.

Dynamic ANN and Its Application on Optimizing the Electric Apparatus

Yundong Cao, **Xiaoming Liu**, **Dong Liu**
Shenyang University of Technology, China

The ANN has the parallel computation capability, which possesses the ability to mimic the intricate nonlinear problems. Moreover, using the ANN, some tedious modeling of the complicated system can be simplified because it is unnecessary to have pre-knowledge of the computation structure. Generally, the ANN can effectively solved the knowledge has the characteristics of fuzziness, deformity and uncertainty, and the mathematical algorithm has the defects of clear analytical analyses. However, for the inverse problem computation of electromagnetic field for optimizing the electric apparatus, there exist the heavy demands of optimization variables, the great demands of computing work, and increased demand of the samples of the computation of the electric field for insuring the precision of the global optimum. Accordingly, for the concrete application cases, such requirement of large samples worked the optimization into difficulty. It is obvious that the conventional ANN can not be effectively applied for optimizing the electric apparatus with multi-variables.

In this paper, the ANN is introduced to optimize the electric apparatus, and a novel dynamic neural network (NN) has been proposed. Based on the application of the nonlinear approaching ability and high efficiency of the ANN, the strategy of the approaching ability, searching space, sample collection and computation precision have been investigated. The validity and the feasibility of the proposed dynamic ANN have been verified by computing a typical testing function and optimizing the disc insulator of a 500 kV GIS.

Parallel Couple Computation of Electric and Flow Field in HV SF_6 Circuit Breaker

Yundong Cao, **Luze Zhao**, **Xiaoming Liu**
Shenyang University of Technology, China

Nowadays, investigation on the interrupting performance and the dielectric recovery characteristic based on the numerical calculation of the electric field and flow field plays a very important role for researching and developing the HVCBs. So, it is necessary to investigate the characteristic of electric field and flow field in uniform viewpoint, and to analyze the dielectric recovery characteristic of the CBs. In which, the meshing in preprocess of the electric field and flow field directly influence the characteristic. Using the traditional finite element method, when the calculating region dynamically moved, the calculation region must be re-meshed to guarantee the elements and the nodes to be continuous. Whilst, the meshing elements in electric field and flow field for the calculation of dielectric recovery characteristic are impossibly completely consistent. For thoroughly solving the above problems, the sub-region meshing method is proposed and employed to parallel calculate the electric field and the flow field, and the dielectric recovery characteristic with higher precision can be obtained.

In this paper, for obtaining the corresponding data to exactly solve the dielectric recovery characteristic of the CB, the parallel couple calculation of electric field and flow field is realized using the sub-region meshing method, and the meshing elements are self-adaptively densified in the interrupting process, then the practical model is done. An effect method for calculating the dielectric recovery characteristic is confirmed.

Optimization on Electrical Apparatus Based on Compensated Fuzzy Neural Network

Yundong Cao, **Feng Li**, **Xiaoming Liu**
Shenyang University of Technology, China

With the increase of the voltage level of power system, higher requirement have been brought forward for insuring the miniaturization and complexity of the electric apparatus. However, the optimization design of electrical apparatus covers many variables, optimization mathematics model is more complex, and the optimization problem has overstepped the scope what the traditional optimization method does. Recently, the compensated fuzzy logic Artificial Neural Network (CFNN) was widely applied in many fields, because it possesses the ability to simulate the intricate nonlinear problems and compute parallel. And the fuzzy logic allows users to response to questions in a very humanlike way. The CFNN is fault tolerant, i.e., it can efficiently be trained from either well-defined initial fuzzy rules or ill-defined initial fuzzy rules, and the convergence speed of the compensatory learning algorithm is faster than that of the conventional backpropagation algorithm.

In this paper, the combination of the fuzzy logic and the ANN has been introduced to optimize the electrical apparatus. And the approaching ability of the proposed method has been investigated using a testing function. The approaching and fault tolerant capability of the ANN has been improved using CFNN. Moreover, the hybrid method of the CFNN and the golden section has been proposed and effectively applied to optimize the electric apparatus.

Computation of Insulating Performance of SF_6/N_2 Mixtures Gas HV Circuit Breaker

Xiaoming Liu, **Lei Li**, **Yundong Cao**
Shenyang University of Technology, China

SF_6 gas, a compound of fluorine and sulfur, features excellent insulation, arc-extinguishing capabilities and stability, pure SF_6 is non toxic and biologically inert as well as being safe to the human body. So in the electric power industry, SF_6 gas is often used for high voltage (HV) gas circuit breakers (GCBs) and gas-insulated switch gears. SF_6 gas has no chlorine radical therefore it does not directly destruct the ozone layer, but it does have a high global warming potential and the byproducts of the SF_6 is toxic. Because an effective insulating gas that substitutes for SF_6 has not found, the electric power industry will continue to use SF_6 with promoting the recovery and recycling of SF_6 to restrict emissions as much as possible. And from the contributions reported, it can be found that, the hybrid SF_6/N_2 is generally widely accepted as the best choice to substitute for the SF_6. So it is very necessary to investigate the electrical and insulating property of the hybrid SF_6/N_2 applied in the HVCB. Consequently, in this paper, the electric field for different hybrid ratio of the SF_6/N_2 have been numerically computed and analyzed. In this paper, the insulating performance of SF_6/N_2 mixtures gas based on the numerical computation of the electric field of a HVCB has been investigated. And 2D mathematical model of the electric field and its numerical analyses are obtained and presented to investigate the electric field and the insulating performance during the interrupting course.

Remote Sensor of Methane Pipeline Leakage Using a Tunable Diode Laser Absorption Spectroscopy

Hong Fan, **Xiaoming Gao**, **Bao Jian**
Xia Wang, **Teng Huang**, **Xiaoyun Li**
Wei Huang, **Zhensong Cao**, **Weijun Zhang**

Anhui Institute of Optics & Fine Mechanics, Chinese Academy of Sciences, China

Natural gas has widely used in our daily life as primary energy-source material. Its main component is methane. Methane is a flammability and explosive gas. The leak of natural gas is not only economic loss and the fountain of dangerous. From the view-point of safety, the detection of CH4 leakage is important. Conventional detection techniques of natural gas pipe leak have lower efficiency and slow respond time, therefore, it is difficult to suit practice application. Optical sensors based on NIR tunable diode laser absorption spectroscopy were widely used because of high sensitivity, small volume and less maintenance, and has narrow linewidth which can determine the leak position and concentration in a short time. In this paper, a portable remote sensor of natural gas pipeline leak at a wavelength of 1.65 μm was reported. The 1.65 μm DFB diode laser has a narrow line width and a wide tune range. The sensor used a ratio between second and first harmonic signals as calibration method, the calibration method shows a good consistent between concentrations and the ratios between second and first harmonic signals. The effect of different topographic scattering targets on the ratio detection was measured and analyzed. The results show the ratio detection between second and first harmonic signals can be used in practice application as a auto calibration method. It was found that the sensor can detect a 10 cc/min city-gas leak with a sensor output equivalent to the range-integrated concentration over 100 ppm $\cdot$m.

Fuzzy Calculation in Non Destructing Testing

S. Calcagno, **F. C. Morabito**, **M. Versaci**
Univ. Mediterranea, Italy

Non Destructive Testing (NDT) in the field of defects identification in metallic elements plays a remarkable role with special regard to those sectors where the integrity of the material is strictly required. As a consequence, the detection of defects in metallic plates together with the relevant shape classification provides the operator useful information on the actual mechanical integrity of the specimen [1]. It should be considered that defects rarely look as well-known geometrical shapes. State-of-the-art Non Destructive identification systems allow to locate a defect but without being capable to determine the shape of it. As an example, in Fig. 1 a typical signal is shown representing a local measurement of perturbed magnetic field on an aluminum plate with an hole in the center; the zero-crossing between the two peaks locate the defect, whereas the peak-to-peak amplitude gives a measure of its deepness. Now, different defects give rise to totally similar signals. This work aims to deal with the problem introducing an approach based on soft computing. For this purpose, Neural Networks (NNs) Fuzzy Inference Systems (FISs) and Neuro Fuzzy Inference Systems (NFISs) with Sugeno's inferences-type is exploited. The use of fuzzy inference techniques allows obtaining banks of IFTHEN fuzzy rules, in virtue of which the system under investigation behaves as a linguistic structure. Once the position of a defect has been located, next step will be to determine the depth of it by introducing fuzzy entropy and mutual entropy concepts, with a parametric index family, whose members have varying sensitivities. This way a more complete summary of a fuzziness family is done, i.e. a continuum of possible fuzziness measures within the fuzzy partition as a function of its. In addition, changing it allows for a vectorial description of the uncertainty in a classified labelling of thematic maps representable by their fuzziness profile. Fuzzy entropy can this way be meant as a parametric measure of the degree of fuzziness of a signal at unknown depth in comparison with a well-known signal. The fuzzy entropy approach translates into a value in the range 0-1 the membership of the depth of a defect to one of a number of predefined classes: a kind of classification of a defect in terms of its depth comes out, being the transition from a depth to another a fuzzy evolution without interruption.

REFERENCES

1. Calcagno, S., et al., "Damage Analysis of Thin Metallic Plates," *Advances in Structural Engineering and Mechanics, ASEM02, voPusan, Korea*, 2002.

The Design of a RF Photonic Bandgap Wideband Filter

Linshu Shi, **Dongwu Lou**
Zhejiang University, China

In this paper, a 1-D microstrip PBG stopband filter working at 2.4GHz is introduced. The use of PBG structure allows a wide stop-band filter to be integrated into the circuit substrate, thus allowing for collocation of other microstrip circuit elements with the filter. The first section describes how the PBG filter was designed and presents the parameters of the filter. The section followed is to describe the simulated results with 3D full wave electromagnetic analysis using HFSS. The last section gives a discussion of the effect of parameters of the 1-D PBG stopband filter especially the depth of the period holds.

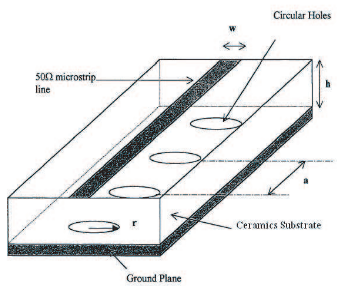

Figure 1: Three dimensional schematic of a one dimensional photonic band-gap structure for microstrip lines

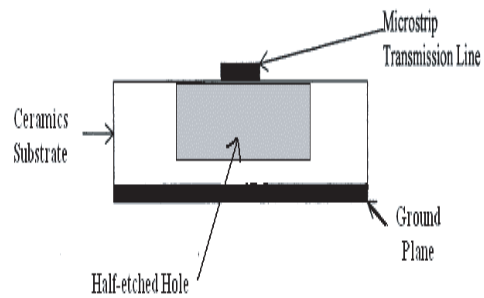

Figure 2: Cross-sectional view of modeled structure half-etched holes

SIMULATION OF HFSS

The bandstop filtering properties of the structure are clearly visible. In the PBG filter, the stopband is 2.4GHz. The 3dB band-width is 790MHz (31.6% of the central band-pass frequency) from 2.06GHz to 2.89 GHz.

DISCUSSION

In order to investigate the stopband effect of the PBG structure, many circuits have been simulated with circles of different distance, radii and depth.

Generally speaking, f0, the stopband center frequency, is a function of the period of the structure [1]. Particularly, the guided wavelength at f0 is twice the length of period a.

For smaller circle radii the stopband is relatively shorter. In the limitation case r=0 (or r/a=0) there is no stopband, and the structure becomes a standard microstrip line. As the circle radius being increased, the stopband becomes more distinctive. A tradeoff is r/a=0.25, with significant stopband width and small passband ripple in S11.

LDPC Based Differential Unitary Space-frequency Coding for MIMO-OFDM Systems

Hai-Ning Jiang, **Han-Wen Luo**, **Ji-Feng Tian**, **Wen-Tao Song**
Shanghai Jiaotong University, China

Multi-antenna assisted space-time coding has generated widespread interest recently. Coherent decoding of space-time codes requires reliable estimation of the underlying multi-channels at the receiver. This is a challenging and costly task, especially when the channel experiences high mobility induced fast channel fading. Differential space-time modulation (DSTM), which circumvents the need for channel estimation, offers an attractive alternative in fast-fading environments. However, most of current DSTM schemes were designed primarily for flat-fading (narrowband) channels. To deal with frequency-selective fading channels, narrowband DSTM schemes can be used with orthogonal frequency division multiplexing (OFDM) on each sub-carrier across the transmit antennas. However, such extensions do not exploit the embedded spectral diversity offered by multi-path propagation in wideband systems. In this paper, we present a novel LDPC based differential unitary space-frequency coding (DUSFC) scheme for MIMO-OFDM systems over frequency-selective fading channels when there is no channel state information (CSI). The new DUSFC strategy basically consists of coding across transmit antennas and OFDM tones simultaneously as well as differential modulation in the time-domain. It can fully exploit the inherent advantages provided by the multi-path fading channels, resulting in a high degree of diversity. We also develop further simplifications by sub-carrier grouping (SG) and illustrate its impact on the performance of DUSFC. Then, the state-of-the-art low-density parity-check (LDPC) codes are concatenated with our DUSFC as channel coding to improve the bit error rate (BER) performance considerably. Owing to the maximum multi-path diversity and large coding advantages, LDPC-DUSFC strongly outperforms the differential unitary space-time coded OFDM techniques recently proposed in literature. Meanwhile, the LDPC-DUSFC scheme is more tolerant to the Doppler spread, which indicates its robustness for the time- and frequency- double selective fading channels. Simulation results illustrate the merits of the proposed scheme.

Sub-Matrix Interleaved Differential Space-Time Modulation for Fast Fading Channels

Jifeng Tian, **Youyun Xu**, **Haining Jiang**, **Wentao Song**
Shanghai Jiao Tong University, China

Differential space-time modulation (DSTM), which circumvents the challenging task of multi-channel estimation in time-varying channels, has generated significant interest recently. However, current DSTM schemes are designed primarily for slowly fading channels. For fast fading channels, the performance of DSTM schemes degrades considerably and suffers an irreducible error floor. In this paper, we present a novel sub-matrix interleaved differential space-time modulation (SMI-DSTM) scheme for multiple-antenna systems when neither the transmitter nor the receiver has access to the channel state information (CSI). The proposed SMI-DSTM scheme employs a differential encoder, a matrix-segmentation, and an interleaving based on sub-matrices, which is designed to yield the full transmit diversity and significant coding gain. The transmission system diagram of SMI-DSTM scheme is depicted in Fig. 1. A sequence of information binary bits is divided into N_s groups. At time $\tau(\tau = 1, 2, \cdots, N_s)$ each group is mapped into an element matrix V_{z_τ}, which is selected from a diagonal unitary constellation group Ω with $L = 2^{RM}$ matrix elements. A differential space-time modulation follows and the transmitted matrix at time τ can be expressed as $X_\tau = V_{z_\tau} X_{\tau-1}, X_0 = I_M$. Based on some segmentation rule, the matrix X_τ is segmented into K sub-matrices $X_\tau(0), X_\tau(1), \cdots, X_\tau(K-1)$, whose dimensions are $r_0 \times M, r_1 \times M, \cdots, r_{K-1} \times M$ respectively, where $r_0, r_1, \cdots, r_{K-1}$ are integers with the constraint $r_0 + r_1 + \cdots + r_{K-1} = M$. And then the sub-matrix $X_\tau(k)'s(k = 0, 1, \cdots, K-1,\ \ \tau = 1, 2, \cdots, N_s)$ are interleaved based on a specific pattern, and sent to the transmit antennas. Compared with conventional DSTM system, SMI-DSTM requires less coherent time intervals and is more tolerant to Doppler spread with comparable decoding complexity. In this paper, we also derive the Chernoff bound for pairwise error probability (PEP) of SMI-DSTM system, which demonstrates that our SMI-DSTM system can achieve the same diversity gain to DSTM system. Through PEP analysis, the code design criteria are also derived over time-selective fading channels. The choice of segmentation rule and interleaving pattern will provide flexibility to tradeoff hardware complexity with performance. Numerical results are presented to illustrate the performance of the proposed SMI-DSTM scheme, which outperforms conventional DSTM schemes considerably in fast fading channels.

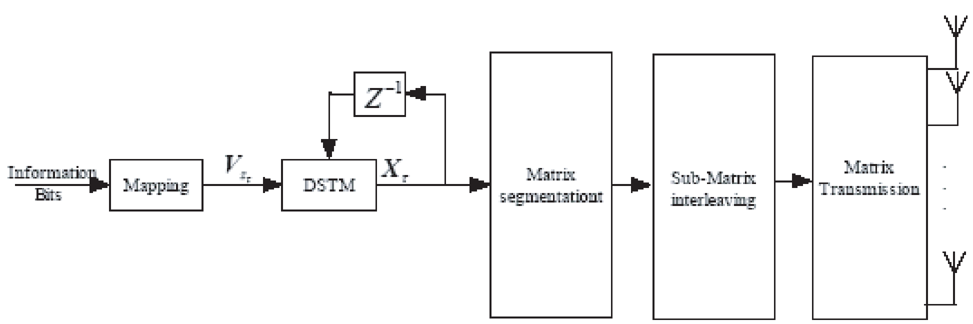

Figure 1

Towards Realizing Devices Based on Lefthanded Materials

P. V. Parimi, **P. Vodo**, **W. T. Lu**, **E. Di Gennaro**, **S. Sridhar**
Northeastern University, U.S.A.

J. S. Derov
Air Force Research Laboratories, U.S.A.

A variety of applications such as band pass filters, beam steerers, leaky wave antennas etc. based on lefthanded materials have been proposed in the literature. Realization of such applications requires experimental demonstration of the proof of principles. Here, we present of the results of near field and far field imaging and slow wave propagation in lefthanded materials in the microwave frequency range. The far field imaging was achieved using a plano concave photonic crystal (PhC) lens. An inverse experiment in which the source was placed at the observed focal point was also performed and resulted in a clean plane wave emerging on the far side. The focal point is observed to move with the radius of curvature of the lens. Different radii of curvature have different frequency ranges of focusing all of which lie in the second band frequencies along Gamma-X propagation direction of the PhC. The near field imaging was achieved using a flat PhC lens. Remarkably slow propagation of microwaves was observed in two different classes of lefthanded materials - a composite material made of split-ring resonators and wire strips and the PhC. Pulse and continuous wave transmission measurements revealed group velocities of the order of c/100, where c is the free space light velocity. The slow group velocities are quantitatively described by the strong dispersion observed in these materials. All the results of group delay dispersion as well as near and far field imaging are in excellent agreement with the theoretical predictions. Slow propagation and tailor made refractive index obtained in these lefthanded materials to the design of delay line filters and ultra sensitive phase shifters. While near field and far field imaging have potential to find applications as antenna elements.

*Work supported by AFOSR and NSF-PHY-0098801

Improved Genetic Algorithm and Its Application on Computation of Electric Field

Xiaoming Liu, **Yundong Cao**, **Erzhi Wang**
Shenyang University of Technology, China

Genetic algorithm (GA) is a random searching algorithm based on the natural selection of the evolutionism, which aims at the optimum using different varying operators in the global space. And GA is widely applied to the continuous variable global optimization for solving the combined optimization problem. Although GA has been widely applied, and different integrating optimization strategies have been put forward and obtained many fruits, in optimizing, the diversity of the population and the optimum normalization is a pair of contradiction. That is, premature normalization cause prematurity, and late diversity directly slow the convergence speed. Consequently, in this paper, for improving the optimizing quality, speed, and tracking control, a fine prematurity criterion in optimizing course is established, and a novel improved GA for solving the continuous combinatorial optimization problems has been proposed. The implementation of the proposed GA differs from other GA implementations in two respects. First, while the prematurity criterion is used to generate new members in the GA population or adjust the operators of the GA for effectively finding the optimum. Second, the tendency to local convergence can be successfully avoid by tracking and control the rank of the population in each step. Moreover, for improving the quality and convergence speed of the optimum, the crossover and the mutation operator are automatically adjusted according the "prematurity criterion" in the optimizing course. The feasibility and practicability are verified by a typical optimization testing function and demonstrated examples.

A Numerical Comparative Experiment of Three CG-FFT Methods for 3D Inhomogeneous Scatterer Problems

Zhenhong Fan, **Rushan Chen**
Nanjing University of Science and Technology, China

The electromagnetic scattering problem of three-dimensional dielectric body can be formulated and solved by using integral equation. By using method of moments (MoM), the resultant integral equations can be converted to a system of linear equations or matrix equation. The matrix equation can be solved with iterative solver in $N_{iter}N^2$ operations where the N_{iter} is the number of iteration and N^2 represents the matrix-vector multiplication in the iterative solver. It is well known that integral equations method will generally produce ill-conditioning matrix and this will give rise to slow convergence, i.e. a large value of N_{iter}. Such computational costs have prohibited the MoM from solving problems with a large number of unknowns.

Fast algorithms such as conjugate gradient fast Fourier transform (CG-FFT), multilevel fast multipole algorithm (MLFMA) and adaptive integral method (AIM), pre-corrected fast Fourier transform (P-FFT) have been proposed to accelerate the matrix-vector multiplication. The computational complexity of the matrix-vector multiplication can be reduced to the order of O(NlogN) by the CGCFFT, MLFMA, AIM and P-FFT method. Besides the matrix-vector multiplication, the Niter also shall be minimized in order to reduce the overall computational time. The reduction of the N_{iter} can be achieved by using a more effective iterative method or by preconditioning techniques.

This paper makes a comparison of three widely used CG-FFT approaches, which are proposed in reference [1-3], corresponding to the techniques using pulse-basis and point-matching, rooftop-basis and razor-matching, and rooftop-basis and rooftop-testing, respectively, by investigating their accuracies and iteration numbers. Further more we apply some other Krylov subspace iterative methods such as QMR, GMRES, and Flexible-GMRES to show the reduction of Niter in scattering problem.

REFERENCES

1. Su, C. C., "The Three-dimensional Algorithm of Solving the Electric Field Integral Equation Using Face-centered Node Points, Conjugate Gradient Method and FFT," *IEEE*, Vol. MTT-41, No. 3, 510, 1993.
2. Catedra, M. F., "A Numerical Scheme to Obtain the RCS of Three-dimensional Bodies of Resonant Size Using the Conjugate Gradient Method and the Fast Fourier Transform," *IEEE*, vol. MTT-37, No. 5, 528, 1989.
3. Zwamborn, P. and P. M. van den Berg., "The Three-dimensional Weak Form of the Conjugate Gradient FFT Method for Solving Scattering Problems," *IEEE*, Vol. MTT-40, No. 9, 1757, 1992.

Computation of Planar Structures Using Nonuniform Fast Fourier Transforms (NUFFT)

L. Zhou, **Z. H. Fan**, **L. Mo**, **R. S. Chen**
Nanjing University of Science and Technology, China

It's know to us, Fast Fourier Transforms (FFT) is a fast algorithm for calculating Discrete Fourier Transforms, it has been widespread applied to numerical analysis and other areas of applied mathematics area as a powerful and practical numerical tool. The FFT, which require the input data must be uniformly spaced. In some applications, however, the input data is not equally spaced. In this case, the FFT must be improved urgently, thus, the Nonuniform Fast Fourier Transforms (NUFFT) is proposed. Different from FFT, the NUFFT is sampled uniformly in time-domain $[-N/2, N/2]$ or frequency-domain $[-\pi, \pi]$. The algorithm requires $o(\alpha N \log_2 N + mN)$, when α is oversampling factor, m is cut_off_parameter, N is the number of data. Usually we choose $\alpha = 2$. In this paper, we will introduce the NUFFT and NUIFFT (Nonuniform inverse fast Fourier transforms) algorithm simply, and we first employed an accelerated algorithm into the general NUIFFT for accelerating the speed of algorithm. We combined NUFFT and SOC (Short and Open Calibration) to analysis anomalistic plane structures, whereby decrease the numbers of grid, save much computational resource. Our numerical results demonstrate that this method is advantageous over CG-FFT in NUIFFT algorithm in terms of memory requirement and CPU time.

A Wideband CPW-Fed Monopole Antenna

S.-B. Chen, **Y.-C. Jiao**, **F.-S. Zhang**, **N.-B. Wang**, **Q.-Z. Liu**
Xidian University, China

As a kind of very simple and efficient radiating elements, monopole antennas are widely used in wireless communication systems. However, the drawbacks of these antennas are their limited bandwidth and distortion radiation characteristics. Some techniques for improving the bandwidth performance have been reported.

A novel compact and wideband coplanar waveguide (CPW)-fed monopole antenna is proposed. To enhance its bandwidth, we add two rectangular stubs in the ground plane according to the idea of the sleeve monopole antenna. The configuration of the proposed antenna seems to be a uniplanar sleeve-shaped monopole antenna. The dimensions and positions of the rectangular stubs in the proposed antenna are optimized by the parametric analysis with the HFSS simulator of Ansoft. A Teflon substrate (RO3210tm) with thickness of 2mm and relative permittivity of 10.2 is used. A properly designed antenna has an operating frequency range from 2.1 to 5.2GHz for the return loss of less than -10dB, shown in Fig. 1. Moreover, the radiation patterns of the antenna are similar to that of the conventional monopole antennas.

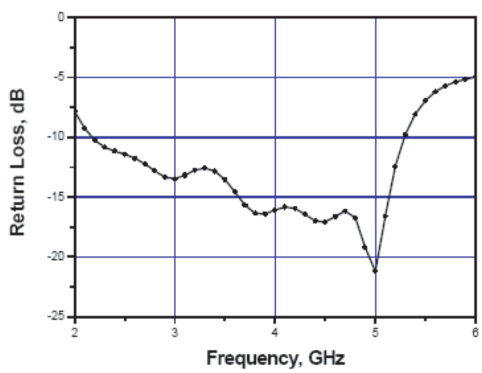

Figure 1: Return losses of the proposed antenna

*This work was supported by the National Natural Science Foundation of China (60171045).

Tunable Compact Feeder Network for Shaped Beam Antennas of Long Range 3D Surveillance Radar

Shubha Elizabeth, **Anil Kumar Singh**, **Y. Mohan**
Defense Research & Development Organisation, C. V. Raman Nagar, India

S. Christopher
Defense Research & Development Organisation, Belur, Yemlur Post, India

Generally, 3-D radar systems uses a shaped antenna pattern to cover the given elevation region. Usually feeder network built on wave guide technology leads to huge and massive constructions. In this paper we discuss the design and analysis of compact corporate feeder network using S - band reduced height wave guide H-plane Tee junction power divider with an additional septum for wide impedance bandwidth and fine amplitude control. A movable vane dielectric phase shifter has been introduced in the individual power divider module to get up to 360° phase shift at all outputs. Since the medium of design is wave-guide it has the inherent capability of high power handling. This hybrid design combining dielectric phase shifters and wave guide feeder network provides an elegant solution for compact broadband high power feeder networks required for long-range surveillance radars to get any desired beam shape. A design of 1:32 hybrid network has been carried out. Simulated results of the feeder network across the band of operation $\sim$ 13% (400 MHz in S band) tuned for a $cosec^2$ pattern with 30° coverage is also discussed.

High power feed network, which will give the suitable amplitude distribution, is achieved through a 32 way in phase corporate network with unequal power division at each level. This is realized using Hplane tee junction power dividers. Usually in H-plane tee power division is achieved through a single septum in the broad wall and two additional septums in the branch guide for impedance matching. While synthesizing a shaped beam pattern with phase alone synthesis, to get a low side lobe outside the shaped beam region large amplitude taper is required from less number of elements. For large amplitude taper distribution or when the number of antenna elements is less, the power division ratio to be handled by a single power divider in a corporate feed network is quite large. This leads to individual power divider modules with less impedance bandwidth. This draw back is overcome thorough the novel design technique where in addition to the main septum (S1), which is in the broad guide, another septum is introduced in one of the output arms nearer to septum S1 so that power flow to that arm is restricted and thereby increasing the power division ratio. The length and offset of the additional septum determines the further power flow. This innovative power divider will give the required impedance bandwidth over 20% (for return loss 18 dB) band for any power division ratio. This addition of septum has an added advantage since for high power handling large amplitude taper power dividers with single septum approach, the length of the septum S1 is very large that it is near to the narrow wall that unless properly sealed will cause arcing. This approach of using double septum will reduce the length of septum S1 that arcing due to high peak power is eliminated to a certain extent. The amplitude distribution at the output ports is as per Taylor distribution to achieve a side lobe level better than 40 dB. The amplitude distribution was carefully studied. An optimized combination of double septum and single septum power divider is chosen to design the 32 way feed network with in phase outputs to get a phase tracking of ±4° across the 13% bandwidth.

The feed network based on H-plane corporate power divider with added septum enables the design of aperture distribution for low side lobe level antennas The integration of 360° movable vane dielectric phase shifters to achieve any desired beam shape with phase alone synthesis will result in lightweight, compact, broadband, low loss feed network for shaped beam antennas.

Session 3A6

Electromagnetic Modeling and Inversion (Einstein)

A Robust Preconditioner for GMRES Method Applied to Finite Network Method

A. Farschtschi, **T. Richter**
University of Technology Chemnitz, Germany

The aim of the autors is the calculation of induction and proximity effects of electric machines in an intermediate frequency range up to 100 kHz by the Finite Network Method (FNM). FNM excludes non-magnetic and non-conductive media (e.g. air) from the numerical calculation and fulfilles the asymptotic boundary conditions for the free space automatically. That's why FNM is prefered since it results in a small equation system compared to finite element programs such as ANSYS. FNM results in a complex and fully occupated system matrix. Since this matrix avoids the application of direct solvers or simple iterative solvers such as SOR or th conjugate gradient method there is need to investigate in fast and robust iterative solver for FNM. In our article we can show that the equation system of FNM can be solved by the preconditioned GMRES method (Generalized Minimum Residual) using a simple Gauss-Seidel preconditioner and an early restart value.

We present a short derivation of FNM for non-magnetic materials from Maxwell's equation. In a first simple model of FNM compact materials were discretised into hexagonal elements with three cartesian current components. By the use of the mesh current method and in the harmonic case FNM results in an equation system with a complex impedance matrix with a fully occupated and symmetric imaginary part and a diagonally dominant real part. We present the applicability of the complex GMRES method in the whole frequency range. In the low frequency limit $f \rightarrow 0$ the impedance matrix reduces to its real part and the equation system can be solved by the Gauss-Seidel method. The real part of of the impedance matrix is used as Gauss-Seidel preconditioner for the GMRES solver. Despite the considerable portion of the imaginary part of the system matrix at higher frequencies the Gauss-Seidel preconditioner is applicable in the whole frequency range. In contrast to the unpreconditioned GMRES method we choose an early restart for the preconditioned GMRES.

As an example we calculated the skin and proximity effect in two parallel copper wires with 200 to 500 degrees of freedom and an early restart value of 5 for the preconditioned GMRES. The preconditioner results in an acceleration of GMRES up to a factor 8.

Futhermore, these efforts in computing time were achieved without an acceleration of matrix-vector products. We point out that the implementation of the approximate calculation of matrix-vector products by hierarchical techniques such as Fast Multipole Method (FMM) should result in an additional acceleration of computing time.

The One Dimensional Stochastic Electromagnetic Field and Applications

Sheng Yan Wang
National Huwei University Of Sciences & Technology, Taiwan

Feng Hsieh
GL Geophysical Laboratory, USA

In this paper, we study a stochastic electromagnetic field simulation. We use one dimensional TE model and TM model analytical form to be a global filed. Next, we look the electromagnetic filed and its parameters to be random filed, by probability and statistics theory, we decomposed the electromagnetic filed into a expected filed and its second order co-variation correction. In the meantime, we decomposed the electromagnetic parameter into a expected parameter and its second order co-variation correction. We successively obtain the expected electromagnetic field, co-variance electromagnetic field, co-variance conductivity, and electromagnetic field and conductivity cross co-variance field. Finally, we develop the high accurate one dimensional stochastic TE model and TM model.

The stochastic electromagnetic field simulation has widely and important applications in the sciences and engineering. In particular, in the laser measurement, nanometer material and super conduct study. In Super conduct study, one dimensional TE model and TM model analytical form were used. However, the stochastic electromagnetic field simulation is lack in super conduct simulation. The physical super conduct phenomena and measurement are random. The stochastic electromagnetic field simulation is important and necessary [1]. Our stochastic electromagnetic field SGILD simulation will be useful in super conduct phenomena study and optical electric sciences and engineering.

REFERENCES

1. Xie Ganquan and Jianhua Li, "New parallel SGILD modeling and inversion," Physics D, Vol. 133, 477, 1999.

A New EM Integrodifferential Equation and GL Method

Ganquan Xie, **Feng Xie**, **Jianhua Li**
GL Geophysical Laboratory, USA

In this paper, we proposed a new electromagnetic integrodifferential equation

$$E(r) = \frac{(\sigma_b + i\omega\varepsilon_b)}{(\sigma + i\omega\varepsilon)(r)} E_b(r) - \frac{1}{i\omega\mu(\sigma + i\omega\varepsilon)} \bigtriangledown_r \times \int_{\Omega} ((\sigma - \sigma_b) + i\omega(\varepsilon - \varepsilon_b)) E^M(r', r) E_b(r') dr'$$

where, $G^M(r', r)$ is the magnetic Green tensor.

$$E^M(r', r) = \frac{1}{\sigma + i\omega\varepsilon} \bigtriangledown_{r'} \times G^M(r', r)$$

$E^M(r', r)$ is a convergent integrable electric Green tensor with weak singularity. The electric integrodifferential equation has the convergent integrable kernel. But the kernel of Hohmann's electric field integral equation is divergent. Based the new electric field integrodifferential equation and a magnetic field integrodifferetial equation, we construct the Global and Local electromagnetic field modeling and inversion in the frequency domain and time domain that is called GL EM modeling and inversion method. There are massive computational cost, large matrices solving and storages, artificial boundary reflection error difficulties in the FDTD and FEM methods. There are inaccurate, low resolution, high frequency, high contrast difficulties in the Born approximation and its variable versions. The new GL modeling and inversion methods overcome these serious difficulties in the FDTD, FEM, and Born like methods. Using GL method, we proved the existence and uniqueness of solution of the 3D and 2.5D Maxwell equation. We proved that GL method can obtain $o(h^4)$ superconvergence if the Gaussian integral points are used. The GL EM method and new EM integrodifferential equation have merits and widely applications in the electromagnetic theory, science, and engineering.

REFERENCES

1. Xie, Ganquan, Feng Xie, Jianhua Li, "Theory of GL EM method and new integrodfferential electromagnetic equation", *Report GLP04009, GLGEO Copyright*, 2004.

Diamagnetic Levitating Rotor

Joe Nhut Ho, **Wei-Chih Wang**
University of Washington, USA

This paper discuses the application of diamagnetism to create a stably levitating rotor. While diamagnetism is weak, it is strong enough to levitate small magnets with no external power input. This paper explains some of the mechanics and demonstrates a way to build such a diamagnetic levitating rotor. Numerical analysis is also used to estimate the torque developed on the rotor by various magnet and coil configurations.

New Computational Mirage

Feng Xie, **Lee Xie**
GL Geophysical Laboratory, USA

Computational Mirage is a complete new research project in the electromagnetic visualization. We search "Computational Mirage" in the Google and Yahoo and do not find any relative information on "Computational Mirage". In the computational graphic, computational visualization, and computational movies, people need reliable visual imagine for a static or dynamic objects. Recently, many researchers try to use mechanical method, finite element method, and FDTD method to do it. However, massive computational cost and storages and boundary resolution are serious difficulties for the computational visualization in the real time. For example, a shell and plate large deformation mechanical model is very difficult to simulate the cloth motion in the wind. The computational mirage and electromagnetic visualization will be a new approach to overcome the above difficulties. The visual imaging is light scattering when the light passes through the object. The mirage is light scattering when the light passes through water fog. Similarly, the desert city is light scattering when the light passes through sand fog. The light is high frequency electromagnetic filed. Therefore, we develop parallel GL and GILD electromagnetic, flow, acoustic, and seismic joint modeling and inversion to simulate mirage and rainbow. The computational mirage technology has widely applications in the computational art, computational movie, games, scene, sciences and engineering.

REFERENCES

1. Xie, Ganquan, Jianhua Li, and Feng Xie, "New Global and Local Electromagnetic Field Modeling And Inversion," To be presented in PIERS 2005, 2004.

New GL and GILD Fast Parallel Computational Visualization

Feng Xie, **Lee Xie**, **Jianhua Li**
GL Geophysical Laboratory, USA

In this paper, we developed a new Global and Local fast parallel algorithm for the computational visualization. The GL algorithm decomposes the Global visual imaging into 2^p Local imaging. Then we use 2^q nodes distribute computer to do parallel imaging. The visual imaging is scattering of the light when it passes through the objects. The light is the high frequency electromagnetic filed. Therefore, new GL and GILD electromagnetic parallel modeling and inversion are powerful methods for explicit and implicit computational visualizations. Traditional visual imaging is full screen scanning. Our new visual imaging is parallel local screen scanning and patching together into the global imaging. Therefore, our method is much fast than traditional imaging method. Our GL parallel imaging has widely applications in the computational movie, games, biological imaging, geophysical imaging and weather imaging etc sciences and engineering.

REFERENCES

1. Xie, Ganquan, Jianhua Li and Feng Xie, "New Global and Local Electromagnetic Field Modeling And Inversion," GLGEO Report GLP04008, GLGEO Copyright, 2004.
2. Xie, Ganquan, Jianhua Li, Feng Xie, "New Global and Local Electromagnetic Field Modeling And Inversion," to be presented in PIERS 2005, 2004.

A New GL EM Modeling and Inversion Based on Dual Boundary Integral Equation

Ganquan Xie, **Jianhua Li**, **Feng Xie**
GL Geophysical Laboratory, USA

In this paper, we develop new GL electromagnetic (EM) surface modeling and inversion by new dual boundary integral equations. The dual integral equations are

$$ME(r)=\frac{\sigma_b+i\omega\varepsilon_b}{(\sigma+i\omega\varepsilon)}E_{pb}(r)+\frac{1}{\sigma+i\omega\varepsilon}\oint_{\partial\Omega} i\omega\mu[G_b^H(r',r)\times H(r')]\cdot dS+\frac{\sigma_b+i\omega\varepsilon_b}{(\sigma+i\omega\varepsilon)}\oint_{\partial\Omega}[E_b^H(r',r)\times E(r')]\cdot dS$$

and

$$NH=\frac{\mu_b}{\mu}H_{pb}(r)+\frac{1}{i\omega\mu}\oint_{\partial\Omega}[(\sigma_b+i\omega\varepsilon_b)G_b^E(r',r)\times E(r')]\cdot dS+\frac{\mu_b}{\mu}\oint_{\partial\Omega}[H_b^E(r',r)\times H(r')]\cdot dS$$

Where M and N is 3×3 matrices, the EM sources are located in the up air half space. Suppose that the earth surface has topography, we develop determined and stochastic curve surface boundary GL EM modeling. Then we use weak regularizing to construct the surface GL inversion for the EM properties and topography. There is no any artificial boundary in our GL surface method. There is no large matrix need to solve in the GL surface method. The GL EM surface modeling and inversion and their stochastic version have widely application in the material sciences, cell phone health, antennas, rough surface, MRI, GPR, medical, geophysics etc sciences and engineering.

REFERENCES

1. Xie, Ganquan, Jianhua Li and Feng Xie, "New Global and Local Electromagnetic Field Modeling And Inversion", *to be presented PIERS2005*, 2004.

Accurate and Efficient Modeling of Monostatic GPR Signal of Dielectric Targets Buried in Stratified Media

I. van den Bosch [1], **S. Lambot** [2], **M. Acheroy** [3], **I. Huynen** [1], **P. Druyts** [3]

[1] Catholic University of Louvain, Belgium
[2] Delft University of Technology, The Netherlands
[3] Royal Military Academy, Belgium

This paper presents an accurate model of a monostatic stepped-frequency continuous-wave (SFCW) ground-penetrating radar (GPR). The model takes into account the multiple reflections occuring between the soil, target and antenna, which is a transverse electromagnetic (TEM) ultra-wide band (UWB) horn. The antenna radiation pattern is accounted for by a Huyghens cosinusoidal distribution of electric and magnetic current located on the aperture. The model is validated by experiments, involving dielectric targets embedded in a sandbox. These experiments validate altogether the radar modeling, as well as the MoM and the dyadic Greens functions (DGFs) used in the numerical algorithms.

Numerical Modeling on Transient Electromagnetic Responses of a 3-D Electric Dipole Source on 2-D Plarizable Earth Surface

Yanjun Chang, **Yanzhong Luo**, **Yongliang Meng**
China University of Geosciences, China

Numerical modeling on transient electromagnetic responses of a 3-D electric dipole source on 2-D earth model, which is called 2.5-D numerical modeling, is an important basis work in electromagnetic geophysics exploration. When the axial transient electrical-field (for short dipole-dipole array) response on the polarizable earth surface is studied in time domain, it is called time spectral resistivity method (TSR). In this paper, 2-dimensional numerical algorithm for TSR is studied. Basic procedures are:

(1) carry out the Laplace transform and the Fourier transform to the partial differential equations of E and H vectors in the 3-D spatial field, and then the boundary-value problems are converted into 2-D partial differential equations for scalar E and H;

(2) turn 2-D boundary-value problems into 2-D problem of calculus of variations, and use finite element technique to seek for numerical solution;

(3) take the inverse Fourier transform and the inverse Laplace transform to obtain transient responses of the electric field.

The main characters of our algorithm are as following.

(1) A 2-D finite element method is adopted in which two diagonal lines are increased in each rectangular net to form triangular networks. Unknown variable at central node of the rectangular net is eliminated by the Gauss elimination. So complex 2-D geoelectric section can be modeled more exactly but computation quantity is much less than that in rectangular network.

(2) A new algorithm of computing secondary field directly is founded, which only needs computing two components of electric and magnetic primary field. Not only the computation accuracy is high, but also the computation time is not increasing much.

(3) The new G-S inverse Laplace transform method based on the delay theorem of Laplace transform is used for the rapid calculation of the transient electromagnetic response with dense samples.

(4) The algorithm can be used for computing the transient electromagnetic response on the conductive and polarizable earth, i.e.the electromagnetic and induced polarization modeling can be realized simultaneously using the algorithm.

Based on established algorithm, time spectral responses of the electric field are computed for one 2-D slab model in the half space. Computed data are drawn to reflect the anomaly characteristic in a kind of figure, the profiling curve map at different time channels.

Study on Characteristics of Transient Electric Field by an Electrical Dipole Source on One-dimensional Polarizable Earth Surface

Yanjun Chang, **Yanzhong Luo**
Quiqing Zhang, **Ying Zhang**, **Zhonglin Cao**
China University of Geosciences, China

Spectral induced polarization (SIP) method or complex resistivity (CR) method, which adopts electric dipole as transmitting source ($n \cdot 10^{-2} \sim n \cdot 10^{2}$Hz) and studies axial electrical field responses(for short dipole-dipole array), has been used widely in environmental and engineer geologic investigation as well as various explorations of mineral resources, oil & gas and so on since 70s of last century. As a kind of frequency-domain electromagnetic method, its exploration effect is commonly accepted or recognized. But the data acquisition takes much time in frequency-spectrum measurement for different frequency one by one, which results in low efficiency and high expense in practical production. In theory, frequency spectral is equivalent with time spectral, and they may be transformed each other. Therefore, when the same array as the SIP method or CR method is used in practical work, and observes the transient step-off responses of the electric field component in time domain, namely time spectral responses, a high producing efficiency is achieved in the work. Imitating the name of CR in frequency-spectral measurements, we name this new method as time spectral resistivity method, for short TSR. Studying the characteristics of transient electrical field by an electrical dipole source over one-dimension polarizable earth surface is one of its basic theory works.

Based on the numerical modeling, we obtain lots of computation results on different polarizable earth models and transient response curves. According to the shape of the curves, we study the time spectral characteristics of electric field component and obtain following conclusions. (1) Spectral parameters of induced polarization (IP) have the same influence rules on the transient response curve in TSR as the frequency spectral (especially, phase spectral) curves. On bi-logarithmic axes, chargeability (m) has mainly an influence on the amplitude of the curve, time constant (τ) mainly influencing on the horizontal position of the curve, and frequency dependence (c) mainly influencing on the curve shape. (2) Electromagnetic effect is primary in the early time and IP effect is primary in the later time, which makes it possible to utilize two kinds of effect respectively. (3) On the condition of one-dimension polarizable earth, Ignoring of the magnitude-value difference and trifling difference, the curve shape of the transient response of the electric field component can be simply classified as two kinds of type. One is D type (including H- and Q-types); another is G type (including K- and A-types).

Inversion Study of Spectral Induced Polarization Based on Improved Genetic Algorithm

Zhonglin Cao, **Yanjun Chang**, **Yanzhong Luo**
China University of Geosciences, China

As a kind of electromagnetic exploration method in frequency domain, spectral induced polarization (SIP) or complex resistivity (CR) technique is widely used in geophysical prospecting. In the theory of SIP or CR data interpret, Cole-Cole model is a basic expression, which has three parameters (m, τ, c) to reflect the spectrum-function characteristic. Chargeability (m) has mainly an influence on the amplitude of the spectral function curve, time constant (τ) mainly influencing on the horizontal position of the curve, and frequency dependence (c) mainly influencing on the curve shape. Due to their respective special character, the inversion of m, τ and c based on the frequency spectral data is usually instable. In this paper, we adopt a kind of improved genetic algorithm to implement inversion computation, the obvious characteristic of which are that it does not depends on the initial model, and only needs giving a proper scope for each inversed parameter.

Inversion computations on one Cole-Cole model show that the algorithm converges fast, and has very good stability and high precision, and even can permits the observed data random error up to 15%. Computations on two Cole-Cole models, which simulate the fact that the effects of electromagnetic and induced polarization exist simultaneously, show the algorithm is still fast convergence and high precision, and permits a few observed data error (say, 5% random error). Only when random error add up to 10%, the results of inversion begin to change worse.

Session 3A7

Electronically Controllable Microwave and Millimeter-wave Devices and Antennas 1

Artificial Transmission Lines in the Design of Broadband Tunable Phase Shifters

I. S. Nefedov
Helsinki University of Technology, Finland

S. A. Tretyakov
Helsinki University of Technology, Finland

A possibility to design tunable phase shifters with reduced frequency dispersion using combined sections of forward-wave and backward-wave transmission lines is discussed. It is shown that inclusion of backward-wave sections into a transmission line always increases the total dispersion. On the other hand, we show that dis- persion can be reduced by means of lines with positive anomalous dispersion and provide an example of such line.

One- and two-dimensional "metamaterials" for the microwave range can be realized without any resonant elements by periodically loading two-dimensional transmission lines with lumped element series capacitors and shunt inductors [1, 2], and such structures can be used in the design of tunable phase shifters and delay lines. The phase compensation idea was proposed by N. Engheta [3], who suggested a sub- wavelength cavity resonator formed by two adjacent material slabs that support forward and backward waves.

The idea of phase compensation was further extended to the design of phase shifters in [4]. That paper discusses a broadband phase shifter formed by connected transmission- line sections with forward and backward waves. This design allows to realize negative phase shift values in comparatively short sections of transmission lines. A natural question arises: Is it possible to reduce the frequency dispersion of phase shifters using this approach, in addition to achieving negative phase shifts? And if possible, what kind of transmission line or filling metamaterial is required? These are the questions that we will address in this presentation.

REFERENCES

1. Silin, R. A. and V. P. Sazonow, "Slow-wave structure", *Staschera, Boston-SPA Eng., National-Landing Science and Technology, 1971. Translated from Russian: R.A. Silin, Slow-Wave structures, Moscow, Sovetskoe Radio, 1966. R.A. Silin, Peri- odic Waveguides, Moscow, Phasis,* 2002.
2. Eleftheriades, G. V., A. K. Iyer, and P. C. Kremer, "Planar negative refractive index media using periodically L-C loaded transmission lines", *IEEE Trans. on Microwave Theory and Techniques*, Vol. 50, 2702, 2002.
3. Engheta, N., "An idea for thin subwavelenght cavity resonators using metamaterials with negative permittivity and permeability", *IEEE Antennas Wireless Propagat. Lett.*, Vol. 1, 10, 2002.
4. Antoniades, M. A. and G. V. Eleftheriades, "Compact linear lead/lag metamaterial phase shifters for broadband applications", *IEEE Antennas and Wireless Propagation Letters*, Vol. 2, 103, 2003.

Applications of Electromagnetic Bandgap and Tunable Left-handed Materials

Viktor Krozer[1], **Elisa Sbarra**[1], **Martin Schüßler**[2], **Christian Damm**[2], **Rolf Jakoby**[2]

[1]Technical University of Denmark, Denmark
[2]Technische Universität Darmstadt, Germany

The paper discusses the applications of electromagnetic bandgap materials and tuneable left-handed materials in microwave and millimetre-wave frequencies. Emphasis is on structures, which offer advantages over traditional approaches, especially for direct implementation in integrated circuits. The structures discussed in detail in the paper are examples of microwave and millimetre-wave filters and phase-shifters, which represent a paradigm change in the design of such circuits.

EBG and LH meta-materials have been discussed in view of their applications in microwave circuits. The emphasis is on demonstration of particular circuit solutions and topologies.

The possibility to realize compact phase shifter circuits with the principle of periodically LC loaded lines with LH wave propagation is demonstrated in this paper. Basic expressions are derived, describing the influence of losses due to tuning activated input mismatch and the quality of the tuneable material. With the help of a figure of merit (FoM), describing the phase shift per attenuation degree, a comparison between a phase shifter with LH- and RH-wave propagation is performed. They reveal that LH lines can have the same FoM as RH lines but with dramatic length reduction, however with the drawback of bandwidth reduction. A phase shifting circuit is developed as a demonstrator exhibiting reasonable accordance with simulation results. The circuit is designed for 2GHz, has the length of $\lambda/3$ and can produce an absolute phase shift of 184° with a FoM of 28°/dB.

Eigenvalue Analysis of Curved Open Waveguides Using a Finite Difference Frequency Domain Method Employing Orthogonal Curvilinear Coordinates

C. S. Lavranos, **G. A. Kyriacou**
Democritus University of Thrace, Greece

The numerical solution of the eigenvalue problems for arbitrary cross section open waveguides constitute one of the most arguable problems of computational electromagnetism. Due to the difficulty of the problem only a few articles have been published toward this aim, e.g. [1], [2], which have employed the Finite Difference in conjunction with the Perfect Matching Layer technique, [3], to confine the solution domain to a finite area. However, to the authors knowledge, none of these techniques can handle curved open geometries. So, a challenging problem refers to handling the proper absorbing boundary condition along with a numerical method, so as to obtain accurate numerical results for the eigenvalues of a given open curved geometry.

The method presented in this paper combines a 2-D Finite Difference Frequency Domain eigenvalue method formulated in orthogonal curvilinear coordinates, [4], with the proper mesh truncation, in order to simulate open curved geometries. The first aim of this technique is to study curved open waveguides or microstrip lines printed on curved substrates either isotropic or anisotropic. Besides, this method is capable of examining leaky waves structures. This is achieved by applying the proper ABC tensor to the 2-D FDFD discretized orthogonal curvilinear grid. The 2-D FDFD analysis is formulated as an eigenvalue problem for the complex propagation constants and it is restricted to structures uniform along the third direction ($u_3 - axis$), along which field propagation is considered. As the method has the capability to handle anisotropic lossy media, a PML absorbing boundary condition, e.g. [3], is easy to implement using the well known PML permittivity and permeability tensors. So, starting from this implementation this paper addresses the three basic issues. How can the PML describe an aperture on a curved geometry? How does the PML boundary influence the mode spectrum of the curved waveguide structure? How accurate can be the description of the leakage effects? Moreover, the use of other mesh truncation methods will be considered, in order to obtain more accurate results and to avoid some of the PML's negative influences.

Numerical results for the eigenvalues of several open structures as described above will be presented at the conference, as well as comparisons with already published results.

REFERENCES

1. Tischler, T. and W. Heinrich, "The perfectly matched layer as lateral boundary in finitedifference transmission-line analysis", *IEEE Transactions On Microwave Theory And Techniques*, Vol. 48, 2000.
2. Marengo, EA, CM Rappaport and EL Miller, "Optimum pml abc conductivity profile in fdfd", *Transactions on Magnetics*, Vol. 35, 1506, 1999.
3. Berenger, J. P., "A perfectly matched layer for the absorption of electromagnetic waves", *J.Comput. Phys*, Vol. 114, 185, 1994.
4. Lavranos, C. S., G. A. Kyriacou and J. N. Sahalos, "A 2-d finite difference frequency domain (fdfd) eigenvalue method for orthogonal curvilinear coordinates", *Progress In Electromagnetics Research Symposium, PISA, Italy*, 2004.

Finite Element Method and FDTD Method for Open Electromagnetic Structures

A. V. Brovko, **A. G. Rozhnev**
Saratov State University, Russia

A. B. Manenkov
Institute for Physical Problems, Russian Academy of Sciences, Russia

The development of the electronically controllable microwave and millimeter wave devices, especially open systems, requires precise numerical modeling of the electromagnetic structures with complex media parameters and complex geometry. Application of standard numerical techniques such as FEM or FDTD method often does not provide desired precision and performance of the software. Sometimes, more relevant results can be obtained using the combinations of standard numerical techniques with additional procedures based on analytical or semi-analytical analysis. In this paper we present several newly developed techniques which exploit combinations of FEM and FDTD methods with other techniques based on variational principles and integral equations.

The paper contains the following topics.

1. The software based on FEM which permits to analyse the eigenmodes of waveguides with general permittivity and permiability tensors has been developed.

2. A method for the calculation of the dispersion characteristics of the helix slow wave systems has been proposed. The problem is solved in the cross section of the slow wave system by the FEM. The helix is modeled as the spirally conducting cylinder.

3. Efficient versions of the FE and integral equation methods have been developed to analyse the guided (surface) modes of an arbitrary shaped optical fibre. The first approach is based on the replacement of the open waveguide by the screen guide structure with an artificial impedance wall. The integral equation is solved by the adaptive collocation technique.

4. A method for scattering analysis of the electromagnetic waves on the end of the dielectric waveguide with arbitrary cross section has been developed. The method is based on the combination of FEM and a variational formula for the reflection coefficient.

5. A method for the analysis of the eigenmodes in the waveguiding systems near cut-off and for the analysis of leaky modes has been proposed. The method is based on the combination of FEM and an integral equation.

6. The problem of the guided mode reflection from the planar dielectric waveguide end and from other discontinuities is studied by the FDTD method. The combination of FDTD method and variational technique is proposed for improvment of the precision of the computations.

Analysis of Wave Diffraction on Irises by the Combined FDTD Method and Variational Technique

A. V. Brovko
Saratov State University, Russia

A. B. Manenkov
Institute for Physical Problems, Russia

In the past few years the FDTD method found wide application for the scattering problems. In particular, it was used for the analysis of the diffraction of the guided modes in the open dielectric waveguides with discontinuities. The method is the effective and universal tool and it permits the analysis for complex enough geometry of the problem. However, the results obtained with the FDTD method often depend on some auxiliary parameters that should be defined during the computation. For instance, the result may depend on the cells sizes, the positions of the reference planes, the sizes of the computational domain (for the open structures), the type and the parameters of the boundary conditions, the parameters of the exitation and so on. It is difficult to set all these parameters so that their influence on the result would be negligible. The demands to the parameters are contradictory, and the compromise values often do not provide high precision taking into account limited computational resources.

In this paper we present a combined method for the analysis of the guided mode diffraction on the irises in the planar waveguide. The method is based on the combination of the FDTD technique and the approach which follows from the theory of the spectral decompositions. When we calculate the reflection and transmission coefficients, we compute the field distributions by the FDTD method, and substitute the results into the functional derived by the eigenmode expansion technique. Due to stationarity the precision of the new results is higher than the accuracy of the ordinary approaches, even if we apply more coarse meshes. Furthermore, this approach reduces the dependence of the result on the auxiliary parameters. The eigenmode expansion approach also permits to compute easily the far zone fields (directivity diagram). The method can be applied to other problems (for example, for the analysis of the mode scattering by mirrors).

Cylindrical Horn Antennas Analysis Using a Hybrid Mode Matching-Auxiliary Sources Technique

S. G. Diamantis, **A. P. Orfanidis**, **G. A. Kyriacou**
Democritus University of Thrace, Greece

J. N. Sahalos
Aristotle University of Thessaloniki, Greece

Horn antennas are widely used as feeds of large reflectors and lens antennas, as elements in phased arrays and as standard-gain components in antenna measurements. A lot of works are devoted in horn antenna analysis during the last decades. However most of them do not take into account the discontinuity between the horn aperture and the free space. Different approaches for the analysis of the discontinuity between the horn aperture and the free space have been used. Up to now the researchers effort was concentrated on the study of the rectangular horn aperture discontinuity. Wriedt et al [1] as well as Liu et al [2] employed the method of moment (MoM) in conjunction with a stepped wavequide approximation to analyze this discontinuity, while Encinar et al, [3] considered a plane wave expansion for the field in the free space which was in turn matched (through the continuity conditions) to the field of the last waveguide section. Our current effort aims at the analysis of the aperture discontinuity for cylindrical horn antennas.

In our previous work [4], a hybrid technique was employed for the analysis of the rectangular horn antenna, including the discontinuity effect between aperture and free space. The transition from the feeding waveguide to the radiating aperture has been analyzed using the mode matching technique (MMT) while the discontinuity between the horn aperture and free space has been modeled combining the method of auxiliary sources with the MMT for the stepped waveguide section. In this paper the method proposed in [4] will be extended in order to analyze a cylindrical horn antenna. Following a similar way, the closed part of the horn (including the conical region) will be approximated by circular waveguide sections, namely employing the stepped waveguide approach. The field in the unbounded region will be described by pairs of orthogonal elementary dipole sources. These sources will be located on a plane inside the horn and at a very small distance from the aperture. The generalized scattering parameters of the discontinuity between the horn aperture and the free space will be obtained by enforcing the field continuity conditions on the aperture surface. This approach although referred as Auxiliary sources technique it is actually a modification of the moment method, where the sources are displaced from the surface on which the boundary conditions are imposed. Moreover, the sources considered are more accurately defined as equivalent sources in the sense of Love's equivalence principle. Summarizing, the study includes the determination of the input reflection coefficient, the antenna input impedance as well as the far field radiation patterns for several cylindrical horns.

REFERENCES

1. Wriedt, T., K. H. Wolff, F. Arndt and U. Tucholke, "Rigorous Hybrid Field Theoretic Design of Stepped Rectangular Waveguide Mode Converters Including the Horn Transitions into Half Space," *IEEE Trans. on Antennas and Propagation*, Vol. AP-37, No. 6, 780, June 1989.
2. Liu, K., C. A. Balanis, C. R. Birtcher, G. C. Barber, "Analysis of Pyramidal Horn Antennas Using Moment Methods," *IEEE Trans. on Antennas and Propagation*, Vol. 41, No. 10, 1379, October 1993.
3. Encinar, J. A., J. M. Rebollar, "A Hybrid Technique for Analyzing Corrugated and Noncorrugated Rectangular Horns," *IEEE Trans. on Antennas and Propagation*, Vol. 34, No. 8, 961, August 1986.
4. Diamantis, S. G., A. P. Orfanidis, G. A. Kyriacou and J. N. Sahalos,"Horn Antennas Analysis Using a Hybrid Mode Matching-Auxiliary Sources Technique," *PIERS 2004, Piza, Italy.*

Development of an Adaptive and a Switched Beam Smart Antenna System for Wireless Communications

F. E. Fakoukakis, **S. G. Diamantis**, **A. P. Orfanides**, **G. A. Kyriacou**
Democritus University of Thrace, Greece

A new technique that aims to improve the capacity and quality of wireless communication systems is the SDMA (Space Division Multiple Access), which is mainly based on the use of Directional Antennas driven by electronically controllable Beamforming Networks (BFNs), [1]. Alternatively, this technique is also known as a Smart Antenna. Our present research activity is focused on the development of Beamforming Networks.

These networks can be developed either at RF or IF level. The use of IF-BFNs results in a Smart Antenna System fully exploiting the advantages of an Adaptive Antenna. Also, their implementation and their digital control is easier. However, IF-BFNs suffer from increased complexity, since they are incorporated into a multichannel topology requiring the development of the system from scratch. On the other hand, RF-BFNs offer decreased complexity despite their harder control requirements. Moreover, RF-Beamforming Networks exploit only some of the Smart Antenna Systems capabilities. Their critical advantage is the easy integration with the existing architectures in Base Stations, since only the replacement of the RF front-end is needed. All the above, have lead us to focus our research on the design and development of RF-BFNs for Wireless Communications, including both Switched Beam and Adaptive systems.

The Switched Beam Systems are the simplest and provide less capability, in contrast to the Adaptive Systems which are more reliable beyond their complexity and cost. This study concentrates on the design of a complete transmit-receive system for Wireless Applications. The Switched Beam System will cover a spherical sector in the azimuth in the elevation direction. The BFNs in both the azimuth and elevation directions will be based on a printed Butler matrix topology [1], [2], [3]. A separate Direction Of Arrival (DOA) unit will be developed to provide the intended-desired user direction. A control unit will be responsible for controlling the above units.

The adaptive system follows a similar approach. The main difference is the use of RF vector modulators for the establishment of a multichannel beamforming network. This in turn enables a very accurate pointing of the antenna beam in the desired direction. This work is supported by the Greek project "Pythagoras". The system design is carried out and some of the modules are already fabricated and tested. The system level design for both switched beam and the adaptive system will be presented at the Symposium, along with some simulated and experimental results of some modules. A comparison of the two systems will be tried.

REFERENCES

1. Litva, J. and T. K-Y Lo, *Digital Beamforming in Wireless Communications. Artech House*, 1996.
2. Hansen, R. C., *Phased array antennas. John Wiley & Sons*, 1988.
3. Hansen, R. C., *Microwave Scanning Arrays. Academic Press*, 1966.

Modulation of mm-waves by an Acoustically Controlled Monocrystalline Hexagonal Ferrite Resonator

M. Y. Koledintseva
University of Missouri-Rolla , USA

To develop mm-wave modulators, high-anisotropy monocrystalline hexagonal ferrite resonators (HFR) can be used. One of the ways to modulate the hexagonal ferrite resonator's resonance frequency is to periodically vary the angle between the equilibrium magnetic moment and the external magnetization field. This angular control can be made by the mechanical (acoustic) oscillations excited in a piezoelectric slab having a good acoustic contact with the HFR.

It is shown theoretically and experimentally that an acoustic control of the resonance frequency of a monocrystalline magneto-uniaxial hexagonal ferrite resonator (HFR) and a corresponding modulation of mm-wave signals is possible.

The quasistatic mathematical model of the uniaxial HFR with angular control of its resonance frequency is considered. An approach using the magnetic susceptibility tensor of the HFR allows analyzing the behavior of the magnetization vector components in the vicinity of FMR at comparatively low frequencies of modulation.

Amplitudes of the modulation frequency harmonics in the magnetization vector components, as well as amplitudes of the harmonics of the modulated mm-wave signals, have been analyzed. They are proportional to the intensity (power) of the input signal, and they also depend on physical parameters of the ferrite, its angle of orientation, the waveguide geometry, as well as on the amplitude and frequency of the modulating signal.

The formulas for finding an optimal angle of orientation and the parameters of the modulation yielding the maximum modulation depth of the mm-wave signal have been obtained, and the results of calculations are represented. The calculated optimal angles of the HFR orientation agree with the experimentally obtained results.

Practical realization of a modulator on the basis of an HFR and a piezoelectric slab (PES) has been proposed. The possibility of modulating the 8-mm-wave signal by an HFR-PES structure has been demonstrated. It has been shown that enclosing the ferrite resonator in a quartz glass capsule, so that the HFR's position is fixed at the optimal angle of orientation, increases the coupling between the HFR-PES structure with the electromagnetic field of the waveguide and leads to the higher modulation depth. The presence of any viscous medium in the quartz capsule decreases the acoustic coupling between the HFR and PES. Presence of water or alcohol decreases electromagnetic coupling between the HFR and the waveguide.

Session 3P1

Meta-materials and Structures with Negative Refraction 2

Characterization of Metamaterials in Terahertz Region by Terahertz Time Domain Spectroscopy

Baogang Quan[1,2], **Xin-Long Xu**[1,2], **Chao Li**[1,2], **Xiao-Xiang Xia**[1,2]
Qiang Wang[1,2], **Li Wang**[1,2], **C. Z. Gu**[1,2]

[1]Institute of Physics, Chinese Academy of Sciences, China
[2]Institute of Electronics, Chinese Academy of Sciences, China

In recent years, the composition of split ring resonators (SRRs) and wires of conducting metal material has been proved to exhibit simultaneously negative permeability and negative permittivity and hence negative refractive index by many results of theoretical and experimental investigations. The magnetic response and negative refraction of metamaterials in terahertz region are very important because they possess potential applications for the magnetic resonance, security imaging, and remote sensing and so on. Until now, Fourier transform infrared spectrum has been the principal tool to characterize the response of SRRs, but there is a limitation in the measurement, that is the detecting generally performed at cryogenic ambient in order to avoid the influence of the black radiation signal. In our work, terahertz time domain spectroscopy (THz-TDS) was introduced to characterize the abnormal phenomena of met materials, including the response of SRRs, in terahertz region at room temperature. Terahertz time domain spectroscopy utilizes a coherent electromagnetic pulse wave as a detecting source. The amplitude and phase of the wave are given by fast Fourier transformation, and then other physical properties can be extracted.

The microstructures of the samples were fabricated on a quartz slab by photolithography technology, magnetron sputtering and lift-off processes. Two absorption peaks were observed in the extracted absorption spectroscopy, which were induced by the surface plasmon resonance at 0.9 THz and by the LC resonance at 2.0 THz, respectively. It was found that the two different resonances showed different phase characteristics in phase spectroscopy. For the surface plasmon resonance, a weak abnormal dispersion and negative group velocity as well as low group delay can be observed while reversely a strong abnormal dispersion and negative group velocity and high group delay were observed from LC resonance. The simulations about the transmission of terahertz time domain pulse were performed using High Frequency Software Simulator, and the results were consistent with the experimental ones. Besides, the difference in phase spectroscopy also indicates that THz-TDS is a very effective tool for the characterization of the metamaterials at terahertz.

Resonant and Negative Index Behavior of Non-reciprocal Omega Media at MW Frequencies

Vasundara V. Varadan
University of Arkansas, U.S.A

Omega media also called pseudo-chiral media consist of a distribution of Ω shaped metallic objects in which the gap at the base of the Ω is smaller than the radius of the circular part. Such media are magneto-electric and obey constitutive relations of the form $D = \vec{\varepsilon} \cdot E + \vec{\alpha} \cdot H$ and $B = \vec{\beta} \cdot E + \vec{\mu} \cdot H$ where ε and μ are the permittivity and permeability tensors. α and β are the magneto-electric coupling tensors, and if they are not equal, the material is pseudo-chiral and non-reciprocal. The material must be anisotropic to be nonreciprocal [1]. Anisotropic Omega media were constructed using the geometrical parameters provided by He et al [2]. Omega patterns were printed on a dielectric sheet with random and fixed orientations and spaced periodically or randomly in the x-y plane. Reflection and transmission coefficients are measured in the frequency range 5-110 GHz using a focused plane wave beam. The H-field of the incident beam is always perpendicular to the plane of the Omega structures. Nonreciprocal behavior is observed for forward and backward wave propagation in these samples, i.e. the propagation properties of the medium are different for waves propagating in the $\pm$z directions. The geometry of the Omega structures is such that there is a plasmon resonance and a negative index is measured for both directions of propagation with the negative behavior occurring at different frequency bandwidths. This non-reciprocal, negative index behavior has not been reported before and does not appear to be restricted to periodic systems.

REFERENCES

1. Weiglhofer & Lakhtakia, *IEEE AP-S Magazine*, Vol. 37, No. 3, 1995.
2. *Phys.Rev.Lett. A*, Vol. 322, 2003.

Engineering Nanostructures for Plasmonic Near-field Optics and Applications

Din Ping Tsai
National Taiwan University, Taiwan

The direct near-field optical imaging of the transmitted laser spots through nanostructured metallic thin film provides much important information, and reveals the local near-field optical interactions of the surface plasmons. The nonlinear absorption and refraction of the nanostructured metallic thin film can be disclosed by the experiments of Z-scan. Many interesting local interactions were found. Measurements of transmission and reflectance indicate complicate transition process of the optical interactions of the structures of nanostructured metallic thin film. Both reverse saturable absorption and saturable absorption happened at different range of input power. Negative nonlinear refraction coefficients were found for nanostructured metallic thin film. The results of the optical pump-probe are able to show the temporal dynamic optical response of the nanostructured metallic thin films which is closely related to the response time. Based on all the various local optical responses observed, interactions of localized surface plasmon are studied. The effects of the localized surface plasmon are considered to be the key issue in many aspects of near-field optical applications.

Impact of Loss on the Performance of a Negative Refractive Index Lens

Kevin J. Webb[1], **M. Yang**[1], **David W. Ward**[2], **Keith A. Nelson**[2]

[1]Purdue University, USA

[2]Massachusetts Institute of Technology, USA

Negative refractive index or left-handed (LH) material has interesting properties [1], and it has been suggested that amplification of the evanescent fields within the negative refractive index slab could result in a perfect lens [2]. Simultaneously negative permittivity and permeability implies frequency-dependent dispersion in these parameters, and, through the Kramers-Kronig relations, loss [3]. We describe the impact of small loss on the imaging potential of a LH lens.

Consider the imaging geometry of Figuer 1. The fields in the object plane ($z = 0$) with wave number $k = 2\pi/\lambda$ can be expanded into a summation of plane wave components through a Fourier transformation along the space-invariant transverse $x-$direction. In considering perturbational loss in the slab, we choose the constitutive parameters: $\epsilon_R = \epsilon'$, $\mu_R = \mu'$, $\epsilon_L = -\epsilon' + i\epsilon''$, $\mu_L = -\mu'$, giving $(\epsilon_L + \epsilon_R)/\epsilon_R = i\epsilon''/\epsilon' = i\delta_i$. Figure 2 shows the transfer function as a function of k_x/k. Notice that even minute loss has a drastic impact on $\|\tau\|$ for sufficiently large k_x/k. This means that for a realistic LH slab having some degree of loss, achieving high resolution is restricted to the near-field. Equivalently, the slab thickness is restricted with loss. The loss results in decaying field power consumption. For the perfect lens, the maximum amplitude of the amplified evanescent field in the slab, which occurs at the right interface ($z = z_0 + d$), reaches its maximum when $z_0 = 0$, and is a minimum when $z_0 = d$. When perturbational loss is introduced, the larger the field amplitude at z_0, the higher the power consumption of the decaying field.

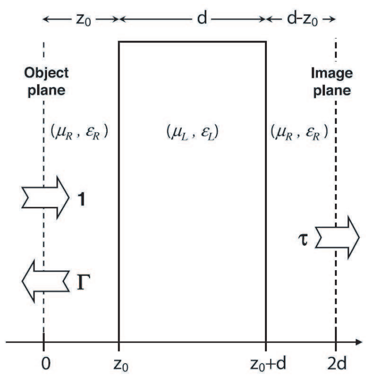

Figure 1: Planar negative refractive index lens schematic.

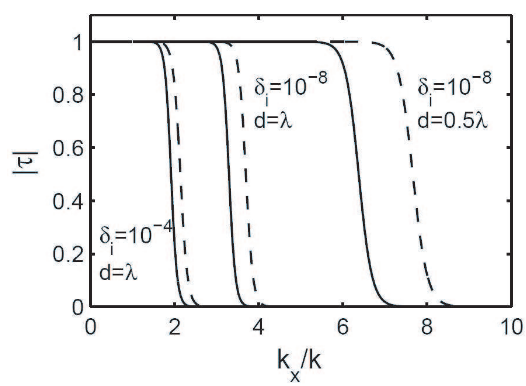

Figure 2: Transfer function of the slab of left- handed material with different slab thickness and perturbational loss. Solid: TM fields (H_y), dashed: TE fields (E_y).

REFERENCES

1. Veselago, V. G., "The electrodynamics of substances with simultaneously negative values of ϵ and μ", *Sov. Phys. Uspekhi*, Vol. 10, 509, 1968.
2. Pendry, J. B., "Negative refraction makes a perfect lens", *Phys. Rev. Lett.*, Vol. 85, 3966, 2000.
3. Webb, K. J., M. Yang, D. W. Ward, and K. A. Nelson, "Metrics for negative refractive index materials", *Phys. Rev. E*, Vol. 70, 035602, 2004.

Study on the Quality of Subwavelength Focusing with a Slab of Left-handed Material (LHM)

Chao Li, **Cixiang Liu**, **Qiang Sui**, **Fang Li**
Institute of Electronics, Chinese Academy of Sciences, China

Subwavelength focusing with LHM slab was first proposed by Prof. Pendry and attracted great attention and hot debate. This paper deals with the study on the quality of focusing using a slab of LHM. The focusing qualities of both the composite LHM slab and the homogeneous LHM slab were studied by FDTD and Spectral Domain Method (SDM), respectively. The composite one is similar to that introduced by D.R. Smith et al. in 2001, which consists of the split-ring-resonators and metallic thin wires.

As we know, Pendrys theory of perfect lens is based on these two strict conditions: the LHM is homogeneous and isotropic and it's relative permittivity and permeability are simultaneously -1 (matched conditions). Our FDTD simulation was done at the frequency on which the real part of the refraction index equal to -1 by phase velocity measurement. The focusing behind the composite LHM slab was obviously observed in the numerical results. However, the image quality was degraded by the attenuation of the composite LHM (The imaginary part of the refraction index), by the unmatched conditions (the wave impedance of LHM is not exactly equal to that of air), by the finite length of the slab, and by the anisotropic of the composite material.

To investigate the dependence of the image quality on these factors, we used the spectral domain method (SDM) to analyze the subwavelength focusing of a homogeneous LHM slab with different conditions such as lossy and unmatched. The super-resolving ability was studied by extract the propagating and evanescent components in the image plane. Results of the two methods (FDTD and SDM) were compared and ways have been found to improve the quality of the focusing by the composite LHM slab.

Low-Frequency Superprism Effect and Hybridization of Transmission-Line Modes in Two- and Three-Dimensional Wire Media

P. A. Belov [1], **C. R. Simovski** [2], **I. S. Nefedov** [3], **S. A. Tretyakov** [3]

[1] Queen Mary University of London, UK
[2] St. Petersburg State University of Information Technologies, Mechanics and Optics, Russia
[3] Helsinki University of Technology, Finland

In the recent years the periodic metallic lattices have found many applications both in optical and microwave ranges. However, some fundamental problems have not been resolved yet, even for typical metallic electromagnetic crystals. One of them is the problem of low-frequency spatial dispersion in wire media (WM). The low-frequency spatial dispersion of a simple wire medium (a doubly periodic regular array of parallel wires) has been studied only recently in [1].

In the present paper this theory is generalized for double and triple wire media, i.e. lattices of perfectly conducting wires comprised of two or three doubly periodic arrays of parallel wires which are orthogonal to one another. An analytical method based on local field approach is used [2]. The explicit dispersion equations are obtained and studied. A possibility to introduce a dielectric permittivity is discussed. The theory is validated by comparison with the numerical data available in the literature.

The study of spatial dispersion effects in the a double and triple wire media has been started in work [3]. However, this study (based on the numerical approach) is far from being complete. Our theory significantly complements the results [3]. It is analytical one, and in order to validate it, a comparison to the results from [3] is carried out.

The materials under consideration could find various applications due to its very unusual properties caused by strong low-frequency spatial dispersion phenomena. We would like to note especially such applications as creation of low frequency super-prism and design of materials with negative refraction.

REFERENCES

1. Belov, P. A., R. Marques, S. I. Maslovski, I. S. Nefedov, M. Silverinha, C. R. Simovski and S. A. Tretyakov, "Strong spatial dispersion in wire media in the very large wavelength limit", *Phys. Rev. B*, Vol. 67, 113103, 2003.
2. Simovski C. R. and P. A. Belov, "Low-frequency spatial dispersion in wire media", *Phys. Rev. E*, Vol. 70, 046616, 2004.
3. Silveirinha M. G. and C. A. Fernandes, "A hibrid method for efficient calculation of the band structure of 3D metallic crystals", *IEEE Trans. Microw. Theory Tech.*, Vol. 52, 889, 2004

Session 3P2

Poster Session 2

Analysis of Metasurface with Periodic Apertures of SRRs or Spiral Structure

Wei Sun, **Yijun Feng**, **Hongying Liu**, **Junming Zhao**
Nanjing University, China

In recent years, metamaterials and metasurfaces have been the subject of study by various research groups due to their unconventional properties, which can offer electromagnetic properties that are difficult or impossible to achieve with natural materials. Left-handed metamaterial with simultaneously negative permittivity and permeability has indicated both theoretically and experimentally the negative refraction of electromagnetic wave. Such metamaterial was first realized by an array of split ring resonators (SRRs) and thin wires in alternating layers. Metasurfaces or artificial frequency selective surfaces, which are usually constructed as planar 2-dimensional periodic arrays of metallic elements with specific geometrical shapes, or as periodic apertures in a metallic screen, have also been widely studied and found a variety of applications in microwaves and optics.

In the presented paper, the SRRs or spiral structure, which is an externally driven L-C resonant element, has been applied to construct frequency selective metasurface. The metasurface is formed by 2-dimentional periodic arrays of apertures with SRRs or spiral structures on a metal plate, as shown in fig. 1. Full-wave analysis utilizing the finite-element method based numerical simulation has been carried out to study the electromagnetic transmission and reflection behavior of the metasurface. Total transmission peak has been observed at frequency corresponding to the resonance of the SRRs or spiral structure when the metasurface is illuminated by a normally incident plane wave. We have also found that such transmission peak is polarization dependent due to the cross-polarization effects in SRRs or spiral, and only occurs for incident wave with a nonvanishing component of the electric field along the y-axis. The periodicity of the aperture array does not have much influence on the frequency of the transmission peak, but affects the bandwidth of the peak. We will also present the transmission coefficient measurement on such metasurfaces, which conforms the numerical analysis. We believe this kind of metasurface with polarization dependent frequency selective phenomenon will find useful applications in practical microwave devices and antennas, since the resonant frequency could be easily tailored by changing the geometry of the aperture.

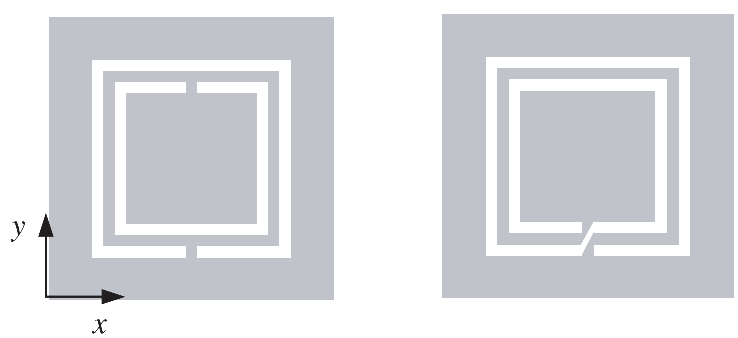

Figure 1: Unit cell of SRRs and spiral aperture in the metasurface

Design and SAR Analysis of Broadband PIFA with Triple Band

D. G. Choi[1], **C. S. Shin**[1], **N. Kim**[1], **H. S. Shin**[2]

[1]Chungbuk National University, Korea
[2]Kunsan National University, Korea

This paper proposed a novel broadband PIFA(Planar Inverted-F Antenna) for IMT-2000/ WLAN/DMB terminal. Two branch lines for meander type were utilized in order to improve the characteristics of PIFA which usually has a narrow band. The shorting strip between the ground plane and meander-type radiation elements were used in order to minimize the size of the antenna. The -10 dB return loss bandwidth of a realized antenna was 38.2%(1.84 $\sim$ 2.71 GHz), which contains the broadband bandwidth with triple band. And the simulated and measured values of 1 g and 10 g averaged peak SAR on human head caused by the triple band PIFA mounted on folder-type handsets were analyzed and discussed. As a result, the measured 1 g and 10 g averaged peak SARs of PIFA were similar to simulated values and were lower than the 1.6 W/kg and 2 W/kg of 1 g and 10 g averaged peak SAR limits.

Internal Monopole Antenna Design for Multi-band Operation and SAR Analysis

C. S. Shin, **D. G. Choi**, **N. Kim**
Chungbuk Na'l Univ., Korea

J. I. Choi
Electronics and Telecommunications Research Institute, Korea

In this paper, the planar monopole antenna mounted on PCS/IMT-2000/WLAN handset for SAR reduction is designed. Frequency characteristics and SAR value optimized with various design parameters are analyzed and discussed. The 1 g and 10 g peak average SARs of internal monopole antenna are 0.656 and 0.387 W/kg respectively. And the internal monopole antenna and external monopole antenna attached on the handset are tested and compared. As a result, internal monopole antenna's 1 g and 10 g peak average SARs are 0.686 and 0.356 W/kg. And external monopole antenna's results are 1.33 and 0.812 W/kg, respectively. So internal monopole antenna has a about 50% SAR reduction in comparison with external monopole antenna.

Two Port Representation in the Frequency Domain of Long Range Guided Waves for Non Destructive Testing of Pipes

F. Bertoncini, **S. Barmada**, **A. Musolino**, **M. Raugi**
Università di Pisa, Italy

Corrosion in pipework is a major problem in the gas, oil, chemical and other industries. Many pipes are insulated, which means that even external corrosion cannot be seen without removing the insulation, resulting in prohibitive additional costs. Ultrasonic guided waves in the pipe wall provide an attractive solution to this problem because they can be excited at one location on the pipe and propagate many metres along the pipe, returning echoes indicating the presence of corrosion or other pipe features. The transducer receives an electric input signal and responds mechanically striking the inspected pipe, and then impulsive elastic guided waves propagating along the pipe are generated.

The study of the scattered field (reflected and transmitted) provides essential features for defect detection. In general numerical modelling of ultrasonic guided waves in solid material is used for examining the generation, propagation and interaction of elastic waves in the pipe for nondestructive evaluation (NDE). Finite element models have been developed including inhomogeneity, anisotropy and three-dimensional (3-D) geometries. Some theoretical and experimental results using FEM [1], BEM [2], have been presented and also FEM-BEM coupled schemes have been proposed [3].

We present a different approach for guided waves applications. We represent the transmitted and received signal as the input and output signal of a system modelled as a two port system characterized by transfer function in the frequency domain. The equivalent representation has been tested in order to verify the accuracy of the results obtained analyzing the actual system in several operating conditions. The numerical results obtained by usual numerical simulations of the complete system under a wide range of input waveforms have been compared with those obtained by using the proposed two port equivalent.

Moreover, the proposed equivalent representation can be obtained also from experimental data. The effectiveness of this kind of representation depends on the accuracy of the measurements only. No requirements on the knowledge of the physics of the system are needed. In this way it is possible to eliminate the uncertainties affecting the precision of the usual numerical models i.e. Finite Elements or other ones.

REFERENCES

1. Lerch, R. "Simulation of Piezoelectric Devices by Two- and Three-dimensional Finite Elements," *IEEE Trans on Ultrasonics Ferr. and Freq.*, Vol. 37, No. 2, 233, 1990.
2. Cho, Y., J. L. Rose, "A Boundary Element Solution for a Mode Conversion Study on the Edge Reflection, JASA," Vol. 99, No. 4, pt. 1, 2097.
3. Kaltenbacher, M., H. Landes, R. Lerch, "An Efficient Calculation Scheme for the Numerical Simulation of Coupled Magnetomechanical Systems," *IEEE Trans. On Mag.*, Vol 33, No. 2, 1646, 1997.

Wavelet Based Characterization of Defects for Long Range Guided Waves Non Destructive Testing of Pipes

F. Bertoncini, **S. Barmada**, **A. Musolino**, **M. Raugi**, **R. Rizzo**
Università di Pisa, Italy

Pipelines are important components of petrochemical industrial plants, nuclear power generation and for the distribution of water and gas, hence their inspection in order to check the corrosion and the presence of defects is an essential aspect for the safety and continuity of operation of industrial plants.

In service inspection are usually carried by NDT whose role is becoming more and more important for condition assessment to optimise maintenance management and safety.

Recently there has been great interest on the possibility of adopting a technique based on ultrasound allowing the inspection of long pipes, the so-called "Ultrasonic long range guided waves" technique. This method allows to inspect entire pipelines by means of a limited number of accessible points. Consequently, the time for the inspection is reduced and the safety can be improved by choosing appropriate inspecting locations.

The ultrasonic wave propagates in the tested material and when impinges on an obstacle or a defect it is reflected and absorbed following the same laws of other wave propagation phenomena. However, the reflected signal coming back to the transducer is very complex and results from a sum of several waves with different frequency and phase. Then the possibility of the method to go beyond detection and location to classification and sizing, is still under investigation by researchers in the field.

Indeed one of the difficult problems about this kind of nondestructive test (NDT) inspection is the multi-mode coexistence. The different modes cannot be distinguished by the waveforms in the time domain. Cawley proposed a two-dimensional (2-D) Fourier Method to distinguish Lamb modes in wavenumber (k)-frequency (f) space. However the 2-D Fourier method needs a large number of spatial samples of Lamb waveform. This requirement makes the 2-D Fourier method difficult to be used in practice. Recently Wavelet Transform has been used for the analysis of guided waves propagation in pipes.

We propose the use of two port equivalent based on the use of wavelet expansion for the interpretation of the reflected ultrasonic guided wave. Wavelet transform is a powerful tool for transient signal processing. Its zooming property makes the resolution of high and low frequency more accurate than other signal processing method. Indeed, the wavelet expansion of a function in space characterizes the "harmonic" content of the function at every coordinate, then wavelet basis functions have very good localization properties in space. The ability of wavelets to focus on short interval for high frequency components and long intervals for low frequency components makes the method effective to represent non-smooth functions since they automatically concentrate in the fast varying regions.

The obtained results show that mode conversion phenomenon can be seen from the wavelet results, and some preliminary potentiality of wavelet transform in the Lamb wave inspection of tubular structures are evidenced.

Optimized Design Method of Microstrip Parallel-coupled Bandpass Filters with Compensation for Center Frequency Deviation

Houle Gan, **Dongxiao Yang**, **Dongwu Lou**
Zhejiang University, China

Microstrip parallel-coupled bandpass filters are widely used in modern microwave systems. Such filters consist of a cascade of coupled-line stages, which in essence are half-wavelength resonators. There are, however, two open ends in each coupled-line stage. The edge field effects of these open ends are usually modeled as parasitic capacitances, and they result in resonant frequency deviation. In practice, it is common to introduce an equivalent end extra line with length Δl, which is cut off at each open end so as to bring the center frequency back to the desired value. This approach requires empirical estimation of the value of Δl, and brings along unavoidable error in the design process.

In this paper, an optimized design method is presented. Assume the desired center frequency of the filter is f_0, while the actual center frequency deviates to f_0' if no effort is made to compensate for its open-end effects. Beginning with the resonant condition of each coupled-line stage, it is shown that f_0' is bound to be lower than f_0. To examine the relationship between f_0 and f_0' in more detail, multiple-port network parameter analysis is given. The coupled-line stage is considered as a four-port network with an impedance of Z_C connected both at ports 2 and 4, where Z_C represents the impedance of open-end parasitic capacitance. The result shows that θ_0', the electrical length of the stage at f_0', decreases when f_0 increases. If dispersion in microstrip lines is neglected, it can be written that $f_0' = 2\theta' f_0/\pi$. In this case, if $f_0' - f_0$ curve is plotted, its slope decreases when f_0 increases, namely, this curve exhibits properties of a convex function.

The key concept of the proposed method is to raise the center frequency f_0 in traditional design procedures to a new value, f_1, which results in an actual center frequency $f_1' = f_0$ at the original desired value, and no extra effort should be made to adjust physical dimensions at each open ends. To obtain the value of f_1, it is shown that analytical approach is possible, which still requires, however, the empirical estimation of C_f, the open-end parasitic capacitance. According to the convex function characteristic of $f_0' - f_0$ curve, EM simulators can be utilized to further simplify this method. A multi-step procedure can be followed to obtain different points on $f_0' - f_0$ curve, and they are connected to extrapolate and determine new points, so as to approach the goal point, namely, N(f_1, f_0). Details on how to decide these points in each step is given, both in a graphical way (on $f_0 - f_0'$ plane) and in an analytical way. Finally, a bandpass filter at 10GHz is designed to show the validity of this method.

New Configuration of Microstrip Coupled SIR and Its Application in Bandpass Filters

Houle Gan, **Dongxiao Yang**, **Dongwu Lou**
Zhejiang University, China

Microstrip Stepped impedance resonators (SIR) are composed of microstrip lines with different characteristics impedances. SIR structure in microstrip bandpass filters provides an effective way to minimize circuit size and push spurious resonant frequencies away from passband. Tapped-line is another useful configuration to save circuit size and optimize filter performances. It is shown in [1, 2] that tapped-line input and output can be incorporated into coupled SIR bandpass filters, and create transmission zeros, due to which the selectivity and stopband attenuation are optimized.

In this paper, a new configuration of coupled half-wavelength microstrip stepped impedance resonators is presented. This back-to-back configuration exhibits same passband performance as face-to-face configuration proposed in [1]. In stopband, however, when tapped-line input and output are used to create transmission zeros, the number and positions of these zeros are significantly different between the two configurations. The back-to-back configuration can be used alternatively with face-to-face configuration to build bandpass filters, offering an additional degree of freedom in the design process. It is shown that the number and positions of zeros can be predicted by multi-port network parameter analysis, and by adjusting the locations of tapped-line input and output, positions of zeros can be further tuned. The coupling configurations used in the filter and corresponding number and positions of zeros are summarized, so as to provide guidance for design of filters with special requirements, such as high attenuation at special frequencies, or steep passband-to-stopband transition. A fourth-order bandpass filter with alternant face-to-face and back-to-back configurations is designed and simulated, and the result agrees well with the theory, showing an optimized performance (two more zeros) compared with the fourth-order bandpass filter with only face-to-face configuration proposed in [1]. The fabrication of this filter is in process, and its measured response will be given during the presentation.

REFERENCES

1. Shih, E. and J. T. Kuo, "A New Compact Microstrip Stacked-SIR Bandpass Filter with Transmission Zeros," *2003 IEEE MTT-S Int. Microwave Symp. Dig.*, 1077, 2003.
2. Huangfu, J., L. Ran, and K. Chen, "A New Microwave SIR Bandpass Filter with Input and Output Tapped Lines," *J. of Circuits and Systerms*, Vol. 8, No. 5, 76, 2003.

The GPR Technology on the Seisimic Damageability Assessment of Reinforced Concrete Building

G. Angiulli, V. Barrile, M. Cacciola
Univ. Mediterranea, Italy

The radar technology, used to perform controls on the reinforced concrete structures, derive from the one used for underground surveys called Ground Penetration Radar (GPR). GPR identifies a radar apparatus used on subsoil, structures and manufactured articles surveying. It is a technique that can reveal in a non-destructive and non-invasive way presence and position of buried objects using the phenomenon of the reflection of electromagnetic waves. The technology is based on the same principle of conventional radar systems, but with any meaningful differences. In fact, in the field of introspection of the ground (propagation of the wave in the ground), the radar generally works on distances of few meters and not on many kilometers as in conventional radars. It is known that all real means absorb some electromagnetic waves proportionally to their electric characteristics (dielectric relative constant er, conductibility s). A transmitter produces an impulsive signal with a determined frequency whose central value determines resolution and maximum depth characteristics of survey. The electromagnetic drawn signal has characterized from a series of peaks whose ampleness mainly depends from three factors: nature of the reflector, nature of the mean between reflector and spar, curve of applied amplification. In this paper the operative methodologies (with a particular reference to the phases of data elaboration and interpretation of experimental tests conducted on a civil building) and the results carried out by employ of this technique are presented. In particular, this technology is employed in structural elements of reinforced concrete buildings, in order to perform non-destructive tests that could allow to contemplate the determination of inside morphology, to search of some inhomogeneities and defectiveness and to determine the position of the steel reinforcements. However, and as described above, the proposed technique can be used in other fields, such as subsoil analysis. The used system (RIS/S System), composed from an apparatus of ground acquisition and an apparatus for deferred elaboration, is able to furnish a good planimetric and three-dimensional result in terms of localization and positioning.

An Integrated GPS-GIS Surface Movement Ground Control System

V. Barrile, **M. Cacciola**
University "Mediterranea" of Reggio Calabria, Italy

The development of the air transport system in the last decades due to a more and more increasing transport demand level, has a constraint in the bounded capacity of the system, that depends on the air control system and the actual specific set of rules. Even of the air transport system can be considered a safe system, however, the risk linked to interferences among aircrafts and/or vehicles during the ground movements is still high with respect to the suitable standards for the system [1]. Actually, different Surface Movement Ground Control Systems (SMGCS) have been proposed to assure safety conditions to the operations occurring in the airport area (as landing, take-off, ground circulation), to optimize the ground movement and to increase airport capacity. The system used to control the ground aircraft movement are based on radar systems and/or underground detectors. But while radar-based systems had limits linked to the wave propagation, the detectorbased systems can detect the movement of the vehicles only at specific points, because the detectors are located in prefixed points of the airside. Moreover, the actual system cannot neither locate and identify the moving vehicles with the needed accuracy nor convert the signals acquired by detectors in analogical data to be used in an automatic computing system [2]. For this reason, we propose a different system in order to integrate the radar control with other apparatus, also by using completely different technologies to guarantee both the ground movement safety and the airport capacity increase. In this paper, an integrated approach GPS-GIS will be described; it follows the new requirements of Intelligent Transport System (ITS) applications. ITS applications use data transmission technologies and data processing methods to obtain an "intelligent" management of the transport system in terms of efficiency, safety and environmental aspects. Goal of our system is to provide a control system for the airport ground movement, in order to obtain an efficient, safe and quick management of the vehicle movements at an airport area (both aircrafts and land vehicles); the GPS component is used to know the aircraft position in real time while the GIS component is used to manage and depict the position geographical information. Particularly, the proposed system considers:

1. location and positioning of airplanes and other vehicles on the square by GPS and transfer of data referred to its position (other data measured by different sensors can also be considered);
2. management and data processing operating in a GIS system;
3. re-transmission of informations to the board-personnel by local transmitters, internet and WAP systems.

REFERENCES

1. Janic, M, "An Assessment of Risk and Safety in Civil Aviation," *Journal of Air Transport Management*, Vol. 6, 43, 2000;
2. AA. VV., "Methods of Preventing Runway Collisions Evolve in Europe and in the United States," *Airport Operations*, Vol. 26, No. 4, 2000.

Analysis of Transient Scattering from 2-D Rough Surface Using Time Domain Integral Equation Method

Siyuan He[1], **Boxun Xiao**[2], **Guoqiang Zhu**[1]

[1]Wuhan University, China
[2]Changjiang Water Resources Committee, China

Because of the need of many engineering applications, the research of rough surface scattering has attracted many researchers' attentions for a long time. The research of the characteristics of transient scattering from rough surface is a project with great theoretical challenges and great value of application. In this paper, the method of time domain integral equation (TDIE) is used to analyze the characteristics of transient scattering from two-dimensional rough surface.

The TDIE is computed numerically by using moment method with marching-on-in-time algorithm. In this work, an efficient, accurate and stable numerical solution is developed for the TDIE. The two-dimensional rough surface was approximated by a set of triangular patches. We use the triangular patch modeling and the RWG vector basis functions. The solution is based on the Galerkin's testing in space and point marching in time. It has no matrix storage thereby eliminating the expensive inveresion step. Furthermore, the method employs a special averaging procedure to contral the late-time oscillations. This numerical solution has been tested and a good agreement is obtained. The diffractions of artificial edges are eliminated by introducing pulse tapered wave as the incident wave.

Specifically, a TDIE model for Transient scattering from 2-D dielectric rough surface is developed: Transient scattering from 2-D dielectric rough surface when illuminated by different polarized pulse tapered wave are computed, then the numerical results are compared with scattering from dielectric plate, and the characteristics of scattering from 2-D dielectric rough surface are analyzed.

Characteristics of Different Kinds of UWB Antennas

Dua-Chyrh Chang, **Ming-Yen Liu**
Da Yeh University, Taiwan

An ultra wideband system is generally defined as having a wide bandwidth. There are some antenna types have such bandwidth. At least four different kinds of UWB antenna developed at Da Yeh University (DYU). By using different characteristic of structures as shown in the following figures, we can obtain good impedance matching for wideband applications. Details of the antenna design and both simulation and experimental results will be presented and discussed.

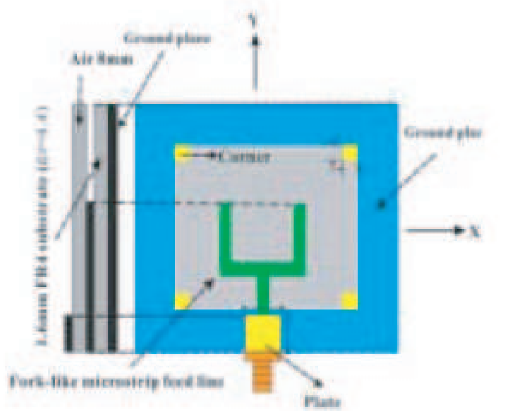

Figure 1: Fork-like microstrip feed line antenna

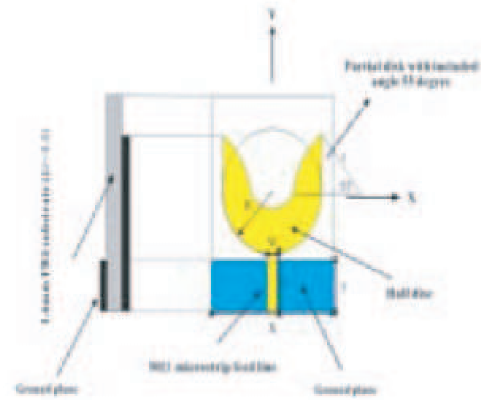

Figure 2: Planar UWB monopole antenna

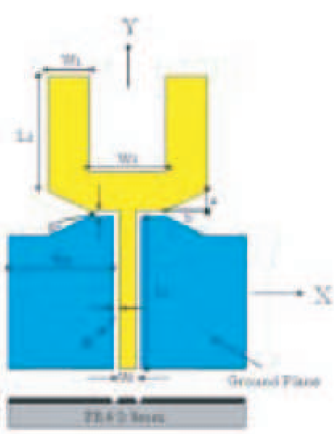

Figure 3: CPW-fed U type monopole antenna

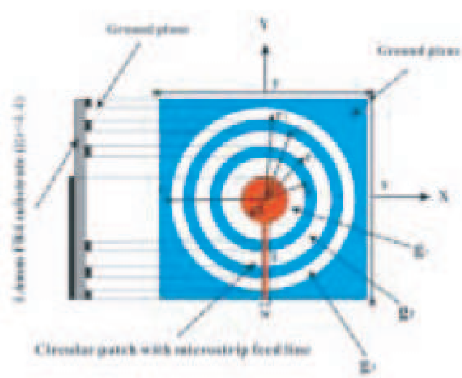

Figure 4: Concentric annular rings antenna

The Roles of UWB TEM Horn in Antenna Measurement System

Dau-Chyrh Chang, **Jr-Hung Lee**, **Shih-Hung Lee**
Da Yeh University, Taiwan

There are compact antenna test range, hybrid near field range, indoor far field range, and two outdoor far field ranges inside campus of Da Yeh University. Most of transmit antennas for these antenna test ranges are narrow band. It is time consuming by changing different bands of transmit probes for wideband antenna pattern measurement.

The TEM horn will have the properties of UWB (Ultra-Wide Band) characteristics. The variation of phase center for each E and H planes at different frequencies are small. The radiation patterns are almost in broadside direction. In this paper, TEM horn antenna with impedance frequency bandwidth 1 GHz $\sim$ 30 GHz is developed. This developed horn antennas are used as the field probes of compact range, near field range, indoor far field range and two outdoor far field ranges. The performance of quiet zone of compact range, correction of near field probe pattern, and performance of far field ranges will be detailed discussed. The design of these kinds of TEM horn will also described during the presentation.

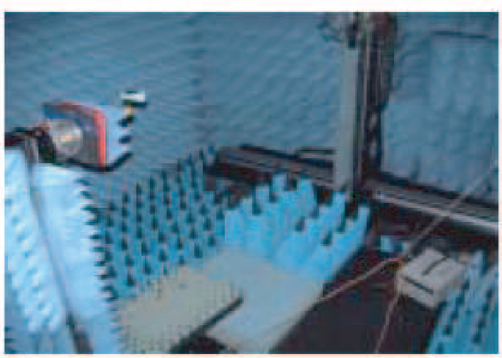

Figure 1: TEM horn antenna is under measured horn antenna

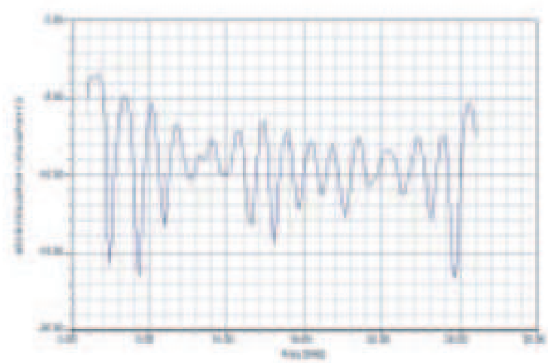

Figure 2: Test result of S11 of the TEM horn antenna

Pictorial Visualization of Antipersonnel Mines Using Ground Penetrating Radar

L. Capineri[1], **P. Falorni**[1], **L. Masotti**[1], **C. G. Windsor**[2]

[1]University of Florence, Italy
[2]116, New Road, East Hagbourne, OX11 9LD, U.K.

Ground Penetrating Radar (GPR) (or UWB-SP Ultra Wide Band Short Pulse) radar are widely used in many industrial and military applications for the detection of buried objects and more recently for detecting antipersonnel mines with low metallic content. In this work we report a new algorithm for extracting the characteristic response of buried mines by processing three-dimensional data sets obtained with a scanning probe placed at the air-ground interface.

The new algorithm requires few assumptions concerning the experimental conditions. The input parameters of the program are the spatial and time sampling steps and a rough estimate of the propagation velocity in the soil. Moreover we introduce the concept of *local echo contrast pattern* for non point-like objects in order to overcome the limitations of standard signal processing approaches based on the assumption of a hyperbolic response from a point-like reflector. The information on the mine shape is derived by the time-flight measurements performed on each contrast pattern. The method is capable of retrieving a series of mine contours and an associated propagation velocity. A pictorial visualization technique in 3-d space is proposed showing the estimated contours and the depth from the top surface and compared to standard C-scan visualization.

The Major Insulation Optimal Design of Power Transformer with the Combined Arithmetic of Sensitivity Analyses and Evolution Strategies

Guoqiang Zhang
Chinese Academy of Sciences, China

Youtong Fang
Zhejiang University, China

Xiang Cui
Department of North China Electric Power University of China, China

Daniel J. Tschudi
H. Weidmann AG, Switzerland

A combined arithmetic for the optimal design of major insulations in power transformers is proposed in this paper. To simplify the process of optimization, after the initial electrical field computation, a succeeding electric field calculation with the increment vector of design variables was performed leading to the sensitivity matrix between safety margins and design variables. This permits the elimination of the variables that have little influence on sensitivity matrix; the evolution strategies will thus be accelerated more effectively. Our example is optimized by (1+1) evolution strategy because it was well founded theoretically and well tested practically. Above combined arithmetic saves calculation cost by 72 percent, according to its actual application for the optimal design of a power transformer. Another innovation described in this paper is to nominate the safety margin as the optimal objective function instead of the maximum electrical field intensity. The safety margin is defined as the ratio between the occurred electrical stress and the permitted one along an equal electric flux line of each oil gap. The previous optimal designs focused on minimizing electrical field intensity on the surface of electrode. However, it had no obvious effect all the time because the electrical field intensity is not the exclusive factor influencing the insulation safety margin. The proposed optimal object is beneficial to promote the partial discharge inception voltage and heighten the insulation reliability of power transformers. The result of our example indicates that the partial discharge inception voltage increases by 20 percent, with the help of proper oil gap division. The analyses for the testing results of two models show the proposed objective function can reflect optimization effect more properly.

Curl-Slot Loaded Microstrip Antennas for Dual-Band and Wideband Operation

C. Y. Huang[1], **Hsueh-Fen Tsai**[2]

[1]National Kaohsiung Normal University, Taiwan
[2]Asia-Pacific Research Foundation, Taiwan

Characteristics of single-layer single-feed dual-frequency and wideband microstrip antennas with embedded curl-slot on FR4 substrate are proposed and demonstrated. This antenna can easily achieve good impedance matching at both frequencies by tuning the feed position. Another advantageous aspect is that it has high polarization purity. The effects of various antenna parameters on two resonant frequencies, frequency ratio, and radiation pattern characteristics of the antenna are analyzed and discussed. The obtained two operating frequencies are of the same polarization planes and by varying the embedded curl-slot size to perturb the surface current, a tunable frequency ratio of the two frequencies ranging from 1.05 to 1.73 is obtained. An effort for wideband design can be greater than 2.2 times that of a conventional rectangular microstrip antenna. Details of the antenna design are described and typical experimental results are presented and discussed.

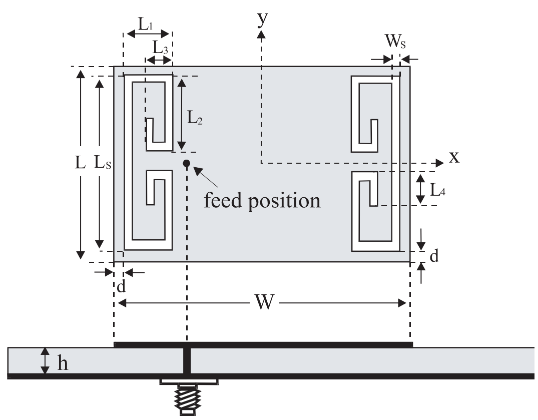

Figure 1: Geometry of rectangular microstrip antenna loaded with curl-slot for dual frequency and wideband operation

Rigorous Approach to Modelling Electromagnetic Characteristic of Finite-size Printed Antennas Based on Surface Integral Equation Methods

Jian Dong, **Shunlian Chai**, **Junjie Mao**
National University of Defence Technology, China

A rigorous full-wave approach, based on surface integral equation method and method of moments for modelling arbitrary shaped printed antennas with finite-size substrate is presented.

For many years, the moment method based infinite stratified media Green's function approach has been a common technique for analyzing printed antennas. Such an approach yields good results for antenna's input impedance and resonant frequency. However, because of the assumption of an infinite substrate and ground plane in the formulation of Green's function, accurate prediction of far-field parameters has been problem. Some works based on the moment method have been carried out for modeling the radiation and scattering characteristics of printed antennas. The idea behind these works is to use free space Green's function and the equivalence principle. The volume integral equation is popular used for solving this problem based on the volume equivalence principle [1]. Another good approach is to use surface integral equation method based on the surface equivalence principle, but it scarcely discussed in literature until recent years.

Based on the surface equivalence principle, the electromagnetic fields inside a homogeneous isotropic and linear region can be expressed in term of the impressed field and equivalent electric and magnetic currents distributed over its boundary surface. By expressing boundary conditions in terms of the impressed fields and equivalent currents, different types of surface integral equations can be obtained. As the finite-size printed antenna structures are composed by the dielectric substrate and metallic patch etched on it, the combine of EFIE and PMCHW formula is a good choice. In [2], the moment method based on the RWG subdomain basic function is used to solve the EFIE+PMCHW integral equation on the assumption that the metallic surfaces is infinitesimally close to dielectric surfaces, but never touch them which cause redundant magnetic current unknowns on the surface between dielectric and etched metallic patches. In [3], a general PMCHW formulation is given to treat combined metallic and dielectric structures, but they construct special basic functions to represent currents distribution.

Our approach is to follow the formulation presented in [3], but we us the RWG basic function to represent equivalent surface currents distributions. And much attention is paid to treat the multiple metallic and/or dielectric surface junctions problems specially on modeling of printed antennas. Many types of finite-size printed antennas have been analyzed using our approach. Numerical examples include microstrip line feed rectangle patch antenna , microstrip line feed circular patch antenna and stripline-feed printed-aperture antenna. The numerical results show good agreement with measurements which will be presented on the conference.

REFERENCES

1. Yee, K. Y. and E. M. Freeman, "Rigorous Approach to Modeling Electromagnetic Radiation from Finite-size Printed Circuit Structures," *IEE Proc-Microw. Antennas Propag.* Vol. 146, No. 1, 29, 1999.
2. Rao, S. M. ,T. K. Sarkar, P. Midya and A. R. Djordjevic, "Electromgnetic Scattering and Radiation from Finite Conducting and Dielectric Structures: Surface/Surface Formulation," *IEEE Trans. Antennas Propagat.*, Vol. 39, No. 7, 1034, 1991.
3. Kolundzija, B. M., "Electromagnetic Modeling of Composite Metallic and Dielectric Structures", *IEEE Trans. Microwave Theory and Tec.*, Vol. 47, No. 7, 1021, 1999.

Interface Heterobond Effects in (hkl) InAs/GaSb Superlattices Solved by Bond Orbital Model

Chun-Nan Chen, **Kao-Feng Yarn**, **Wei-Chih Chien**
Sheng-Hsiung Chang, **Meei-Ling Hung**
Far-East College, Taiwan

For the (hkl)-oriented InAs/GaSb quantum wells and superlattices: the in-plane anisotropy, the in-plane zero-field spin splitting (ZFSS), and the Dresselhaus-like spin splitting are found in this paper. Moreover, it is due to the microscopic symmetry reduction, which originates from the existence of heterobonds (In-Sb and Ga-As) inside the interfacial unit-cells.

The lifting of the two-fold spin degeneracy in the absence of a magnetic field is an important topic for semiconductor quantum devices. In this work, we will study the transport and optical phenomena associated with the ZFSS of the subbands in semiconductor quantum devices.

The intracell perturbations at the atomic scale are neglected in the bond orbital model (BOM) due to the unit-cell-scale orbitals. This makes the breakdown of the higher symmetry Hamiltonian of BOM used for calculating the microscopic phenomena. To improve this problem, the intracell effects is introduced into the BOM by expanding the BOM basis in terms of the tetrahedral (anti)bonding orbitals and using the potential operator instead of the scalar potential for the extraction of the microscopic information.

This microscopic interface effect can play a crucial role in dominating the quantum semiconductor behaviours. According to the theoretical modeling in this paper, the heterobonds are proved to dominate the semiconductor optical and electrical behavior in three ways: one is the in-plane anisotropic property due to the interface-induced mixing of heavy hole and light hole at the zone center on the lower symmetry heterojunction, the second is that the inversion asymmetry interfaces leads to a new mechanism for contributing the in-plane ZFSS, and the third is a Dresselhaus-like ZFSS along the growth direction.

The possibility of tailoring the electronic and optical properties of semiconductor quantum devices can be obtained through symmetry breaking. Apart from the growth direction, the structure asymmetry, and the strain effect, the interface heterobonds may offer another degree of freedom for varying the symmetry. It may open a new frontier for future application to optical and electrical quantum devices.

The Dynamic Performance Analysis Model of EMS-MAGLEV System Utilizing Coupled Field-Circuit-Movement Finite Element Method

Yingying Yao, **Youtong Fang**, **Guanzhong Hu**
Zhejiang University, China

In EMS-Maglev system such as the German Transrapid, the propulsion is defined by a Longstator linear synchronous motor which stator (armature) is fixed all along the track and the moving poles with the excitation (suspensive magnets) are on the vehicle. The attractive force between the motor stator and the moving poles creates the levitation forces. And linear generator supplies the on-board electric power. The LSM windings are energized by three-phase alternating voltage over a power supply section. Obviously the excitation current has to satisfy an accurate levitation force and a high power factor. To find the current and optimize the system, analysis of the electromagnetic field is necessary. Because the external system is complex, analytical method can hardly obtain the dynamic performance. With ordinarily transient finite element method, it is also difficult to consider the external power supply of linear synchronous motors and the working status of linear generator. Moreover, the eddy current induced by movement produces an effect on dynamic performance. In this paper, a new 2D transient finite element algorithm for the performance analysis of magnetically levitated vehicles of electromagnetic type is proposed. The algorithm incorporates external power system and vehicle's movement equations into FE model of transient magnetic field computation directly. The eddy current induced by movement is calculated by using upwinding technique. Sliding interface between stationary and moving region is used during the transient analysis. The periodic boundaries are implemented in an easy way to reduce the computation scale. Using the proposed modeling method, the factors affecting levitation and propulsion forces can be easily investigated. Through computations of an EMS-MAGLEV system, it is shown that the algorithm gives reasonable results.

Dynamic Monitoring of Indigenous Coking Sites in China by Using Multi-temporal Landsat Images

Xiangsheng Kong[1,2], **Fang Miao**[1], **Hongfu Liu**[2], **Yuyang Dong**[2]

[1]Chengdu University of Technology, China
[2]Taiyuan University of Technology, China

In recent years the Chinese government has carried out some serious investigations and expended considerable effort to shut down indigenous coking sites, but effective control has not been achieved. There are still many problems and the situation is still severe. One important measure in tackling this problem has been improvements in the level of monitoring. The largest producing province, southeast of Shanxi in China, was chosen as the study area for this paper. Using two muti-temporal Landsat5 images of this area acquired in 1999 and 2004, information about indigenous coking sites was extracted through digital image process. The analysis of TM channels showed that TM channel 7 was the most sensitive to indigenous coking sites, where the reflectance value manifested the "peak" configuration as a flag for indigenous coking sites. TM channel 5 was the second most sensitive to coking sites. Using the spectral profiles, TM7 and TM5 critical values for areas of indigenous coking sites were discovered. The higher the coke-making temperature, the nearer the band was to TM5 channel. TM751 RGB("Red", "Green", "Blue") false colour images can be used to interpret indigenous coking sites with 95% accuracy, confirmed by ground checking. Over a period of 5 years(1999-2004), the quantity of new indigenous coking sites points, distributed mainly on the plain in districts of population concentration, increased by 10 times and the indigenous coking sites has caused serious pollution to the environment. Some control strategy was proposed in the last paper. These findings contributed to the scientific foundation for accurately monitoring the dynamics of indigenous coking sites at large scale, and offered a kind of brand-new, quick technological method for the Chinese government monitoring indigenous coking sites.

Transient GPR Signals Modelling for Non-destructive Testing of Pavement

F. Liu, **L. Laguerre**
Laboratoire Central des Ponts et Chaussées, France

In the field of civil engineering, Ground Penetrating Radar (GPR) systems are commonly used to recover geometrical characteristics and material properties, as pavement thicknesses or near-surface concrete degradation. Simple analytical models dealing with plane-wave approximations are generally used but they are not well adapted to the specific configuration of Ground Penetrating Radar measurement system, that is, the one of a radiating dipole close to the surface of the material under evaluation. Here, we develop a transient electric field physical model of a horizontal dipole radiating over a horizontally stratified pavement medium. We investigate the transient electromagnetic response with two semi-analytical methods derived from integral transforms of the fields in the wave number and frequency domains (Sommerfeld integrals) using Debye series expansion of the medium transfer function. The first consists in the Cagniard-de-Hoop method which has been proved to be efficient and stable numerically, but which is restricted to the non-dispersive or non-attenuating medium case. The second one is concerned with the Branch-Cut integration method, which is a simple and direct method able to treat both lossy and lossless medium cases. Different arrangement of geometries and materials are considered here (a two homogeneous half-space medium case and a two-layered homogeneous subsurface medium case, each with or without loss). For the lossless medium, results from both methods are compared. Simulation and experimental results are illustrated with the Common-Middle-Point (CMP) representation to identify the different wave arrivals which are explicitly described by the model as the direct wave, lateral and guided waves.

Wave Propagation in a Composite Metamaterial Cylinder

Cixiang Liu, **Chao Li**, **Qiang Sui**, **Fang Li**
Institute of Electronics, Chinese Academy of Sciences, China

The finite-difference time-domain (FDTD) method was used to simulate the wave propagation in a composite metamaterial cylinder with a line source in it's center. The perfectly matched layer (PML) absorbing boundary condition was applied in x and y direction, and periodic boundary condition (PBC) in z direction, so the cylinder is infinitely long along z axis. The structure of the metamaterial is the well-known periodic arrangement of rods and split-ring resonators, and some change has been done to make it more symmetric in x-y plane. A line source generating the monochromatic wave at 12.5G Hz was put in the center of the cylinder, outside the cylinder is air. From our result, it can be obviously observed that the phase fronts are approximately circular no matter in or out of the metamaterial cilynder. This means the structure has a very low spatial dispersion and can be treated as almost isotropy. It can also be observed that the circular phase fronts move inward in the metamaterial cylinder, but outward in the air. This is in good agreement with the backward-wave property of the left-handed metamaterial. Figure 1 and 2 shows the electric field in z direction and its phase in different time step at stable station.

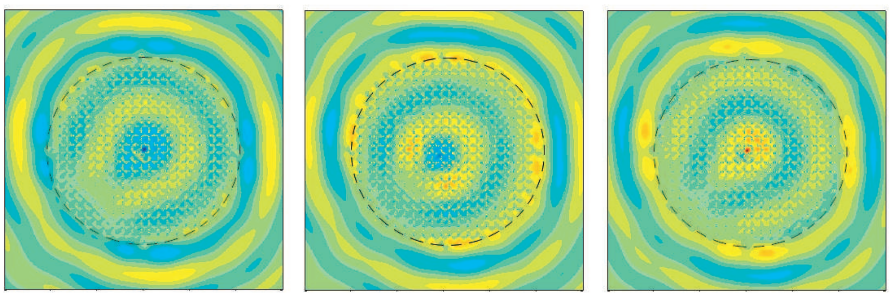

Figure 1: the electric field captured at time steps of 39900, 39950, 40000, respectively, the dashed circle is the interface of the metamaterial cylinder and the air.

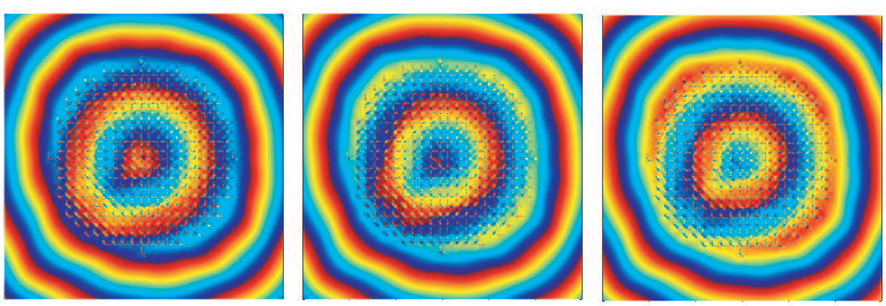

Figure 2: the phase calculated at time steps of 39900, 39950, 40000.

The Effect of Whole Body Exposure of 50 GHz Microwave Radiation on Reproductive Patterns in Male Rats

Jitendra Behari, **Yadwinder Singh**
Jawaharlal Nehru University, India

The objective of this study is to investigate the effects of 50 GHz microwave radiation on sperm counts, wet weights of testes and accessory reproductive organs, rectal temperature etc. of rats. Male rats(n=24) of Wister strain, of age group 80-90 days, were divided into two main group-Group I Control (two subgroups of 6 rats each) and Group II Experimental (microwave exposed). The rats were housed in temperature-controlled room (20-24°C) with constant humidity (40-50%) and received food and water ad libitum. The animals were kept on 12/12-h light/dark schedule. During exposure rats were placed in Plexiglas cages with drilled holes and kept in anechoic chamber. The animals were exposed 2 h a day for 60 days continuously at power density 0.95 mW/cm^2. After the exposure period the rats were sacrificed and sperm counts determined by haemocytometer method. Rectal temperature was measured using fiber optic probe. The sperm counts decreased significantly in epididymus of exposed animals, being $211 \pm 7 \times 10^6$/ml in cauda and $103 \pm 6.5 \times 10^6$/ml in caput regions as compared to control i.e. $246 \pm 16.4 \times 10^6$/ml (cauda) and $119 \pm 5.8 \times 10^6$/ml (caput) respectively. The one-way ANOVA test was used for statistical comparison of groups.

Is Electronmagnetic Force a Possible Means for Life Transmission in the Universe

V. V. Tchernyi, **Sergey V. Kapranov**
General Physics Institute, Russia

Organic molecules recently found in the interstellar material are almost systems that could have superconductivity. The idea of possible superconductivity of some cell structures and biomolecules is also relatively long discussed. Despite the lack of reliable facts of superconductivity, there are attempts to realize this idea experimentally. They are based on fact that superconductive state is indicated by anomalous high conductivity of media. There is number of experimental results where magnetic measurements data of biological and organic media are interpreted as presence of molecular or subcellular domains of superconductivity. Properties of molecular conductors and semiconductors put a number of questions. Interrelation between molecular structure of these materials and their measured electrical properties can not be easily deduced. There are two large groups: molecular crystals and polymers. Metalphtalocyanines are referred to the first group. Its molecules possess superconductive properties with a wide range of conductivity.

Electric properties of doped organometallic materials are usually close to those of metalphtalocyanines. Platinum oxidized complexes also were mentioned as structure of "exciton superconductor". Under certain condition sulfur polynitride becomes to be superconductive. At the same time superconducting particles in space may be enforced by levitation force which move them in the direction of low intensity of external magnetic field.

Determination of the CFL Number for FD-ADI-FDTD Based on the Required Accuracy

Arnaud Thiry, **Fumie Costen**
University of Manchester, U.K.

Ultra WideBand (UWB) systems have a wide range of applications from microwave imaging to communication purposes. Major advances towards the realisation of these applications require a system modeling which produces UWB signal waveforms after propagation in a lossy media. The Frequency Dependent (FD) Finite Difference Time Domain (FDTD) method is a popular method to do so which works by discretising both space and time. The Courant-Friedrichs-Levy (CFL) condition limits its time discretisation size according to the space discretisation, which can lead to unpractically small computation times.

The Alternating Direction Implicit (ADI) method has been introduced to FDTD to remove that CFL condition and trade accuracy for faster simulation times. This speed up in simulation time is interesting for the simulation of UWB signals because of the high spatial resolution required to accomodate the higher frequencies. The problem is that UWB simulation requires frequency dependent material because of its high frequency and ultra large bandwidth and thus a FD-ADIFDTD method has to be used for UWB simulations. To be able to make sensible choices between FD-FDTD and FD-ADI-FDTD for UWB simulations, the effects of spatial and time discretisation need to be better understood.

This paper takes a novel approach to investigate the effects of temporal and spatial discretisation on accuracy on the FD-ADI-FDTD formulation presented in [1]. Moreover, based on the results, it proposes a way of determining the CFL Number (CFLN), that is, how many times the time discretisation can be increased compared to the maximum one from the FDTD method, from the viewpoint of accuracy.

REFERENCES

1. Costen, F. and A. Thiry, "Alternative Formulation of Three Dimensional Frequency Dependent ADI-FDTD Method", *IEICE Electron. Express*, Vol. 1-17, 528, 2004.

Efficient Absorbing Boundary Condition for UWB Simulation in Frequency Dependent ADI-FDTD

Arnaud Thiry, **Fumie Costen**
The University of Manchester, UK

The Finite-Difference Time-Domain (FDTD) method has become interesting for electromagnetic simulations since the wide availability of computer resources. Its key features are its simplicity both in implementation and in representing the simulation space. One of its teething problems, though, is that the computation space needs to be terminated by an Absorbing Boundary Condition (ABC) which aims at absorbing the outgoing wave as if it was still travelling outward.

The latest ABC technique consists in surrounding the computation space by an artificial anisotropic media. It was first introduced by Bérenger and it is called the Perfectly Matched Layer (PML) ABC. It is the most versatile of the ABCs, effectively absorbing any outgoing waves, from any direction and any frequency. Because PML emulates a media, it increases the size of the computational space by the size of the absorbing media and moreover the PML media is updated like the computational space and requires some computation.

One of the problems of the original PML is that the media parameters proposed are not general enough to fit some simulations. This problem has been taken care of by Gribbons et al. by introducing a stretched coordinates system inside the PML media so that evanescent waves spend enough time in the PML to get absorbed. Another shortcoming of the original PML is that when simulations involve long grids or signals with long time signature late time reflections can show up. Kuzuoglu et al. increased the causal nature of the scheme by shifting the frequency dependent pole of the PML media parameters off the real axis into the negative-imaginary half of the complex plane to solve that problem.

Gedney et al. proposed an efficient alternative formulation by using stretched coordinates and recursive convolution called Complex Frequency Shifted (CFS) PML. They successfully implemented CFS-PML for FDTD and ADI-FDTD and demonstrated the validity of their method and increase in efficiency for little computational cost over the original PML. This is the most complete and most efficient formulation of PML.

Ultra Wide Band (UWB) signals are used for a diverse range of devices, from ground penetrating radars to high speed data transmission. When dealing with these signals using ADI-FDTD, the wide bandwidth in high frequency range involved requires the modelling of frequency dependent media. A Debye model for the ADI-FDTD method has already been proposed but only uses Mur's ABC which is computationally efficient but provides very poor performance. The alternative approaches to the FD-ADI-FDTD utilise regular PML.

This paper proposes a formulation of CFS-PML to be able to use Debye media in ADI-FDTD for the simulation of UWB signals.

A Joint Timing and Frequency Synchronization Used in DVB-T System

Jun Zhou, **Haibin Zhang**, **Wentao Song**
Shanghai Jiaotong University, China

OFDM, which has high frequency spectral efficiency and lower multi-path distortion, is a popular technology for industries and academics. The modulation scheme was chosen for the two European terrestrial broadcasting standardsdigital audio broadcasting (DAB) and digital video broadcasting (DVBT) for its virtue.

Frequency synchronization is very important to an OFDM system, since little frequency offset may lead to loss of orthogonality between subcarriers. In that case, each subcarrier regards the adjacent carriers as noise, which is called inter-carrier interfere (ICI). Usually, there are three basic methods, which utilize pilots (including continual pilots and scatted pilots), training sequence, and cycle prefix (CP) respectively, to estimate frequency offset.

For DVB-T, because the frequency distance is no more than 4kHz, very little frequency error will lead to serious interfere. That means in order to achieve perfect performance, the allowable rest frequency offset is only about several hertz. This really is a challenge.

In this paper, we propose a novel joint timing and frequency synchronization method used in DVB-T System. This process is divided into three phases, one for coarse fractional, one for integer and one for fine-tuning. Firstly, we utilize CP (accurate symbol synchronization is not necessary) to estimate the fractal frequency offset and time delay(joint ML estimation algorithm); then the differential signal of continual pilots for adjacent OFDM symbol are used to estimate integer frequency offset; last, in order to improve the performance, differential signal of scattered, instead of continual pilots, are used to determine the residual fractional frequency error. The performance analysis is presented in this paper. We also create the simulation link based on DVB-T standards. Theory analysis and simulation results show that this method, can perfectly satisfy the request of DVB-T standards and can be easily realization.

*This project was supported by the National Nature Science Foundation of China under Grants 60332030 and National Hi-tech Research and Development program(863) of China (No. 2003AA123310).

A Fading Channel Model Based on Complex M-Distribution

Jun Zhou, **Haibin Zhang**, **Wentao Song**
Shanghai Jiaotong University, China

Nakagami distribution [1], also named m-distribution, is an important distribution as a generic model of fade statistics used in the study of mobile radio communications [1] [2]. Due to its great versatility, the Nakagami fading channel model has received considerable attention recently.

Nevertheless, most of these works about Nakagami-m distribution assume that the channel only has amplitude fading. Few of them consider the fading coefficient as a complex. In SISO or SIMO systems, this assumption is reasonable because the phase of complex gain cannot affect the received signal envelope and it has little influence on the performance if only the amplitude is considered. In MISO or MIMO systems, since each antenna of a receiver sums the signals from all antennas of a transmitter, the phase of the complex gain of fading channels greatly affects the value of received signal, which means that assumption is not suitable. On the other hand, fading amplitude distribution is considered when amplitude modulation is only used. In order to obtain higher frequency efficiency, joint amplitude-phase modulation are used in practical radio communication system, such as QPSK and QAM. Thus, phase distribution of fading gain is another key factor. Consider gain of fading channels as a complex, where amplitude and phase obey an m-distribution and a special distribution respectively, and its distribution of corresponding real and imaginary parts, is necessary and interesting.

In this paper, we consider a complex channel fading distribution in which amplitude follows m-distribution and angle follows a uniform/arbitrary distribution. The probability density functions (including marginal PDF and joint PDF) of the real and imagine part of fading gain for different phase distribution are derived. In addition, some of the prominent features of this complex distribution, which are essential and useful in its applications, are presented as well. The proposed formulation can be efficiently used in the analysis of channel capacity and performance of MIMO systems, modelled by the complex Nakagami fading.

*This project was supported by the National Nature Science Foundation of China under Grants 60332030 and National Hi-tech Research and Development program(863) of China (No. 2003AA123310).

REFERENCES

1. Nakagami, M., "The M-distribution: a General Formula of Intensity Distribution of Rapid Fading," *Statistical Mathods in Radio Wave Propagation, W. C. Hoffman, Ed., New York, Pergamon*, 3, 1960.
2. Braun, W. and U. Dersch, "Physical Mobile Radio Channel Model," *IEEE Trans. Veh. Technol.*, Vol. 40, 472, 1991.

Study on the Interaction of Electric Field and Gas Flow for HV SF6 Circuit Breaker

Xiaoming Liu, **Yundong Cao**, **Erzhi Wang**
Shenyang University of Technology, China

With gradually increase of electrical capacity and the highly concerned function of urban areas, the high reliable and economical power system is demanded urgently. And because the future extra, ultra line and the difficulty in acquiring land for substations, underground substations with high voltage (HV) line, HV SF6 circuit breakers CBs with higher reliability and stability are required and the interrupting current is also demanded to exceed. And the numerical calculation of the electric field and the flow field with aid of computer technique is an indispensable tool in various electricity-concerned applications, especially, for analyzing the insulation property and interrupting characteristic of CB and designing HV equipments. In this paper, the couple model of the electric field and flow field has been established based on the N-S equation and turbulent model, taking the influence of temperature and pressure of the arc and the effect of gas flow on the arc and self-adaptive adjustment of the current into consideration, for reflecting the interaction of the dynamic arc and gas flow under the short circuit interrupting course. And the gas flow field of 1-break 500kV SF6 circuit breaker with complex flow path, supersonic nozzle, active, viscous, compressible, variable boundaries has been solved. Moreover, the simulation results qualitatively present the feature of arc-flow interaction and the presence of a localized form of arc choking of the gas flow, and obtain the variation of the mass flow and pressure around the arc region.

Numerical Simulation of Unbounded Electric Field Using the Improved Charge Simulation Method

Xiaoming Liu, **Yundong Cao**, **Erzhi Wang**
Shenyang University of Technology, China

Charge simulation method (CSM), FEM, FDM and BEM are commonly used for computing electric field of high voltage insulation systems. In which, CSM is very effective in calculating electric field with open boundary and floating conductors, and many concerned contributions have been reported in literatures. However, the disadvantage of the conventional CSM is that simulation charges are difficult to be exactly located and require modifying by experiences repeatedly. Furthermore, computation precision is also greatly influenced by matching relationship of simulation charges and contour points. Aiming at these problems, for improving the calculation precision of the electric field, a hybrid method of genetic algorithms (GA) and (CSM) is proposed for effectively calculate the electric field with open boundary. In which, the allocations and quantities of optimized charges can be obtained using GA, and higher calculation precision can be achieved. The feasibility, practicability and efficiency of the proposed optimized CSM have been verified by the demonstration examples. And higher calculation precision can be achieved. Moreover, less number of the simulation charges and faster convergence are achieved by using the combined CSM comparison with the conventional CSM.

Fast Analysis of Microwave Integrated Circuits Using Preconditioned SMCG Method

X. P. Feng, **J. Q. Chen**, **L. Mo**, **R. S. Chen**, **W. Zhuang**
Nanjing University of Science and Technology, China

In recent years, analysis and design of planar structures such as microwave monolithic integrated circuits (MMIC) became a very important topic. Full-wave electromagnetic analysis of microstrip structures is especially significant. Due to the complexity of this scheme, efficient numerical tools are required for their analysis. For these planar structures, a mixed-potential integral equation (MPIE) formulation solved with the Method of Moments (MoM) is often used, while the RWG triangular discretization is employed to analysis the microstrip structures of arbitrary shape. One of the most popular techniques for analyzing this scheme is the sparse-matrix/canonical grid (SMCG) method. The impedance matrix of SMCG method can be decomposed into near-interaction portion and far-interaction portion. During the iterative process, the near-interaction portion of the matrix-vector multiplication is computed directly as the conventional MPIE formulation. The far-interaction portion of the matrix-vector multiplication is achieved by a Taylor series expansion of the Greens function about the grid points of a uniformlyCspaced canonical grid overlaying the triangular discretization. In this paper, we propose a preconditioned SMCG (PSMCG) iterative solution for analyzing arbitrary microstrip structures, which is based on near-field precondition. The preconditioning of the PSMCG method is used to improve the condition number of the matrix rendered by premultiplying Z_s^{-1}(Z_s impedance matrix of the near-interaction portion) in the both side of matrix equation ZI=V . The original matrix equation transforms to $\hat{Z}I = \hat{V}(\hat{Z} = Z_s^{-1}Z, \hat{V} = Z_s^{-1}V)$, and this matrix equation can converge very fast with sparse iterative method. Our numerical calculations show that the PSMCG can converge much faster than the conjugate gradient (CG) method and SMCG method. Some typical microstrip structures are analyzed and the good results demonstrate the validity of the proposed algorithm.

Application of Adaptive Integral Method (AIM) for Analyzing Microstrip Structures

W. Zhuang, **L. Mo**, **R. S. Chen**
Nanjing University of Science and Technology, China

In this paper, we illustrate the analysis of microstrip structure with a large number of unknows using the adaptive Integral Method. We employ the Mixed-Potential Integral Equation (MPIE) formulation in conjunction with RWG triangular discretization. The full impedance matrix is decomposed into sparse matrix with corresponds to near interactions and its complementary matrix which corresponds to far interactions, defined in terms of a sparse coefficient matrix and the Green's function stored as a two-level Toeplitz matrix which will calculated by using discrete fast Fourier transforms (FFT). During the iterative process, the near-field portion is computed, directly using the Galerkin method employing a set of N arbitrary basis functions, and the calculation of the far-field matrix element also used the Galerkin method, with a set of N auxiliary basis functions, which are constructed as superpositions of pointlike current elements located on uniformly Cartesian grid nodes and are required to reproduce the far field, equal to what generated by the original basis functions. Compared with the conventional MOM, the storage requirements are reduced from $O(N^2)$ to O(N), and the computation complexity is reduced from $O(N^2)$ to $O(N \log N)$, where N denotes the number of unknowns.

Three schemes of far-field approximation are introduced, the multipole expansion based on a least squares approximation, the multipole expansion using the analytical function, and the far field expansion based on a least squares approximation. Compared with the multipole expansion ,the far field expansion based on the a least squares approximation provide a better accuracy(for grid spacing a$\sim \lambda/7$ or larger,compared to a$\sim \lambda/10$ in the multipole expansion, a is the size of the Cartesian grid) and the smaller distance(as small as 0.5λ, typically smaller than the multipole expansion).

The ADI-FDTD Method for Planar Circuits Analysis

Y. Yang, **R. S. Chen**, **Z. B. Ye**
Nanjing University of Science and Technology, China

It is well known that the conventional FDTD method has been successfully used to simulate a lot of modern microwave and millimeter-wave planar circuits. Howeverone of the major limitations of this method is that the maximum time step is limited by the minimum spatial discretization interval defined by the Courant-Friedrich-Levy (CFL) condition. In recent years, an unconditional stable three-dimensional (3-D) alternating direction implicit finite-difference time-domain (ADI-FDTD) method has been developed [1]. The main advantage of this method is that the CFL condition can be totally removed. Hence, the time-step size can be set arbitrarily and in simulation it is no longer restricted by stability but by accuracy of this algorithm. For the analysis of planar circuits, the proper applications of an absorbing boundary conditions (ABCs) and a proper source excitation scheme are the critical factors in successful ADI-FDTD simulations. Hence in this paper two kinds of ABCs are first jointly employed for ADI-FDTD algorithm. The Gedney's uniaxial PML (UPML) scheme based on an **E-H** field formulation is implemented into the ADI-FDTD algorithm in propagation directions [2]. For decrease the cost of computation, we implement the Mur's first-order ABC to truncate the other outer surfaces. On the other hand, the setting of excitation in ADI-FDTD is different from the conventional FDTD. Numerical results indicate that the excitation scheme should be forced at several sequential source planes at the same time corresponding to the increased time-step size in order that the field components are accurate enough.

Several examples are considered: a simplified microstrip grounded via, a microstrip T-junction, a coplanar stripline and a microstrip meander configuration. The results demonstrate the validity of this ADI-FDTD scheme. Both time-domain waveforms and scattering parameters are presented by different time-step size. The results show that the number of iterations with this algorithm can be six times less than that with the conventional FDTD without the large loss of accuracy. It is also found that the numerical dispersion error increases with the increasing time-step size.

REFERENCES

1. Namiki, T., "3-D ADI-FDTD MethodUnconditionally Stable Time-domain Algorithm for Solving Full Vector Maxwell's Equations," *IEEE Trans. Microwave Theory Tech*, Vol. 48, 1743, 2000.
2. Zhao, A. P., "Uniaxial Perfectly Matched Layer Media for an Unconditionally Stable 3-D ADI-FDTD Method," *IEEE Microwave Wireless Compon. Lett*, Vol. 12, 497, 2002.

Parallel Realization of Algebraic Domain Decomposition for the Vector Finite Element Analysis of 3D Time-harmonic EM Field Problems

X. W. Ping, **R. S. Chen**
Nanjing University of Science and Technology, China

E. K. N. Yung, **C. H. Chan**
City University of Hong Kong, Hong Kong

When solving large sparse linear systems resulting from FEM, FDTD etc, the domain decomposition method (DDM) is a popular choice. With DDM, a large problem can be divided into several smaller pieces that are much easier to solve. Whats more, domain decomposition method (DDM) is a very natural framework to develop solution methods for parallel computing. An algebraic domain decomposition method (ADDM) is similar to domain decomposition, but the solution procedure of ADDM is mainly based on the operation of the coefficient matrix. In this paper, we investigate the parallel realization of algebraic domain decomposition method to solve the large sparse linear systems, which derived from the vector finite element method (FEM) for three dimensional Helmhotz equations in electromagnetic problems based on message passing interface (MPI) distributed-memory network. The proposed method segments the problem into several smaller sub-problems, solves each sub-problem in each node (i.e. computer) by direct method, exchanges related data between nodes with MPI cluster network, and then reassembles the sub-problem solutions together to get the global result. Multifrontal method is applied to solve intermediate equations associated with each sub-problem. The reduced interface system is solved by Krylov subspace iterative method. To test the efficiency of ADDM, we divided each problem into 2-5 sub-problems, and we also tried different methods (CG BCG GMRES) to solve the reduced problem. The simulation results demonstrate that the proposed parallel computing can save much more memory and CPU time than sequential computing. Furthermore, it can solve larger system in reasonable time and get excellent performance vs. price ratio

The Perturbed RIC2 Preconditioning of Finite Element Equations for the Three-dimensional Helmhotz Equations

X. W. Ping, **X. X. He**, **R. S. Chen**
Nanjing University of Science and Technology, China

E. K. N. Yung, **C. H. Chan**
City University of Hong Kong

The Krylov subspace method (CG BCG etc) is a kind of popular iterative method for solving large sparse linear systems. However, they are much affected by the condition number of the linear systems. One efficient method to solve this problem is preconditioning technique. In this paper, we consider the fast solution method of large sparse complex symmetric non-Hermitian systems resulting from the analysis of waveguide device by use of edge-based finite element method (FEM). The anisotropic media and active properties of the perfectly matched layer (PML) absorbers significantly deteriorate the finite element method (FEM) system condition and as a result, convergence of the iterative solver is substantially slowed down. We consider the second order incomplete Cholesky decomposition(RIC2) preconditioning strategies combined with conjugate gradient method for the iterative solution of the problem. For the open boundary problems, the standard RIC2 may fail when applied to highly-indefinite matrix when a zero pivot is encountered or the obtained triangular is unstable. A perturbed diagonal matrix is added to the matrix before the RIC2 factorization process to make the real part of the coefficient matrix more diagonally dominant. The main purpose of this study is to evaluate the efficiency of the perturbed RIC2 preconditioner applied to highly indefinite matrix obtained by discretize Helmhotz equations. The numerical efficiency of the preconditioner are illustrated on a set of model problems arising both from academic and from industrial applications. Experimental results show that the RIC2 preconditioner is fairly robust and can reduce the number of CG iterations substantially.

Sea-wave Fractal Spectrum and Scattering Coefficient Evaluation from an Improved Two-Dimensional Fractal Sea Surface

Lixin Guo, **Yunhua Wang**
Xidian University, China

In this paper, an improved fractal sea surface model is proposed for modeling the two-dimensional time-varying rough sea surface. The important contribution of this work is to develop the classical fractal sea surface model to a new one, which is more consistent with the actual sea spectrum. It is well known that the spectrum of the general fractal rough surface shows the negative power behavior, but the spectrum of the sea surface takes the same form only for the spatial wavenumber is larger than the spatial fundamental wavenumber K_0, once the spatial wavenumber is less than K_0, the spectrum is the positive power spectrum rather than the negative power spectrum, thus the fractal spectrum of the general fractal sea surface model cannot fit the classical sea spectrum such as fully developed Pierson-Moskowitz spectrum very well. We start from a new definition of the fractal sea surface model, the spatial autocorrelation and the spectrum of our new model are derived and calculated, it is observed the two-dimension fractal spectrum also includes the δ- functions, which is similar to the result of one-dimension fractal spectrum given by Jaggard. We can also get a continuously approximated and limited fractal sea spectrum in the case of the scale factor approaches unity and the slope of the new continuous spectrum heavily depends on the fractal dimension. It is found that the omnidirectional sea-wave spectrum of the 'fractal sea spectrum' evaluated from our improved fractal sea surface model fitting the PM spectra well, and the spreading function of the 'fractal sea spectrum' has the same properties as those given by Cote and Mitsuyasu models.

The solution of the scattering coefficient and the average intensity coefficient from this new fractal surface model is studied based on the Kirchhoff theory, the effect of the different wind speed and wind direction on angular distribution of the monostatic and bistatic scattering coefficients are calculated and analyzed, the relationship between the fractal dimension of the time series of the backscattering coefficient and the fractal dimension of the sea surface is discussed in detail.

REFERENCES

1. Jaggard, D. L., Y. Kim, "Diffraction by Band-limited Fractal Screens," *J. Opt. Soc. Am. A*, Vol. 4, No. 6, 1055, 1987.
2. Berizzi, F., E. Dalle Mese, "Sea-wave Fractal Spectrum for SAR Remote Sensing," *IEE Proc-Radar, Sonar Navig.*, Vol. 148, No. 2, 56, 2001.
3. Berizzi, F., E. Dalle Mese, "Scattering Coefficient Evaluation from a Two-dimensional Sea Fractal Surface," *IEEE Transactions on Antennas and Propagation*, Vol. 50, No. 4, 426, 2002.

Analysis of an Electrically Small Cylindrical Monopole Surrounded by Double Negative Materials Using FDTD Method

N.-B. Wang, **Y.-C. Jiao**, **F.-S. Zhang**
Xidian University, China

Double negative (DNG) materials have simultaneously negative permittivity and permeability over a certain band. Due to their unique properties that may lead to unconventional phenomena in transmission, radiation, and scattering of electromagnetic wave, DNG materials have recently received much attention from various research groups, and may find potential applications in many domains. Recently Ziolkowski introduced an idea of the potential use of DNG materials to enhance the radiation characteristics of electrically small antennas [1]. The theoretical analysis of the reactive power within the dipole-DNG shell system indicates that the DNG shell acts as a natural matching network for the dipole.

In this paper an electrically small cylindrical monopole, surrounded by a cylindrical shell of DNG material on a finite circular ground, is analyzed numerically using the two-dimensional frequency-dependent finite-difference time-domain (FDTD) method in cylindrical coordinate. Both the negative permittivity and permeability are realized with the Lorentz medium model, and the auxiliary differential equation (ADE) method is used to implement frequency dependence in the FDTD algorithm [2]. A second-order accurate FDTD equation at dispersive medium interfaces is presented and applied to simulate this monopole-DNG shell combination. The numerical results show that a properly designed monopole-DNG shell combination increases the real power radiated by more than an order of magnitude over the corresponding free space case. Moreover, the resistance of this antenna increases, while the corresponding reactance decreases. The radiation characteristic of this electrically small antenna is very similar to that of a conventional monopole antenna. This theoretical study indicates that the monopole surrounded by a cylindrical shell of DNG material is an efficient way for realizing the miniaturization of the monopole antenna.

*This work was supported by the National Natural Science Foundation of China (60171045).

REFERENCES

1. Ziolkowski, R. W. and A. D. Kipple, "Application of Double Negative Materials to Increase the Power Radiated by Electrically Small Antennas," *IEEE Transactions on Antennas and Propagation*, Vol. 51, 2626, 2003.
2. Taflove, A. and Susan C. Hagness, *Computational Electromagnetics: The Finite- Difference Time-Domain Method, Second Edition, Boston, MA: Artech House*, 2000.

An Assessment of Ionospheric Faraday Rotation Using Total Electron Content GPS Measurements

Wei Zou, **Deting Hou**, **Jianhong Yang**
Dongfang Zhou, **Zhongxia Niu**
Information Engineering University, China

Frequency re-use by means of orthogonal polarizations is often used to increase the capacity of space telecommunication systems. This technique is limited, however, by the depolarization produced by a number of elements along the transmission path, which include both antenna and propagation contributions. Various mechanisms, Faraday rotation, rain and ice particles along the propagation path produce depolarization. Faraday rotation is an effect brought about by the free electrons present in the ionosphere and results in depolarization of linearly polarized signals. This effect will become an important consideration in satellite systems designing. To assess this effect, it is necessary to compute the amount of rotation angle over a given path across the ionosphere. The Faraday rotation angle is approximately proportional to the integrated electron content along the path, to the magnetic field strength at the heights of the ionosphere, and to the cosine of the angle between the satellite-to-ground path and the magnetic field lines. The calculation is simplified in this paper by using the average value of the magnetic field and the integrated electron content, namely the total electron content (TEC) along the path. Simple analytic expression for Faraday rotation is given in this paper.

TEC is defined as the total number of electrons in a column with a cross sectional area of $1m^2$ along the ray path. The TEC measurement can be used for calibration of ionospheric Faraday rotation. In this paper we discuss the method of TEC measurement using a dual-frequency GPS Navigation receiver which utilize differential delay. The contribution of plasmospheric TEC to the total GPS TEC is considered. In using GPS TEC for ionospheric purposes, we estimate and deduct the plasmospheric TEC component. The data obtained from the TEC measurement is used to estimate the Faraday rotation angle.

The magnitude of the Faraday rotation angle depends on time of day, solar activity and the observatory location. In the last of the paper, the relationship between the variability of the Faraday rotation and the spatio-temporal TEC variability is analyzed.

Guideline for a UWB Waveform Robust to the Numerical Dispersion in FDTD Schemes

Arnaud Thiry, **Fumie Costen**
The University of Manchester, U.K.

Research and development of Ultra WideBand (UWB) systems require model simulations to verify algorithms applied to the systems. In this field, the finite difference time domain (FDTD) method is widely used for simulation of the transient wave propagation. The waveforms obtained from FDTD do not perfectly match to the theoretical ones. This imperfection comes from the nature of the spatial discretization, boundary conditions and the waveform of the source excitation. The introduction of higher order discretization schemes, the complex boundary conditions with higher absorption of signals are the standard devices to reduce the numerical dispersion as well as the use of the higher spatial resolution. The voxel size determines the cutoff frequency for transmission in the system. The frequency components close to the cutoff frequency propagate slower than the other components. This implies that the waveforms vulnerable to the numerical dispersion have relatively large frequency components in magnitude close to the cutoff frequency.

Many works utilize a Gaussian pulse because of its smoothness in both time and frequency domains and some use a raised cosine pulse because of its minimum amount of transients. However, to the authors' knowledge, no report has so far been found which studies the influence of the source excitation on the waveform distortion from the viewpoint of the numerical dispersion in FDTD.

This paper has novelty in revealing the relationship between the frequency spectrum of the source excitation and the numerical dispersion and in proposing a guideline to the production of UWB waveforms relatively robust to the numerical dispersion.

The Two or More Scale Models in Heterogeneous Media Electrodynamics

V. S. Travkin
Hierarchical Scaled Physics and Technologies, U.S.A.

The multiscale modeling in electrodynamics never been recognized as the strongly relative to the most of the problems or the important one. Through the years the models for complicated media were used as based on the Lorents's predicament of the same scale effective coefficients, while using the same scale, but said the second (upper) scale Maxwell's governing equations with coefficients determined by variety of the same one scale methods.

Advancements in optical engineering and networking, experimental confirmation of existence of composites with properties of negative refractive index media (NRIM) elevated the old and mostly neglected multiscale description area in electrodynamics and optics to a new "level" of significance.

As soon as this field in electrodynamics remains to be very much misunderstood and underdeveloped, the few first mathematically correct steps in this direction must have a lot of beneficial consequences as, for example, the issue of modeling and simulation of effective properties of heterogeneous and scaled media. In spite that to this topic being attached many books and hundreds (in not thousands) papers, the current situation calls for re-evaluation even of basic definitions as - what is the effective property for inhomogeneous and heterogeneous media? What is the difference between both if any?

Those are not recognized and understood issues in electrodynamics, in spite that in other physical disciplines these questions debated many years ago and have found resolutions.

The new field of NRIM (or left-handed materials, media) is the marvelous example of the situation of how unprepared is the theoretical and mathematical determination of major acting physical fields in these materials (composites). Without this determination, the efforts to study and analyze the experimental results will remain impaired, even incorrect.

The present talk will be recognizing the one scale and two scale mathematical definitions and governing equations for complicated, heterogeneous media such as superlattices, composites, materials demonstrating unusual electric and optical characteristics in conjunction with goals for modeling and data reduction for these media electrodynamics.

Adaptive Integral Method (AIM) Combined with the Enhanced GMRES Algorithms for Planar Structures Analysis

L. Mo, **P. L. Rui**, **W. Zhuang**, **R. S. Chen**
Nanjing University of Science and Technology, China

The design of planar structures such as microwave monolithic integrated circuits (MMIC) and microstrip antenna has become a very important topic in current electromagnetics. Due to the complexity of these devices, efficient numerical tools are required for their analysis. One of the most popular techniques for analyzing these devices is the integral equation method. To discretize the integrate equations by using of method of moment (MoM) with Rao-Wilton-Glisson (RWG) basis functions can model arbitrarily shape planar structures but usually leads to a fully populated matrix. The adaptive integral method (AIM) can map these basis functions onto a rectangular grid then the Toeplitz property of the Green's function would be utilized, which enables the calculation of matrix-vector products by use of the fast Fourier transform (FFT). The resultant algorithm reduces the memory requirement from $O(N^2)$ to $O(N)$ and the operation complexity from $O(N^2)$ to $O(N \log N)$, where N is the number of unknowns. Several kinds of Krylov subspace iterative solvers are applied to the resulting matrix equations such as the generalized minimal residual method (GMRES), Loose-GMRES, Augmented-GMRES, Nested-GMRES, inner-outer Flexible-GMRES, etc. All these enhanced GMRES methods converge much faster than the conventional Conjugate Gradient method (CG). Some typical microstrip circuits and microstrip antenna arrays are analyzed and the good results demonstrate the validity of the proposed algorithm.

Comparison of Real Formulations to Solve Complex Linear Systems Arising in Computational Electromagnetics

G. Angiulli, **M. Versaci**
Univ. Mediterranea, Italy

Method of Moments (MoM) is a standard technique to solve integral equations in computational electromagnetics [1]. It permits to evaluate the current density distribution on a scattering objects by solving a complex matrix linear system. Unfortunately, for electrically large obstacle the moment matrix equation is quite time consuming to solve using direct inversion. Thus, in order to reduce the computational effort iterative methods in conjunction with preconditioning techniques are currently employed [2], [3]. As well known by technical literature on numerical linear algebra most preconditioned iterative methods can be employed to both real and complex linear systems. It can be useful to transform a complex linear system in a real one since many available software packages employed currently in numerical computations are specialized to manage only real systems [4]. This work has two main objectives. The first is to discuss the properties of the dierent real formulations. The second is to compare their performances. All the formulations have been coded using MATLAB© and numerically tested. Results are presented for the linear systems arising by MoM treatment of the Electrical Field Integral Equation (EFIE) for the plane wave scattering by conducting objects as metallic cube and sphere.

REFERENCES

1. Harrington, R. F., *Field Computation by Moment Methods, Macmillan*, 1968
2. Chew, W. C., J-M. Jin, E. Michielssen, *J. Song (editors), Fast and Efficient Algoritms in Computational Eletromagnetics, Artech House*, 2001.
3. Greenbaum, A., *Iterative Methods for Solving Linear Systems, Frontiers in Applied Mathematics, SIAM*, 1997.
4. Day, D., M. Heroux, "Solving Complex-Valued Linear System via Equivalent Real Formulations," *SIAM J. Sci. Comput.*, Vol. 23, 480, 2001.

Time Domain Numerical Calculation of Wave Spread in Electric Power Cable and Its Application in Fault Positioning

Shizuo Li, **Yuanzhong Liao**, **Hanyi Huang**
Guangxi University, China

Transmission line have been researched for a long time, but those researches usually concentrate on frequency domain, and only simple cases in time domain such as wave spread under step or impulse activating have been investigated. This is enough for some application, but a more accurate numerical calculation is needed to study the character of wave spread in transmission line. In fault positioning of electric power cable, high voltage strike circuit (shown as Fig.1) usually is used, and Fig.2 illustrates the equivalent circuit. Differential equations are derived as:

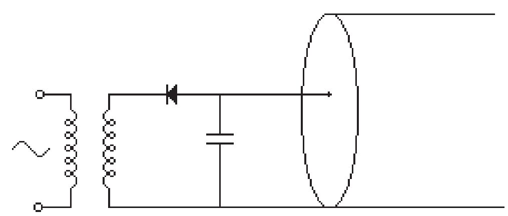

Figure 1: Strike Circuit

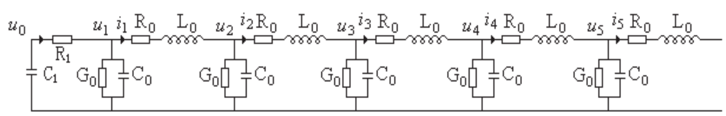

Figure 2: Equivalent Circuit

$$C_1\frac{du_0(t)}{dt} = -\frac{u_0(t)-u_1(t)}{R_1} \quad C_0\frac{du_1(t)}{dt} = \frac{u_0(t)-u_1(t)}{R_1} - i_1(t) - G_0u_1(t)$$

$$L_0\frac{di_j(t)}{dt} = u_j(t) - u_{j+1}(t) - R_0i_j(t) \quad j = 1, 2, \ldots$$

$$C_0\frac{du_j(t)}{dt} = i_{j-1}(t) - i_j(t) - G_0u_j(t) \quad j = 2, 3, \ldots$$

Numerical calculation of these differential equations in many kinds of fault is done by Euler method, and actual waves are recorded to compare with the numerical results.

Based on numerical result and actual wave, the relationship between fault position and wave spread have been studied detailedly and a fault positioning method is developed.

The Correct Solution for the Upper (Bulk) Scale Two-Phase Multilayer Media Electrostatics and Electrodynamics Problems

V. S. Travkin
Hierarchical Scaled Physics and Technologies, USA

The recent results in heterogeneous media electrodynamics scaling formulation were utilized to address the local, non-local, and two-scale modeling (and experimental) EM diffraction fields in superlattices and two-phase regular layered structure composites. Derived and compared various non-local and heterogeneous scaled models for diffraction in infinite and finite 2D two-phase composites.

The structure of the half space medium specimen accepted to be organized as the 1D or 2D layered medium with periodic fast-oscillating or two-phase heterogeneous media. This is considered as the well known and solved long ago problem. We show that it is not true even in terms of the lower scale traditionally taught in almost every technical discipline statements. These problems have been recently solved considering them as the two-scale tasks with the local conventional statements and the upper (second) scale problems, those inherently connected to the lower scale physics and mathematical statements. More complicated are 2D heterogeneous media combining their separate local, non-local and two-scale models. We show the range of difference in simulation models results for various physical models of phase and interface phenomena. Heterogeneity and scaled description of interface and phase related fields bring up previously unreachable features to include into the diffraction picture.

Some of these phenomena as, for example, when the phase coefficients are homogeneous (constant) revealed, the interface surficial and the phase fields exchange components. The effective dielectric permittivity and transmittivity as well as experimental local and non-local data reduction methods for homogeneous and heterogeneous (composite) materials outlined and explained the reasons to relate strictly the scale of measurements and data reduction. Given the examples of scaled treatment.

Session 3P3

Electronically Controllable Microwave and Millimeter-wave Devices and Antennas 2

Modeling Fronzen Modes in Finite Three-Dimensional Magnetic Photonic Crystals

Seung-Cheol Lee, **Jin-Fa Lee**
Ohio State University, USA

Recently, Figotin and Vitebskiy have studied electromagnetic wave propagates within nonreciprocal magnetic photonic crystal (MPC) structures. The primitive cell of the MPC consists of three layers, and the material properties of the three layers can be summarized as

$$[\varepsilon_r^{(a1)}] = \begin{bmatrix} \xi + \delta\cos 2\varphi_1 & \delta\sin 2\varphi_1 & 0 \\ \delta\sin 2\varphi_1 & \xi - \delta\cos 2\varphi_1 & 0 \\ 0 & 0 & 1 \end{bmatrix}; [\mu_r^{(a1)}] = \begin{bmatrix} \mu + \Delta\cos 2\varphi_1 & \Delta\sin 2\varphi_1 & 0 \\ \Delta\sin 2\varphi_1 & \mu - \Delta\cos 2\varphi_1 & 0 \\ 0 & 0 & 1 \end{bmatrix}$$
$$[\varepsilon_r^{(a2)}] = \begin{bmatrix} \xi + \delta\cos 2\varphi_2 & \delta\sin 2\varphi_2 & 0 \\ \delta\sin 2\varphi_2 & \xi - \delta\cos 2\varphi_2 & 0 \\ 0 & 0 & 1 \end{bmatrix}; [\mu_r^{(a2)}] = \begin{bmatrix} \mu + \Delta\cos 2\varphi_2 & \Delta\sin 2\varphi_2 & 0 \\ \Delta\sin 2\varphi_2 & \mu - \Delta\cos 2\varphi_2 & 0 \\ 0 & 0 & 1 \end{bmatrix}$$
$$[\varepsilon_r^{f}] = \begin{bmatrix} \varepsilon & j\alpha & 0 \\ -j\alpha & \varepsilon & 0 \\ 0 & 0 & 1 \end{bmatrix}; [\mu_r^{f}] = \begin{bmatrix} \mu_f & j\beta & 0 \\ -j\beta & \mu_f & 0 \\ 0 & 0 & 1 \end{bmatrix} \tag{1}$$

It is found through transfer matrix of layered medium that a so-called frozen mode exists within such a MPC structure so long as $\varphi_1 - \varphi_2 \neq 0, \frac{\pi}{2}$. The frozen mode also corresponds to a stationary inflection point on the dispersion relation between the frequency and the Bloch wave vector, namely

$$\frac{\partial\omega}{\partial k}|_{k_0} = \frac{\partial^2\omega}{\partial k^2}|_{k_0} \neq 0; \frac{\partial^3\omega}{\partial k^3}|_{k_0} \neq 0 \tag{2}$$

Subsequently, for electromagnetic waves propagating through the MPC in the vicinity of the frozen mode frequency, the group velocity of the wave can be slowed significantly. Moreover, the frozen mode phenomena, unlike resonances in resonator structures such as photonic band gap, exhibits finite wave impedance and thus allowing energy to couple into the MPC structure. Therefore, in the vicinity of the frozen mode frequency, the electromagnetic wave not only experiences the slow-down effect but also its field amplitude will increase drastically.

The finite MPC structures in three-dimensional space, which include non-reciprocal material properties and large variations of field intensity within small regions, do impose significant difficulties in numerical computations. In this talk, we shall address the difficulties that we have encountered and the remedies that have been adopted. Moreover, the effect of the "finiteness" on the "frozen modes" with the MPC structures will also be discussed.

Figure of Merit and Limiting Characteristics of Tunable Ferroelectric Microwave Devices

Irina Vendik, **Vladimir Pleskachev**, **Orest Vendik**
St. Petersburg Electrotechnical University, Russia

Microwave application of ferroelectrics is very promising for electrically tunable microwave devices due to electric field dependence of the dielectric permittivity. Tunable filters and controllable phase shifters are successfully designed as integrated circuits based on the multilayer structure containing a thin epitaxial ferroelectric (FE) film. As a rule lumped ferroelectric capacitors are used as the tunable components. In order to evaluate quality of these components and compare them with other widely used tunable components (p-i-n-diodes, varactor diodes etc.), the commutation quality factor (CQF) was introduced and defined as

$$K = \frac{(X_2 - X_1)^2}{R_2 R_1} \tag{1}$$

where $R_{1,2}$ and $X_{1,2}$ are the real and imaginary parts of the impedance of the tunable components in two different states corresponding to two levels of the biasing control signal. The CQF as applied to the FE tunable components looks as

$$k = \frac{(n-1)^2}{n \tan\delta_1 \tan\delta_2} \tag{2}$$

where $n = \varepsilon_1/\varepsilon_2 = C_1/C_2$ is the tunability of the material (FE capacitor) and $\tan\delta_{1,2}$ is the loss factor. The higher K, the higher is the quality of the device. For practical applications 500 K$\geq$ 500. Let us introduce the figure of merit (FM) of the tunable device. For the tunable resonator

$$F = \frac{\omega_2 - \omega_1}{\Delta\omega} \tag{3}$$

for the tunable filter

$$F = \frac{\omega_2 - \omega_1}{\Delta\omega} \cdot \frac{1}{L(dB)} \tag{4}$$

for the phase shifter

$$F = \frac{\Delta\phi}{L}\left(\frac{degree}{dB}\right) \tag{5}$$

where $\omega_2 - \omega_1$ is the shift of the resonant/central frequency of the resonator/filter while tuning $\Delta\omega$ is the width of the resonant curve/passband of the resonator/filter, L is the insertion loss in dB, N is the filter order (number of resonators), and $\Delta\phi$ is the phase shift in degree. The figure of merit of these devices is determined by the tunability and loss-factor of the tunable FE component. One can proof that the maximum of the FM, which is considered as the limiting characteristic, is a function of the CQF. For the resonator

$$F_{max} = 0.5\sqrt{K} \tag{6}$$

for the filter

$$F_{max} = \frac{\sqrt{K}}{8.68N} dB^{-1} \tag{7}$$

and for the phase shifter

$$F_{max} = 6.6\left(\sin\frac{\Delta\phi}{2}\right)^{-1}\sqrt{K}\left(\frac{degree}{dB}\right) \tag{8}$$

The FM defined by (6)-(7) describe the maximum achievable value of the FM, which is determined by the CQF, depending on the quality of the FE material.

Novel High-power Electronically Tunable Helical Resonator Filter

Rui-Feng Xue[1], **Bin Yuan**[1], **Jun-Fa Mao**[1], **Chang-Hong Liang**[2]

[1]Shanghai Jiao Tong University, China
[2]Xidian University, China

Tunable filters have always been a focus of research due to their wide applications. As the key component of the multi-channel transmitting system in commercial and military HF radio communication, high-performance tunable filters with high tuning speed, high-Q factor, high power capacity, and broad tuning range are needed. A novel design of high-power electronically tunable helical resonator filter suitable for applications in HF radio communication is proposed.

First, the helical resonator is loaded in the middle of the helix instead of conventional end position. This relieves the requirements of withstand voltage and power capacity of the tuning element greatly, and makes the filter own the ability to tune over a broad spectrum of frequencies. Second, the tuning element is set outside the cavity. We can get more assembly space for tuning elements, less dissipation, better heat emission, without interfering with the electromagnetic fields within the cavity. Third, a special CMOS power switched capacitor is exploited as the tuning element, which can be utilized for high frequency large signal transmission.

Theoretical analysis and experimental verification are demonstrated. A prototype is manufactured and tested. The results show that the filter can be realized with properties of high tuning speed, high-Q factor, high power capacity, and broad tuning range. It is believed that the proposed techniques offer an attractive way to implement the high-power electronically tunable filter.

Design of the PLL Module for Dual-band Repeater

Jin-Sup Kim, **Sang-Gi Byeon**, **Yong-Cheol Kang**
Korea Electronics Technology Institute, R.O.Korea

The dual-band RF technology for applications to the wireless repeater for CDMA and WCDMA mobile communications has been developed in this paper. The dual-band PLL module consisted of dual-band VCO and one PLL IC has been developed. The main technological efforts for the dual-band PLL module is to suppress the interference signals by applying the miniature ceramic filter using the slow wave characteristics.

The CDMA & WCDMA dual-band PLL module shows the phase noise of -95dBc/Hz at 10KHz offset and locking time of 1.4ms which meets the required specification. The dual-band miniature RF module including dual PLL module and one MCU controller is very attractive for applications to the miniature dual-band RF mobile repeaters.

Broadband THz Generation from Photoconductive Antenna

Qing Chang, **Dongxiao Yang**, **Liang Wang**
Zhejiang University, China

Since the observation of radiation in the Terahertz (THz) frequency range from photoconductive antennas exited by femtosecond (fs) laser pulses, considerable efforts have been made to understand the mechanism responsible for THz generation, and to develop applications in THz Time-Domain Spectroscopy (THz-TDS). In this paper, the calculation of THz radiation from biased photoconductive an- tenna is reported, given some amelioration of the calculation model and classical Drude-Lorentz theory. Some simulation results based on the new calculation model are shown.

Nonlinear Loaded Loop Antennas with a Dielectric Core

T. M. Zaboronkova
Technical University of Nizhny Novgorod, Russia

A. A. Gorbachev, **A. A. Vasenkov**
Radiophysical Research Institute, Russia

Specific features of electromagnetic wave scattering by objects with nonlinear characteristics are of interest because they can be used for solving a number of applied radar problems unsolvable by conventional methods. Nonlinear electromagnetic wave scattering is inherent in any man-made object containing electronic components or imperfect contacts. The difficulties of the theoretical analysis of nonlinear scattering and obtaining information on the properties of nonlinear scatterers give rise to experimental techniques and methods for recognizing such objects. During such studies, one often analyzes the adequate simplified models of the actual objects rather than the objects themselves.

We consider a model problem of electromagnetic wave scattering by a circular loop with a dielectric core. The loop contains a nonlinear local load in the form of a semiconductor diode with the known (preliminary measured) current-voltage characteristic. The operation regime of the nonlinear load is determined by setting the operating point of the current-voltage characteristic and can be tuned by varying the electric field of the sounding signal. We restrict ourselves to the case of weak nonlinearity, which allows us to consider only the second harmonic of the nonlinearly reflected signal. The case where an electromagnetic wave is scattered by the nonlinear-loaded loop without a dielectric core is discussed in [1]. Here, we present the results of experimental and theoretical studies of the influence of the following parameters on the signal at the second harmonic: (i) the core electrical size, (ii) the core permittivity, (iii) the diode location on the loop, (iv) polarization of the signal incident on the loop, and (v) the loop electrical sizes. During the experiment, we considered the core of spheroidal form with a length of up to one wavelength of the sounding signal in free space. We also obtained the rigorous solution of the problem in the case of a circular loop with a core in the form of a dielectric sphere. The radii of the loop and the sphere were assumed coinciding. For the case where the core possesses the spherical form, the experimental results are in good agreement with the theoretical calculations.

We have thus considered the influence of the dielectric core on the backscattering field produced by the antenna with a nonlinear local load at the second harmonic of the sounding signal. In particular, it has been shown that the presence of a dielectric core leads to a significant increase in the double-frequency signal for a certain range of the core electrical size. Preliminary experimental results obtained in the decimeter-wavelength range can be extended to the centimeter-wavelength range. The features of nonlinear scattering can be used for detection of marked objects as well as for development of nonlinear markers.

REFERENCES

1. Gorbachev, A. A., T. M. Zaboronkova and S. P. Tarakankov, “Scattering of electromagnetic waves by nonlinear antennas in the presence of a two media boundary”, *J. Electromagn. Waves Appl.*, Vol. 9, No. 10, 1285, 1995.

Application of Scatterers Loaded by a Parametric Contour with Self-modulation as Markers of Objects

T. M. Zaboronkova
Technical University of Nizhny Novgorod, Russia

P. A. Gorbachev
Radiophysical Research Institute, Russia

Application of passive nonlinear scatterers as markers of objects meets a number of restrictions, including in particular the necessity of the second frequency channel for reception of a nonlinear product created by the scatterers. Moreover, false alarms can arise from external nonlinear scatterers such as household radio electronics. Subharmonic scatterers down-conversioning the frequency of the sounding signal allow one to avoid background noise and false alarms in most cases but also require the second frequency channel for signal reception [1], which is inconvenient in certain cases. The present communication discusses the possibilities of application of half-wave subharmonic scatterers operating in the self-modulation regime as markers of objects. The parametric contour of a subharmonic scatterer provides modulation of the effective scattering cross section at the sounding-signal frequency and ensures the criterion allowing identification of objects (due for example to modulation of the scattering cross section by the known frequency). As a result, the second frequency channel is not required. The operation regime of subharmonic scatterers can be tuned by varying the sounding-signal Poynting flux. As is known [2], if the value of this flux in the place of location of scatterers is greater than the threshold of excitation of the parametric contour but smaller than the threshold of breakdown, then subharmonic scatterers are capable of generating subharmonics.

As in [1], we consider a subharmonic scatterer in the form of a half-wave oscillator loaded with a high-frequency diode in parallel to which a metal half ring (of 1 to 3 cm in diameter) is connected. The excitation threshold is about $10^{-4} - 10^{-3} W/m^2$ and satisfies the above-mentioned condition. After introducing two additional elements with active resistance R and capacitance C in the scatterer parametric contour, the regime of interrupted generation is possible. In the case of a monochromatic sounding signal, the scattered signal at the subharmonic frequency represents a sequence of pulses with the known frequency determined by the values of R and C. Accordingly, at the sounding-signal frequency, the scatterer can be considered as the object with parametrically varying effective scattering cross section. Thus, it is possible to use the frequency of amplitude modulation as the individual criterion for identification of the object. The performed measurements show that a subharmonic scatterer can give the response at the sounding-signal frequency in accordance with such an criterion. The related experimental results will be reported and discussed for particular cases.

REFERENCES

1. Gorbachev, P. A., T. M. Zaboronkova and A. A.Vasenkov, "Nonlinear electromagnetic wave scattering by objects located near water surface," *17th Wroclaw Symp. on Electromagnetic Compatibility*, www.emc.wroc.pl, 2004.
2. Gorbachev, P. A., "Nonlinear subharmonic scatterers of electromagnetic waves," *Radiotekh. Élektron.*, Vol. 44, No. 10, 1164, 1999.

Session 4A1

Advances in Detection and Classification Techniques by Radar

Automatic Detection of Buried Pipes from Ground Penetrating Radar Data

P. Falorni, **L. Capineri**, **L. Masotti**
University of Florence, Italy

G. Alli, **G. Pinelli**
I.D.S. S.p.A, Italy

In previous works [1][2] the authors presented a method for the detection of hyperbolic patterns in radar B-scans by using the gradient-sigmoid filter. The processing of these patterns by a modified Hough Transform allows to estimate lateral position (y), depth (z) and propagation velocity (v) of targets.

In this work we will present a further step towards the automatic detection of buried pipes/cables exploiting the 3d spatial tracking of sequences of hyperbolic patterns positions as obtained by the modified Hough Transform method on a number of adjacent B-scans.

The capability of the full automatic process has been tested on experimental data acquired with a 200 MHz IDS-RIS radar on a test field containing 18 distinguishable pipes/cables (plastic or metal) arranged in different positions (deep and/or shallow, isolated and/or clustered). Obtained results are the correct detection of 17 out 18 pipes/cables with only 2 false alarms; the missed target being a single large deep pipe.

The 3d spatial tracking is based on the assumption that a pipe is nearly orthogonal (within an assigned solid angle) to the B-scan plane and that a pipe is defined by a series of hyperbolic patterns positions belonging to different B-scans. In order to declare a pipe, the feasible sequences are checked to satisfy the following 5 properties: serialization, directionality, continuity, straightness and minimum energy (Dijkstra algorithm).

The robustness of this pipe detection method has been tested on simulated data where false hyperbolic patterns and some degree of true target misplacement were introduced.

The computational complexity of this type of algorithms is generally a problem for practical applications; in this case it has been limited to a linear factor working on small sequences of five apexes. A Matlab program has been executed in 43 s on a 1.5 GHz laptop PC on 18 B-scans of 20 meter length each and corresponding to an area of $140m^2$.

REFERENCES

1. Falorni P., L. Capineri, L. Masotti, G. Pinelli, "Reliable detection of hyperbolic diffraction patterns in Radar scans for computerized topographic mapping of buried utilities", *invited work at PIERS 2004, Pisa, Italy*, 2004.
2. Falorni P., L. Capineri, L. Masotti, G. Pinelli, "3-D Radar imaging of buried utilities by features estimation of hyperbolic diffraction patterns in radar scans", Tenth *International Conference on Ground Penetrating Radar, 21-24 June, 2004, Delft, The Netherlands*, 2004.

Detection and Characterization of Targets Buried Below a Rough Surface

O. Cmielewski[1], **M. Saillard**[2], **H. Tortel**[1]

[1]Institut Fresnel, CNRS, France
[2]Universite du Sud Toulon-Var, France

The problem of detection and characterization of an object buried at very low depth beneath a rough surface is addressed. At least two approaches have been proposed to solve such an inverse problem. One of them consists in reconstructing simultaneously both the scatterer and the surface profile. One can also proceed in two steps: first, the surface profile is reconstructed from the early-time response to ultra-wide band signals, and the corresponding Green's function is built numerically. The second step deals with the reconstruction of a scatterer embedded in a (rough) stratified medium. However, both methods assume that the buried object has been previously detected and localized, since only a small area around the scatterer is considered. Here, we mainly focus on this preliminary step.

A new way of detecting buried objects from wide band near-field multi-static data is presented. The so-called near-field configuration corresponds to a set of N transmitters and receivers located along a piece of line in the vicinity of the surface. From the N×N matrix of multi-static data, we suggested to compute the correlation C(X) between columns (or lines) associated with two transmitters located symmetrically from the point X under test, and average over all such pairs. Indeed, a theoretical study in the frame of a low frequency approximation predicts an enhancement of the correlation peak resulting from the cross terms combining surface and target contributions, confirmed by rigorous computations. Lorentz reciprocity ensures the same result if a single transmitter is used but measurements performed at two receivers located symmetrically from X. This technique has been numerically tested in various configurations, and the performance of the detector has been estimated against roughness parameters through computation of the receiver operating characteristic curves (probability of detection versus false alarm rate). This technique can be improved if a network of more than two transmitters/receivers can be used, since it is demonstrated that the weight of the terms contributing to the correlation peak increases when the number of correlated data sets is increased.

Combining multi-static data and wide band signals can also be viewed as an averaging process over surface roughness, aimed at smoothing its contribution and let the scatterer auto-correlation peak clearly appear in C(X). Therefore, we think that a reconstruction process based on a minimization of a cost function built with C(X) instead of the scattered field, as is usually done, could be more robust against clutter. The inversion algorithm is currently under construction.

Progress in the Research of Ground Bounce Removal for Landmine Detection with Ground Penetrating Radar

Renbiao Wu, **Jiaxue Liu**, **Tang Li**, **Qian Gao**, **Hongyu Li**, **Bei Zhang**
Civil Aviation University of China, China

Downward looking ground penetrating radar (GPR) has been considered a viable technology for landmine detection. For such a GPR with the antennas positioned very close to the ground surface, the reflections from the ground surface, i.e., the ground bounce, are very strong and can completely dominate the weak returns from shallowly buried plastic mines. Hence, one of the key challenges of using GPRs for landmine detection is to remove the ground bounce as completely as possible without altering the mine return.

In this paper, we first review existing ground bounce removal algorithms. Then two newly devised adaptive ground bounce removal algorithms, ASaS (Adaptive Shifted and Scaled algorithm) and RLP (Robust Linear Prediction) will be presented. Both ASaS and RLP are based on a flexible ground bounce data model applicable to rough ground surface, and hence are robust. We have also presented several new effective selection methods of secondary data samples, which is vital for all ground bounce removal algorithms, including conventional nonadaptive algorithms as well as adaptive algorithms. Finally, some experimental examples are provided to demonstrate the performance of the proposed methods.

Localized Parametric Electromagnetic Inversion for Pavement Profiling with Ground Penetrating Radar

Weikun He, Jiaxue Liu, Renbiao Wu
Civil Aviation University of China, China

The estimation of layer thickness and permittivity is very important for the routine maintenance of the road, highway, and airport runways. Ground penetrating radar (GPR) has proven to be an effective non-destructive tool for pavement profiling. Layer thickness and permittivity can be estimated by using an inverse scattering approach to the echoes collected by GPR. Two effective methods have been proposed for this purpose, one is called layer-stripping and the other is called parametric electromagnetic (EM) inversion. Layer-stripping is based on tracking and analyzing the estimates of amplitude and time of delay of reflected echoes, while parametric EM inversion is based on minimizing a cost function based on the difference between measured and simulated signals (by parametric modeling) in every spatial location. Layer-stripping is less accurate but is computationally more efficient than parametric EM inversion. In practice, layer-stripping is used as a prescreening method for rough inspection of a large area, and parametric EM inversion is used for fine inspection of some interested small area.

Existing parametric EM inversion approach didn't take into account the discontinuity (non-homogeneous) of the permittivity profile along the survey direction. In this paper, we have proposed a localized parametric EM inversion approach which can effectively overcome the above drawback. Numerical examples provided have shown that the proposed method can work well in non-homogeneous multi-layered environment and is computationally more efficient than existing parametric EM inversion algorithm.

The Estimation of Buried Pipe Diameters by Generalized Hough Transform of Radar Data

C. G. Windsor
116, New Road, East Hagbourne, OX11 9LD, UK

L. Capineri, **P. Falorni**
University of Florence, Italy

The generalised Hough transform method is applied to the measurement of the diameters of buried cylindrical pipes by Ground Penetration Radar (GPR). 600 MHz radar scans across long pipes, buried in one metre or so of soil, show complex reflection patterns consisting of a series of inverted hyperbolic arcs. The time of flight $t(y)$ as the probe is scanned along an axis, y, perpendicular to the pipe, shows an arc whose shape depends on 4 unknown variables: y_0, the position of the centre of the pipe along the scan, z_0, the depth of the pipe centre, R, its radius and V the velocity in the medium. Analytic expressions for the solution of these variables have been obtained. They use sets of between 1 and 4 times t_i at corresponding positions y_i, along the arc, depending on the number of variables to be determined. In the generalised Hough method many such sets of times are chosen randomly from points on the arcs. The results are presented for example as peaks in an accumulator space for each variable. The method is demonstrated for a 0.18 m radius concrete pipe buried at a nominal 1 m depth in a road. Using data acquired at 600 MHz frequency (around 0.16m wavelength in soil) the estimated radius was 0.174 ± 0.059 m.

Application of Tomographic Inverse Scattering Techniques to Microwave Imaging Radars

Rui-Feng Xue, **Bin Yuan**, **Jun-Fa Mao**
Shanghai Jiao Tong University, China

The application of tomographic inverse scattering techniques to imaging radars is presented to realize high quality radar imaging in this paper. Diffraction tomography is applied to ultra wideband synthetic aperture radar (UWB SAR) and ground penetrating radar (GPR) with the comprehensive consideration of the electromagnetic scattering mechanisms, the data acquisition system and the image reconstruction algorithms.

Radar imaging is treated from the viewpoint of tomographic inverse scattering. Multistatic data acquisition and the matching reconstruction algorithms are presented to exploit diffraction tomographic techniques into both SAR and GPR imaging. Diffraction tomography has the optimum imaging ability since it is based on the wave equation and takes more scattering mechanisms into consideration. Multistatic illumination and reception can increase the measured information content, especially the low spectrum coverage in the spatial spectral domain which is important for radar to perform penetration imaging.

The application of diffraction tomography to UWB SAR is investigated. The fundamental differences between UWB SAR and conventional narrowband SAR are analyzed from the electromagnetic scattering mechanisms. The theoretical limitation of the point-target imaging in the UWB case is pointed out. The imaging model and the reconstruction algorithm suitable for UWB SAR are discussed.

Similarly, diffraction tomographic technique is applied to GPR imaging. The multistatic configuration is presented to realize the fast and effective data acquisition and the influence of low spatial spectral information which is neglected by the usual collection way is studied.

Theoretical and numerical results validate the feasibility. Some encouraging conclusions are drawn. This research has the important significance and the great potential value for novel imaging radar systems.

Microwave Imaging via Adaptive Beamforming Methods for Breast Cancer Detection

Bin Guo[1], **Yanwei Wang**[1], **Jian Li**[1], **Petre Stoica**[2], **Renbiao Wu**[3]

[1]University of Florida, U.S.A
[2]Uppsala University, Sweden
[3]Civil Aviation University of China, China

Ultra-wideband (UWB) Microwave imaging (MWI) is a promising breast cancer detection technique which can exploit the significant contrast in dieletric properties between normal breast tissue and tumor. Previously, data-independent methods, such as delay-and-sum (DAS) and space-time (ST) beamforming, have been used for microwave imaging. However, the low resolution and the poor interference suppression capability associated with the data-independent methods restrict their use in practice, especially when the noise is high and the backscattered signals are weak. In this paper, we develop three data-adaptive methods for microwave imaging, which are referred to as the robust weighted Capon beamforming (RWCB), singular value decomposition with least squares fitting (SVD-LS), and the maximum likelihood method (MLM). Due to their data-adaptive nature, these methods outperform their data-independent counterparts with improved resolution and lower sidelobes. We compare these algorithms and illustrate their performance by using a complex three dimensional (3-D) breast model with a small embedded tumor. The backscattered signals are simulated by using the finite-difference time-domain (FDTD) method.

Experiment on Artificial Frozen Soil Boundary GPR Detection During Cross-passage Construction in Tunnels

Yong-Hui Zhao, **Xiang-Dong Hu**
Tongji University, China

Guo-Qiang Zhao
Shanghai No.2 Municipal Engineering Co., China

Based on analyzing disadvantage of routine estimate on frozen soil boundary in freezing method construction and comparing the dielectric difference between artificial frozen soils and natural soils, experiment on estimating artificial frozen soils boundary using Ground Penetrating Radar (GPR, EKKO-4) was discussed during the connected aisle construction of Shanghai East Fuxing Road tunnel engineering. For knowing the amplitude and phase features of GPR reflected wave from frozen soils boundary, forward modeling was also developed. The electromagnetic disturbance could be removed form primal GPR profiles using non-linear filtering, and the reflected wave from froze soils boundary would be amplified. By tracing the in-phase reflected wave the boundary could be estimated from GPR profile. The estimated results of frozen soils boundary using GPR were consistent with the temperature field distribution derived from temperature supervising datum. Experimental and modeling results show that GPR can supply a gap of temperature supervising method, such as the less temperature supervising holes and data lost due to some supervising sensors damaged. GPR should be a quickly and effective assistant supervising method for estimating the frozen soils boundary during connected aisle construction in tunnel using freezing method.

Detection of Groundwater by Ground Penetrating Radar

Said I. Elkhetali
The Higher Institute of Electronics, Libya

This paper addresses the application of ground probing radar (GPR) to detection of groundwater from relatively deep aquifers in a desert environment. Tests of signal processing techniques to improve the detectability of a weak signal in noise and interference are reported. The study is based on simulated images from structures that have the potential of storing groundwater. Highly attenuation weak echoes from deeper ground strata are difficult to detect because they are contaminated by noise, interference, filtering (selective attenuation of higher frequencies), direct coupling between antennas and dispersion. All these effects are included in the simulation.

To increase the signal to noise ratio to achieve a reasonable probability of detection and false alarm, various processing schemes are possible, typically employing analogue, binary (double threshold) and digital processing Different system architectures are compared to improve detectability. First impulse and stepped frequency systems were compared. Then there is more emphasis on the stepped frequency and different architectures are compared.

Monograms showing how losses vary as functions of depth and attenuation and how the signal to noise ratio is improved by processing are provided.

The difficulty of detecting a weak signal being reflected from a deep interface in the presence of noise and interference is compounded by electronic components being non-ideal. System effects are studied. A successful detection is obtained when the SNR are adequate to provide an acceptable probability of detection and false alarm. Automatic detection and classification by artificial neural networks is tried to classify geologic subterranean features for aiding and speeding the process and to overcome lack of experts on the field.

Urban Road Network Extraction from Spaceborne SAR Image

Guangzhen Cao, **Yaqiu Jin**
Fudan University, China

A two-step method of road segments detection and linking is developed for automatic extraction of the main road network in dense urban area using *fused data* of infrared Landsat ETM+ and microwave ERS-2 SAR images. In the first step of road segments detection, the edge detector and image classification are combined together. The coefficient of variation detector, as a constant false alarm rate of the edge detector, is first applied to find the potential area, which might contain flat road, river as well as other homogeneous surfaces. Then, image classification based on the back-propagation artificial neuron network and genetic algorithm (BP-ANN/GA) for the fused Landsat ETM+ and SAR images is developed to eliminate most of the non-road surfaces, e.g. river which is morphologically similar to road. Finally, the acceptable segments of roads are detected using the morphological thinning algorithm.

In the second step, the road linking is carried out to the detected road segments. In order to reduce the connection complexity, the road segments are clustered into five classes according to their directions and are connected by the distance and orientation between the endpoints of different segments, respectively. The connection results are synergized together. The main road network is finally obtained after some post-processing depending on the geometrical characteristics of the roads and their relationships, such as continuity, linearity and mutual intersections.

As an example, detection of main road network in Shanghai Pudong area is presented to show our approach as effective and accurate.

Numerical Simulation of Targets Deorientation and Its Application to Unsupervised Classification in Polarimetric SAR Images

Feng Xu, **Ya-Qiu Jin**
Fudan University, China

The advancement of the SIR-C and Radarsat-2 SAR technology has promoted the study of fully polarimetric scattering and applications of information retrievals from polarimetric SAR imagery. Different scatter surfaces might produce similar scattering due to complex scatter size, shape, dielectric and many other properties, and confuse the surface classification.

We present a deorientation theory which transforms the spatially oriented targets into a certain orientation or status, i.e. at the minimum cross polarization. In this system, four parameters Ψ,u,v,w, which have functional dependence upon deorientation, ratios of co-polarized and cross-polarized echoes, are defined, respectively. These functional parameters are adopted to analyze characteristics of the eigen-vectors of the coherence matrix from polarimetric scattering vector. Based on these parameters and the entropy extracted from eigen-values of coherence matrix, an unsupervised classification method for terrain surface is presented.

Numerical simulations of various models, i.e. a layer of random non-spherical scatters as a terrain surface model, are applied to validating this new methodology.

As an example, a SIR-C polarimetric image over China's Guangdong Hui-Yang district is classified by our new method of deorientation and four parameters, which demonstrates the advantage of our approach over the conventional alpha-entropy method.

Session 4A2

Plasmonic Nanophotonics 1: Experimental Research

Light Scattering and Absorption by Plasmonic Resonances of Metallic Nanoparticles

Hiroharu Tamaru[1,2], **Kenjiro Miyano**[1]

[1]The University of Tokyo, Japan
[2]Japan Science and Technology Agency, Japan

Localized surface plasmon polaritons (LSPP) in metal nanoparticles are increasingly gaining attention due to their strong interaction with light. With recent progresses in the area of nanofabrication such as those realized by electron beam lithography, it has become a promising candidate as the key element for room-temperature nanophotonics, and it is of major interest to investigate for an optimal nanostructure that brings out their strong confinement and field enhancement. For this, a means to calculate accurate spectral and spatial behaviors for detailed morphologies is in great demand. In this talk, our current results from a series of experiments, simulations and analytical discussions performed in order to certify each other will be presented.

Finite-difference time-domain (FDTD) calculations with a capability to take the complex dielectric dispersion of silver and gold into account were employed. The scattering spectra for a series of spheres and spheroids were calculated. By comparing the results with an analytical formula derived from Mie theory by expanding the coefficients in terms of the size parameter, a simple practical formula which describes the resonant behavior with respect to their size and morphologies (depolarization factors), is proposed.

Darkfield microspectrometry of individual nanoparticles, together with the results from scanning electron microscopy (SEM) of the same particle, allow us to analyze the LSPP with respect to their morphologies and dimensions. It is seen that even a subtle anisotropy of the morphologies are readily observable in the polarization controlled scattering spectra.

The experimental results are very well explained by these numerical and analytical discussions; the resonance peeks and linewidths calculated from the morphologies observed with SEM reproduces the experimental spectra.

Nevertheless, it is found that scattering phenomena is easier to handle, whereas a more detailed numerical analysis revealed that absorption poses more difficulties for the FDTD method. This is mostly due to the discretization scheme that is necessary for the FDTD method, and our ongoing efforts in this respect will be discussed.

Metal Nano-shelled Three-dimensional Photonic Lattices

Hong-Bo Sun[1,2,3], **Koshiro Kaneko**[1], **Satoshi Kawata**[1,3]

[1]Osaka University, Japan
[2]Jilin University, China
[3]RIKEN, Japan

The progress in molecular structure design/synthesis and in crystal growth has enabled a huge amount of optically functional materials for novel applications on nonlinear optics, optoelectronics and bio-photonics. Nevertheless, some desired performance is all the same neither available in existing materials nor synthesizable. Artificially structured materials become a more and more important solution. A typical example is photonic crystal (PhC), a novel optical material or structure that has periodic distribution of refractive indexes, which could be used to precisely control the light emission and manipulate photon propagation. When metal is used for constructing PhCs or added as a PhC component, one has the concept metallic photonic crystal. Compared with general dielectric PhC, a metallic photonic crystal has been considered as even promising type of devices due to its much wider photonic bandgap arising from cutoff frequency, three-dimensional modulation to surface plasmon wave for novel sub-diffraction-limited nanophotonic devices, and the huge enhancement of nonlinear effects in a PhC cavity.

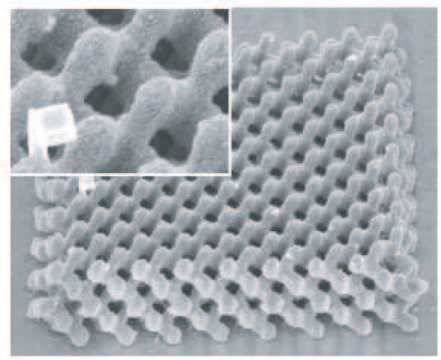

Figure 1: Silver-coated diamond lattice PhC structure. The lattice constant is 2.5 μm (4 layer)

In our research, we fabricated arbitrary-shape three-dimensional PhCs with two-photon photopoly merization-based laser nanofabrication approach. The polymer PhCs are then metal-coated via electroless plating. The method consists of modifying the surface of the polymerized structures with Sn^{2+} ions and then carrying out a redox reaction, wherein the Sn^{2+} ions are oxidized to Sn^{4+} and at the same time Ag^{+} ions are reduced into metallic Ag. The silver stays attached on the polymer surface. The thickness of the coated layer is precisely controllable by adjusting the dipping duration. When it is larger than the skin depth, the coated polymer skeleton behaves like a structured bulk metal. Experimentally it is observed that a broad photonic bandgap opens from a 63-nm-thick silver coated 2.5-μm lattice constant diamond structure PhC [Fig.1] from 2.5 μm to larger than the detection range, 5 μm. Such metal lattices are very promising as 3D plasmonic devices or as high-efficiency light emitter at arbitrary infrared wavelength.

Plasmonic Coupling in Corrugated Metallic Microcavity

H. L. Tam[1], **R. Huber**[2], **K. F. Li**[1], **W. H. Wong**[3], **Y. B. Pun**[3], **J. B. Xia**[1], **K. W. Cheah**[1]

[1]Hong Kong Baptist University, China
[2]Lawrence Berkeley National Laboratory, USA
[3]City University of Hong Kong, China

Coupling of surface plasmon to an internal luminescence source in hexagonal textured metallic microcavity was studied. The texture we used is two-dimensional hexagonal lattice with sub-micron periodicity and the organic green emitter tris(8-quinolinolate) aluminum (Alq_3) was used as the internal luminescence source. The six-fold symmetry of the hexagonal lattice enables more photons within the microcavity to escape through couple with the surface plasmon via Bragg scattering through all the in-plane directions. The optical characteristics of the textured microcavity samples were obtained by angle resolved transmission and photoluminescence measurements. The experiment showed that the transmission through the top corrugated silver layer is enhanced due to the surface plasmon coupling. The extraction enhancement was estimated and found that the textured microcavity have 10% more light extracted than the planar microcavity. In fact at selective direction, the enhancement can be as much as 12 times greater (Fig.1). The dispersion of the emission peak was simulated by scatter matrix method and it agreed with the experimental results. Also, simulation of the surface plasmon modes showed that metal/air interface modes dominate in the coupling. In summary, this work demonstrates that constructive surface plasmon coupling can effectively extract light from microcavity.

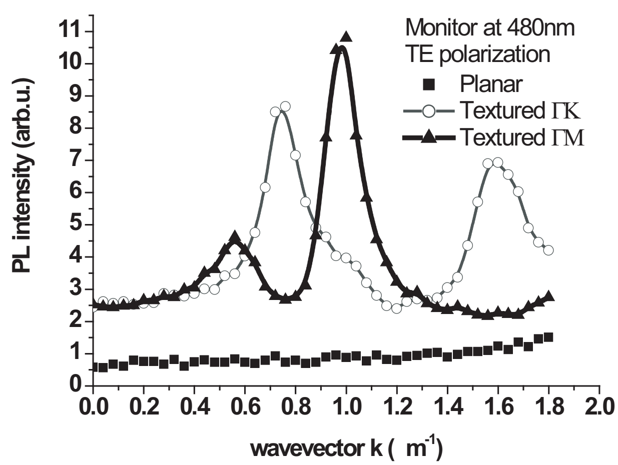

Figure 1: PL intensity at different in-plane wavevector for different samples

Optical Properties of Metal and Metal-semiconductor Hybrid Nanoparticles in Polymer Matrix

Xuan-Ming Duan[1], **Zheng-Bin Sun**[1], **Xi-Ming Xia**[2], **Xian-Zi Dong**[1], **Wei-Qiang Chen**[1]

[1]Technical Institute of Physics and Chemistry, Chinese Academy of Sciences, China
[2]Wuhan University, China

Nanoparticles of metal and semiconductor have been an attractive class of representative nanoscale materials for optical applications due to their unique optical properties. The optical properties of these nanoparticles are sensitively influenced by the environment, including chemicals, temperatures, and so on. Hybrid materials, which are consisted by two or more kinds of materials, usually perform new properties comparing with their original materials. This kind of materials gives us many chances to discover some new properties which could not be observed from non-hybrid materials. One of interesting hybrid nanoscale materials is metal-semiconductor hybrid nanoparticles. In particular, since the optical properties of metal-semiconductor hybrid nanoparticle should be influenced by the plasmonic effect from metal core or shell, the synthesis and evaluation of metal-semiconductor hybrid nanoparticles have become to be critically important. On the other hand, polymer matrix including this kind of hybrid nanoparticles should play an important role in fabrication of two-dimensional and three-dimensional (2D & 3D) structure, which could be fabricated by one-photon or two-photon photopolymerization, for photonic applications, i.e. photonic crystals, optical waveguide, and so on. Using techniques of laser micro/nanofabrication and nanoparticle synthesis, it will become to be possible to fabricate micro/nanoscale photonic devices of polymer including metal-semiconductor hybrid nanoparticles, which could be expected to perform unique properties.

In this paper, we propose a new strategy to fabricate 2D & 3D structures of polymer including metal-semiconductor hybrid nanoparticles. The metal-semiconductor hybrid nanoparticles were directly synthesized in photopolymerized matrix and the optical properties of metal-semiconductor hybrid nanoparticles in polymer matrix were investigated. The details will be reported at the meeting.

A Planar Metallic Collimator Based on Controlling Surface Plasmons's Phase

Pei Wang, **Xiaojin Jiao**, **Ling Tang**, **Douguo Zhang**
Yonghua Lu, **Jianping Xie**, **Hai Ming**
University of Science and Technology of China, China

Surface plasmons (SPs) are waves that propagate along the surface of a conductor. Since T.W.Ebbesen reported the extraordinary optical transmission through a 2D hole array perforated on a metallic film in 1998, many theoretical and experimental works have been made to search the physical explanations, and many potential applications in subwavelength optics are being explored. By altering the structure of a metals surface, the properties of surface plasmons can be tailored, which offers the potential for developing new types of photonic device. The properties of SP devices are intimately linked to the activity and the distribution of SPs on the metal surface.

In this paper, We have performed analysis of optical transmission through the metallic film with very narrow slits and a novel planar metallic collimator is numerical designed by 2D FDTD. The Fabry-Perot-Like phenomenon of SPs resonant transmission has been found through numerical analyzing the influence of the slits depth. The slit depth navigates the transmission peak of the SPs resonant mode, which is consistent with the behavior of the long-range coupled surface plasmons (LRSP, waveguide) mode. The essential different between two modes is due to the different phase change on the aperture of slits, which represents the different light coupled process. The different mode can be used to the different purpose, such as subwavelength photolithography corresponding the SPs mode or polarized beam splitter corresponding the LRSP mode. It is directive and important for many application to give a clear description of the role of the surface plasmons .

Based on each subwavelength slit element transmits light with phase retardation controlled by metal thickness in the aperture region, Metallic lenses with convex-shaped array surfaces structure have been designed. But the fabrication of this structure is not easy. According to our above analysis, utilizing the phase change of SPs propagation on the surface of metallic film, a novel planar metallic collimator is designed. This structure with appropriate space between the slits can collimate the output beam even after 2-3 wavelengths of propagation, which is useful in the applied fields of optical storage, optical coupler et al.

REFERENCES

1. Ebbesen, T. W., H. J. Lezee, H. F. Ghaemi, et.al., *Nature*, Vol. 391, 667, 1998.
2. Yu, Zhaoning, Paru Deshpande, Wei Wu, et.al., *Appl.phys.Lett.*, Vol. 77(7), 927, 2000.
3. Lezec, H. J., A. Degiron, E. Devaux, et.al., *Sceince*, Vol. 297, 820, 2002.
4. Barbes, W. L., A. Dereux and T. W. Ebbesen, *Nature*, Vol. 424, 824, 2003.
5. Pendr, J. B., L. Martin-Moreno, F. J. Garica-Vidal, *Science*, Vol. 305, 847, 2004.
6. Luo, Xiangang and Teruya Ishihara, *Appl. Phys. Lett.*, Vol. 84(23), 4780, 2004.
7. Sun, Zhijun and Hong Koo Kim, *Appl. Phys. Lett.*, Vol. 85(4), 642, 2004.

Design, Fabrication and Characterization of Very Small Aperture Lasers

Jiying Xu, **Jia Wang**, **Qian Tian**
Tsinghua University, China

Fabrication of a very small aperture in an opaque metallic film is one effective method to obtain a near-field nanometric light source. Its integration with a semiconductor laser diode which is called the very small aperture laser (VSAL) is more attractive in various fields such as near-field scanning optical microscopy, near-field optical data storage, nano-photolithography and near-field spectroscopy. The near-field nanometric light source not only should have an ultrahigh resolution light spot in nanometer scale, but also should have sufficient output power for practical applications. We calculate some apertures with different shapes in the metallic film by the method of 3D finite-difference time-domain (FDTD), and present an L-shaped apertures strong field enhancement effect which can compare favorably with C and bow-tie apertures. Based on a commercial edge-emitting semiconductor laser, some very small apertures with different shapes are fabricated in our laboratory. The confined optical field of VSALs is detected by scanning near-field optical microscope (SNOM) with fiber probe. The variation of the emission spot size and the intensity distribution in different distance apart from the aperture are mapped, from which the work distance of VSALs can be determined. The emission patterns of VSALs with different aperture shapes are compared and analyzed. The experimental results indicate that the unconventional apertures such as L-shaped aperture and C-shaped aperture have stronger intensity than the conventional square or circular aperture while the sub-wavelength confined optical field is comparable. In addition, the experimental results will be compared with the numerical simulation results, and the agreement and differences will be analyzed considering the simplification of theoretical simulation and the situation of the practical fabrication. The enhancement mechanism, including local surface plasmon enhancement effect and resonant effect of the metallic film thickness, will be discussed based on the experimental results.

Nanolithography Structure Using Surface Plasmon Interference with a Planar Silver Lens

Xiaojin Jiao, **Pei Wang**, **Douguo Zhang**
Ling Tang, **Hai Ming**, **Jianping Xie**
University of Science and Technology of China, China

The nanolithography technology employing the surface plasmons (SPs) resonant interference has been proposed and the sub-100nm lines were patterned photolithographically in the optical near field excited by a wavelength of 436nm[1]. This technology uses the interference of SPs to generate the high resolution field and need short exposure time because of the near-field enhancement of SPs[2]. But through analyzing the distribution of the output field versus the distance between the lithography structure and the photoresist, we find that the performance of this technology strongly depend on the distance, which limits its applications. On the other hand, Melville has achieved submicron image using a planar silver lens, where the silver lens acted as "perfect lens"[3]. Through imaging with the silver lens, this method does not require the intimate contact between the structure and the photoresit, which means that the limitation of the lithography distance decreases in this process. Base on the works described above, we propose a novel nanolithography scheme, which utilizes the image of the interferential field of SPs through a planar silver lens. The structure is shown in Fig.1. This method can not only generate the high resolution distribution of field, but also reduce the limitation of lithography distance, which is more convenient for practical applications.

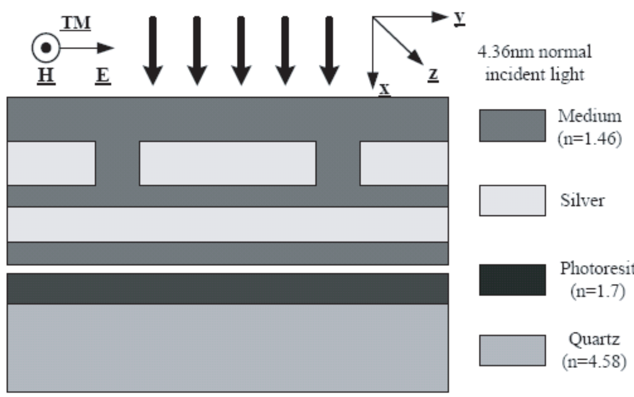

Figure 1: Schematic representation of surface plasmon interference lithography with a planar silver lens.

REFERENCES

1. Luo, Xiangang and Teruya Ishihara, *Appl. Phys. Lett. 84*, 4780, 2004.
2. Luo, Xiangang and Teruya Ishihara, *Opt. Expr. 12*, 3055, 2004.
3. Melville, David O. S., Richard J. Blaikie and Conrad R. Wolfc, *Appl. Phys. Lett. 84*, 4403, 2004.

Session 4A3a

EMC Analysis, Spectrum Efficiency, and Wireless Communication

Planning Future Heterogeneous Wireless Networks

Jijun Luo[1], **Xuemin Huang**[2]

[1]Siemens AG, Germany
[2]LS telcom AG, Germany

In this paper, based on the analyzed emerging challenges encountered by the future radio network, we focus on several candidate techniques targeting at a more spectrum-efficient and cost-effective solution. Among them, spectrum management is one special topic covering fields of technique, regulation and politics. We point out the high tendency of spectrum liberation in terms of spectrum allocation for services and radio technologies even between dierent network providers. In the network planning topic, we address a number of solutions w.r.t. some typical dominating factors. A solution reducing the risk of high expenditure in conjunction with the flexibility of spectrum management is also given. To further enhance the efficiency, advanced radio resource management allowing interworking among heterogeneous radio technologies is also presented.

A New Neural Blind Beamforming Algorithm for Cyclostationary Signals

Hongsheng Li, **You He**, **Rijie Yang**
Naval Aeronautical Engineering Institute, China

Beamforming is another name for spatial filtering where an array of sensors together with appropriate signal processing can either direct or block the radiation or the reception of signals in specified directions. Conventional beamforming approaches require a reference signal or accurate knowledge of the array response vector corresponding to the desired signal. If the array response vector is not known precisely, the performance of conventional beamforming techniques can be severely degraded. For this reason there has been much interest in blind beamforming techniques which do not require a reference signal or knowledge of the array response. In this paper a blind beamforming algorithm based on a neural network is presented according to the cyclostationarity of wireless communication signals. This method transforms the question of estimating beamformer weight vectors into the one of computing the singular value decomposition (SVD) of the cross correlation matrix of the array input signals and their frequency shift signals. A cross correlation neural network is introduced to compute the SVD of the cross correlation matrix so as to reduce the computational complexity and carry out the blind beamforming more efficiently. On the other hand, an improved cross-coupled Hebbian learning rule is presented in this paper based on defining a learning rate by the eigenvalues of the autocorrelation matrix of the input signal and choosing the initial weight values by the orthogonalization. The new learning rule can make the weights of the neural network converge much fast. Moreover, the other advantages of our algorithm are that the neural network performs beamforming without the need of prior information about the directions of arrival or reference signals and can extract and separate the desired signals simultaneously. Simulation proves its correctness.

Improved Iterative Receiver for Turbo Coded G-STBC MIMO-OFDM System

Le Zhang, **Youyun Xu**, **Hanwen Luo**, **Xingzhao Liu**
Shanghai Jiaotong University, China

OFDM is an effective technique for combating multipath fading and for high data rate transmission over wireless channels. COFDM(Coded Orthogonal Frequency Division Multiplexing) has become an important modulation technique in a wide range of digital communication applications. Information theory shows that a multiple-input multiple-output (MIMO) communication system can efficiently increase system capacity in rich scattering wireless channel environment. Turbo processing has been employed in many areas of coding and signal processing to obtain near-optimum performance in a specific wireless communication system.

In this paper, a Turbo coded G-STBC MIMO-OFDM system is described and an iterative receiver design scheme for this system is proposed to realize reliable wireless transmission with high spectral efficiency. A joint soft PIC and instantaneous MMSE filter based soft MIMO demodulation and Turbo decoding is applied to improve the reliability of multiple antenna wireless communication over fading channels. This algorithm is applicable to not only MPSK but also MQAM signal constellations. The effect of different number of groups, different number of subcarriers, different number of transmitter and receiver antennas and Doppler spread on the performance of the algorithm is reported and compared. Simulation results show that significant gains can be achieved over the traditional noniterative receiver both in quasi-static channels and Jakes fading channels and this algorithm is robust to above different parameters. Since max-log-MAP approximation is used to simplify MIMO demodulation, a weighted max-log-MAP algorithm whose optimum weights are calculated based on LLR combining is employed to improve the performance of the system. It is achieved by scaling the a priori information by correction weights at each iteration. Simulation results show that this algorithm has achieved better performance than the max-log-MAP algorithm and approach the optimum MAP algorithm.

Analysis of the Frequency Reuse Efficiency for the Reverse Channel in a DS-CDMA System

Halysson Barbosa Mendonça, **Adaildo Gomes d'Assuncao**
Federal University of Rio Grande do Norte, Brazil

Lately, a great number of cellular mobile systems, including those of the third generation, use the code division multiple access (CDMA) technique, because it usually provides a better system capacity than the other techniques. This higher capacity of a CDMA system is related to the reuse of the same frequency spectrum in all cells.

In a CDMA system all the users have access to the same available bandwidth simultaneously, in such a way that we can say that this system is interference limited. In multicell systems, the received interference in a base station will consist of interferences from mobiles within the same cells and, in addition, of these due to mobiles in the surrounding cells. The frequency reuse efficiency (F) is a measurement of these interferences.

In this work the reverse link capacity of a CDMA system is determined after the calculation of F. The results are achieved from analytic solutions and simulation methods. The frequency reuse efficiency is determined for several propagation conditions, power control errors, and non-uniform cell loading. Besides, the capacity system is also analyzed for sectorized cells. It has been found that, for non-ideal conditions, the system capacity may be reduced.

Usually, the works reported in the literature use a simple exponential law to model the path loss. This exponential law doesn't describe properly the modern cellular system channels. In this work, empirical and theoretical models are used to model the path loss, providing a better accuracy in the determination of the system capacity. The sectorization effect was also investigated by other authors, but only for real pattern antennas. To show how these real antenna patterns modify the CDMA system capacity, the frequency reuse efficiency was also estimated for theoretical pattern antennas, which provide well-behaved radiations pattern. This comparison, helps to show how the capacity of a CDMA system depends of the antenna pattern choice.

Comparative Study of Perfluorinated Polymer and Silica Multimode Fibre System Operating at 850 nm for Local Area Networks

Goffin Andre, **Lethien Christophe**
Royal Military Academy, Belgium

The potentials of perfluorinated polymer based graded index polymer optical fibre (fibre A4g 120/230 PF GIPOF as specified in the IEC69793-2 document) and A1b silica multimode fibres (fibre 62.5/125) intended to be used in wired and wireless LAN have been evaluated. A comparison between both fibres has been made to demonstrate the enormous potentials of PF GIPOF in LAN applications using low COTS transceivers at 850 nm.

The study highlights the differences of both physical layers, in terms of bandwidth, dispersion penalty, BER (Bit Error Rate), EVM (Error Vector Magnitude), IQ constellation analysis and eye pattern when being used in a Gigabit Ethernet transmission or when being used to enhance the coverage of WLAN (Wireless LAN) indoor networks.

Session 4A3b

Antenna Technology for UWB

Dual-polarized Broadband Aperture-coupled Stacked Patch Antenna Array

Wei Wang[1,2], **Shun-Shi Zhong**[2], **Xian-Ling Liang**[2]

[1]East China Research Institute of Electronic Engineering, China
[2]Shanghai University, China

An 8-element dual-polarized slot-coupled microstrip antenna array for X-band application is presented, which obtains a wide bandwidth, high-isolation and low cross polarization. The good characteristics of the array are achieved benefited from several methods adopted in radiating element and feed network design. The stacked patch antenna is used to obtain a wide bandwidth. And the eight-element linear array constructed using the antenna is fed with a corporate-series network, in which the power dividers are simple microstrip T-junctions. For a single patch antenna, the H-shaped coupling slots for the two linear polarizations are arranged in a “T” configuration. This configuration achieves high isolation between the ports because the center slot couples via magnetic field and the edge slot couples via electric field. Furthermore, the two microstrip feed lines terminated in open are constructed in straight and T-shaped forms respectively instead of the conventional bended ones. This makes the feeds symmetric and improves the isolation between ports. The elements are placed so that the center slots are perpendicular and the edge slots parallel to the array. Pairs of elements work together to increase the polarization isolation, in which the edge slots of such pairs of elements are fed by corporate feed network in phase, while the center slots are fed with 180° out of phase. A uniformly excited linear array is designed, fabricated and measured. The measured input impedance bandwidths of the two ports exhibits 20% for return loss less than -10dB. The cross polarization level is at least 25dB below the main lobe level at all frequencies. The isolation between ports is better than 35dB over the whole frequency band. The measured results are in a good agreement with that of calculation, verifying the validity of the design. With the T/R module used, the array is suitable for wide band dual-polarization active phased antenna arrays.

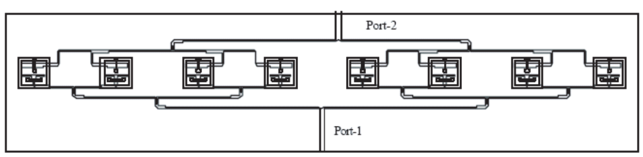

Figure 1: Configuration of the dual-polarized aperture coupled stacked patch antenna array

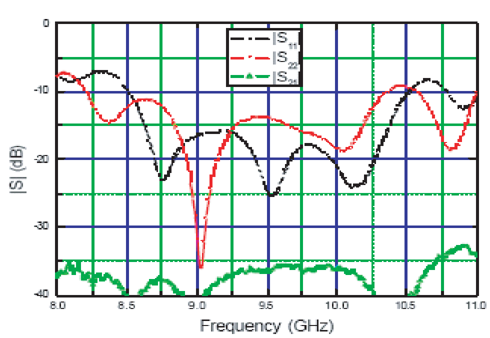

Figure 2: Measured S-parameters of the array

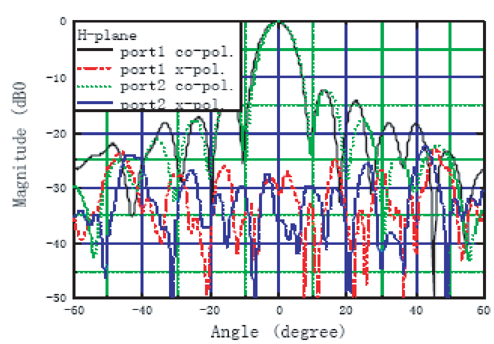

Figure 3: Measured radiation patterns and cross-polarization at 9.5GHz

The Design and Analysis of Wide-Band Dual Polarized Probe Antenna

Yun-Hi Choi, **Jung-Hwan Choi**, **Seong-Ook Park**
Information and Communications University, Korea

The tapered slot antenna (TSA) is very attractive for wide band probe applications with using the optically modulated scatterer. Its potential for wide band and small size makes it a prime candidate for high-performance probe antenna with dual mode operation. The probe antenna with TSA is motivated by the need for a broadband probe for a small antenna measurement. The classical vivaldi antenna is a printed exponential type of TSA. It has been shown to produce a good performance over a broad bandwidth which is usually limited by the feed structure. However, achieving a successful design is usually costly and time consuming since the relationships between antenna parameters and their performance are not well understood. This is especially true for designing dual-mode probe antenna since mutual coupling between the antenna elements is one of significant factors for the isolation of cross-polarization.

This paper presents the design of a dual polarized vivaldi antenna with each associated parameters of the probe sturcture. Finally, the numerical results are presented and compared to those of the experimental results to validate the model.

The probe antenna covers a bandwidth of 1-6 GHz with the structure of two displaced co-located linear polarized elements. Because of the need for accurate and fast measurement of antenna characteristics, it is desirable to have the modulated scatterer and a receiving antenna that can be electronically switched to receive E_ϕ and E_θ. It consists of a slot line with gradually increasing slot width, a bilateral vivaldi antenna element fed by a symmetric stripline, and the dual-mod dipole scatterer with two photodiodes. The element design was optimized by wave guide simulator methods, using the CST software and fabricated. In order to increase the discrimination of the cross-polarization, we will present the simulated and measured results of the notched techniques and receiving probe with an optically modulated scatterer.

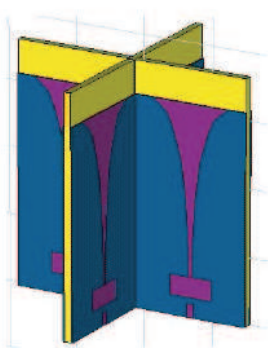

Figure 1: The geometry of the proposed antenna

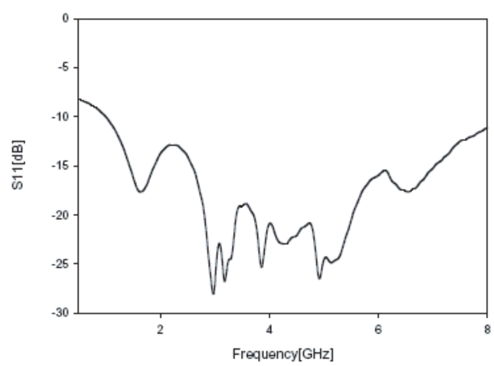

Figure 2: Return loss by the simulation

Interference Suppression in Ultra-wideband Adaptive Array Antennas

Junjie Chen[1], **Ronghong Jin**[1], **Xiaojing Huang**[2]

[1]Shanghai Jiaotong University, China
[2]University of Wollongong, Australia

Ultra-wideband antenna technology has recently attracted both scientific and commercial interests. Due to its specialty in physical profile and signal processing, ultra-wideband antenna differs from the conventional narrowband ones. The design and analysis of ultra-wideband antenna are also great challenges.

An adaptive array antenna points a main beam toward a desired signal, and suppresses interference and noise from other look directions simultaneously. The operation of such an antenna system is controlled by an adaptive signal processing algorithm that is designed to meet specific performance criteria for a desired signal. This concept of adaptive array is also applicable to the emerging ultra-wide band radio communications.

Interferences such as ISI (intersymbol interference) and NBI (narrow band interference) limit the performance of an UWB system significantly. This paper analyzes interference and noise in an UWB antenna array and provides ways to suppress them. As we know, the multipath in wireless channel causes various delays in received signals, which will lead to the ISI in communication systems. Because the delay could be much longer than the chip period in a high-speed UWB system, the spatial signature which is derived for narrowband channel would not be suitable in an UWB channel. Therefore, the effects of signal delays must be considered in the analysis and design of UWB systems. Since ISI must be taken into account, the best weighting vector may not be the same as that used for narrowband system. Suppose that there are an SOI(signal of interest) with DOA(Direction-Of-Arrival) θ and several interferences from different directions among all the signals received by an antenna array. The objective is trying to suppress all the interferences into zero, while keeping the power of SOI unchanged. That is, we want the mainlobe of array pattern aims to θ, whereas the zeros of the array pattern aim to these interferences. Under this condition, we can then calculate the weighting vector. In this paper, several different UWB signals and interferences will be used to test the weighting vector and thus to draw the conclusions. An algorithm to calculate the weighting vector for UWB adaptive antenna will be proposed, and the simulation results of suppressing the interference and noise in UWB system will also be given.

A Conformal Archimedean Spiral Antenna for Ultrawide-band Systems

Qi Wu[1], **Ronghong Jin**[1], **Xiaojing Huang**[2]

[1]Shanghai Jiaotong University, China
[2]University of Wollongong, Australia

Ultrawide-band (UWB) technology has been widely used in various radars, and attracted much attention recently for communication systems. The design of an antenna is one of the most exciting challenging tasks in those systems. For UWB systems, successful signal transmission and reception need minimized of ringing, spreading and distortion. This minimization requires sufficient impedance matching and near constant group delay (linear ungrouped phase) throughout the entire bandwidth. These requirements for UWB antennas make the design process complicated and time-consuming.

This paper will introduce an improved Archimedean Spiral antenna for UWB systems, which can be conformal to a helmet. The Archimedean Spiral antenna is a classic wideband antenna usually backed by a lossy cavity, which is frequency independent and has a suitable operating frequency range. Although the lossy cavity improves the low frequency impedance and axial ratio of the spiral by reducing the reflections from the end of each arm, it will increase the size of the antenna and make it harder to construct or to be conformed to a helmet. Furthermore, in an Archimedean Spiral antenna, the higher frequency components radiate first, followed by the lower ones. The mechanism causes frequency dispersion. This dispersion affects the impulse signals and cause a chirp duration, which makes it unacceptable for UWB applications. To overcome these shortcomings, an Archimedean Spiral without the lossy cavity is presented in the paper. A high gain of this Archimedean Spiral is also obtained. The structure of the antenna is improved and some capacitors are added to the antenna. These capacitors are critical to improve the performance of a Spiral antenna; especially it could get rid of the frequency dispersion. The important parameters of this improved antenna such as the inner radius, width of each arm, spacing between each turn and position of capacitors are optimized by using Genetic Algorithm (GA). The radiation pattern of this improved Archimedean Spiral antenna has been simulated and the VSWR has also been measured. The results show that this antenna with improved structure performs well and has suitable parameters for UWB systems. The frequency dispersion is also been gotten rid of. Furthermore, this improved Spiral antenna can be conformal to a helmet, so we can forecast that it has a good perspective in future wireless communications.

A Conformal Vivaldi Array Antenna for Ultrawide-Band Aystems

Qi Wu[1], **Ronghong Jin**[1], **Xiaojing Huang**[2]

[1]Shanghai Jiaotong University, China
[2]University of Wollongong, Australia

The Federal Communications Commission (FCC) has allocated the 3.1-10.6 GHz frequency spectrum for ultra wideband applications, which has presented a myriad of exciting opportunities and challenges. For UWB systems, successful signal transmission and reception need minimized ringing, spreading and distortion. This minimization requires sufficient impedance matching and near constant group delay (linear ungrouped phase) throughout the entire bandwidth. These requirements for UWB antennas make the design process complicated and time-consuming.

This paper will introduce an omni-directional Vivaldi array for UWB systems, which can be conformal to a helmet. Vivaldi is a slow-wave, leaky, end-fire and traveling-wave antenna. Theoretically, the Vivaldi antenna has an unlimited bandwidth, with constant beamwidth over the entire bandwidth. Therefore, the Vivaldi antenna is a good choice for UWB systems. However, in practical applications, the bandwidth of a Vivaldi antenna is mainly limited by the feeding arrangement, and its dimension also should be taken into account. Usually a Vivaldi antenna is excited by a slot line. Thus feeding a Vivaldi requires a transition between slotline and the microstrip line. Thus a microstrip line is an unbalanced line and slot line is a balanced line, feeding a Vivaldi needs a balanced to unbalanced transition (balun) to avoid compromising the antenna's performance. For UWB use, the feeding part needs small parasitic inductance and capacitance over the whole bandwidth. So we choose the double-Y balun to do this job because it has no inherent bandwidth limitation. Another problem is that a single Vivaldi antenna can't achieve omni-directional transmission, so a Vivaldi array is needed here. This array is made up of eight Vivaldi elements that are allocated uniformly on the surface of a helmet. Each element is identical, which has been optimized by using HFSS. The radiation pattern of this omni-directional Vivaldi array has been simulated and the VSWR has also been measured. The results show that this array performs well and has suitable parameters for UWB systems. Furthermore, this array can be conformal to a helmet, so we can forecast that it has a good perspective in future wireless communications.

The Characteristic of Sleeve Antenna

Jian-Ying Li, **Yeow Beng Gan**
National University of Singapore, Singapore

Sleeve antenna has many advantages, such as mechanical simplicity, broadband, and omnidirectional radiation in horizontal plane, etc. It is widely used in mobile communication systems and broadcast systems. In the past decades, many papers have been published on the analysis of the sleeve antenna. The main work in this paper focuses on the VSWR performance of normal sleeve antenna and open-sleeve antenna.

For the normal sleeve antenna (Fig. 1a), it is obvious that each VSWR curve has basically three null frequencies (Fig. 2). If the length of the driven dipole L_1 is $0.5\lambda_0$ at f_0, the first frequency is almost f_0, the third frequency is slightly above $2.88f_0$ for the case $L_3 = 0$. The effects of the sleeve on f_1 and f_3 are very small. The driven dipole has minimal impact on f_2. However, the second null frequency f_2 changes for different types of sleeve antenna. The wavelength at f_2 is related to the length of the sleeve L_2 and the distance R, and lies between f_0 and $2.88f_0$. Sleeve antenna with broad bandwidth can be easily designed by adjusting L_2, R and a. It is shown when the height L_2 is increased, the second resonance frequency f_2 shifts to lower band. Conversely, shorter L_2 shifts f_2 to the higher band.

For the case of $L_3 \neq 0$, characteristics similar to the case of $L_3 = 0$, ie. with three null regions, are observed. The first null region remains near f_0, but the third null region shifts to $2.77f_0$ for L_3 between $0.01\lambda_0$ and $0.02\lambda_0$. The bandwidth is therefore reduced. At the same time, f_2 shifts to lower frequency. The VSWR is obviously improved for $L_3 \neq 0$.

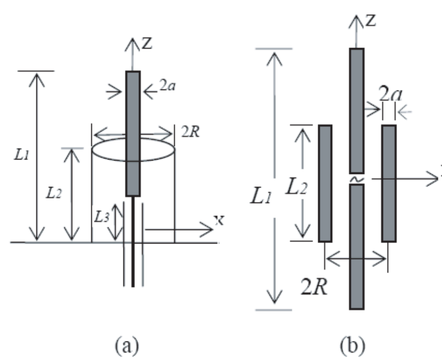

Figure 1: The structure of the sleeve antenna

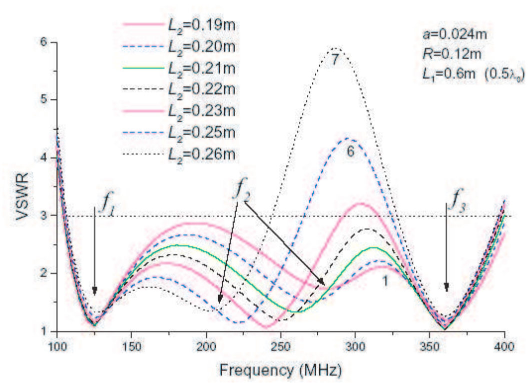

Figure 2: VSWR of the sleeve antenna

Numerical results showed that the open sleeve antenna (Fig. 1b) also has three null regions. If the length of driven dipole is $0.45\lambda_0$ (wavelength at f_0), the first frequency would correspond to f_0, and the third frequency is just above $3f_0$. The frequency f_2 is changed for different types of open sleeve antennas. This frequency is due to the length of the sleeve L_2 and the distance R, and lies between f_0 and $3f_0$. By choosing appropriate values of L_2, R and a, open sleeve dipoles with good broadband performance can be easily designed.

Session 4A4

Nanostructures and Systems

Scattering Properties in Quantum Waveguide for Nanoelectronic Devices

Yupeng Chen, **Thomas X. Wu**
University of Central Florida, USA

It is well known that quantum mechanical effects restrict further scaling of semiconductor devices below 50 nm [1]. The miniaturization trend of electronic devices following Moores law will cease without novel devices. Consequently, there have been a lot of research efforts to investigate novel quantum devices [1], which have the potential to operate at ultra-high speed and high chip density under the dimensions of nanometer level (hence Nanoelectronics). Quantum waveguide is a nano-structure in which the electron wave is locally trapped and is guided along an arbitrary direction and is expected to be an important building block of the next generation electronics [1-3]. The wavelike behavior is dominant in nano-devices so that the transport of electrons through the heterostructure device is analogous to the propagation of electromagnetic waves in dielectric waveguides. As a result, advanced numerical microwave techniques have been applied to quantum waveguide modeling [2-3]. Transport and scattering properties of quantum waveguide are important because not only they can determine the conductance of the device but also they are useful to investigate discontinuity for quantum interface. Based on our pervious research [2-5], a further study of scattering properties in novel quantum waveguide structures will be presented. In this paper, theoretical equations governing the electron wave in the device are introduced at first. Rigorous mode matching method based on microwave transmission line theory is presented to model the step discontinuities in terms of the boundary conditions. Then finite element method (FEM) formulism is given in detail to solve system model numerically. Finally, numerical results are displayed to explain the underlying physics of the structures.

REFERENCES

1. *Technology Road Map for Nanoelectronics, European Commission IST programme Future and Emerging Technologies*, 2000.
2. Chen, Y. and T. X. Wu, "Modeling of Electron Waveguide for Nanoelectronic Devices", *(invited) The 8th World Multi-Conference on Systemics, Cybernetics and Informatics*, 2004.
3. Chen, Y. and T. X. Wu, "Numerical Modleing of Quantum Waveguide Device", *(invited) The 7th International Conference on Solid-State and Integrated-Circuit Technology*, 2004.
4. Wu, T. X. and D. L. Jaggard, "Scattering of Chiral Periodic Structure", *IEEE Trans. on Antennas and Propagation*, Vol. 52, No. 7, 1859, 2004.
5. Yang, X. and T. X. Wu, "Physical Properties of Wave Scattering by a Chiral Grating", *Journal of Optical Society of America A*, Vol. 21, No. 11, 2109, 2004.

Electromagnetics Properties of Nanocomposites Powder Compacts

Philippe Talbot, **Christian Brosseau**
Université de Bretagne Occidentale, France

One of the most fascinating purposes of nanotechnology is to accomplish the local modification of material properties on the nanometer scale. The resulting physics is remarkably complex and multifaceted. In the search for magneto-dielectric nanostructured systems, a tempting strategy is to use nanomaterials produced by the compacting of powders. Here, the materials considered were dispersions of ferro-and ferrimagnetic nanoparticles into otherwise nonmagnetic particles. The electromagnetic response at microwave frequencies, of cold-pressed powder compacts made of Ni, $\gamma - Fe_2O_3$, Co, and ZnO nanosized powders, have been investigated using frequency domain network analysis. The effective complex permittivities and permeabilities of magnetic/nonmagnetic composites were studied over a broad frequency range (0.1 -10 GHz) as a function of composition. Within this frequency range of measurement the real and imaginary parts of the effective permitivity of nanocomposites exhibit spectra which can be analytically well represented by power laws. The associated Jonscher exponents, which are similar for the real and imaginary parts of the permittivity, are in the range 0.05-0.20 in agreement with data in the published literature. The dependences of the effective permittivity versus composition are compared to those obtained from the effective medium theory of Bruggeman and found to be not adequate for all nanocomposites studied. Results show also that the nanocomposite samples display a prominent gyromagnetic resonance in the GHz region of frequency which can have a more or less complex structuration. Interestingly, the Ni/$\gamma - Fe_2O_3$ nanocomposites exhibit a composition dependence of the effective permeability which is quite different from the Co/ZnO, Ni/ZnO and $\gamma - Fe_2O_3$/ZnO nanocomposites. From the microwave data collected, it is found that a mean-field approach (effective medium approximation) is appropriate for understanding the permeability of composite materials characterized by submicrometer inclusion length scales. The relevance of the Bruggeman and McLachlan models are tested against experimental data over a large range of composition. From these comparisons, although there are some systematic discrepancies to a certain extent, we conclude that the overall agreement of the spectral dependence of the complex permeability of Ni nanocomposites with the Landau-Lifshitz-Gilbert prediction is fairly good in view of the simple asssumption. It seems that this phenomenology is also applicable to Co nanocomposites by assuming a double Lorentzian form for the gyromagnetic resonance. Analysis of the gyroresonance linewidths strongly suggests a large dispersion in the local field which presumably reflects the disordered physical nanostructure.

Magnetization Curve Characteristic Changes of Nano-Magnetic Structures in Irradiated Thin Films

D. Bajalan
Vienna University of Technology, Austria

Determining the properties of nano-magnetic structures is extremely important for the development of data storage devices that contains these nano-magnetic shapes and structures[1,2]. It is an interesting task for micromagnetic modeling to find a relation between particle shape and magnetization direction. Different loops have been identified due to angel variation of the applied magnetizating field (φ is the angle between H and M or the direction of magnetization field). In perpendicular recording from the point of view of transition demagnetization it could be true that: the ultimate recording density for perpendicular recording is therefore not limited by the transition self-demagnetizing effect. The total demagnetizing factor is important for calculations. One of the serious problems in conventional magnetic recording media is this superparamagnetic [3] limit when making the grain volume smaller. Thermal stability is one of the main issues for developing high density recording and thus much effort has been made to overcome this problem.

REFERENCES

1. Bajalan, D., H. Hauser, P. L. Fulmek, "Magnetic Nanostructure in Thin Film Multi-Layer", *Progress in Electromagnetic Research Symposium*, 667, 2004.
2. Bajalan, D., H. Hauser, P. L. Fulmek, "Modeling of the ion irradiation effect on the nanostructured thin", *Physical B*, Vol. 343, 384, 2004.
3. Bajalan, D., H. Hauser, P. L. Fulmek, "Calculations of Magnetic Nanostructure Hysteresis Loops for Modified Thin by Ion Irradiation", *Progress in Electromagnetic Research Symposium*, 468, 2004.

First-Principles Calculation of Electrical Forces among Nanospheres in a Uniform Applied Electric Field

Xiangting Li
Tel Aviv University, Israel

David J. Bergman
Tel Aviv University, Israel

David G. Stroud
The Ohio State University, USA

We present a unified framework for a first-principles calculation of the electric force acting on dielectric or metallic nanospheres suspended in a dielectric host and subject to a uniform external electric field. The calculation is based on the spectral representation of the local electric field in a composite medium. The result is an explicit expression for the force acting on any sphere, which can be used for arbitrary configurations of nanosphere clusters with arbitrary (i.e., non-equal) sphere radii. Even when the spheres are metallic (the dielectric permittivity is then infinite) no infinities appear, and the resulting expression is even simpler then.

The expressions obtained are not limited to dilute collections of spheres—they are valid even when the gaps between neighboring spheres are much smaller than their radii. Therefore the forces are not limited to dipolar forces. Moreover, the force acting on any sphere is not a simple sum of two-body forces: When the inter-sphere gaps are small, complicated many-body forces appear. This is due to the fact that, when a sphere center is displaced slightly, the electric polarization of all the other spheres is changed. Consequently, the total electrical energy is changed in a way that cannot be represented as a sum of two-body energy changes.

Explicit calculations of these forces for a few selected sphere clusters are presented and discussed. The results are quite different from what is obtained in the dipole approximation. We also calculated the forces acting on spheres in these clusters when, instead of applying an external electric field, the cluster is in one of its quasi-static eigenstates (these are the so-called "surface plasmon resonances").

A Novel Lane Detection Algorithm Based on Support Vector Machine

Hao Zhang, **Dibo Hou**, **Zekui Zhou**
Zhejiang University, China

In this paper a novel lane detection algorithm for horizontal shape recognition based on support vector machine (SVM) was proposed. In the last few decades, problems concerning traffic efficiency, safety and energy consumption have become more serious in most developed counties. So research on intelligent vehicles and intelligent transportation systems (ITS) has come in for a great deal of attention worldwide. Lane detection is a basic and important research task because it is a prerequisite for automatic pilot in the intelligent vehicles system project. The so called lane detection of intelligent vehicles is defined as a process of analyzing images obtained by vehicle-mounted camera to obtain meaningful information such as relative position of vehicle, road marking, road boundaries, direction of vehicle's heading and the vehicle's deviation angle. The acquired data was used to support road keeping of intelligent vehicle. The main steps for road horizontal shape recognition, which is divided into straight, curve, curve-in, curve-out four models relating to the vehicle control action, was as follows: transforming a monochromatic image from an original image to a bird-eye view image, image enhancement to eliminate noise and distinguish lane marking, image edge detection for lane marking, getting edge support points (ESP) which can represent lane marking edge using less points, regress the edge support points by support vector machine. Relative to traditional lane detection which acquiring less information through images directly, the algorithm can describe almost all kinds of lane model by function expression through which we can extract all kinds of road characters indirectly and conveniently by mathematical methods, then automatic pilot of intelligent vehicles will be supported better. Experiments on real images show the algorithm can complete the lane detection faster and more precisely relative to laser-based sensors and millimeter-wave radar which classified as active sensors. Experimental results also show the vision-based passive sensor has an advantage that it acquires data in a noninvasive mode and will not alter the environment.

Matrix Converter Control System

Jiri Lettl, **Stanislav Fligl**
Czech Technical University in Prague, Czech Republic

The presented paper deals with the designed concept of the matrix converter control system employed in the hybrid traction drive with electric power splitting.

Matrix converters provide an all-silicon solution to the problem of converting AC power from one frequency to another, offering almost all the features required of an ideal static frequency changer. They possess many advantages compared to the conventional voltage or current source inverters. A matrix converter does not require energy storage components as a bulky capacitor or an inductance in the DC-link. It enables the bi-directional power flow between the power supply and load. The most of the contemporary modulation strategies are able to provide practically sinusoidal waveforms of the input and output currents with negligible low order harmonics, and to control the input displacement factor. The solution is advantageous especially with regard to the above mentioned reactive component reduction.

The special “Host PC - Target PC” digital control system was developed for the realised experimental test bed. The matter consists in the processor throughput. While in case of the digital signal processors it can be as far as 100 MIPS at 16 bit DSP with fixed point, 200 MIPS at 32 bit DSP with fixed point, 20-200 MIPS/MFLOPS at DSP with floating point only, in case of processors for PC it can reach e.g. 9000 MIPS and 2600 MFLOPS.

The basis of the control system consists of two common personal computers. The first one (Host PC) should be equipped with any multitasking operating system and the MatLab programme must be installed on this PC. It serves for compiling of the target real-time applications and for monitoring purposes only, such as downloading and displaying of measured waveforms, commands entry, etc. One serial port of the RS232 standard and one parallel port enabling operation in the ECP mode are inevitable. The second one (Target PC) works in real time and the matrix converter control programme is processed on it only. The most important component of this PC is the Multi I/O PCI card Meilhaus ME-2600i containing A/D and D/A converters and digital inputs and outputs. All the signals are reprocessed and adjusted in interface cards situated in the control rack. Here is also placed the IGBT’s switch pulses generating card based on a FPGA device. To make the work easy, the firmware for the Target PC and the monitoring programme for the Host PC were prepared. The firmware consists of the libraries set programmed in the ASSEMBLER and C language enabling faster algorithm implementation and testing. It has the real-time kernel with 50 - 200 microseconds period and contains synchronisation, communication, and I/O card specific routines. The monitoring programme consists of the set of the mutually communicating programmes programmed in the MatLab, JAVA, and C languages. However, from the user sight it seems to be one application only. This software is very important for easy control application developing.

The matrix converter realised on the base of new progressive semiconductor elements (IGBT’s modules) is used to treat the electrically transmitted power part of the hybrid traction drive with electric power splitting. The electrical torque split device consists of a special electric generator with both stator and rotor rotating. The rotor is connected to internal combustion engine and its torque is via air gap electromagnetic forces transmitted to the stator. The torque and the output shaft angular speed constitute the mechanically transmitted power. The remaining part of the internal combustion engine power is transformed into the electric power and represents the input power of electrical transmission.

The developed matrix converter control hardware and software makes it possible to achieve greater throughput of the digital control system and its variability. The results obtained on the built-up experimental test bed have proved proper function of the designed conception of the matrix converter control system.

Advanced Modeling Technology of RF SAW Packages

Hao Dong, **Thomas X. Wu**
University of Central Florida, USA

In the RF section of cellular phones, electronic packaging has become an important integral part of device design as the requirements of the market are trending toward smaller size and higher frequency of operation. Package parasitics plays a significant and increasing role in determining the total device performance. In the past few years, ceramic duplexers have been replaced by smaller and less expensive SAW duplexers. This size reduction requires extensive EM modeling tools for characterizing the performance of the SAW packages.

In our research, we have developed a comprehensive methodology for the analysis and design of SAW filter and duplexer package. Ansoft High Frequency Structure Simulator (HFSS), based on the finite element method (FEM), is used for the characterization of the duplexer package, die busbars, bonding wires and PCB. The die acoustics model is obtained using the Coupling-of-Modes (COM) techniques. This method can take into account of the mutual coupling among the package, die busbars, bonding wires, PCB and give us the accurate model. An excellent agreement between the simulation and measurement can be found.

Small insertion loss and high isolation in stop band are very important specifications in the SAW filter and duplexer package design. Based on our methodology, four novel methods, (1) cut on the inner ground plane; (2) new bonding wire scheme; (3) Adding vias between the ground bonding pad and inner ground plane; (4) adding vias between the inner ground plane and PCB ground, are proposed to significantly improve the isolation for the KPCS duplexer package [1]. For the flip chip package, we redesign the package and optimize the die, 10 dB improvement of the isolation is achieved.

Our methodology is effectiveness and can be applied to various RF SAW device packages. It reduces the design cycle time significantly.

REFERENCES

1. Dong, H., T. X. Wu, K. S. Cheema, B. P. Abbott, C. A. Finch and H. Foo, "Design of miniaturized RF SAW duplexer package", *IEEE Trans. Ultrason., Ferroelect., Freq. Contr.*, vol. 51, no. 7, 849, 2004.

Modeling the Effects of Randomly Rough Surface of Conductors on Wave Propagation in Interconnects in the GHz Range

Xiaoxiong Gu[1], **Leung Tsang**[1], **Henning Braunisch**[2]

[1]University of Washington, U.S.A
[2]Intel Corporation, Components Research, U.S.A

A method for modeling the impact of randomly rough conductor surface on the propagation loss of high-speed interconnects is presented. The roughness of the interface, especially in microelectronic packaging based on organic materials, is often used to facilitate the adherence of the copper structures to the dielectric layers. Since the speed of interconnects is rapidly increasing to the multi-GHz region, the propagation and radiation at the shorter wavelength can cause the roughness of the surface to have significant effects on signal integrity. Existing commercial software tools do not allow users to model the surface roughness of the substrates accurately. There only exist simple empirical models with limited or unknown validity.

We model a planar waveguide structure with two metal layers on both sides and a dielectric layer in between. The interface between the dielectric and the metal is randomly rough. When excited by a magnetic line source, the guiding structure supports TM wave propagation. The layered medium Green's function is that of a dielectric layer sandwiched between two metallic layers with flat interfaces, where the impedance boundary condition (IBC) is used. We use this layered medium Green's function to formulate a surface integral equation for the case when the interface between the dielectric layer and the metallic layer is randomly rough. The propagation loss of the waveguide is quantified through the development of the solution of electromagnetic fields and surface currents on the rough dielectric-metal interface. The analysis leads to the extraction of frequency-dependent power attenuation for each given metal roughness profile.

We demonstrate the method for random Gaussian rough surfaces. Results are illustrated for the frequencies of interest that extend up to 30 GHz. Statistical results are further obtained from Monte-Carlo simulations. The roughness profiles are up to 4 microns in RMS height with correlation lengths 1 to 3 times the RMS heights. We also use a fast matrix solver to solve the integral equations for cases with a large number of surface unknowns.

Design of Microwave Chaotic Colpitts Oscillator Module with a 25 GHz Bipolar Junction Transistor

Zhiguo Shi, **Lixin Ran**
Zhejiang University, China

Chaotic Colpitts oscillators with fundamental frequency f^* beyond 1 GHz were studied by circuit experiment using Philips' broadband transistor with threshold frequency of 25GHz. A chaotic oscillator module, which will output chaotic signal in microwave band without tuning any circuit parameters when the power supplies switch on, was implemented. For the basic configuration of Colpitts circuit with f^* of about 1.6GHz, broadband continuous power spectrum could be obtained from this module. The harmonics of the observed signal from Agilent PSA/ESA Spectrum Analyzer are noticeable as far as 12GHz, which is the highest one reported till now.

Figure 1 shows the prototype board of the chaotic oscillator module. The core chips in the prototype is the two BFG425w, one of which is for oscillation generation and the other one is for output signal buffering. The power supplies to this module are one +15V and one -15V voltage sources. Chaotic signal can be outputted via two different SMA interfaces or one two-header interface.

Figure 2 shows the output signal spectrum of this module when the power supplies switch on. Continuous power spectrum indicates that chaotic oscillation has been established in this module. The fundamental frequency marked in Figure 2 is about 1.6 GHz, and the harmonics are noticeable as far as about 12 GHz.

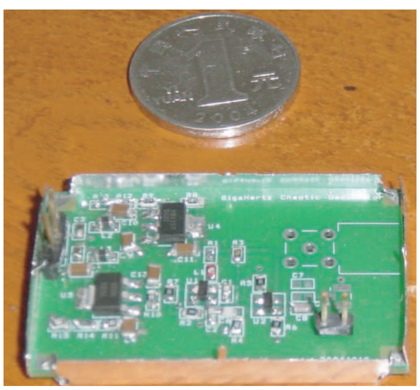

Figure 1: Chaotic Colpitts oscillator module.

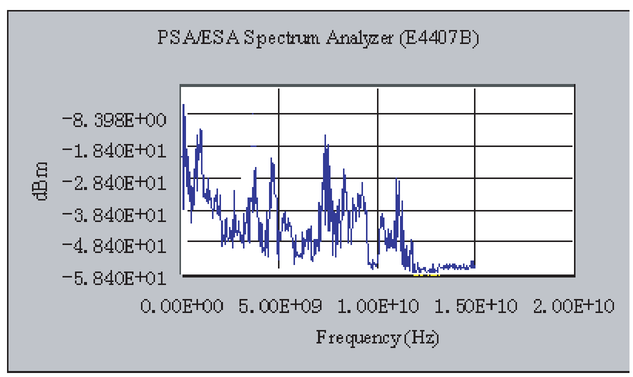

Figure 2: Output chaotic signal spectrum.

Session 4A5a

Electromagnetic Theory 1

Fourier Transformation and Boundary Conditions in the Special Domain

Jan Zehentner, **Jan Mrkvica**, **Jan Machac**
Czech Technical University, Czech Republic

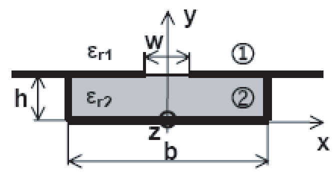

Figure 1: Cross-section of the guide

The method for separating variables in the plane transversal to the field propagation on planar transmission lines is very often not usable. The Fourier transform into the spectral domain provides a solution resulting in the wave equation, where the searched quantity depends only on one variable. Boundary conditions are auxiliary equations enabling the integral and separation constants to be determined. They cannot be formulated easily and clearly, particularly when radiation from the bound region to the boundless region is investigated.

Calculating the propagation constant of a leaky wave propagating in the rectangular waveguide with a longitudinal slot cut in the middle of its wider wall, Fig.1, demonstrates the approach to this problem.

Let $\Psi(x, y)$ represent some strength or potential of the field. Then the Fourier integral fransform is used in the 1st region, and in the x-direction

$$\tilde{\Psi}_1(\xi, y) = \int_{-\infty}^{\infty} \Psi_1(x, y) e^{-j\xi x} dx \tag{1}$$

while in the 2nd region the Fourier finite interval transform is applicable

$$\tilde{\Psi}_2(\xi_n, y) = \frac{2}{b} \int_{-b/2}^{b/2} \Psi_2(x, y) e^{-j\xi_n x} dx \qquad \xi_n = \begin{cases} 2n\pi/b & \text{even modes} \\ (2n-1)\pi/b & \text{odds modes} \end{cases} \tag{2}$$

The distribution of the field in the space domain is obtained by the backward transform. Imposing boundary conditions in the plane y=h transformed to the spectral domain requires, e.g., continuity of the tangential electric field components in the slot $E_{x1}(x, h) = E_{x2}(x, h)$. Of course, $\tilde{E}_{x1}(\xi, h) \neq \tilde{E}_{x2}(\xi_n, h)$ where $\tilde{E}_{x1}(\xi, h), \tilde{E}_{x2}(\xi_n, h)$ are expressed in terms of basis functions. Let us consider $E_{x2}(x, h)$ as the finite function $E_{x2f}(x, h)$ when $|x| \leq b/2$ and $E_{x2f}(x, h)$ equals zero for $|x| > b/2$. After a short manipulation

$$\tilde{E}_{x1}(\xi, h) = \frac{b}{2} \sum_{n=-\infty}^{\infty} \tilde{E}_{x2}(\xi_n, h) \cdot Sa[\frac{b}{2}(\xi - \xi_n)] \tag{3}$$

where the sampling function

$$Sa[\frac{b}{2}(\xi - \xi_n)] = \frac{\sin[\frac{b}{2}(\xi - \xi_n)]}{\frac{b}{2}(\xi - \xi_n)} \tag{4}$$

Parseval's theorem enables current density on the metallization to be eliminated from the boundary conditions. In the end, the standard Galerkin procedure and a complex root search is applied in order to find the propagation constant of the mode.

*This work has been supported by the Grant Agency of the Czech Republic under project 102/03/0449 "New circuit devices for communication technology".

Axisymmetric Spherical Travelling Electromagnetic Waves in Isotropic Medium

Yuri A. Zyurykin
Saratov State Technical University, Russia

Mariya V. Pavlova
Saratov State Technical University, Russia

The scientific interest to the models of spherical electromagnetic waves arises in the theory of radio-wave propagation, in the analysis of UHF spherical resonators, in optics, in problems of lasers initiation of an thermonuclear synthetic reaction, etc. The conventional and established today essence of the theory for spherical electromagnetic waves is represented by a relatively small number of works published at the end of 40-th and at the beginning of 50-th previous century. However in these works the theory was founded on a little bit formal solution of the Helmholtz's equations relative to components of Hertz's vector, and solution are expressed through transcendental functions and insufficiently detailed. These functions describe as rule the standing spherical waves, and among theirs multitude are selected these that have not peculiarities in centre as infinity. The functions that describe travelling spherical waves was not analyzed in detail because of the same infinity in centre take place. What is more there is opinion that the converging spherical waves have not physical meaning that is they are not existing though the diverging spherical waves are supposed existing as an radiation from the point source (for example from Hertz's dipole).

The aim of present works is the consideration of the propagate problem for travelling spherical electromagnetic waves and, in particularity, for converging waves. Converging and diverging spherical waves are considered here as independent ones and both existing, and then they are represented as transformation the first one in the another at transiting converging waves through the centre. The analytical expressions, defining components travelling spherical E- and H-waves, and also equations of lines of force for various modes are obtained. The numerical solution of these equation has allowed to calculate and to present graphically pictures of lines of force for travelling spherical waves in time current. Thus it is shown how the converging wave transforms into the diverging wave at the transit of first one through free centre. The all consideration is realized in axisymmetric assumption.

Electromagnetic Field Generated by a Horizontal Electric Dipole in a Spherical Earth Covered by N-Layered Dielectrics

Kai Li
Zhejiang University, China

Yilong Lu
Nanyang Technological University, Singapore

The problem of the electromagnetic (EM) field from a dipole source located on or near the surface of the spherical earth has been a subject of interest for many years. The early classic harmonic-series solution for a dipole in the presence of a homogeneous sphere was begun by Watson. The subsequent further developments were made by other pioneers, such as Van del Pol, Fock, Bremmer, Norton, and Wait. Despite the remarkable progress that had already been made on this problem, some aspects of it remained in the dark. The problem was recently reexamined by Houdzoumis and Margetis. The exact formulas are obtained for the complete EM field on the surface of the spherical earth when vertical and horizontal electric dipoles are located on that surface.

When the spherical earth is covered with layered dielectrics, the derivations of the EM field radiated by a dipole source are in general much more complicated. Recently, the complete explicit formulas have been derived for the EM field of a dipole source over the spherical conducting or electrically earth coated with a dielectric layer. Furthermore, the general case of the EM field radiated by a dipole source near the surface of the spherical earth coated with N-layered dielectrics has been treated.

In what follows, we will attempt to determine the EM field from a horizontal electric dipole located in the spherical electrically earth. The starting point is based on the formulas for the EM fields in air due to vertical electric and magnetic dipoles situated in air above the surface of the earth coated with N-layered dielectrics. By using boundary conditions, the formulas of the EM fields in the earth due to vertical electric and magnetic dipoles located in air are derived readily. Based on the above results, using the reciprocity theorem, the formulas are obtained for the six components of the EM field from a horizontal electric dipole located in the earth. To illustrate the applications of the formulas obtained, computations are carried out when the layered dielectrics are composed of successive 2 spherically bounded layers, each with the thickness $l/2$.

Electromagnetic Scattering from an Anisotropic Uniaxial-coated Conducting Sphere

You-Lin Geng[1,2], **Xin-Bao Wu**[3], **Bo-Ran Guan**[2]

[1] Xidian University, China
[2] Hangzhou Dianzi University, China
[3] Shanghai Research Institute of Microwave Technology, China

Scattering fields from an anisotropic uniaxial-coated conducting sphere by a plane wave are derived. The electromagnetic fields in uniaxial anisotropic medium and free space can be expressed in terms of spherical vector wave function in uniaxial anisotropic media and in an isotropic medium. Applying the continue boundary condition in the interface between the uniaxial anisotropic medium and free space, and tangential part of electric field vanishing in the surface of the conducting sphere, the expansion coefficients of electromagnetic fields in uniaxial anisotropic medium and that of scattering fields in free space are obtained. Numerical results between this method and Mie theory are in good agreement as we expect. Some numerical results are obtained in this paper.

*This work is partially supported through No. Y104539 by the Natural Science of Zhejiang Province of China and a Research Grant No. 60071025 by the National Natural Science Foundation of China (NSFC).

REFERENCES

1. Sheng, X. Q., J. M. Jin, J. M. Song, C. C. Lu and W. C. Chew, "On the Formulation of Hybrid Finite-Element and Boundary-integral Methods for 3-D Scattering", *IEEE Trans.*, Vol. AP-46, No. 3, 303, 1998.
2. Geng, Y. L., X. B. Wu, L. W. Li and B. R. Guan, "Mie scattering by a uniaxial anisotropic sphere", *Physical Review E*, Vol. 70, No. 5, 056609/1-8, 2004.

Losses in Frequency Selective Surfaces

Maurizio Bozzi, **Luca Perregrini**
University of Pavia, Italy

Frequency selective surfaces (FSS) are planar periodic structures, widely used as filters from the microwave to the infrared region [1,2]. They consists either of a periodic array of metal patches printed on a dielectric substrate (capacitive FSS) or a metal screen perforated periodically with holes (inductive FSS).

The loss of power due to dissipation determines a degradation of the reflection and transmission performance of the FSS.Moreover, the issue of power loss is particularly critical in the case of high power handling, due to the heating of some parts of the device, which could eventually melt or burn. Losses in FSS arise from two different effects: ohmic losses (due to the finite conductivity of the metal) and dielectric losses (due to the electric loss angle in the dielectric substrate).

In general, when using a numerical method based on the periodic method of moments (like the MoM/BI-RME method [3,4], the effect of dielectric losses can be readily incorporated in the Green's function representation. Conversely, the calculation of ohmic losses is usually more difficult.

In the case of capacitive FSS, ohmic losses can be easily included in the analysis, under the hypothesis of infinitely thin metal patches and skin effect. A better estimation can be obtained by considering metal patches with finite thickness, which can be represented by considering different current densities on the top and bottom surfaces of the metal patch, and possibly also on its side wall.

The calculation of ohmic losses in inductive FSS is usually more difficult than in capacitive FSS. This is due to the formulation of the electromagnetic problem in terms of an integral equation, where the unknown is the magnetic current density at the terminal cross–section of the hole [3], whereas the losses are physically related to the electromagnetic field on the metal surface. A possible technique for calculating the dissipated power in inductive FSS is based on the perturbation approach. In this approach, the electromagnetic problem is solved without considering ohmic losses, and the magnetic current density is determined at the terminal cross–sections of the holes. Once the magnetic current density is known, the magnetic field on the metal surface can be calculated by a Green's integral, and the lost power density can be obtained.

All these topics will be discussed through numerical and experimental results at the conference.

REFERENCES

1. Besso, P., M. Bozzi, L. Perregrini, L. Salghetti Drioli, and W. Nickerson, "Deep Space Antenna for Rosetta Mission: Design and Testing of the S/X–Band Dichroic Mirror", *IEEE Trans. Antennas & Propagat.*, Vol. AP-51, No. 3, 388, 2003.
2. Bozzi, M., L. Perregrini, J. Weinzierl, and C. Winnewisser, "Design, Fabrication, and Measurement of Frequency Selective Surfaces" ,*Optical Engineering*, Vol. 39, No. 8, 2263, 2000.
3. Bozzi, M., L. Perregrini, J. Weinzierl, and C. Winnewisser, "Efficient Analysis of Quasi–Optical Filters by a Hybrid MoM/BI–RME Method", *IEEE Transactions on Antennas and Propagation*, Vol. AP-49, No. 7, 1054, 2001.
4. Bozzi, M., and L. Perregrini, "Analysis of Multilayered Printed Frequency Selective Surfaces by the MoM/BI–RME Method", *IEEE Transactions on Antennas and Propagation*, Vol. AP-51, No. 10, 2830, 2003.

About Magnetic Field Distribution in Granular Superconductors

M. V. Belodedov, **V. V. Tchernyi**, **P. V. Makhno**
Russian Academy of Sciences, Russia

It is generally adopted point of view that magnetic field penetrate into superconductors by vortices each of which contain simple magnetic flux quantum $\Phi_0 = hc/2e$. This phenomenon take place both in bulk superconductors of II kind (abrikosov vortices, [1]) and in distributed josephson junctions (josephson vortices, [2]). The grate interests of in-vestigator are directing now to high-temperature superconductors (HTSC), which may be consider as multiple josephson medium. For HTSC technical applications it is necessary to study particulars of magnetic field penetration in it. The majority of authors researching this question suppose that magnetic field penetrate into HTSC also by vortices with simple quantum of mag-netic flux [3].

Granular superconductors electrodynamics was investigated in [4]. There material equation of granular superconducting medium was obtained by microscopic parameters averaging (in volume that is grater then single granules dimensions but is small enough for macroscopic pa-rameters been constant in it). In stationary case this equation ties current density $\vec{\jmath}$ and magnetic vector potential $\vec{A}$:

$$\vec{\jmath} = -I\rho\frac{\pi^2 a^2}{4\Phi_0}\vec{A}\exp(-\frac{\pi^3 a^2}{4\Phi_0^2}A^2),$$

where I is the mean critical current density of the josephson junctions in granular medium, ρ - there concentration in the medium, a - mean granules dimension. By this equation with Maxwell equation $rotrot\vec{A} = (4\pi\mu/c)\vec{\jmath}$ stationary current density and magnetic field distributions in granular superconducting medium where obtained. These distributions (central symmetry is supposed) are shown on the figure.

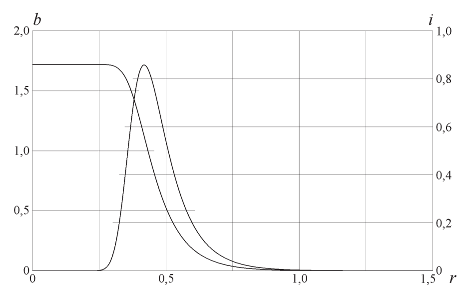

Figure 1: Magnetic field b and current density I distri-butions (arbitrary units) in magnetic vortex in the granular superconductor.

The formations obtained by the modeling described are correspond to the magnetic vortices in kind II superconductors.

Magnetic flux containing in the vortices obtained is determined by the medium parameters and therefore is not equal to both Φ_0 and integer amount of Φ_0. This fact may be explained: stable magnetic formations in the complicated josephson structures may contain a lot of magnetic flux quanta.

The results obtained emphasize that it is necessary to investigate in detail the granular superconducting medium electrodinamics.

REFERENCES

1. Abrikosov, A. A., *JETP*, Vol. 32, 1442, 1957.
2. Ferell, R. and R. Prange, *Phys. Rev. Lett.*, Vol. 10, 479, 1963.
3. Sonin, E. B., *JETP Letters*, Vol. 47, No. 8, 415, 1988.
4. Belodedov, M. V. and V. K. Ignat'ev , *Superconductivity: Physics, Chemistry, Technics*, Vol. 3, No. 6, 1170, 1990.

Session 4A5b

EM Methods for VLSI

Optimization for the Locations of Decoupling Capacitors in Suppressing the Ground Bounce by Genetic Algorithm

Kai-Bin Wu[1], **An-Shyi Liu**[1], **Guang-Hwa Shiue**[1], **Chien-Min Lin**[2], **Ruey-Beei Wu**[1]

[1]National Taiwan University, Taiwan
[2]Taiwan Semiconductor Manufacturing Company Ltd., Taiwan

As clock frequency increases and rise time decreases in high-speed digital printed circuit boards, noise on power bus will be incurred due to a sudden change during the high-to-low and low-to-high transition, called simultaneous switching noise, delta-I noise or ground bounce. This noise may result in signal integrity and electromagnetic interference problems in high-speed digital systems, such as wrong judgment of digital system logic.

This paper investigates the optimal placement of the decoupling capacitors in suppressing the input and transfer impedances of power-ground plane vias. First, the cavity model is employed to calculate the n-port impedance matrix among the vias and possible locations of the decoupling capacitors in the power-ground plane. In view of the time-consuming doubly innite series of the Green's function in the cavity model, a simplied form has been derived to speed up the computation. Then, the genetic algorithm (GA) is applied to search for the optimal locations of the decoupling capacitors, in order to minimize the input and transfer impedance over a desired frequency range. Finally, some numerical examples based on the present approach will be presented, and from which some of the ecient ways in suppressing ground bounce by decoupling capacitors will be discussed.

Collocation Method based RC/RLC Extraction with Process Variation

Janet M Wang, **A. Mitev**, **N. Kankani**
University of California at Berkeley, USA

Interconnect models must take into account the following uncorrelated geometric parameters: metal layer thickness, metal line width, line-to-line space, and ILD thickness. These geometric parameters are variables that account for manufacture uncertainties in the extraction tools. Current research techniques16-19 usually assume constant geometric parameters i.e. they neglect possible variations. To the best of the PI's knowledge existing industry extraction tools follow the same methodology. Very recent discoveries show that this constant geometry approach may have a delay that is 45% less than the real delay. In order to better estimate the delay, we proposes a new extraction program based on the collocation method.

The new extraction method writes geometry changes in the input technology files as percentages. The approach models the metal and the dielectric layers as 2D or 3D domains with internal sub-domains for maximum and minimum layer geometries. As is well known, interconnect parasitic extraction solves Maxwell equations by using multi-grid finite difference or finite element methods. The sub-domains with the maximum metal geometries and with the minimum dielectric geometries act as initial conditions for the Maxwell equation solvers. The width (W), the height (T) of wires and the spacing (S) between every two wires are not constants any more. They are changing inside ranges given by the process designers. Collocation method is to provide an array of important geometric sampling points that are important to over all performance. The sampling points (also referred as collocation points) are offered in a top-down manner: interconnect networks on the critical path whose delays have high sensitivity to certain geometric parametric values. With the given collocation gemometric samples, we then denote the region outside the biggest possible cross section of wires as sub-domain A, the region inside the smallest cross section of wires as sub-domain C. The changing region between A and C is denoted as B. The corresponding coefficient matrices of sub-domain A and C will be constant. The coefficient matrices corresponding to B, interdependancy between A, C and B, C, and the right hand side vector may be varying. The unknowns represent charges in A, B and C domains respectively. Iterations between the maximum and minimum sub-domains yield the resistance, capacitance, and inductance polynomial functions with respect to layer geometries as well as the upper/lower bounds of resistance, capacitance, and inductance per unit length of the interconnect wires. Because of the small size of region B and the positive definite property of the coefficient matrices, the convergence speed is relatively fast. To further speed up the extraction procedure, we plan to apply memory sharing and parallel computation techniques. Our preliminary results show 30x speedups over the traditional Monte Carlo based approaches while maintaining the similar accuracy.

ICCAP: A Linear Time Sparse Transformation and Reordering Algorithm for Three-dimensional BEM Capacitance Extraction

Rong Jiang
University of Wisconsin, USA

Charlie Chung-Ping Chen
National Taiwan University, Taiwan

With the reduced feature size and the increased operation frequency, extracting self and coupling capacitances associated with on-chip interconnects and packages has become increasingly important for determining the functionality and performance of very large scale integration (VLSI) design.

Many fast algorithms have been proposed in the literature to solve the dense linear system associated with boundary element capacitance extraction. FastCap is based on fast multipole method (FMM) for accelerating the dense matrix-vector multiplications required by iterative matrix solvers. HiCap is also FFM algorithm with kernel-independent hierarchical panel refinement. Normally, those iterative algorithms require $\mathrm{O}(n^2)$ per iteration since the potential coefficient matrix is of order n^2. Other well-known algorithms include the precorrected fast Fourier transformation (FFT) method and singular value decomposition (SVD) method, they are of $\mathrm{O}(n \log n)$ complexity and with O(n) memory requirement.

Recently, PHiCap proposes to construct cost-efficient preconditioners by applying an orthogonal sparsification transformation. Albeit the iteration number is greatly reduced, the orthogonal matrix generation still requires $\mathrm{O}(n \log n)$ operation and hence becomes the bottleneck of the entire algorithm. Furthermore, the transformation matrix needs extra storage spaces and makes the memory budget even tighter for large scale design applications.

This paper presents an efficient, simple, hierarchical, and sparse 3D capacitance extraction algorithm, ICCAP. Most previous capacitance extraction algorithms introduce intermediate variables to facilitate the hierarchical potential calculation but still preserve the basic panels as basis. In this paper, we propose a completely different perspective and discover that those intermediate variables are fundamentally much better basis than leaf panels. As a result, we are able to explicitly construct the sparse potential coefficient matrix and solve it with linear memory and linear runtime in comparison with the most recent hierarchical $\mathrm{O}(n \log n)$ approach in PHiCap.

Furthermore, the explicit sparse formulation of potential matrix not only enables the usage of preconditioned Krylov subspace iterative methods but also the reordering technique. A new reordering technique, Level-Oriented Reordering, is proposed to further reduce over 20% of memory consumption and runtime compared with no reordering techniques applied. In fact, LOR is even better than the state-of-the-art minimum degree reordering and more efficient. Without complicated orthonormalization matrix computation, ICCAP is very simple, efficient, and accurate. Experimental results demonstrate the superior runtime and memory consumption over previous approaches while achieving similar accuracy.

A Real-Time Wireless Physiological Monitoring System for Nursing Center

Jeng-Pang Wang[1,2], **Fok-Ching Chong**[2]

[1]National Taiwan University, Taiwan
[2]National Taiwan University Hospital, Taiwan

Physiological monitoring system in nursing center that the subject is mobile, ideally , has to be able to monitor vital signs data continuously, wirelessly, monitor all the subjects simultaneously, as well as communicate on demand in real-time. This report describes the design and implementation of a nusing center that meets the above requirements. The function of this system is to monitor individual physiological parameters such as body temperature, blood pressure, heart rate and EKG real-time via wireless radiofrequency communication channel and wired local area communication network. Several devices have been built:

1. A portable multi-channel physiological monitor with expandable sensor interface. This device performs signal conditioning, data logging, data acquisition, data transmission to a base station (wired or wireless).
2. Wireless data and voice communication interface.
3. Wireless base unit streaming data to the base station (via BlueTooth$^{\mathrm{TM}}$ or other modalities).
4. Display base station and network management center computer.

All collected data are stored in the network management center computer for further processing, and analysis, facilitate the staffs in the nursing center to monitor in real-time and track the physiological changes in longer term. It could. operate in coordination with Internet related communication protocol to provide data exchange for nursing centers and medical institutes. In order to to make it more friendly and easy to use, the design process starts from opinions of the medical staffs about easy and convenient usage and aiming to reduce the loading of the staffs and . This system bas been clinically tested and tuned to its optimal performance. This system could improve the service quality of nursing center. And is also applicable to other clinical, first responder, or home health monitoring. in-house or ambulatory care.

Session 4A6

Optics and Photonics, Lasers, Gyrotrons

Research of ATP Technology for Underwater Laser Communication System

Jun Ma, **Xing Jing**, **Faliang Ao**
Guilin University of Electronic Technology, China

Underwater Laser Communication (ULC) has become a hot subject for recent years in the world. However, it makes the job extremely difficult because the communication channel underwater is very complicated and unsteady. In order to handle with this problem, a new methodology based on more mature techniques of Free-Space Communication (FSO) is proposed.

Acquisition, Tracking and Pointing (ATP) technology is one of more mature techniques of FSO. The work of laser communication in the atmosphere is well done by use of ATP technology. Moreover, many successful military and commercial products used this technology have been seen in the market. From a theoretical point of view, the situation is analogical between ULC and FSO. Both of them have reflection, attenuation, refraction and scattering to laser signal. Nevertheless, it is more serious and complex to the communication channel underwater than under atmosphere. So a new methodology has to be proposed for the special environment.

For tracking and pointing, the primary step is to acquire laser signal on receiver. Because of the effect of the channel underwater, laser signal will be distorted and become faint when it comes to the receiver. Through a Charge-Coupled Device (CCD) with high resolution and high sensitivity, we can observe a black-white image which includes distorted signal and noises on the terminal. By use of opto-electronic image processing algorithms, it is likely to extract and restore the laser signal from the image. Furthermore, we can estimate the position of transmitter and use them as parameters of control devices to accomplish auto tracking and pointing. In order to validate the feasibility and availability of the methodology, many experiments have done on the sea. And also an experiment environment, which has a 50m tunnel filled with water, is established for convenience . The obtained results through these experiments prove the availability of the methodology mentioned above.

Stability Analysis of Mode Locked Figure-Eight Fiber Laser

M. K. Islam
City university of Hong Kong, Hong Kong

P. L. Chu
City university of Hong Kong, Hong Kong

Mode locked fiber lasers, as a source of short pulse generation find applications in Telecommunications and Optical signal processing where low noise and stable pulse train is the main requirement. It is therefore important to analyze shot to shot pulse amplitude stability and timing jitter of the pulse trains quantitatively before using these sources practically. By introducing a gradual twist in fiber and use of normal dispersion EDF to stretch and amplify the pulse, high energy, stable pulse train generated from a figure eight pulse has been analyzed. Fluctuations of pulse repetition time, pulse energy and pulse width jitter occur simultaneously. All these types of noise have been characterized quantitatively by examining the higher harmonics of the rf spectrum [1,2]. The measured peak to peak stability of 99.2% and a timing jitter of 5.59 psec for 2.2 MHz pulse train has been optimized for the total dispersion and length of the cavity which is quite remarkable, whereas the variation of cavity parameters results in increased timing jitter and peak pulse instability.

REFERENCES

1. Linde, D. Von der, "characterization of the noise in continuously operating mode locked lasers", *Appl. Phys. B*, Vol. 39, 201, 1986.
2. Fuss, I. G., "an interpretation of the spectral measurements of optical pulse train noise", *IEEE J. Quantum Electron.*, Vol. 30, 2707, 1994.

A Routing Algorithm for ASON

Xiaoyun Gong
Guilin University of Electronic Technology, China

Faliang Ao
Guilin Institute of Electronic Technology, China

The recommendations for ASON(Automatic Switched optical Networks) are proposed by ITU-T. Among them the G7715 is the routing protocol which provides the routing service. But it not give the routing method in G7715. At present time, there are many routing protocols for IP network, for example, OSPF(open shortest path first). If we use those methods for ASON, it may need some improvements. As there are some differences between IP network and ASON.

Consider the characteristics of ASON, for example, there may be many wavelengths in an optical fiber link, or there are the necessary condition for wavelengths, we propose a new routing algorithm for ASON in this paper. We call this method as comprehensive cost minimum.

Comprehensive cost minimum method is based on a routing protocol of OSPF, and it takes available wavelengths of every fiber into account. This paper realizes this algorithm by VC^{++} programs, and verifies the feasibility of this algorithm.

REFERENCES

1. ITU-T Recommendation G.8080/Y.1304-2001, "Architecture for the automatic switched optical networks(ASON)", 2003.
2. Xue, Yong, et al.: "Architecture and Requirements for Routing in the Automatically Switching Optical Network", ITU-T G.7715 v0.6.4, 2002.
3. Moy, J.: *Open Shortest Path First Version 2,* RFC2328, 1998.

40 GHz Distributed Amplifier for OEIC Optical Receiver

Shilong Jiao[1], **Feng Qian**[2], **Yuan Zheng**[2], **Tangsheng Chen**[2], **Yutang Ye**[1]

[1]University of Electronic Science and Technology, China
[2]Nanjing Electronic Devices Institute, China

The growing demands for large capacity and long haul data transmission has resulted in a rapid development of optical communication. There are two ways to enhance the capacity: one is time division multiplex (TDM) or wavelength division multiplex (WDM) technology, that means increasing the channels of single optical fiber; the other is boosting the operational speed of a single channel, for example, from 10 Gb/s to 40 Gb/s.

For 40 Gb/s application, the lower limit of the system bandwidth is estimated to be less than 100 kHz, and the upper limit is about at least 28 GHz for NRZ[1]. But for the chip design of the preamplifier of optical receiver, there must be some bandwidth margin for interconnections and package, so the upper limit of bandwidth should be more than 30 GHz. The distributed amplifier (DA), which incorporates the input and output capacitances of transistors into artificial transmission line (ATL) structures, overcoming the broadband match problem inevitable to lump amplifier design, can get very large bandwidth[2], so its a hopeful selection for high speed optical communication applications.

In this paper, a kind of DA, based on 0.2 m GaAs low noise PHEMT process, is designed, which consist of seven-stage cascode units for gain-bandwidth production and six-stage active load units for bias. The DA has a measured -3dB bandwidth beyond 40 GHz, with transimpedance gain about 45.6dBΩ. The return losses of input and output ports are both less than 10dB. On the condition of 300 mW power dissipation, the minimal equivalent input noise current density is $22pA/\sqrt{Hz}$. The measured output eye diagram for 40 Gb/s pseudo-random code stream is clear and satisfying. As an example, the simulated output eye diagram of OEIC optical receiver front end is also presented. All the results show that the DA is suitable for 40 Gb/s optical communication.

REFERENCES

1. Tsugumichi Shibata, Shunji Kimura, Hideaki Kimura, Yuhki Imai, Yohtaro Umeda, and Yukio Akazawa, "A Design Technique for a 60 GHz-Bandwidth Distributed Baseband Amplifier IC Module," *IEEE J. Solid-State Circuits*, Vol. 29, 1537- 1544, Dec. 1994.
2. Robertson, I. D. and S. Lucyszyn, *RFIC AND MMIC Design and Technology*, London: The Institute of Electrical Engineers, 2001

The Application of PIM in Laser Communication System

Ming-Song Chen, **Tian-Song Li**, **Fa-Liang Ao**
Guilin Institute of Electronic Technology, China

The paper try to introduce one of the methods how to realize the PIM modulation by the use of PIC. At first, this technique can effectively improve the synchronization puzzles confronted during the process of modulation and demodulation. The second, the method can improve the coding efficiency of the laser communication system. The third, according to the principle of PCM, it could be integrated into one system by using PIC controlling mode. For the system communicate data with computer via asynchronous series port so that the demodulator can be made simple and cheap, can be fulfilled code by PIC and can be separated apart from the computer. At the end , the paper conclude the advantages for this application such as simple circuit design, stable working reliability.

REFERENCES

1. Kahn M J, R J. Barry, "Wireless infrared communications .Proceedings", *the IEEE*, Vol. 85, No. 2, 265, 1997.
2. Ghasse, mlooy Z, A R. Hayes, "Digital pulse interval modulation for IR communications systems", *a review. int. J. Commun. Syst, special issue*, Vol. 13, 519, 2000.
3. Proakis, G J., "Digital Communications.3^{rd}", *New York: Mcgraw - Hill*, 201 -206, 254-272, 1995.
4. Hayes, A R, Ghasse mlooy Z, Hayes A R, et al, "Base-line wander on the performance of digital pulse-interval modulation", *IEE Proc-Optoelectron*, Vol. 147, No. 4, 295, 2000
5. Martin, Roden, "Analong and digital communication system[M]", *New York: Prentice-Hall*, 2002.
6. Huang, Yuan, Jianjun Sun, "Spectum for pulse frequency modulation[J]", *Semiconductor Photonic and Technology*, NO. 8, 65, 2002.

The Implementation for Synchronization Controlling Set of the Laser Underwater Imaging System

Ming-Song Chen, **Wei-Ping Cao**
Guilin Institute of Electronic Technology, China

The research to laser underwater imaging technology is always one of the up-to-day researching fields in the world. The implementation for synchronization controlling set of the imaging system is one of the key techniques. The one programmable pulse width controlled laser imaging system used in the distance-triggered model by using single chip computer AT 89C51 as the controlling center as long as combining 8253 programmable counter/clock is carefully introduced in this paper. We try to use the synchronization set to fulfill this distance-triggered model, and take a study on the scheme for programmable controlling method to the pulse width and delayed time of the controlled pulse. We apply the digital camera as the imaging equipment , use the pulsed laser as the light source and adopt the controlled system as the controlling part to realize the laser distance-triggered model imaging system. We have been trying our best to put forward the corresponding solving method of the whole laser underwater imaging system.

REFERENCES

1. Dixon G. J ., Contributing Editor, "Laser radars produce three-dimensional pictures", *Laser Focus World*, Vol. 34, No. 8, 137, 1998.
2. John W. Mclean and James T. Murray, "Streak-tube lidar allows 3-D ocean surveillance", *Laser Focus World*, Vol. 34, No. 1, 171, 1998.
3. WORLD NEWS, "Portable fluorometer tracks pollutants", *Laser Focus World*, Vol. 34, No.10, 38, 1998.
4. WORLD NEWS, "Mine-locating lidar system delivered to US Navy", *Laser Focus World*, Vol. 33, No. 2, 26, 1997.
5. George Williams and James Janesick, "Cameras with CCDs capture new markets", *Laser Focus World*, Vol. 32, No. 3, S5, 1996.
6. Mark Gitin and Seaton, "Laser manufacturers target commercial markets(Underwater imaging)", *Laser Focus World*, Vol. 32, No. 11, 153 1996.
7. WORLD NEWS, "Laser system charts Australias coastline", *Laser Focus World*, Vol. 32, No. 4, 24, 1996.

Simultaneous Measurement of Pressure and Temperature Using a Single Fiber Bragg Grating

Shilie Zheng, **Xianmin Zhang**
Zhejiang University, China

Fiber Bragg grating (FBG) has been extensively used in fiber sensor applications owing to its compactness in structures, simplicity in fabrications and wavelength coding in measurements. However, in temperature and pressure sensor applications, it is difficult to distinguish between the temperature and pressure effects as FBG is sensitive to both. In this paper, a novel sensor based on a single fiber Bragg grating is described. The sensor is configured by encapsulating the right half of a fiber Bragg grating in a polymer filled metal cylinder and fixing the other half to the metal cylinder. Since the two ends of the left half of the FBG is fixed, this part of the FBG will not respond to the axial strain and thus only the right half of the FBG is sensitive to the applied pressure. As the right half of the FBG is coated with a thick polymer, which has a small Young's modulus, the pressure sensitivity is significantly increased. When the temperature varies, the thermal expansion of the polymer will add another thermal effect on the right half of the FBG, and hence the left half and right half of the FBG respond to the thermal effect differently. As a result, in practical, when both pressure and temperature change, the Bragg wavelength of the origin bare FBG will split in the two Bragg wavelengths, which shift accordingly. By measuring the shift of the two Bragg wavelengths, this sensor is able to measure pressure and temperature simultaneously. Using a novel tactic to transfer the applied pressure to the axial extended-strain on the fBG, the pressure sensitivity reaches to 9.65×10^{-3} MPa^{-1}, which is about 4700 times larger than that of the bare fiber Bragg grating. The accuracy of the pressure measuring can also be improved through introducing a fixed Bragg wavelength as a reference.

High Speed Low Loss Fiber Optic Switch

Xiaofeng Jin, **Shilie Zheng**, **Xianmin Zhang**
Zhejiang University, China

Sub-microsecond and multiple-port fiber switches with low loss and low cost are in great demand for use in modern defense systems and optical communication networks. However, high-speed switch with response time of sub-microsecond can only be achieved by solid-state beam steering technology. In this paper, high performance of 2x2 fiber optical switch is built out by further developing this novel solid-state switching technology, which uses new crystal materials having large electro-optic effect and excellent thermal stability to act as optical switching rotator. The structure of the fiber switch consists of the switching rotator and two polarization splitting collimators. Switching control is achieved by the switched 90 polarization rotation. This design of the optical switch eliminates the need for mechanical movement, organic materials, and waveguides, which introduce intrinsic drawbacks. Moreover, the design is simple, compact, and cost effective.

The E-O switch responses and the E-O switchs optical performance covering a wide temperature range of 65° to -75° are experimentally measured for reliability and space applications. The results show that the switch speed changes from 0.8 μs to 2.5 μs as temperature changes from 65° to below -75 °, and the E-O switch has high extinction ratio and relatively small temperature dependent insertion loss covering this temperature range, which assures this type of device operating in space environment. Typically the insertion loss is around 0.8 dB with polarization dependent loss less than 0.1dB. The isolation for this kind of one-stage 2×2 switch is better than 20dB.

This novel technology provides the optic switching with state-of-the-art performance attributes of electro-optic high-speed operation, polarization insensitivity and low optical insertion loss. The optical switches will be of great potential with the maturation of the production method.

*This work was supported by the National Natural Science Foundation of China (Grant No. 60477025).

Session 4P1a

Remote Sensing

Review of Electromagnetic Inverse Scattering and Subsurface Sensing

W. C. Chew[1], **G. L. Wang**[1], **A. Hesford**[1], **A. A. Aydiner**[2], **T. J. Cui**[3]

[1]University of Illinois at Urbana-Champaign, USA
[2]Intel Corporation, USA
[3]Southeast University, China

This paper will review some of the activities in subsurface sensing in our research group in recent years. A successful solution to the inverse problem is instrumental in many applications such as remote sensing, biomedical imaging, subsurface sensing, as well as geophysical exploration. Past methods in this arena are usually based on approximate models so that the range of validity is limited. More rigorous models can be developed for inverse scattering, but they usually give rise to intensive numerical computations. Ways to reduce the computational resource needed have been the preoccupation of researchers in recent years.

Our interest has been in devising inverse scattering method that can reconstruct images of buried objects as well as deducing their electromagnetic properties. A general way to solve this problem is via a numerical inverse scattering approach. We will review the distorted Born iterative method (DBIM), where two forward scattering solutions are needed for each iteration in the inverse scattering solution. Laboratory experiments have confirmed that the use of DBIM in processing experimental data can give rise to super-resolution compared to just the simple Born approximation. Simple Born inversion does not account for multiple scattering effect within the scatterer, but DBIM accounts for multiple scattering, which ultimately makes the inverse scattering problem a nonlinear problem.

We will also illustrate the use of 1D inverse scattering solution to process data collected in 3D space. Since the 1D inverse solution is very rapid, massive amount of data can be processed within reasonable time. Our recent attempts have been the use of 3D inverse solution to process data collected in the real world. This tends to be computational intensive as the solution of the 3D forward problem is expensive. A way around this is to use fast algorithm as a forward solver, so as to expedite the inverse scattering solution. Another way is to use improvised inverse scattering algorithm whereby only approximate solution to the forward problem is needed, such as the extended Born approximation.

We will also discuss alternative inverse scattering solution such as the linearized inverse solution based on the Born approximation which is related to diffraction tomography. Another method is the linear sampling method, but this method allows the reconstruction of the shape of an object, but not its electromagnetic properties. Some comparisons between linear sampling method, diffraction tomography, and nonlinear inverse scattering method such as DBIM will be undertaken.

Surveillance of Sub-Surface Sanctuaries Using Earth-Penetrating Radiators

John Norgard, **Randall Musellman**
US Air Force Academy, U.S.A.

Electromagnetic (EM) imaging techniques are being developed to survey strategic sub-surface sanctuaries. The overall goal of this study is to develop and demonstrate techniques for sub-surface profiling from ground based and/or airborne (or even space) platforms.

This surveillance scheme combines and utilizes bistatic RCS measurement techniques, broadband GPR antenna technologies, and far-field SAR remote sensing techniques. The combined RCS/GPR/SAR surveillance technique is used to extract target signatures concealed in measured RCS data and to remove thermal nose and ground clutter at the earth/air interface from the SAR data.

The combined RCS/GPR/SAR surveillance process utilizes ground contact and airborne transmitting (TX) and receiving (RX) antennas. Small, but efficient, ultra-wideband (100:1 bandwidth) conformable GPR antennas are being designed and developed to operate over the HF/VHF bands.

Planar wire-grid bowtie antennas are being developed as broadband GPR radar antennas. These antennas are 2D approximations to frequency independent, i.e., ultra-wideband, 3D solid biconical antennas. The antennas are truncated to finite lengths, which reduce the bandwidth to a finite range that is adjusted to cover the HF/VHF bands. 2D cross-sectional versions of the bowtie antennas were built and tested at the AFRL/RRS sub-surface antenna range and were compared to an adjustable standard-gain half-wave dipole antenna.

Experiments were conducted at an abandoned Zinc mine in New York. Two bowtie antennas were used to collect data over a grid containing 121 points on the surface. The transmitter remained stationary while the receiver was moved to cover 121 equally spaced points on the ground. A manmade drift (mine) 150-160 feet below the surface was detected and imaged using an experimental setup developed at AFRL/RRS-Sensors Directorate.

Remote sensing using an elevated GPR system, as used in the mine experiment, provides a safe stand-off distance, but reduces the surface penetration of the transmitted wave and radar resolution. Ground foliage and the mismatch at the earth/air interface further reduce the transmitted energy available in the wave propagating in the earth. Therefore, a new concept is proposed to use a subsurface radiator, delivered as an earth penetrating non-explosive, electronic bomb (e-bomb), for the source of the transmission and ground contact or airborne receivers.

Most notable in the Zinc mine data were extensive unfocused clutter spanning from 20 to 40 feet below the ground. Using a subsurface e-bomb transmitter, the unfocused clutter at or near the air-earth interface would be significant reduced. Modeling and simulation of this scenario showed a 15 dB improvement in received signal.

The overall goal of this work is to achieve improved subsurface surveillance of buried objects, target detection and identification, wide-area surveillance, targeting, battle damage assessment, and buried facility parameters (lateral location, depth, size, shape, and portals). This technique will improve the detection process of locating deeply buried objects.

Physical and Mathematical Understanding of High-Resolution Synthetic Aperture Radar

Yunhua Zhang[1], **Haibin Li**[1,2], **Jie Wu**[1,2]
Xiangkun Zhang[1], **Jingshan Jiang**[1]

[1]Center for Space Science and Applied Research, CAS, China
[2]Graduate School of the Chinese Academy of Sciences, China

Synthetic Aperture Radar (SAR) is a kind of radar, which utilizes coherent processing of echoes of successive pulses from target (both point target and distributed target) in a range of aspect angles, so as to achieve a big equivalent antenna aperture.

In a physical point of view, SAR imaging is a mapping of scattering centers, which is equivalent to solving an inverse electromagnetic scattering problem. The formed scattering centers are much related to the target geometry and the wavelength of transmitted electromagnetic wave. The shorter the wavelength, the weaker the multi-scattering effect, so the easier the scattering centers can form, and the clearer the radar image we can obtain.

In a mathematical point of view, SAR imaging is equivalent to a problem of solving an integral equation by applying Fourier transformation, so the spatial resolution is inverse proportion to the bandwidth of observed spatial spectrum obtained by illuminating the target with wide-band radar signal in wide aspect angles. We can obtain a wide-band spatial spectrum for a target both by a single radar system, which is the case of ordinary SAR system, and by distributed radar systems, which is much more complicated than a single SAR system.

In a practical wide-band imaging radar system, motion compensation and electromagnetic calibration are two never avoidable issues when high resolution imaging is intended to achieve. After deriving the physical optics method to calculate the electromagnetic scattering from target, we clearly show the physical meaning of motion compensation and electromagnetic calibration for wide-band imaging radar.

Numerical simulations support our understandings about SAR. In the end, we propose a new algorithm for processing multi-aperture SAR signal to obtain high resolution radar image.

Locating Multiple Objects in the Radar Volume Using Multiple-receiver Radar Interferometry

Jenn-Shyong Chen
Chienkuo Technology University, Taiwan

With multiple receivers at different locations, it is capable of detecting the angles of arrival of the radar echoes scattered/reflected from objects. This technique, used with mesosphere-stratosphere-troposphere (MST) coherent radar, has been applied to the atmosphere to locate multiple echoing centers in the radar volume, provoking plenty of research topics such as irregularity structure, gravity wave activity, interaction of radio wave with the atmosphere, and so on. One of the proper algorithms dealing with multiple-receiver signals is Copan method. To implement the above researches, a 30-MHz radar, with five receivers, is now constructing on the Chung-Li radar site (121.18°E, 24.97°N; Taiwan), apart from the exited 52-MHz radar. For the new radar, we made a numerical study on various antenna configurations, which suggests a better arrangement of receiving antennas. To validate our computing procedure and codes, we applied the codes to the atmospheric echoes observed by the German-OSWIN (11.8°E and 54.1°N) and Chung_Li VHF radars. The OSWIN radar has six receivers, which enable us to find the condition of multiple scattering centers in the radar volume. A study of polar mesosphere summer echoes (PMSE) observed by the OSWIN radar was demonstrated here. For the Chung_Li radar, however, three receiving channels are available at the moment, which limits the radar to identifying only one object in the radar volume. In view of this, we used the radar echoes reflected from airplane and demonstrated that the location of airplane could be found easily.

Variability Analysis of Ka Band Rain Attenuation in Taiwan

Chi-Huei Tseng[1], **Kun-Shan Chen**[1], **Chih-Yuan Chu**[1]
Yu-Chang Tzeng[2], **Pay-Liam Lin**[1]

[1]National Central University, Taiwan
[2]National United University, Taiwan

As the communication services are demanding rapidly access for higher frequencies up to Ka-band and beyond, a model to predict the propagation through rain is required in order to estimate the link budget and communication performance. The rain drop size distribution (DSD) is the most important parameter in the attenuation prediction model. In this paper, we establish the DSD model from measurements, followed by presenting an attenuation model using the DSD model.

A two year observation (2002-2003) using two 2D optical distrometers at different locations were recorded. The DSD were measured and analyzed for different seasons under various rain rates. The variability of DSD in both space and time was clearly shown even in the not so large area of North Taiwan. It follows that a relationship between rain rate and DSD was established. From statistical regression, it was also found that the DSD follows the Gamma distribution best in most cases.

Long-term rain attenuation measurements using a Ka band (28GHz) CW system at vertical polarization were conducted in northern Taiwan. An optical rain gauge which has resolution of 0.01mm and can collect the rain rate every 5 seconds measured the rain rate at the same location. The attenuation due to rain can be estimated by calculating the extinction coefficient over all of the rain drops within the antenna beam volume. Two methods were used to estimate the extinction coefficient. First, assuming that the scattering mechanism follows the Mie scattering approximation, and the rain drops are all sphere. Second, using T-Matrix method and the oblateness of the rain drops vary from 1.0 to 0.8. Making use of the Gamma-distribution for DSD model, a semi-empirical rain attenuation model was then developed. To validate the model, we compared it with the measured data. For the purpose of cross referencing, we also compared it with the ITU-R and Crane models. The results show that the proposed model matched very well with in-situ measurement from a two-year data set. Both the Crane model and the ITU-R model were inadequate, as expected, for a correct interpretation of the accumulated measurement data producing overestimates.

Session 4P1b

RF Multipath Environments

Experimental Field Statistics Validation in a Cubic Reverberation Chamber with Mechanical Mode Stirring & Bistatic Illumination

M. Piette, K. Moesen, S. Montezuma
Royal Military Academy, Belgium

The cubic shape is generally claimed to be quite inconvenient for reverberation purpose, because of its high degree of symmetry and the degeneration of the cavity mode frequencies [1]. But notwithstanding this resonance frequency degeneration, the corresponding eigenfunctions are still different, so that the combination of their field distributions can yield good field homogeneity, so far all these modes are effectively excited into the chamber. This can only be achieved with a mode stirrer of high quality, able to reflect and diffract the incident waves in various and time dependent directions, so that sufficient modes resonating at the same frequency can be generated [2]. Mode number and stirring efficiency are indeed key parameters to obtain a good field uniformity. The ultimate test on that point of view is the CDF test by which the experimental cumulative probability density function of the field component amplitudes is compared to the theoretical distribution, in the sense of a statistical hypothesis test, taking into account the number of statistically independent samples.

The present paper gives an critical overview of the measurements carried on in the small cubic reverberation chamber at Royal Military Academy (2,5 x 2,5 x 2,5 m^3) equiped with a homemade mechanical mode stirrer. The system used for field measurements consists of a small broadband triaxial E-field probe, an optical fiber cable, an electro-optical convertor and a spectrum analyser. A couple of small ultra-wideband TEM horns is used to generate the microwave energy into the cavity. Although the mode stirrer rotation makes that the fields exhibit no definite polarization over one stirrer rotation, the two illumating horns are set in cross-polar configuration, so that the mode stirrer is illuminated bistatically and simultaneously in both polarizations, in order to enhance the unpolarized character of the stochastic fields.

The frequencies of interest are between 900 MHz and 2,5 GHz. Though the whole validation of the chamber as immunity testing facility and antenna calibration room is still on progress, the set of results presented here points out what can be firstly seen as a drawback - the cubic shape - can be effectively overcome by the quality of the mode stirrer. The space homogeneity of all field components, the stirring ratio in different space locations and the CDF measured at 900 MHz and 1800 MHz (GSM, DECT and DCS mobile radio systems) will be presented and critically commented.

REFERENCES

1. Leferink and van Etten, "Optimal Utilization of a Reverberation Chamber," *EMC Symp. 2000, Bruges*, Vol. 1, 2000.
2. John, S., "From Cubic Faraday Cage to HIRF Testing Reverberation Chamber," *EuroEM '04, Magdebourg*, 2004.

Propagation Path Loss Prediction for Outdoor Environment Using Adaptive Neuro-fuzzy Inference Systems

Supachai Phaiboon, **Pisit Phokharatkul**
Mahidol University, Thailand

Suripon Somlurnpanic
Kingmonkul Institute of Technology Ladkrabang, Thailand

This paper proposes method to predict path loss in cellular mobile communication systems using Adaptive Neuro-Fuzzy Inference Systems (ANFIS). The propagation mediums are classified into propagation environment densities defined as input sets namely, X1 = building density, X2 = house density, X3 = Tree density. These crisp inputs are classified by fuzzifier to fuzzy sets of the ANFIS, trained with measurements. The advantage of the ANFIS with hybrid least squares and gradient descent algorithms is fast convergence compared with original neural network. The K-means algorithm for selection of the training patterns was also presented. For this study, we classified the environments into 4 difference terrains namely, high density urban area, urban area, suburban area, and garden area. Comparison of our predicted results to measurements indicate that improvements in accuracy over conventional empirical models are achieved.

Antennas and Propagation for Wireless Body-centric Networks

Yang Hao[1], **P. S. Hall**[2], **A. Alomainy**[1]
Y. I. Nechayev[2], **C. Parini**[1], **C. C. Constantinou**[1]

[1]Queen Mary University of London, UK
[2]University of Birmingham, UK

Wireless Body-Centric Networks consist of a number of nodes and units placed on the human body or in close proximity, such as on everyday clothing. Currently it is used to receive or transmit simple information which requires very low processing capabilities. However, some high performance and complex units are needed in the future to provide the facilities for powerful computational processing with high data rates for applications such as video streaming and heavy data communications. These have led to increasing research and development activities in the field of body area network applications for many purposes with the main interest being health care and patient monitoring and task-specific/fully compatible wearable body networks (e.g. wearable computers) that have been applied in fields such as construction and medicine. There are three primary criteria for wireless modules for Wireless Body-Centric Networks. Firstly, they must support high data rates and secondly, they must be small, both of which suggest the use of high frequencies. Thirdly they must consume the minimum of power, which implies highly efficient links. In terms of antennas and propagation, efficient design requires, firstly, good understanding of the properties of the propagation channel involved, and secondly the development of optimised antennas. This paper presents results from studies at Queen Many University of London and the University of Birmingham, on the characterisation of on body radio wave propagation paths and the optimum choice of antenna for these systems.

A Measurement System Using Dual-phase Lock-in Amplifier for Optically Modulated Scattering Microwave Fields

Jung-Hwan Choi, **Seong-Ook Park**
Information and Communications University, Korea

Microwave fields are generally measured with an open-ended rectangular waveguide type of probe or coaxial type of probe. The accuracies of the conventional measurement method are affected by a feeding cable and near-by conducting objects. Conventional probes may produce too much distortion of the field to be measured because a probe must be connected to the receiver by a transmission line or a cable. Thus, such a parasitic factor degrades the accuracy of the measurement significantly. In order to minimize the perturbation of microwave fields and improve the accuracies, the modulated scattering technique has been popularly used for measuring microwave fields. The modulated scattering microwave fields can be discriminated from unmodulated parasitic signals. The modulated component includes the amplitude and phase information that characterized microwave fields at the probe's location.

The conventional system for measurements of the modulated scattering microwave fields have an unstable measurement ability and a measurement limitation in terms of a frequency range because a homodyne receiver utilized a coupler to make quadrature phase component. An important factors, which limits the used of in-phase and quadrature coupler in wide band performance, are relatively narrow bandwidth and inaccuracy due to imperfect characteristics of a quadrature coupler in the entire operating frequency range. To overcome such a drawback, we propose the improved system. The directional coupler and quadrature coupler which limit the operating frequency range are eliminated from the proposed system. Instead of this, the detecting part uses a dual-phase lock-in amplifier. The signal frequency of $f_1 - 2f_m$ is used to demodulate the received signal instead of the coupled signal component of f_1. The dual-phase lock-in amplifier makes in-phase and quadrature phase components of only one component whose frequency is f_m. Therefore, the proposed system has more accurate and broadband than one with a conventional system.

To validate the accuracy of the measurement system, the measured amplitude and phase distributions of the double-ridged horn antenna in far field region are compared with those of the conventional system in the commercial band (0.8∼6.0 GHz).

The measurement system in a bi-static configuration is composed of Tx and Rx antennas, a modulated dipole scatterer, controller, and detecting parts. Double-ridged horn antennas (0.8∼6.0 GHz) are used for Tx and Rx parts. A 7 kHz modulated laser signal feeds a photodiode to modulate the received fields at the center of a dipole scatterer by optical fiber. The motion controller automatically adjusts the distance between Tx antenna and a modulated dipole scatterer, which has the fixed distance with Rx antenna. The detecting part consists of mixer and dual-phase lock-in amplifier using the modulating low frequency signal as a phase reference.

Session 4P1c

Subsurface Identification & Modelling

Diagnosis of Concrete Structure Using Microwave

Toshiyuki Tanaka, **Syogo Kijima**, **Kenzo Nagatomi**
Takayuki Ohnishi, **Takashi Takenaka**
Nagasaki University, Japan

Though concrete structures are made having a useful long life, they starts to be degraded and will be in deteriorated condition within twenty to thirty years. Therefore, it is necessary to make a close investigation of the condition of concrete structures with respect to cracks, cavities, and corrosion of reinforcing steels in order to prevent dangerous accidents such as drop of a flake or mass of concrete. Additionally, not only reinforcing steels but also various cables are buried in the concrete. Confirmation of the accurate positions of the reinforcing steels and cables is necessary for repair and reconstruction of the concrete structure. The existence of the reinforcing steel near the surface of the concrete can be confirmed at the good accuracy with conventional concrete radars. However, it is very hard to estimate the accurate position of the reinforcing steel, if the electric constant of the concrete has not been known. Also, when several grids of reinforcing steels are in the concrete, though it is possible to confirm a grid near the surface, the confirmation of the grids at the deeper position is difficult.

In this paper we propose two methods about the diagnosis of concrete structure. One is a method for estimating the electric constant of the concrete, when any objects exist in the concrete. A transmitting antenna radiates the pulse similar to the modulated Gaussian pulse, and a receiving antenna observes the pulse response. This measurement is performed at many locations in straight line on the surface of the concrete. The average subtraction processing is carried out in observed data, and the effect of the reflection from the surface of the concrete is removed. The data after average subtraction processing is the time response of the reflection and scattering from reinforcing steels. The average electricity constant of the concrete is estimated by the application of the nonlinear least squares method using these data. The other is a method for confirming the reinforcing steel at the deeper position, when some reinforcing steels exist at several depths in the concrete. Changing the interval of the transmitting antenna and the receiving antenna, the above-mentioned measurements are performed repeatedly. The synthetic aperture processing is carried out using all the observation data. The effectiveness of the presented method has been confirmed using real measured data.

Steel Bars Identification in Reinforced Concrete Structures by Using ANN and Magnetic Fields

N. P. de Alcantara Jr., **M. E. L. Gasparini**
São Paulo State University, Brazil

This paper proposes a new type of Non-Destructive Testing (NDT) for reinforced concrete structures, in order to identify the components of their reinforcement.

In the proposed methodology a sufficiently strong magnetostatic field is generated close to the structure by electromagnetic devices specially designed for this purpose. The presence of ferromagnetic materials (the steel bars of reinforcement) immersed in the concrete disturbs the magnetic field in the region of the structure. These field alterations can be detected by hall sensors placed along of its surface. Variations in the bar position, bar's cross section and number of bars in the structure originate slightly different patterns for the magnetic induction curves at the surface of the structure.

In this paper the curves for the deviations of the magnetic induction (difference between magnetic induction curves with and without the presence of ferromagnetic materials) were used to generate the training vectors for multilayer perceptron artificial neural networks. The curves were obtained by simulations with a finite element program. Thousands of simulations were done, and the neural networks were used to solve two kind of problems: (1) the position and cross section of a bar immersed in the concrete and, (2) the array topology and cross section of the bars in a complex concrete structure.

The paper presents aspects of the electromagnetic devices, neural networks architectures, and obtained results. The results strongly encourage the construction of real devices, based upon the methodology proposed here.

Measurement of Layer Thickness and Permittivity Using a New Multi-Layer Model from GPR Data

Chien-Ping Kao, **Jing Li**, **Richard Liu**
University of Houston, U.S.A.

For many years, a conventional method for estimating the depth and permittivity of layered media from ground-penetrating radar (GPR) data is common-middle point (CMP) method. When the distance between transmitter and receiver is relatively small, CMP is an effective method. However, with the increasing of antenna separation, CMP method will result in noticeable errors in depth, thickness, and permittivity readings. To improve the measurement accuracy, a new mathematical model is presented covering multi-layer GPR measurement problem, including one or two-layer cases. In the new model, we first consider all the possible paths when the GPR signal propagates in the multi-layer environment. We not only consider the effects from the air-ground interface but also introduce a ray-path-searching process in the GPR measurement using Fermat's shortest path law. The shortest path is then used in the process of GPR data inversion in order to calculate the depth and permittivity of each layer. After establishment of the new model, we used the transmission-line matrix method (TLM) to simulate the propagation of GPR signal in the multi-layered formation. By comparing the results from numerical simulation and measured results using a pulsed GPR with the results from proposed new model, it is found that the layer thickness and permittivity inversion data from the new model agrees well with both of simulation and measurements. It proves that the new model can be applied to the GPR measurement in multi-layer cases.

Inverse Electromagnetic Modeling of a Submerged Source in Shallow Sea Water

O. Thongsamouth, **M. Piette**
Royal Military Academy, Belgium

Modern smart mines can nowadays identify a class of ships by examination of their acoustic and electromagnetic signatures. The understanding of the electromagnetic ship signature is of greater interest in defence-related science since it can be used as a method of detecting a vessel and thus pose a substantial threat to it. Primary sources of time dependent electromagnetic fields are electrical currents generated by corrosion processes or power supplies and electrical equipment on board. The fields are found to be in the ELF (Extremely Low Frequency) range.

In this paper the forward problem is solved by a model, using a spectral domain technique, adapted for low frequencies in stratified conducting media. The present results take into account four layers composed of air, sea water, wet sand and rocks. The source is an array of oscillating punctual sources or an array of dipoles located in the sea. The fields are observed near the seabed in order to simulate what a mine could measure.

The problem of inverse modeling consists, in our case, to determine the underwater source strength distribution from measured field data by minimizing the L2 norm of the residuals for a given source number and a given spatial configuration of the sources. The inverse problem is in general ill-posed, sensitive to noise and measured data inaccuracies, and its solution is not unique. We compute the current intensity distribution for synthetic data generated from known source distributions and for real signatures. The accuracy of the results and the stability of the inversion algorithm with various source arrays are discussed.

Session 4P2

Plasmonic Nanophotonics 2: Theoretical Research

Evaluation of Tunneling Excitation Transfer and Dissipation in Plasmon-related Optical Near-field Interactions Based on Angular Spectrum Representation

Hirokazu Hori
University of Yamanashi, Japan

Tetsuya Inoue
Yamanashi Industrial Technology Junior College, Japan

Yasuo Ohdaira
Niigata University, Japan

Excitation transfer and dissipation govern the quantum mechanical operation and signal transport properties in nanophotonics devices. One of the basic issues is optical near-field interactions of excited electronic systems with surface plasmon, where tunneling excitation transfer into/through metallic structure and associated energy loss govern dissipation processes including observation processes and interactions with reservoir.

We have established a theoretical treatment of optical near-field interactions of oscillating electric and magnetic multipoles based on angular spectrum representation and tunneling picture of electromagnetic excitations via evanescent electromagnetic fields. The quantum optical properties of near-field radiation have been analyzed on the basis of novel second quantization theory of electromagnetic fields employing detector modes [1]. To produce a comprehensible model of optical near-field interactions, we have introduced the tunneling picture based on evaluation of Poynting vector and show that the energy transfer of tunneling regime is described by the overlap integral of evanescent waves of same penetration depth and pseudo-momentum [2]. Because of the universality of angular spectrum representation, the tunneling picture is applicable to the theoretical evaluation of general nanometer-sized photonic devices.

In this work, we study the dissipation processes in optical near-field regime, considering a metallic layer and evaluating tunneling energy transfer from an oscillating electric dipole. Our theoretical description based on angular spectrum representation and tunneling current provides us with a clear identification of plasmonic excitation transfer, transmission loss in metallic layer, energy dissipation or quenching of excitation at the metallic surface, and so on, in relation to the characteristic complex wave number of evanescent waves. We have analyzed the energy transmission from oscillating electric dipoles through three and four layers system including a single metallic layer. One of the remarkable results obtained is the transmission energy spectrum dependent on the thickness of dielectric layer placed between oscillating electric dipole and metallic surface, which explains the experimental results showing spectral shift and transmission energy variation depnding on the distance between fluorescent molecule and metallic surface.

REFERENCES

1. Hori, H. and T. Inoue, *Phys. Rev. A*, Vol. 63, 063805, 2001.
2. Inoue, T. and H. Hori, *Progress in Nano-electro-optics*, (in press).

Design of Metal-claded Near-field Fiber Probes with a Dispersive Body-of-revolution Finite-difference Time-domain Method

Sailing He, **Liu Liu**
Zhejiang University,China

Near-field scanning optical microscopy (NSOM) can give images of subwavelength or sub-diffraction-limited resolution, which conventional optical microscopes can not achieve [1]. A near-field optical probe is employed in an NSOM, and the size of the probe end is typically smaller than the working wavelength. When the scanning probe is placed very close (with a distance less than the working wavelength) to a sample, some optical and topographic images of the sample near the probe can be detected with subwavelength resolution. These subwavelength images can only be detected in the near field since they are carried by non-propagating waves. The near-field optical probe is the most important part of an NSOM since its structure and shape will have a significant impact on the response and resolution of the whole NSOM system. It is thus important to analyze the light propagation in an NSOM probe and make an optimal design of the probe.

a typical NSOM probe employs a tapered, metal-claded optical fiber. Such a probe has a rotational symmetry. For scattering from a structure of rotational symmetry, 3D Maxwell's equations can be discretized only along the radial and propagation directions and thus the computational effort can be reduced greatly. Such a simplified FDTD algorithm is called body-of-revolution (BOR) FDTD method in order to distinguish it from the conventional 3D FDTD method. In the present paper, a dispersive BOR FDTD method is developed to analyze the propagation of optical fields in some NSOM probes. A linearly dispersive model is incorporated to characterize the optical properties of the metal used in the NSOM probes. This dispersive BOR FDTD method is first verified for a simple structure, and then used to simulate and design some practical NSOM probes.A dispersive body-of-revolution finite-difference time-domain method is developed to simulate metal-claded near-field scanning optical microscopy (NSOM) probes. Two types of NSOM probes (aperture and plasmon NSOM probes) are analyzed and designed with this fast method. The influence of the metal-cladding thickness and the excitation mode on the performance of the NSOM probes is studied. A new scheme of illumination-mode NSOM is introduced by employing the plasmon NSOM probe with the TM01 mode excitation. Such an NSOM probe is designed, and its advantages over the conventional aperture NSOM probe are demonstrated by scanning across a metallic object.

Surface Plasmon Polaritons Computed by the Approach of an Interfacial Operator

Chien-Cheng Chang, **Ruey-Lin Chern**, **Chien-Chung Chang**
National Taiwan University, Taiwan

It has been difficult to obtain the dispersion relations for periodic structures with metallic components due to the existence of modes of surface plasmon polariton. In considering the real metal effects where the dielectric function is frequency-dependent, solution of the band structures poses a non-linear eigenvalue problem, and cannot be easily attacked by some commonly used methods such as plane wave expansions. Moreover, the localized nature of modes of surface plasmon polariton denies accurate representation by the sum of a small number of plane waves. However, a few methods have been applied for this frequency-dependent eigenvalue problem, e.g. KKR method, augmented plane waves and methods based on scattering matrices. But they have been mainly used to band computation of photonic crystals with spherical symmetries. The multiple multi-pole method is another choice, but requires a careful definition of cost function in detection of resonant frequencies. The method of looking for eigenfrequencies by detecting resonance peaks is also applicable to the finite-difference-time-domain method. In this study, we present a direct method for obtaining the modes of surface plasmon polariton. By introducing an interfacial operator in a finite difference formulation, we are able to formulate the problem for computing modes of surface plasmon polariton in the format of standard eigenvalue problems. The validity of the presently proposed approach is confirmed by comparing the numerical results and analytical results obtained for a one-dimensional periodic structure. The method is readily extended to be applicable to two-dimensional problems with several demonstrations for periodic structures with corrugated interfaces between metals and dielectric materials, and other classes of interfaces. Interesting results including mode branching and degeneracy with one-dimensional crystals, band broadening associated with corrugated surfaces, and dependence of surface plasmon bandgaps on interfaces of different metals and dielectrics and geometric parameters will be discussed.

Shaping Surface Plasmon Modes with Weakly-distorted Metallic Surfaces

Wei-Chih Liu
National Taiwan Normal University, Taiwan

The excitation of surface plasmon polariton in a plane metallic surface has been well studied and has many applications. Periodic or isolated structures on a metallic surface can modify the resonant condition and the surface plasmon modes. In this research, we studied how nano-scale surface geometry affects the properties of the surface plasmon modes and investigated the mode properties of plasmonic structures. The coordinate-transformation differential method [1,2] was used to numerically calculate surface plasmon modes in a weakly disordered metallic surface. Here an air-silver surface profile was assigned as $h\cos(K_d x)$, where $K_d = 2\pi/d$, with a nano-scale height h and a very short period d less than 100 nm. With TM polarization (the magnetic-field vector is perpendicular to the plane), the magnetic field H of a surface plasmon mode was written as $H(x, y) = e^{iKx} H_K(x, y)$, where K is the Bloch wave number and H_K is the periodic magnetic field of the surface plasmon mode associated with K. It was found that the Bloch wave numbers and field distributions of the surface plasmon modes were highly sensitive with the distortion height h of only a couple nanometers.

Surface plasmon in sinusoidal aluminum surfaces with 500 nm period at 650 nm wavelength has been studied by Popov et al[3]. At such period only slightly smaller than the wavelength, the complex Bloch wave number K changed little if h is smaller than 20 nm. On the contrary, for a weakly distorted sinusoidal silver surface with period d=50 nm at 650 nm wavelength, when h reached several nanometers, K increased rapidly and reached a resonance at $h = 6.2$ nm at the resonance condition $Re[K] = K_d/2$. Here K were much larger then the surface plasmon wave number K_{sp} of a plane silver surface and the corresponding surface plasmon mode was highly localized compared with the surface plasmon mode of the plane metallic surface. Different surface profiles exhibited different surface plasmon modes of wide variations. The exploration of these surface plasmon modes will result in the discovery of novel optical properties of both fundamental and practical importance and will help to manipulate the surface plasmons in metallic nanostructures.

REFERENCES

1. Chandezon, J., M. T. Dupuis, G. Cornet and D. Maystre, *J. Opt. Soc. Am.* Vol. 72, 839, 1982.
2. Li, L., J. Chandezon, G. Granet and J.-P. Plumey, *Appl. Opt.*, Vol. 38, 304, 1999.
3. Popov, E., L. Tsonev and D. Maystre, *J. Mod. Opt.*, Vol. 37, 379, 1990.

Optical Tunneling Effect of Surface Plasmon Polaritons: a Simulation Study Using Particles Method

Yung-Chiang Lan
National Cheng Kung University, Taiwan

The phenomenon of optical tunneling through thin metal films with periodic narrow grooves has drawn a lot of attention for its potential applications in optical and plasmonic devices [1]. This tunneling effect is attributed to excitation of surface plasmon via the periodic structure coupler at the metal surface. Traditionally, the excitation of surface plasmon polaritions (SPP) was studied by means of solving the Maxwell equations numerically, e.g. finite-difference time-domain method [2] and scattering matrix approach [3]. In these models, the electron gas in metal film is viewed as a uniform material with a complex dielectric constant described by Drude or Lorentz dispersion model and plasma frequency. But these approaches neglect the nonlinear interaction between electromagnetic fields and electron gas.

In this work, we will adopt a new viewpoint to investigate the SPP excitation. We consider the electron gas in metal as real plasma accompanied with immobile background ions and using the particle-in-cell plasma simulation method [4] to study it. The particle-in-cell method is a time-domain scheme to calculate self-consistently the interaction between electromagnetic fields and plasma particles. The fields are advanced in time at each time step. In each time step, the charged particles are moved according to the Lorentz equation using the fields advanced in each time step. The weighted charge density and current density at the grids are subsequently calculated. And then, the obtained charged density and current density are used as sources in Maxwell equations for advancing the electromagnetic fields.

Initially, the plasma is uniformly distributed in the thin silver film with periodic Gaussian-shaped grooves on both surfaces. The plasma density is assigned according to silver's plasma frequency. And a momentum collision-frequency method is employed to model the collision dissipation. Our simulation results exhibit that, for the silver film with periodic grooves in both surfaces, the TM-polarized plane waves will tunnel through the film with high transmission coefficients at some particular frequencies. The transmission coefficients become very low if the film is grooved in one side only. The plasma in the interface will be heated by the strong coupling between the light and the surface plasma. But the temperature of the plasma has little effect on the transmission coefficients and the tunneling mechanism.

REFERENCES

1. Barnes, W. L., A. Dereux and W. Ebbesen, *Nature 424*, 824, 2003.
2. Liu, W. C. and D. P. Tsai, *Phys. Rev. B 65*, 155423, 2002.
3. Hooper, I. R. and J. R. Sambles, *Phys. Rev. B 66*, 205408, 2002.
4. Birdsall, C. K. and A. B. Langdon, *Plasma Physics via Computer Simulation, IOP Press*, 1991.

Size Effects of Localized Surface Plasmon Induced by Embedded Silver Nanoparticles in Near-field Optical Disk

T. C. Chu[1], **W. C. Liu**[2], **D. P. Tsai**[1]

[1]National Taiwan University, Taiwan
[2]National Taiwan Normal University, Taiwan

As the demand of data storage capacity grows up, optical data storage technologies are driven to ultrahigh recording densities. In 1998, a multilayer structure was demonstrated to overcome the diffraction limits and subsequently was named as "super-RENS"- super-resolution near-field structure [1]. In previous studies, we found that the super-resolution capacity of the AgO_x-type super-RENS disk is related to the localized surface plasmon of silver clusters dissociated from the AgO_x layer and the complicated interactions between the nonlinear near-field optical enhancements and the subwavelength recording marks [2-5]. Metallic nanoparticles of subwavelength size exhibit numerous optical resonant phenomena relate to geometry-dependent surface plasmon resonances. These plasmon resonances are the interaction between incident electromagnetic waves and induced charges in metallic particles, and the enhanced electric field induced by plasmon resonance are confined with in a few nanometers near the surface of nanoparticles. The surface plasmon resonant behaviors are significantly affected by the size of metallic nanoparticles.

In this report, we used the two-dimensional finite-difference time-domain (FDTD) method to study the near-field properties of the AgO_x-type super-RENS disks with different sizes of silver nanoparticles embedded in the AgO_x layer. Localized enhancements were found around the edges of silver nano disks in the near fields, and the enhanced fields highly increase with the size of nano scatters. The far-field signals confirmed the super-resolution capability of the AgO_x-type Super-RENS and the far-field signals increased with the enhancements induced by nanoparticles in the near field. The behaviors of far-field signals indicated the correlation between the enhanced localized surface plasmons and the super-resolution capabilities of AgO_x-type super-RENS.

REFERENCES

1. J. Tominaga, T. Nakano and N. Atoda, *Appl. Phys. Lett.*, Vol. 73, 2078, 1998.
2. W.-C. Liu, C.-Y. Wen, K.-H. Chen, W. C. Lin and D. P. Tsai, *Appl. Phys. Lett.*, Vol. 78, 685, 2001.
3. F. H. Ho, H. H. Chang, Y. H. Lin, B.-M. Chen, S.-Y. Wang and D. P. Tsai, *Jpn. J. Appl. Phys.*, Vol. 42, 1000, 2003.
4. W.-C. Liu, Ming-Yaw Ng and D. P. Tsai, *Jpn. J. Appl. Phys.*, Vol. 43, 4713, 2003.
5. T. C. Chu, W.-C. Liu and D. P. Tsai, *Opt. Comm.*, (in press).

2D Simulation of Surface Plasmon Resonance

J.-W. Liaw[1], **M. K. Kuo**[2], **J.-K. Wang**[1,2]

[1]Industrial Technology Research Institute, Taiwan
[2]National Taiwan University, Taiwan

In the paper, interactions of an electromagnetic wave with a metallic nanoparticle in the optical range for a two-dimensional TM mode (*p*-polarization) are investigated by a set of new surface integral equations. A critical case of triangular silver is studied by the new integral equations to exhibit a strong local enhancement of the electric field at the sharp edges; the amplification of silver is around 300, which is much stronger than a dielectric nanoparticle. In addition, the surface plasmon resonance (SPR) in elliptical silver is demonstrated, and the results indicate the red shift of SPR can be caused by increasing the aspect ratio of the particle and the permittivity of the host.

Focusing the Enhanced Near-field by Manipulating the Nano-Plasmon-Driving Intensifiers

Sheng Chung Chen[1], **Tieh Ming Chang**[2], **Din Ping Tsai**[2]

[1]Far East College, Taiwan
[2]National Taiwan University, Taiwan

When light incidents on a system of the plasmonic nanoparticles, it is well known that the optical near fields will be locally enhanced by the driving of the surface plasmons, thus, we call the nanoparticle as the nano-plasmon-driving intensifier. If one can control the surges of the near fields by manipulating the configurations of the nano-plasmon-driving intensifiers, then many novel photonic devices will be able to be developed. In order to understand how to focus the enhanced near fields, we use the three-dimensional Finite-Difference Time-Domain (3D FDTD) method to investigate the distributions of the enhanced waves in the systems of the nano-plasmon-driving intensifiers.

In consideration of the spherical nano-plasmon-driving intensifiers at near-field region, we find that there are two kinds of enhancement, one is the surface mode excited by the local surface plasmons, the other is the propagating mode comes from the interferences of scattered, reflected and incident fields. The enhancement factor of the surface mode is many times than the propagating mode. The surface mode is localized, and its location is polarization-dependent. Though the surface mode can not radiate, it can be derived by coupling with another intensifiers very closely. The distributions of the propagating mode are dependent on the configurations of the particles, that is, the propagating mode could be guided. Based on the interactions of these two modes of enhancement, a near-field surge is possibly controlled by manipulating the configurations of nano-intensifiers. We will compute a series of configurations to deduce the rules of focusing enhanced near field.

Plasmon Resonances of Spherical and Ellipsoidal Nanoparticles

Jiunn-Woei Liaw
Industrial Technology Research Institute, Taiwan

M. K. Kuo, **C. N. Liao**
National Taiwan University, Taiwan

Surface plasmon resonance (SPR) of a single metallic nanoparticle is analyzed and simulated via multi-multipole method for 3D problems. The excitation, at optical frequencies, of the SPR leads to an extremely strong field in the vicinity of the nanoparticle. Numerical results indicate that a red shift of SPR is induced for an ellipsoidal nanoparticle, compared to a spherical one. Two structures of core-shelled spherical nanoparticles are also studied; one is a nanosphere of Ag shell with an oxide core, and the other one is Ag core with an oxide shell (ZrO_2 or SiO_2). Numerical results illustrate the SPR of these two core-shelled structures are quite different from each other and different from that of a solid one. It suggests that one can manipulate the optical response on demand by tuning the core/shell ratio and the permittivity of shell or core.

Session 4P3a

Special Session on Radar Polarimetry and Polarimetric SAR Interferometry

Polarimetric SAR Interferometry: Applications in Ground Based Remote Sensing of Vegetation

Zheng-Shu Zhou, **Shane R. Cloude**
University of Adelaide, Australia

The combination of imaging radar polarimetry and interferometry (called POLInSAR) is a promising new technology for the quantitative remote sensing of vegetated land surfaces. Originally developed using space-borne SIR-C data it has more recently been successfully applied to the estimation of forest height and biomass using L-band airborne sensors [1, 2].

In this talk we consider application of this technology to ground based radar imaging. Such a facility has a limited field of view but provides wide band coverage with none of the problems of poor temporal sampling associated with space sensors. In this way it can potentially be used to monitor vegetation dynamics and extract parameters such as growth rates, plant water content and surface moisture with high spatial and temporal resolution.

To demonstrate this potential, we show analysis of the estimation of vegetation structure parameters for maize plants using data from the European Microwave Scattering Laboratory (EMSL) and conclude with a survey of possible future developments and research trends. We also outline our proposed ground based (GB-POLInSAR) activities at the University of Adelaide.

REFERENCES

1. Papathanassiou, K. P., S. R. Cloude, "Single Baseline Polarimetric SAR Interferometry", *IEEE Transactions Geoscience and Remote Sensing*, Vol. 39/11, 2352, November 2001.
2. Cloude, S. R., K. P. Papathanassiou, "A 3-Stage Inversion Process for Polarimetric SAR Interferometry", *IEE Proceedings, Radar, Sonar and Navigation*, Vol. 150/03, 125, June 2003.

The Dependence of Forest Biomass on the Order Parameter of K-distribution of High-resolution Airborne Polarimetric SAR Images of Forests

Haipeng Wang[1], **Kazuo Ouchi**[1], **Manabu Watanabe**[2]
Masanobu Shimada[2], **Takeo Tadono**[2], **Ake Rosenqvist**[2]
Shakil Ahmad Romshoo[3], **Masayuki Matsuoka**[4], **Seiho Uratsuka**[5]

[1]Kochi University of Technology, Japan
[2]Japan Aerospace Exploration Agency, Japan
[3]The Energy and Resources Institute, India
[4]Research Institute for Humanity and Nature, Japan
[5]National Institute of Information and Communications Technology, Japan

The purpose of this paper is to quantify the relation between the Pi-SAR polarimetric data and the parameters of the Tomakomai forests in Hokkaido, Japan; and the present paper is a summary of the results based on the data acquired in November, 2002 and August, 2003. It is found that there are fairly well-defined relations between RCS (radar cross section) and tree biomass, and "age" of trees within certain ranges. At X-band, the VV-polarization images are found to show largest RCS, followed by HH- and cross-polarization images. While at L-band, the HH-polarization images have the largest RCS followed by VV- and cross-polarization. The X-band RCS increases with biomass and saturates at about 20 tons/ha; and the saturation limit of L-band RCS is about 40 tons/ha. These saturation values are in agreement with the result of several previous results [e.g. 1,2].

Close inspection indicates that the high-resolution L-band Pi-SAR images of the Tomakomai forests do not simply consist of classical Gaussian speckle, but rather the image fluctuations are "textured" and appear to obey non-Gaussian statistics. These textures reflect the structures of individual trees, and as such they contain information on the scattering objects. Thus, a statistical analysisis is carried out to investigate the relation between the non-Gaussian statistical properties of Pi-SAR images and tree parameters. A preliminary result indicates that the K-distribution is found to fit best to the image amplitudes, though Weibull distribution equally fits well [3]. The order parameter of K-distribution tends to increase with biomass and age for all polarizations. In particular, there is a strong correlation between the tree biomass and the order parameter of the cross-polarization data than co-polarization data. It is also found that X-band data show weaker statistical dependencies on the tree parameters than L-band data [4].

REFERENCES

1. Toan, T. L., A. Beaudoin, J. Riom and D. Guyon, "Relating Forest Biomass to SAR Data," *IEEE Trans. Geosci. Remote Sens.*, Vol. 30, 402, 1992.
2. Imhoff, M. L., "Radar Backscatter and Biomass Saturation: Ramifications for Global Biomass Inventory," *IEEE Trans. Geosci. Remote Sens.*, Vol.33, 511, 1995.
3. Sekine, M. and Y. H. Mao, *Weibull Radar Clutter, Peter Peregrinus Ltd.: London, United Kingdom*, 1990.
4. Wang, H., K. Ouchi, M. Watanabe, M. Shimada, T. Tadono, A. Rosenqvist, S. A. Romshoo, M. Matsuoka and S. Uratsuka, "On the Quantitative Relation between Tree Parameters and Pi-SAR Polarimetric Data over the Tomakomai Forests: Preliminary Results," *Proc. 37th Japanese Conf. Remote Sens., Hitachi*, 61, 2005.

On the Need of Developing Multi-band Differental (Multiple Pass) POLinSAR Theory and Algorithms for Remote Sensing and Monitoring Severe Environment Stress Changes (Disarters)-Such as Earthqukes, Severe Storms, Typhoons and Floods

Wolfgang-Martin Boerner, **Jorge J. Morisaki**
University of Illinois at Chicago, U.S.A.

Alberto Moreira, **Kostas P. Papathanassiou**, **Irena Hajnsek**
DLR (German Aerospace Centre), Germany

Eric Pottier, **Laurent Ferro-Famil**, **Andreas Reigber**
IETR, UMR CNRS-6164, France

Motoyuki Sato, **Takeshi Hamasaki**, **Koichi Iribe**
Tohoku University, Japan

Shane R. Cloude, **Zheng-Shu Zhou**
University of Adelaide, Australia

Yoshio Yamaguchi, **Hiroyoshi Yamada**
Niigata University, Japan

Jong-Sen Lee, **Tom L. Ainsworth**, **Dale L. Schuler**, **Mitchell Grunes**
Naval Research Laboratory (NRL), U.S.A.

Kun-Shan Chen, **Chih-Tien Wang**, **Chung-Pai Chang**
National Central University, Taiwan

Jeffrey K. Weissel, **Kristina Rodriguez-Czuchlewski**
Columbia University, U.S.A.

Wooil Moon, **Sang-Eun Park**
Seoul National University, Korea

Joong-Sun Won, **Seung-Kuk Lee**
Yonsei University, Korea

Worldwide, medium- to short-term earthquake prediction is becoming ever more essential for safeguarding man due to an un-abating population increase, but hitherto there have been no verifiable methods of reliable earthquake prediction developed - except for a few isolated examples. In comparing the various approaches and especially the local tectonically active regions within which the current studies are being conducted, based on the extensive travels with site assessment, currently Taiwan ranks out to be the best and ideally suited compact region for conducting such "*integrated Searches for Earthquake Precursor Signatures*", and for setting up the pertinent ground-based metrological networks plus conducting aeronomic and satellite imaging studies. The work performed in Taiwan hitherto is well reviewed on the URL of their ongoing 4-year study [http://www.ss.ncu.edu.tw/ istep]. In comparison with other suitable sites, it was found that Taiwan is ideally and best suited for studying ERPS. In this context the development of complete Differential Repeat-Pass POLinSAR theory, algorithm development and surface change assessment become of highest urgency as may be verified with the 1999 Chi-chi (September 21: M = 7.4) and Chai-Yi (October 23, M = 6.8) earthquakes and the subsequent catastrophic mud-slides during two major typhoons of April and July 2004.

On the Need of Development High-Altitude Drones (UAVs) for Implementation of Multi-band Single and Multiple Pass Differential POLinSAR Technology towards in Situ Montoring of Severe Environmental Stress Changes

Wolfgang-Martin Boerner, **Jorge J. Morisaki**
University of Illinois at Chicago, USA

Alberto Moreira, **Kostas P. Papathanassiou**, **Irena Hajnsek**
DLR (German Aerospace Centre), Germany

Eric Pottier, **Laurent Ferro-Famil**, **Andreas Reigber**
IETR, UMR CNRS-6164, France

Motoyuki Sato, **Takeshi Hamasaki**, **Koichi Iribe**
Tohoku University, Japan

Yoshio Yamaguchi, **Hiroyoshi Yamada**
Niigata University, Japan

Shane Cloude, **Zheng-Shu Zhou**
University of Adelaide, Australia

Jong-Sen Lee, **Tom L. Ainsworth**, **Dale L. Schuler**, **Mitchell Grunes**
Naval Research Laboratory (NRL), USA

Kun-Shan Chen, **Chih-Tien Wang**, **Chung-Pai Chang**
National Central University, Taiwan

Jeffrey K. Weissel, **Kristina Rodriguez-Czuchlewski**
Columbia University, USA

Wooil Moon, **Sang-Eun Park**
Seoul National University, Korea

Joong-Sun Won, **Seung-Kuk Lee**
Yonsei University, Korea

In this overview, reasons are provided on why we do need to place multi-modal, multi-band single and multiple pass POLinSAR monitoring platforms next to space and lower altitudes at highest possible altitudes. The questions "*on what POLinSAR monitoring can provide that POL-SAR and IN-SAR by themselves cannot accomplish*" is assessed; whereupon facts and justifications on developing Differential Repeat-Pass POL-IN-SAR platforms on high-altitude drones and/or UAVs are provided. Reasons for this technology becoming a basic requirement for current, near-future and much more so for future *all-day & night year around* monitoring of severe abrupt environmental stress changes - such as earthquakes, typhoons, severe storms, landslides, floods, and so on - within the terrestrial covers are analyzed in view of the un-abating and uncontrollable terrestrial population explosion, which is going to continue on a global although not necessarily localized scale.

Session 4P3b

Remote Sensing of Ionosphere and Ocean

The Survey of Ionospheric Scattering Function

Zhengyu Zhao, **Gang Chen**
Wuhan University, China

Because of its advantages, such as broad sounding range and real-time sounding, etc, ionospheric oblique back sounding has been regarded as one of the most important ionospheric sounding means. Just one ionospheric oblique back sounding instrument is able to provide the information of ionospheric and oceanic state within a radius of thousands of kilometers. Up to now, there is no other ground-based measurement techniques, which can cover such broad ionosphere, land and ocean. Ionospheric oblique back sounding is capable to get ionospheric state as well as features of HF back scatting channel in real-time and the whole information of features will be shown by the Frequency-Time delay-Amplitude 3D graphics in the form of scattering function. The Doppler frequency shift f_d, the multidiameter spread according to time and channel fading can be obtained directly by surveying the scattering function of the HF channel. Consequently, under the conditions of a particular time and in a certain HF channel determined by antenna tilt, the area covered and scattering echo amplitude of the given frequency radio wave can be achieved, and then the channel quality can be diagnosed correctly.

The new type ionospheric oblique back sounding system (IOBSS) developed by Wuhan University put pseudo-random phase-coded pulse compression in use. This system, compared with traditional oblique back sounding radar can not only get general ionospheric oblique back sounding information (front edge of echo, MUF, $P' - f$ curve, etc), more importantly, but also get ionospheric bi-time response, scattering function, and the valuable engineering information about ionospheric Doppler frequency shift in real-time.

One example of the sounding results by IOBSS is shown in the following:

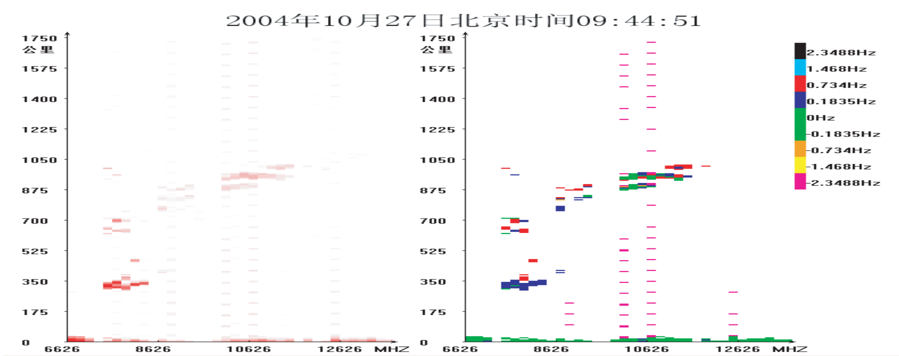

Left figure: Distance-Frequency-Amplitude $(P' - f - A)$
Right igure: Distance-Frequency-Doppler frequency shift$(P' - f - f_d)$

Radioemission by a Modulated Electron Beam Injected into the Ionosphere from Spacecraft

Yong Yang, **Zhengyu Zhao**
Wuhan University, China

I. O. Anisimov
Taras Shevchenko National University of Kyiv, Ukraine

Excitation of electromagnetic waves occurs when modulated electron beams are injected into anisotropic plasma. This phenomenon has been observed in both space and laboratory experiments. A possible mechanism to produce this excitation is transition radiation on the metal-plasma border, e.g. injecting the beam along the geomagnetic field. Transition radiation has been studied in laboratory experiments, where the transverse length of the formation zone of the transition radiation is considerably small relative to the dimensions of the injector. In this paper, we address the opposite case which is typical of ionosphere experiments. It corresponds to the radiation caused by the longitudinal restriction of the beam.

Cylindrical semi-restricted thin modulated electron beam with radius a is injected from the spacecraft board into the ionosphere plasma along the geomagnetic field. The density of the beam decreases exponentially along z-axis with.

Pointing vector was calculated numerically with typical parameters in ionosphere ($\omega = 2 \cdot 10^6 rad/s$, $\omega_H = 7 \cdot 10^6 rad/s$, $\omega_p = 6 \cdot 10^7 rad/s$) when frequencies fall into the whistler band ($\omega_p \gg \omega_H \gg \omega$). In these conditions, all the three modes corresponding to the stationary phase points are present at small angles. Fig.1 shows the angular dependence of the Pointing vector. Interference between the three modes with different wave numbers results in the oscillatory radiation pattern at these small angles.

For the angles larger than some critical value, two of the stationary phase points vanish and the directivity diagram is determined by one mode. As a result, the angular dependence of the Pointing vector increases monotonically with the angle. Fig. 2 shows the angular dependence in a wide band of angles. One can see that the radiation efficiency greatly increases near the angle of the resonant cone. Therefore, the radiation at smaller angles shown in Fig. 1 becomes negligible. Radioemission at even larger angles falls into the resonant cone and vanishes. Fig. 2 proved that the radiation pattern has a sharp peak when the Cherenkov resonance condition for the beam modulation wave number χ is satisfied.

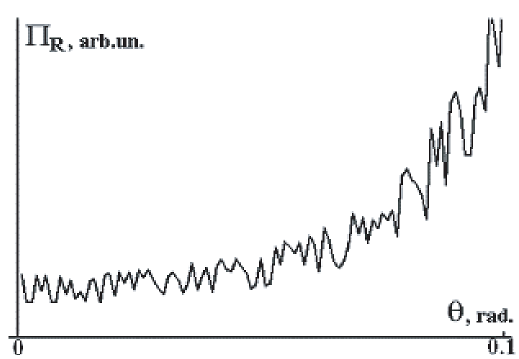

Figure 1

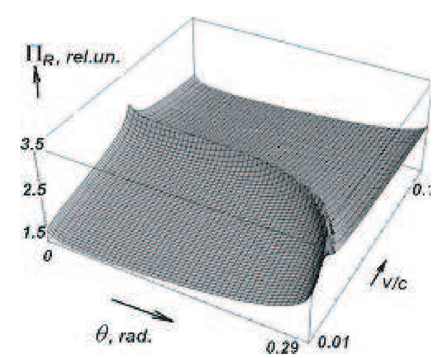

Figure 2

The Approach Based on Cumulant of Received Signals' Increment in Spaced Antenna Wind Measurements

Weiping Shu, **Zhengyu Zhao**
Wuhan University, China

This paper presents an approach to measure wind field with cumulant of spaced antenna Radar signals increment for the best estimates of real wind field on the nonlinear and non-stationary conditions. It results from structure-function-based approach to decrease the non-stationary effect and uses the characteristics of the high order cumulant in signal processing to remove Gaussian noise and detect nonlinear process. The procedure and parameters of the approach are described and discussed in the paper. One can get mean horizontal wind speed and turbulence characteristics of scattering medium with zero-lag cumulant of increment. The computer simulations based on atmospheric scattering model are in agreement with theoretical investigations well. Theoretical analysis and simulations show that the approach can be adaptable to locally stationary and/or homogeneous random process and fields; the too long or too short sample time will bring great estimation errors, but the former more remarkable. It is also concluded that the approach is more suitable for large mean horizontal wind speed and the estimate of the mean horizontal speed is not very sensitive to the size of spaced antennas. The high order ($k \geq 3$) cumulant of increment are proposed to study the nonlinear interactions between atmospheric waves and high order estimations of turbulence characteristics, which can not be obtained from the general 2^{nd} order methods (Full Correlation Analysis in time domain and Full Spectral Analysis in frequency domain).

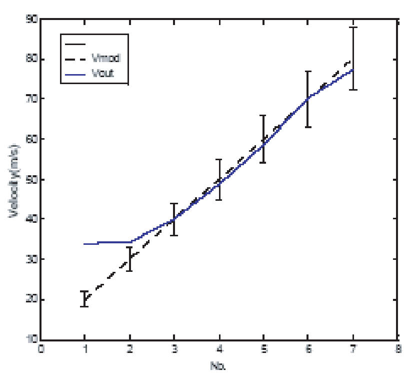

Figure 1: the comparison of input model mean speed (solid line) and simulation results (dashed line) when one can simulate with different input model mean speed. The X and Y axes denote respectively the number of simulation test and velocity. The error bars (10%) indicate the standard deviation of input speed.

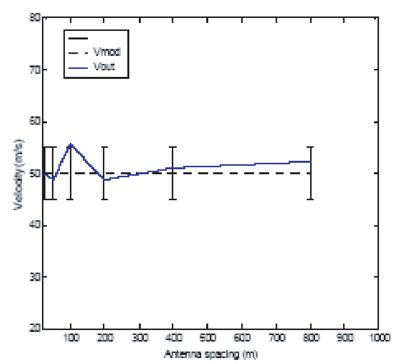

Figure 2: the comparison of input model mean speed (solid line) and simulation results (dashed line) when one can simulate with different spacing of spaced antenna. The X and Y axes denote respectively the spacing of spaced antenna and velocity. The error bars (10%)indicate the standard deviation of input speed.

Mars Advanced Radar for Subsurface and Ionosphere Sounding (MARSIS)

G. Picardi[1], **R. Seu**[1], **J. Plaut**[2], **W. T. K. Johnson**[2]
R. Orosei[3], **O. Bombaci**[4], **D. Calabrese**[4], **E. Zampolini**[4]

[1]University of Rome, Italy
[2]Jet Propulsion Laboratory, U.S.A.
[3]CNR/IAS, Italy
[4]Alenia Spazio ALS, Italy

According to the Mars Express mission, the MARSIS primary *scientific objectives* are to *map the distribution of water, both liquid and solid, in the upper portions of the crust of Mars.* Detection of such reservoirs of water will address key issues in the hydrologic, geologic, climatic and possible biologic evolution of Mars, including the current and past global inventory of water, mechanisms of transport and storage of water.

Three *secondary objectives* are defined for the MARSIS experiment: *subsurface geologic probing, surface characterization, and ionosphere sounding.*

According to the previous scientific objectives, this paper provides a description of the design approach and expected performances of the MARSIS.

The principle of operation of MARSIS the following: the transmitted radar pulse will reach the top of the Mars surface producing a first reflection echo which propagates backward to the radar. However, due to the long wavelengths employed, a significant fraction of the e.m. energy impinging on the surface is transmitted into the crust and propagates downward. Additional reflections, due to subsurface dielectric discontinuities, will occur and the relevant echoes will propagate backward to the radar. As consequence time domain analysis of the strong surface return, eventually after multi-look non-coherent integration, will allow estimation of surface roughness, reflectivity and mean distance, just like in classical pulse limited surface radar altimeters. The presence of weaker signals after the first strong surface return will enable the detection of subsurface interfaces, while the estimation of their time delay from the first surface signal will allow the measurement of the depth of the detected interfaces.

The detection of these subsurface echoes is limited by the surface echoes (especially if surfaces are rough), for this reason three different methods was implemented in MARSIS: Doppler Beam Sharpening, Secondary Monopole Antenna, and Dual Frequency Processing.

Finally, the Marsis frequency-agile design will allow to tune the sounding parameters in response to changes in sun illumination condition, latitude etc., allowing global coverage to be achieved within the currently accepted Mars Express baseline orbit and mission duration.

A Study on the Relation between Ocean Surface Coherence Time and Speckle Cross-correlation in Multilook SAR Images Produced by Partially Overlapped Subapertures

Haipeng Wang, **Kazuo Ouchi**
Kochi University of Technology, Japan

The purpose of multilook processing of SAR data is to equalize the resolution in both the range and azimuth directions, and more importantly, to reduce speckle noise by adding the multilook images on an intensity basis. This technique of speckle reduction is based on the assumption that the speckle patterns are uncorrelated [1]. In general, multilook images are produced by processing the SAR raw data using two or more non-overlapping subapertures, so that the corresponding speckle patterns are not correlated with each other. For the case of sea surface, small-scale waves are principal scattering elements; and these waves have decorrelation times that are shorter (about 0.05-0.1s) than the SAR integration times (order of 0.5-2s) [2]. The inter-look speckle patterns may then decorrelate at time separation of sea surface coherence (decorrelation) times, and it may be possible to produce multilook images with uncorrelated speckle patterns by using partially overlapped subapertures whose center times are separated by the scene coherence time [3].

Thus, the purpose of this paper is to investigate the dependence of the sea surface coherence time on the inter-look CCF (cross-correlation function) of Gaussian speckle patterns produced by partially overlapped subapertures. In the first part of the paper, a general integral expression is derived and discussed for the CCF of speckle patterns in the SAR images of randomly moving sea surfaces processed by using partially overlapped subapertures of arbitrary Doppler center frequencies (or equivalent azimuth times). With theassumption of the white noise approximation for the backscattered field, it is shown that the CCF of the interlook Gaussian speckle intensity patterns is given by the squared modulus of the autocorrelation function of the amplitude weighting function of subapertures, where the time lag is the center time difference. It is also shown that the interlook CCF of Gaussian speckle is independent of the surface coherence time of sea surface [4]. The integral expression for the intensity CCF is then evaluated for a rectangular weighting function to illustrate the dependence of CCF on the interlook time difference. To verify our theory, experiments were carried out by using JERS-1 L-band and RADARSAR-1 C-band SAR data. The CCFs computed from the JERS-1 SAR data show excellent agreement with the theory, and good agreement is obtained by the RADARSAT-1 data [5].

REFERENCES

1. Goodman, J. W., "Statistical Properties of Laser Speckle Patterns," *Laser Speckle and Related Phenomena (ed. J.C.Dainty)*, 19, 1975.
2. Crande, R. E., "Estimating Ocean Coherence Time Using Dual-baseline Interferometric Synthetic Aperture Radar," *IEEE Trans. Geosci. Remote Sens.*, Vol. 32, 846, 1994.
3. Raney, R. K. and P. W. Vachon, "Synthetic Aperture Radar Imaging of Ocean Waves from an Airborne Platform: Focus and Tracking Issues," *J. Geophy. Res.*, Vol. 93, C 10, 12,475, 1988.
4. Ouchi, K. and R. E. Burge, "Speckle Cross-correlation Function in Multilook SAR Images of Moving Discrete Scatterers," *Int. J. Remote Sens.*, Vol. 12, 1933, 1991.
5. Ouchi, K. and H. Wang, "Interlook Cross-correlation Function of Speckle in SAR Images of Sea Surface Processed with Partially Overlapped Subapertures," *IEEE Trans. Geosci. remote Sens.(accepted for publication)*, 2005.

Two-dimensional Ocean Surface Doppler Spectrum at Microwave Frequency

G. Soriano[1], **M. Joelson**[2], **M. Saillard**[3]

[1]Université Paul Cézanne, France
[2]Université d'Avignon, France
[3]Université du Sud Toulon-Var, France

Previous numerical simulations on one-dimensional surfaces have shown that the non-linear aspect of the ocean surface is of prime importance in the Doppler spectrum of the backscattered signal [1,2]. We look into extending these studies to two dimensional surfaces.

Time-harmonic integral equation-based numerical method that provides exact evaluation of the scattered field has recently known rapid progress, and their use has been extended to Monte Carlo Doppler simulations. However, grazing angles are reached only through hundred wavelength-long enlightened surfaces. Multiple numerical solution of the complete integral equation for such two-dimensional surfaces would be prohibitive in both computer time and central memory. As the ocean surface shows moderate slopes, a Meecham-Lysanov approach can be applied, resulting in an approximate integral equation [3]. This equation can be solved at a numerical cost of order $N\log_2(N)$, where N is the number of surface unknowns.

Rough surfaces generation for Monte Carlo simulations has never been a difficulty compared to the solution of Maxwell equations, until today. As a matter of fact, the ocean surface is both multi-scale and non-linear. The simplest models for this surface are the Barrick and Weber second order perturbative model [4] and the Creamer et al. non-linear surface model [5]. Since their numerical cost is of order N^2, they cannot be applied efficiently to two-dimensional surfaces. We have expanded the Creamer formula as a series with respect to the linear surface, up to second order. With such a development, we generate non linear ocean surface samples at a numerical cost of order $N\log_2(N)$.

At Ultra High Frequency, the empirical ocean surface spectra cannot be used to generate the linear part of ocean surface profile. Indeed, the resulting non-linear surface would exhibit unrealistic height and slope root mean squares. The ocean spectrum has to be *undressed* of its non-linear part before it can be used to generate a linear surface. We present comparisons of Doppler spectra obtained on linear and on non-linear, *dressed and undressed*, ocean surfaces.

This work is motivated by experimental measurements of ocean surface Doppler using a coastal radar at L band in December 2003 and in December 2004 at *Batterie de la Renardière* near Toulon, Var, France.

REFERENCES

1. Toporkov, J. V., G. S. Brown, "Numerical of Scattering from Time-varying, Randomly Rough Surfaces," *IEEE Trans. G.R.S*, Vol. 38, 1616, 2000.
2. Johnson, J. T., J. V. Toporkov, G. S. Brown, "A Numerical Study of Backscattering from Time-evolving Sea Surfaces: Comparison of Hydrodynamic Models," *IEEE Trans. G.R.S*, Vol. 39, 2411, 2001.
3. Saillard, M., G. Soriano, "Fast Numerical Solution for Scattering from Rough Surfaces with Small Slopes," *IEEE Trans. Antennas Propag*, vol. 52, 2799, 2004.
4. Barrick, D.E. and B.L. Weber, "On the Nonlinear Theory for Gravity Waves on the Ocean's Surface. Part II: Interpretation and Applications," *J. Phys. Oceanogr*, Vol. 7, 11, 1977.
5. Creamer, D .B., F. Henyey, R. Schult, J. Wright, "Improved Linear Representation of Ocean Surface Waves," *J. Fluid Mech*, Vol. 205, 135, 1989.

Focusing Infrared Beams Out of Sea Surface Found in Satellite Thermal Pattern in the Ocean

Shigehisa Nakamura
Kyoto University, Japan

This is a note to a passive signal of local sir-sea interaction in the satellite thermal pattern in the ocean directly monitored at a station. A satellite signal was directly received by a set consisting a cross-bar antenna and a personal computer. Normal operation of this monitoring gave us to see what could be a dynamical background of focusing infrared beams out of the sea surface must be noticed.

Numerical Simulation of Concentration Field Distribution of Non-corona High-Temperature Electrostatic Cyclone Precipitation

Guanghua Tang, **Shiming Wang**
South East University, China

Zhongzhu Gu
Nanjing Normal University, China

With the increasing development of technology and consciousness of protecting environment, the technology of high-temperature precipitation is more and more widely used. Though moving granular bed filter and cyclone dust catcher are mainly used abroad for high-temperature dust removal, for their limitations especially the weak performance of removing microparticles, people are seeking an innovative technique for cleaning up high-temperature flue gasesnon-corona high-temperature electrostatic cyclone precipitation which has the advantage of low resistance, high current density and high efficiency etc. It utilizes the negative electrode made of some particular material which emits a large number of electrons when heated, instead of the corona discharge in traditional ESP, to charge dust particles.

Based on similar experimental results by others, numerical simulations on dust charging, particle diffusion, flue gas flow and ash collection are completed. The influence of variables including temperature, pressure, voltage, flow velocity, particle concentration in flow, dust resistance and its diameter on ash collection effect is theoretically analyzed. In the article, the author mainly gives the flow field and concentration field distribution in different conditions such as change the inlet velocity and the voltage of removing particles using RSM(second-moment Reynolds stress model)and SIMPLEC methodology (Semi-Implicit Method for Pressure Linked Equation consistent) considering the high anisotropy. By comparing with concentration field in different conditions and study the particle tracks and the particle distribution of different diameters, we can more reasonably design the configuration of dust catcher and the dimension and position of the electron emitting pole and most of importance and then we can improve the efficiency of dust catcher.

Session 4P4a

NIM & EBG

Simulation of a Novel Structure for Two-dimensional Left-handed Material

Jiangtao Huangfu, **Lixin Ran**, **Hongsheng Chen**
Xianmin Zhang, **Jin Au Kong**
Zhejiang University, China

In this paper, a design for two-dimensional left-handed material is introducted. The unit cells used to construct two-dimensional left-handed metamaterial generally composed of one rod and several SRRs to produce negative permittivity in one direction and negative permeabilities in other two directions. In figure 1, we present a different unit cell, which is constructed by four folded Ω-like metal strips.

When an eletromagnetic wave is incident upon such structure, electrical resonance occurs when the electric field is along the Z direction and the magnetic resonance occurs when the magnetic field is located in the X-Y plane. The inductive currents in the metal strips can be easily coupled into nearby loops via the small gaps between the four loops. In such a way, this unit cell works equivalently to the two one-dimensional left-handed material we have reported, and therefore can exhibit two-dimensional left-handed properties.

In Figure 1, the width of the strip is 0.6 mm, the radius of the loop is 1.5 mm, the gaps between loops are 0.4mm, the height of the unit cell is 5 mm, and the periods of the cell are 5mm in X and Y direction, respectively.

Figure 2 shows power transmission simulation results. For a metamaterial composed of 5×5 unit cells, for a wave incident along along X or Y direction, a passband due to LH property can be found at 7 to 8 GHz frequency band.

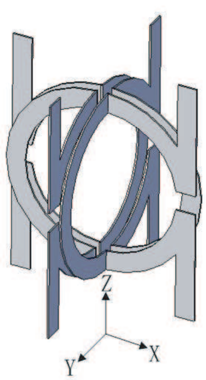

Figure 1: The unit cell.

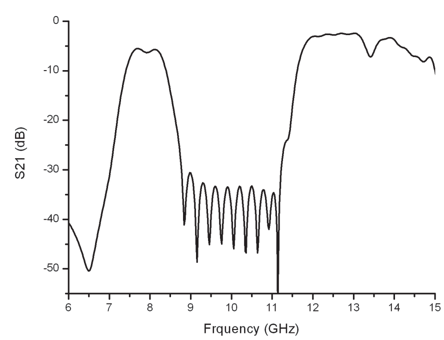

Figure 2: Power transmission simulation.

A Microwave Coupler Filled with Left-handed Material

Yu Yuan, **Lixin Ran**, **Hongsheng Chen**, **Jiangtao Huangfu**
Dongxing Wang, **Xianmin Zhang**, **Jin Au Kong**
Zhejiang University, China

In this paper, we design and fabricate a microwave coupler by filling left-handed and right-handed material samples into a rectangular waveguide based coupler, as shown in Fig.1, where the electromagnetic wave is fed into port 1, propagates in the waveguide filled with left-handed material and then edge-coupled into a waveguide filled with right-handed material. The left-handed material is composed of the S-shaped resonator that exhibits negative index of refraction in the frequency band of 11$\sim$13 GHz. At the interface of the right-handed material and the left-handed material, the wave vectors within both layers have the same directions due to phase matching conditions but the Poynting vectors are contra-directional, which lead to backward coupling. Measurements show that the power detected in port 3 is about 8 dB larger that that detected in port 4, in 11$\sim$13 GHz.

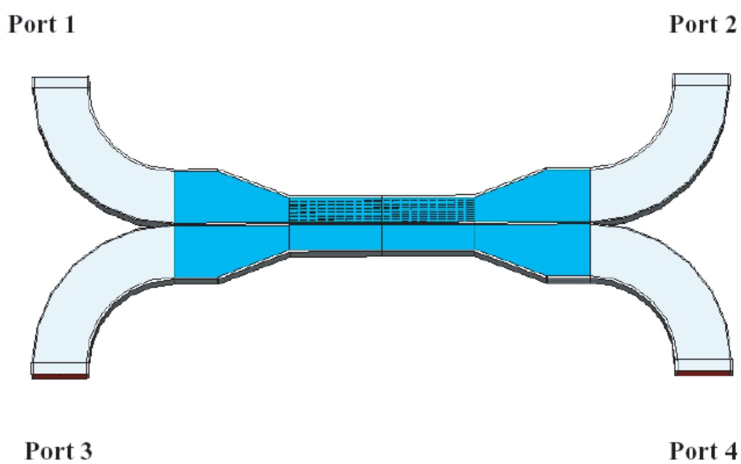

Figure 1: Backward waveguide coupler using left-handed material

Direct Measurement of Negative Permittivity and Permeability of a Left-handed Material

Dongxing Wang[1], **Jiangtao Huangfu**[1], **Hongsheng Chen**[1], **Lixin Ran**[1], **Yu Zhong**[1]
Xianmin Zhang[1], **T. M. Grzegorczyk**[2], **Jin Au Kong**[1,2]

[1]Zhejiang University, China
[2]Massachusetts Institute of Technology, U.S.A.

The measurement of the negative effective permittivity and permeability of a left-handed material is a direct way to verify its left-handed property, and is the basis for more applications of left-handed material. In this paper, a transmission experiment for a left-handed material sample is performed. The effective permittivity and permeability are retrieved from the experimental S_{11}, S_{21} data. The results show that in the frequency range of negative refraction, the effective permittivity and permeability are simultaneously negative.

Figure 1 shows the experimental S_{11} and S_{21} of the LHM sample in 8GHz-10Ghz

Figure 2 shows the experimental retrieval results of effective permittivity and permeability of the LHM sample

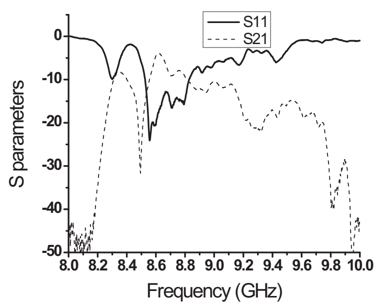

Figure 1: The S_{11} and S_{21} of the LHM sample

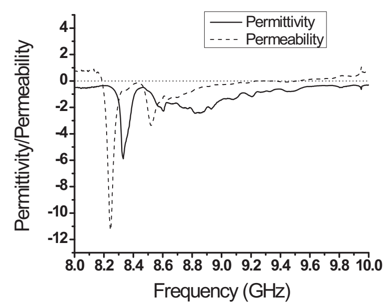

Figure 2: The experimental retrieval results of effective permittivity and permeability of the LHM sample

Analysis of Radiation Characteristics for Step Discontinuity in Planar Left-handed Waveguide

Xiaobo Wang, **Shanjia Xu**
University of Science & Technology of China, China

The radiation characteristics of step discontinuity in planar left-handed waveguide as shown in Fig. 1 are analyzed by a method, which combines the rigorous mode-match method with the multi-mode network theory. Unlike the conventional method to treat the radiation as a "source-field" problem, in the present approach the radiation problem is transferred to the propagation problem of a series of surface and space waves from the viewpoint of scattering. The dispersion property of the grounded planar left-handed waveguide is carefully examined. It can be found from the dispersion curve given in Fig. 2 that in a lower frequency band the propagation constant β is negative or the phase velocity of the wave is negative which indicates that in this frequency band the discontinuity structure appears the left-handed characteristics. In this case, the radiation pattern should be in the backward direction. On the other hand, as increasing of frequency the dispersion curve enters a right-handed region in which the propagation constant β and the phase velocity of the wave are both positive; then the radiation pattern should be in the forward direction. Fig. 3 clearly shows the relationship between the dispersion curve and the radiation pattern. When the frequency is respectively 40GHz, 43GHz and 45 GHz, which is in the left-handed region and the stepped structure radiates backward. With increase of frequency, at 55GHz, 60GHz and 65 GHz, β is positive and the left-handed discontinuity structure is operating in the right-handed region so that the radiation pattern is in the normal forward direction.

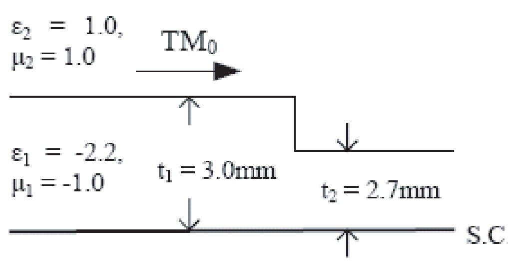

Figure 1: Step discontinuity in planar left-handed waveguide

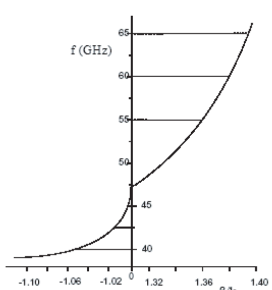

Figure 2: Dispersion curve of the stepped structure

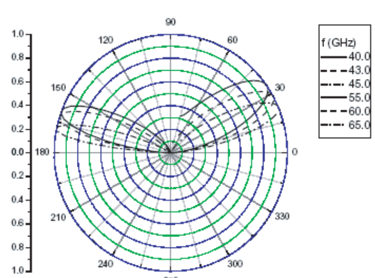

Figure 3: Radiation patterns at different frequency

*Supported by the National Natural Science Foundation of China (No. 60471037) and (No: 60371010).

Session 4P4b

Electromagnetic Theory 2

Accurate Numerical Modeling Method for Ceramic/Polymer Composites

L. Jylhä[1], **J. Honkamo**[2], **H. Jantunen**[2], **A. Sihvola**[1]

[1]Helsinki University of Technology, Finland
[2]University of Oulu, Finland

Effective permittivity was modeled and measured for composites (Fig.1) that consist of up to 35 Vol.% of Titanium dioxide powder dispersed in a continuous epoxy matrix. The study demonstrates a method that enables fast and accurate numerical modeling of the effective permittivity values of ceramic/polymer composites. The model is based on the accurate modeling of the finestructure of the composite. The elementary shape of inclusions is calculated from the lattice structure of Titanium dioxide in rutile phase.

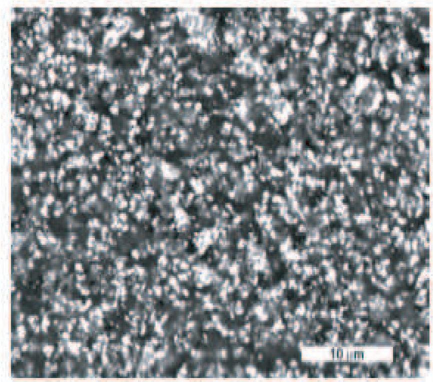

Figure 1: Microstructural image of ceramic/epoxy composites with a ceramic loading of 25 vol. %.

The method requires electrostatic Monte-Carlo simulations, where randomly oriented homogeneous prism-shaped inclusions occupy random positions in the background phase.

The computation costs of solving the electrostatic problem by a finite-element code is decreased by the use of an averaging method[1] where the same simulated sample is solved three times with orthogonal field directions. This helps to minimize the artificial anisotropy that results from the pseudo-randomness inherent in the limited computational domains. It also allows to reduce the size of the computation domain, then the finestructure can be modeled accurately. The same method could also be used with other numerical techniques.

The results show significantly better agreement with measurements compared with the predictions of basic effective medium models. They are in a good agreement with measruements in all volume fractions, because of the accurate modeling of the finestructure.

REFERENCES

1. Jylhä, L. and A. Sihvola, "Numerical Modeling of Disordered Mixture Using Pseudorandom Simulations", *IEEE Transactions on Geoscience and Remote Sensing*, Vol. 43, No. 1, 2005.

A Single Arm Phase Tracking Interferometer Based on a Plate Beamsplitter-Quarter Waveplate Combination and Using a Linearlyn Polarized Source

G. P. Riblet
Microwave Development Laboratories, Inc., U.S.A.

With the conventional Michelson interferometer, which uses an unpolarized light source, only the transmitted power P_t is detected. There is no point detecting the power reflected back to the source P_r since it cannot provide additional information. The situation changes if a polarized source is used however. Recently, a novel phase tracking interferometer which used a linearly polarized source and two detectors was described [1]. It was based on a polarizing cube beamsplitter-quarter waveplate combination. Let θ be the phase difference of the paths in the two arms of the interferometer. It was demonstrated experimentally that if the power measured in one of the transmitted polarization states has a $\cos\theta$ dependence, then the power measured in one of the reflected polarization states may have a $\sin\theta$ dependence. In this way the phase ambiguity inherent in the Michelson interferometer can be resolved.

In the experimental interferometer roof mirrors may be used in the secondary arms to reflect waves with E vectors polarized at 45° to the S and P directions of the cube beamsplitter [1]. Wire grid mirrors with the grid wires oriented at 45° to the S and P directions could also be used. Such mirrors which work in the optical portion of the spectrum have recently become commercially available. The thought occurred to me to use one such wire grid mirror in front of a standard mirror in one arm of the interferometer only. The phase difference θ then becomes that due to the small path difference between these closely spaced mirrors! Further investigation showed that this approach won't work if a polarizing cube beamsplitter is used. However, it has been determined that this concept can be employed if the beamsplitter cube is replaced by a non-polarizing plate beamsplitter.

An experimental single arm phase tracking interferometer has been constructed using inexpensive optical components. The linearly polarized diode laser of the previous experiment was used. The beam is split now by a non-polarizing plate beamsplitter. A commercial wire grid linear polarizer (420–700 nm) is included in one arm of the interferometer as a mirror. A standard mirror is adjusted to within one coherence length behind it. This mirror is aligned to provide beam overlap with the beam reflected by the wire grid mirror. A PZT is used to vary the separation of the mirrors over a half wave length. The overlapping beams in the transmitted direction pass through a quarter waveplate as in the original experiment. The rest of the experimental arrangement, including the two detectors to measure the powers P_t and P_r also duplicates that of the original experiment. By applying the two resulting voltages to the X and Y axis of an oscilloscope, the phase tracking feature of this novel single arm interferometer has been confirmed.

REFERENCES

1. Riblet, G. P., "A Compact Phase Tracking Interferometer Based on a Quarter waveplate-polarizing Cube Beamsplitter Combination and Which Uses Polarized Beams," *PIERS 2002*, 311, 2002.

Wave Polarization and Left-handed Materials in Metallic Magnetic Thin Films

Ruixin Wu
Nanjing University, China

Xiaokai Zhang, **John Q. Xiao**
University of Delaware, U.S.A.

Recently, negative index materials have attracted much attention since the negative refraction has been observed in some artificial materials [1–2]. These materials have extraordinary properties [3] and have many potential applications [4–5]. For example, Pendry [6] predicted that lossless negative index slab could act as a perfect lens, which overcomes the resolution limitation in conventional imaging system. Later, Garcia [7] pointed out that the negative index slab couldnt act as a perfect lens since the actual negative index materials are lossy and dispersion. However, more recently studies show that nearly perfect image is still possible to realize in the negative index slab if its loss is very small [8], and its thickness is much thinner than the wavelength of incident radiations [9]. Therefore finding a material with low loss and thin thickness is the basic task to realize the nearly perfect imaging. For this purpose, the films and the film composite materials have been developed [10–11].

In this work, we study the ways to realize the negative refraction in layered dielectric/conductor-ferrite film composites. For the composite with symmetric configuration, we have derived the effective complex permeability and complex permeability, and found that even if real parts of complex permeability ϵ' and complex permeability μ' are not negative at same time, the material also have effective negative refraction index. The negative refraction index depends on the configuration, and the component materials used. Under certain conditions, the left-handed material (i.e. double negative) can be achieved. We also have studied the power loss of the composite, and found in some ways the loss of the composite could be greatly reduced.

Improved Analysis of the Coupling of Optical Waves into Multimode Waveguides Using Overlap Integrals

M. Stallein, **C. Kolleck**, **G. Mrozynski**
University of Paderborn, Germany

Future computing hardware will operate with on-chip clock rates up to 10 GHz and needs an optical interconnection technology based on board-integrated optical channel waveguides of arbitrary cross section guiding a large number of modes [1]. The system design of optical interconnects requires an effective set of design tools with each basic algorithm being efficient with respect to time needs and memory requirements. The aim of this paper is to present an effective approach in this context to describe the coupling of optical waves into a highly multimodal step index waveguide based on simple overlap integrals.

Ray optical methods are preferred in analyzing optical interconnects, but it is not precisely known for which geometries the are applicable. Investigation by full-wave analysis using the mode matching technique is very extensive, as a lot of reflected and transmitted modes have to be regarded. Thus a large linear system of equations has to be solved. An often used approximation is to neglect the reflected waves. In this case evaluating the boundary conditions for the transverse field components by means of the mode orthogonality leads to explicit expressions for the amplitudes of the transmitted modes involving overlap integrals. That is, no system of equations has to be solved any more. In our approach we use both boundary conditions for the transverse electric field and for the transverse magnetic field to calculate the amplitudes C_k of the forward propagating modes.

$$|C_k|^2 = T\,\mathrm{Re}\left\{C_k^{(1)} C_k^{(2)^*}\right\} \quad \text{with} \quad C_k^{(1)} = \frac{1}{2Q_k}\int \mathbf{E}^i \times \left\{\mathbf{h}_k^t\right\}^* \mathrm{d}\mathbf{a}\,, \quad C_k^{(2)} = \frac{1}{2Q_k}\int \mathbf{e}_k^t \times \left\{\mathbf{H}^i\right\}^* \mathrm{d}\mathbf{a}$$

Here $\mathbf{E}^i$, $\mathbf{H}^i$ represent the incident waves while $\mathbf{e}_k^t$, $\mathbf{h}_k^t$ describe the k-th mode of the considered waveguide. Q_k corresponds to the normalized power of each mode. With $T = 1$ this approach conserves the power through the waveguide interface. In order to determine a mode independent T that minimizes the error caused by neglecting reflected waves, we compared the results of the approximate method with those of a full-wave analysis using the mode matching technique. In this way we have shown that quite accurate results are achieved, if T is equal to the transmission factor of a plane wave impinging on a dielectric half space.

The waveguide design we want to analyze consists of waveguides with rectangular cross section. As no analytical expressions for the modes of these waveguides are known, we look at two basic waveguides with known mode spectra to verify our approach. The first one is a planer slab waveguide, and the second is a cylindrical fiber. In our calculations the incident waves are assumed to be a Gaussian beam, which irradiates the waveguide interface with varying angles of incidence and lateral displacements. As we apply the method of mode matching we considered closed geometries with perfectly electric conducting walls. The incident field is expanded into a set of hollow waveguide modes formed by these walls. Results are shown and give rise to apply the method to interconnects of arbitrary cross section.

REFERENCES

1. Schrage J., T. Bierhoff, "Embedded Optical Waveguides for On-board Interconnections", Frontiers in Optics, 87th OSA Annual Meeting, Tucson, Arizona, USA, October 2003.

Model for Differential Model Delay Distribution in Multimode Fibers

Nishi Sharma, **Abhijit S. Chitambar**, **Charles H. Bianchi**, **K. Sivaprasad**
University of New Hampshire, U.S.A.

A band-limited fixed frequency linearly polarized optical signal excites several modes of propagation when it is launched into a multi-mode dimensioned optical fiber waveguide. This signal will therefore propagate over multiple paths along the transmission medium resulting in different propagation time for each mode. Thus replicas of the input pulse launched into the multimode fiber arrive at the output at different times, with the fundamental mode arriving first. A Differential Modal Delay (DMD) distribution is thus produced at the output of the fiber. The mode distribution, and consequently the modal delay distribution, are both a function of the physical attributes (geometry, distance, launching angle) of the optical waveguide. In optical communication systems this DMD distribution creates signal distortion that limits system designs (power, modulation, noise) and network performance (reach, rate, capacity). Accurate quantification of this DMD distribution is therefore essential to the prediction and improvement of performance.

Zero-filling Technique in Fresnel Transform Image Reconstruction for MR Image Denoising

Bin Rong Wu, **Satoshi Ito**, **Yoshitsugu Kamimura**, **Yoshifumi Yamada**
University of Utsunomiya, Japan

The effectiveness of magnetic resonance imaging (MRI) is rising as a diagnosis way in the medical treatment field. However, it is a traditional problem to get high signal to noise ratio (SNR) (quality) images.

We proposed the Fresnel transform imaging method [1], which use a nonlinear field gradient for phase encoding. The Fresnel transform imaging method has a great property that it can diffuse the noise contained in NMR signal, because the noise is modulated numerically in image reconstruction process. But we cannot find any diffuseness of the noise when we fix the signal matrix size to reconstruct images. However, if we prepare suitable area for noise diffusing by zero-filling technique [2] before reconstructing images in this method, the spectrum of noise will evenly distribute over the zero filled area. On the other hand, we can obtain a multi-resolution type image that consists of distribution on which the image information locally concentrates. Returning to the beginning signal space by taking a series of inverse-processes after the noise removing by a threshold filter in multi-resolution image space, and reconstructing the denoised signal by usual Fresnel transform image reconstruction method, we can obtain an MR image which the noise is greatly improved, whereas the deterioration in spatial resolution is hardly caused.

In this study, we present a new MR image denoising method using zero-filling technique in the Fresnel transform imaging method; and describe the effectiveness from comparing with standard Wiener filtering and Wavelet Wiener filtering on SNR improvement and deterioration in spatial resolution.

REFERENCES

1. Yamada, Y., K. Tanaka and Z. Abe, "NMR fresnel transform imaging technique using a quadratic nonlinear field gradient", *Rev. Sci. Instrum.*, Vol. 63, No. 11, 5348, 1992.
2. Wu, B. R., S. Ito, N. Kobari and Y. Yamada, "SNR improvement method using noise spreading effect in NMR Fresnel transform imge roconstruction", *IEICE Trans. Info. Syst.*, Vol. J86-D-II, No. 7, 1099, 2003.

A New Model for the Computation of Differential Group Delay from Polarization Distortion in Single Mode Fibers

Abhijit S. Chitambar, **K. Sivaprasad**, **Charles H. Bianchi**, **Nishi Sharma**
University of New Hampshire, USA

Linearly polarized signals, when propagating over long lengths of single mode fiber, become randomly polarized at the output. Irregularities along a fiber, such as stress and strain, give rise to longitudinal non-homogeneity resulting in birefringence and causing continuous and random scrambling of the polarization states. This polarization behavior has been explained by the evolution of Principle States of Polarization (PSP) along the length of propagation. Since birefringence varies along the length of a single mode fiber, the linearly polarized input polarization is effectively transformed into elliptically polarized output through the accumulation of distributed mode coupling and random polarization scrambling effects in long birefringent fibers. This sequential coupling and scrambling phenomenon along the segments of the fiber randomizes the resultant delay distribution of the polarization components at the output. The resulting random distribution may be mathematically characterized by smooth and continuous Gaussian or Maxwellian envelopes. The mean value may then be determined in order to estimate the system penalties and outage probabilities caused by dispersion that results from this polarization-induced delay distribution (polarization-mode dispersion, PMD).

This paper will investigate a new method for characterizing the delay distribution for polarization-mode dispersion that results from evolution and scrambling of polarization caused by random inhomogeneity along a single- mode fiber.

In this model, a long fiber may be represented as concatenation of birefringent sections with random orientations of polarization axes (fast and slow axes). The Electric fields emerging from each segment are projected onto the polarization axes of the following segment. The incremental lengths of propagation may be expressed as multiples of beat length 'L_b'. A beat length is defined as a section of fiber with fixed birefringence and axes of polarization. The entire length of propagation then becomes a concatenation of fused segments having lengths 'L_b'. A randomly polarized signal at the input of the first beat length segment will transmit energy that may excite both the spatial modes (fast and slow axes) of that segment. The two distinct output signal components will then transmit energy and excite the next segment, doubling the number of delayed signal components. The intensities of the signal components will depend upon the interaction of the input modes to a segment with the polarization axes of the segment at the coupling interface. The differential propagation delay between the signal components traveling along a fiber is then a function of individual propagation delays of each beat length segment traversed. Concatenation of large number of beat length segments, each with random orientation of polarization axes and distinct birefringence, results in differentially delayed polarization components with random power intensities at the farend. Such a discrete approach allows for greater control of the distribution of polarization-induced differential delay and allows direct evaluation of the impact on optical transmission systems in terms of signal distortion, channel capacity, and system performance.

Session 4P5

Novel Mathematical Methods in Electromagnetics I

A Preconditioner for Solving the Finite Element-Boundary Integral Matrix Equation of Scattering by Three-Dimensional Cavity

Yong-Ling Ban, **Zaiping Nie**, **Yan-Wen Zhao**, **Shengbo Wu**
University of Electronic Science and Technology of China, China

The finite element-boundary integral (FE-BI) method [1]-[3] is a powerful tool for solving infinite open-region scattering problems. Since in this method the boundary integral equation produces a full matrix equation, the final system consists of a partly full, partly sparse matrix. On account of ill-conditioned peculiarities of this system, commonly it's difficult to solve efficiently by iterative methods based on general algebraic preconditioning techniques such as SSOR [4]. Recently, a highly effective preconditioner based on a physical approximation for this system is proposed by Liu and Jin [3]. It is constructed from the finite element method using an absorbing boundary condition (ABC) on the truncation boundary. To implement this preconditioner, a truncation boundary surface away from the object must be added and hence the FEM computational region when the FE-BI method is employed is enlarged, which is a main disadvantage of this preconditioner [3] and to a certainty limits the wide use. In our work, a simple preconditioner devoted to efficiently solving the FE-BI matrix equation is proposed, where while the Householder version of GMRES [6] is employed. It's constructed by directly extracting the sparse part of the FE-BI system and discarding the remaining part of the BI matrix. The constructing procedure doesn't change the FEM computational region and also needn't additional computational cost besides forming the FE-BI system. Its efficiency will be illustrated by the following example.

REFERENCES

1. Jin, J. M., "The Finite Element Method in Electromagnetics," *John Wiley & Sons, Inc., New York, Second Edition*, 2002.
2. Liu, J. and J. M. Jin, "A Special Higher Order Finite-element Method for Scattering by Deep Cavities," *IEEE Trans. Antennas Propagat.*, Vol. 48, No. 5, 694, 2000.
3. Liu J. and J. M. Jin, "A Highly Effective Preconditioner for Solving the Finite Element-boundary Integral Matrix Equation of 3-D Scattering," *IEEE Trans. Antennas Propagat.*, Vol. 50, No. 9, 1212, 2002.
4. Chen, R. S., E. K. Yung, C. H. Chan, et al, "Application of the SSOR Preconditioned CG Algorithm to the Vector FEM for 3-D Full-wave Analysis of Electromagnetic-field Boundary-value Problems," *IEEE Trans. Microwave Theory and Techniques*, Vol. 50, No. 4, 1165, 2002.
5. IIic, M. M. and B. M. Notaros, "Higher Order Hierarchical Curved Hexahedral Vector Finite Elements for Electromagnetic Modeling", *IEEE Trans. Microwave Theory and Techniques*, Vol. 51, No. 3, 1026, 2003.
6. Saad, Y., "Iterative Methods for Sparse Linear Systems," *Soci. Ind. Appl. Math., Second Edition*, 2003.

Numerical Technique for the Analysis of MEMS Structures including the Complex Motion Effect

Michiko Kuroda
Tokyo University of Technology, Japan

The accurate knowledge of the electromagnetic field evolution around a moving or rotating body is very important for the effective modeling of new optical devices or microwave devices such as RF MEMS structures. But due to the limitations of the conventional numerical technique, it is tedious to solve these moving boundary problems numerically. In this paper, a novel numerical method for the analysis of the time dependent moving boundaries in the electromagnetic field is proposed. Employing this transformation, it is possible to apply the grid generation technique for the analysis of geometries with time-changing boundary conditions [1].

RF MEMS technology is developing rapidly in RF field [2] and the accurate design of RF MEMS structures require the computationally effective modeling of their transient and steady-state behavior including the accurate analysis of their time-dependent moving boundaries. RF MEMS structures have many complex motions such as non-uniform motions or rotating motions. Using this numerical technique, it is possible to analyze such complex motions easily. In this paper, some complex motions are shown to simulate the MEMS devices, such as switches or capacitors. And the relation between the acceleration, the velocity and the displacement of the capacitors are shown. Also, the MEMS antenna is simulated and the relation between S11 parameters and the velocity of the plate is shown. It is concluded that this technique can demonstrate its unique computational advantages in the modeling of microwave devices with moving boundaries.

REFERENCES

1. Kuroda, Michiko, Noriyuki Miura, Manos M. Tentzeris, "A Novel Numerical Approach for the Analysis of 2D MEMS-Based Variable Capacitors Including the Effect of Arbitrary Motions," *ACES Journal*, Vol. 19, No. 1b, 133, 2004
2. Rebeiz, Gabriel M., "RF MEMS Theory, Design, and Technology," *John. Wiley* & *Sons Publication*, 2003.

Element Free Method with Numerical Grid Generation for Large Complicated Waveguide Analysis

G. Zhao, **B. L. Ooi**, **D. X. Xu**, **M. S. Leong**
National University of Singapore, Singapore

Waveguides with complicated cross sections have many applications in the electromagnetic modeling. In literature, a number of methods for waveguide analysis have been reported, such as the finite element method (FEM), finite difference method (FDM), finite difference time domain method (FDTD) and surface integral-equation method (SI). The conventional mode-matching method can be used when the waveguide geometric shapes are simple. When the cross section becomes complicated, the finite element method (FEM) or other numerical techniques have to be adopted. The finite element method, which is a powerful method for waveguide analysis, usually shows high computation cost whenever the re-meshing is needed and most especially for problems that involve large geometrical changes.

Recently a novel kind numerical method, named mesh free method, has been widely used for the numerical solution of partial differential equations. Most of the application areas are focused on the mechanical problems, such dynamics, fluids, shells and so on. The mesh free methods have very good features, such as requiring only a scattered set of nodes, fast convergence, ease of adaptive refinement, trivial rising of the consistency order and the continuity of derivatives up to the desired order, etc. Mesh free methods have been used for the hollowing conducting waveguide analysis. However, when the cross sections become very large and complicated, these methods still have large computation burden. Thus the mesh free method coupled with numerical grid generation method is proposed. Through the numerical grid generation method, the complex domain in the Cartesian coordinate system can be transformed into a rectangular domain or a combination of rectangular sub domains in the curvilinear coordinate system. An idealized waveguide of cross section approximating that of a vehicular tunnel with conducting walls is investigated.

Influence of Parameters Uncertainties in Equivalent Circuit Modeling of 3D Electromagnetic Devices

S. Barmada[1], **G. Becherini**[2], **A. Musolino**[1], **M. Raugi**[1]

[1]Università di Pisa, Italy
[2]Accademia Navale di LivornoViale, Italy

Uncertainties in the parameters can greatly influence the circuit's behaviour, particularly in data lines, producing a substantial variation in the voltages and currents. This problem is also present as far as simulations are concerned: the accuracy of the utilized model is fundamental to produce results in good agreement with the real performance of the circuit. Generally the model is composed by a set of resistances, capacitances and inductances mutually coupled, whose parameters are obtained by measurement on the physical structure. The accuracy in such measurement determines the quality of the simulation results. In very complex systems the equivalent model is composed by a great quantity of parameters that have a different influence on the circuit response. The knowledge of each parameter's influence (on the output) allows establishing the accuracy of the measurements: it must be improved for those quantities that have a great influence on the circuit response and can be lower on the others. It is often possible to define a range of variation of each single parameter, and the goal is to determine the correspondent variation in the circuit output. Montecarlo methods are the most common technique, but requires a great number of simulations, hence a high CPU time consumption.

In this work we consider a system composed of an Electrical Fast Transient surge generator, a clamp, a shielded cable over a ground plane terminated in a shielded box that simulates a data transmission interface. Measurements have been performed on this setup [1] allowing the construction of an appropriate model to predict the noise introduced in a shielded cable for data transmission when a disturbance, is introduced. Simulations executed by the circuit simulator SPICE [1] and by a wavelet based technique [2] gave the same results. Here we attribute a ±10% variation to each parameter and determine the influence in the output. The bounds of the output variation by a sensitivity approach [3] are then determined. The output variation due to a single parameter is expressed by: $dV = \frac{\partial V}{\partial x} dx$. The bounds (with respect to the nominal output) are determined considering the worst case, i.e. adding all variations.

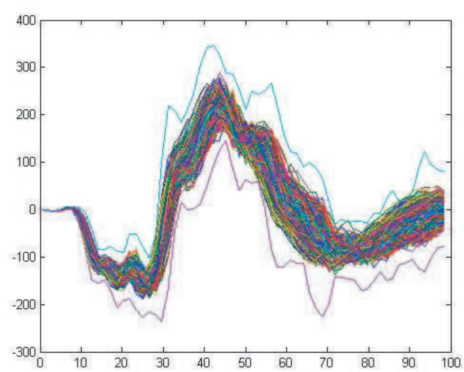

Figure 1: output bound and Montecarlo cloud

The procedure is validated by a Montecarlo techniques. Some results are showed in fig.1

REFERENCES

1. Caniggia, S., L. Vitucci, M. Acquaroli and A. Giordano, "Measurements and SPICE Models for Data Signal Lines Under Electrical Fast-Transient Test", *EMC 2000 Brugge*, 2000.
2. Barmada, S., G. Becherini, S. Caniggia, F. Maradei and M. Raugi, "A Wavelet Based Solver for Simulation of Fast Transients in signal Data Lines", *EMC 2002 Sorrento*, 2002.
3. Barmada, S., G. Becherini, A. Musolino and M. Raugi, "A Sensitivity Approach to Determine the Response of Transmission Line with Random Parameters", *2004 IEEE International Symposium on Electromagnetic Compatibility, Santa Clara*, 2004.

Image Reconstruction from Experimental Data Using the Forward-backward Time-stepping Method

Takashi Takenaka, **Toshiyuki Tanaka**, **Yoshinori Tanaka**, **Eiichiro Iwaya**
Nagasaki University, Japan

Inverse scattering problems of determining the electric properties of scattering objects are very important, and have been attracting the attention of many researchers because of their potential applications in a variety of fields such as medical imaging, geophysical exploration, nondestructive testing, and target identifications. Many nonlinear inversion techniques have been proposed for imaging high-contrast objects both in the frequency domain and in the time domain. Taking into account the fact that the time domain data has much more information about the unknown scattering objects than a single frequency scattering data, we have proposed a time-domain inverse scattering imaging technique, the forward-backward timestepping (FBTS) method, to reconstruct the electrical parameters such as the permittivity and conductivity profiles of scattering objects [1]. We have shown their effectiveness in several numerical simulations for inhomogeneous anisotropic as well as isotropic objects [2, 3].

In this paper we apply the FBTS method to experimental data to show their usefulness in real situations. Step-frequency measurements are conducted using a vector network analyzer. The scattering data is collected with an array of eight identical dipole antennas arranged along a measurement circle. All the transmission responses, S_{ji}, between the ith transmitting antenna and the jth receiving antenna (i, j=1,2,$\cdots$,8), are recorded for image reconstruction using the FBTS algorithm. Reconstructed images of different types of objects are shown to be in good agreement with the true objects. The inversion method will be reported in the presentation with the experimental arrangements and reconstructed results.

REFERENCES

1. Takenaka, T., H. Jia and T. Tanaka, "Microwave Imaging of Electrical Property Distribution by a forward-backward Time-stepping Method", *J. Electromagn. Waves Appl.*, Vol. 14, 1609, 2000.
2. Takenaka, T., H. Jia and T. Tanaka, "Microwave Imaging of an Anisotropic Cylindrical Object by a forward-backward Time-stepping Method", *IEICE Trans. Electron.*, Vol. E84-C, No. 12, 1910, 2001.
3. Takenaka, T., H. Zhou and T. Tanaka, "Inverse-scattering for a Three-dimensional Object in the Time Domain", *J. Opt. Soc. Am. A*, Vol. 20, No. 10, 1863, 2003.

An Accurate Solution of Time-domain Magnetic Integral Equation Using Higher Vector Order Basis Function

Yanwen Zhao, **Shengbo Wu**, **Zaiping Nie**
Xi Luo, **Jianghua Xu**
University of Electronic Science and Technology of China, China

Time Domain Integral Equation (TDIE) method for transient scattering analysis has received considerable attention in the past few years. Recently, several classes of high order vector basis function methods are proposed for the method-of-moments solution of frequency-domain and/or time-domain integral equations [1]-[4] because of their ability to represent fields/currents and model geometries more accurately than conventional low-order methods. Kang et al.[3] presents a set of novel, grid-robust, high order vector basis function. These basis functions are defined over curvilinear triangular patches and represent the unknown electric current density within each patch using the Lagrange interpolation polynomials. The highlight of these basis functions is that the Lagrange interpolation points are chosen to be the same as the nodes of the Gaussian quadratures. Secondly, the surface of an object to be analyzed can be easily meshed because these basis functions do not require the side of a triangular patch to be entirely shared by another triangular patch, which is very stringent requirement for traditional vector basis functions. In our work, the high order vector basis function in [3] is used for solving three-dimensional time-domain magnetic integral equations (TDMFIE), and thus the tedious evaluation of the space-time integrals in the method-of-moments of the time-domain integral equations is greatly simplified and accelerated. The point matching methods in space and time are implemented for the solution of TDMFIE. Several numerical results that demonstrate the accuracy and efficiency of this method will be presented at the conference.

REFERENCES

1. Graglia, R. D., D. R. Wilton and A. F. Peterson, "Higher Order Interpolatory Vector Bases for Computational Electromagnetics," *IEEE Trans. Antennas Propagat.*, Vol. 45, 329, 1997.
2. Canino, L. S., J. J. Ottusch, M. A. Stalzer, J. L. Visher and S. Wandzura, "Numerical Solution of the Helmholtz Equation in 2D and 3D Using a High-order Nystrom Discretization," *J. Comput. Phys.*, Vol. 146, 627, 1998.
3. Kang, Gang, Jinming Song, W. C. Chew, K. C. Donepudi and Jian-Ming Jin, "A Novel Grid-robust Higher Order Vector Basis Function for the Method of Moments," *IEEE Trans. Antennas Propagate.*, Vol. 49, No. 7, 908, 2001.
4. Wildman, R. A., G. Pisharody, D. S. Weile, B. Shanker and E. Michielessen, "An Accurate Scheme for the Solution of the Time-domain Integral Equations of Electromagnetics Using Higher Order Vector Bases and Bandlimited Extrapolation," *IEEE Trans. Antennas Propagat.*, Vol. 52, No. 11, 2973, 2004.

Solitary Waves in Unbounded Cubic-nonlinear Media

Yury Shestopalov
Karlstad University, Sweden

It is well known that in some cases one can reduce the system of Maxwell equations to ordinary differential equations and obtain then their particular solutions that are important for modeling certain one-dimensional phenomena, e.g. the wave propagation in plane-parallel layers filled with homogeneous and inhomogeneous media, both linear and nonlinear [1–3]. The cubic-nonlinear Helmholtz equation on the line [2, 3] is one of such equations; it describes waves propagating in a lossless, nonmagnetic, isotropic medium exhibiting a local Kerr-type dielectric nonlinearity, where the linear component of the permittivity is modeled by a continuous real-valued function of the transverse coordinate. A plane-parallel layer filled with Kerr-nonlinear inhomogeneous dielectric is an example of such a dielectric waveguide (DE). The existence of waves propagating in this DE is shown in [2, 3], particularly, in terms, of the Weierstrass function. In this study, we develop a different technique, also in order to study the problem for a wider class of permittivity functions. We show that there exist soliton-type waves for different dielectric nonlinearities and determine the corresponding solutions solving the cubic-nonlinear Helmholtz equation by the method of parametrization: the Helmholtz equation is transformed to another semilinear ordinary differential equation; its solutions are then evaluated for different parametrization functions. Using this approach, we determine explicitly various particular soliton-type solutions for different parametrization functions that model the permittivity, including rational functions of exponents, logarithmic functions, and splines based on their various combinations. We also solve the equation numerically. The technique is tested for the case of constant permittivity by reproducing some well-known soliton-type solutions [4, 5].

REFERENCES

1. Agrawal, G., *Nonlinear Fiber Optics, Second Ed., New York, Academic Press*, 1995.
2. Schürmann, H. W., V. Serov and Y. Shestopalov, “TE-polarized Waves Guided by a Lossless Nonlinear Three-layer Structure”, *Physical Review E*, Vol. 58, No. 1, 1040, 1998.
3. Schürmann, H. W., V. Serov and Y. Shestopalov, “Solutions to the Helmholtz Equation for TE-Guided Waves in a Three-Layer Structure with Kerr-Type Nonlinearity”, *J. Phys. A: Math. Gen.*, Vol. 35, No. 50, 10789, 2002.
4. Arfken, G. B. and H. J. Weber, *Mathematical Methods for Physicists, Fifth Ed., New York, Harcourt/Academic Press*, 2001.
5. Schürmann, H. W., V. Serov and Y. Shestopalov, “Propagation of TE Waves through a Layer Having Permittivity Depending on the Transverse Coordinate and Lying between Two Half-Infinite Nonlinear Media”, *Dokl. Ros. Akad. Nauk, Maths.*, Vol. 60, No. 2, 286, 1999.

Location of Zeros of Electromagnetic H-waves on the Complex Plane

Masahiro Hashimoto
Osaka Electro-Communication University, Japan

In the early work [1], we presented a new approach to describe electromagnetic waves in terms of zeros of the far-zone field patterns on the complex plane. For EM waves scattered by N-polygonal cylinders, the distributions of zeros on the complex plane extend up to a point of infinity. The directions of such infinite sequences of zeros just correspond to the directions of N polygonal sides and the lengths of N sides, which means that the exact distributions of zeros are predicted when the polygons are specified in space. Mathematical expressions for EM fields that cover the entire region from the near- to far-zones can be obtained by determining the location of zeros. The EM fields in real space and the corresponding distributions of zeros in spectral space are now related mathematically by a new integral transform just like a Fourier transform. Therefore the theoretical rigor of electromagnetic fields will be discussed in the "spectral domain". It was pointed out [1] that the spectral-domain-tracks of zeros starting from the unit circle whose center is located at the origin of the complex plane and lastly terminating at infinity are quite similar in both cases of E and H waves. However, some additional zeros appear in case of H waves. These zeros are known to be located near the unit circle and they are observed as the null points of the far-zone field pattern plotted in real angular space. Thus they are studied from geometrical optics considerations including the effects of diffraction. In the present paper, we focus our mind on these additional zeros inherent in H waves. Principal behaviors are characterized by means of physical optics.

REFERENCES

1. Hashimoto, M., "Locations of Zeros for Electromagnetic Fields Scattered by Polygonal Objects," *IEICE Trans. Electron.*, Vol. E87-C, No. 9, 1595, 2004.

Statistical Aspects of Radar & Sar Polarimetry

Wolfgang-Martin Boerner
University of Illinois at Chicago, U.S.A.

Dedicated to late Ernst Lüneburg
EML Consultants, Georg-Schmid Weg 4, Germany

A comparison between the Kennaugh matrix and the covariance matrix formulation of second- order moment radar polarimetry reveals fundamental relationships between power and variance aspects of bi-static and mono-static radar scattering from randomly distributed targets.

In radar and in optical polarimetry there exist essentially two different methods to characterize the polarimetric scattering properties of plane fully polarized electromagnetic waves by randomly distributed targets using second-order multivariate statistics: the Kennaugh matrix and the covariance matrix formulations. They are generally considered to be different and independent, although formally they involve the same second-order multivariate moments. The Kennaugh approach is used for finding solutions for maximal and minimal power transfer between the transmitting and receiving antenna whereas the covariance matrix analysis is used for entropy and variance considerations and for the generation of uncorrelated random variables. Second-order statistics involve complete information for multivariate Gaussian distributions and in general provide sufficient information for sub- and super-Gaussian distributions.

In the far field of any scattering object the elements of the 2×2 polarimetric scattering matrix S in a linear appropriately chosen linear transmit and receive basis for the domain and range of the scattering operator are correlated random variables where t stands for time or ensemble value and first and second index denote receiver transmitter polarization basis vectors

$$S(t) = \begin{bmatrix} S_{x_r x_t}(t) & S_{x_r y_t}(t) \\ S_{y_r x_t}(t) & S_{y_r y_t}(t) \end{bmatrix}$$

Assuming ergodicity ensemble averages can be replaced by time averages and will be denoted by sharp brackets $< \ldots >$. For the sake of simplicity we take $< S(t) = 0 >$ which implies the removal of the means. A coherently scattering target, also called a point or a deterministic target will be denoted by the same symbol but without round brackets. Using a common polarization basis system for the interesting and important case of backscattering (the BSA convention) the Sinclair backscattering matrix is symmetric due to reciprocity for all instants of time.

Lüneburg, E., W-M Boerner, "Statistical Aspects of Radar Polarimetry," 43-52 in: P. Russer, M. Mongiardo (Editors), Fields, Networks, Computational Methods, and Systems in Modern Electrodynamics A Tribute to Leopold B. Felsen (the Proceedings of the Symposium on Fields, Networks and Computation: A Modern View of Engineering Electrodynamics, 2004 June 01-02, Technical University of Munich (in dedication to Leopold B. Felsen for his bestowment of the Dr.-Ing. E-h. of TUM, Munich), Springer-Verlag Berlin-Heidelberg-New York, 2004.

Integral Approach to General Eddy Currents in Linear Structures

Ivo Doležel[1], **Pavel Karban**[2], **Bohuš Ulrych**[2]

[1]Institute of Electrical Engineering ASCR, Dolejškova 5, Czech Republic
[2]Faculty of Electrical Engineering UWB, Univerzitní 26, Czech Republic

Eddy currents in metal structures and their effects such as electrodynamic forces, Joule losses and consequent temperature rise play very important role in many domains of electrical engineering, particularly in power applications. Nowadays, their investigation is mostly performed by means of FEM or other suitable differential techniques. The related professional codes are powerful, reliable and yield results of very good quality. Despite of this fact, however, there exists a group of tasks whose processing by these methods may appear disadvantageous and from time to time can even fail. Mentioned can be arrangements with elements that are geometrically incommensurable (for example thin conductors versus air) or that move with respect to one another, which requires remeshing of the whole domain at each time step. Difficulties may also be caused by ignorance of boundary conditions, which is quite typical for tasks of this kind.

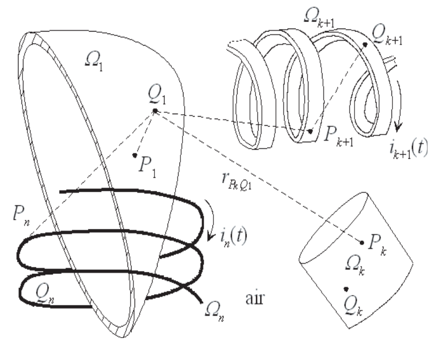

Figure 1: General arrangement with field coils and linear electrically conductive bodies

Consider a linear system in Fig. 1 consisting of free electrically conductive bodies Ω_i, $i = 1, \cdots, k$ and inductors Ω_i, $i = k+1, \cdots, n$. The inductors are supposed to be supplied from sources of generally time dependent currents $i_i(t)$, $i = k+1, \cdots, n$. All elements of the system can move at sufficiently low velocities (so that the corresponding component of eddy currents due to velocity may be neglected). Distribution of the total current densities in massive bodies is given by integral equations in the form

$$J_j(Q_j, t) + \frac{\mu_0 \gamma_j}{4\pi} \cdot \sum_{i=1}^{n} \int_{\Omega_i} \frac{\frac{\partial J_i(P_i, t)}{\partial t} \cdot dv}{r_{p_i Q_j}} = J_{0j}(t), \quad j = 1, \cdots, n$$

where γ_j denotes electrical conductivity of the $j - th$ body and $J_{0j}(t)$ a function of time that is in a given body not known in advance. The other symbols follow from Fig. 1. These equations are supplemented with conditions

$$\iint_{S_j} J_j(Q_j, t) dS = 0 \;\; for \;\; j = 1, \cdots, k \;\; and \;\; i_j(t) \;\; for \;\; j = k+1, \cdots, n$$

where the integration is carried out over a suitable cross-section of the body (or inductor).

The paper presents a general derivation of the continuous mathematical model in 3D. Its next processing (discretization, formation of numerical schemes and algorithmization) is performed in details, however, only in typical 2D arrangements. Computations are carried out by a code fully developed and written by the authors. Presented is an illustrative example demonstrating capabilities of the suggested algorithm and the results are compared with values obtained by other ways. Discussed are advantages and drawbacks of the approach and further possibilities of its improvement.

*This work has been financially supported from the Grant Agency of the Czech Republic (projects No. 102/04/0095 and 102/03/0047).

Method of Integrodifferential Equations for Solving Three-dimensional Diffraction Problems Using Supercomputers

Yu. G. Smirnov
Penza State University, Russia

There are many electromagnetic diffraction problems which require large and complicated calculations on computers. We consider two families of such three-dimensional problems of the electromagnetic field diffraction by (1) anisotropic dielectric or magnetic bodies in free space, in a waveguide, or in a box, and (2) perfectly conducting surfaces and screens in free space. Both problems can be reduced to integrodifferential equations on bodies or surfaces: volume singular integral equation (VSIE) for the first family of problems and the electric field integral equation (EFIE) for the second family.

The main difficulties in the method of integrodifferential equations are (a) very large time of calculations of matrix elements with sufficiently high accuracy and (b) occurrence of large and dense matrices in systems of linear algebraic equations obtained after discretization of the problems.

If one uses the Galerkin method for the problem discretization, the matrix elements may be calculated independently. A natural way to calculate the matrix elements is utilization of parallel computations using supercomputers or clusters. Note in addition that the structure of matrices is not arbitrary: in many diffraction problems we have the so-called structured matrices with O(n) different elements, where n denotes the matrix dimension.

We have created and elaborated efficient solvers for several types of systems with structured matrices on the basis of algorithms of parallel computations.

*This study is carried out under the support of the Russian Foundation for Basic Research, grant no 03-07-90274.

Session 4P6

Coherent Effects in Random Media

Spectral Theory of Time Dispersive and Dissipative Systems

Alexander Figotin
University of California at Irvine, U.S.A.

Jeffrey Schenker
Institut für Theoretische Physik, Switzerland

We study linear time dispersive and dissipative systems. Very often such systems are not conservative and the standard spectral theory can not be applied. We develop a mathematically consistent framework allowing: (i) to constructively determine if a given time dispersive system can be extended to a conservative one; (ii) to construct that very conservative system, which we show is essentially unique.

We illustrate the method by applying it to the spectral analysis of time dispersive dielectrics and the damped oscillator with retarded friction. In particular, we obtain a conservative extension of the Maxwell equations which is equivalent to the original Maxwell equations for a dispersive and lossy dielectric medium.

Scattering of TE Plane Wave from Periodic Grating with Defects

Kazuhiro Hattori, **Junichi Nakayama**
Kyoto Institute of Technology, Japan

The wave scattering from periodic grating has been studied by many authors. However, to find defects in a periodic structure such as metal parallel lines of VLSI, it is necessary to know the effect of defects in the scattering propertics. This paper deals with the scattering of a Teplane wave from a periodic grating with defects. As a simple example of such a grating, we consider a case shown in Fig.1, which is a periodic array of rectangular grooves, but there are some defects where grooves are not formed. We will study two cases of periodic grating with defects: one with a single defect at a know position, and the other with randomly distributed defects. In the former case with a single defect, the wave field above the x axis is represented by a sum of three components: the incident plane wave, the diffracted wave by a periodic groove is written by a sum of guided modes. Solving the boundary condition, we will give an optical theorem and the scattering cross section. In the latter case, randomly distributed defects are mathematically modeled by a stochastic binary sequence b_m taking only ± 1. Taking the shift invariance of the stochastic binary sequence in the probability theory, the scattered wave is shown to be a periodic stationary process. Since the average of a periodic sationary process is a periodic function of x, the coherent wave is a sum of diffracted waves into discrete directions given by the grating formula. The scattered wave is regarded as a stochastic functional of the binary sequence and is written by a sum of orthogonal binary functionals with unknown binary kernels determined from the boundary condition. Assuming that the probability of defect existence is low, we approximately determine the binary kernels, in terms of which the coherent diffraction and incoherent scattering will be discussed.

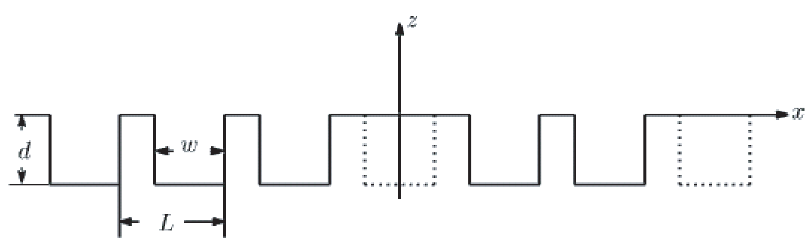

Figure 1: Period grooves with defects. L is the period, ω is the width of a groove and d is the depth.

Dicke Effect for Strongly Copled Quantum Dots

Richard Berkovits
Bar-Ilan University, Israel

Felix von Oppen
Freie Universität Berlin, Germany

Jan W. Kantelhardt
Martin-Luther-University Halle-Wittenberg, Germany

It is well known that the number of electrons in a weakly coupled quantum dot changes discretely as function of the chemical potential. This phenomenon is the basis for the application of such dots as single electron transistors. When the coupling to the external leads is weak, it may be treated as a perturbation and results in a broadening $\Gamma = \pi N \nu |V|^2$ of the states of the uncoupled dot. (ν is the density of states (DOS) in a lead, N the number of leads, and V is the overlap matrix element between a state in the dot and a typical state of the leads.) Usually, one expects the discrete features of the dot to be lost once the broadening is larger than the typical level spacing Δ in the dot. This corresponds to the requirement that the dimensionless conductance through the dot, $g_{\text{dot}} = \Gamma/\Delta$, should be larger than one.

In this picture the only relevant condition for the the appearance of discrete features in the dot is $g_{\text{dot}} < 1$. Nevertheless, one may extrapolate from the Dicke effect that a quantum dot strongly coupled to a lead will also show sharp resonances. In an extreme strong coupling limit, we can think of the dot levels as degenerate, analogous to the identical resonances of the atoms in the Dicke effect. These degenerate levels are coupled via the continuum of lead states which is akin to the coupling of the atoms by the radiation field.

In our talk we show that in the limit $g_{\text{dot}} \to \infty$, the relevant parameters in determining the number of bound states in the dot for generic dot-lead coupling is the number of channels N of the leads, and the number oof states in the dot N_{dot}. At strong coupling $N_{\text{dot}} - N$ states remain bound to the dot, except when the coupling matrix elements between leads and dot are independent of either dot level or channel index. For the latter cases, $N_{\text{dot}} - 1$ states remain bound to the dot. Using numerical density-matrix renormalization group (DMRG) as well as analytical arguments, we show that these bound states exhibit discrete charging as well as Coulomb blockade except for very large charging energies. Thus, in order to wash out all discrete features of a dot in the limit of strong coupling, one or more leads of total dimensionless conductance $g > N_{\text{dot}}$ must be connected. With increasing coupling strength, a dot coupled to leads will evolve from N_{dot} bound states at very weak coupling, to no bound states at intermediate coupling and finally to $N_{\text{dot}} - N$ bound states at strong coupling. Criteria for the different regimes and experimental realizations will be discussed.

Optical Properties of Complex Photonic Materials

Riccardo Sapienza[1,2], **Stefano Gottardo**[1], **Costanza Toninelli**[1]
Dominique Delande[2], **Diederik Wiersma**[1]

[1]European Laboratory for Nonlinear Spectroscopy (LENS) and INFM, Italy
[2]École Normale Supérieure et Université Pierre et Marie Curie, France

We will give an overview on the latest developments on light transport in complex photonic systems, focusing on the special cases when the translational or rotational scattering symmetry is broken. We will address in this talk 3 dimensional structures.

In particular we will discuss the transport of optical waves in a range of materials going from fully ordered, like photonic crystals, to partially disordered systems like quasi-crystals, and liquid crystals, and to completely disordered structures. There are many examples of wave phenomena where interference effects play a crucial role both in the optical and the electronic case. Often these processes are easier to study with light because the coherence length of an optical wave packet is usually much longer than that of an electronic wavepacket.

We will go in detail into the case in which optical waves exhibit localization effects. One of the most robust two-waves interference phenomena is weak localization of light in disordered media. We will present experimental results on anisotropic light transport and anisotropic interference [1] and recent Monte Carlo simulations [2].

REFERENCES

1. Sapienza, R., S. Mujumdar, C. Cheung, A. G. Yodh and D. Wiersma, "Anisotropic Weak Localization of Light," *Phys. Rev. Lett.*, Vol. 92, 033903, 2004.
2. Sapienza, R., D. Delande and D. Wiersma, "Anisotropic Weak Localization of Light: from Isotropic Scattering to Ordered Nematic Liquid Crystals," *Mol. Cryst. Liq. Cryst.*, in the press, 2004.

Light Propagation through Randomly Spaced Partial Reflectors in a Single Mode Optical Fiber

H. Pérez, **N. Lizárraga**, **E. I. Chaikina**, **E. R. Méndez**
Centro de Investigación Científica y de Educación Superior de Ensenada, México

J. A. Sánchez-Gil
Instituto de Estructura de la Materia, CSIC, Spain

Multiple scattering in all kind of disordered system is currently an active area in both fundamental and applied research. Single and multimode waveguides represent systems that have been widely employed in recent years in investigations of the propagation of waves through disordered media, and studies of localization and transport phenomena. Here, we present an experimental and theoretical investigation of the propagation of light through a single mode optical fiber that contains randomly spaced partial reflectors, in the form of Bragg gratings. For the transport properties of the light, the system can be considered one-dimensional, and has negligible losses. Both, uniform and chirped gratings were fabricated along the fiber with a well-known mask technique using commercially available Ge doped fibers. Since the fibers are photosensitive in the UV, as a source we used an Argon ion LEXEL 95 CW laser with an intracavity crystal to generate second harmonic light. The spacing between two successive gratings varies from several wavelengths to a few centimeters. We study the dependence of the transmitted intensity as a function of the number of gratings in the fiber, and as a function of the wavelength of the propagating light in the range 1520-1580 nm.

The Scattering of Light from a Moving Metal Surface

T. A. Leskova, **A. A. Maradudin**
University of California, U.S.A.

We study the scattering of p-polarized light of frequency ω, whose plane of incidence is the x_1x_3 plane, from a one-dimensional random metal surface that is moving parallel to itself with a constant speed v in a direction perpendicular to the generators of the surface. The equation of the surface can then be written as $x_3 = \zeta(x_1 - vt)$, where the surface profile function $\zeta(x_1)$ is a single-valued function of x_1, that is differentiable, and constitutes a stationary, zero-mean, Gaussian random process defined by $\langle\zeta(x_1)\zeta(x_1')\rangle = \delta^2 \exp[-(x_1 - x_1')^2/a^2]$. The angle brackets here denote an average over the ensemble of realizations of $\zeta(x_1)$, and δ is the rms height of the surface. The single nonzero component of the total magnetic field in the vacuum region $x_3 > \zeta(x_1 - vt)_{max}$ is the sum of an incident plane wave and scattered waves,

$$\begin{aligned} H_2^{>}(x_1, x_3; t) &= \exp[i(kx_1 - \alpha_0(k,\omega)x_3 - \omega t)] \\ &+ \int_{-\infty}^{\infty} \frac{dq}{2\pi} \int_{-\infty}^{\infty} \frac{d\Omega}{2\pi} R(q|k) \exp[i(qx_1 + \alpha_0(q,\Omega)x_3 - \Omega t], \end{aligned}$$

where $\alpha_0(q,\Omega) = [(\Omega/c)^2 - q^2]^{\frac{1}{2}}$, with $Re\alpha_0(q,\Omega) > 0$, $Im\alpha_0(q,\Omega) > 0$. The reduced Rayleigh equation satisfied by the scattering amplitude $R(q|k)$ is derived, and is solved as an expansion in powers of the surface profile function through terms of third order. This solution is used to calculate the contribution to the mean differential reflection coefficient from the light that has been scattered incoherently (diffusely), as a function of the speed v. The dispersion of the surface plasmon polaritons supported by the vacuum-metal interface depends on v: for a given frequency of the incident light ω the forward and backward propagating surface plasmon polaritons have different wavenumbers. This results in a shift of the enhanced backscattering peak from the retroreflection direction in the direction of larger (smaller) scattering angles for positive (negative) v. The shift is a function of the ratio v/v_g, where v_g is the group velocity of the surface plasmon polariton, and is larger in magnitude the larger is v/v_g. From the magnitude and sign of this shift it is possible to obtain the speed v of the moving surface.

Time Reversal and Detection in Random Media

Guillaume Bal
Columbia University, U.S.A.

Olivier Pinaud
Columbia University, U.S.A.

We consider the detection and imaging of inclusions buried in highly heterogeneous media, where wave propagation may be modeled by a macroscopic (radiative transfer or diffusion) equation for the wave energy density. We show that inclusions can be detected and reconstructed provided that we have access to statistically stable measurements. Furthermore we show that time-reversal techniques can be used to significantly reduce the signal-to-noise ratio in the presence of background noise. This is a direct consequence of the enhanced refocusing properties that characterize time reversed waves propagating in heterogeneous media. Finally we present numerical simulations of acoustic waves propagating in heterogeneous two-dimensional media that illustrate the theoretical predictions.

Conductance of Photons in Disordered Photonic Crystals

A. A. Asatryan, **L. C. Botten**, **M. A. Byrne**, **T. N. Langtry**, **N. A. Nicorovici**
University of Technology, Australia

R. C. McPhedran, **C. Martijn de Sterke**, **P. A. Robinson**
University of Sydney, Australia

One of the fundamental problems in electromagnetic wave propagation in disordered media is the phenomenon of Anderson localization[1]. In this phenomenon, initially discovered for electrons in disordered solids, the transport of electrons is inhibited due to the random scattering of electrons. The same phenomenon also occurs for photons, with wave amplitudes decaying exponentially as they propagate in a strongly disordered medium. Despite much research in the area, a completely rigorous theory of Anderson localization has still be be developed. One of the general theories that describes this phenomena is scaling theory [2], according to which the localization properties can be characterized by the scaling properties of a single parameter g, the conductance. Even though scaling theory relies on only the scaling of a single parameter, nevertheless it is able to predict general localization properties of waves in different dimensions. According to scaling theory, waves for all wavelengths are localized for the one and two dimensional problems ($d \leq 2$), while for three dimensional problems, there is a transition point (the mobility edge) that marks the boundary between diffusion and localization. Subsequently it was discovered that conductance (in disordered media) is a highly fluctuating quantify [3], raising doubts about the applicability of scaling theory. In turn, the phenomenon termed universal conductance fluctuations (UCF), in which the variance of the conductance is independent of the size of the medium and the disorder of the sample, was observed.

In this paper, we outline a comprehensive study of photon conductance, and its properties, in two-dimensional disordered photonic crystal systems. In this, we have used Landauer's formula for electronic conductance[4] $g = \mathsf{Tr}\ \mathbf{T}\mathbf{T}^{\dagger}$ to characterize photon conductance. Here $\mathbf{T}$ is the transmission scattering matrix for the sample, calculated using our rigorous technique based on multipole expansions[5]. From a comprehensive study of the average of the conductance, its variance, and distribution for both polarizations, we observe UCFs for electromagnetic waves and show that the variance and the distribution of g is remarkably similar for both polarizations. We also show that the distribution of the conductance in the diffusive regime is Gaussian, while in the localization regime the distribution of g is well characterized by a log-normal distribution. We will also discuss the distribution of the conductance at the transition to localization together with the results of our numerical study of the applicability of scaling theory.

REFERENCES

1. Sheng, P., "Scattering and Localization of Classical Waves in Random Media," *World Scientific, Sing.*, 1990.
2. Abrahams, E., et. al, *Phys. Rev. Lett.*, Vol. 42, 673, 1979.
3. Lee, P. A., et al, *Phys. Rev. Lett.*, Vol. 55, 1622, 1985; Altschuler, B. L., *JETP Lett.*, Vol. 41, 648, 1985.
4. Fisher, D. S., et al, "Relation between Conductivity and Transmission Matrix," *Phys. Rev. B*, Vol. 23, 6851, 1981.
5. Botten, L. C., et al, *J. Opt. Soc. Am A*, Vol. 17, 2165, 2000; *ibid*, Vol. 17, 2177, 2000.

The Twilight Zone in the Over-barrier Scattering: between Perturbation Theory and Quasiclassics

N. M. Makarov
Universidad Autónoma de Puebla, México

K. Yu. Bliokh
Institute of Radio Astronomy, Ukraine

V. D. Freilikher
Bar-Ilan University, Israel

As is known, in solving the problem of electron/wave backscattering one can employ the perturbation theory if the scattering potential is small or the WKB (quasiclassical) approximation when the potential is smooth. The dimensionless parameters of smallness δ and smoothness ε^{-1} of the potential are defined, respectively, by the ratio of its amplitude to the electron/wave energy and by the ratio of its variation scale to the wave length. Therefore, for simultaneously small ($\delta \ll 1$) and smooth ($\varepsilon \ll 1$) potential both of approaches seem to be applicable with the same result. In this contribution we show that in general it is not the case.

We discuss the applicability of WKB and Born (small perturbations) approximations for one-dimensional over-barrier scattering problem with different types of potentials, both deterministic and random, within the ballistic and localized regimes. The dependence of the reflection coefficient R and the localization length ℓ_{loc} on the dimensionless amplitude δ and lengthwise variation scale ε^{-1} of the scattering potential is studied.

It is shown that perturbation and WKB theories are inconsistent with each other for the over-barrier backscattering. The quasiclassical reflection coefficient is extremely sensitive to the shape of the potential profile. When the potential has small amplitude and long variation scale there is no universal dependence $R(\delta, \varepsilon)$, and this function is quite individual for each given potential. This is in contrast to the case of tunneling ($\delta > 1$), when WKB approximation results in the transmission which is determined by the characteristic height and width of the barrier and practically independent of the details of its shape. The surprising fact is that for the over-barrier scattering even the location and shape of the line, separating the WKB and Born domains in the (δ, ε) plane, are essentially different for different potentials. In the case of a random potential the line turns into a finite area where neither of two approaches is valid. The form and size of this region in the (δ, ε) plane depend drastically on the statistic properties of the potential.

Revealed high sensitivity of the reflection coefficient to the details of the potential is not of theoretical interest only. It must be taken into account in processing of experimental data for their comparison with theoretical models. In real experiments, the shape of the scattering potential is known, at best, in a set of discrete points, but most commonly just the typical scales, δ and ε, are available. While it is sufficient to estimate the tunnelling transmission, for the over-barrier backscattering, a small deviation in the shape of the fitting function could give rise to a dramatic difference in the predicted value for R and its dependence on the parameters of the problem.

Tunneling and Localization in Two-level Systems Subjected to an Electromagnetic Field

M. Gitterman
Bar-Ilan University, Israel

A nontrivial example of tunneling and localization induced by a classical electromagnetic wave is provided by a two-level system. The Hamiltonian of the system is reduced to that describing a particle interacting with the vibrational excitations of a classical field. Just as for the small-polaron problem (electron dressed by phonons), the Hamiltonian can be transformed by applying an appropriate unitary operator to eliminate a linear interaction of a particle with the classical-field boson excitations. A large "effective mass" of a particle "dressed" by a large number of classical-wave excitations, prevents the particle from the tunneling to a second state. For appropriate values of the amplitude A and frequency ?of the electromagnetic field one finds a localization of a particle ("coherent destruction of tunneling") in a double-well potential, or the suppression of photon emission from a single molecule. In the latter case, the finite width of the excited energy level destroys this suppression.

Localization of Transverse Waves in Randomly Layered Media at Oblique Incidence

K. Yu. Bliokh[1,2], **V. D. Freilikher**[2]

[1] Institute of Radio Astronomy, Ukraine
[2] Bar-Ilan University, Israel

Localization of classical waves and quantum particles in one-dimensional (1D) disordered systems is well studied theoretically. Important application of the theory is the propagation of radiation in randomly layered media where the refractive index depends on a single coordinate, z. In general, however, this is a three-dimensional problem, and the field, $\psi(r)$, of a monochromatic wave at oblique (with respect to z-axis) incidence can be presented as $\psi(r) = \exp(ik_x x + ik_y y)\chi(z)$. The equation for $\chi(z)$ takes the form

$$-\frac{d^2\chi(z)}{dz^2} + k^2\delta\varepsilon(z)\chi(z) = (k^2 - k_x^2 - k_y^2)\chi(z)$$

where $k = \sqrt{\varepsilon_0}\omega/c$, ω is the frequency, , $\delta\varepsilon(z) = -\Delta\varepsilon(z)/\varepsilon_0$, and the dielectric constant of the medium is given by $\varepsilon(z) = \varepsilon_0 + \Delta\varepsilon(z)$ with $\Delta\varepsilon(z)$ being a random function of the coordinate. Obviously the "energy", $k^2 - k_x^2 - k_y^2$, may take any positive value, in particular can be less "potential" $k^2\delta\varepsilon$. It gives rise to an additional mechanism of localization, which is due to the internal reflection and tunnelling. Another new effect, which is absent in pure 1D random systems, comes about at oblique propagation of transverse vector waves. In this case the symmetry with respect to the direction of propagation is broken, and the localization length depends significantly on the polarization of the radiation. Here we present an approximate method for calculating the localization length in randomly layered medium based on the assumptions of the exponentially small transmission and complete phase randomization, and use this method to calculate the localization length for two orthogonal linear polarizations. It is shown that the localization length of a wave with the vector of the electric field orthogonal to the plane of incidence (S-wave) is always larger than that of P-waves (with the electric vector in the plane of incidence), for which a sort of stochastic Brewster effect takes place. As the result, the radiation transmitted through a long enough randomly layered sample is always P-polarized (with an exponential accuracy). The effect on the localization length of the internal reflection at the interfaces between random layers is also studied. Some examples of randomly layered media have been considered.

Session 4P7a

Wavelet Application and Other Computational Method

Fast Solution of Electromagnetic Integral Equations Using BCR Non-Standard Wavelet Decomposition

Hai Deng
University of North Texas, U.S.A.

Wavelet basis has been widely used to reduce the computational complexity of solving electromagnetic integral equations. However, the traditional wavelet-based method is based on the tensor-product decomposition, i.e. the standard wavelet transform, of moment matrix, which leads to the strong interactions between different scales and thus more non-zero elements in the transformed matrix. In this work, the Beylkin-Coifman-Rokhlin (BCR) non-standard wavelet decomposition is used for fast solution of moment equations for electromagnetic scattering problems. The BCR non-standard wavelet decomposition was initially proposed by Beylkin, Coifman and Rokhlin to compress linear integral operators. In this work the method is further expanded to solving electromagnetic integral equations.

Using the traditional tensor wavelet transform, the number of the non-zero elements in the transformed moment matrix is about $O(N^{1.7})$ with a problem size of N, and thus the computational complexity of iteratively solving the transformed moment equation is about $O(N^{1.7})$. However, if the BCR non-standard waveform decomposition is applied to a smooth moment matrix, the transformed matrix will have about $O(N)$ non- zero elements. Therefore, with the new method, the cost to solve an electromagnetic problem could be potentially reduced to $O(N)$ operations.

Consider a moment equation as follows:

$$[Z]J = E \tag{1}$$

Using the traditional tensor wavelet transform the transformed moment equation is:

$$[M]^T[Z][M][M]^TJ = [M]^TE \tag{2}$$

where [M] is the wavelet basis matrix. The above equation can be represented in wavelet basis form as:

$$[\tilde{Z}]\tilde{J} = \tilde{E} \tag{3}$$

For BCR wavelet transform, the wavelet basis matrix in (2) is different from scale to scale. The transformation of a moment matrix is similar to the quadtrature decomposition of an image, but the components with low-frequency band basis functions in both horizontal and vertical directions are repetitively decomposed the same way until the coarsest level. The excitation vector E in (1) is similarly decomposed using BCR transform. Once the induced current vector in wavelet basis is solved by using an iterative solver from (3), the actual J can be found using inverse transform with little cost.

Preliminary numerical results based on a two-dimensional scatterer indicate the new method results in significant cost reduction for solving electromagnetic integral equations.

Data Hiding Method Apply to the Wireless Network

Wen-Chung Kuo[1], **Yu-Chih Huang**[2]

[1]National Formosa University, Taiwan
[2]Tainan Woman's College of Arts & Technology, Taiwan

1984, the prisoners' problem of data hiding was proposed by Simmons. Then, there are many experts and scholars invested this question. Recently, Wu and Liu apply that find the hidden pixels and odd-even mapping methods to achieve the goals of data hiding. It is very difficult to find the difference between cover-image and stego-image by human eyes. Unfortunately, Wu and Liu assumed a technique of shuffling to prevented attack in frame of data hiding, but the method of shuffling can't was shown in public. Wu and Liu were not proposed the mathematical property of shuffling in their literary and how to achieve it?

Thus we will research the presently method of shuffling and achieve the technique of shuffling by RSA, then design algorithms of data hiding based on RSA. At the same time, we propose the method not only focus on algorithm of RSA, but also achieve data hiding in space domain. However, the data hiding technical skills still are not used in the wireless due to the computational capabilities of mobile devices.

In this paper, we will attempt to combine some wireless technical (such as IEEE 802.11) and our proposed method to apply the data hiding on the Wi-Fi. The proposed mechanism mainly includes four functions: shuffling, signature, detection and authentication. In shuffling component, the sender calculates the character of image data and combined the RSA method to generate the cover image. Then, the sender embeds the secret data into the cover image and uses his private key and the receiver's public key to generate stego-image. Thus, the receiver station can use the WEP to detect the stego-image contents when it received the stego-image. In final, the receiver can use his private key and sender's public key to check the secret data whether it comes from the sender. If the stego-image signal has no authorized right, its illegal use will be easily detected by the WEP or receiver. Thus, our method not only can increase security of data hiding to reduce space and shuffling in public but also except receiver can decode property of shuffling. It can prevent compress or malicious attack.

REFERENCES

1. Bender, W., D. Gruhl, N. Morimoto and A. Lu, "Techniques for Data Hiding," *IBM Syst. J.*, Vol. 35, 313, 1996.
2. Katzenbeisser, S. and F. A. P. Petitcolas, *Information Hiding Techniques for Steganography and Digital Watermarking*, Artech House Publishers, 2000.
3. Mantin, Itsik, "Analysis of The Stream Cipher RC4," *school Weizmann Institute of Science*, 2001.
4. Marvel, L. M., C. G. Boncelet and C. T. Retter, "Spread Spectrum Image Steganography," *IEEE Trans. Image Processing*, Vol. 8, 1075, 1999.
5. Rivest, R., A. Shamir and L. Adleman, "A Method for Obtaining Digital Signatures and PublicKey Cryptosystems," *Communications of the AMC*, Vol. 21, No. 2, 120, 1978.
6. Simmons, G. L., "The prisoners problem and subliminal channels," *Proc. Annu. Int. Cryptology Conf., SantaBarbara, CA*, 51, 1984.
7. Wu, M. and B. Liu, "Digital Watermarking Using Shuffling," *In Proc. IEEE ICIP'99, Kobe, Japan*, Vol. 1, 291, 1999.
8. Wu and B. Liu, "Data Hiding in Binary Image for Authentication and Annotation," *IEEE Transactions on Multimedia*, Vol. 6, No. 4, 528, 2004.

Aeromagnetic Search using Genetic Algorithm

A. Sheinker, **N. Salomonski**, **B. Ginzburg**
R&D Integrated Systems Section, Propulsion Division, Soreq NRC, Israel

L. Frumkis, **B. Z. Kaplan**
Ben-Gurion University of the Negev, Israel

Airborne Magnetic Anomaly Detection (MAD) is used for decades to detect underwater targets, such as sunken ships. The concept of localization is based on the assumption that the magnetic field generated by the target is a dipole like, which produces an anomaly in the Earth magnetic field. Various noise sources reduce MAD performance. The major source is due to the aircraft maneuvers through Earth magnetic field. Another important source of interference is natural environmental noise. Known methods for noise reduction have limited capacity. That is why further investigation of effective noise cancellation is of great importance. Basing on modern nonlinear mathematical methods, we propose Genetic Algorithm (GA) for detection and localization of an underwater target by airborne MAD. The approach was simulated on a personal computer, obtaining promising results.

The measured magnetic field by the airborne magnetometer $\vec{B}(\vec{m},\vec{r})$ is a sum of the target magnetic field approximated by a dipole, and Earth's magnetic field $\vec{B}_{Earth}$assumed as a known constant:

$$\vec{B}(\vec{m},\vec{r}) = \frac{\mu_0}{4\pi}[\frac{3(\vec{m},\vec{r})\vec{r}}{r^5} - \frac{\vec{m}}{r^3}] + \vec{B}_{Earth} \tag{1}$$

Our aim is to solve Equation (1) for $\vec{m}$ and $\vec{r}$, which are the target magnetic moment, and the vector to the target respectively. By taking $N > 6$ samples of the measured magnetic field we get a nonlinear over-determined set of equations. The next step will be to define the solution domain and the needed resolution, thus transforming an analytical problem to a discrete problem. As a consequence there is no need to solve analytically the nonlinear over-determined equation set. Instead we can search for the (sub) optimal solution in a finite set. Checking all possible solutions one by one is a time consuming task, far behind up-to-date real time systems capabilities. For this reason we proposed the GA as a rapid search method. The stop condition of the GA has been 2,500 generations and the population was set to 50 chromosomes. Selection of those parameters results in execution time of 25 sec, which indicates that the proposed method can be implemented in real time. Preliminary results show high localization characteristics in noisy environment: for SNR=0.2 the scatter radius is about 60m, which is acceptable for practical needs. Further investigation will be made concerning various noise characteristic, gradiometric measurements, and enhanced detection capabilities.

Frames and Dual Frames in Computational Electromagnetics

A. R. Baghai-Wadji
RMIT University, Melbourne, Australia

A. S. Kahttab
Vienna University of Technology, Austria

In previous works we have shown that employing the fundamental solution of Laplace equation we can construct a scaling function and the associated wavelet which satisfy the criteria of the multiresolution analysis. A remarkable fact about this result is that while the utilized Green's function possesses a logarithmic singularity at infinity the constructed scaling function and the wavelet are devoid of any singularities. Even more, the latter two functions can be interpreted as potential responses of collections of overall charge-neutral line charges. More recently we have shown that also quasi-static asymptotic tails of general Greens functions in spectral domain can be utilized to construct scaling functions and wavelets, which satisfy the axioms of the multiresolution analysis. Furthermore, we have shown that arbitrary impulse responses of linear time invariant systems and general Green's functions permit the construction of orthonormal bases but not wavelets or wavelet-like systems of analyzing and synthesizing functions. These considerations have led us to the present work. In this presentation we consider a generalization of the concepts of bases and wavelets which is known as frames. Frames are overcomplete systems of functions, which, in conjunction with their dual frames, allow the analysis and reconstruction of finite energy functions. Related to a given frame and the associated dual frame there are the frame operator S and the corresponding dual frame operator $\tilde{S}$. However, the construction of dual frames involves the determination of the inverse of large dense matrices. To remedy this drawback, iterative algorithms have been suggested which can be employed. Frame algorithm, Chebyshev and conjugated gradient methods have been proposed in literature. This work is an attempt to further popularize the powerful concepts of frames and dual frames in computational electromagnetics by establishing a connection between shift-invariant spaces, frames and Green's functions. Following a brief review of the frame concept several classic and modern iterative techniques will be compared in view of their suitability for constructing dual frames. Apart from the aforementioned techniques the Gauss-Jacobi, Gauss-Seidel, successive relaxation, and the multi-preconditioned conjugated gradient algorithm will be discussed. Many examples throughout the discussion shall make the discussion accessible to an audience with no background in the theory of frames. The presentation will conclude with brief comments on irregular frames of translates, frames of exponentials, Gabor frames, wavelet frames and frame multiresolution analysis.

Finite Element Based Transformer Operational Model for Dynamic Simulations

O. A. Mohammed, **Z. Liu**, **S. Liu**, **N. Y. Abed**
Florida International University, U.S.A.

L. J. Petersen
Office of Naval Research, U.S.A.

Accurate electromagnetic transient studies, such as, harmonic loadCflow require accurate modeling of network elements and their components. The modeling of iron-core transformer plays an important role in the dynamic simulation of power system transients such as inrush currents, short circuits, and fault conditions.

The key point of iron core transformer modeling is the representation of nonlinear magnetization of iron core. Two commonly used methods are the piece-wise linear curve and the simple saturated reluctance function. These approaches consider the effects of average excitation level on the flux/inductance but ignore the fluctuating ac excitation itself. For cases requiring high-precision modeling, this is not adequate.

The transformer model proposed in this paper considers the effects of the average excitation levels as well as the periodic fluctuations of ac excitation on the winding self and mutual inductances during dynamic operation. Each inductance is described using a 2D profile, which is obtained from sequential FE solutions covering a complete ac cycle at various excitation levels. During dynamic simulation of power systems, the selection of the inductance value is performed using table-look-up technique. Technical details on the transformer modeling are provided, including the transformer equation, inductance calculation, 2D inductance table establishment, as well as Simulink implementation. As an example, a 60-kVA, 288/232-V three-phase power transformer is studied. Simulation results show that the established model is capable of restoring the nonlinear magnetization phenomena of transformer iron core. The significance of this model is its accuracy and its applicability for dynamic simulation of interconnected components in a power system.

Session 4P7b

Antennas

Fast FEM Frequency Sweep of Patch Antenna Using Robust Well-Conditioned Asymptotic Waveform Evaluation

Li-Ping Hu, **Yong-Ling Ban**, **Zaiping Nie**, **Feng Yang**
University of Electronic Science and Technology of China, China

Recently, a well-conditioned asymptotic waveform evaluation (WCAWE) moment-marching process [1][2] is proposed for matrix equations (like the frequency-domain finite element-boundary integral method) that have polynomial variations in the MORe parameter. Unlide regular AWE methods [3][4], the WCAWE process is well-conditioned, and therefore is robust and doesn't stagnate. Furthermore, unlike the linearized Krylov subspace methods [5], WCAWE doesn't require the neglection of higher order terms or the introduction of extra degrees of freedom; therefore, the approximation can be accurate in a wider bandwidth with just one expansion point and the memory required to store the MORe vectors doesn't become prohibitive for large-scale FEM problems. In [6], The WCAWE is integrated into MOM to calculate RCS of 3-D perfectly electric conductor (PEC) bodies, and furthermore an automate multipoint well-conditioned asymptotic waveform evaluation (AMWCAWE) technique was proposed by the same authors in [7]. In our work, firstly the vector finite element-boundary integral (FE-BI) method [8] is adopted to formulate the radiation model of a cavity-backed patch antenna, where the higher order hexahedral vector basis functions [9] are employed to expand the unknown field. And then the WCAWE with only a frequency expansion point is used to realize the fast frequency sweep for the response of input impedance over a wider frequency band. Numerical results for input impedance are presented to illustrate the robustness of the WCAWE.

REFERENCES

1. Slone, R. D., "Fast Frequency Sweep Model Order Reduction of Polynomial Matrix Equations Resulting from Finite Element Discretizations," *Ph.D Dissertation, Ohio State Univ., Columbus*, 2002.
2. Slone, R. D., R. Lee, and J. -F. Lee, "Well-conditioned Asymptotic Waveform Evaluation for Finite Elements," *IEEE Trans. Antennas Propagat.*, Vol. 61, No. 9, 2442, 2003.
3. Tong, C. -M. and W. Hong, "Fast Calculation of Wide Angle Mono-static RCS Pattern of Conducting Cylinders Based on Asymptotic Wave Evaluation Technique," *Acta Elec. Sinica*, Vol. 29, No. 9, 1198, 2001.
4. Sun, Y. -F. and S. -J. Shan, "Fast Computation of Wide-band Radar cross Section Using Asymptotic waveform Evaluation Technique," *Journal Infrared Millim. Waves*, Vol. 21, No. 6, 469, 2002.
5. Balk, I., "On a Passivity of the Arnoldi Based Model Order Recuction for Full-wave Electromagnetic Modeling," *IEEE Trans. Advanced Packaging*, Vol. 24, No. 3, 304, 2001.
6. Wan, J. -X. and C. H. Liang, "Fast Calculations of Scattering Response over a Wide Frequency Band Using WCAWE," *ACTA Elec. Sinica*, Vol. 32, No. 6, 1001, 2004.
7. Wan, J. -X. and C. H. Liang, "AMWCAWE-MNM for a MoM Fast Entire Frequency Sweep", *ACTA Elec. Sinica*, Vol. 32, No. 6, 911, 2004.
8. Jin, J. M., *The Finite Element Method in Electromagnetics*, New York, Wiley, Second Edition, 2002.
9. IIic, M. M., and B. M. Notaros, "Higher Order Hierarchical Curved Hexahedral Vector Finite Elements for Electromagnetic Modeling," *IEEE Trans. Microwave Theory and Techniques*, Vol. 51, No. 3, 1026, 2003.

Analysis of Probe-fed Conformal Microstrip Antennas on Finite Ground Plane and Substrate

Ning Yuan, **Tat Soon Yeo**, **Xiao-Chun Nie**
Yeow Beng Gan, **Le-Wei Li**
National University of Singapore, Singapore

The prediction of radiation and scattering from realistic microstrip antennas is essential to the design of many communication systems. In practice, microstrip antennas are usually probe-fed and fabricated on conformal, finite-sized ground plane and substrate. However, most studies on microstrip antennas considered infinite ground plane and substrates. In this paper, an accurate approach to analyze probe-fed microstrip antennas on finite ground plane and substrate based on the Volume-Surface-Wire integral equation (VSWIE) is presented.

In the VSWIE approach, the entire structure comprising the patch, ground plane, dielectric substrate and probe feed are included in the solution domain. The dielectric materials (substrate) are replaced by equivalent volume current and the conducting bodies (patch, ground plane and probe feed) are replaced by equivalent surface and wire current respectively. All currents radiate in free space, and hence the free space Green's function is used in the formulation. The Volume-Surface-Wire integral equation is established by enforcing the following two conditions:

(1) In the dielectric substrate, the total electric field is the sum of the field due to the impressed source and the scattered field;

(2) On the surface of the patch, ground plane and probe feed, the tangential components of the total electric field are zero.

The method of moments (MoM) is used to solve the integral equation. The unknown currents on the material bodies, conductive surfaces, and wires are expanded using three triangular-type basis functions. A special basis function [1] is applied to both patch and feed for the probe feed modeling. This attachment mode can be employed in any surface-wire junction. It ensures the continuity of electric current from the feed to the patch, and models the rapidly varying patch current in the vicinity of the connection point.

Our approach is best suited for irregularly shaped patches on conformal, finite-sized ground plane, since the approach is based on the free space Green's function and sub-domain basis functions. As the current on the probe feed is rigorously accounted for, the input impedance, radiation pattern and RCS of loaded patches can be accurately evaluated. This method can also be used to treat arbitrary configurations with conducting wire-surface junctions, e.g. wire antennas mounted on the surface of aircraft or satellite. Numerical results will be presented to verify the method and demonstrate its capability.

REFERENCES

1. Champagne, N. J., W. A. Johnson, D. R. Wilton, "On Attaching a Wire to a Triangulated Surface," *IEEE APS Int. Symp. Dig.*, 54, 2002.

Analysis of a Strip Monopole Mounted Near an Edge or a Vertex

Xiaofeng Que, **Zaiping Nie**
University of Electronic Science and Technology of China, China

The strip monopole model is used in the conjunction between the thin wire and the conducting bodies. The strip width equals to four times the radius of the thin wire. The wire/surface junction can be changed to the surface/surface junction. Planar triangular patches and RWG base function are used with the Moment Method. This method can avoid the difficulties caused by other methods for the junction problems which use additional attachment basis functions. In this paper, some segmentation methods for the triangular patches in the vicinity of the attachment point are described when the junction is near an edge or a vertex. Through adjusting the position of the junction, fewer triangular patches on the surface are segmented to get more equilateral triangles. The feeder model on the common edge of two RWG basis functions is obtained. The advantages of applying these segmentation methods are illustrated with several representative examples, which show good versatility and efficiency for solving these problems of wire/surface junctions.

REFERENCES

1. Newman, E. H. and D. M. Pozar, "Electromagnetic modeling of composite wire and surface geometries," *IEEE Trans. Antennas Propagat.*, Vol. 26, 784, 1978.
2. Pozar, D. M. and E. H. Newman, "Analysis of a monopole mounted near an edge or a vertex," *IEEE Trans. Antennas Propagat.*, Vol. 80, 401, 1982.
3. Mtthews, J. C. G. and G. G. Cook, "An efficient method for attaching thin wire monopoles to surfaces modeled using triangular patch segmentation," *IEEE. Trans. Antennas Propagat.*, Vol. 51, 1623, 2003.
4. Rao, S. M., D. R. Wilton and A. W. Glisson, "Electromagnetic scattering by surfaces of arbitrary shape," *IEEE Trans. Antennas Propagat.*, Vol. 30, 409, 1982.

Strip-Type AMC Structure and Analysis to Its Band-Gap Characteristic

Dunbao Yan, **Qiang Gao**, **Chao Wang**, **Naichang Yuan**
National University of Defense Technology, China

Because of its two unique characteristics: suppressing surface wave and reflecting plane wave in phase, mushroom-like artificial magnetic conductor (AMC) structures are widely studied recently. However, when vias are removed, the characteristic of suppressing surface wave disappear too. But the structure still reflect plane wave in phase, and it is found that the reflection phase band-gap is relative to only the size in the direction parallel to polarization direction of incident plane wave. Therefore the strip-type AMC structure is introduced, which is shown in Fig.1, and its reflection phase band-gap and surface wave band-gap are analyzed. Different surface wave characteristics compared with mushroom-like structure are found. Fig.2 shows the reflection phase characteristic of strip-type AMC structure for the plane wave with y polarization. When p_x is infinite, which means the structure becoming strip-type, the reflection phase characteristic is the same with mushroom-like AMC structure. In fact, reflection phase is not effected by vias. Therefore, when a fixed direction polarization in-phase reflection is required, a very simple strip-type structure without vias can be used. Moreover, because g_y is very small, TE surface wave in y direction can nor be established. Horizontal monopole antenna can be built on AMC closely, and the surface wave mode is TE mode mainly in the direction vertical to monopole. So the strip-type AMC is very simple and useful for some antenna application.

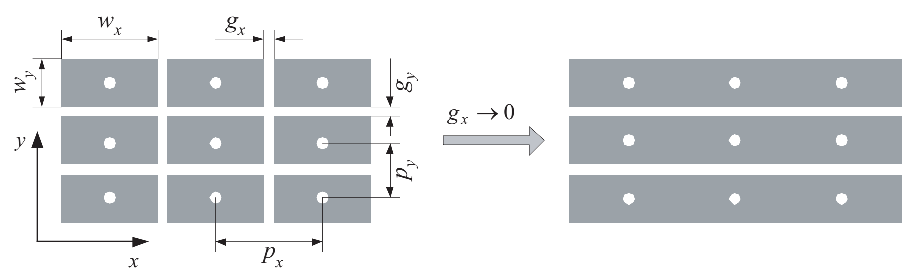

Figure 1: Geometry of strip-type AMC structure

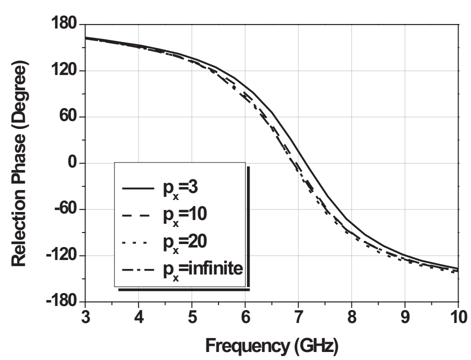

Figure 2: Reflection phase characteristic of strip-type AMC structure

A Critique and New Concept on Gain Bandwidth Limitation of Omnidirectional Antennas

Johnson J. H. Wang
Wang Electro-Opto Corporation, U.S.A.

It has been well-known and well-established for over half a century that the gain bandwidth of an omnidirectional antenna is fundamentally limited by its electrical size measured in wavelength (Chu, L. J., "Physical Limitations of Omnidirectional Antennas," *J. Appl. Phys.*, Vol. 19, 1948). The theory has been verified and amplified both theoretically and experimentally by many prominent engineer scholars, and is here collectively referred to as the Chu theory. The present paper is to point out the severe shortcomings of the Chu theory and offers a new concept which enables the design of omnidirectional antennas with gain bandwidth exceeding the limitations imposed by the Chu theory.

The severe shortcomings of the Chu theory are rooted in its basic assumptions which are overly narrow and inconsistent with most real-world problems. First, an omnidirectional antenna is rarely an object isolated in space. Its specific size becomes ambiguous when it is mounted on a platform. Second, the problem was formulated overly restrictively (strictly speaking, inadequately) as an antenna with an external matching network, with single-port connections between them and the transceiver. Third, the Chu theory is applicable only to high-Q narrowband antennas, such as the resonant antennas, since the relationship between Q (quality factor) and bandwidth, a key cornerstone of the Chu theory, is valid only for the case of high Q (say, $Q > 4$). Fourth, the unrealistic assumption of zero dissipative loss often ended up with hardware having unexpectedly low efficiency and gain, especially when it is applied to resonant antennas.

The above observations are straightforward, and readily obvious, upon a close examination of the Chu theory. They have also been verified experimentally recently using refined models of the mode-0 SMM (spiral-mode microstrip) antenna (Wang, U.S. Patent #5,508,710, April 16, 1996; U.S. Patent #5,621,422, April 15, 1997). This antenna is a traveling-wave antenna (Wang, *Electromagnetics*, July-Aug, 2000) with good omnidirectional patterns like that of the monopole. It is in the shape of a disk 1.06-inch or 0.09 λ_L in height, and 5.7-inch or 0.48 λ_L in diameter, where λ_L is 11.8 inch, the wavelength at f_L (1 GHz, the low end of the operating frequencies).

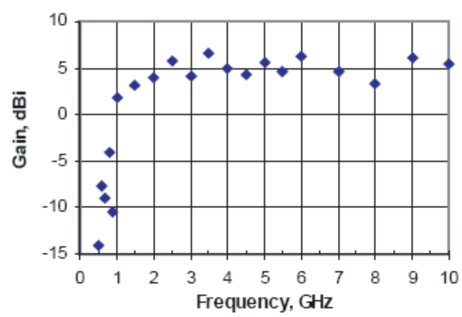

Figure 1: Measured gain of a mode-0 SMM antenna.

Fig.1 shows measured data obtained in WEO's anechoic chamber for this antenna mounted on a ground plane 12-inch in diameter. As can be seen, a 10:1 gain bandwidth (1-10 GHz) with minimum gain of 1 dBi was achieved. The measured gain bandwidth far exceeds the prediction of the Chu theory; this is not surprising since the four assumptions of the Chu theory are invalid for this antenna. Note that a large gain bandwidth exceeding the limitations of the Chu theory can be achieved, as demonstrated here, by circumventing the narrow and often impractical assumptions on which the Chu theory rests.

Multi-Band Meander Antenna

The-Nan Chang
Tatung University, Taiwan

In this paper, we discuss a kind of meander antenna shown in Fig.1 which is designed for FM (88-108MHz) and DAB (upper band of Band III) reception. Two resonators were constructed on the topside of a printed circuit board. The resonator with a longer length is responsible for an FM band, while the shorter one is for DAB use. Since the second higher order mode FM frequency range is roughly within the bandwidth of a DAB signal, the structure is expected to be able to enhance the DAB bandwidth. It is shown in Fig.2 that a two-resonantor behavior is observed within the DAB band. The 216MHz resonant frequency in DAB band is twice that of 108MHz.

Based on this idea, different coupling resonators can be introduced to tune resonant frequencies to the required pass-band. Resonators with different lengths are resonated at different frequencies and these multiple resonances are responsible for an enhancement in bandwidth. We may also add resonators on the backside of the present structure. We found that it is easy to tune multiple frequencies to the required pass-band.

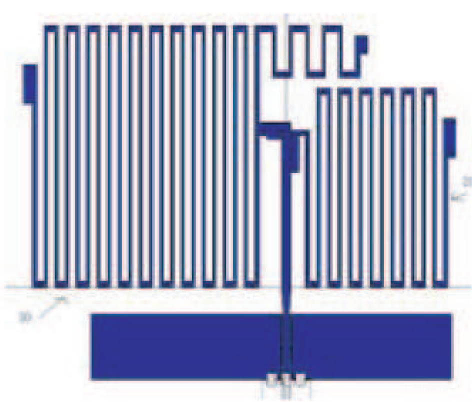

Figure 1:

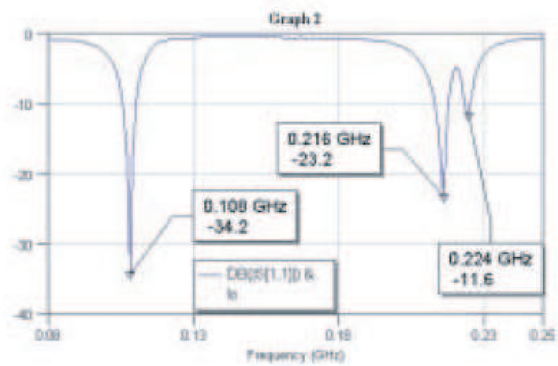

Figure 2:

Wearable Antennas Adopted at Mobile Terminal in MIMO System

Wei-Hong Xiao, **Zaiping Nie**, **Yan Cheng**
University of Electronic Science and Technology of China, China

Multiple-input multiple-output (MIMO) technique employs multiple transmit antennas and multiple receive antennas simultaneously, which can greatly increase the capacity and spectrum efficiency of wireless communication systems. It is a key technique for the new generation of mobile communication.

It has been demonstrated that the system's capacity increases linearly with the increasing of min(M,N). Compared with integrating antennas within the terminal, taking the antennas out of the mobile terminal by adopting the technique of wearable antenna can increase the min(M,N) remarkably. Since the wearable antenna system explores the space resource adequately, more diversity gain can be achieved.

In this paper, a new type of wearable antenna system is presented and its characteristics are evaluated. This antenna system is integrated on a strap, and it is composed of four rectangular microstrip patches made by flexible copper attached to flexible dielectric substrate. The central operating frequency of this antenna system is 2.14GHz. Each of the antennas is horizontally polarized and fed by EM coupling. Four rectangular microstrip antennas are arranged in the azimuth plane around the strap, and the distance between each antenna is about 1λ. Since wide angle spread occurs in outdoor urban and indoor environments at the mobile terminals, spatial diversity gain, as well as pattern diversity gain, will be achieved. As the strap is putted around human's body, the influences of curved-surface profile and different size of humans body should not be neglected. Designs taking into account these influences are also presented in this paper.

Printed Dipole Antenna Designed with Microstrip Balun on V-shaped Ground Plane

Zhiguang Fan, **Lixin Ran**, **Kangsheng Chen**
Zhejiang University, China

Based on improving the feeding structure of microstrip balun, a printed dipole antenna is designed with microstrip balun on V-shaped ground plane. Compared with the original microstrip balun feeding structure, such printed dipole antenna features a broader impedance bandwidth in excess of 33% (under VSWR < 2 and a center frequency of 2.4GHz), an increased gain by 2dB, a backward radiation suppression greater than 7dB and a good consistence of radiation pattern in the whole operating band. This antenna is therefore a good selection as a basic radiating element for a complex antenna system.

Figure 1 shows the structure of the dipole antenna . It is printed on both sides of a FR4-type PCB substrate with a thickness of 1.6mm and a relative dielectric constant of 4.6. In the figure, black color denotes one side of the PCB substrate and gray color denotes the other one. The RF signal is fed into the antenna by SMA interface. The dimensions of the antenna are designated as d, theta, L1, L2, L3, W1, W2 and W3. For the experimental setup we have d = 5mm, theta = 45°, L1 = 19.9mm, L2 = 16mm, L3 = 10mm, W1 = 6mm, W2 = 5mm and W3 = 15mm.

Figure 2 shows the results of the simulation and experiment. The impedance bandwidth is larger than 33% (under VSWR < 2 and a center frequency of 2.4GHz).

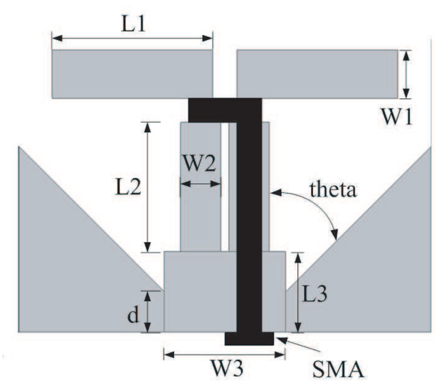

Figure 1: Structure of the antenna

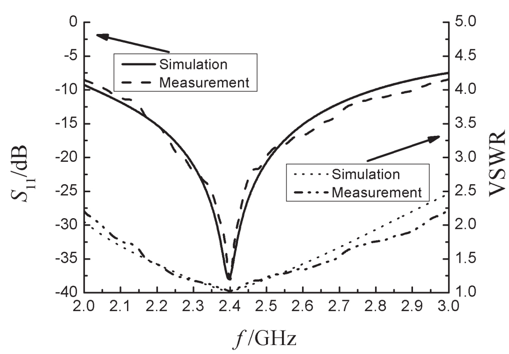

Figure 2: Results of the simulation and experiment

Session 5A1

Passive Microwave Imaging Technology and Applications

Research Activity on Synthetic Aperture Radiometry in CSSAR/CAS

Ji Wu, **Hao Liu**, **Shouzheng Ban**, **Xiaolong Dong**, **Jingshan Jiang**
Center for Space Science and Applied Research, Chinese Academy of Sciences, China

Interferometric synthetic aperture radiometry is a relative new technique in the area of microwave earth observation to measure the brightness temperature distribution of the earth. It can enhance the spatial resolution of the passive microwave remote sensing effectively. Steady progresses of this technology have been achieved in both one dimensional and two dimensional cases since 1990's. The typical instruments are ESTAR and MIRAS.

Relative research in China was mainly conducted by National Microwave Remote Sensing Laboratory (NMRS Lab), Center for Space Science and Applied Research (CSSAR), Chinese Academy of Sciences (CAS).

Under the support of the National High Technology Research and Development Program of China (863 Program), NMRS/CSSAR/CAS started its own preliminary research on this topic from the middle of 1990's. A C-band instrument has been developed as a demonstrator by 2001, which can achieve 4 degree spatial resolution with 6 channels and 11 analogue correlators. Many experiences and lessons were achieved in this progress. After that, NMRS/CSSAR/CAS developed an airborne X-band 8 channel synthetic aperture radiometer during 2002∼2004, which can achieve higher spatial resolution about 2 degrees. Both analogue and digital correlation scheme are adopt in this system design to permit the direct comparison between them. The X-band instrument got a good performance in its first flying experiment in April, 2004. Furthermore, by utilizing different antenna array arrangement and digital correlation design, this one-dimensional X-band instrument can even be switched to a two-dimensional experimental system.

In this paper, the development of the C-band and X-band instruments will be reviewed, and the system upgrade plan of them will be prospected. The latest experimental results of the digital correlation X-band instrument, including two-dimension imaging results, will also be presented.

SMOS In-Orbit External Calibration and Validation

M. Martín-Neira, **M. Suess**, **J. Kainulainen**
European Space Agency, The Netherlands

SMOS is ESA's second Earth Explorer mission with the objective of producing global maps of Soil Moisture and Ocean Salinity over the Earth. Launch date is expected in the beginning of 2007. The only instrument on-borad SMOS is an L-band Microwave Imaging Radiometer with Aperture Synthesis (MIRAS).

This paper describes what is believed to be the optimum strategy to calibrate and validate MIRAS in-orbit using external targets. The method ensures the generation of valid and calibrated visibilities from raw measurements with minimum impact from instrument errors, in particular, antenna errors. Central to the method are the flat target response and the flat target transformation of the Corbella equation.

It has been possible to devise this strategy only after the derivation of the Corbella equation, published recently, which correctly describes how MIRAS works. The proposed in-orbit calibration and validation approach is fully based on this equation. The paper provides the theoretical background of the calibration and validation approach as well as some preliminary simulation results on the improvement gained.

Evaluation of Imaging Performance for Sub-Y-type Interferometric Synthetic Aperture Radiometer

Ho-Jin Lee, **Hyuk Park**, **Sung-Hyun Kim**, **Yong-Hoon Kim**
Gwangju Institute of Science and Technology, Korea

The two-dimensional interferometric synthetic aperture radiometer measures the brightness temperature distribution using two-dimensional antenna array without scanning. This type radiometer is developed for meteorology, earth observation like atmosphere or ocean monitoring applications, such as MIRAS developed by ESA for ocean monitoring. It has been reported that Y-type array configuration with equally spaced antennas are optimal in terms of a narrow 3dB beamwidth and wide synthesized field-of-view.

The interferometric synthetic aperture radiometer with sub-Y-type antenna array was suggested to improve the spatial resolution than that of conventional Y-type with the same number of antenna elements. To evaluate it, 37 GHz 2-channel interferometric radiometer demonstration model is developed. This model consists of microstrip patch antennas, an antenna mounting structure and two channels correlation radiometer. The visibility samples for interferometric aperture synthesis are measured by sequentially spacing two antenna elements in required pairs of positions in the near-field condition. The measured visibility samples are for sub-Y-type with 40 antennas. The angular resolution of sub-Y-type array with the 40 antennas was compared with that of Y-type array with the 40 antennas. The imaging characteristics of sub-Y-type array for the single point source were analyzed not only theoretically, but also experimentally. From the experiment the angular resolution of the sub-Y-type is enhanced by about 23% enhancement than that of the conventional Y-type. In this paper, the performance of sub-Y-type was evaluated under the some two-dimensional targets such as a square object and contiguous square objects. The images of sub-Y-type and Y-type array were simulated. The imaging features were compared.

FY3 Microwave Radiometer Image(MWRI) Surface Parameters Inversion Algorithm and Validation in China

Yang Hu
National Satellite Meteorological Center, China

Jiancheng Shi
University of California, Santa Barbara, U.S.A.

FY3 is new generation polar orbit meteorological satellite of China plan to launch in 2006. There is total of 11 different remote sensing sensor onboard it, design to get the geophysical parameters of atmosphere, land, and ocean surfaces at the same time all day and night and in all weather conditions. The MWRI is a 10-channel five-frequency linearly polarized, passive microwave radiometer imager system onboard the FY3, which measures atmospheric, ocean, and terrain microwave brightness temperatures at 10.65, 18.7, 22.3, 36.5, and 89 GHz. In this paper, in order to derive surface temperature and soil moisture from the MWRI data, a new developed microwave RT model, AIEM was used to simulate the microwave emission characteristic of bare soil, and an new surface soil moisture inversion algorithm was established, which is only need the 10.65GHz V and H channel data. Applying the algorithm to AMSR-E orbit data, which is very similar with the FY3/MWRI, the daily globe soil moisture distribution was derived. The surface temperature was also derived by using a empirical model. To compare the inversion results with insitu data, the meteorological data in china area was collected, and points were interpolated to area with the resolution of MWRI by using a new interpolate model of complex terrain.

Application of Synthetic Aperture Radiometer Technology in Solar Wind Remote Sensing

Ji Wu, **Hao Liu**, **Weiying Sun**, **and Chi Wang**
Center for Space Science and Applied Research, Chinese Academy of Sciences, China

Shui Wang and Chingsheng Wu
Chinese University of Science and Technology, China

Synthetic aperture radiometer technology used nowadays in earth remote sensing is an extended development from ground based radio astronomy once used for star observation. However, once the technology is developed in the earth remote sensing field, it can certainly be applied back in its original field or other field. In this paper, we will discuss the rotational phased array of time shared synthetic aperture technology application in solar wind remote sensing area. The main idea is to send a spacecraft to the orbit of solar polar orbit. From this orbit, one can look down to the ecliptic plane solar wind propagation. In fact the most interested and useful information of the interplanetary solar wind is the Corona Material Ejection (CME) since it can cause sever geospace storms and result man made technical system such as satellite failure. The main scientific initiatives and technical system conceptual design will be explained in this paper.

Optimization of Fourier Plane Coverage of Antenna Arrays for SPORT

Weiying Sun[1,2], **Baoyu He**[1], **Ji Wu**[1]

[1]Center for Space Science and Applied Research, Chinese Academy of Sciences, China
[2]Graduate School of the Chinese Academy of Science, China

The fidelity of image reconstruction of SPORT depends on samplings in the Fourier transform domain of the scene performed by its antennas array. Research in this paper aims at finding the optimal layout of the receiving elements which is fitting for SPORT. Simulated annealing is applied to finding solutions for $N = 8, 10, 12, 14$. The simulation results show that centers of gravity of optimized antenna arrays are situated on center of the circle. Spatial frequency domain is covered evenly by the sampling points after rotation of the optimized antenna array. Moreover, the redundancy of baselines is minimized. The length values of the baselines of the optimized antenna array are also evenly distributed on the interval [0, 1].

On-board Calibration Instruments of MIRAS

Andreas Colliander[1], **Josu Uusitalo**[2], **Lasse Ruokokoski**[2]
Ville Kangas[2], **Aleksi Aalto**[1], **Janne Lahtinen**[2], **Martti Hallikainen**[1]

[1]Helsinki University of Technology, Finland
[2]Ylinen Electronics Ltd, Finland

New radiometric techniques have been developed as we have deigned, manufactured and tested a reference radiometer and a noise distribution network (NDN) for calibration of the MIRAS (Microwave Imaging Radiometer Using Aperture Synthesis) instrument of the SMOS satellite at Ylinen Electronics Ltd and Laboratory of Space Technology of Helsinki University of Technology. The performance of these subsystems is a decisive factor of the MIRAS performance. In this paper we present the operation principles of the NIR and the NDN and the related design guidelines and test methods, which we have been following in the developing of these subsystems. Additionally, an overview on the development process of the subsystems is given.

The MIRAS (Microwave Imaging Radiometer Using Aperture Synthesis) instrument is the single payload of the SMOS (Soil Moisture and Ocean Salinity) mission of European Space Agency (ESA). The MIRAS is an interferometric radiometer, or synthetic aperture radiometer, providing brightness temperature images of Earth's surface at L-band.

The calibration procedure of the MIRAS involves three reference radiometers. The reference radiometer is a fully polarimetric noise injection radiometer (NIR) with the capability to measure the noise temperature level of the NDN, as its purposes are: (1) Measurement of fully polarimetric antenna temperature; (2) Measurement of noise temperature of the NDN; (3) Measurement of a MIRAS baseline with any other receiver units. The purpose of the NDN is to calibrate the following parameters of the LICEF units: (1) Receiver noise temperature and gain; (2) Total phase shift experienced by the signal as it travels from the receiver input to the receiver output (the phase shifts of different receivers are not identical, so so-called in-phase errors exist between the receivers); (3) Quadrature phase error: the amount by which the phase difference of the I and Q outputs of a LICEF unit differs from 90 degrees.

The NIR and NDN subsystems are being developed, manufactured and tested by Ylinen Electronics Ltd (Ylinen) and Laboratory of Space Technology of Helsinki University of Technology (HUT). The work was started with prototyping in year 2001 and the flight model of both subsystems is to be finished in year 2005. The SMOS satellite is to be launched in the beginning of year 2007. In the process we have developed new radiometric techniques for the NIR and ensured the high performance of the NDN.

Image Simulator for One Dimensional Synthetic Aperture Microwave Radiometer

Qiong Wu, **Hao Liu**, **Ji Wu**
Center for Space Science and Applied Research, CAS, China

Calibration for a one-dimensional synthetic aperture microwave radiometer is critical. A numerical image retrieving method using an intermediate transformation matrix called the gain matrix or simply G-matrix is considered to be a good method. This matrix takes into account all the couplings and un-uniformed amplitude and phase between the channels. However, measuring the G-matrix is not an easy job. One has to set up a point source in the far field and rotate the system in the fan beam direction. The difficulty is mainly due to the incomplete test environment.

In this paper,a measurement set-up called image simulator is present. It is a circuit network composed of a number of high accurate microwave I-Q vector modulators and a noise generator. It simulates the incoming waves to the thinned antenna array corresponding to any image scene to be measured.

The design and test of the image simulator are presented followed with test results of G-matrix. The image simulator can also simulate a point source in the two dimensional aperture case which discussed in the paper too.

Wavelet Interpolation Algorithm for Synthetic Aperture Radiometer

Chunxia Fu[1,2], **Ji Wu**[1]

[1]Center for Space Science and Applied Research, CAS, China
[2]Graduate School of Chinese Academy of Sciences, China

In this paper, we propose a wavelet-based-interpolation algorithm, which improves the effect of Fourier image reconstruction for 2_D synthetic aperture radiometer. The core idea is to get the VF (Visibility Function) data on grid points by using the interpolation algorithm. Along with the problems that Fourier transform meets being solved, the reconstruction precision improved. Comparing with the traditional interpolation methods, this algorithm has the advantages to take the correlation of the whole image into account, to keep fine details of the image, and to avoid the saw-tooth and smoothing effects associated with traditional image interpolation techniques. Accordingly, we present experiments to demonstrate the effectiveness of the algorithm.

Design and Implementation of Digital Correlator for CAS Synthetic Aperture Radiometer

Jingye Yan, **Ji Wu**, **Hao Liu**
Xiaolong Dong, **Jingshan Jiang**
Center for Space Science and Applied Research, Chinese Academy of Sciences, China

This paper is focused on the problem that the analog correlator unit of Synthetic Aperture radiometer is becoming too complex, so that have a inverse effect on the implementation of spaceborne synthetic aperture radiometer. There is a new digital correlator, which uses the technology of direct intermediate frequency(IF) sampling and digital phase shift.

The synthetic aperture radiometer comprises eight elements, one element is composed of a antenna and a receiver. Output IF signals from these receivers are fed to digial correlator. Digital correlator down-samples IF signals(Inphase signal, I) and delay one sample interval for 90 degree phase shift(Quadrature signals, Q) in the digitalized IF. Based on same method as analog correlation, the digitalized I/Q's are processed in a FPGA chip.

Due to the fact that the digital correlators are realized with the help of Analog-Digital Converter (ADC) chips and the FPGA technology, the realized volume, mass, power consumption and complexity turned out to be greatly reduced compared with that of the analog correlator's. Simulations show that the resolution of ADC has an influence on the synthesized antenna patterns, but it is very closed to the analog correlator's result if more than 2bit is used. Experiences conducted in April 2004 gain satisfying images based on our design.

Tsunami Detection Using the PARIS Concept

M. Martin-Neira, **C. Buck**
European Space Agency, The Netherlands

S. Gleason, **M. Unwin**
University of Surrey, U.K.

M. Caparrini, **E. Farrés**, **Olivier Germain**, **G. Ruffini**, **F. Soulat**
Edifici de l'Observatori Fabra, Muntanya del Tibidabo, Spain

On December 26th 2004 a tsunami generated by an earthquake with epicentre on the Indian Ocean West of Indonesia caused a real human and material catastrophe in this region. After the event some proposals to establish a network of sensors for tsunami detection were put forward.

The present paper presents an alternative concept that can be applied from satellite, aircraft or from the coast, and which can complement such network of sensors for fast tsunami detection. The concept makes use of GNSS signals reflected from the ocean's surface to perform mesoscale ocean altimetry. The technique, designated PARIS (Passive Reflectometry and Interferometry System), aims at capturing fast topographic events happening on the ocean surface, as eddies and fronts.

PARIS is a very wide swath altimeter, of near 1000 km, as it picks up reflected signal from several GNSS satellites (typically 6 GPS and 6 Galileo when available). This wide swath means that a constellation of 10 PARIS satellites with an orbital inclination of 45° could cover the most populated central part of the Earth (from 45°S to 45°N in latitude) with a revisit time of less than an hour. A 30-60 cm 100 km wavelength tsunami wave in this region would be observable as the typical resolution of PARIS is 5-10 cm in height and 20-50 km in spatial resolution.

The paper describes some aircraft experiments that demonstrate the capability of the system, a technique which could also be used from commercial aircraft and from the coast.

Session 5A2

Periodic Structures I: Photonic Crystals and Related Topics

Research on the Wide-angle and Broadband 2D Photonic Crystal Polarization Splitter

Y. Y. Li, **P. F. Gu**, **M. Y. Li**, **H. Yan**, **X. Liu**
Zhejiang University, China

With the conventional polarizing beam-splitter, which utilizes the 1D photonic crystal made of thin films, only at the Brewster angle the unpolarized incident light is absolutely splitted into two orthogonal polarized beams, which are the reflected light polarized perpendicular to the plane of incidence and the transmitted light polarized parallel to that plane. Recently a novel 2D photonic crystal polarization splitter was described. It was based on the deposition of multilayer films onto a grating. By virtue of automatic shaping mechanism, the multilayer films were corrugated, which formed the rectangular lattice. It was demonstrated experimentally that for the near-infrared wavelengths the propagation of the transverse electric (TE) mode was forbidden and the transverse magnetic (TM) mode transmitted when the light incidented normally. The explanation in theory is that the partial band gap of TE mode overlap the passing band of TM mode for the wavevector $\bar{k}$ from Γ to X. It is considered an opening to the wide-angle and broadband 2D photonic crystal polarization splitter. If the partial band gap of TE mode is replaced by the complete band gap which also overlaps the complete passing band of TM mode for all the direction of wavevector $\bar{k}$, it means the omnidirectional polarization splitter is obtained.

So, in this paper, a 2D photonic crystal of corrugated multilayer films is designed with the materials of SiO_2 and a-Si, which realizes omnidirectional polarization splitting with TM mode complete passing window from $\lambda = 1.48$ to $1.52\mu m$ which is the complete band gap of TE mode. Plane-wave expansion method(PWM) is used to calculate the band structure. After the optimization, we find that both the slope angle of the layers and the width of a-Si layer have wide variable ranges which is of great benefit to the manufacture. The finite-difference time-domain(FDTD) method is employed to simulate the propagation of the TM mode and calculate both the insertion loss and the extinction ration as a function of the incidence angle. An arrow-head like 2D photonic crystal which is the deformation of the corrugated multilayer films is also designed for comparison. It can only work as a wide-angle polarization splitter not an omnidirectional one for the wavelength from 1.28 to $1.31\mu m$. The comparison of the band structures of these two different 2D photonic crystals leads to the method of extending the incidence angle of the 2D photonic crystal polarization splitter.

REFERENCES

1. Kawashima, T., T. Sato, et al., "Tailoring of the Unit Cell Structure of Autocloned Photonic Crystals," *IEEE Journal of Quantum Electronics*, Vol. 38, 899, 2002.
2. Hanaizumi, O., K. Miura, et al., "Frontiers Related with Automatic Shaping of Photonic Crystals," *IEICE Trans. Electron.*, Vol. E83-C, 912, 2000.

Tunable Study of Frequency Selective Filter Based on Photonic Crystal

Gang Bi, **Yongjin Zhang**, **Huajuan Wang**
Zhejiang University, China

An effective design of frequency Selective Filter in a two-dimensional (2-D) photonic-crystal (PC) is proposed. At first, a branch-missing-line photonic-crystal waveguide by inserting three different PC materials to the crotch was researched. By analyzing band gaps of the filter, the characteristics of a frequency selective filter were discussed. Second, by choosing different radii of PC rods in the crotch of a branch waveguide, we can similarly obtain the required frequency of the electromagnetic wave. Finally, by using Thermo-optical effect to change dielectric constant, the operating wavelength of the device can be tuned.

Superprism Effect in Thin Film Fabry-Perot Filter

Xue-Zheng Sun, **Pei-Fu Gu**, **Hai-Xing Chen**, **Bo Jin**, **Hai-Feng Li**, **Xu Liu**

Zhejiang University, China

The superprism phenomenon has been studied nearby the forbidden band in photonic crystal, where the phase and group velocity change rapidly with wavelength and it caused the large spatial separation for beam of different wavelength after exiting the photonic crystal device; this effect could be used for achieving large light deflection in different wavelength as the prism-like component. Thin film Fabry-Perot filter could be simply regarded as the 1-D thin film photonic crystal, which has drastic change in phase around the transmittance peak wavelength and exhibit large group delay. Herein, we investigated such effect in thin film Fabry-Perot filter and observed the large spatial separation with different wavelength nearby the transmittance peak by deploying its large group delay, the exiting shift for different wavelength outside the device was simulated and calculated by characteristic matrix method used in thin film theory and the spot splitting phenomenon of the incident Gaussian beam was also observed, we analyzed the Gaussian beam propagating in the device by Fourier decomposition in angular field and gave the interpretation of this phenomenon. The thin film device was fabricated by e-beam deposition in vacuum and measured from 782nm to 787nm achieved by the tunable Ti-sapphire laser; the maximum shift could reach to $65\mu m$ at transmittance peak wavelength which consist well with the designed one. The total thickness of the thin film stack of the device is only $3.3\mu m$, it shows a very large deflection angle about $1.8°$/nm compared with the traditional prism. This device is very useful for making compact light deflection system or the spatial de-multiplexer device in optical communication system.

Difference between Homogeneous and Inhomogeneous Methods While Simulating Nonlinear Kerr Type Photonic Crystals

J-J. Bonnefois, **G. Guida**, **A. Priou**
GEA, France

Photonic crystals exhibit strong confinement of the light and lead to an important exaltation of the electromagnetic field. As a consequence, it has been judged an interesting Kerr material by the scientific community [1], the major objective being to obtain a switching and/or bistable behaviour for bulk or integrated optic.

Many methods to simulate 2D Kerr Photonic Crystals rely on the assumption that, if small enough, the Kerr inclusions can be seen as homogeneous and their permittivity is then linked to the spatial average of the field inside them. This concern methods such as, but not restricted to MSM [2] or Green function based [3].

Methods which can rigorously simulate inhomogeneous Kerr PCs are eigenmodes expansion approach [4,5] well suited for waveguide, PWM which concern unlimited PCs [6,8] and FDTD which is very versatile but needs huge amount of computing time and storage capacity [7] while having its own problems with non-linear PCs [6].

We developed a new extension of MSM able to cope with inhomogeneous Kerr inclusions while retaining its versatility to simulate limited, unlimited, disordered or complex PCs geometry. We also used the FFF algorithm [9] and wrote another program able to tackle depth limited inhomogeneous Kerr PCs. The two ab-initio frequency domain methods, having only the Maxwell equations in common, produced results in perfect agreement and needed only a fraction of the computer power and storage capacity necessary to FDTD. Using this new MSM method we explore the difference produce by the use of the homogeneous simplification versus a strict inhomogeneous model. Surprisingly, as 2D-PC constituted by cylinders as small as $\lambda/9$ were thought to be safely assumed as homogeneous we found that when used as cavity border such as in [2], the difference could become drastically important. Indeed this difference can even exceed 100% while predicting the device's switching intensity threshold if cylinders no bigger than $\lambda/6$ are used.

REFERENCES

1. Slusher, R. E. and B. J. Eggleton (eds), "Nonlinear Photonic Crystals", *Springer-Verlag*, 2003.
2. Centeno, E., D. Felbacq, "Optical bistability in finite-size nonlinear bidimensional photonic crystals doped by a microcavity", *Phys. Rev. B*, Vol. 62, No. 12, 2000.
3. Mingaleev, S. F., Y. S. Kivshar, "Self-Trapping and stable localized modes in Nonlinear Photonic Crystals", *Phys. Rev. Letters*, Vol. 86, No. 24, 2001.
4. Bienstman, P., R. Baets, *Opt. Quantum. Electron*, Vol. 33(4-5), 327, 2001.
5. 1998B.Maes et al., "Rigorous modelling of non-linear wavelength-scale$\cdots$", *OWTNM 2003, 11, Czech Republic*, 98, 2003.
6. Panoiu, N. C., M. Bahl, R. M. Osgood Jr, "Ultrafast optical tuning of a superprism effect in nonlinear photonic crystals", *JOSA B*, Vol. 21, No. 8, 2004.
7. Taflove, A., ed., "Advances in Computational Electrodynamics: The Finite-Difference Time-Domain Method". *Norwood, MA: Artech House.*
8. Lousse, V., J. P. Vigneron, "Self Consistent photonic band structure of dielectric supperlattices containing nonlinear optical material", *Phys. rev. E*, Vol. 63, 2001.
9. Neviere, M., E. Popov, "Light propagation in periodic Media, Differential theory and design", *Marcel Dekker Inc.*

Unification of Gap Soliton Classes

Xunya Jiang[1,2], **Mingrui Zhang**[1], **Chuanhong Zhou**[1], **J. D. Joannopoulos**[2]

[1] Institute of Mircrosystems and Information Technology, CAS, China
[2] Massachusetts Institute of Technology, USA

We studied the gap solitons in nonlinear photonic crystal systems and constuct a new physical picture, the local Bloch wave picture, to discribe the complex interplay between the periodicity and the nonlinearity in such systems. From the picture, we can see that the nonlinearity not only is amplified by the periodicity, but also tunes the local Bloch functions. Such a feedback between the nonlinearity and the periodicity generates the new nonlinear effect (highorder nonlinear effect). New nonlinear equations are derived for the envelope of gap soltions and can explain all forms of gap soltions. Based on such equations, the new dynamical instability of the gap solitons is discovered.

Lamb Shift of Sources Embedded in Finite Two-dimensional Photonic Clusters

A. A. Asatryan, **L. C. Botten**, **N. A. Nicorovici**
University of Technology, Australia

Spontaneous emission and Lamb shift of energy levels of atoms are amongst the most fundamental effects of quantum electrodynamics. While these were studied originally for atoms in free space, it is now well known that both the emission rate and source frequency can be modified by the environment. The effects can be particularly strong in photonic crystals[1]—microstructures, with a periodic refractive index distribution, having ranges of propagating states (pass bands) as well as ranges of inhibited states (band gaps) in their frequency spectrum. In the case of infinite photonic crystals it has been shown that, at the edge of the gap, there exists a photon-atom bound state as well as an enhancement of the Lamb shift[2], assuming an isotropic dispersion model. On the other hand, assuming an anisotropic dispersion model, smaller energy shifts (relative to vacuum) have been reported[3]. There also appears to be some controversy in the literature concerning the size of the Lamb shift at the edge of the band gap, with Li[4] finding no significant change in the Lamb shift (compared with that observed in free space) for a hydrogen atom embedded in an infinite photonic crystal, and Wang[5] reporting the opposite conclusion.

Until now, all calculations for the Lamb shift have been undertaken at separate points inside of an infinite photonic crystal. In reality, however, all photonic crystals are finite and it is important to understand the effect of both the finite size and cluster shape on the spatial distribution of the Lamb shift.

In this talk, we consider a two-dimensional photonic crystal cluster composed of a finite number of cylinders of infinite length, irradiated by a line (dipole antenna) source embedded in the structure. We follow the approach reported in[6] where the frequency shifts are found for a dipole oscillator located near a metallic interface. The scattering problem for the Green function G is solved using a rigorous multipole theory and, from that, the Lamb shift is calculated from the real part of G. Our calculations show that the Lamb shift is strongly enhanced at the gap edge and is a strong function of both the size of the cluster and its position. The Lamb shift is also a very sensitive function of the shape of the cluster. An animation showing the Lamb shift as a function of position and wavelength will be presented.

REFERENCES

1. Joannopoulos, J. D., R. D. Meade, and J. N. Winn, "Photonic Crystals," *Princeton University Press, Princeton, 1995*, 1995.
2. John, S., J. Wang, *Phys. Rev. Lett.*, Vol. 64, 2418, 1990.
3. Zhu, S.-Y, et al, *Phys. Rev. Lett.*, Vol. 84, 2136, 2000.
4. Li, Z.-Y., Y. Xia, *Phys. Rev. Lett.*, Vol. 63, 121305, 2001.
5. Wang, X.-H., Y. S. Kivshar, and B. Y. Gu, arXiv:quant-ph/0406183 Vol. 1, 25, 2004.
6. Morawitz, H., *Phys. Rev.*, Vol. 187, 1792, 1969.

A Theoretical Study of the Chirped and Apodized Photonic Crystals

Gang Bi, **Huajuan Wang**
Zhejiang University, China

The photonic crystal with two-dimensional chirped structure and apodized structure were analysed, and the transmission characteristics of them were studied by FDTD method and PML technology. The photonic band gap can be achieved wider with different chirped coefficient or apodized function. This can provide an effective method to control the photonic band gap in the photonic crystal applications.

Dielectric 2-D PBG Sheet Used as Substrate or Superstrate of Patch Antennas

Zhi-Chen Ge, **Wen-Xun Zhang**
Ying-Ying Gu, **Zhen-Guo Liu**
Southeast University, China

The dielectric PBG structure consisting of periodical cells prohibits the passage of electromagnetic wave with the frequency within some proper bands, which depend on the geometric sizes and dielectric permittivity of the cell. However, this electromagnetic band-gap property is sensitive to the direction of wave propagating. In the case of MIC application, a 2-D dielectric PBG substrate with air holes is effective for suppressing the surface wave and then increasing efficiency and reducing side-lobe-level. In the case of antenna application, the radiated wave forward to substrate should be reflected, by means of a ground plate (with spacing), or a 3-D multi-layer grating PBG structure (with larger thickness); on the other side, by using appropriate 2-D dielectric PBG superstrate over the radiator, the outward wave from radiator may be concentrated around the normal direction with enhanced directivity. As practical designed examples, let us put the microstrip patch antenna accompanied with dielectric 2-D PBG sheet acting as substrate or superstrate into comparison. For this purpose, a 2-D PBG sheet with permittivity of 10 and thickness of 1.27 mm is employed, which bandgap involves the resonant frequency 14 GHz of a microstrip patch radiator. When it is used as a substrate, the surface wave is reduced remarkably, which results in the improvements of 3 dB in the front-back ratio and 1.7 dB along the surface, compared to the traditional substrate. However, the resonant frequency is shifted down and bandwidth is narrower because the effective permittivity is lower; but the directivity is almost same. In this paper the authors treat the 2-D PBG sheet as superstrate of the radiator of patch with traditional substrate and ground plate. By means of increment in total thickness (height), we are looking for enhancing the directivity cover a similar bandwidth. To make comparison among a number of simulated examples by employing Microwaves Studio CST code, some results can be summarized as: (1) By using $\sim$l/4 thickness of superstate, whatever solid PBG sheet or a pair of thin (1.27 mm) PBG sheets, placed apart $\sim$l/2 from the patch, the directivity may be obviously increased up to 18 dB (corresponding to the aperture efficiency increase from $\sim 5\%$ to $\sim 67\%$) accompanied with improved side-lobe-level and front-back ratio. (2) If non-PBG superstrate are used as one of or both the sheets, though a similar directivity can also be obtained, the backward lobe become visibly larger (corresponding to the front-back ratio decrease from $\sim$23 dB to $\sim$12 dB) due to the stronger reflection from the inner-surface of the non-PBG superstrate and the unsuppressed surface wave inside the superstrate. In general, the demands for the dielectric material used as a substrate or a superstrate are different. For antenna application, the substrate of high permittivity should be avoided, which decrease the bandwidth and cause more surface wave; however, a high permittivity dielectric must be used in superstrate to enhance the directivity of antenna. On the other side, the dielectric PBG is always associated with high permittivity. So the dielectric PBG structure should be used as a superstrate rather than substrate.

Session 5A3

Antenna Design and EMC Problems for the Car-based Communications

A Vehicle-mounted Conformal Dual-band GPS/GSM Antenna

Wen-Jiao Liao
Yuan Ze University, Taiwan

Yan-Chun Peng
Yuan Ze University, Taiwan

A conformal dual-band GPS/GSM antenna suitable for mounting on vehicle chassis is proposed in this work. This antenna is designed for the vehicle positioning system (VPS), which requires positioning information from the global positioning system (GPS) and mobile data communication via existing GSM/GPRS systems. A desired VPS antenna design should meet following requirements: dual or multi-band coverage, individually specialized gain patterns, and conformal antenna structure. Because the VPS system not only receives the L-band GPS signal for vehicle positioning, but also provides connections to other communication systems such as the GPRS network, the VPS antenna must be capable of handling dual or multi-band signals. Furthermore, the VPS antenna must yield specified gain patterns and field polarizations for signals of applicable bands. For example, GPS signals may come from any direction of the upper hemisphere with circular polarization while linearly polarized GSM signals are more likely to appear at the horizontal directions. Finally, due to concerns on aerodynamics and vehicle styling, the VPS antenna should be made in planar structure so that it can be conformally mounted or integrated within the car chassis. Other factors such as durability, cost and physical volume are also of great importance. In this work, we integrate two types of antennas into a planar module so that it can be mounted on vehicle top. One is a patch antenna for GPS reception while the other is a cavity-backed slot antenna for GPRS/GSM signals. Because the two antennas are planar and the patch is expected to be smaller than the slot, they can be packed into the same space by overlapping the patch on top of the slot structure. We also employ dielectric loading to further reduce the physical volume of this dual-band antenna. In ideal conditions, the two antennas can be operated independently at the same time since the separation in operation bands and the required antenna patterns are different. Simulation and prototype measurement results are provided to demonstrate the feasibility of the mobile antenna. Performance degradation due to mutual coupling of closely spaced antenna elements are accessed. Techniques developed in this work can be forwarded to future research development on integration of multiple antennas.

Applications of Mounted Horns and R-cards to Improve the Radiation Performance of Microstrip Antennas Installed on the Car Roof

Hsi-Tseng Chou, **Chung-Yi Chung**, **Yu-Ting Hsiao**
Yuan Ze University, Taiwan

The demand of integrating wireless communications into mobile car has increased the utilization of antenna systems mounted on the car structures. In many situations, car antennas can experience destructive interferences due to the multi-path effects from front hood or back trunk when they are installed near the edge of the top roof. It is therefore motivated in this paper to design antenna systems that can improve the multipath effects caused by the car structure itself.

Among the popularly employed antenna types, microstrip antenna is one of excellent candidates that attracted most attentions because of its capability to remain small sizes. However, microstrip antenna's characteristics of broad main beam and side lobe patterns have increased the possibility of destructive multipath effects. Note that the multipath effects generally arise from the reflections of the trunk/hood surfaces and interference with main beams in some angles of interest. Those null angles have therefore caused problems in practical communication systems such as the reception of satellites might occur in these angles.

This paper intends to improve the radiation performance of microstrip antenna based on a hybrid combination of mounted horn structure and resistive card (R-card). The new antenna structures potentially reduce the sidelobes and wide angle main beam patterns, and as a result, increase the gains without significantly impacting the operation frequency. Experimental examinations are presented to demonstrate the concepts.

Currents Induced in Human Bodies Sitting inside a Vehicle Exposed to Lightning Electromagnetic Pulse Waves

Hsing-Yi Chen
Yuan Ze University, Taiwan

Yu-Feng Kuo
Yuan Ze University, Taiwan

Studies of vehicle's electromagnetic interference/compatibility (EMI/EMC) has become increasingly important due to the growing use of highly sensitive electronic devices in an automobile platform for wireless communications. On the other hand, one may pay special attention to the topic of currents induced in a human body sitting inside a vehicle exposed to lightning electromagnetic pulse (LEMP) waves. Because the fast rise time of $1 \sim 2\mu s$ for a very high magnitude LEMP wave may induce very high currents in a human body sitting inside a vehicle and may cause the human in mismanaging the vehicle. However, there is still a great deal unknown about the current or current density induced in a human body sitting inside a vehicle due to the exposure of LEMP waves. Because life is invaluable, it is very difficult to directly obtain an experimental descriptions of currents induced in a human body exposed to LEMP waves. Therefore, it is important for researchers to concentrate more on work associated with analytical and numerical quantification of these effects and to further study their potential hazards. Data from Fourier analysis show that the Fourier amplitude of the LEMP wave decreases very quickly for frequencies above 1MHz. But from Gandhi's study, the predominant components of the induced current are at frequency close to $40 \sim 45MHz$, which is near the resonant frequency of an adult human. In this paper, the finite difference time-domain (FDTD) method is used to study currents induced in human bodies sitting inside a car exposed to LEMP waves at frequency ranging from 10 Hz to 50 MHz. The human body is simulated by a realistic model with homogeneous muscle permittivity. The model of the human was constructed with 10,002 cubical cells of dimension 2 cm. The dielectric constant and conductivity of the human muscle at various frequencies were obtained from published literatures. An electric field of the LEMP wave $E_0(t) = 40(e^{-1.42\times10^4 t} - e^{-4.9\times10^6 t})$ kV/m is adopted for the simulation. The vehicle is divided into 266,004 cubical cells of dimension 2 cm. Obtained results of current and current distribution in human bodies will be presented in figures. Finally, remarks on health effects according to the calculation data and some sources obtained by scientific and public health communities will be made.

A Compact CPW-Fed Monopole Antenna for WLAN Systems

Yuehe Ge, **Karu P. Esselle**
Macquarie University, Australia

Trevor S. Bird
CSIRO ICT Centre, Australia

With the rapid growth in applications operating at the internationally available unlicensed ISM bands, future wireless systems are required to be multiband. Examples of the applications include Bluetooth or wireless local area networks (WLAN) at 2.4 GHz and WLAN systems at 5.2 and 5.8 GHz. Therefore, it is desirable for a single wireless device to provide multi-band operation, and multi-band antennas are needed for such multi-standard wireless devices. On the other hand, in order to meet size requirements, small antennas are essential for these wireless systems. In this paper, we present a compact multi-band monopole antenna for potential use in the wireless PCMCIA card and other similar small portable wireless devices.

In this paper a novel design of a quad-band small internal antenna is presented. This antenna covers IEEE 802.11a (5.2 and 5.8 GHz), 802.11b (2.4 GHz), 802.11g (2.4 GHz) and 802.11j (4.9 GHz) WLAN bands. The proposed antenna is fed by a 50-Ω CPW line and both lines as well as the ground plane are etched on a low-cost FR4/Epoxy substrate, which has a thickness of 0.8 mm and a dielectric constant of 4.4. Since the antenna is printed on a substrate, it can be easily integrated with the associated microstrip circuits, which are printed on the same substrate.

The radiating element is composed of two metal strips, which operate in two frequency bands. The two metal strips have the same, uniform width and are folded to make the element's shape like a rectangle. The total area of the element is less than 11×11 mm^2. The shorter metal strip is designed to operate in the upper frequency band, which is from 4.9$\sim$6 GHz, while the longer strip operates in the lower 2.4 GHz band. In the upper band, the starting point of the strip design is at the feed point, which is located at the end of the CPW transmission line and directly above the end edge of the ground plane. The resonant length of the shorter strip is around a quarter wavelength at the centre frequency ($\sim$5.5 GHz). For this kind of monopole antenna, a frequency band of over 20% can be obtained. In the lower band, the length is also about a quarter wavelength, but this longer strip is bent around the shorter one, leaving a small separation between the metal strips. The antenna has been designed by using Ansoft HFSS, fabricated in-house, and tested in the antenna facilities at CSIRO.

The measured return loss shows two operating frequency bands. The lower band bandwidth, determined by a return loss greater than 10 dB, covers the frequency range from 2.34 GHz to 2.55 GHz. The bandwidth in the upper band is about 2.6 GHz, from 4.64 GHz to 7.24 GHz, which cover the IEEE 802.11a, 802.11b, 802.11g and 802.11j WLAN frequency bands. The measured radiation patterns of the antenna will be described in the presentation at the Symposium.

Signal Modulation Recognizer Based on Method of Artificial Neural Networks

M. Richterova
University of Defence, Czech Republic

Communication signals travelling in space with different modulation types and different frequencies fall in a very wide band. Usually, it is required to identify and monitoring these signals for many applications. Some of these applications are for civilian purposes such as signal confirmation, interference identification and spectrum management. Automatic modulation recognition of communication signals is a rapidly evolving area of signal analysis. In recent years, interest from the academic research institutes has focused around the research and development of modulation recognition algorithms. In this paper is described the new original configuration of a subsystems for the automatic modulation recognition of digital and analog signals. The signal recognizer being developed consists of five subsystems: (1) adaptive antenna arrays, (2) pre-processing of EM signals, (3) key features extraction, (4) modulation recognizer and (5) output stage. The choice of maximum value of spectral power density of the normalised-centred amplitude, standard deviation of the absolute value of the centred non-linear component of the instantaneous phase, standard deviation of the absolute value of the normalized-centred instantaneous amplitude, standard deviation of the absolute value of the normalized-centred instantaneous frequency, spectrum symmetry measure as key features for the digital and analog modulation recognizer based on the artificial neural networks (ANNs). The new original structure of the recognizer of digital and analog signals is described. The modulation recognizer using two ANNs with two hidden layers. The results are summarized for real EM signals.

Dual-Band(PCS/IMT-2000) Mobile Handset Antenna

Ho-Jun Lee, **Se-Hwan Choi**, **Jae-Young Lee**, **Jong-Kyu Kim**
Korea Electronics Technology Institute, Korea

Byungje Lee
Kwangwoon University, Korea

In this paper, we propose a novel internal antenna design with a small size and low profile could be achieved. The proposed antenna obtained bandwidths cover the personal communication services(PCS : 1750-1870 MHz), international mobile telecommunication 2000(IMT-2000 : 1920-2170 MHz) bands within a VSWR of 2.0:1. The internal antenna has compact dimensions 9.1×5.8 mm and is mounted on the printed circuit board(PCB, 75×45 mm) an FR4 substrate (thickness 1.67 mm and relative permittivity 4.7), which can be treated as the circuit board of a practical mobile phone. To increase the bandwidth of a single layer antenna, parasitic elements have been added on the same substrate. Many configurations, having different dimensions and different numbers of elements have been tried experimentally in order to determine the most possible compact geometry. A considerable number of simulations, by modifying the parameters one by one, have been conducted to optimize the design that ensures satisfying the requirement of the frequency sweep for the dual-bnad mobile handset antenna. The proposed antenna is tested with the actual mobile phone. It is clearly seen that two wide operating bandwidths are obtained. Figure 1 shows the proposed dual-band internal antenna for PCS/IMT-2000 mobile phones. The proposed antenna is designed by using CST MWS(MicroWave Studio) simulator and tested by using the VNA(vector network analyzer, Agilent 8753ES), Satimo(Stargate-32) measurement system. The measured antenna gain for the PCS and IMT-2000 bands. The proposed antenna has the maximum gain of 1.84dBi and the average gain of -2.35dBi. For the PCS band the antenna gain is about 1.84∼ -5.61 dBi; for the IMT-2000 band the antenna gain ranges from 1.05∼ -4.67 dBi. Details of the proposed antenna designs are described, and typical experimental results are presented and discussed.

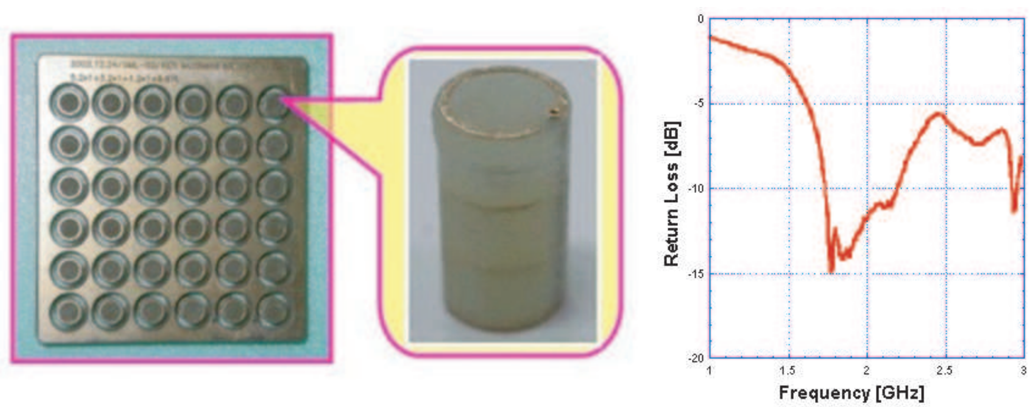

(a) The geometry of the internal antenna (b) Measured return loss

Figure 1: The proposed internal antenna.

Determination of Resonant Frequencies of Triangular and Retangular Microstrip Antennas, Using Artificial Neural Networks

E. R. Brinhole[1], **J. F. Z. Destro**[2], **A. A. C. de Freitas**[2], **N. P. de Alcantara Jr.**[3]

[1]Londrinense Metropolitan Faculty-UMP, PR- Brazil
[2]CEFET at Cornélio Procópio, PR-Brazil
[3]São Paulo State University-Unesp, Bauru-SP-Brazil

Triangular and retangular microstrip antennas are widely used in mobile communications devices (cell phones). For obvious reasons, these kinds of antennas must operate only in the vicinities of their resonant frequencies. Due to their very narrow bandwidth, the resonant frequencies must be determined with very high precision.

Deterministic mathematical models involve extensive numeric computations, subject to truncation errors, are time consuming and may need further experimental adjustments in relation to theoretical results previously obtained.

The resonant frequency of microstrip antennas is a phenomenon governed by laws whose behavior can be determined from input-output samples, obtained from real or simulated cases. ANN based models, trained with such data, are able to preliminary estimate, without the need of any mathematical expression, the resonant frequency of microstrip antennas in a fabrication process.

This paper uses Artificial Neural Networks (ANN) to compute the resonant frequencies of retangular and triangular microstrip antennas, used in mobile communications. The methodology consists in to develop models to estimate the resonant frequencies, and to compare them with deterministic and ANN based empirical models from the literature.

Perceptron Multi-layers (PML) and radial base functions (RBF) models are used. For retangular antennas PML networks was used with the Quasi-Newton method proposed by Broyden, Fletcher, Goldfarb and Shanno (BFGS). For triangular antennas PML networks used the Resilient Propagation (Rprop) Algorithm. In both cases the results was superior to others reported in the studied literature. However RBF based models used in this paper presented much better than PML models for both, reatangular and triangular antennas.

Finally, the proposed models are also able to be embedded in CAD (Computer Aided Desing) environments.

A LTCC-MLC Balance Filter with Two Transmission Zeros Using Image Parameter Method

Yng-Huey Jeng, **Yi-Ming Chen**
Sheng-Fuh Chang, **Hsiao-Kuang Lin**
National Chung Cheng University, Taiwan

A low-temperature co-fired ceramic (LTCC) differential bandpass filter is presented for applications in differential CMOS RF transceiver on a chip. The conventional bandpass filter is usually in a single-ended structure, which requires an additional balun to connect to the differential RF low-noise amplifier or balanced mixers. The differential signal format is often used in Silicon CMOS circuits for their excellent rejection of common-mode substrate noise. In this differential bandpass filter design, the balun is incorporated into the bandpass filter circuitry such that a miniaturized fully-integrated LTCC bandpass filter can be used directly between the antenna and single-chip differential CMOS RF transceiver. The differential bandpass filter is decomposed into a bandpass filter circuitry and a Marchan balun circuitry. The bandpass filter is designed by the image parameter method, which provides a simple and accurate technique to add extra transmission zeros in the stopband. The Marchand balun is realized with two sets of folded broadside-coupled lines to fully utilize the LTCC multilayer advantage. The circuit is simulated by 3D EM simulator to optimize the bandpass performance with two transmission zeros in the lower and upper stopbands. The EM simulation results show that the insertion loss is less than 1.8 dB and the return losses are greater than 12.5 dB in the 2.35-2.50 GHz. The amplitude imbalance is less than 0.23 dB and phase imbalance is less than 1.9°. The stopband rejection is greater than 35 dB over the 3.5-to-6.0 GHz range due to the incorporation of transmission zeros. The circuit is implemented by a sixteen layers LTCC process and the measured results agree very well with simulated results. This shows great application potentials of the proposed differential LTCC bandpass filter in wireless single-chip RF transceivers.

REFERENCES

1. Leong, Y. C., K. S. Ang and C. H. Lee, "A derivation of a class of 3-port baluns from symmetric 4-port networks," *IEEE MTT-S Digest*, 1165, 2002.
2. Tang, C. W., "Harmonic-suppression LTCC filter with step-impedance quarter-wavelength open stub," *IEEE Trans. Microwave Theory Tech.*, Vol. 52, No. 2, 617, 2004.
3. Hasler, M. and J. Neirynck, *Electric Filters, Boston, MA: Artech*, 1986.
4. Shea, T. H., M.S., *Transmission Networks and Wave Filters. New York: D. Van Nostrand Company, Inc.*, 1930.
5. *em user's manual, Sonnet Software Inc., Liverpool, NY.*
6. Hasler, M. and J. Neirynck, *Electric Filters. Boston, MA: Artech*, 1986.

A Miniaturized Dual-mode Bandpass Filter Using Self-coupled Step-impedance Resontaors

Yi-Ming Chen, **Yng-Huey Jeng**, **Sheng-Fuh Chang**
National Chung Cheng University, Taiwan

A miniaturized dual-mode bandpass filter using self-coupled step-impedance ring resonators is proposed. The self-coupled step-impedance resonator provides the same mode-separation effect as a perturbation stub in the regular smooth-impedance ring resonator. This offers an advantage of simpler circuit layout and the ring resonator size reduction, compared with the regular one-wavelength ring resonator. The even-mode and odd-mode analysis of step-impedance resonator is conducted to obtain the mode separation effect and the design formula. Furthermore, the coupled line analysis of step-impedance resonator is performed to estimate transmission zeros location. Then two step-impedance half-ring resonators are broadside-coupled with each other to reduce the circuit area and form a high harmonic-rejection bandpass filter. The 3D electromagnetic simulator HFSS is performed to optimize the passband insertion loss and stopband suppression. A prototype circuit was implemented with three layers of 25N substrate with the dielectric constant of 3.38, loss tangent of 0.002 and thickness of 18 mils and 30 mils, respectively. The circuit area is less than half of the filter implemented with the regular smooth ring resonators. The measured result shows 1.4dB insertion loss at 2.5 GHz. Three transmission zeros are distributed across the lower and upper stopbands, which locate at 1.65 GHz, 4.6 GHz and 6.3 GHz. Thus the harmonic rejection is at least 30 dB on the second and the third harmonics. The measured result agree very well with the simulation, showing great application potentials of proposed dual-mode bandpass filter in wireless communications.

Step-impedance Pseudo Interdigital Bandpass Filter with Multi Octave Stop-band Suppression

Sheng-Fuh Chang, **Chia-Chan Chang**, **Sheng-Chi Hsieh**
Yi-Ming Chen, **Gong-Hong Chou**
National Chung Cheng University, Taiwan

A microstrip pseudo-interdigital bandpass filter using inter-coupled step-impedance resonator is presented. A compact and high-selectivity microwave bandpass filter has become a must for high-performance RF measurements. By parallel-coupled microstrip bandpass filters, using open-ended $2/\lambda$ resonators, have been widely used for its advantages of planar structure, low cost, and ease of design. However, it suffers from poor stop-band suppression due to its inherent spurious passbands, particularly the nearest two harmonics at $2f_0$ and $3f_0$, where f_0 is the desired passband frequency. The microstrip interdigital filter, which is extremely compact by using $4/\lambda$ shot-circuited resonator, has nearest spurious harmonic at $3f_0$. But they require via holes, which are not compatible with the planar fabrication process. Hong et al. [1] proposed pseudo-interdigital structure without via-hole grounds, which offers a transmission zero near passband by nonadjacent inter-stage coupling. In this paper, a pseudo-interdigital filter, using inter-coupled step-impedance resonator and tapped I/O, enhance is designed to improve the skirt characteristics and increate the stop-band suppression. The advantage of step-impedance resonator removes the spurious harmonics farther away to higher frequency and the I/O tapping scheme helps eliminate, the spurious harmonic level. The electromagnetic simulation shows that spurious levels are reduced below 50dB up to 10GHz for a 4.5% bandwidth and 2.4dB insertion loss with at least 50dB suppression up to 10GHz for a 2.41GHz bandpass filter. The electromagnetic simulation shows that a 2.45GHz bandpass filter has at least 50dB suppression up to 10GHz, which is a significant, five-fold-stop-band suppression. The passband loss is 2.4dB and return loss reduced than 20dB. The circuits were implanted with FR4 board and its size is 21mm by 12.4mm. The measurement results show very good agreement with the simulation, showing great potentials in high-performance electromagnetic compatibly equipments.

Development of Prime Feed Reflector Antenna for Site Survey Applications

Dau-Chyrh Chang
Da Yeh University, Taiwan

Chao-Hsiang Liao
Da Yeh University, Taiwan

In order to develop an antenna for site survey applications with the frequency from 4.5 GHz to 5 GHz, an offset reflector antenna is developed. In order to reduce cost and easy manufacture, the feed with dipole antenna is used as shown in Fig. 1. The feed is with the corner reflector dipole antenna is shown in Fig. 2. The offset reflector is with an existing DBS (Direct Broadcasting Satellite) antenna. The diameter of the offset reflector is 35cm. The F/D of the offset reflector is 0.6. Fig. 3 shows the final antenna system measured by compact range. Fig. 4 shows the measurement result of H-plane pattern. The specification of the offset reflector antenna is with gain 21 dBi. The test results are agreed with that of the theoretical simulations.

Session 5A4a

Device

Design and Simulation of RSFQ/RISC Computer System

Zhong-Hai Zhang[1,2], **Bo-Ran Guan**[2]

[1]Xidian University, China
[2]Hangzhou Dianzi University, China

The RSFQ technology is expected for the high speed digital computer system because of its picosecond gate delays and low power consumption. Until now, there are many achievements in this filed, such as the HTMT project and the FLUX project. But to get a RSFQ chip is very expensive and will cost a long time. We can now get many good softwares to simulate the RSFQ digital circuit and this will bring people convenience. They will bring out another problem, the low speed of circuit level simulation for these softwares to be used for verification of function and timing of large RSFQ circuits.

We can get another way from semiconductor digital circuit design, which can simulate a circuit at the logic instead of the circuit (transistor or junction) level. We can write the functional model of the RSFQ digital basic gates using a hardware description language (HDL) such as Verilog HDL. Then a large RSFQ circuit composed of hundreds gates and thousands Josephson junctions can be simulated using standard semiconductor industry CAD tools. We have developed a library of Verilog models for the basic RSFQ gates needed. Using these basic modules, we describe a RSFQ/RISC computer system. This system is different from the common semiconductor computer systems in the system architectural, timing distribute, the data reading out, etc. This paper presents the system and the simulation results.

REFERENCES

1. Likharev, K. K. and V. K. Semenov, "RSFQ Logic/Memory Family: A New Josephson-Junction Technology for Sub-Terahertz-Clock-Frequency Digital Systems", *IEEE Trans, Appl, Superconductivity*, Vol. 1, 1, 1991.

Characterization of a Quasi-optical NbN Superconducting Hot-Electron Bolometer Mixer

L. Jiang, **W. Zhang**, **Q. J. Yao**, **Z. H. Lin**, **S. C. Shi**
Purple Mountain Observatory, NAOC, CAS, China

Y. B. Vachtomin, **S. V. Antipov**, **S. I. Svechnikov**, **B. M. Voronov**, **G. N. Gol'tsman**
Moscow State Pedagogical University, Russia

We have successfully demonstrated that phonon-cooled NbN superconducting hot-electron bolometer (HEB) mixers are able to work with close-cycled mechanical 4-K cryocoolers [1]. The temperature fluctuation and mechanical vibration of such a cryocooler, however, still have some effects on the mixer performance. Fig. 1 exhibits the measured IF-output-power responses, corresponding to a 300-K and a 77-K load, as well as the pumped and unpumped I-V curves for a quasi-optical NbN superconducting HEB mixer (of relatively low quality as a testing device). Although the I-V curves looks smooth, we can observe clear fluctuation from the IF-output-power curves. The preliminary result gives a DSB noise temperature of 2450 K at 510 GHz and IF-output-power stability around 2%.

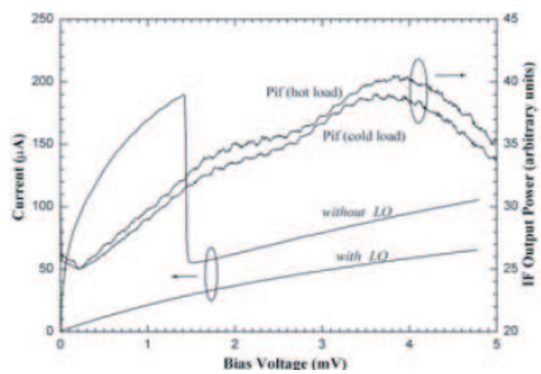

Figure 1

In this paper, we focus on the further investigation of the noise performance of this quasi-optical NbN superconducting HEB mixer at the 500- and 850-GHz bands. Its IF-output-power characteristic is also studied. Furthermore, here we introduce a hot-spot mixer model [2] to describe the heat-exchange physics of quasi-optical NbN superconducting HEB mixers. This model includes the terms of the temperature fluctuation and mechanical vibration in the heat balance equation of NbN superconducting HEB mixers to describe the measured mixer characteristics, including the mixer I-V curves, conversion gain, and noise which consists of the thermal fluctuation, Johnson noise, and quantum noise.

REFERENCES

1. Jiang L., J. Li, Q. J. Yao, Z. H. Lin, W. Zhang, and S. C. Shi, S. I. Svechnikov, Yu. B. Vachtomin, S. V. Antipov, B. M. Voronov, N. S. Kaurova, and G. N. Gol'tsman, "Characterization of NbN Hot-Electron-Bolometer Devices Cryogenically Cooled by a Close-Cycled 4-K Refrigerator," *Progress in Electromagnetics Research Symposium, Nanjing, China,* 2004.
2. Merkel Harald, Pourya Khosropanah, pavel Yagoubov, Erik Kollberg, "A hot spot mixer model for superconducting phonon-cooled HEB far above the quasiparticle bandgap," *Proc.* 10^{th} *International Symposium on Space Terahertz Technology, Charlottesville*, 592, 1999.

Study of Flicker Noise for Zero-IF Receiver

Jun Gao, **Jin-Sheng Tang**, **Ke-Min Sheng**
Southwest Jiaotong University, China

Zero-IF receiver has some advantages, such as small factor, low cost and easily-integrated on a chip. They make it competitive of RF receivers. However, DC offset and flicker noise have profound effects in zero-IF receiver ,which would not be considered in superheterodyne receiver. In particular, since the downconverted signal centers at zero frequency, the flicker noise of device has a profound effect on the signal, a severe problem in MOS implementation. With an important 1/f character, meaning that the noise spectral density is inversely proportional to the frequency, the flicker niose is also called 1/f noise. Although there is no unifying mechanism for flicker noise, measurement on CMOS device shows that it has much higher flicker noise than bipolar device, possibly due to the random trapping in the oxide-silicon surface conduction of CMOS. In heterodyne receivers, the signal has been amplified to the full swing amplitude before it reaches the baseband circuits, so the low frequency noise is not a mayor problem. Our solution to the flicker noise issue is involved with adopting the passive mixer to remove flicker noise during frequency transfer and the special low-flicker noise opamp as post-buffer. When active mixer is used as a reference, which is a normal low bias active mixer, the advantage of using passive mixer becomes prominent . At 100KHz, active mixer has already 5dB higher noise figure than the passive one. It will further go to 20dB higher at 10KHz.Using passive mixer can reduce flicker noise effectively in CMOS technology.

An Improved Design for Ka-Band Phase Shifter Using Distributed MEMS Transmission Line Structure

Bo-Shi Jin[1], **Yu-Ming Wu**[1], **Qun Wu**[1]
Hao-Yuan She[1], **Le-Wei Li**[1,2]

[1]Harbin Institute of Technology, China
[2]National University of Singapore, Singapore

MEMS phase shifter is being paid more attention for the advantages of low insertion loss, high isolation and low cost in millimeter wave band applications. MEMS phase shifters fabricated at Ka-band have been reported [1]. With increasing interests in millimeter wave, millimeter wave phased array antenna is being attached more importance, as the core of phased array antenna, phase shifter at Ka-band is the key technology. Phase shifters using traditional devices such as ferrite, PIN and MMIC provide good performance at Ka-band, but it is difficult to make the system miniaturization. So far, several MEMS phase shifter structures have been proposed, such as switched delay line phase shifter, interdigital capacitor phase shifter and distributed MEMS transmission line (DMTL) [2].

In this paper, a DMTL design approach is proposed for Ka-band application. In DMTL structure, a coplanar waveguide (CPW) transmission line is loaded periodically with the MEMS bridges, the applied bias voltage between the MEMS bridges and bottom electrodes changes the height of the MEMS bridges, which in turn varies the distributed MEMS capacitance. This results in a change in the loaded transmission line impendence and phase velocity, which in turn causes phase shift. In the traditional design method, a metal-insulator-metal (MIM) capacitor between the bridge and the signal line on symmetry CPW structure is used. After analysis and simulation, the performance of DMTL is beyond that of other structures at millimeter wave band.

However, in the newly-developed design, an improved structure of DMTL is proposed. The asymmetry CPW structure and the irregular signal trace are used so that the characteristic impedance can be changed to raise the Bragg frequency[3]. We also can replace the MIM capacitor with the MAM capacitor to increase the ratio of C_{down}/C_{up} to increase phase shift per dB loss, but we should pay attention to control the height of bridge for bridge will be pulled down at $2g_0/3$. Simulation results have predicted that the reasonable height should be between $2g_0/3$ and $3g_0/4$, and the insertion loss of the phase shifter will be below 2dB and the bias voltage decreases by 1/3 compared with traditional design, final test results will be given later. References

REFERENCES

1. Barker N. S. & G. M. Rebeiz, "Distributed MEMS True-Time Delay Phase Shifters and Wide-Band Switches", *IEEE Trans.on Microwave Theory and Technology*, Vol. 46, No. 11, 1998.
2. Barker N. S. & G. M. Rebeiz, "Optimization of Distributed MEMS Phase shifters", *1999 IEEE MTT-S Digest*, 1999.
3. Gupta K. C., Ramesh Garg, "Inder Bahi and Praksh Bhattia", *Microstrip Lines and Slotlines, Artech House, Boston*, London, 1996.

Improving Design of Symmetrical Six-Port Microstrip Coupler

Yuan Chen, **Ji-Jun Yao**, **Swee Ping Yeo**
National University of Singapore, Singapore

The symmetrical six-port coupler has been singled out for special purposes. Different designs have already been proposed for such a coupler. Of particular interest in the present paper is the coupler which ideally yields the performance characteristics encapsulated in the following scattering matrix:

$$\mathbf{S_{ideal}} = \begin{bmatrix} 0 & \alpha & 0 & \tau & 0 & \alpha \\ \alpha & 0 & \alpha & 0 & \tau & 0 \\ 0 & \alpha & 0 & \alpha & 0 & \tau \\ \tau & 0 & \alpha & 0 & \alpha & 0 \\ 0 & \tau & 0 & \alpha & 0 & \alpha \\ \alpha & 0 & \tau & 0 & \alpha & 0 \end{bmatrix}$$

where $|\alpha|=|\tau|=1/\sqrt{3}$ and $\arg(\alpha/\tau) = \pm 2\pi/3$. Among the various microstrip designs reported in the literature for this coupler, the prototype which achieved the best performance thus far is based on the design proposed by Yeo *et al* [1] but their coupler only yields a (measured) bandwidth of 25%. We shall utilize this paper as our reference.

We have attempted a variety of improvements for the design described in [1]. The coupler structure we finally obtained combines the double-ring topology, the central star, the $\pi/6$ angular displacement for the six ring-to-ring links, and the tapered lines employed for impedance matching. The first-order eigenmode model employed in [1] has to be expanded, in order to take into account the additional features incorporated into the improved design. Based on the finally optimized result by our software package, a practical microstrip coupler has also been fabricated to verify our prototype. It is evident from the measured performance plots that the coupler we fabricated meets the design specifications over the 1.24-1.88 GHz range (41% fractional bandwidth). In comparison, the design adopted in [1] yields only 25% fractional bandwidth. Moreover, the close agreement, between the data generated by our software package and the measured data taken by the HP8510C network analyzer, validates the accuracy of our circuit model, for both magnitude of scattering-coefficients and phase differences.

REFERENCES

1. Yeo, S. P., B. Tan and E. H. Kwek, "Improved design for symmetrical six-port microstrip coupler (based on double-ring-with-star structure)", *IEEE Trans. Microwave Theory & Tech.*, Vol. 48, No. 6, 1074, 2000.

Research on the Method of Neural Network Modeling Based on FCM Algorithm and Its Application on Vision-based Sensors

D. B. Hou, **D. Yu**, **Z. K. Zhou**
Zhejiang University, China

This paper proposes a novel neural network model base on fuzzy kernel clustering method. The model can accept continuous and discrete inputs together, but traditional neural network models usually only accept continuous inputs, the discrete inputs, for example, scenario A, B, C, etc., should be transferred or quantified to continuous value. The discrete input to the model is divided into several clusters by using fuzzy c-mean clustering algorithm (FCM), and each input sample are gave membership degrees belong to each cluster, a membership degree matrix is presented as a result. A fuzzy clustering neuron (FC-neuron) then is constructed using the input membership degree matrix. The function of the FC-neuron is to output a membership degree value belong to one cluster for each discrete input. The number of FC-neurons to each discrete input lies on the cluster number, that is, if a discrete input has N clusters after some fuzzy clustering method there should have N FC-neurons to give every possibility to input. A four-layer hybrid neural network is designed; first layer is input layer, input nodes transfer modal inputs to next layer's inputs; second layer is fuzzifier layer, there are two kinds of neurons, one is Fuzzy-neuron which deal with continuous inputs, each node compute a membership degree, another is FC-neuron which deal with discrete inputs, each node compute a member ship degree also by the predefined matrix. Fuzzy-neurons and FC-neurons construct the antecedent part of fuzzy rules include continuous and discrete conditions; the third layer is rule layer, rule nodes construct the consequent part of fuzzy rules by product; the last layer is output layer, the weighted sum of active value of all rules is taken as the model output. A multi-input multi-output hybrid neural network was designed by the novel modeling method and applied to vision-based passive sensors. Vision-based passive sensors were used in intelligent vehicles system to recognize road status, but many road statuses are hard to quantify. With the proposed modeling method a few road statuses were taken as neural network' discrete inputs. Simulation results show this method is superior to the traditional neural network model in road pattern recognition.

Session 5A4b

Medical Applications

Theory of Evanescent Mode Applicators

Jan Vrba[1], **Jakub Cvek**[1], **Ladislav Oppl**[1]
Josef Kvěch[2], **Jiří Kubeš**[2]

[1]Czech Technical University in Prague, Czech Republic
[2]Institute of Radiation Oncology in Prague, Czech Republic

In this contribution we would like to describe our new results dealing with evanescent mode waveguide hyperthermia applicators, typically used for cancer treatment. We have developped theoretical basis of this technology and designed & evaluated different versions of these applicators working below waveguide cut-off frequency.

In our contribution we would like to discuss what happens, when the frequency f of hyperthermia apparatus is either very different (i.e. much higher or lower) from the cut-off frequency f_c or very near (even equal) to the cut-off frequency f_c of the used waveguide applicator. This special case of our interest can happen when either the hyperthermia apparatus is tunable in broader frequency range or the cut-off frequency f_c of the applicator is changed by different dielectric parameters of various types of biological tissues.

There is a substantial difference between the two ways of the waveguide applicator excitation (i.e. above or under the cut-off frequency f_c) and in the propagation and "behaviour" of the EM field inside such applicator also. Basic differences would be explained during the presentation.

For the following discussion we have chosen the case of the rectangular applicator with a flange. But similar results is possible to obtain for other important cases like e.g. rectangular applicators without flange or for the family of circular applicators.

Waveguide flange is in our approach considered as an electric wall, dashed line going into the biological tissue determines the magnetic wall of our model. The distance between these walls determines the cut-off frequency f_c of the applicator aperture. Of course, f_c is influenced by the tissue permittivity also.

The results we would like to describe in our contribution are interesting from theoretical point of view of the knowledges about the general properties of the waveguide applicators. And are very important also for the treatment - our results demonstrate very substantial changes of SAR distribution in the treated biological tissue. If f is going to f_c then so called hot spots complicating the treatment can arise.

*This research is supported by the Grant Agency of the Czech Republic and by the Ministry of Education, Youth and Sport of the Czech Republic.

Arrays of Waveguide Applicators for Microwave Thermotherapy

Jan Vrba[1], **Roman Chovanec**[1], **Hana Trefná**[1]
Jan Herza[1], **Josef Kvěch**[2], **Jiří Kubeš**[2]

[1]Czech Technical University in Prague, Czech Republic
[2]Institute of Radiation Oncology in Prague, Czech Republic

In this contribution we would like to describe our new results dealing with waveguide hyperthermia applicators, typically used for cancer treatment. We have designed and evaluated a water filled lens applicator (aperture of a the rectangular waveguide applicator is divided into 3 or 5 sectors with shifted excitation).

We would like to present theoretical model of this applicator, results of numerical modelling and experimetal evaluation as well. Focusing principle of the lens applicator enables to increase the depth of efficient heating in comparison with waveguide applicators.

The basic schematics of the discussed type applicator is shown in the following figure. The aperture of lens applicator is divided into 3 or 5 sectors with shifted excitation (i.e. different amplitude and phase). To achieve deep local treatment by aid of this applicator we can thus use a focusing principle.

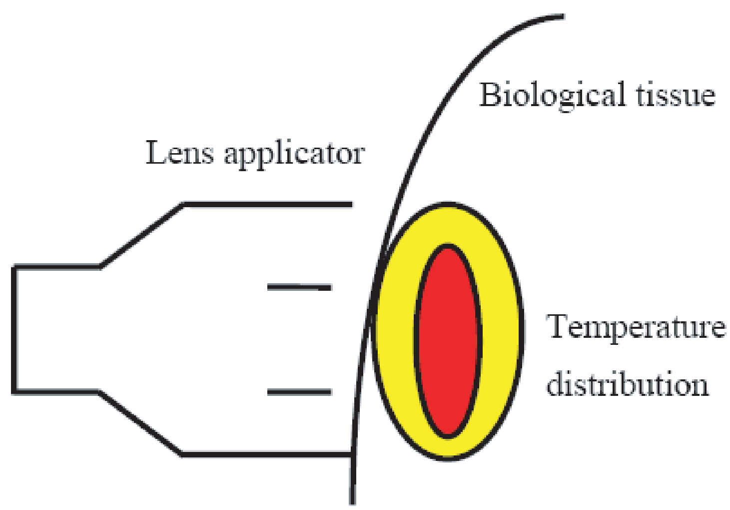

In our contribution we will discuss our results with the design of this type applicator and also some first experiments will be presented.

*This research is supported by the Grant Agency of the Czech Republic and by the Ministery of Education, Youth and Sport of the Czech Republic.

Comparison of Two Different Absorbing Boundary Conditions in Numerical Dosimetry of Animals Using FDTD Code

Y. Alfadhl, **X. Chen**
Queen Mary University of London, UK

The finite difference time domain (FDTD) technique has been used widely as an accurate and efficient tool for solving Maxwell's equations within inhomogeneous regions. Evaluations of the interactions of electromagnetic (EM) fields with animals are typically made by measuring the specific absorption rate (SAR). Assessments of the SAR distributions induced inside inhomogeneous animal models have been carried out in several studies using a widely used code ([1]-[2]). The algorithm implemented in this original code was based on the separation of the incident and scattered fields combined with the second order 'Mur' absorbing boundary conditions (ABC) [3]-[4]. The separation of the incident and scattered fields eliminates the incident fields from the radiation hitting the outer boundaries. This improves the reflection profiles; however, the utilisation of the 'Mur' ABC within this program has raised some concerns about the accuracy especially in the lower frequency band where the fixed distance between the object and the outer boundaries becomes smaller relative to the wavelength.

In this study, a PML (Perfect Matched Layer) ABC has been applied to improve the accuracy of the FDTD numerical dosimetry program. The results have shown that the difference between the results obtained using the 'Mur' ABC relative to the results from the PML varies with the radiation frequency. A good correlation has been observed for the SAR computed at frequencies above 900MHz ($\sim 10\%$). Conversely, the relative difference between the SAR calculated using the two boundary implementation shows a significant increase of the difference at lower frequencies. It has been noted that the relative difference factor for the models of smaller rats is much larger than for the models of larger ones. This is due to the fact that the larger rat models are achieved by increasing the voxel sizes creating a bigger gap between the model itself and the outer boundary. It is believed that the PML ABC works better than the Mur method at the lower frequency when the object is closer to the boundary. However, further analysis is required to verify the results obtained.

REFERENCES

1. Mason, P. A., W. D. Hurt, T. J. Walters, J. A. D'Andrea, P. Gajsek, K. L. Ryan, D. A. Nelson, K. I. Smith, J. M. Ziriax, "Effects of Frequency, Permittivity, and Voxel size on predicted specific absorption rate values in biological tissue during electromagnetic-field exposure", *IEEE trans. on microwave theory & tech.*, Vol. 48-11, 2050, 2000.
2. Alfadhl, Y., C. C. Chiau, Z. Wang, X. Chen and C. Gabriel, "Assessment of SAR distributions inside 10, and 70 days old rats exposed to 900MHz RF: Influence of tissue dielectric properties", *Int. Symposium on Antennas and Propagation (ISAP i-02)*, 2002.
3. Kunz, K. S., R. J. Luebbers, "The Finite Difference Time Domain Method for Electromagnetics", *CRC press, ISBN:0-8493-8657-8*, 1993.
4. Mur, G., "Absorbing boundary condition for the finite-difference approximation of the time-domain EM field equations", *IEEE trans. on EM Comp.*, Vol. 23(4), 377, 1981.
5. Berenger, J-P, "A perfectly matched layer for the absorption of electromagnetic waves", *J. of computational physics*, Vol. 114, 185, 1994.

Development of a Miniature Sensor for the Temperature Follow-up Using Microwave Radiometry in Chronobiology

L. Dubois[1], **C. Ricard**[1], **L. Beghin**[2], **P.-Y. Cresson**[1], **J. Pribetich**[1]

[1]Université des Sciences & Technologies de LILLE, France
[2]Centre d'Investigation Clinique du Centre Hospitalier Régional et Universitaire de Lille Hôpital Cardiologique, France

The medical field is a sector particularly interested in non invasive techniques for the measurement of human temperature. In fact, the corporal temperature is proved to be a pertinent parameter in the scope of diagnosis, monitoring of many pathologies and for the posology of some medicines. For example, the circadian rhythm corresponding to a 24 hours cycle control the metabolic, physiological and psychological functions. Ruled by a biological metronome situated in the brain near the hypothalamus, this cycle is correlated to the human corporal temperature variation which has nearly the shape of sine curve characterized by parameters such as amplitude and phase. So a misfunctioning of the biological rhythm due to medical, environmental or social factors can de detected by the measurement of the human temperature. As a non-invasive way for measurement of temperature, microwave radiometry can bring a precious assistance in the research in chronobiology. This paper is concerning the realization of new miniature sensors allowing to measure the human central temperature or the temperature of an internal organ (such as the liver or the medulla oblongata) by microwave radiometry.

The techniques most currently used for temperature measurements among men are built on the use of thermocouples, optical fibers or infrared sensors. Their drawbacks are to give a superficial or a punctual information and are sometime traumatizing. They can be put in several places of the human body such as the rectum, the esophagus, the mouth and the axillary armpit. However, these different techniques and locations for measuring the temperature are reflecting more or less the central temperature of a person located in the hypothalamus considered as the regulating center of the corporal temperature. At present, the rectal temperature is considered by all clinicians as the best reference of the central temperature. However, the variation of this temperature shows certain inertia with respect to the central temperature. The first phase of the clinical study in collaboration with the Center of Clinical Investigation (CCI) of the CHRU/INSERM of Lille (protocol 'TEMPIL 1') was to demonstrate the feasibility and the consistency of the measurement of human temperature by microwave radiometry. For this study, we make use of a "cold" sensor connected to a radiometer working around 3.2 GHz with a bandwidth of 500 MHz. Although the results have proved the coherence of the measurements compared to classical techniques mentioned above, two important points must be mentioned: the transitional state due to putting in temperature of the sensor which is directly in contact with the skin and the deficiency of the volume of tissues in depth contributing to the radiometric temperature. So, in order to compensate these drawbacks, it is necessary to work at a lower frequency (around 1.575 GHz): it will be also necessary to develop new sensors with a reasonable size (about 1 to 2 cm^2).

We have chosen a technique of reduction of antennas proposed by par R. AZADEGAN and applied to dissipative structures. The sensor has been realized on an epoxy substrate (permittivity $\varepsilon_r = 4.9$) of thickness 1.58 mm. The geometrical dimensions have been calculated from a software based on the moment's method (IE3D) in order to be used at a distance from the skin equal to 3 mm as to reduce thermal exchanges. The volume of tissues contributed to the determination of the radiometric temperature with such a sensor agrees to our expectation. A campaign of measurements on phantoms equivalent to human tissues is now in progress. A second clinical study (TEMPIL 2) which goal is to follow up the thermal cycles of internal organs such as the liver is in preparation with the CCI.

Session 5A5

Novel Mathematical Methods in Electromagnetics II

An Accurate and Stable Solution of Time-domain Integral Equation for Electromagnetic Scattering from 3-D Dielectric Bodies

Xi Luo, **Yan-Wen Zhao**, **Shengbo Wu**, **Zaiping Nie**
University of Electronic Science and Technology of China, China

For the solution of a time-domain integral equation (TDIE), the marching-on in time (MOT) is usually employed. But, two serious drawbacks are the occurrence of late-time instability and expensive computational complexity. More recently, the PWTD-enhanced MOT algorithms considerably reduce the costs for analyzing surface-scattering phenomena. One of the earlier and most popular approaches to stabilize TDIEs consists of time-averaging to filter out the high-frequency component of the solution that is thought to cause the instability. Although time-averaging and filtering techniques are simple to implement, they result in inaccurate solutions and often fail for geometrically complicated structures. It is shown that properly choosing spatial and temporal interpolation functions (such as higher-order functions) can improve the accuracy and stability of the MOT scheme. In practice, the principal reasons of MOT instabilities are the numerical round-off errors or analytical and numerical approximations made in discretization procedure of TDIEs. Therefore, the late-time stabilities can be improved considerably by accurate evaluation of the impedance matrix elements, specially the self-term elements.

We propose a time-domain electric field integral equation formulation for analyzing the transient electromagnetic response from three-dimensional dielectric bodies. The solution is based on the Galerkin's testing in space and point marching in time. The RWG vector basis functions are used for spatial expansion and the temporal bases are chosen to be triangular functions. In our work, the transformations of the parametric coordinates and general Duffy coordinates transformation are employed to transform the singular integrals of TDIE into non-singular integrals, which can be accurately and efficiently evaluated by dividing the transformed domain of integration into sub-domains. This method provides more accurate and very stable solution, because it eliminated the principal source of the numerical error. The proposed method is suitable to any causal temporal basis functions and can be extended to curvilinear patch and high-order spatial basis functions in a straightforward way.

A Method of Solution for a Large-sized Least-squares Problem with a Block-diagonal Jacobian

M. Ohtsu[1], **Y. Okuno**[1], **T. Matsuda**[2]

[1]Kumamoto University, Japan
[2]Kumamoto National College of Technology, Japan

We describe an effective method of solution for a large-sized least-squares problem with a blockdiagonal Jacobian matrix, which arises in solving the problem of diffraction by a multilayered bigrating by using Yasuura's modal expansion method [1]. An outline of Yasuura's method can be itemized as follows: 1. Define approximate solutions in each layer as finite linear combinations of modal functions with unknown coefficients; 2. Locate sampling points on boundaries separating the layers, where the number of sampling points should be a few times the number of unknowns (modal functions); 3. Apply boundary conditions at each sampling point to obtain an over-determined set of linear equations with respect to the unknowns; 4. Solve the set of equations in the sense of least-squares to find the coefficients. For a 2-D problem, in which the grating is periodic in one direction and the plane of incidence is perpendicular to the grooves, the number of unknowns is relatively small and we can solve the least-squares problem on a personal computer without much trouble. In a 3-D problem (e.g., the problem of conical diffraction or bigrating), however, we often employ hundreds or thousands of modal functions and face the problem of large-sized set of linear equations.

If we solve the set of linear equations directly, we should pay a huge amount of computational cost, which is defined by computer storage times computation time. Fortunately the Jacobian (the coefficient matrix of the linear equations) that appears in the problem of a layered grating has a block-diagonal structure: making use of this, we can employ a technique called sequential accumulation [2] in solving the least-squares problem to save a big amount of computational cost.

After formulating a least-squares problem with a block-diagonal Jacobian, we explain how to solve the problem by QR decomposition with the sequential accumulation taking the Jacobian structure into account. We then show numerical examples comparing the present method with a conventional QR method (direct solution of the linear equations). This makes clear that the present method is superior to the conventional method in computational cost and even in computational accuracy.

REFERENCES

1. Yasuura, K., "A view of numerical methods in diffraction problems", *Progress in Radio Science 1966- 1969 (W.V. Tilson and M. Sauzade, eds.), URSI, Brussels*, 257, 1971.
2. Lawson, C. L. and R. J. Hanson: *Solving Least Squares Problems, Prentice-Hall, Englewood Cliffs, NJ*, 1974.

Analysis of Strip Gratings Using a Parametric Modal Method by Fourier Expansions

G. Granet[1], **J. P. Plumey**[1], **N. Yashina**[2]
F. Tinasoa[3], **K. Raniriharinosy**[3]

[1]Université Blaise Pascal, France
[2]I.R.E.N.A.S of Ukraine, Ukraine
[3]Université de Fianarantsoa Madagascar, Madagascar

The problem of the diffraction of electromagnetic waves by strip gratings has been extensively studied in the past, since strip gratings can model such devices as photolithographic masks or frequency selective surfaces either in the optical or in the microwave domain. A possible way to obtain the solution is to express the fields in terms of the Rayleigh expansions above and below the strips and to apply the combined boundary conditions method (C.B.M) introduced in [1]. The advange of this method is its simplicity due to the use of Fourier series. Furthermore it offers the numerical possibility to easily mix strip gratings and lamellar gratings provided that they are analysed with the modal method by Fourier expansion and that they share the same periodicity. However the main drawback of most Fourier based methods is that they are not able to describe efficiently electromagnetic fieds with sharp variations. As a consequence, convergence is achieved with rather large matrices. Here, the tangential component of the field that points toward the axis of periodicity is singular at the edge of the strips! Therefore, we are concerned with a case where a Fourier basis is certainly not the best choice.

This presentation is devoted to show that it is possible to overcome this drawback by introducing a new coordinate system that has previously been used succesfully by Granet in [2]. This system is chosen such that coordinate lines become constricted around the strip edges. Doing so, we preserve the simplicity of the method of [1] but we dramatically improve the convergence speed. This very new approach has been compared favorably with other rigorous methods [3]. We shall illustrate the effectiveness of the method by analysing the surface wave resonances that appear on strip gratings deposited on thin dielectric layers.

REFERENCES

1. Montiel, F. and M. Nevière, *Optics Comm.*, Vol. 101, 151, 1993.
2. Granet, G., *J. Opt. Soc. Am. A*, Vol. 16, 2510, 1999.
3. Panin, S., A. Ye. Poyedinchuk, "The plane wave diffraction by a grating over chiral medium", *Telecommunication and Radio Engineering*, Vol. 53, 4-5, 98, 1999.

Efficient Computation of Z-parameter for the Rectangular Planar Circuit Analysis

Ping Liu
Shanghai Jiaotong University, China

Zhengfan Li
Shanghai Jiaotong University, China

With the operating frequencies increasing and working voltage decreasing in high-speed digital systems, the model and design of power/ground (P/G) planes are becoming more and more critical. In order to develop a systematic P/G design strategy, the fundamental properties of P/G plane structures need to be explored.

The conventional eigen-mode expansion method is a commonly used approach to compute Z-parameter of a rectangular planar circuit. However the formula in the method involves a summation of a double infinite series, which may consume much time and computer storage to obtain sufficiently good accuracy. To improve the computation efficiency, this paper proposes a new convergence-accelerating algorithm, which is based on a trigonometric Fourier series formula and the η-algorithm. The trigonometric Fourier series formula can transform the double infinite series into a single one. And the η-algorithm is able to accelerate the convergence of the single infinite series.

The technique is easy to catch on and has high efficiency and good accuracy. A numerical example testifies that the new accelerating algorithm can achieve the same accuracy with 21 terms as the conventional eigen-mode expansion method with 366×366 terms at least and the computation time is only about 0.3 percent of that of the eigen-mode expansion method for the same accuracy. The example also shows that the new accelerating algorithm possesses good accuracy since its results agree well with those of the eigen-mode expansion method with 2000×2000 terms.

The new technique greatly improves the computation efficiency of the conventional eigen-mode expansion method. With it the eigen-mode expansion method can be applied more extensively.

Bistatic Scattering Enhancement Phenomenon in a Random Medium

Z. Q. Meng[1], **M. Tateiba**[2]

[1] Fukuoka University, Japan
[2] Kyushu University, Japan

When a body is embedded in a random medium, the radar cross-section (RCS) of the body may be remarkably different from that in free space. This special phenomenon is called backscattering enhancement, and has been one of the important subject for radar engineering, remote sensing, astronomy and bioengineering. Backscattering enhancement has been investigated from an academic point of view and thereby been said to be a fundamental phenomenon in a random medium and to be produced by statistical coupling of incident and scattered waves. If the body is regarded as a single point and the backscattering enhancement occurs prominently, RCS of the body has generally been taken to be nearly twice as large as that in free space.

To make clear numerically the scattering characteristics for a practical body scattering, we analyzed a bistatic RCS of a conducting body in a random medium. Our approach is based on general results of both independent studies on the surface current on a conducting body in free space and on the wave propagation and scattering in a random medium. A non-random operator, called current generator, is introduced to get the surface current from any incident wave. The operator depends only on the body surface and can be constructed by Yasuuras method. On the other hand, the wave propagation in a random medium is expressed by use of Greens function in the medium. Here, a representative form of the Greens function is not required but the moments are done for the analysis of average quantities concerning observed waves. We apply a two-scale asymptotic procedure to get the fourth moment of Greens functions. As a result, we have obtained numerically results agreed with the law of energy conservation, and shown some interesting behaviors of bistatic RCS caused by statistical coupling between incident and scattered waves.

Recently, our new numerical results show that the scattering enhancement phenomenon may not occur in the backward direction but in the other directions in some cases. Here we discuss the new phenomenon by analyzing a bistatic RCS of a conducting circular cylinder embedded in a random medium.

Effect of Absorption on the Resonances in One-dimensional Random Systems

K. Yu. Bliokh[1,2], **Yu. P. Bliokh**[3], **V. Freilikher**[1], **A. Genack**[4]
B. Hu[4], **J. Klosner**[4], **P. Sebah**[4,5]

[1]Bar-Ilan University, Israel
[2]Institute of Radio Astronomy, Ukraine
[3]Department of Physics, Technion, Israel
[4]Queens College of CUNY, USA
[5]Universite de Nice-Sophia Antipolis Nice, France

One of the manifestations of strong disorder-induced localization is the appearance of high Q-factor resonators in sufficiently long samples. The striking feature of this resonator is that the region of energy localization is not bounded by walls or regular potential barriers, and the effective cavity appears due to the interference of multiply scattered fields. The size of the cavity is much smaller than the total length, L, of the sample, and is of order of the localization length, l_{loc}, that is defined as $l_{loc} = L < \ln T(L) >^{-1}$ where $< \ln T(L) >$ is the ensemble-averaged value of the transmission coefficient. The transmission coefficient at a resonance is anomalously high. It does not depend on the total length and is determined only by the localization length and the location of the effective cavity. Therefore, generally speaking, the resonances can be detected and their location inside the sample can be determined by measuring the transmission coefficient as a function of frequency. Though relatively small absorption is inessential at off-resonance frequencies, it leads to huge loss of energy at resonances inside the effective cavities. It dramatically suppresses resonant transmission, so that the measurements of the transmitted intensity becomes inadequate. In this case the measurements of the intensity at the input of the system come to the rescue of those who wants to detect inner resonant cavities by means of external measurements. A model has been developed that enables us to account for the absorption and to calculate both transmission and reflection coefficients. Based on this model, we show that losses at resonances give rise to well-pronounced singularities in the dependence of the reflected intensity on frequency. We demonstrate how measurements of intensity on the input side of the sample can be used as a tool for the detection and analysis of the resonances, in particular, of the so-called necklace states. As an example of a one-dimensional random system the one-mode microwave waveguide had been used. Experimental measurements are in good agreement with theoretical predictions.

A Nonlinear Eigenvalue Hybrid FEM Formulation for Two Dimensional Open Waveguiding Structures

P. C. Allilomes, **G. A. Kyriacou**
Democritus University of Thrace, Greece

During the last years a particular research effort is directed towards the solution of the eigenvalue problem of arbitrary cross-section waveguiding structures in a unified and general way.

All of the techniques developed towards this direction try to convert the open-radiating problem to an equivalent closed one and in that way truncating the solution domain. This can be achieved either by making use of an artificial boundary transparent to the solution or by combining the Finite Element Method (FEM) with methods, such as the method of moments, capable of modeling the unbounded region. When the artificial boundary is considered one method to truncate the solution domain is to impose on it either the Absorbing Boundary Conditions (ABCs) or employ the Perfect Matching Layer (PML). An alternative method is to express the field in the unbounded region as an expansion of eigenfunctions satisfying both the Maxwell equations an the radiation conditions. However, for the two dimensional (2D) open waveguides, the already proposed techniques performance in the solution of the corresponding eigenvalue problem, is very poor. In particular, while PML is quite efficient in the estimation of the field distribution generated by a specific source, when this is used in the solution of eigenvalue problem leads to spurious (or corrupted) solutions. Moreover, all these techniques leads to a non linear eigenvalue problem yielding an inefficient approach.

In the present work a hybrid finite element method capable of handling problems considering open arbitrary shaped waveguides is described. The problem at a first stage is modelled approximately by means of a linear eigenvalue formulation. The formulation is derived by combining the finite element method and an approximate expansion in cylindrical harmonics [1]. Namely, the radial wavenumber in the unbounded media is considered approximately equal to than of free space. This is reasonable for the spectral region around cut-off. The eigenvalues calculated using this approach were in good agreement with experimental results. However, aiming at a more generally valid method, the present effort considers the accurate radial wavenumber, which unfortunately (as it is already expected) yields a non-linear eigenvalue problem. The final nonlinear algebraic system is formulated employing a full electric field FEM formulation discretized by mixed edge/node triangular elements. The final nonlinear system is solved using the Regula Falsi technique [2] and using as an initial guess the solution of the linear approach.

REFERENCES

1. P. C. Allilomes and G. A. Kyriacou, "An eigenvalue hybrid fem formulation for 2d open structures using mixed type node/edge elements and a cylindrical harmonics expansion", *PIERS 2004, Piza, Italy.*
2. Hager, P., "Eigenfrequency analysis. fe-adaptivity and nonlinear eigen- problem algorithm", *PhD Thesis. Dept Struct. Mech., Chalmers University of Technology, Geteborg*, 2001.

Comparative Study of Synchrotron and Cherenkov Radiations - Tutorial Review

Toshiyuki Shiozawa
Chubu University, Japan

Synchrotron radiation and Cherenkov radiation have been playing an important role for the radiation sources in the region of the far infrared through the visible to the ultraviolet and the X-ray wavelengths, and for the detection of high-energy elementary particles falling on the earth from deep space.

In classical electrodynamics, it is well known that a charged particle emits radiation when it is accelerated. For an electron moving with extremely relativistic velocity, in particular, the radiation due to the longitudinal acceleration is negligible as compared with the radiation due to the transverse acceleration. In other words, if the direction of motion of a relativistically moving electron is deflected by a transverse force such as the Lorentz force due to a static magnetic field, it emits sharp intense radiation in the instantaneous direction of its motion. This radiation is generally referred to as synchrotron radiation.

On the other hand, a charged particle moving uniformly in a material medium can also emit radiation if it is moving with a velocity greater than the velocity of light in the medium. This radiation is possible only if the velocity of light in the material medium is less than that in vacuum, or equivalently, the refractive index of the medium is greater than unity. This radiation is called the Cherenkov radiation after the discoverer of this phenomenon.

This paper presents a tutorial review of the analytical treatment for these important radiation schemes of synchrotron and Cherenkov radiations from a relativistically moving charged particle.

Rigorous Representations of Source-excited Electromagnetic Fields in Cylindrically Stratified Gyrotropic Media

A. V. Kudrin, **E. Yu. Petrov**, **L. L. Popova**
University of Nizhny Novgorod, Russia

T. M. Zaboronkova
Technical University of Nizhny Novgorod, Russia

We consider methods for representing electromagnetic fields excited by spatially bounded arbitrary given sources in the presence of a radially inhomogeneous gyrotropic cylinder surrounded by a homogeneous gyrotropic background medium. The axis of symmetry of such a cylindrically stratified structure, here taken as z axis, is parallel to the gyroelectric axis of the medium described by a dielectric tensor in the form $\hat{\varepsilon} = \epsilon_0(\varepsilon\hat{\rho}_0\hat{\rho}_0 - ig\hat{\rho}_0\hat{\phi}_0 + ig\hat{\phi}_0\hat{\rho}_0 + \varepsilon\hat{\phi}_0\hat{\phi}_0 + \eta\hat{Z}_0\hat{Z}_0)$, where ρ, ϕ, and z are cylindrical coordinates. The behavior of source-excited electromagnetic fields in the presence of such structures attracts considerable interest in view of many applications including, in particular, those concerned with the excitation and propagation of whistler-mode waves in density ducts in laboratory and space plasmas, helicon waves in magnetized metals and semiconductors, waves in fibers with a gyrotropic cladding, etc.

The total field is sought in terms of the vector modal solutions of homogeneous Maxwell's equations. The transverse (with respect to the z axis) components of the field can be expressed via two axial components which satisfy two coupled second-order partial differential equations. By demanding the completeness of the modal spectrum and using a continuity argument, we determine the content of the modal spectrum and obtain an eigenfunction expansion for the field. Then we derive the orthogonality relations and excitation coefficients for modes of the discrete and continuous parts of the modal spectrum. Note that continuous-spectrum modes in the considered case are grouped into two categories, "ordinary" and "extraordinary", related to the presence of two normal waves in a homogeneous background gyrotropic medium, which makes the obtained solution substantially different from that in the case of an isotropic background region [1]. Next we particularize our analysis to consideration of two cylindrical guiding structures immersed in a magnetoplasma, in the light of a recent upsurge of interest in this subject (see, e.g., [2] and references therein). Namely, we consider (i) a perfectly conducting cylinder excited by a given voltage applied across a circumferential gap on the cylinder surface and (ii) a magnetized plasma column excited by given currents. Although the emphasis, throughout, is placed on the modal (or z-transmission) representation, some discussion will also be given of an alternative, radial transmission, representation which can be furnished by using methods pertaining to a Green's function technique.

A detailed comparison of the above-mentioned field representations will be made and advantages of each of them for analysis of particular problems will be discussed.

REFERENCES

1. Manenkov, A. B., "Irregular magneto-optical waveguides", *IEEE Trans. Microwave Theory Tech.*, Vol. MTT-29, No. 9, 906, 1981.
2. Kondratev, I. G., A. V. Kudrin and T. M. Zaboronkova, *Electrodynamics of Density Ducts in Magnetized Plasmas, Gordon and Breach, Amsterdam*, 1999.

Session 5A6a

Metamaterials & Novel Structures

Realization of PEMC (Perfect Electromagnetic Conductor) Boundary

I. V. Lindell, **A. Sihvola**
Helsinki University of Technology, Finland

Perfect electromagnetic conductor (PEMC) is a nonreciprocal generalization of both the perfect electric conductor (PEC) and the perfect magnetic conductor (PMC). Because PEMC does not allow electromagnetic energy to enter, it can serve as boundary material. Possibilities for the realization of a PEMC boundary are studied in terms of a layer of certain nonreciprocal materials resting on a PEC plane. It is shown that the parameters of a bi-isotropic or a gyrotropically anisotropic medium can be chosen so that the interface of the layer acts as a PEMC boundary to normally incident waves. After a modification of medium parameters the same is shown to be asymptotically valid for arbitrary plane waves. A structure for the realization of such a boundary is suggested.

The structure is based on a material labeled as gyrotropic guiding medium. Electromagnetic properties of such a medium are studied. It is shown that the electromagnetic fields satisfy equations of the transmission-line type which can be applied to transfer dyadic boundary impedances through a slab of medium. In particular a slab of guiding medium can transfer a PEC boundary to a PEMC boundary which is valid for any electromagnetic sources.

REFERENCES

1. Lindell, I. V. and A. Sihvola, "Perfect electromagnetic conductor", *J. Electromag. Waves Appl.*, to appear.

Split Ring Resonators and Complementary Split Ring Resonators: Left-handed Lines and Applications in Microwave Planar Technology

M. A. G. Laso[1], **T. Lopetegi**[1], **F. Falcone**[1], **E. Jarauta**[1]
J. D. Baena[2], **J. Bonache**[3], **J. García-García**[3], **J. Illescas**[4]
A. Marcotegui[1,4], **F. Martín**[3], **R. Marqués**[2], **M. Sorolla**[1]

[1]Universidad Pública de Navarra, Spain
[2]Universidad de Sevilla, Spain
[3]Universitat Autònoma de Barcelona, Spain
[4]Pol. Plazaola F-Nave 1, Spain

A new particle, the Complementary Split Ring Resonator or CSRR, obtained by etching a conventional Pendry's SRR on a metal plate, has been recently proposed by these authors [*Physical Review Letters, Vol. 93, No. 19, Nov'04 by these authors*]. By applying duality it can be easily inferred that the vertical E-field lines present in a microstrip line can excite the CSRRs if they are etched on the ground plane, leading to a strong electric response. It can be also demonstrated that CSRRs would hence exhibit negative-ε values in the vicinity of the quasi-static resonant frequency. In order to simultaneously obtain negative μ in a microstrip line, an array of T-shaped capacitive elements may be added on the central conductor strip as shown in the layout of Fig. 1. Backward power coupling, and therefore left-handedness, can be experimentally demonstrated through a novel coupler consisting of a conventional microstrip line and the novel modified microstrip line smoothly approaching each other (Fig. 2). Dispersion diagrams of the modified line allow us to design the frequencies at which it behaves as a left-handed line and backward coupling (from input port 1 towards output port 2) occurs. For instance, if two sections of left-handed transmission lines with different unit-cell dimen-sions are cascaded (Fig. 3), power would be coupled backwards at the frequency where the CSRRs with *Size* 1 are tuned and, simultaneously, at the frequency where CSRRs with *Size* 2 are designed following the procedure in [*IEEE Transactions on Microwave Theory and Techniques, Vol. 53, No. 4, Apr'05 by these authors*]. Fig. 4 shows the simulated behavior of the structure in Fig. 3. Following a similar approach, left-handed lines were also proposed in coplanar waveguides [*Applied Physics Letters, Vol. 83, No. 22, Dec'03 by these authors*], and filtering and radiation effects have been investigated in both technologies taking benefit from the left-handedness effect or the sub-wavelength resonant SRR/CSRR behavior by itself. During the conference, the authors will summarize their latest advances concerning this original approach.

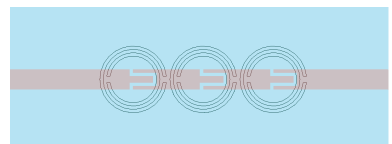

Figure 1: Left-handed microstrip transmission line.

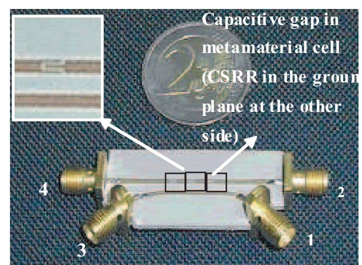

Figure 2: Photograph of a three-cell backward coupler. This coupler is composed of a conventional microstrip and a left-handed line with 3 metamaterial cells.

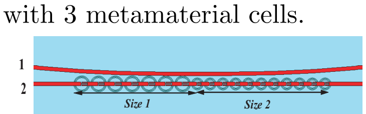

Figure 3: Layout of a backward coupler working at two frequencies.

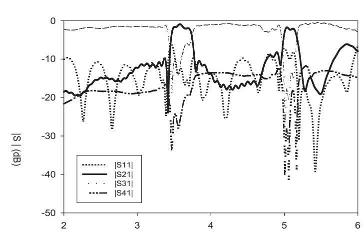

Figure 4: Simulated S-parameters for the backward power coupler working at two frequencies.

Stability and Quality Factor of Sub-wavelength Rectangular Cavity Partially Filled with Left-handed Material

Tian Jiang, **Yijun Feng**, **Yan Chen**
Nanjing University, China

Increasing interest in metamaterials started after Pendry et.al. predicted that certain artificial composite structure could possess, in a given frequency interval, both a negative permeability and a negative permeability[1]. Such materials known as the left-handed materials (LHM) exhibit many unique properties that may lead to unconventional phenomena in guidance, radiation, and scattering of electromagnetic waves and have been proposed in a number of applications. N. Engheta proposed an idea of a one-dimensional cavity resonator formed by a pair of conventional and LHM slabs between two perfect conducting walls, and demonstrated theoretically that in such a 1D cavity a resonant mode can still exist even when the thickness of the slabs is electrically very thin[2]. Its stability and quality factor have also been analyzed in the vicinity of Engheta's resonant condition, and it is shown that Engheta's resonant condition is unstable and gives zero resonating frequency in most cases[3].

In earlier work, we have theoretically investigated a rectangular cavity partially filled along z axis with a LHM slab. It has been shown that there exists resonant modes with frequency much lower than the cut-off frequency of the waveguide (along z axis). In this presentation we will show our analysis of the stability and the quality factor of the TE resonant modes and their dependences on the material characteristics and the geometric parameters of the cavity.

We have analyzed the quality factor of the cavity when a small dielectric loss or magnetic loss is considered in the LHM. We have found that the magnetic loss has much more influence on the quality factor than the dielectric loss. Numerical simulation results show that when the cavity's dimension d along z axis decreases, the stability and the quality factor decrease, therefore d should be comparable to the dimensions along x and y axes for tolerable stability and quality factor. The compactness of the resonator (λ/d, the ratio of the resonant wavelength in vacuum and d) is also restricted by both the stability and the quality factor. Considering all these factors, we can find a balance point, which is not restricted to the vicinity of Engheta's resonant condition, and construct a useful rectangular cavity of sub-wavelength dimensions with tolerable stability and quality factor.

With the acceptable stability and quality factor, this kind of cavity can provide exciting future applications in design and miniaturization of compact devices and components in the microwave and millimeter wave circuits based on left-handed material.

REFERENCES

1. Pendry, J. B., A. J. Holden, D. J. Robbins, W. J. Stewart, *IEEE Trans. MTT*, Vol. 47, No. 11, 2075, 1999.
2. Engheta, N., *IEEE Antennas and Wireless Propagat. Lett.*, Vol. 1, No. 1, 10, 2002.
3. Shen, Linfang, Sailing He, Sanshui Xiao, *Phys. Rev. B 69*, 115111, 2004.

SRRs' Artificial Magnetic Metamaterials Modeling Using Transmission Line Theory

Ming-Feng Wu[1], **Fan-Yi Meng**[1], **Qun Wu**[1], **Jian Wu**[2], **Le-Wei Li**[1,3]

[1]Harbin Institute of Technology, China
[2]National Key Laboratory of Electromagnetic Environment, China
[3]National University of Singapore, Singapore

Metamaterials represent a dielectric medium that exhibits negative refractive index phenomenon and has simultaneously negative permittivity and negative permeability [1]. To artificially realize it, it is vital to achieve the electromagnetic media with negative permeability.

The negative value of effective permeability was first reported using an array of the metallic implants called Split Rings Resonators (SRRs) [2]. These materials comprised small metallic SRRs periodically embedded into a dielectric host, and SRRs just behaved as the elementary "atoms" of these electromagnetic media, at the mutual distances much shorter than a wavelength. The implants may alter both the dielectric and magnetic properties of the original material yielding new values of the macroscopic effective permittivity and permeability.

However, there are still some performances to be improved, such as the anisotropy and bandwidth with the SRRs' structure metamaterials [3]. It is promising to arrive at the motive through improve the geometrical structure or the sizes of the single SRR. The presented methods are always powerful enough to describe the macroscopical performances of the SRRs' arrays, but it is difficult to probe the microcosmic electromagnetic effects of the single SRR.

In this paper, an approach to analyze a single SRR effect by using equivalent circuit model, which based on the transmission line theory, is proposed. In the model, the distributions of the electric charge and electric current in the SRR have been considered, which develop the equivalent circuit. After that, the constitutive relations on the magnetic metamaterial are processed using the parameters provided by the equivalent circuit model. Numerical simulation results of the permeability have shown that the proposed model is valid to describe the single SRR characteristics.

REFERENCES

1. Veselago V. G., "The electrodynamics of substances with simultaneously negative values of ϵ and μ", *Soviet Physics Usp*, 10(4), 509, 1968.
2. Pendry J. B., A. J. Holden, D J Robbins and W J Stewart, "Magnetism from conductors and enhanced nonlinear phenomena", *IEEE Trans. MTT*, 47(11), 2075, 1999.
3. Yao Hai-Ying, Qun Wu, Wei Xu and Le-Wei Li, "Recent research and development on metamaterials: theory, design and realization", *in proceedings of the 2004 China-Japan Joint Meeting on Microwaves, Harbin, China*, August 5, 2004.

Session 5A6b

Nanophotonics and Surface-enhanced Raman Scattering

Surface-plasmon-enhanced Optical Transmission through Planar Metal Films

L. Lin, **R. J. Blaikie**, **R. J. Reeves**
University of Canterbury, New Zealand

Currently, surface-plasmon-enhanced optical transmission through thin metallic films with periodic subwavelegth structures has attracted a great deal of interest. Much attention has been devoted to metal films perforated with subwavelength hole arrays, single apertures surrounded by periodic textures and metallic gratings with subwavelegth slots. We report here on the optical transmission properties of diffraction gratings closely coupled to planar metallic films, showing that this can also give rise to plasmon-enhanced transmission.

A schematic diagram of the structure used in this study is shown in Fig. 1. It consists of a thin, planar metallic film, a dielectric layer and a rectangular metallic transmission grating on the top. The grating and the dielectric layer provide the required transverse momentum and metal/dielectric interface respectively for optical excitation of surface plasmons (SPs) on the planar film beneath. We study the zeroth order transmission properties of Ag film-SiO_2-Ag grating structures: the thickness of the Ag film is 25-35 nm, which is considerably larger than its skin deep in the visible region; the thickness of the SiO2 layer is 100-200 nm; the Ag grating height is 40-120 nm and the grating period is 450-800 nm. The desired zeroth order optical transmission characteristics can be obtained by altering these parameters.

Simulations based on the rigorous coupled-wave analysis technique reveal that the optical transmission properties of the structure, such as centre wavelength, bandwidth and transmission efficiency, are critically determined by the geometry of the structure. The overall transmission is a result of the coupling between light, SP modes and waveguide modes. With the appropriate arrangement, the transmission efficiency can exceed 75% with the bandwidth (FWHM) narrowed down to less than 15 nm. Figures 2 and 3 show the effects of the grating height and grating duty cycle (DC) on the transmission of the structure, respectively. The incident light is TM-polarized and the angle of incidence is 0 degrees. The structure configuration for Fig. 2 is: Ag film = 25nm, SiO_2 = 200nm, Ag grating period = 700nm and DC = 0.7. The configuration for Fig. 3 is: Ag film = 30nm, SiO_2 = 200nm, Ag grating period = 700nm and height = 90nm.

The process for fabricating these structures involves vacuum deposition of the planar thin films, interference lithography for grating pattern definition and reactive ion etching for pattern transfer. The spectral transmission of the samples is analysed in a spectrophotometer at normal incidence. The details of the fabrication process, together with experimental results will be discussed further in the paper.

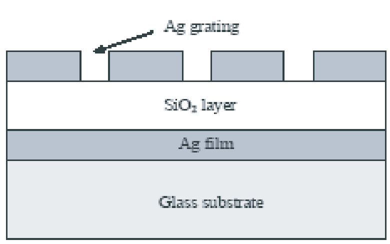

Fig. 1: Schematic diagram of the structures studied here.

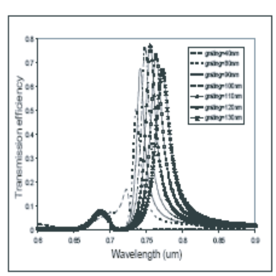

Fig. 2: Simulated transmission spectra for varying grating thickness

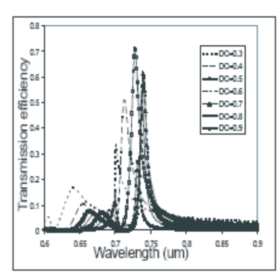

Fig. 3: Simulated transmission spectra for varying duty cycle

A Model for Surface-Enhanced Raman Scattering

Kevin J. Webb, **J. Li**
Purdue University, USA

Surface-enhanced Raman scattering (SERS) [1] has been attributed to large electromagnetic fields near nanostructured metallic surfaces, in particular, recessed regions such as occur in the region between two dimer particles. Consequently, there have been many numerical studies (see [2, 3, 4, 5]), and large fields have been found. Lacking has been a simplified physical model that describes the phenomenon. We propose an analytic model to explain the SERS effect, which in turn leads to material and geometry requirements.

The presence of a large field in recessed regions external to the particles is not consistent with the geometry-independent small particle Mie resonance, as in that case there would be significant field throughout the particle. The phenomenon has been linked to surface plasmon-polaritons from the small particle resonance [6, 7] (plasmons from the free charge and polaritons from the bound charge), but this view does not yield specific geometry requirements. It has been proposed that plasmon modes trapped between surfaces cause the effect and that they exist in the electrostatic approximation [2]. However, electrostatic fields within recessed regions in conductors approach zero, as do the electromagnetic fields as the free charge increases to the limit of a perfect conductor. Large fields exist close to tips, but this short range effect produces a small dipole moment and hence would not be expected to result in a significant Raman signal.

The linear intensity dependence of SERS experimental data suggests a spontaneous effect [7]. If both the excitation and Stokes fields are equally enhanced, then the enhancement factor is proportional to the fourth power of the excitation field [6].

We have studied the scattering from various two-dimensional silver nanoparticle geometries using the finite element method, and indeed, for certain wavelengths and geometries, we find enhanced fields in dimer-like recessed regions. We also found similar enhancement in a simplified notch geometry in the silver particle, thereby achieving a more convenient parameterization. To explain these results, we have developed an analytical model based on the electromagnetic modes of the structure. This analytical model produces results that fit the numerical data nicely. We are therefore led to believe that the description is complete, and that the concept can be used in the design of experiments.

REFERENCES

1. Moskovits, M., "Surface-enhanced spectroscopy", *Rev. Modern Phys.*, Vol. 57, 783, 1985.
2. Garcia-Vidal, F. J. and J. B. Pendry, "Collective theory for surface enhanced Raman scattering", *Phys. Rev. Lett.*, Vol. 77, 1163, 1996.
3. Xu, H., E. J. Bjerneld, M. Kȧll, and L. Bȯrjesson, "Spectroscopy of single hemoglobin molecules by surface enhanced Raman scattering", *Phys. Rev. Lett.*, Vol. 83, 4357, 1999.
4. Kottmann, J. P. and O. J. F. Martin, "Retardation-induced plasmon resonances in coupled nanoparticles", *Opt. Lett.*, Vol. 26, 1096, 2001.
5. Hao, E. and G. C. Schatz, "Electromagnetic fields around silver nanoparticles and dimers", *J. Chem. Phys.*, Vol. 120, 357, 2004.
6. Otto, A., *Light Scattering in Solids, Chap. 6 (M. Cardona and G. Guntherodt, eds.)*, (Springer-Verlag, Berlin), Vol. 4, 1984.
7. Haslett, T. L., L. Tay, and M. Moskovits, "Can surface-enhanced Raman scattering serve as a channel for strong optical pumping?", *J. Chem. Phys.*, Vol. 113, 1641, 2000.

Plasmon Enhanced Near-Field Optical Lithography

D. O. S. Melville, **R. J. Blaikie**
University of Canterbury, New Zealand

There has been an increasing amount of interest in the utilisation of plasmonic resonances to enhance near-field optical lithography [1, 2, 3]. These techniques attempt to use optically-stimulated electrical resonances on layers of silver to expose photosensitive resists. Although the manner it which the resonances are generated differ, they all rely on the silver layer's ability to sustain plasmonic waves down to a few nanometres in wavelength enabling the possibility of sub-100nm features to be exposed. Ref [2] has achieved 50nm features by using a combination of resonant and interference lithography.

Recently, work has been done that builds on the concepts described in a controversial paper describing a "perfect lens" [4]. This paper claimed that a planar layer of silver could act as a lens that could produce sub-diffraction-limited images. We have investigated the ability of a planar layer of silver to image sub-wavelength features in a near-field optical lithography regime. Features at a pitch of 250nm have been achieved through a 50nm thick silver layer. This is an improvement from previously reported results which achieved 700nm pitch features through 120nm thick silver [3]. Figure 1 shows a range of results produced with this technique. The performance increase is related to better processing that reduced losses by allowing a reduction in the silver layer's thickness. Although current resolution does not currently match interference or standing wave techniques, the imaging technique holds an advantage of being able to produce isolated features.

Modifications to the technique in Ref [3] have been made which promise even higher fidelity results without reducing the silver thickness. In this talk the details of this approach and current results will be presented.

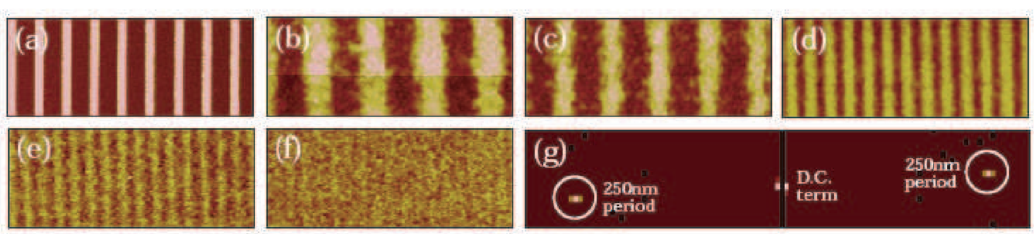

Figure 1: Atomic force microscope scans show resist profiles exposured through a $25nm|50nm|10nm - PMMA|Ag|SiO_2$ mask stack. Feature fidelity at (a) $1\mu m$, (b) $500nm$, (c) $420nm$, (d) $350nm$, (e) $290nm$, and (f) $250nm$ periods are shown. Figure (g) shows the two-dimensional Fourier transform of fig. (f) confirming the presence of the 250nm period features.

REFERENCES

1. Luo, X. G. and T. Ishihara, *Japanese Journal of Applied Physics Part 1-Regular Papers Short Notes & Review Papers 43*, 4017, 2004.
2. Luo, X. G. and T. Ishihara, *Applied Physics Letters 84*, 4780, 2004
3. Melville, D., R. Blaikie, and C. Wolf, *Applied Physics Letters 84*, 4403, 2004.
4. Pendry, J., *Physical Review Letters 85*, 3966, 2000.

Session 5A7

RF Safety Issues

The State of the Science of Radiofrequency Health Effects

M. L. Swicord, **J. A. Elder**, **J. J. Morrissey**
Motorola Florida Research Laboratories, USA

There are more than 1320 peer reviewed publications in the radiofrequency (RF) database as listed on the WHO website at http://www.who.int/peh-emf/research/database/en/. This database contains publications dating back more than 50 years. Many of these studies exposed animals, cells or other biological samples to thermal as well as non-thermal levels of RF energy. A review of these published studies does not reveal any consistently and independently repeatable non-thermal effect because attempts at replication or confirmation of reported effects have failed to support the original finding.

Some replication studies are currently underway and the outcome of these studies will help address the necessity for further research. However, the extant database does not provide any testable hypotheses to pursue with the exception of a few studies that are currently under investigation. This is particularly true of long-term animal studies with all 20 publications since 1998 showing no effect of RF exposure on cancer, body weight or survival.

In the absence of experimental evidence to guide research on non-thermal effects, theoretical postulates might give useful guidance. However, the hypotheses regarding non-thermal effects that have been put forward have been found, upon examination by other theoreticians, to be implausible.

Reviews of the RF database by numerous national and international expert bodies, including WHO, conclude that there is no credible evidence that RF exposure within the internationally accepted limits recommended by ICNIRP cause any adverse health effects. Most panels go on to state that more research is needed and it is estimated that currently planned RF research to be conducted around the world in the next 3-5 years will exceed 100 million (US$).

In summary, the state of the science regarding RF exposure supports the following points.

- The only established adverse health effects of RF exposure are thermal effects.
- Reports of low-level (non-thermal) biological effects are not being replicated/confirmed and, furthermore, are not consistent with results of studies of animals exposed for long durations, including lifetime exposure of two years, i.e., all 20 long-term exposure studies published since 1998 report no difference in health of RF-exposed animals and control (sham exposed) animals.
- The weight of evidence in epidemiology studies does not provide evidence of cancer in human populations exposed to RF energy including users of mobile phones.
- The general consensus of expert panels and governments around the world is that a) RF exposure within the limits of the ICNIRP standard is safe and b) there are no adverse health effects associated with use of mobile phones.
- The results in recently published papers strengthen the support for the general consensus of expert panels and governments from around the world regarding RF exposure.

Studies in the Radiofrequency Literature Relevant to the Use of Mobile Phones by Children

J. A. Elder
Motorola Florida Research Laboratories, USA

The concern for use of mobile phones by children is based in part on concern for radiofrequency (RF) effects on their developing nervous system and the potential for exposure throughout most of their lifetime. This review focused on studies in the RF database that exposed animals during critical periods of nervous system development. Some studies exposed the animals throughout gestation while other studies involved lifetime exposure including prenatal exposure. The health endpoints investigated included birth defects, brain cancer and structure and function of the central nervous system (CNS) including blood-brain barrier permeability and neurobehavioral development.

Studies investigating birth defects in the offspring of pregnant animals exposed to RF energy are important because exposure occurred during the most sensitive in utero stages of CNS development and the results addressed the question of whether or not the head and brain developed normally. Some studies included almost continuous RF exposure throughout pregnancy. Results show that RF exposure can cause birth defects if the exposure caused a significant increase in body temperature of the pregnant animal.

Exposure to mobile phone signals from late gestation through 24 months of age (lifetime exposure) did not increase the incidence of either spontaneous primary CNS tumors or chemically-induced CNS tumors. The results of these long-term exposure studies provide no support for the hypothesis that RF energy acts as a carcinogen or a cancer promoter in CNS tissues, including the brain, during critical periods of CNS development and through adult life. Another lifetime study examined blood brain barrier (BBB) permeability in mice exposed for two years at exposure levels up to 4 W/kg. The mobile telephone-type signal produced no significant effect on the BBB. These results are consistent with the weight of evidence showing that changes in the BBB are induced by exposures above 4 W/kg causing significant elevation in brain temperature.

In another long-term study, monkeys were exposed to three exposure levels beginning the second trimester of pregnancy. Mothers and offspring were exposed for an additional 6 months after parturition and the offspring were exposed for another 6 months. In the offspring, a wide array of endpoints were measured including growth rate, EEG, biochemistry, hematology, and five tests of behavioral development. RF exposure at SARs up to 3.4 W/kg did not affect neurobehavioral function of non-human primates. Other studies found that RF exposure in utero did not affect brain organogenesis or cognition in animals tested as adults.

The RF literature does not provide support for the developing animal, as a surrogate for the developing human, being more sensitive than adults to RF exposure. This conclusion is in agreement with the recent report from the Health Council of the Netherlands stating that there is "$\cdots$ no reason to recommend limiting the use of mobile phones by children" [1] and advice from the U.S. Food and Drug Administration (FDA) stating that "The scientific evidence does not show a danger to users of wireless phones, including children and teenagers" [2].

REFERENCES

1. *Bioelectromagnetics*, Vol. 25, 142, 2004.
2. http://www.fda.gov/cellphones/qa.html#31.

Effects of Microwaves from GSM Mobile Phones on the Blood-brain Barrier and Neurons in Rat Brain

Bertil R. R. Persson, **Jacob Eberhardt**, **Lars Malmgren**
Mikael B Persson, **Arne Brun**, **Leif G Salford**
Lund University Hospital, Sweden

Our group has since 1988 studied the effects of different intensities and modulations of 915 MHz microwaves in a rat model where the exposure takes place in a TEM-cell during various time periods and post exposure recovery times. The effective microwave power fed into TEM-cells was 0.125, 1.25, 12.5 or 125 mW corresponding to whole body SAR (determined experimentally): 0.2, 2, 20 or 200 mW/kg. The rats were awake and not restrained during exposure and after the recovery period the animals were anaesthetized and sacrificed by perfusion-fixation with 4% formaldehyde. Paraffin embedded 5 mm. thick brain slices were stained for albumin by applying albumin antibodies (Dakopatts), by which albumin is revealed as brownish discolorations. Dark neurons were revealed by staining for RNA/DNA with cresyl violet. The occurrence of blood-brain barrier leakage and damaged (dark) neurons in different parts of the brain is judged blindly in a semi-quantitative way by the neuropathologist by given ranking values of increasing degree of albumin leakage: 0 (for no leakage); 0.5; 1.0 (for weak leakage); 1.5; 2.0 (for moderate leakage); 2.5 and 3.0 (for severe leakage).

In series of more than 1800 Fisher rats, we have proven that sub thermal power levels from both pulse-modulated and continuous RF fields - including those from real GSM mobile phones - have the potency to significantly open the BBB for the animals own albumin (but not fibrinogen) to pass out into the brain and to accumulate in the neurons and glial cells surrounding the capillaries. Albumin extravasations are most prominent at the lower SAR values. This dose-response behaviour suggests some kind of energy or electromagnetic field strength windowing effect. A linear dose-response relationship for dark neurons was found at 50 days after exposure, with most prominent occurrence at SAR 200 mW/kg.

The possible risks by radiofrequency electromagnetic fields exposure of the human body, is a major concern for the society. A new, third generation of mobile communication is becoming increasingly important, but the health impact of this radiation modality is largely unknown. Epidemiological studies will not be able to answer this question until after 10 - 15 years from now. It is therefore of greatest importance to study in the laboratory biological effects that can lead to health impairment. It is of great importance both to quantify the leakage of albumin through the BBB and to study the toxicological effects of this leakage. This new knowledge can be used as a foundation for new exposure limits that take into account non-thermal biological effects of microwaves radiation from mobile telephones and base stations.

REFERENCES

1. Salford, L. G., A. Brun, K. Sturesson, J. L. Eberhardt, and B. R. R. Persson, "Permeability of the Blood-Brain barrier Induced by 915 MHz Electromagnetic Radiation, Continuous Wave and Modulated at 8, 16, 50, and 200 Hz", *Microscopy Research and Technique*, Vol. 27, 535, 1994.
2. Persson, B. R. R., L. G. Salford, and A. Brun, "Blood-brain barrier permeability in rats exposed to electromagnetic fields used in wireless communication", *Wireless Networks*, Vol. 3, 455, 1997.
3. Salford, L. G., A. E. Brun, J. L. Eberhardt, L. Malmgren, and B. R. R. Persson, "Nerve cell damage in mammalian brain after exposure to microwaves from GSM mobile phones", *Environmental Health Perspectives*, Vol. 111, 881, 2003.

Toxicity Effects of 4T Superconductive Static Magnetic Field on Rat and It's Embryo

Xiao-Yun Zhang, **Yu Zhang**
Shenzhen University, China

The current study investigates the effects of 4T static magnetic field(SMF) exposure on acute toxicity in rats and it's embryo, in order to prove the security of SMF and give some references to safe intensity limit of country. Method We have used 4T superconductive static magnetic field was made of Institute of Electrical Engineering Chinese Academy of sciences and Conventional SD rat was got from Laboratory Animal Department of Peking University Health Science Center. There are three different dosage group, After treatment of magnetic field 24 hours, 48 hours and 72 hours, through observed general states, pathological dissection, biochemical parameters measure, check micronucleus and karyotype search after safety of 4T SMF. We take above indexes again 12 hours and 30 days later after treatment of SMF 72 hours and reproductive toxicity test. In embryonic test we adopt three dosage group, they were treated in MF 0.5h, 1h, 2h everyday, a negative group and positive group. Then we take sperm malformation test, traition malformation test and micronucleus test. In these test we have observed figure of sperm, growth of rat offspring, G strip of chromosome and percent of micronucleus. Result After treatment of 4T SMF most parameters have not any changes in above tests, have no toxicity of rat sperm, gravid rat, growth of rat embryo and chromosome. Conclusion 4T SMF have not any acute toxicity about rats and reproduction toxicity of it's offspring.

In Vivo Exposure Setup for Large Scale Toxicity/Carcinogenicity Studies with Rats at 900/1800MHz

S. Ebert, **N. Nikoloski**, **V. Berdiñas**, **J. Fröhlich**, **N. Kuster**
Foundation for Research on Information Technologies in Society (ITIS), Switzerland

Two types of *in vivo* exposure setups for studies within the context of the health risk assessment of low level exposure to the RF of mobile phones have been developed. They have been used in (1) two combined toxicity/carcinogenicity studies with 900 MHz GSM & 1800 MHz DCS wireless communication signals in WISTAR rats at RCC in Switzerland and in two studies evaluating DMBA-induced mammary tumors in Sprague Dawley rats exposed to 900 MHz GSM signals at (2) the Austrian Research Centers Seibersdorf in Austria and additionally also at (3) Zhejiang University in Hang Zhou in China.

The objectives were to develop, optimize and build two exposure setups for rats and perform a detailed dosimetric evaluation. The setup at 900 MHz operates at the mid band of the GSM 900 uplink at 902 MHz, the other at the mid band of the DCS 1800 uplink at 1747 MHz. The rat exposure setup provides excellent exposure homogeneity for different animal sizes. The realized concept of the rat setup is a circular cascade of 17 sectorial waveguides, all excited by a loop antenna placed in the center, delivering a H-polarization in animal orientation. A specially designed loop antenna which handles 200 W CW / 400 W peak provides a homogeneous circular field distribution, low losses and well matched impedance. For 1800 MHz the concept was further enhanced by reducing the distance of the plates to certain diameter around the exciting antenna in order to guarantee single-mode excitation and by developing a more sophisticated setup shielding. The distance between the short and the rats as well as the diameter of the inserted circular plates for the 1800 MHz band have been optimized for maximum uniformity of exposure. Electromagnetic sealing of the openings is achieved using easy to handle, custom-made stainless steel covers. The setup design furthermore provides enough light for the animals and the same airflow for all 17 animals. All relevant technical and biological parameters during the experiment (e.g., temperature, humidity, oxygen, field strength) were monitored every ten seconds and recorded with the control software. A feedback control was implemented with two E-Field sensors which monitors the exposure and were used for drift compensation. The setups fulfill GLP conditions. The setups have been carefully evaluated, optimized and verified by numerical and experimental means using the FDTD simulation platform SEMCAD and the near-field scanner DASY4 equipped with the latest probe technology.

A detailed dosimetry and uncertainty assessment was performed and showed excellent performance of the exposure setup. The experiments were conducted double blind at three different power levels (4 W/kg, 1.3 W/kg, 0.4 W/kg, sham). The dosimetry for the weekly whole-body averaged SAR for the entire group showed an uncertainty of ± 1.2 dB (for k=2) when evaluated according to NIST TN 1297, with an instant SAR variation (standard deviation) of ± 1.1dB. Considering the up to two year long-term exposure of the rats and the applied rotation scheme, the SAR variations reduces to ± 0.6dB. Furthermore, a detailed analysis of the organ specific SAR values was performed using high-resolution numerical rat models of different sizes and strains. The study was supported by the 5th Framework Program of the European Union, the Swiss Government (BBW), the Mobile Manufacturers Forum (MMF) and the GSM Association.

Energy Absorption in Layered Biological Tissue and Its Consequences on the Compliance Testing of Body-Mounted Wireless Devices

A. Christ, **A. Klingenböck**, **N. Kuster**
Foundation for Research on Information Technologies in Society, Switzerland

Recent years have seen a steady increase of cellular phone usage. In addition, novel wireless devices such as WLAN transmitters in laptop computers and body-mounted health support systems further increase user exposure to electromagnetic radiation. The absorption mechanisms of the electromagnetic fields caused by cellular phones have been intensively studied, and standardized methods for compliance testing have been established. However, additional factors must be considered for the compliance testing of body-mounted wireless devices. These include:

- a large frequency range (30 MHz—6 GHz),
- variation in usage patterns (positions and distances from the body),
- other compositions of the body tissues at the exposed locations and
- different output powers, amplifier characteristics and modulation schemes.

This study aimed at a rigorous analysis of the energy absorption mechanisms considering these conditions and at the assessment of an appropriate phantom size required for a conservative SAR assessment. The tissue composition of the human body at different locations was studied with respect to worst-case energy absorption considering anatomically correct tissue distributions. Because of the high frequency range and typical distances between 5 mm and 200 mm from the body, coupling effects in the near field and in the far field were considered. The absorption was assessed both analytically using generic antenna types and body models and numerically using the FDTD platform SEMCAD for the simulation of real world devices and anatomical high-resolution models. The absorption in these body models is compared to the SAR assessed with liquid filled flat phantoms of different sizes and shapes.

The results show that the presence of a tissue layer with low water content such as fat between two tissues with high water content (skin, muscle) has a significant impact on the energy absorption. Under far field exposure conditions, standing wave effects can cause an SAR increase in the skin, whereas reactive electric field components can penetrate the low permittivity fat tissue in the near field. Both effects can lead to higher SAR, depending on the frequency, distance, antenna type (dipole, helix, patch) and tissue distribution in comparison to homogeneous tissue or liquid filled phantoms.

In conclusion, it could be demonstrated that an elliptical phantom with a surface of $600 \times 400\,\mathrm{mm}^2$ as defined in [1] is well suited to exclude influences from the phantom shape and size within the frequency and distance range of interest. However, due to layering effects, additional considerations such as a safety factor between 2 and 3 may be necessary to assert a conservative SAR assessment using a homogeneous liquid filled phantom.

Study of SAR Reduction in the Human Head with Metamaterials

Jiunn-Nan Hwang, **Fu-Chiarng Chen**
National Chiao Tung University, Taiwan

The influence of EM waves from cellular phones has been discussed recently. The growing number of cellular users and the way cellular phone placed close to human head both arouse public concerns about the interaction between human body and EM waves. The specific absorbing rate (SAR) is a defined parameter for evaluating power deposition in human tissue. For the cellular phone compliance, the SAR values must be below the limits recommended by international safety guidelines. Therefore, many researchers are working on reducing SAR distribution in human body.

Recently, metamaterials have inspired great interests in their unique physical properties and novel application. Two important parameters, electric permittivity and magnetic permeability determine the response of the materials to the electromagnetic propagation. A negative permittivity can be obtained by arranging the thin metallic wires periodically. On the other hand, an array of split ring resonators (SRRs) can exhibit negative effective permeability.

In this paper, the metamaterials are covered on the portable telephone to reduce the EM interaction between portable telephone and human head. The human head in this study is modeled as an anatomically based human head model and the portable telephone is modeled as a monopole on a metal box. First, simulation of metamaterials is performed by 3-D FDTD method with Drude model. The effective medium parameter is chosen to be negative at PCS band of the cellular phone. Then, we construct metamaterials from periodical arrangement of split ring resonators. With properly choosing geometry parameters of SRRs, the stop band can also be shifted around PCS band. The peak 1-g averaged SAR values in the human head can be reduced with metamaterials. The performances of the portable telephone with metamaterials are also studied. Numerical results are demonstrated to validate the efficiency of the proposed metamaterials.

Harmonization of International RF Safety Standards

C-K. Chou, **J. A. D'Andrea**, **R. A. Tell**, **E. R. Adair**, **M. L. Swicord**
Sakari Lang, **John DeFrank**, **R. C. Petersen**
Institute of Electrical and Electronics Engineers, USA

During the past 60 years, the dramatic increase in technologies that produce electromagnetic fields (EMF) in the environment has led to public health concerns in many parts of the world. Specifically, questions have been raised on the safety of exposure to EMF emitted from microwave ovens, video display terminals, high voltage power lines and from antennas used for radar, TV, radio, and most recently, mobile telephones and base stations. Since the 1950's, scientists and health officials around the globe have dealt in different ways with the EMF health issue. Various maximum permissible exposure (MPE) values with up to a thousand-fold difference between Eastern and Western countries have caused confusion and added to the debate. Currently there are two major exposure standards accepted by countries around the world. While the IEEE RF safety standard has a much longer history (since 1966), many countries have adopted the 1998 International Commission on Non-Ionizing Radiation Protection (ICNIRP) guidelines, which are endorsed by the WHO. A lack of uniformity between the IEEE and ICNIRP MPEs and basic restrictions for localized exposures has led to confusion in regulation and product compliance as well as decreased public confidence in the scientific community that sets the limits. Harmonization of EMF safety standards will eliminate these problems and could help minimize electrophobia. If EMF standards continue to be determined by local governmental politics and not by sound scientific data, there will never be a world harmonized EMF safety standard. Likewise, arguments about biological significance among scientists of different countries continue to make harmonization more difficult. Harmonization of IEEE standards and ICNIRP guidelines is a first step toward a global EMF safety standard.

The IEEE C95.1 standard "IEEE Standard for Safety Levels with Respect to Human Exposure to Radio Frequency Electromagnetic Fields, 3 kHz to 300 GHz," was published in 1991 and modified in 1999 with essentially no changes in the exposure limits and without updating and reevaluating the supporting scientific literature. A complete revision of the standard is now in progress. The revision is based on the literature published through 2003 and is listed in a database containing more than 1300 references on biological effects. New insights, gained from a better understanding of the effects of acute and chronic RF electromagnetic field exposures of animals and humans and the associated dosimetry through improved experimental and theoretical analysis methods, are included. The recommendations for limiting the potential for adverse health effects from RF exposures are based on a comprehensive and critical review of the scientific data. An important criterion established for the revision of C95.1 was "The RF standard should be harmonized with other international standards to the extent where scientifically defensible." The latest draft revision of C95.1 retains the same whole-body-average SAR basic restrictions and MPE values as before for the upper tier. However, new peak spatial-average SAR limits are harmonized with those of ICNIRP, although the parts of the body to which these limits apply are not identical. The MPE values for the lower tier are harmonized with the ICNIRP general public exposure guidelines for frequencies greater than 300 MHz. For the first time, this standard includes a requirement for RF safety programs. Similarities and differences between IEEE and ICNIRP, including arguments for and against the adoption of a single tier of exposure limits safe for all, will be discussed at the meeting.

Session 5P1a

Application of Remote Sensing Techniques in Earth Sciences

The Effect of Tree Crown Structure on Radar Backscatter Using Model Analysis

Zhifeng Guo[1,2], **Guoqing Sun**[3], **Xuan Li**[4]

[1]Institute of Remote Sensing Applications, Chinese Academy of Sciences, China
[2]Graduate School of the Chinese Academy of Sciences, China
[3]University of Maryland, USA
[4]National Meteorological Center, China

In this study, a larch forest stand, which is the dominant species in Daxingan Mountains, was established according to the results from forest growth model, with an emphasis on the construction of the three-dimensional larch tree model using parametric and stochastic Lindenmayer system (L-system). Then a forest backscatter model is described and is used to calculate the incoherent backscatter from the established larch stand composed of realistic geometry of tree crown. The forest growth model can provide statistical information of larch forest and derive stands parameters for radar model. Combining with forest growth model, we generate different 3-D tree crown architectures faithful to the real stand using L-system, which provide realistic and detailed canopy structure information for radar model. Through the simulated tree model, we can get exact position information of canopy architecture and analyze its effect on radar backscatter using radar model. Here, we define five major backscatter components: direct crown backscatter, direct ground backscatter, direct trunk backscatter, multi-path interactions between crown and ground and double-bounce trunk-ground interactions. Total backscatter from a simulated larch stand is computed by incoherent summation of these five components.

In this paper, polarization radar returns of different larch stands under 10 years old, 30 years old and 80 years old conditions, that correspond to the young, mid-age, and mature forests commonly used in forest management practice in Northeastern China, are simulated and analyzed at C-, L-band. The results show that the discrepancy between larch stands with the same tree age is not evident, for the conifer canopy structures with same age are similar. But the discrepancy between larch stands with different age is large and distinct. The differences calculated from modeled data are 3.665dB between 10 years stand and 30 years stand, and 2.845dB between 30 years stand and 80 years stand at L band HH polarization, which have an agreement with the JERS-1 images of larch forest stands in Daxingan Mountain and indicate that tree crown architecture plays an important role in determining the radar backscatter.

Radiometric Cross-calibration of MODIS and CMODIS Based on Dunhuang Test Site

Xuan Li[1], **Zhifeng Guo**[2,3]

[1]National Meteorological Center, China
[2]Institute of Remote Sensing Applications, Chinese Academy of Sciences, China
[3]Graduate School of the Chinese Academy of Sciences, China

With the enhancement of launching, China launched meteorology and earth resource satellite in recent years. Launched on March 25,2002, the first Chinese Moderate Resolution Imaging Spectroradiometer (CMODIS) aboard the SZ-3 spacecraft has 34 bands with wavelength in the range of 403-12500nm. CMODIS is mainly applied to aspect and so on land utilization, land cover, water pollution monitor and resources investigation research. In-flight period CMODIS has obtained the massive data. In-flight calibration is imperative to quantities the data with higher accuracy and enable wide application, which is the subject of this paper.

This paper presents a methodology for radiometric cross-calibration of the solar reflective spectral bands of Moderate Resolution Imaging Spectroradiometer (MODIS) and Chinese Moderate Resolution Imaging Spectroradiometer (CMODIS) sensors based on analysis of two difference time image pairs for Dunhuang test site on July 27,2002. With the well-calibrated MODIS as a reference, we derive top-of-atmosphere (TOA) reflectance using MODIS data and then use these TOA reflectance to compute TOA radiance for CMODIS taking into account the effect of spectral band difference and the changes in solar zenith angle due to any temporal differences in the overpass times as well as differences in the view angles between the sensors. These TOA radiance, which are correlated with the sensor digital number (DN) output, determine the in-fight calibration coefficients of CMODIS. The average difference between the cross-calibration and vicarious calibration results is 7-8%. Results show that the cross-calibration approach can provide a valuable contemporary calibration for CMODIS in visible and near-infrared spectral bands based on the excellent radiometric performance of MODIS.

New Model of Atmospheric Radio Noise at Low and Very Low Frequencies in the Atlantic Area

Sophie Fieve, **Philippe Portala**
DGA/CTSN, France

Louis Bertel
Université de Rennes 1, France

The atmospheric noise originates mainly from the lightning discharges and is a major source of interference at low and very low frequencies. Noise measurements have been undertaken for now 8 years by the CTSN at different locations in Europe and around the Atlantic ocean and for different LF and VLF frequencies. The results have been analyzed and related to the current ITU model. It showed that the current model is not sufficient to describe accurately the atmospheric noise [1, 2].

The objective is now to propose a new model based on the description and the interpolation of the CTSN measurements in the time, frequency and spatial domains. This study is at the moment limited to the Atlantic area.

The low variability of the noise over the years, which was a condition for the creation of a model, was first verified. A precise description of the levels and the impulsivity of the atmospheric noise, and of their dependency to the frequency, the period of the day and the period of the year was then realized, giving a good understanding of the phenomena. Finally different methods were used to develop a model of the variations in the different domains : In the time domain a prediction based on a 'sliding median' with a monthly basis and an interpolation of the hourly measurements was proposed. A particular attention was given to the sunrise and sunset times, when quick changes in levels occur. In the frequency domain the spectra of the noise, recorded at specific times, could be directly extrapolated. The spatial domain was the critical part. Indeed it is not possible to make measurements in sufficient places, especially over the ocean. Two technics were then combined, a spatial interpolation from the different measurement sites and an addition of information from satellite maps of lightning.

The combination of the different domains gives a complete model of the atmospheric noise and its variability in the Atlantic area. Future developments are in progress to extend the area of the model and to add a real time component.

REFERENCES

1. Portala, P., "A Comparison of the CCIR Noise Model in VLF and Acquisitions of the CTSN Network," *PIERS 2001 Proceedings.*
2. Fieve, S., P. Portala and L. Bertel, "Study of Some Characteristics of Atmospheric Noise at 17.4 kHz Over a Tropical Area," *PIERS 2003 Proceedings.*

The Landslide Analysis of Taiwan in 2004

Long-Shin Liang, **Kun-Shan Chen**
National Central University, Taiwan

Chin-Lun Wang
National Chung Hsing University, Taiwan

Taiwan Island poses very rough and steep terrain along the Central Range to east coast with only about 30% of plain area along the west coast. It suffers from strikes from typhoon and flush storms almost every year. The Mindulle typhoon in 2004 July carried heavy rainfalls and raged viciously to the several counties in Middle Taiwan. The aim of this project was to understand and document the caused landslides in the seven counties by means of change detection using satellite images in order to assess the potential risk, to build up the attribution properties, and to compare with the past analysis result by Soil and Water conservation Bureau (SWCB) in earlier this year. It is hoped that we may improve our understanding about the status and trend of the catchments, drainage network, and watersheds.

From the analysis results, it was found that the new developed landslide area was 23,748.37 hectares. Among them, the increased counties were Miaoli, Taichung, Nantou, and Jiayi, while the decreased counties were Taichung city, Zhanghua, and Yunlin; only 11%(2607.23 hectares) belong to mountain-side range, the others were part of forest area. In terms of the scale by numbers of landslide, mostly were fallen between 0.1 to 0.5 hectares, or about 33.4% in total; if terms of area, areas between 2 to 10 hectares had 33% of the total; gradient at most number is 53% between 30 with 45 degree. It was also found that most landslides were in between 45 to 60 degrees and 25% of them were between 1,500 to 2,000 meters in altitude. It was worth mentioning that Nantou County, the 921 great earthquake site, wrap up a total of 13,270 hectares, increasing 1,792 hectares from previous report, while the most area decreasing county was Yunlin, amount to 204 hectares in reduction.

An Advanced Technology for Multi-layered Cloud Properties Retrievals

J. Huang[1], **B. Lin**[2], **P. Minnis**[2], **Y. Yi**[3], **T. F. Fan**[4], **R. Arduini**[4]

[1]Lanzhou University, China
[2]NASA Langley Research Center, USA
[3]Analytical Service & Material Inc., USA
[4]SAIC, One Enterprise Parkway, USA

This study has developed an advanced technology for multi-layered cloud retrievals. A two-layer cloud model is used to simulate multi-layered cloud radiative characteristics at spectra of visible (VIS), near infrared (NIR), thermal infrared (IR) and microwave (MW) wavelengths. The lookup tables of top-of-atmosphere (TOA) radiances at these wavelengths for the multilayer cloud systems are developed. For a ice-over-water cloud system, microwave satellite measurements are used to estimate cloud liquid water path and cloud water temperature of the lower level water cloud. The cloud properties of the upper-layer ice cloud are then derived using the MCRS algorithm based on satellite VIS, NIR and IR measurements for the two-layered clouds. The preliminary results from multiple sensor TRMM data, namely VIRS and TMI measurements, suggest that the MCRS may significantly improve the accuracy of ice cloud properties of multilayer cloud systems and reduce the overestimation of optical depth and IWP. The combination of different instruments covering broad wavelengths from VIS to MW provides great potentials in improving the estimation and understanding of radiative feedbacks of multilayer clouds.

Session 5P1b

Randomly Rough Surface and Volume Scattering

Reduced Rayleigh Equations in the Scattering of Light from and Its Transmission through a Film with Two One-dimensional Randomly Rough Surfaces

T. A. Leskova, **Alexei A. Maradudin**
University of California, Irvine, USA

The theoretical study of the scattering of light from a one-dimensional rough surface is significantly simplified if the electromagnetic field within the scattering medium can be eliminated from consideration, so that it is only the field in the medium of incidence that has to be calculated. The method of reduced Rayleigh equations [1] effects this elimination, and yields a single integral equation for the scattering amplitude, rather than the pair of coupled integral equations for the scattering and transmission amplitudes obtained from a straightforward application of the Rayleigh method to the scattering problem. It is desirable to extend this simplification to the study of the scattering of light from, and its transmission through, a film both of whose surfaces are one-dimensional rough surfaces. Thus, in this paper we consider p- and s-polarized light incident on a structure consisting of a medium characterized by a dielectric constant ϵ_1 in the region $x_3 > \zeta_1(x_1)$; a film characterized by a dielectric constant ϵ_2 in the region $-H + \zeta_2(x_1) < x_3 < \zeta_1(x_1)$; and a substrate characterized by a dielectric constant ϵ_3 in the region $x_3 < -H + \zeta_2(x_1)$. The light is incident from the region $x_3 > \zeta_1(x_1)$, and the plane of incidence is the x_1x_3 plane. Each of the surface profile functions $\zeta_{1,2}(x_1)$ is assumed to be a single-valued function of x_1 that is differentiable. A single integral equation (a reduced Rayleigh equation) for the scattering amplitude and for the transmission amplitude is derived for incident light of both polarizations. We also derive an expression for the transmission amplitude in each polarization as an integral transform of the corresponding scattering amplitude. Finally, we obtain a pair of coupled integral equations for the scattering and transmission amplitudes in each polarization.

REFERENCES

1. Toigo F., A. Marvin, V. Celli, and N. R. Hill, *Phys. Rev. B* **15**, 5618, 1977.

Non-local Effective Medium for the Electromagnetic Response of Colloidal Systems: a T-matrix Approach

Rubén G. Barrera, **Alejandro Reyes-Coronado**, **Augusto García-Valenzuela**
Universidad Nacional Autónoma de México, México

The concept of an effective medium for the description of the linear electromagnetic response of an inhomogeneous system has attracted, since long, the attention of many researchers and it has been extended to other different fields of physics. The idea is to replace the inhomogeneous system by an equivalent homogeneous one with the same electromagnetic properties. This is achieved by defining an effective response in terms of the parameters characterizing the inhomogeneous medium (mixing formulas). The main advantage is that one can calculate all different electromagnetic properties of the system using the whole power of continuum electrodynamics. The effective-medium concept has been extremely useful for the treatment of colloidal and granular systems when the size of the inclusions is much less that the wavelength of the incident radiation. When particles are not small compared to this wavelength the system becomes optically turbid. That is, in addition to a coherent field there is also a diffuse field. In this case there have been attempts to derive an effective refractive index to the random medium which describes the propagation of the coherent wave. This effective refractive index is in general complex and the imaginary part takes into account optical absorption and scattering of light.

Recently we developed a scattering-theory model for the coherent reflectance of light from a half-space of a composite material consisting of a uniform matrix material with randomly embedded particles. The model is formulated in terms of the scattering properties of individual particles and is restricted to systems with low particle density. Nevertheless it is applicable to systems with particles of sizes small, comparable, or larger than the wavelength of the incident radiation. We found that the reflection amplitudes for a colloidal half-space derived from our model are not consistent with the use of Fresnel's relations together with an effective index of refraction, when the particles are large. Also, when we try to derive an effective response from our scattering-theory model we find that there is an effective electric permittivity as well as an effective magnetic susceptibility (effective optical responses), even when the colloidal components are not magnetic. We also found, as an uncomfortable peculiarity, that these effective optical responses depend on the angle of incidence. Here we show that this peculiarity disappears when one recognizes that the effective medium of a colloidal system with large inclusions is actually nonlocal (spatially dispersive). We found explicit expressions for both, the effective nonlocal optical responses in terms of the longitudinal and transverse components of the transition operator of an isolated sphere. First we discuss the physical origin of the magnetic response in terms of induced closed currents within the spheres, and then we present an innovative procedure for the calculation of the transition operator. We apply this procedure to the case of a system of randomly located spheres and we show the results obtained for the nonlocal effective optical responses. Finally we discuss the extremely restricted utility of a nonlocal effective medium by calculating the surface impedance and the reflectance of the colloidal system for a particular model of the surface.

Surface Effects on the Coherent Reflection of Light from a Polydisperse Colloid

A. García-Valenzuela, **C. Sánchez-Pérez**
Rubén G. Barrera, **Alejandro Reyes-Coronado**
Universidad Nacional Autónoma de México, México

In recent works we developed a scattering-theory model for the coherent reflectance of light from a half-space of a composite material consisting of a uniform matrix material with randomly embedded particles. The model is restricted to dilute systems of particles but it is applicable to systems of particles with sizes smaller, comparable, or larger than the wavelength of the incident radiation. When particles are not small compared to the wavelength of the incident radiation the system becomes optically turbid. That is, in addition of a coherent field there is also a diffuse field. In this case it is known that one can assign an effective refractive index to the random medium which describes the propagation of the coherent wave. The refractive index is in general complex and the imaginary part takes into account optical absorption and scattering of light. However, in the scattering-theory model the effective refractive index does not appear explicitly. The model is formulated in terms of the scattering matrix elements of individual particles. Therefore it is not surprising that the scattering-theory model of the coherent reflectance does not coincide with the reflection amplitude derived from Fresnel relations together with an effective refractive index, when the particles size is not small compared to the wavelength of the incident beam. We have been looking for ways to confirm experimentally whether the Fresnel relations are in fact not valid and test the validity of our theory. The main difficulty is that for dilute colloids, the contribution of the particles to the coherent reflectance, is in general very small compared to the contribution of the matrix interface. An exception to this, is when the reflectance is measured in an internal-reflection configuration near to the critical angle of the incident-medium/matrix interface, in a similar way the modern critical-angle refractometers operate.

In this work we present the results of a series of experiments where we measure the coherent reflectance of light from a turbid colloid in an internal-reflection configuration. We compare the experimental data with our scattering model and with the predictions of the Fresnel relations. We show that the results obtained up to date confirm that the Fresnel relations are not valid when the colloidal particles are not small compared to the wavelength of the incident beam. This means that the use of a modern critical-angle refractometer with a turbid colloid will generally lead to inconsistencies. On the other hand, the experimental data can be reproduced well by our scattering-theory model and support its validity. We conclude that a possible method to characterize turbid colloids is to measure the coherent reflectance about the critical angle, but instead of relying on the Fresnel relations one should fit the scattering-theory model to the experimental curve. By doing a multi-parameter fit it is possible to obtain the size of the particles, their refractive index, and the refractive index of the matrix. Then we analyze the sensitivity of the coherent reflectance with respect to particle size and refractive index of the particles providing estimates for the precision of such method in practical cases. Finally, we discuss the extension of our model and the sensitivity to polydisperse systems of particles.

Measurement of the Effective Refractive Index of a Turbid Colloidal Suspension Using Light Refraction

Alejandro Reyes-Coronado, **Augusto García-Valenzuela**
Celia Sánchez-Pérez, **Rubén G. Barrera**
Universidad Nacional Autónoma de México, México

The measurement of the effective refractive index of a colloidal suspension has been studied experimentally over the past 40 years. However, in these works, they had used critical angle refractometers. The problem with these measurements is that one has to assign a critical angle to a prism-colloid interface. In general, the effective refractive index of a random system of spheres in suspension is complex, and the reflectance near the critical angle in a prism-colloid interface does not have a sharp transition to total internal reflection. This implies that one requires a model for the reflectance as a function of the angle of incidence. However, it has been now recognized that the reflectance of a half-space of a random system of large particles does not follow the expressions for the reflection amplitude given by Fresnel together with an effective refractive index. Thus, further analysis is needed to validate the procedure for the determination of the effective refractive index through measurements of reflection near the critical angle. A suitable alternative is to avoid any reflection measurements.

Here, we propose to measure the angle of refraction at a plane interface to determine the real part of the effective refractive index. One would expect that the coherent wave at a plane interface of a turbid medium should refract according to the usual laws for homogeneous media with an index of refraction corresponding to the propagation of the coherent wave through the bulk of the medium. Therefore, by measuring the angle of refraction of the coherent wave at a plane interface, one may determine the effective refractive index of a turbid medium. In practice, due to turbidity, such a simple measurement will be limited to dilute systems. Despite its simplicity, one has to recognize that there are not many other alternatives, and these measurements are not only interesting but also potentially useful. Besides providing a direct experimental verification of the laws of refraction of the coherent wave according to a well-defined effective refractive index and Snell's law, they provide a determination of the real part of the effective refractive index without the support of a multiple-scattering theory. Furthermore, one could use these measurements, together with a specific model, to determine some parameters of the particles in suspension, like their particle-size distribution and their refractive index.

In this work we propose a simple method to measure simultaneously the real and imaginary parts of the effective refractive index of a dilute suspension of particles, through measurements of the angle of refraction and transmittance of a laser beam that traverses a hollow glass prism filled with a colloidal suspension. We present results of experiments using an optically turbid suspension, which consists of polystyrene spherical particles suspended in deionised water. The diameter of the particles is comparable to the wavelength of the laser beam. We compare the results obtained with theoretical predictions taken from van de Hulsts effective-medium theory. As a corollary, we also report experimental evidence showing that the refractive behavior of the diffuse component of light coming from a suspension depends on filling fraction of the colloidal particles.

Ellipsometry of Inhomogeneous Media Interfaces

E. R. Méndez
Centro de Investigación Científica y de Educación Superior de Ensenada, México

A. García-Valenzuela, **A. Reyes-Coronado**, **Rubén G. Barrera**
Universidad Nacional Autónoma de México, México

The propagation and scattering of electromagnetic waves through random, heterogeneous media has been a subject of long-standing interest. In general, the optical heterogeneity of the sample originates from spatial fluctuations of the refractive index, and the amplitude and size of these fluctuations determine the turbidity of the sample.

In this work, we study the coherent reflectance of a system of single-sized, randomly positioned spherical particles whose size is comparable or larger than the wavelength, embedded in an otherwise homogeneous semi-infinite medium. The experimental system consists of latex particles in water illuminated through a glass hemisphere using a He-Ne laser ($\lambda = 0.633\mu$m). The coherent reflectance of the system depends on the polarization of the incident light, on the refractive indices of the media involved, and on the filling fraction and size of the particles.

We present measurements of the ellipsometric parameters Ψ and Δ for different angles of incidence. First, it is shown that, for relatively large particles, the measurements are not consistent with the reflection coefficient of a hypothetical effective medium characterized solely through its refractive index [1]. The measurements are then compared with theoretical results for the reflectivity of a half-space of particles based on the effective medium approach, and on the multiple scattering theory of Barrera and Garca-Valenzuela [2].

REFERENCES

1. Hulst HC, van de, "Light Scattering by Small Particles". *New York NY: John Wiley & Sons Inc*, 1957.
2. Barrera, R. G., A. García-Valenzuela, *J. Opt. Soc. Am. A*, Vol. 20, 296, 2003.

Reconstruction of Small Inclusions

H. Ammari
CMAP, France

The aim of our talk is to explain recent developments in inverse problems to detect small electromagnetic inclusions and calculations of effective properties of dilute composite materials. The central concept in these developments is the generalized polarization tensors and the main tool is the boundary integrals expressed in terms of layer potentials. Most of the material is from our recent book with H. Kang [1].

REFERENCES

1. *Lecture Notes in Mathematics, Springer-Verlag, Berlin*, Vol. 1846, 2000.

Nanosecond Laser Pulse Scattering from Arbitrarily Shaped Objects with Rough Surfaces

Gérard Berginc
Thalès Optronique, France

This paper discusses the trends in High Temporal Resolution Ladar (Laser Detection And Ranging) development. The incoherent ladar concept, based on the direct detection and analysis of the light backscattered by the target, has demonstrated interesting capabilities. Nanosecond pulse ladar utilizes 1-dimensional laser signatures or range profiles for enhanced, long-range identification of target. Previous papers have shown the range profiles at near infrared wavelengths are dominated by diffuse scattering and have desirable stability with observation angle.

Two major objectives are discussed. One is the modeling of nanosecond laser pulse scattering from objects with randomly rough surfaces. The other thrust includes experiment design and comparison with theoretical results.

The design of high temporal resolution ladar and the determination of laser signatures of various targets require accurate modeling software that will take surface reflectance representation as an input, and combine this representation with geometrical models to develop the laser cross-section of a nanosecond laser pulse. The surface reflectance representation is obtained by using the second order small-slope approximation for polarized incident laser wave. The formulas of coherent and incoherent scattering cross-sections have been obtained. This paper describes the main features of the simulation and the basis for its validity.

The fundamental concept of 1-D imaging is described as following: each scattering center of the target is interrogated at time proportional to its range as the short laser pulse sweeps across the target. The profile signature is the sum of all scattering centers. These range profiles are unique to each target. Preliminary experiments, using short laser pulses, fast single element detectors will be presented. The primary goals of these experiments are to compare theoretical modeling and measure and to investigate nanosecond laser pulse scattering from randomly rough surfaces.

Session 5P2

Periodic Structures II

Improving the Fourier Modal Method for Crossed Gratings with C_4 Symmetry by Use of a Group-theoretic Approach

Benfeng Bai, **Lifeng Li**
Tsinghua University, China

Using a group-theoretic approach that we developed recently we reformulate the Fourier modal method for crossed gratings with C_4 symmetry, i.e. the two-dimensionally periodic structures that are invariant after rotations about the normal of the grating plane through angles $n\pi/2$ where n is any integer. With this approach we decompose a crossed-grating problem in some Littrow mountings into four symmetrical basis problems whose field distributions are the symmetry modes of the grating. Then the symmetrical basis problems are solved with symmetry simplifications, whose solutions are superposed to get the field of the original problem. Theoretical and numerical results show that the reformulation improves the computation efficiency effectively: the memory occupation and time consumption are reduced to 1/4 and 1/16 of the original formulation, respectively; for normal incidence, the time-saving ratio is further reduced to 1/32.

Plasmon Resonance-absorption in a Metal Grating and Its Application for Refractive-index Measurement

T. Suyama[1], **Y. Okuno**[1], **T. Matsuda**[2]

[1] Kumamoto University, Japan
[2] Kumamoto National College of Technology, Japan

A metal grating has an interesting property known as the resonance absorption [1] : partial or total absorption of incident light energy occurs in TM incidence (p polarization). This is related to excitation of surface plasmons and an abrupt change of efficiency caused by the excitation is termed the resonance anomaly. [1, 2, 3]

For a grating placed in planer (or classical) mounting (the plane of incidence is perpendicular to the grooves) this phenomenon can be seen in TM incidence alone. While in conical mounting (the plane of incidence is not perpendicular to the grooves) the absorption is observed in both TM and TE incidence; and the absorption is accompanied by enhanced TM-TE mode conversion. Although the mode conversion always occurs in conical mounting, it is enhanced by the excitation of surface plasmons.

Numerical computation is carried out for a commercial UV grating made of aluminum. Computational results in reflected total, TM, and TE efficiency and the ratio are compared with experimental data. Enhancement of TM-TE mode conversion accompanying the excitation is examined. When a TM wave is incident on a metal grating, enhanced TM-TE mode conversion occurs at angles of incidence at which the surface plasmons are excited. The strength and sharpness of the mode conversion depends strongly on the azimuth angle (the angle between the plane of incidence and the direction of periodicity) of the mounting. The results of numerical computation predict that a maximum conversion ratio is available at an azimuth angle. This is verified by experiment and an application for refractive-index measurement is suggested.

REFERENCES

1. Raeter, H., "Surface Plasmon and Roughness," in V. M. Argranovich and D. L. Mills eds., *Surface Polaritons, North-Holland, New York,* chap. 9, 331, 1982.
2. Nevièr, M., "The Homogenous Problem," in R. Petit ed., *Electromagnetic Theory of Gratings, SpringerVerlag, Berlin*, chap. 5, 123, 1980.
3. Barnes, W. L., T. W. Preist, S. C. Kitson, J. R. Sambles, N. P. K. Cotter and D. J. Nash, "Photonic Gaps in the Dispersion of Surface Plasmons on Gratings," *Phys. Rev. B*, Vol. 51, 11164, 1995.

Resonant Scattering by a Multilayered Grating

T. Matsuda[1], **Y. Okuno**[2], **T. Suyama**[2], **M. Ohtsu**[2], **A. Wakahara**[3], **T. Nakamura**[4]

[1] Kumamoto National College of Technology, Japan
[2] Kumamoto University, Japan
[3] Toyohashi University of Technology, Japan
[4] Kushiro National College of Technology, Japan

We describe resonant scattering [1] in a multilayered grating, which is a stack of dielectric or metal thin-films periodically corrugated in one direction. The phenomenon is associated with the excitation of two kinds of surface waves, surface plasmons excited on metal surfaces and guided waves supported by dielectric thin-films: the incident light couples with the surface wave via an evanescent spectral order generated by the periodic structure. We employ Yasuura's modal expansion method [2] in solving the problem of plane-wave diffraction by a multilayered grating placed in conical mounting, in which the plane of incidence is not orthogonal to the grooves of the grating. In the results of numerical computation we observe partial or total absorption of incident light energy, which is seen as a dip (or an abrupt change) in an efficiency curve. It is numerically demonstrated that the absorption is related to the coupling of an evanescent diffracted mode with surface plasmons or guided waves. We show interesting behavior of the resonance absorptions in a multilayered grating such as the enhancement of polarization conversion [3] and coupled surface plasmons [4]. In the enhancement of polarization conversion, a TM (or TE) component of the incident light is strongly converted into a TE (or TM) one of the relfected light through the excitation of surface waves[3]. A periodically corrugated thin metal film supports surface plasmons that are simulatenously excited on both the upper and lower surface of the film. The two surface plamson waves interfere with each other and produce a symmetric or an antisymmetric coupled mode[4]. We fabricate a multilayered grating that consists of a stack of sinusoidal metal and dielectric film pairs and experimentally investigate the resonance absorptions in the grating.

REFERENCES

1. Hessel, A. and A. A. Oliner, *App. Opt.*, Vol. 4, 1275, 1965.
2. Ikuno, H. and K. Yasuura, *IEEE*, Vol. AP-21, 657, 1973.
3. Bryan-Brown, G. P., J. R. Sambles and M. C. Hutley, *J. Moderan Optics*, Vol. 37, 227, 1990.
4. Raether, H., *Physics of Thin Films (Academic Press, New York, 1977)*, Vol. 9, 145, 1977.

Realization of EM-wave Localization Using a Left-handed Transmission-line Super Lens

T. J. Cui[1], **Qiang Cheng**[1], **Zhi Zhong Huang**[1], **Yi Jun Feng**[2]

[1]Southeast University, China
[2]Nanjing University, China

We realize the localization of electromagnetic (EM) waves and energies using a left-handed (LH) transmission-line (TL) super lens. A detailed procedure is given to design the right-handed (RH) and left-handed transmission-line media, which correspond to the vacuum and the slightly- mismatched anti-vacuum. After properly designed and properly matched with terminal loads, we can generate a LHTL super lens. With the aid of microwave circuit simulations using the Agilent's Advanced Design System (ADS), we show that nearly all EM fields and energies are confined in a region between two voltage sources when they have the same amplitude and anti-phases and are placed at the image points of the super lens. In the simulation results, strong surface waves are clearly observed, which are coincident with the theoretical analysis for a homogeneous LH medium super lens. We also show that the ideal LHTL super lens cannot be realized due to the spatial dispersion of the TL networks, and the performance of the realizable LHTL super lens is very sensitive to the circuit parameters.

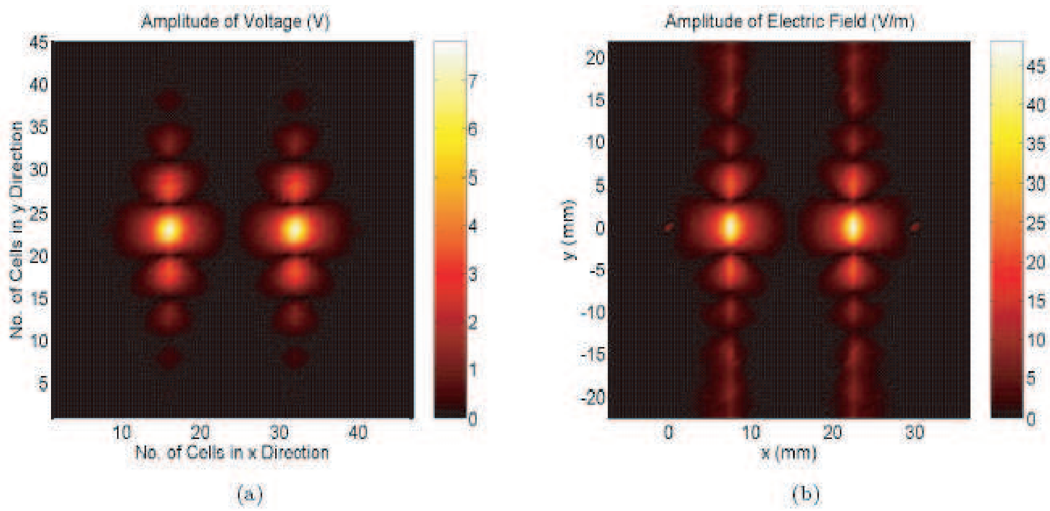

Figure 1: Simulated voltage amplitude in the LHTL super lens for two voltage sources when d = 1 mm and $\delta = -10^{-4}$ and its comparison with the equivalent homogeneous LHM super lens. (a) TL simulation result. (b) Theoretical result for homogeneous LHM super lens.

Nano-magnetic Structures Characterization in Thin Films

D. Bajalan
Vienna University of Technology, Austria

Over the past several decades, amorphous and more recently nano-crystalline materials have been investigated for applications in magnetic devices [3]. Demands for the continuous increase in the data storage density bring the challenge to overcome physical limits for currently used magnetic recording media [1, 2]. The benefits found in the nano-crystalline alloys is from their chemical and structural variations on a nano-scale which are important for developing optimal magnetic devices with high properties. Magnetic nano structures are subjects of growing interest because of their potential applications in high density magnetic recording media and their original magnetic properties. Investigations on nano-magnetic structures becoming very important for designing modern magnetic devices that contains these nanomagnetic shapes and structures. Fundamental calculations with sensitive models to identify the properties of the nano-structures are too important. It must be taken in count parallel with the surface, shape, and size properties identification (through correct microscopy) before the manufacturing process of the nanostructured devices begins [4]. The aim of this paper is mainly to discuss the use of structural characterizing tools like:

1. Atomic force microscopy (AFM)
2. Magnetic force microscopy (MFM)
3. Scanning tunneling microscopy (STM)
4. Lorentz transmission electron microscopy (LTEM)

REFERENCES

1. Solzi, M., M. Ghidini and G. Asti, *Magnetic Nanostructures*, Vol. 4, 123, 2002.
2. Bajalan, D., H. Hauser and P. L. Fulmek, *4th Int. Symposium on HMM, University of Salamanca*, Vol. 8, 78, 2003.
3. McHenry, Michael E., Matthew A. Willard and David E. Laughlin, *Progress in Materials Science*, Vol. 44, 291, 1999.
4. Bajalan, D., H. Hauser, P. L. Fulmek, , *Physical B*, Vol. 343, 384, 2004.

Nano Segregation Effects on Nano Magnetic Properties in Multi-layer Thin Films

D. Bajalan
Vienna University of Technology, Austria

Nanocrystalline systems attract more and more interest due to their applications on chemical catalysis and magnetic recording [1]. Magnetic nanostructures have become centre of great interest in the scientific community and in industry as the core technologies behind magnetic recording devices [2]. The magnetic properties of thin films are strongly influenced by their structure [3]. Small changes in the way a thin film is produced often give rise to large changes in some of the magnetic properties of the thin film [4]. The presence of (nanostructures) non-magnetic (or less magnetic) inhibits or hampers exchange interaction between adjacent grains, and hence increases the dipolar character of the magnetic interactions between grains[5]. This is best understood by observing how the microstructure of the film changes with processing and then correlating the microstructure directly with the properties of the thin film [4]. Experiments shows that segregation of non-magnetic elements (like Cr or Ta) in co enhances the magnetic property of thin films (such as $CoCrTa$). The saturation magnetization M_s and the Curie temperature of the alloy are substantially reduced. From the signal point of view, adding non-magnetic elements into Co poses a disadvantage, that is the substantial reduction of signal-to-noise ratio due to the drop in M_s.

REFERENCES

1. Bastos, C. S. M., M. Bahiana, W. C. Nunes, M. A. Novak, D. Altbir, P. Vargas, M. Knobel, *Physical Review B*, Vol. 66, 214407(1-8), 2002.
2. Mathuna, Diarmaid Mac, *Trinity College, Physics Department*, 2002.
3. Sellmyer, D. J., C. P. Luo, Y. Qiang, *Handbook of Thin Film Devices Magnetic, 5, Nanomaterials And Magnetic Thin Films, Academic Press*, 337, 2000.
4. Laughlin, D. E., Bin Lu, *Seagate Research Center, Materials Science and Engineering Department and Data Storage Systems Center, Carnegie Mellon University, Pittsburgh*, 1, 2001.
5. Jia, H., J. Veldeman, M. Burgelman, *J. Magn. Magn. Mater*, Vol. 223, 73, 2001.

Light Propagation in Random Waveguide Systems

Akira Komiyama
Osaka Electro-Communication University, Japan

Propagation properties of light in a one-dimensional waveguide system have been discussed in relation to the crosstalk between cores in an image fiber [1,2] which permits the direct transmission of an optical image. In an ordered system composed of identical cores of equal spacing light leaks out into neighbouring cores and spreads over the entire system. The spreading angle is $\vartheta_c = \tan^{-1} 2\kappa d$ where κ is the mode coupling coefficient and d is the spacing between cores. In a disordered system composed of randomly different core in size mode waves are localized in a narrow region of several number of cores [3]. Consequently light propagates along an illuminated core and does not almost leak out into neighbouring cores. When the system has random geometrical imperfections along the fiber axis the behaviour of light differs strongly from those [4].

In this paper propagation properties of light in random waveguide systems are presented. A starting point of the discussion is the mode coupling equations and the propagation constants of the modes are a random function of the propagation distance with zero mean and variance $\delta\beta^2$. The correlation function is assumed to be Gaussian. We assume that $D \ll 1/\kappa$ where D is the correlation length. The mode amplitude can be divided into the coherent part and the incoherent part. Equations for both parts can be theoretically derived from the perturbation solution of the coupled mode equations [5]. The coherent part has the same behaviour as light in an ordered system except for the exponential damping. The damping factor is given by $\alpha = \sqrt{\pi} D \delta\beta^2$ and the mean free path is $l = D/\sqrt{\pi}$. Light propagates coherently over the distance l. Since l is small the contribution of the mean free path is neglected in the following description. For small α the spreading angle of the incoherent part agrees with that for an ordered system. For $\kappa/\alpha \ll 1$ the spreading angle becomes small. Then the equations describing the behaviour of the incoherent part are reduced to the well-known coupled power equations and the power coupling coefficient is $d_c = 2\kappa^2/\alpha$.

REFERENCES

1. Komiyama, A. and M. Hashimoto, *Opt. Comm.*, Vol. 107, 49, 1994.
2. Komiyama, A. and M. Hashimoto, *IEICE Trans.*, Vol. E77-C, 1808, 1994.
3. Komiyama, A., *Opt. Comm.*, Vol. 151, 25, 1998.
4. Komiyama, A. and M. Tokimoto, *IEICE Trans.*, Vol. E83-C, 1849, 2000.
5. Komiyama, A., *Proceedings of 2004 URSI EMT-S*, 260, 2004.

A Recursive Solution of a Linear Equation System and Its Application to Wave Scattering

Junichi Nakayama[1], **Lan Gao**[2], **Kazuhiro Hattori**[1]

[1]Kyoto Institute of Technology, Japan
[2]5 Calmwater Crescent, Oyster Cove, Hope Island, Qld 4212, Australia

Scattering problems are often reduced to solving a linear equation system:

$$\sum_{m=1}^{N} D_{lm} A_m = E_l, \qquad (l = 1, 2, \cdots, N). \tag{1}$$

Under the assumption of the unique existence of the solution, numerical solutions have been discussed extensively. However, it is difficult to understand the physical scattering processes from numerical solutions. To obtain an explicit representation of the solution, this paper presents a recursive method, which divides (1) into two parts of equations for any m

$$\sum_{\substack{n=1\\n\neq m}}^{N} D_{ln} A_n = E_l - D_{lm} A_m, \ \ (l \neq m), \qquad \sum_{\substack{n=1\\n\neq m}}^{N} D_{mn} A_n + D_{mm} A_m = E_m. \tag{2}$$

We solve the $N-1$ equations in the left-hand side as a function of A_m and then substitute the result into the equation in the right-hand side to obtain A_m the mth element of the solution. To obtain the solution of the $N-1$ equations, however, we use the solution of the $N-2$ equations, and so on. This recursive process gives an explicit solution of (1) that is represented by a combination of finite continued fractions. The recursive process is also written as

$$A_m^{[L]} = E_m^{(1)}(m)/D_{mm}^{(1)}(m), \quad (L, m = 1, 2, \cdots, N) \tag{3}$$

$$D_{mn}^{(M)}(p_1, p_2, \cdots, p_M) = \begin{cases} D_{mn} - \displaystyle\sum_{\substack{l=1\\ l\neq p_1, p_2, \cdots, p_M}}^{N} D_{ml} \frac{D_{ln}^{M+1}(p_1, p_2, \cdots, p_M, l)}{D_{ll}^{M+1}(p_1, p_2, \cdots, p_M, l)}, & (M = 1, 2, \cdots, L-1) \\ D_{mn}, & (M = L) \end{cases}, \tag{4}$$

$$E_{m}^{(M)}(p_1, p_2, \cdots, p_M) = \begin{cases} E_{m} - \displaystyle\sum_{\substack{l=1\\ l\neq p_1, p_2, \cdots, p_M}}^{N} D_{ml} \frac{E_{l}^{M+1}(p_1, p_2, \cdots, p_M, l)}{D_{ll}^{M+1}(p_1, p_2, \cdots, p_M, l)}, & (M = 1, 2, \cdots, L-1) \\ E_{m}, & (M = L) \end{cases}, \tag{5}$$

where L is the depth parameter. Starting with $L = 1$, we obtain a sequence of approximate solutions: $A_m^{[1]}$, $A_m^{[2]}$, $\cdots$, $A_m^{[L]}$, $\cdots$, $A_m^{[N]}$. however, it may be proved formally that $A_m^{[N]}$ becomes the solution of (1). Some applications of (3)-(5) to scattering and diffraction problems will be presented.

Wave Propagation in Periodically Stratified Inhomogeneous Media by Fourier Series Expansion Methods

Tsuneki Yamasaki, **Kastuji Isono**, **Takashi Hinata**
Nihon University, Japan

Recently, the scattering and guiding problems of the inhomogeneous media have been considerable interest, such as optical fiber gratings , photonic band-gap crystals , frequency selective devices, and a negative refraction media. For the one of a powerful method based on the Fourier series expansion method in inhomogeneous media, it did not obtain the propagation constants for the plasma medium mixes it with the positive/negative in the oblique angle incidences of the TM wave. Therefore, it have been proposed to the modified multilayer approximation method(MMA) in the positive and negative area by using the solution of a linear profile. However, when the permittivity was positive and contained the singular point (zero), MMA has not applicable to the profiles. On the other hand, there was not also applicable to the same profiles though the homogeneous multilayer approximation method(HMA) using extrapolation methods.

In this paper, we proposed a new method for the wave propagation in inhomogeneous medium mixed the positive/negative by the combination of improved Fourier series expansion method using the extrapolation method. Numerical results are given for the complex propagation constants in the stratified inhomogeneous media the region of the positive and contained the singular point (zero) for the case of TM wave using the eigenvalue and eigenvectors obtained by the extrapolation method. Main process of our methods are as follows:

In the periodically inhomogeneous region in Fig.1(a), the structure is uniform in the y-direction and the permittivity $\varepsilon_d(z)$ including singular points at $z = z_1$ and $z = z_2$ (see Fig.1(b)). (1) To the obtain the correct solution in the analysis, $\varepsilon_d(z)$ is adding the expressed loss term σ, (2) Electromagnetic fields are expanded appropriately by a finite Fourier series using the eigenvalues, and the corresponding eigenvectors obtaied the extrapolation methods, (4) Finally, using the periodically boundary conditions in the region $(0 < z < d)$, we get the complex propagation constants.

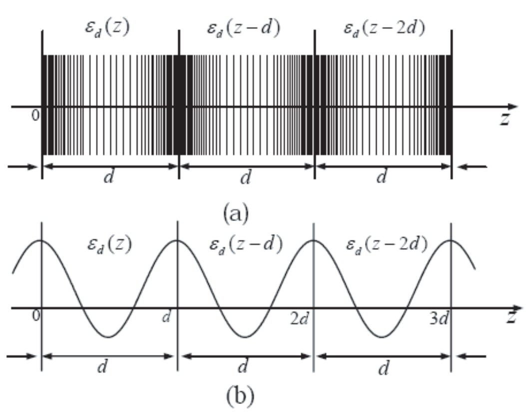

Figure 1: Periodically stratified inhomogeneous media.

(a) Coordinate system , (b) Permittivity profile $\varepsilon_2(z)$ mixed in positive/negative.

Session 5P3a

Volume and Rough Surface Scattering in Remote Sensing

Analysis of Brightness Temperature Data from a Corn Canopy with Vertical Temperature Gradient and Leaf Stress

S. Paloscia[1], **P. Pampaloni**[1], **M. A. Karam**[2], **W. J. Massman** [3]

[1]Institute of Applied Physics -IFAC- CNR, Italy
[2]Northrop Grumman Navigation and Space Sensors Division, Litton Systems, Inc., USA
[3]USDA/Forest Service, Rocky Mountain Station, USA

This study presents the results of analysis of brightness temperature data acquired over a corn canopy with vertical temperature gradient and leaf stress, close to Florence, Italy. The data were acquired at 10 GHz over several days of the vegetation cycle of the canopy. Both vertical and horizontal polarizations were measured over the angle range of $10°$ to $60°$. For each day of observation, vertical profiles of the air and leaf temperatures (of the upper and lower leaf surfaces) and of leaf stress were measured. Other ground truth affecting the brightness temperature data such as plant height, stem diameter, plant water content, leaf area index, leaf area, number of leaves per plant were measured for each day. Also, the soil moisture was measured at depths of 3 and 10 cm below soil surface.

For analysing the brightness temperature data, a brightness temperature formulation based on the stochastic radiative transfer equations and a canopy turbulence model is used [1]. The stochastic radiative transfer equations relate the brightness temperature data to the temperature gradient stress. The stochastic radiative transfer equations treat the canopy as a discrete binary medium, and they permit different thermal temperatures for canopy and air segments. The canopy turbulence model formulates the profiles of temperature gradient in terms of leaf stress. The turbulence model uses localized near-filed Lagrangian theory in formulating thermal temperature profiles within the canopy.

In adapting the corn ground truth for input to the brightness temperature formulation, the corn canopy was treated as a layer of elliptic discs and finite dielectric cylinders above a rough interface representing the leaves, the stalks, and the soil surface respectively. The discs and cylinders were taken to be respectively horizontally and vertically oriented with inclination distribution function $p(\beta)$ (β is the angle between the disc or cylinder axis and the vertical direction). The dielectric constant of the leaves and stalks was obtained from the plant water contents by using a semi-empirical formula [2]. Soil surface was assumed to be Gaussian with height standard deviation and correlation length taken from ground measurement.

Numerical simulations are performed to validate the brightness temperature formulation and to achieve the data analysis. The results of the numerical simulations showed a good agreement with the data, pointed out the impacts of the detailed description of the vegetation layer (including air and leaf nonuniform temperature profiles and leaf stress) on the trends of the brightness temperature.

REFERENCES

1. Karam, Massman, Paloscia, and Pampaloni, *submitted to Radio Science*, 2004.
2. Ulaby and El-Rayes, *IEEE Trans. Geosience and Remote Sensing*, Vol. GE-25, 550, 1987.

Effect of Wave Polarization on Radar Cross Section of Conducting Targets in Random Media

Hosam El-Ocla
Lakehead University, Canada

Scattered waves propagating in continuous random media are calculated efficiently by a method that uses a current generator to clarify the medium effects on radar detection. In earlier investigation, spatial coherence length (SCL) of incident waves around target was proved to have a key effect on the radar cross-section (RCS) of conducting convex bodies. In this work, we analyze numerically the effect of wave polarization on the RCS of target of different parameters. We consider targets are taking large sizes for linear polarizations including E- and H-polarizations and circular polarization (C-polarization). We have made clear the effects that have observed influence on the RCS, they are: the target configuration and the SCL in addition to the conventional double passage effect. These characteristics realize apart from the incident angle and incident wave polarization. In a low frequency limit, the interference between the direct and creeping waves deep in the shadow region that occurs in case of H-polarization results in large increase in the backscattering wave intensity that leads to anomalous RCS. However such phenomenon is much less with C-polarization and absent in case of E-polarization. On the other hand, in the high frequency limit, only the specularly-reflecting points at the surface contribute the scattered fields and therefore the effect of creeping waves become almost negligible.

Impact of Volume Scattering from Tilled Soil Using a 2D Numerical Model

C. Onier, **A. Chambarel**, **A. Chanzy**, **H. Bolvin**
INRA/CSE, France

M. Chanet, **R. Rouveure**
Cemagref, France

The soil tillage is the last work before sowing and has a large effect on plant emergence [1]. Thus, tilled soils should be properly prepared along the whole field unless the impact of spatial heterogeneous property of the soil. One of the main characteristics of tilled soils is the size of the generated clods lying in fine earth. The main goal of this study is then, to estimate the clods' size thanks to a measurement of the scattered electromagnetic waves created by their interactions in the microwave domain. To fulfil this goal, a numerical approach is led by resolving the Maxwell's equations in time domain with finite element method.

In this paper, a microwave scattering simulator is developed. It consists in two main parts:

- a soil structure generator to produce dielectric field of data to included in the domain of the electromagnetic computations. It is based on the a seedbed generator developed by C. Dürr [2]. Thus, the clods are modelled by ellipses which are randomly deformed and located in the fine earth which is the bulk medium. The clods are affected by a different dielectric property than the fine earth which is supposed to model a mix between earth materials and air pockets.
- the core of the electromagnetic propagating simulator is based on an original finite element formulation of the Maxwell's equations developed by A. Chambarel [3,4] thanks to the FAFEMO (Fast Adaptive Finite Modular Object) platform. PML (perfectly matched layer) absorbers, a NFFT (near field to far field transform) and focused beam waves have been implemented in order to propose a complete powerful easy-to-use simulator. Thus, the entire signal (form, incidence angle...) can be controlled with minimization of borders' artefacts.

Finally, after Characterizing some performances of the simulator on canonical targets, simulation results will be presented with varying clods' size and contrast of the clods' permittivity with the bulk medium. In particularly, the analyses will first focus on the quantification of the volume scattering with respect to the surface scattering. Then, the influence of the clods' size with respect to different incidence angles and frequencies will be considered.

REFERENCES

1. Dürr C. and J. N. Aubertot, "Emergence of seedlings of sugar beet (Beta vulgaris L.) as affected by the size, roughness and position of aggregates in the seedbed ", *Plant and Soil*, No. 219, 211, 2000.
2. Dürr C., J. N. Aubertot, G. Richard, P. Dubrulle, Y. Duval and J. Boiffin, "SIMPLE, a model for SIMulation of Plant Emergence", *Soil Science Society of America Journal*, No. 65, 414, 2001.
3. Chambarel A. and E. Ferry, "Finite Element formulation for Maxwell's equations with space dependent electric properties", *Application to Time Domain Reflectometry probe. Revue Européenne des Eléments Finis*, Vol. 9, No. 8, 941, 2000.
4. Chambarel A. and D. Fougère, "A General Parallel Computing Approach Using the Finite Element Method and the Objects Oriented Programming by Selected Data Technique", *PaCT2001, Lectures Notes in Computer Science*, Vol. Springer Verlag 2127, 428, 2001.

Efficient Analysis of Periodic Structures with Arbitrary Shape Using Volume-surface Integral Equation Method

Da-Zhi Ding, **Edward Kai-Ning Yung**, **Dao-Xiang Wang**
City University of Hong Kong, China

Rushan Chen
Nanjing University of Science and Technology, China

In this paper, the combined volume-surface integral equation based on periodic green functions is presented for the electromagnetic wave scattering from periodic structures composed of dielectrics and conducting objects. The triangular patches and tetrahedral elements are used to mesh the dielectric and conducting objects, respectively. The combined integral equations is discretized through surface and volume Rao-Wilton-Gillison (RWG) functions and solved by the method of moments (MoM). To rapidly generate the impedance elements, a hybrid algorithm based on Shank transformation and Ewald's method is used to speed the computation of the periodic Green function due to the fact that the periodic Green function, which is a summation of series, converges very slowly. Further, the flexible inner-outer preconditioning GMRES iterative algorithm (FGMRES) is applied to accelerate the convergence of the resulting matrix equation. Numerical results are presented to demonstrate the efficiency and accuracy of the proposed technique for analyzing the scattering problem of arbitrarily shaped 3-D periodic structure. The proposed technique can also be extensively applied to analyze the periodic structure consisted of inhomogeneous dielectric material and conducting body.

A Statistical Integral Equation Model for EM Scattering from Rough Surface

Yang Du, **Zhuoyuan Wang**, **Liang Peng**, **Wenzhe Yan**
Zhejiang University, China

J. A. Kong
Massachusetts Institute of Technology, U.S.A

Recent years have witnessed rapid progress in modeling of EM scattering from rough surface. One such appealing model is the integral equation model (IEM), which is shown to be able to bridge reasonably well SPM and Kirchhoff models such as PO and GO. However, IEM also suffers from several drawbacks. First of all, it makes implicitly an assumption that both the Kirchhoff term f_{qp} and the complementary one F_{qp} are linear in surface partial derivatives Z_x and Z_y, which immediately leads to determinististization of the otherwise random surface norm $\hat{n}$, and subsequently $f_{vv} = 2R_{\|}/\cos\theta_i$ and $f_{hh} = -2R_{\perp}/\cos\theta_i$ for the backscattering case, which clearly indicates problematic behavior as θ_i approaches near grazing incidence. Mostly for such consideration, the scattering coefficient is defined as $\lim\limits_{r\to\infty} 4\pi r^2|E^2_{qp}|^2/A_0|E^i|^2$, which by convention is used for finite body scattering whereas is needed in the denominator for surface case. Moreover, due to several approximations made in f_{qp} and F_{qp}, accuracy of crosspolarization is compromised. Lastly, shadow function is incorporated in an ad hoc manner in the scattering coefficients.

In this work, we propose a statistical integral equation model (SIEM) where we discard the linearity assumption of f_{qp} and F_{qp} in Z_x and Z_y, instead treat specifically the local terms $\hat{n}$, $\hat{t}$, $\hat{d}$, $R_{\|}$ and $R_{\perp}$ statistically over the orientation distribution of surface unit norm $\hat{n}$ as characterized by the joint probability distribution function of its spherical coordinates (θ_n, ϕ_n). In addition, we incorporate rigorously the shadow function in the Kirchhoff and complementary fields through a careful treatment of the Poggio & Miller equation. No approximation is made about either f_{qp} or F_{qp}.

SIEM thus possesses several advantages over IEM. First, it provides a well behaved $< f_{qp} >$ at near grazing incidence. Consequently, the scattering coefficient can be defined in a way consistent with convention. It also predicts more accurate crosspolarization. Moreover, since in IEM for f_{qp} the surface norm $\hat{n}$ reduces to $\hat{k}_s$ for the backscattering case, which definitely can be viewed as the joint pdf $p(\theta_n, \phi_n)$ being a delta function, and similar treatment applies to F_{qp}, it is clear that IEM is a special case of SIEM. In the same light, the small slope approximation (SSA) at 0^{th} order can also be viewed as a special case of SIEM.

Scattering of the Transmitted Light by Randomly Rough Dielectric Surface

D. A. Rogatkin, **V. V. Tchernyi**
Russian Academy of Science, Russia

With the use of the diffraction theory of scattering of electromagnetic waves by a randomly rough surface it was obtained the analytical solution for the transmitted light scattering by a dielectric rough surface in the case of normal illumination. The solution is formulated in the terms of the photometry indicatrix. As it was estimated by numerical calculation the transmitted light has no strong scattering by a dielectric randomly rough surface even in the case of the so-called "Lambert surface". One of the practical applications of the obtained solution can be the classical theory of the light transport in the turbid dielectric media, biological tissues for example. Today in the classical transport theory the boundary conditions of the plane surface are used more often. But the real dielectric scattering media usually have the non-plane, randomly rough surface, so the randomly rough surface boundary conditions are needed in the transport theory in the common case.

Session 5P3b

Detection & Characterization of Aerosol (or Small Airborne Particles) by Optics

Aerodynamic Sorting and Regrouping of Bioaerosols Cue from Their UV-LIF Spectroscopy

Yong-Le Pan, **Richard K. Chang**
Yale University, USA

Environmental and occupational monitoring of hazardous aerosols, especially bioterrorism threats by way of dispersal of pathogenic bioaerosols, requires advanced systems that can classify air-borne particles in real-time and in-situ. Laser-induced intrinsic fluorescence spectra are capable to, at least partially, distinguish bioaerosols from various kinds of ambient aerosols. Unfortunately, some non-biological aerosols, such as soot particles, have the similar fluorescence spectrum as bioaerosols. Therefore, further specific analysis as a secondstage identifier, such as biochemical assay, Raman spectroscopy, or FTIR spectroscopy is required for the verification of suspect bioaerosols, particularly for the determination of specific species of bioaerosols. When the ratio of non-bioaerosols to bioaerosols is too high, the more specific analysis is adversely affected. A technique for enrichment or sorting of bioaerosols would then be essential. In order to get high speed and sensitivity, we require that the sorted bioaerosols be regrouped into a small area to match the requirement of the second stage identifier.

We present here a system that can deflect, regroup, and thereby enrich bioaerosols that are selected by real-time detection and spectral analysis of single-shot UV-laser induced fluorescence (UV-LIF) of single flowing aerosols (1-10 μm in diameter). Once an aerosol is found to have a characteristic suspect fluorescence spectrum, a trigger signal is generated and sent to a pulsed valve to produce a fast directional puff of gas that deflects this particular bioaerosol onto a region and regroup onto a small area to deposit on the collecting substrate. Laboratory and field test results show the large enrichment factor of biospecies from the mixed aerosols or ambient aerosols can be achieved at least as high as 10^3. Furthermore, the sorted aerosols have been regrouped into an area as small as 1 mm in diameter.

The basic concept of the rapid aerodynamic sorting and regrouping system is as follows. Ambient air is first drawn into a virtual-impactor particle concentrator. Aerosol particles (1 to 10 μm in diameter) are concentrated ($\sim$300 times) and formed into a laminar air stream ($\sim$600 μm in diameter, flowing at a speed $\sim$20 m/s) by an aerodynamic focusing input nozzle. A single-shot of a pulsed UV-laser (263 nm, 4^{th} harmonic of Q-switched Nd:YLF laser) illuminates each particle after it has passed through a trigger volume ($\sim$ 300 μm $\times$ 300 μm). The trigger volume is determined by the intersection of two CW diode lasers at different wavelengths (635 nm and 675 nm). Further downstream, the puffer is triggered as soon as a flowing particle is found to exhibit UV-LIF spectral signatures of suspect bioaerosols (i.e. bacillus subtilis (BG, the stimulant for Anthrax)) that have been predetermined. After the puffer is triggered, it emits an air-packet to deflect that aerosol out of the main stream. All the deflected aerosols are then regrouped in order to be deposited on a substrate within a spot around 1 mm for the high density and small localization requirement for further secondstage identifier. This enriching factor (the ratio of the concentrations of the sorted particles to the concentration of the aerosol mixture before sorting) is larger than 10^3 in this test. The localization of the deflected particles, and thereby enriched in a one millimeter spot size is ideal for FTIR, Raman scattering, or other biochemical analyses. This aerodynamic sorting technique demonstrates a unique capability for selectivity and efficiency in sorting suspect particles from background aerosols. It appears that this system is a viable front-end instrument for sorting out "wanted or suspect" aerosols from ambient or background aerosols.

*We acknowledge the support by the RAAD program (Dr. Jay Eversole) through U.S. Army Research Laboratory (ARO DAAD19-02-0003), the DARPA SUVOS program (Lt.Col. John Carrano) through Brown University, and the DOE program through SRTC (Dr. Justin Halverson).

Study on the Thermophoretic Deposition Efficiency of PM2.5 Using Grey System Theory

Tao Zhou, **Ruichang Yang**, **Lei Zhao**
Tsinghua University, China

The synthesized dynamic model that the influencing factor is relative each other is established with minimal processed data (4) and multi-sequence of number differential coefficient mode in the main contents of grey system theory. The influencing factors are interacting or relating one another and complicated, and maybe not very clear and definite for PM2.5. This is kind of characteristic of the typical gray system with definite information and undefined information. In this paper, the experiment data are analyzed by the grey system theory. At first, the main parameters of influencing thermophoretic deposition efficiency, for example temperature difference or density ratio between PM2.5 and gas in the gas mixture or gas characteristic (viscidity coefficient, density, heat conductivity) or PM2.5 characteristic (density, heat conductivity) and so on, are analyzed by using the grey incidence analysis method, and they are ordered according to influencing magnitude. Then, the experimental data are regularly handled by the grey method. The GM(1,1) and GM(1,h) model are established for the thermophoretic deposition efficiency. The thermophoretic deposition efficiency values are predicted by GM (1,1) model and GM(1,h) model. The predicted thermophoretic deposition efficiency values are agreed with the experimental data well. Finally, the grey model is compared with the traditional method -Multiple Regression method and current mathematics model. Obviously, the grey model is excellent with the traditional method. The good model may be founded with seldom experimental data by the grey system theory. The grey model is excellent when the data are short. The model will become better than last time with more data and feedback. The grey model figure that is made up of the interval points is fit for real the experimental data of PM2.5. A new way that study on thermophoretic deposition efficiency is founded by using the grey system theory. There are special and important significance for predicting PM2.5 thermophoretic deposition efficiency for far the research.

Experimental Research on Real-time Detection for Aerosol Particle Aerodynamic Diameter

Fenping Cui, **Xiaoming Gao**, **Fang Li**, **Haiyang Zheng**, **Wei Huang**
Shixin Pei, **Weizheng Li**, **Weijun Zhang**
Anhui Institute of Optics & Fine Mechanics, Chinese Academy of Sciences, China

Aerosols play an important role in atmospheric chemical and physical processes. The effects of aerosol particles on human health are related to their diameter. There are many methods to detect aerosol particle aerodynamic diameter, but these methods can not measure in-situ and online. In this paper, we use flight time of aerosol particle to detect aerosol particle aerodynamic diameter and can give you fast, extremely precise aerosol measurements. The characteristic of the system is that a diode laser is split into two closely spaced elliptic gauss beams with an optical shaping system. Light is scattered as each particle crosses through the overlapping beams. An elliptical mirror, placed at 90 degrees to the laser beam axis, collects the light and focuses it onto an avalanche photodetector (APD). The APD then converts the light pluses into electrical pulses. With stationary pumping pressure, the kinematic velocity of the different size particle is discrepant, so the transit-time of particle through two beams is different. The time of flight of individual particles is measured in an accelerating flow field. Processing electronics measure the time of flight of the particle using a single high-speed timing processor. And then the aerodynamic diameter of aerosol particle can be determined. The system can detect 0.5$\sim$20μm aerosol particle with two important parameters: time of flight and light scattering intensity. We can obtain the chart plotting particle flight time and light scattering intensity with respect to aerodynamic particle diameter. The particle size distribution of the monodisperse aerosol and polydisperse aerosol, such as dioctyle phthalate (DOP), air and bacterial, has been got. The system can be applied in atmospheric studies and ambient air monitoring.

The Research of Magnetorheological Fluid Damper

Yan Yang, **Qi-Lin Tang**, **Jing Zhou**, **Hui Li**
Chongqing Institute of Technology, China

Magnetorheological (MR) fluids consist of stable suspensions of micro-sized, magnetizable particles dispersed in a carrier medium such as silicon oil or water. When an external magnetic field is applied, the polarization induced in suspended particles results in the magnetorheological effect of the MR fluids. The magnetorheological effect is direct influences on the mechanical properties of the MR fluids. The suspended particles in the MR fluids become magnetized and align themselves, like chains, with the direction of the magnetic field. The formulation of these particle chains restricts the movement of the MR fluids, thereby increasing the yield stress of the fluids.

In this paper the fundamental design method of the MR damper is investigated theoretically. Bingham model is used to characterize the constitutive behavior of the MR fluids subject to an external magnetic field strength. The theoretical method is developed to analyze the shear stress by the MR fluid within the damper. An engineering expression for the shear stress is derived to provide the theoretical foundations in the design of the damper. Based on this equation, be algebraically manipulated, the volume and thickness of the annular MR fluid within the damper is yielded.MR fluid damper is a device to give damping by the shear stress of MR fluid.

The key question in the design of MR fluid damper is to establish the relation between the damper and the parameters of the structure and magnetic field strength. As the magnetic field is applied, the damping F developed by MR fluid can be calculated:

$$F = 2\pi L\tau_B r^2 + \frac{2\pi\eta L r^3 V}{h}$$

The Equation shows that the damping developed in the cylindrical MR fluid damper can be divided into a magnetic field dependent induced yield stress component and a viscous component.

The active volume of annular MR fluid in the cylindrical MR damper can be obtained through the integration the radius of annular MR fluid as follow:

$$V = (\frac{\eta}{\tau_B^2})(\frac{F_B}{F_\eta})(F_B\omega)V$$

The geometric design method of a cylindrical MR fluid damper is investigated theoretically in this paper. The damping developed by MR fluid within the damper under different magnetic field strength conditions was analyzed. The engineering design calculations of the volume, thickness and width of the annular MR fluid within the damper are derived. The parameters of the thickness and width of the fluid in the damper can be calculated from the equations obtained, when the required mechanical power level, the speed of the piston, and the desired control damping ratio are specified.

Algorithm of Numerical Calculation on Lorentz Mie Theory

Jianqi Shen, **Xiaoshu Cai**
University of Shanghai for Science and Technology, China

Methods for the performance of a Mie calculation have been discussed for several decades. The Mie calculation has been well developed due to the important contributions from Mie, Infeld, Dave, Lentz, Wiscombe, and etc. A well-tested and widely used Mie code is Wiscombe's MIEV0 code in FORTRAN. This code provides accurate results for small and large particles with size parameters up to 20,000. But the algorithm used in MIEV0 has to treat small particles and large particles separately, and the calculation of the logarithmic derivative, $d \log \psi_n(m\alpha)/d(m\alpha) = \psi'_n(m\alpha)/\psi_n(m\alpha)$, is complicated. Later, Grehan and Gousbet developed the Mie calculation by evaluating the continued fraction with the Lentz's algorithm. The calculation is robust for small and large, transparent and absorbent particles. However, the calculation is time-consuming, especially for the calculation of large absorbent spherical particles.

In this work, a new algorithm is put forward. By combining the Lentz's method with a downward recurrence of the logarithmic derivative, this algorithm provides exact Mie results with controllable accuracy. The method is proven to be stable, accurate and efficient for both large and small particles. Testing results are given in detail, comparing with those obtained by other methods.

Elastic Scattering of Irregular Aerosol Particles

Gorden Videen
Army Research Laboratory AMSRD-ARL-CI-EM, USA

Building effective detectors that can differentiate between threat and natural aerosols is a top priority, both in the US through Homeland Security and abroad. NATO, for instance has made threat prevention their primary consideration in determining science funding. Three primary design considerations drive much of the research: cost, automation, and speed. Unfortunately, no magic feature has been discovered that fulfills these criteria, but elastic scattering techniques satisfy all requisites. In this presentation I will discuss current techniques that may be employed to obtain information about a particle system from its elastically scattered light.

Session 5P4a

Optical Fibers and Photonic Crystals

Exact Modelling of Defect Modes in Photonic Crystal Structures Using the Fictitious Source Superposition Model

L. C. Botten
University of Technology, Australia

S. Wilcox, **R. C. McPhedran**, **C. M. de Sterke**
University of Sydney, Australia

Many exciting properties of photonic crystals (PC) rely on photonic band gaps—frequency and direction ranges in which the propagation of light is suppressed through Bragg reflection. While band gaps provide the basic building block of a "mirror", the real potential of PC structures is unlocked through defects in otherwise periodic structures, e.g., line defects leading to waveguides, point or localized defects forming resonators, and, for photonic crystal fibres (PCF), a localized defect forming the core of the fibre. The introduction of defects into a structure gives rise to defect modes, the frequencies of which lie in the band gap of the surrounding PC, and thus are localized.

To date, the modelling of defect modes in non-periodic structures has been undertaken using techniques that assume a finite structure—either explicitly or implicitly, as in supercell methods which periodically replicate a finite structure. While such methods work well for strongly confined modes, difficulties arise when a mode becomes extended. The computational requirements of modelling a sufficiently large structure can then become overwhelming and lead to inaccurate results if the mode is poorly confined. To handle such problems, as typically arise in studying a mode near cutoff, we have developed an exact theory, the fictitious source superposition (FSS) method, for computing defect modes in an infinite 2D lattice. Not only does the theory handle structures with an infinite cladding, but also it is computationally more efficient than other techniques when the size of the structure becomes large.

This paper outlines the FSS method which combines the use of fictitious sources with Brillouin zone averaging. The fictitious sources provide the mechanism by which response fields are modified, allowing defects to be introduced, while the Brillouin zone averaging forms a superposition of field problems that models the defect mode exactly. For 2D photonic crystals, the averaging over the 2D Brillouin zone can be reduced to a 1D integral by using the properties of semi-infinite photonic crystals that are summarized in a single scattering matrix. Combining these concepts allows the defect eigenstate to be written as a superposition of the states of the perfectly periodic structure. We go on to demonstrate the strengths of the technique in dealing with the genuinely difficult case of spatially extended modes (e.g., modes in the vicinity of cutoff) in which methods which assume a finite structure fail. We focus on the controversy concerning the existence, or otherwise, of a cutoff for the fundamental mode of a PCF and demonstrate conclusively that the structure is endlessly single mode (i.e., the fundamental has no cutoff).

Guided-Mode Analysis of an Optical Waveguide Using the Imaginary-distance Beam-propagation Method with Efficient Absorbing Layers

J. Shibayama, **T. Yamazaki**, **J. Yamauchi**, **H. Nakano**
Hosei University, Japan

The imaginary-distance beam-propagation method (ID-BPM) [1] has recently been used to analyze a guided mode of an optical waveguide. In the practical analysis, reasonable results can be obtained without using an absorbing layer, provided that a large computational window is adopted. This is due to the fact that for the guided mode the field in the cladding region is dominated by an evanescent wave that rapidly decays toward the computational window edge. However, if a reliable and efficient absorbing layer is available for the ID-BPM, the computational region can be reduced with a subsequent reduction in the computational time. The reduction will be significant particularly for the analysis of a three-dimensional problem.

A perfectly matched layer (PML) [2] is widely used as an efficient absorbing layer in numerical simulations of electromagnetic waves. Unfortunately, we have often encountered stability problems, when carrying out the guided-mode analysis using the ID-BPM with the conventional PML. This is because the conventional PML may be less effective in absorbing an evanescent wave.

Very recently, two alternative absorbing layers have been used for the guided-mode analysis with the ID-BPM, which are based on modifications to stretching coordinate variables (s) of the conventional PML: one approach is to choose s to be a real value [3], and the other is to adopt only the real part of $1/s$ [4]. However, detailed theoretical descriptions of these absorbing layers have not been provided and their possible advantages have not yet been fully investigated.

In the presentation, based on the plane wave solutions, we provide theoretical backgrounds of the above-mentioned absorbing layers for the guided-mode analysis using the ID-BPM. We also investigate the effectiveness of the layers through the analyses of several two- and three-dimensional problems, in comparison with earlier techniques.

REFERENCES

1. Yamauchi, J., *Propagating beam analysis of optical waveguides, U.K.: Research Studies Press*, 2003.
2. Berenger, J. P., "A perfectly matched layer for the absorption of electromagnetic waves", *J. Comput. Phys.*, vol. 114, 185, 1994.
3. Saitoh, K. and M. Koshiba, "Full-vectorial imaginary-distance beam propagation method based on a finite element scheme: application to photonic crystal fibers", *IEEE J. Quantum Electron.*, vol. 38, No. 7, 927, 2002.
4. Shibayama, J., T. Yamazaki, J. Yamauchi and H. Nakano, "Eigenmode analysis of a light-guiding metal line loaded on a dielectric substrate using the imaginary-distance beam-propagation method", *IEEE/OSA J. Lightwave Technol.*, vol. 23, No. 3, 2005.

Development of Fiber-optic Waveplates and Their Application in All-fiber Electric Current Sensing Architectures

Hung-Chia Huang[1,2], **Shou-Qiuan Yao**[1], **Ming-Jue Tang**[1]

[1]Shanghai University, China
[2]Zhejiang University, China

This paper reports the research and development of fiber-optic waveplates and their applications conducted in our laboratory during the past years, with particular emphasis laid on the practical side (fabrication, measurement, fiber circuitry design, experimentation, etc.) of the major results we have achieved in this endeavor. The original concept of fiber-optic waveplates is due to the first author, who has held three early US invention patents[1–3] during the years of early 90's, and a new US Pending Invention Patent[4], entitled "Broad-band fiber-optic waveplates", in 2004.

Among the fiber-optic waveplate varieties, our main effort has been directed to the quarter waveplate version by the preform-spinning technological approach[1], with the micro-heater technique[2] taken as an auxiliary means. By the previous half of this year, our laboratory was able to fabricate fiber waveplate samples in small-scale quatity, whose SOP (Sate of Polarization) transformation performances were tested by the National Center of Measurement and Test for East China, certifying that qualification of most of our samples described by extinction ratio of the transformed linear light exceed 30 dB, with insertion loss at (or less than) 1 dB.

In our laboratory, we have made extensive experiments on the use of fiber-optic waveplates in structuring current sensors of both the polarimetric and the interferometric types. We have borrowed the well-established technology having been used earlier elsewhere in the art of gyroscope, but with the distinctive difference in our sensing architecture that employs fiber-optic quarter waveplate of our invention to function as linear-to-circular SOP transformer to meet the requirement of acquiring a circular light passing the sensing loop. A test report by the East China Electric Power Test & Research Institute certified that our current sensing setup has achieved 0.5% accuracy for measuring large current ranging up to 2000 Amperes.

REFERENCES

1. *US Patent*, No. 4,943,132 (1990);
2. *US Patent*, No. 5,096,312 (1992);
3. *US Patent*, No. 5,452,394 (1995);
4. *US Pending Patent*, No. 10/919,9702 (2004).

The Application of Photonic Bandgap Structure in Microwave Filters

Qiang Gao, **Dun-Bao Yan**, **Guo-Hua Zhang**, **Nai-Chang Yuan**
National University of Defense Technology, China

In recent times, many papers dealing with a one-dimensional (1-D) microstrip photonic bandgap (PBG) were presented[1-3]. The majorities of them have holes in the substrate or etched patterns in the ground plane. This structure has a disadvantage of packing problem: the etched ground plane must be far enough away from any metal plate in order to keep etched patterns in the function. For overcoming the above defect and realizing MMICs, a new structure based on adding the shunt cells to the microstrip and without etching in the ground plane is presented in this paper.

The proposed microstrip filters was realized on the substrate, ε_r=2.65 and $h = 0.5mm$. The layout and parameters of the structure was presented in Figure 1(a). Simulation of S-parameters and measured S-parameters for the structure was presented in Figure 1(b). Simulation and measurement were basically in agreement. The slow-wave factors were showed in Figure 1(c).

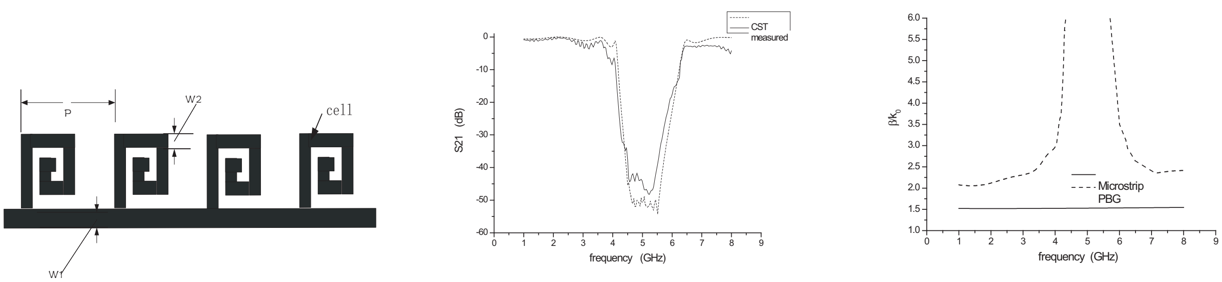

(a) Period $p = 8mm$, width $w_1 = 1.4mm$, $w_2 = 0.8mm$

(b) Simulated S_{21} of the proposed structure

(c) Slow-wave factors of the proposed structures in comparison with a convertional microstrip line

Figure 1: The type of PBG structure.

REFERENCES

1. Tirapu, J., T. Lopetegi, M. A. G. Laso, M. J. Erro, F. Falcone and M. Sorolla, "Study of the delay characteristics of 1-D photonic bandgap microstrip structure", *Microwave Opt Technol Lett.*, Vol. 23, 346, 1999.
2. Chang, C.C., R. Coccioli, Y. Qian and T. Itoh, "Numerical and experiment characterization of slow-wave microstrip line on periodic ground plane", *2000 IEEE MTT-S Digest*, 1533, 2000.
3. Yang Fei-Ran, Yongxi Qian, Roberto Coccioli and Tatsuo Itoh, "A Novel Low-Loss Slow-Wave Microstrip Structure", *IEEE Microwave Guided Wave Letters*, Vol. 8, No. 11, 372, 1998.
4. Sor, J., Y. Qian and T. Itoh, "A novel low-loss slow-wave CPW periodic structure for filter application", *2001 IEEE MTT-S Digest*, 2001.
5. Nesic Dusan, "A new type of slow-wave 1-D PBG microstrip structure without etching in the ground plane for filter and other applications", *PMicrowave and Optical Technology Letters*, Vol. 33, 440, 2002.

Novel Compact Inter-embedded AMC Structure for Suppressing Surface Wave

Dunbao Yan, **Qiang Gao**, **Chao Wang**, **Naichang Yuan**
National University of Defense Technology, China

Artificial magnetic conductor (AMC) structures are widely studied recently because of its two valuable properties: suppressing surface wave and reflecting plane wave in phase. The feature of surface wave suppression helps to improve antenna array's performance by reducing the mutual coupling between antenna elements. Meanwhile, the in-phase reflection property leads to low profile antenna design. However in practical application to antenna array, the space between neighboring elements allows only two or three cells to be used, and evidently, that is not enough. In this abstract, an inter-embedded AMC structure is proposed. This novel structure can be looked as a modified conventional AMC structure, which is a resonant electromagnetic band-gap (EBG) structure. Inter-embedded structure cell has four meandered branches extended from patch side, and the branches are embedded into neighboring cells, as shown in Fig.1. Therefore, the mutual coupling between neighboring cells is enhanced greatly, and the resonant frequency is decreased greatly.

The simulated surface wave dispersion diagrams are given in Fig.2, in which the shadowed regions represent band-gap. For conventional structure, the resonant frequency is about 6.5GHz and the band width is about 1.5GHz. However, for inter-embedded structure, a 0.13GHz band-gap centered at 2.45GHz is achieved. The resonant frequency is decreased about 62%. So the inter-embedded AMC structure is more effective than conventional structure in practical applications to suppress surface wave.

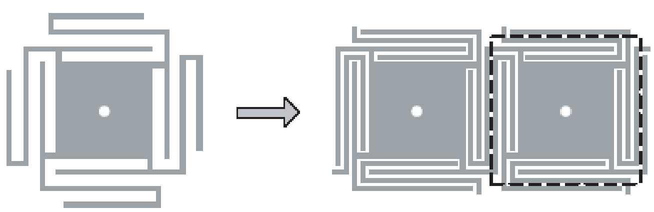

Figure 1: Geometry of inter-embedded structure.

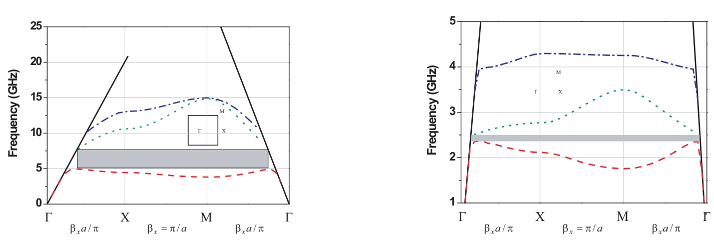

(a) conventional structure (b) inter-embedded structure

Figure 2: Simulated surface wave dispersion diagram for both structures.

Resonance of Compact Frequency Selective Surface Arrays

Qiang Gao, **Dun-Bao Yan**, **Nai-Chang Yuan**, **Yun-Qi Fu**
National University of Defense Technology, China

Frequency Selective Surfaces (FSSs), which have the bandpass or bandstop characteristics, find widespread applications as filters for microwaves in radomes and subreflectors. Conventional surfaces comprise periodically arranged resonant cells in two directions. The resonant cell may be metallic patch element or aperture element within a metallic screen, and have larger unit cell size. In order to meet the miniaturization, this paper introduce Compact FSSs and their resonant characteristics are analyzed in detail.

Three proposed resonant cells are realized on the substrate, $\varepsilon_r = 3.0$ and $h = 0.5mm$. The Finite Element Method[3] is employed to compute the characteristics of these arrays. Figure 2 shows the transmission coefficients of figure 1(b) and (c) at normal incidence, and those of figure 1(a) are given in contrast. It is evident that figure 1(b) and (c) have smaller resonant frequencies comparing to figure 1(a), and especially (c) has the smallest one.

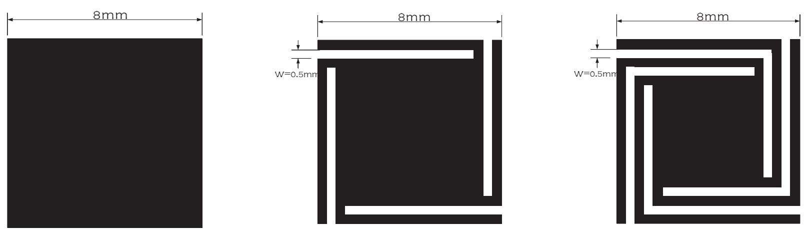

(a) no splits (b) unbent splits (c) L splits

Figure 1: The shapes of resonant cells based on square patch(unitsmm).

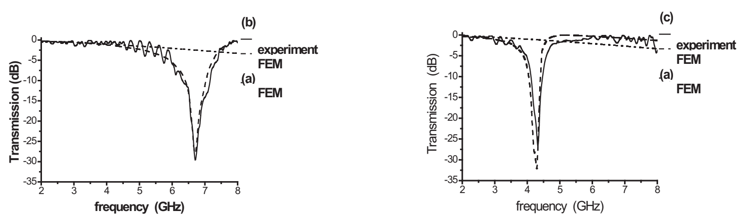

(a) the comparision of figure 1(b) and (a)

(b) the comparision of figure 1(c) and (a)

Figure 2: The transmission coefficients at normal incidence.

REFERENCES

1. Munk, Ben A., "Frequency Selective Surfaces", *Theory and Design (Wiley, New York, 2001)*, 2001.
2. Contopanagos, H., L. Zhang and N. Alexapoulos, "Thin Frequency-Selective Lattices Integrated in Novel Compact MIC, MMIC, and PCA Architectures", *IEEE Transactions on Microwave Theory and Techniques*, Vol. 46, 1936, 1998.
3. Bardi, I., R. Remski, D. Perry and Z. Cendes, "Plane Wave Scattering from Frequency Selective Surfaces by the Finite Element Method", *Compumag Conference Proceedings, Evian France, July 2001*, 2001.

Session 5P4b

Periodic Structures and Their Relation to Negative-Refractive-Index Structures

Waveguide with Transversely Periodic Walls

S. T. Peng, **R. B. Hwang**
National Chiao Tung University, Taiwan

The advances of microelectronic technology have made it possible to create crystal-like materials with a rich variety of lattice patterns that are expected to enrich the electromagnetic properties achievable for device design.The propagation of electromagnetic waves in a crystal-like structure requires sophisticated mathematical analysis of the structure as a boundary-value problem, and the mathematical complexity often hinder the understanding of the physical processes taking place in the structure.For example, a waveguide that is formed by a pair of periodic structures operating in their stopbands had been studied theoretically and experimentally at microwave frequencies and the same concept of utilizing periodic structures of one or more dimensions to form waveguide walls had attracted considerable attention in the optics community, under the general term of photonic band-gap structures.Though simple and amendable to an analytic treatment as a rigorous boundary-value problem, the class of waveguides with one-dimensional (1-D) periodic structures as their sidewalls remains to be investigated to the full extent, so that many basic concepts can be established or clarified. In this work, we present a systematic and thorough study of the wave processes involved in such a simpler structure, in order for a better understanding of possible physical mechanisms that may take place in more complex cases with periodic structures of two or more dimensions.

Excitation of TE Mode in the Left Handed Slab Waveguides

Makoto Tsutsumi
Fukui University of Technology, Japan

This paper treats excitation problem of TE wave mode in the left handed (LH) waveguides, one of which are grounded LH slab waveguide and other is air gap waveguide sandwiched by semi-infinite negative permittivity and permeability media. Dispersion curves of TE mode were derived from Maxwell's equation under estimating constitutive equation of negative permeability and permittivity media. Typical backward wave characteristic of volume and surface wave modes was found from distribution of poynting power to the transverse direction of waveguide. Based on the dispersion relation, excitation characteristic of TE mode by using microstrip line transducer was analyzed under transforming electromagnetic fields into Fourier integral form, and radiation resistance was derived. Radiation reactance was also derived after Hilbert transform of radiation resistance. As a result, insertion loss characteristic of waveguides were estimated as a function of frequency and waveguide thickness. Thus propagation of TE mode in the LH waveguides was confirmed at low frequency below 1 GHz. Experiments were carried out using LH slab waveguide which was made by composed structure of the sprit ring resonator and fine wire planar circuits having dimensions of $147\times110\times10mm^3$. Guided wave propagation characteristic of LH mode at 1GHz was measured using network analyzer, which has been expected by theory.

Compact Bandpass Filter Using Left-Handed Transmission Line

Chao Li, **Cixiang Liu**, **Fang Li**
Institute of Electronics, Chinese Academy of Sciences, China

Composite Left-handed (LH) metamaterials, which are characterized by simultaneously negative ε and μ, were originally developed using thin wire strips and split-ring resonators. More recently, a compact dual transmission line (TL) network was developed that exhibits both negative ε and μ, and it's peculiar properties on refraction and guide waves have been experimentally demonstrated. The dual TL can be realized by interchanging the series inductors and shunt capacitors in the conventional TL model. This approach has the advantages of low insertion loss, broad bandwidth and the ease with which it can be applied in planar microwave circuits. In this paper, a compact band-pass filter was proposed using dual LH TL structure. The unit cell of LH TL was realized by loading a section of conventional TL with lumped series capacitors and shunt inductors. The electrical length per unit cell was made sufficiently small. Periodic analysis was applied to the LH TL structure and dispersion relations have been investigated. Design equations were presented for the determination of the lumped element parameters. By optimizing the structure of unit cell, the response of the filter can be adjusted to a given specification. Compared to a conventional microstrip bandpass filter the proposed one provides the advantages of harmonic suppression and compactness in size.

The Characteristics of Parallel-connected Transmission Lines

Jan-Dong Tseng
National Chin Yi Institute of Technology, Taiwan

Parallel-connected transmission lines are widely used in microwave & millimeter circuits for their frequency dependent characteristics can be applied in frequency selected applications. Parallel-connected transmission lines could be treated as ring circuits or loop circuits for they possessing similar planar geometrical structures.

In this research, the electrical characteristics of two parallel connected lines, shown in Figure 1, are analyzed by using transmission matrix (ABCD matrix) and conversion formula of ABCD to scattering parameters to obtain the overall scattering parameters in terms of the circuit parameters. By given appropriated scattering parameters values, the band pass and band stop circuit design can be obtained. Based on these conditions three circuit designs, band pass, band stop and cascaded band pass, are calculated and analyzed by microwave simulation tools. The circuits of band stop and band pass type are also fabricated to verify the validity of the derived results by experiment. The theoretical and the experimental results show very good agreement in the frequency band from 1 to 5 GHz.

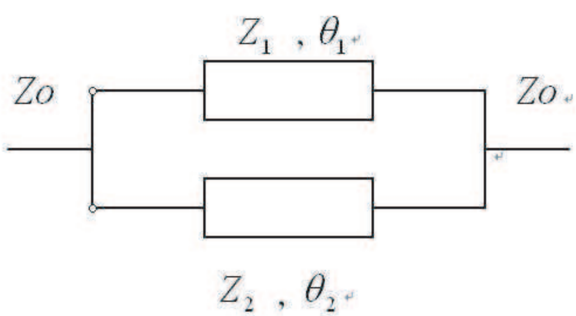

Figure 1: the schematic of parallel-connected circuit

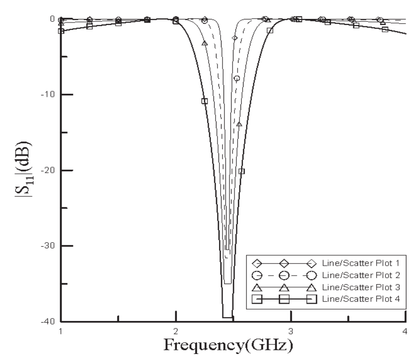

Figure 2: the simulation results of band pass property

The Correlation between Negative-group-delay and Slanted Stop-band in a Two-dimensionally Periodic Structure

R. B. Hwang
National Chiao-Tung University, Taiwan

In this paper, we employed the rigorous mode-matching method to carry out the calculation for the scattering characteristics of a two-dimensionally periodic structure made up of metallic rectangular cylinders. The interesting phenomenon concerning the negative group delay in such a class of 2-D periodic structures was observed. In order to explain their underlying physics, the band structure for the corresponding structure but in infinite in extent was calculated. It is interested to note that the negative group delay merely occurs in the vicinity of the slanted-stop band that is due to the combined effect of the periodicities in both two directions. For the first time, a close connection between the negative group velocity (delay) and the slanted stop-band of a 2-D periodic structure was established.

Ultrarefractive Effect in a Dielectric and Metallic PBG-prisms at Microwave Frequencies: Calculation and Experimental Verification

S. Massaoudi, **A. Ourir**, **A. de Lustrac**
Université Paris-Sud, France

The study concerns the ultra-refractivity phenomenon in dielectric and metallic Photonic Band Gap (PBG) at microwave frequency range. We seek to show this phenomenon using prisms between 7 GHz and 16 GHz. This property leads to very interesting applications, such as compact antennas with high directivity, lens with very short focal length or compact demultiplexer for WDM [1-2]. The dielectric and metallic PBG-prisms, which we studied, are made of dielectric or metallic rods disposed in an isosceles right-angled triangle.

I. The results of the Dielectric PBG-prism: The figure 1(a) shows the radiation pattern measured at 16 GHz of a prism without defect. The dielectric prism is made with 16 by 16 Nylon's rods disposed in an isosceles right-angled triangle. The figure 1(b) gives the radiation pattern measured at 16 GHz of a prism with three defects on the surface of the dielectric. The figure 1(c) shows the dispersion diagram of a square array of dielectric rods with r = 0.357 *a, where r is the radius of the rod and a is the step of the lattice.

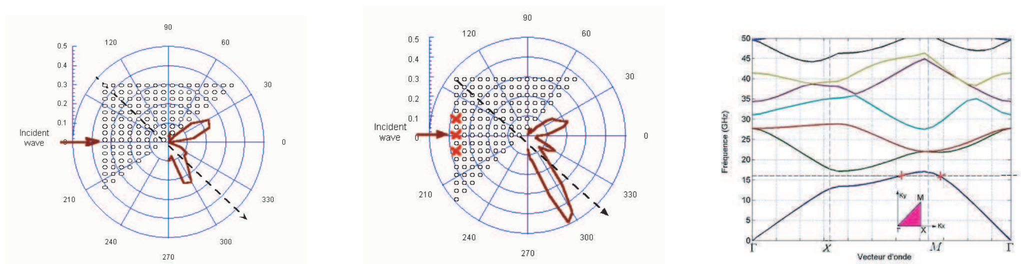

(a) (b) (c)

Figure 1: (a) Measured near field radiation pattern at 16 GHz of the perfect PBG-prism (b) Measured near field radiation pattern at 16 GHz of the PBG-prism with three cavities (in red) placed on the surface (c) The dispersion diagram of a square array of dielectric rods with r = 0.357 *a. The polarization is transverse magnetic.

II. The results of metallic PBG-prism: The metallic PBG-prism is made of copper rods disposed in an isosceles right-angled triangle. The figure 2(a) gives the three-dimensional dispersion diagram. The circle in the plan (kx; ky) represents the projection of the 3D dispersion diagram for one authorized frequency (f=7 GHz). The figure 2(b) shows the calculated far field radiation pattern at 6.6 GHz of the metallic PBG-prism (plasma frequency). The figure 2(c) shows the variation of the measured effective index in the first authorized frequency band (between 7 and 9 GHz). The measurements are taken in TM polarization. The effective index tends to zero at 6.6 GHz (out of our frequency measurement range).

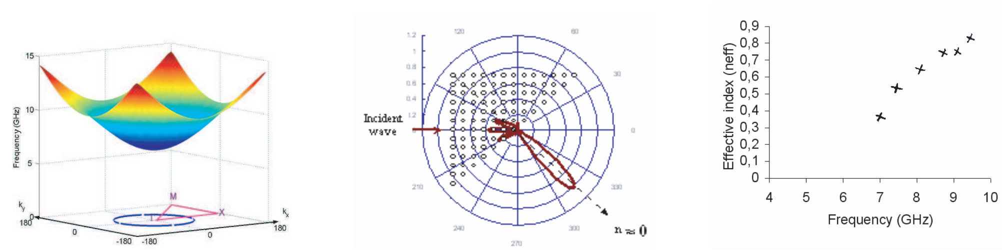

(a) (b) (c)

Figure 2: (a) the three-dimensional dispersion diagram. (b) far-field radiation pattern calculated at 6.6 GHz for the perfect metallic PBG-prism (c) measured effective index of the PBG-prism according to the frequency.

References

[1] H. Kosaka, T. Kawashima, A. Tomita, M. Notomi, T. Tamamura, T. Sato and S. Kawakami, Phys. Rev. B, 58,

10096, 1998.
[2] B. Gralak, S. Enoch and G. Tayeb, Journal of Optical Society of America A 17, 1012-1020, 2000.

An Omni-directional Stop-band by Using Composite 2-D Photonic Crystals

R. B. Hwang, D. C. Pu
National Chiao-Tung University, Taiwan

ESA's Soil Mositure and Ocean Salinity (SMOS) Mission, planned for launch in 2007, will exploit an innovative instrument designed as a two-dimensional interferometer fro acquireing brightness temperature observations at L-band (1.4 GHz) globally and with a revisit time of less than 3 days. SMOS observations will be used to estimate Soil Moisture and Ocean Salinity fields, key-varibales used in weather, climate and extreme-event forecasting.

A number of scientific questions related to the physics of the signal, the perturbing effects and the retrieval concept by accounting for the SMOS observational characteristics were performed to prepare for the mission. This includes specific studies and campaigns dedicated to assess synergistic and complementarity aspects of passive and active sensor systems covering the microwave, the thermal infrared and the optical range of the electromagnetic spectrum. This paper intends to introduces the various activities, to outline the approaches used and to present preliminary results.

Session 5P5

Novel Mathematical Methods in Electromagnetics III

Electromagnetic Scattering and Polarization : Theory and Application

R. Talhi[1,2], **A. Lebrere**[1,2]

[1]University of Tours, France
[2]C.N.R.S-UMR 6115, France

Electromagnetic wave propagation in random media such as terrestrial ionosphere, clouds, fog, and biological tissues, is governed as is well known by the radiative transfer theory which takes into account scattering and absorption due to inhomogeneities present in the medium. We consider here propagation over long distances with respect to the wavelength, weakly fluctuating random media, and the most general case of anisotropic scattering. Our investigation attempted to focus upon understanding of the electromagnetic response due to scattering from these inhomogeneities in the case of random atmospheric effects on wave propagation.

The problem of multiple scattering by random inhomogeneities is rigorously described by the Bethe-Salpeter equation. This equation should be used to derive a radiative transfer equation. However this task is very difficult, and that is why one prefers the application of the Wigner Distribution (W.D) (particularly in the high-frequency asymptotic limit), earlier applied in acoustic and elastic wave problems. It may be noted in passing that the W.D is an interesting mathematical tool which connects the specific intensity (or radiance) of the phenomenological radiative transfer equation (R.T.E) to the fundamental wave fields. Besides, two important elements can be deduced from the W.D : the energy density and the Poyinting vector of the wave, which result respectively from integration of the W.D and calculation of the first moment of the W.D, with respect to the wave vector. In this context, we consider the 3D-vector RTE for electromagnetic waves propagating in the atmosphere, taking into account the polarization state of these waves before and after scattering by using Stokes's representation in terms of four parameters forming a 4-vector. A Monte-Carlo method, based on a probabilistic interpretation of the RTE, is introduced to solve this vector-equation. In order to characterize and estimate some parameters like the distribution of phase-function (or amount of scattered power), intensity and degree of polarization, we firstly tested our method with a Gaussian model which is a theoretical but interesting model taking into account only the anisotropic aspect of inhomogeneities and its consequences on wave scattering. The phase function distribution is investigated versus the wave incidence , and show a quite good agreement when compared to published results. In case of unpolarized incident wave, some other results concerning the behaviour of intensity and degree of polarization with respect to the wave incidence in single and multiple scattering are also reported and discussed. In single scattering, the medium may create a polarization, while in multiple scattering it may reduce and even cancel it.

Furthermore, we also tested our method with a more realistic but complicated medium, that is turbulent ionosphere at high latitude in presence of the terrestrial magnetic field. In this medium we assumed a Chapman profile to describe the electron density, and a Kolmogorov model (power-law form) to describe the power spectrum of ionospheric irregularities. In a first approach, the statistical behaviour of the intensity fluctuation, seems to follow a lognormal distribution for large incidences, and a Weibull distribution for small incidences (few degrees); while the degree of polarization seems to follow a Hill distribution particularly for small incidences. However, additional work is needed to make our method a practical tool for studying complicated media like terrestrial ionosphere.

Analysis of Electromagnetic Absorption and Scattering Characteristics of Conducting Elliptic Cylinder Coated with Absorber Film Using Conformal Mapping Method

Yasumitsu Miyazaki
Aichi University of Technology, Japan

Electromagnetic compatibility is very important technical problem for wireless communication including mobile communication and high speed information system with G bps micro-processors. As one of these electromagnetic compatibility problems, electromagnetic shield and radio absorber for protecting of signals from undesired noises and interferences in information and communication systems.

Fundamental electromagnetic shield and radio absorption characteristics are studied for planar multi-layered panel structures. However, for practical application, general geometrical structures are important factors for electromagnetic shield and absorption in electronic parts, equipments and systems. Electromagnetic eigen impedances of general boundaries are most important factors. In this paper, for analysis and fundamental design of electromagnetic shield and radio absorption, electromagnetic boundary problem on conducting elliptic cylinder with absorber and shield film are generally studied by using conformal mapping method for circular cylinder. Elliptic cylinder includes circular and strip structures, with proper elliptic parameters.

In conducting elliptic cylinder coated with absorber film of complex material constants for dielectric constants, $\tan\delta$ and permittivity, layered elliptic cylinder are mapped to layered circular cylinder by analytic function $\dot{Z} = \dot{z} + \frac{1}{\dot{z}}$. In the mapped new space, new wave equation with inhomogeneous function concerned with space metric parameter is derived, using Green's formula with Green's functions, integral equation is derived for the electromagnetic field in exterior region of layered circular cylinder. A plane wave of linear polarization of general incident angle is incident from far distance position. Electromagnetic fields are analyzed for integral equation with inhomogeneous function of space metric parameter. Iterative method of modified Born approximation for integral equation yields scattering field and transmitted field in layered film. Equivalent impedance, electromagnetic shield and radio absorption effects are discussed for several incident angles and geometrical parameters compared with wavelengths.

REFERENCES

1. Miyazaki, Y. *Trans. IEE Japan*, Vol. 116-C, No. 1, 90-95, 1996.
2. Miyazaki, Y., *Proc. of Int. Symp. on Electromagnetic Compatibility, Tokyo*, 518-528, 1984.
3. Masuda, T. and Y. Miyazaki, *Tech. Report of IEICE*, Vol. EMCJ-99, 2001.

Computation of Wave Scattering Problems from a Spheric Body: Derivation of the New Sommerfeld-Watson Transformation

Hai-Long Wang[1], **Qun Wu**[1], **Xun-Jun He**[1], **Le-Wei Li**[2]

[1] Harbin Institute of Technology, China
[2] National University of Singapore, Singapore

To find a solution of wave scattering from a sphere is a traditional problem. Many scientists have focused on this topic for its broad applications. The exact solution in the form of the partial wave expansion, which is known as Mie series, has been established for a long time[1]. However, with the frequency goes higher, in order to get an accurate solution, the number of the summation must become larger, which is proportional to $k^2a + c(ka)^{1/3} + b^2$ (where k is the wave number and a is the radius, c is equal to 4 or 4.05, b is equal to 1 or 2, depending on the number of ka), so it is difficult to solve this problem using a personal computer directly. Some methods have been presented to overcome the difficulty such as the traditional Sommerfeld-Watson transformation[2][3]. However the physical meaning is not clear in the transformation.

Recently, a new Sommerfeld-Watson transformation[4] have been studied and proven to be a better understanding for it's application to solve wave scattering problems. In the transformation, a residue series using the spherical wave was presented, the number of the summation terms is greatly reduced compared with the traditional Sommerfeld-Watson transformation but a better physical picture has been revealed.

In this paper, the new Sommerfeld-Watson transformation is summarized and a new derivation processing is given. Unlike the original one, this new derivation directly starts from the solution of the traditional Sommerfeld-Watson transformation. The result is instantly reached using the relation between $Q_l(\cos\theta)$ and $P_l(\cos\theta)$ which represent traveling wave and standing wave respectively. So the mathematical processing is shorter and simpler than the original derivation approach. After the derivation, the same residue series using the spherical wave is obtained and the same results are obtained. The detailed discussions will be presented to prove the correctness of this approach during the conference.

REFERENCES

1. Kong Jin Au, "Electromagnetic Wave Theory", *Publishing House of Electronics Industry.*
2. "A Sommerfeld Partial Differential Equation in Physics", *New York: Academic*, 1949.
3. Watson G.N., "The diffraction of electric waves by the earth", *in Proc. Royal Society of London, London, U.K.*, 83, 1918.
4. Li Mao-Kun and Weng Cho Chew, "A New Sommerfeld-Watson Transformation in 3-D", *IEEE Antenna and Wireless Propagation Letters*, vol. 3, 1, 2004.

The Problems of Numerical Solution of Many-dimensional Integral Equations of Electromagnetics

A. B. Samokhin
Moscow Institute of Radiotechnics, Electronics and Automatics, Russia

We consider the problems of numerical solution of many-dimensional integral equations with the kernels depending on the difference of arguments. Many important classes of problems of mathematical physics can be described by equations of this form; for example, this is the case for problems of electromagnetic and acoustic scattering on two and three-dimensional transparent bodies. Below, we will consider numerical solution of integral equation, which is reduced to a system of linear algebraic equations (SLAE) of a very high order N. In this case, we can use only iteration methods. The main efficiency criteria of any numerical algorithm is number T of arithmetic operations which is to be performed to obtain the solution for the initial problem with a prescribed accuracy and memory M required to implement the algorithm. Multiplication of the SLAE matrix A by a vector is the most laborious operation of iteration methods. Therefore, the number of multiplications that should be performed to implement the algorithm will be called the number of iterations. Then, the value of T is estimated by the formula $T \approx LT_A$. Our main purpose consists in the minimization of the values T_A, L and M.

First, we deal with the discretization method applied to the integral equations, that is, the procedure reducing it to a SLAE. The kernel of the integral operator depends only on the difference of Cartesian coordinates of x and y. Therefore, in the discretization, it is desirable to take account of this fact so as to obtain a matrix of the SLAE with the corresponding symmetry properties, especially in the case of curvilinear surface of the body. Then applying the discrete Fourier transform techniques we may obtain that $T_A \approx N \log_2 N$.

The next important problem in solving integral equations is minimization of number L of iterations needed to obtain a desired accuracy. The dimension of SLAE is huge, hence it is reasonable to use the iteration methods, convergence of which depends only on physical characteristics of the problem and doesn't depend on discretization method. Such iteration methods: GMRES and its modification; QMR and its modification; method of simple iteration. The choice of the particular iterative algorithm essentially depends on the specific features of the problem, for example the method of simple iteration is rather effective for the electromagnetic scattering problems in the quasistatic wavelength range. In case of slow convergence of the iterative algorithm it is advisable to use the preconditioners which are able to significantly decrease quality L.

REFERENCES

1. Samokhin A.B., "Integral equations and iteration methods in electromagnetic scattering", *Utrecht: VSP*, 2001.

The Problems of Numerical Solution of Many-dimensional Integral Equations of Electromagnetics. Numerical Examples.

A. B. Samokhin
Moscow Institute of Radiotechnics, Electronics and Automatics, Russia

A. S. Samokhina
Institute of Control Science of Russian Academy of Sciences, Russia

We consider the problems of numerical solution of many-dimensional integral equations with the kernels depending on the difference of arguments. Many important classes of problems of mathematical physics can be described by equations of this form; for example, this is the case for problems of electromagnetic and acoustic scattering on two and three-dimensional transparent bodies. We present the examples of numerical solution of such integral equations, which are reduced to the systems of linear algebraic equations (SLAE) of a very high order N. The dimension of SLAE is huge, hence it is reasonable to use the iteration methods, convergence of which depends only on physical characteristics of the problem and practically doesn't depend on discretization method. For numerical solution we use iteration methods: GMRES and its modification, method of simple iteration We analaze the main parameters of solution such as the number of iterations and dimension of SLAE needed to obtain a desired accuracy in dependence of physical characteristics of initial problem.

Analysis of Electromagnetic Field in Inhomogeneous Medium by Fourier Series Expansion Methods

Tsuneki Yamasaki, **Kastuji Isono**, **Takashi Hinata**
Nihon University, Japan

Recently, the scattering and guiding problems of the inhomogeneous media have been considerable interest, such as optical fiber gratings , photonic band-gap crystals , frequency selective devices, and a negative refraction media. For the plasma medium mixes it with the positive/negative, it have been proposed to the modified multilayer approximation method(MMA) in the positive and negative area by linear profile to the oblique angle incidences of the TM wave. However, when the permittivity was positive and contained the singular point (zero), MMA has not applicable. On the other hand, there was not also applicable to the electromagnetic field in the inhomogeneous layer though the homogeneous multilayer approximation method(HMA) using extrapolation methods.

In this paper, we proposed a new method for the electromagnetic fields with inhomogeneous medium mixed the positive/negative by the combination of improved Fourier series expansion method using the extrapolation method. Numerical results are given for the reflection and transmission coefficients, and the electromagnetic fields in the inhomogeneous region of the positive and contained the singular point (zero) for the case of TM wave using the eigenvalue and eigenvectors obtained by the extrapolation methods. Main process of our methods are as follows:

In the inhomogeneous region $S_2(0 < z < d)$ in Fig.1(a), the structure is uniform in the y-direction and the permittivity $\varepsilon_2(z)$ including singular points at $z = z_1$ and $z = z_2$ (see Fig.1(b). (1) The inhomogeneous layer $(0 < z < d)$ consists periodically stratified layers which is the iteration of the permittivity $\varepsilon_d(z)[= \varepsilon_2(z)]$ in the original region $(0 < z < d)$, (2) To the obtain the correct solution in the analysis, $\varepsilon_d(z)$ is adding the expressed loss term σ, (3) Electromagnetic fields are expanded appropriately by a finite Fourier series using the eigenvalues, and the corresponding eigenvectors obtained the extrapolation methods, (4) Finally, using the boundary conditions, we get the electromagnetic fields in the inhomogeneous in the region $(0 < z < d)$.

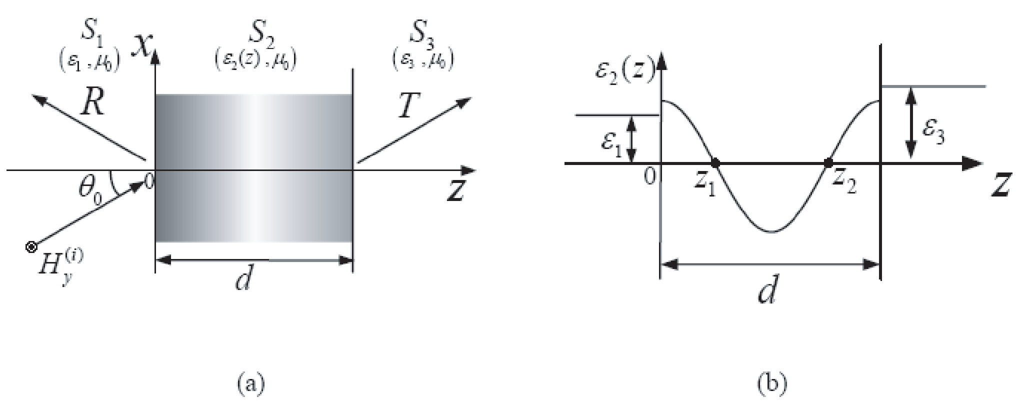

Figure 1: Structure of the inhomogeneous media with a dielectric constant mixed in positive/negative. (a) Coordinate system, (b) Permittivity profile $\varepsilon_2(z)$

Virtual Ray-Tracing in Composite Wedge and Constructing the Diffraction Coefficients

Se-Yun Kim
Korea Institute of Science and Technology, Korea

In high-frequency electromagnetic scattering, one of hot issues is that no rigorous solution to the diffraction by penetrable wedge and cone is available. The ordinary ray-tracing provides the geometrical optics(GO). Applying the physical optics(PO) approximation to the corresponding integral equation, one may obtain the complete form of the PO field consisting of the GO term and the edge-diffracted field. The PO diffraction coefficients are expressed by finite series of cotangent functions, of which amplitudes and poles are equal to the amplitudes and propagation directions of the ordinary rays, respectively. It should be noted that there is one-to-one correspondence between the geometrical rays and the PO diffraction coefficients. However the PO diffraction coefficients cannot satisfy the boundary conditions at the wedge interfaces and the edge condition at the wedge tip.

Recently we suggest a systematic way to correct the error posed in the PO diffraction coefficients. The key idea is inspired from the fact that the exact diffraction coefficients of the perfectly conducting wedge consists of four cotangent functions with angular period $2\pi v_\infty$, where v_∞ is the minimum value satisfying the edge condition at the tip of the conducting wedge. In contrast, the corresponding PO diffraction coefficients consist of two cotangent functions with angular period 2π. Then one may guess that the remaining two cotangent functions among the exact diffraction coefficients may be generated from two virtual rays in the complementary region. Assume that both boundaries of a perfectly conducting wedge are always illuminated by an incident plane wave. We found that the amplitudes and propagation directions of two virtual rays can be obtained only by extending the ordinary ray-tracing technique.

In this paper, both trajectories of actual rays in the physical region and virtual rays in the complementary region are illustrated in case that an E-polarized plane wave is incident on a composite wedge composed of perfect conductor and lossless dielectric. According to the one-to-one correspondence, one may routinely construct the diffraction coefficients consisting of the cotangent functions. Then the angular period of the diffraction coefficients is changed from 2π to $2\pi v_\varepsilon$, where v_ε satisfies the edge condition at the tip of the composite wedge. The validity of the above method is assured by showing that the diffraction coefficients approach zero in the complementary region.

FDTD Analysis of Dynamic Characteristics in Er-Yb Codoped Garnet Waveguide-Type Optical Amplifier

Yasumitsu Miyazaki[1], **Nobuaki Himeno**[2], **Nobuo Goto**[2]

[1]Aichi University of Technology, Japan
[2]Toyohashi University of Technology, Japan

The amplifiers consisting of ion-doped crystalline waveguides have potential of higher gain compared with non-crystalline waveguides such as glasses or silica waveguides. The authors reported an experimental result with Nd doped YGG thin film waveguide on YAG substrates, where 16dB/cm was achieved at the signal wavelength of 1064nm. Steady state and dynamic characteristics in Er-Yb codoped waveguides using rate equations were also reported.

In this report, dynamic characteristics of pulse amplification in Er-Yb codoped YGG waveguide on a YAG substrate is numerically studied using finite difference time domain (FDTD) method. The device consists of an entrance directional coupler for coupling pump and signal lights, an amplifying waveguide and another directional coupler for pump light separation. The FDTD analysis is also used to design waveguide coupler for pumping light. The FDTD analysis was performed along the coupling region and the amplifying region separately. The waveguides are modeled with two-dimensional slab type waveguides. It was found that the pump wave is coupled to the other waveguide whereas the signal wave is coupled back to the incident waveguide when the length is set at 85μm. Next, the amplification characteristics was analyzed in the amplifying region. When 10μW signal pulse with a Gaussian shape is propagated with 0.1mW pump light, the signal light is amplified with amplified gain of 0.36dB along the propagation distance of 200μm Here The ion density of Er and Yb are assumed to be $N^{Er} = 2.0 \times 10^{26}$ ions/m^3, and $N^{Yb} = 1.0 \times 10^{27}$ ions/m^3. This gain of 0.36dB/200mm is in good agreement with the result calculated by the rate equation. The gain characteristics is improved by doping Yb. Larger gain is obtained with small pump power for Yb-Er codoped waveguide than the Er alone doped one. The gain is saturated with smaller pump power for Yb-Er codoped waveguide. We also evaluated the dynamic variation of the ion densities at excited level during the pulse signal propagation.

FDTD simulation in longer waveguide such as 10mm will be investigated by employing spatial segmentation of the medium in future. Also, pulse distortion along the waveguide will be investigated in the longer propagation length.

An Efficient Optical Soft Memory Hardware Description through Optical Device Level Programming

Dipnarayan Guha, **Jun Kyun Choi**
Information and Communications University, Republic of Korea

This paper describes the co-evolving architecture of a $LiNbO_3$ based optical soft memory hardware system for cluster computing through soft decision algebraic polynomial algorithms that are used to instantiate the individual device level crystals. The logic diagram in Fig.1 shows the realization of a co-evolving architecture of a $LiNbO_3$ based optical soft memory hardware system in a Network Processor. The reconfigurable optoelectronic parallel computing system has a multilayer architecture that eliminates data transfer bottlenecks between optical signal processors that have two-dimensional VCSEL and PD array by reconfigurable free-space optical interconnections. The optical soft memory system employs a $LiNbO_3$ spatial light modulator (SLM) for the re-configurability to provide an appropriate interconnection topology matched with the given applications. We design the chip in such a way that it has a massively parallel interconnection to outer computational resources. This is one of the essential features of co-evolving optical systems hardware and forms the link to optical soft memory design being the basis of our hypothesis. We have defined an Optical Generalized Virtual Algorithm (Optical GVA) that forms the core of instantiating the device crystals by external programming logic and maps the hardware computation units into the Single-Instruction-Multiple-Data (SIMD) based processing element array of the SLM. The results and noted and the resulting co-evolving optical system hardware layout is drawn.

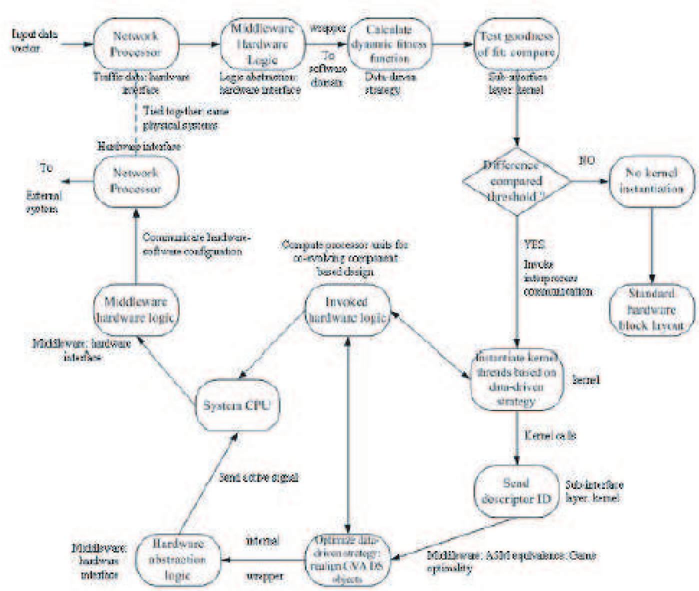

Figure 1: Logic diagram of realizing a co-evolving architecture of an optical soft memory hardware

Session 5P6a

Electromagnetic Theory 3

Multipole Expansion Factorization of Electromagnetic Fields in Cylindrical Coordinates without Utilizing the Addition Theorem

A. R. Baghai-Wadji
RMIT University, Australia

In earlier works we have introduced a formal procedure for the diagonalization of the electromagnetic field equations in cartesian coordinates and suggested a simple recipe for its realization. Also in previous works we have successfully demonstrated that the diagonalization is an enabling concept in engineering applications with numerous consequences in both analytical manipulations (algorithm design, decomposition of operators, and factorization of fields in multipoles) and numerical computations (construction of Green's functions, regularization of singularities, and tempering ill-conditioned problems). In this presentation several new results concerning the diagonalization are addressed: (1) A plausible explanation for the existence of the diagonalized form in cylindrical coordinates in the radial direction has been provided along with an easy-to-apply construction procedure. (2) Dissipative losses in the media has been included in the analysis. (3) It is shown that the diagonalized form corresponds to an algebraic eigenvalue equation in the spectral domain. The resulting eigenvalue equation only involves a minimum number of field components which enter into the equations accounting for jump discontinuities. (4) A physical interpretation for this non-trivial result is provided. (5) The structure of the resulting eigenvalue equation and the asymptotic properties of the eigenvalues and the corresponding eigenvectors have been thoroughly illuminated. (6) It is shown that an intriguing interplay of the low-frequency asymptotic expansion terms of the eigenvectors leads to a cancellation of infinities in our cylindrical problem. This fact provides us with a powerful tool for the regularization of singular surface integrals arising in scattering, or more generally, in direct and indirect problems (renormalization). (7) It is pointed out that some of core calculations have to be interpreted in distributional sense, and that the diagonalization naturally paves the way to this end. (8) Finally it is shown that the factorization of fields, which is central to obtaining multipole expansions, emerges automatically from our formulation without utilizing the Addition Theorem. Conversely, the latter result suggests a constructive procedure for obtaining new Addition Theorems, which are valuable on their own right. Besides the relevance of the diagonalization technique in integral equations it is shown how the diagonalization permits the construction of functionals for the finite element method and the finite difference method implementations. Even more important, its power is examined for the conservative finite-difference method implementations in curvilinear logically rectangular grids. Examples including the electromagnetic scattering and photonics applications will demonstrate the simplicity and elegance of our technique.

Multiquantum Magnetic Vortices in Complicated Josephson Structures

Mikhail Vladimirovich Belodedov, **Makhno Pavel Viktorovich**
Russian Academy of Sciences, Russia

It is generally adopted point of view that magnetic field penetrate into superconductors by vortices each of which contain simple magnetic flux quantum $\Phi_0 = hc/2e$. This phenomenon take place both in bulk superconductors of II kind (abrikosov vortices, [1]) and in distributed josephson junctions (josephson vortices, [2]). The grate interests of in-vestigator are directing now to high-temperature superconductors (HTSC), which may be consider as multiple josephson medium. For HTSC technical applications it is necessary to study particulars of magnetic field penetration in it. The majority of authors researching this question suppose that magnetic field penetrate into HTSC also by vortices with simple quantum of mag-netic flux.

However more complicated magnetic structures are possible in multiple josephson medium. Let's consider system of some ($n = 1, 2, \dots, N$) semi-infinity junctions with one common point $x = 0$. Magnetic field in each junction of system H_n may be wrote by phase difference of order parameter φ_n: $H(x) \sim d\varphi(x)/dx$. Let's find magnetic field distribution in this system by demand that it diminish on infinity: $H_n(x)|_{x\to\infty}$=0. This distribution may be find by solving the Ferell-Prange equation [2] $d^2\varphi_n(x)/dx^2 = \sin\varphi_n(x)$ for each junction with boundary conditions:

$$\begin{aligned}
&\varphi_n(\infty) = 0;\\
&\varphi_1(0) + \varphi_2(0) + \ldots + \varphi_N(0) = 2\pi k;\\
&\frac{d\varphi_1(x)}{dx}|_{x=0} = \frac{d\varphi_2(x)}{dx}|_{x=0} = \ldots = \frac{d\varphi_N(x)}{dx}|_{x=0}.
\end{aligned}$$

Typical magnetic field distribution obtained by the method described by $N = 5$ is shown on figure.

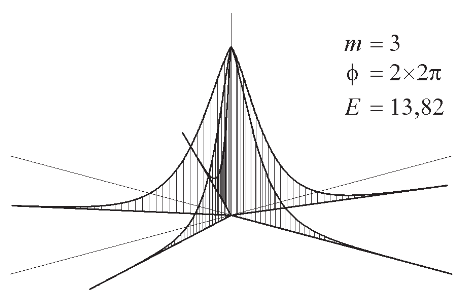

It is necessary to note that the whole magnetic flux in case shown on figure is equal to two quanta: $\Phi = 2\Phi_0$. By numerical modeling of equation

$$\frac{d^2\varphi_n(x,t)}{dx^2} - \frac{d^2\varphi_n(x,t)}{dt^2} = \sin\varphi_n(x,t)$$

it is may be proved that magnetic field distribution similar to that shown on figure contain integer amount of magnetic flux quantum Q and is stable in case $Q \le N/2$.

Granular superconductors, as multiple josephson medium, consist of a lot of distributed josephson junctions which are coupled together by stochastic connections. Results obtained by resent modeling obey to approve that magnetic vortices are possible in granular superconductors with quanta amount more then one. Concrete magnetic flux quanta amount contained in hypervortex (term of [3]) must be defined by medium parameters.

REFERENCES

1. Abrikosov, A. A., *JETP*, Vol. 32, 1442, 1957.
2. Ferell R. and R. Prange, *Phys. Rev. Lett.*, Vol. 10, 479, 1963.
3. Sonin E. B., *JETP Letters*, Vol. 47, No. 8, 415, 1988.

Exact Formulas for Lateral EM Pulses Excited by a Horizontal Electric Dipole on the Boundary between an Isotropic Medium and One-Dimensionally Anisotropic Medium

Kai Li
Zhejiang University, China

Yilong Lu
Nanyang Technological University, Singapore

The frequency-domain electromagnetic (EM) fields from horizontal and vertical electric dipoles located on or near the planar interface between two electrically different media like earth and air or sea water and rock have many useful applications in subsurface and closed-tothe- surface communication, radar, and geophysical prospecting and diagnostics. In the monograph titled "Lateral Electromagnetic Waves, Theory and Applications to Communications, Geophysical Exploration, and Remoting Sensing" by King, Owens and Wu (Springer-verlag, 1992), the approximate formulas have been obtained for lateral EM pulses from vertical and horizontal electric dipoles with delta excitation and Gaussian pulse excitation near or on the boundary between two dielectrics. It is well known that it is very difficult to present the exact solution of the EM field from a dipole source near or on the boundary. Fortunately, the important development on this problem has been made in the monograph by King, Owens and Wu, and the exact formulas were derived in detail for the components E_z and B_ϕ of the transient EM field generated by a delta-function current in a vertical electric dipole on the boundary between two dielectrics. Recently, the authors had derived the exact formulas for the transient EM field from a horizontal dipole with delta-function excitation on the boundary between two dielectrics.

When a horizontal dipole is located on the planar boundary between a homogeneous isotropic medium and one-dimensionally anisotropic medium, the problem of the exact solution on the transient EM field will be in general more complicated. In this paper, it is assumed that the horizontal electric dipole and the observation point approach the boundary between a homogeneous isotropic medium and a anisotropic medium from below and from above, respectively. The exact formulas are derived in the time domain for the electromagnetic field generated by a delta-function current in a horizontal electric dipole located on the planar boundary between a homogeneous isotropic medium and one-dimensionally anisotropic medium. Similar to the isotropic case, the amplitude of the tangential pulsed electric field along the boundary is $1 = \rho^2$, which is characteristic of the surface-wave or lateral pulse. The tangential electric field consists of a delta-function pulse travelling in Region 2 (anisotropic medium), a oppositely directed delta-function travelling in Region 1 (isotropic medium), and a final static electric field due to the charges left on the dipole. The pulsed field consists of the first pulse in Region 2 with the velocity $c/\sqrt{\varepsilon_L}$ and the second pulse in Region 1 with the velocity $c/\sqrt{\varepsilon_1}$ for the component E_ρ. Similarly, the pulsed field consists of a first pulse in Region 2 with the velocity $c/\sqrt{\varepsilon_T}$ and the second pulse in the Region 1 with the velocity $c/\sqrt{\varepsilon_1}$ for the component E.

Electronic Conductivity, Scattering Theory, Quantized Fields, and Coherent States

A. R. Baghai-Wadji[1], **S. W. Yang**[2], **V. B. C. Tan**[3]

[1]RMIT University, Melbourne, Australia
[2]Institute of High Performance Computing, Singapore
[3]National University of Singapore, Singapore

In an accompanying work in this proceedings we investigate the feasibility of frames and dual frames for solving electromagnetic problems [1]. Therein, we address frames which are deduced from the Green's functions associated with given boundary value problems. Frames are, in general, overcomplete sets of analyzing functions, and possess a number of desirable properties. Green's functions, on the other hand, being fundamental solutions, convey the complete information contained in the associated operators subject to specified boundary conditions. Consequently, it can be concluded that the frames discussed in [1] are derived from the operators, which characterize our boundary value problems. From a theoretical and also an application point of view, these ideas are appealing, since we can expect that (overcomplete) analyzing functions, which are tightly connected to our problems, would lead to more efficient and possibly more robust algorithms and, thus, to better and faster solutions. Yet there is another technique known in quantum physics for constructing overcomplete systems of functions, which relies on a fundamentally different point of view, and results in analyzing functions called coherent states. Coherent states in their mathematically modern formulations are known for more than four decades, however, mostly among quantum physicists, quantum chemists and theoreticians in photonics. According to Glauber [2] coherent states can be constructed from any of the following definitions: (i) Coherent states are eigenfunctions of the harmonic-oscillator annihilation operator. (ii) Coherent states can be constructed by applying a displacement operator to the vacuum state of the harmonic oscillator. (iii) Coherent states are quantum states with a minimum-uncertainty relations. Our approach for constructing coherent states is based on a generalization of the group theoretical method in [3]. Our interest in coherent states and related localized fields is twofold: On the one hand we are interested in the *ab initio* quantum mechanical solution of electronic conductivity in molecular structures. On the other hand we are interested in constructing analyzing and synthesizing functions (frames, coherent states) which are constructed from the underlying operators. In achieving these objectives we believe to have filled a gap between physicists and engineers. The common theme are Green's functions and integral equations, even though the solutions have to be interpreted fundamentally differently. In terms of simplified examples we explain notions of groups and algebras, annihilation and creation operators, field quantization, and their relevance to the construction of coherent states and the computation of electronic conductivity in molecular structures.

REFERENCES

1. Baghai-Wadji, A. R. and A. S. Khattab, "Frames and Dual Frames in Computational Electromagnetics", *this proceedings.*
2. Glauber, R. J., *Phys.Rev.*, Vol. 131, 2766, 1963.
3. Zhang, W. M., D. H. Feng and R. Gilmore, "Coherent Staes: Theory and Some Applications", *Rev. Mod. Phys.*, Vol. 62, No. 4, 1990.

Distribution of Poles Affected by the Object Surface Discontinuity

Anxue Zhang, **Zhensheng Shi**, **Xueping Xu**, **Yansheng Jiang**, **Wenbing Wang**
Xi'an Jiaotong University, China

EMS poles of radar target have considerable application potential in target recognition and identification. To identify the complex target, this paper studies the distribution of poles affected by the object surface discontinuity. Scattering data of conductor ball and column with concave or convex on surface are acquired with FDTD simulation. Then MPM (Matrix pencil method) is used to calculate the objects' poles. Results show that when there is a convex on the smooth surface of conductor ball, poles' imaginary will be smaller than the smooth conductor ball. Higher of convex, smaller of poles' imaginary. If a concave exists on the smooth conductor ball, poles' imaginary will become larger. However, when the concave depth is deeper than a value, the distribution of poles will be not effected by the change of concave depth.

Results show that when there is a convex on the smooth surface of conductor ball, poles' imaginary will be smaller than the smooth conductor ball. Higher of convex, smaller of poles' imaginary. If a concave exists on the smooth conductor ball, poles' imaginary will become larger. However, when the concave depth is deeper than a value, the distribution of poles will be not effected by the change of concave depth.

Effective Propagation Constants for Sparse Media Containing Pairs of Dielectric or Chiral Spheres

Yukihisa Nanbu
Sasebo National College of Technology, Japan

Daisuke Ochi
Nippon Telegraph and Telephone Corporation, Japan

Tsuyoshi Matsuoka
Kyushu Sangyo University, Japan

M. Tateiba
Kyushu University, Japan

Materials in nature have been used to design many kinds of electromagnetic devices or functional elements, while artificial materials are studied in order to develop more sophisticated devices. Some artificial materials have been proposed by mixing many particles. In the future utilization, it will become more important to examine electromagnetic properties of them at high frequencies. This means that multiple scattering of waves between particles plays a central role in the determination of material properties; hence, the shape and size of particles also affect the properties.

One of important parameters to know the electromagnetic properties of composite material is the effective propagation constant of the medium. It has been numerically analyzed for media containing dielectric particles and chiral particles. Such composite media are highly expected to apply to some kinds of devices like antennas, optical waveguides, and some sort of filters for electromagnetic waves. However, most researches have dealt with simple composite medium of particles having just one kind of property or symmetry shaped like a sphere or a cylinder. If materials are composed of particles with several kinds of properties and/or with complex shapes, the composite materials are expected to possess more interesting characteristics.

In this paper, we assume a composite medium containing pairs of chiral or dielectric spheres (aggregate spheres) and numerically evaluate the effective propagation constant of the medium. For chiral materials, it is common to discuss its characteristics by decomposing into the left- and right-handed polarizations and we proceed on this condition because we finally deal with a random distribution of the spheres. First, we obtained a T-Matrix of the aggregate sphere by using recursive algorithm. Second, multiple scattering equations with the T-Matrix are solved by applying Effective Field Approximation (EFA) to estimate the effective propagation constants for left- and righthanded polarizations. The characteristics of the effective propagation constants are made clear by changing the electromagnetic properties of particles, and compare with those obtained by mixing formula.

Session 5P6b

EMHD, Gravito-Electrodynamics, and Electrobiology

Chasma Perturbations

Dirk K. Callebaut[1], **Geoffrey K. Karugila**[2], **Ahmed. H. Khater**[3]

[1]University of Antwerp, Belgium
[2]Faculty of Science, SUA, Tanzania
[3]Cairo University, Egypt

In a plasma one has by definition quasi-neutrality over distances of the order of the Debye length. In some situations one has no quasi-neutrality over many times the Debye length. E.g. in certain discharges or in the multipactor regime occurring in the cavities of linear accelerators. Such a non-quasi-neutral plasma or charged plasma has been called chasma. The basic equations are:

$$\partial_t \rho_\pm + dvi \rho_\pm \nu_\pm = \pm p \tag{1}$$

$$m_\pm (\partial_t + \nu_\pm . \bigtriangledown) \nu_\pm = \mp e \bigtriangledown \varphi \tag{2}$$

$$\Delta\varphi = -\frac{\rho_+ + \rho_-}{\varepsilon} \tag{3}$$

with conventional notations. We obtained a steady state with constant electron beam density (ρ_-) and constant ion density (ρ_+). We have investigated the stability of the electron beam when parallel to the electrodes (y-axis). Separation of variables in the perturbed electron density ρ_{-1} leads to

$$\rho_{-1} = Cx^l e^{i(\omega t + ky)} \tag{4}$$

with the dispersion relation

$$\omega^2 + (\nu_{-00} k + il\omega_{ch})\omega - \omega_e^2 = 0 \tag{5}$$

where k and l are wavenumbers (l is dimensionless), ν_{-00} is the constant beam velocity in the steady state,

$$\omega_e^2 = \frac{n_- e^2}{m_- \varepsilon}$$

is the well-known electron plasma frequency and

$$\omega_{ch} = e\sqrt{\frac{n_{+0} - n_{-0}}{m_- \varepsilon}} \tag{6}$$

may be called the chasma frequency. It is a strange combination of the quantities occurring in the usual plasma frequencies. There is always instability unless $l\omega_{ch} = 0$ and for some particular relation between the parameters.

REFERENCES

1. Callebaut D. K. & Knuyt G. K., "Ion Density in Ionizing Beams. 1.", *Plasma Phys. Contr. Fusion*, vol. 20: (6), 511, 1978.
2. Knuyt G. K. & Callebaut D. K., "Ion Density in Ionizing Beams. 2. Applications", *Plasma Phys. Contr. Fusion*, vol. 20: (6), 525, 1978.
3. Callebaut D. K. & Knuyt G. K., "Chasmas in the laboratory and in space", in 'relation between Laboratory an Space Plasmas' (Ed. H. Kikuchi) Reidel Publ. *Co, Dordrecht, The Netherland*, 207, 1981.

Powerful Nonlinear Plasma Waves from Moderate First Order Perturbations

Dirk K. Callebaut
University of Antwerp, Belgium

Geoffrey K. Karugila
Sokoine University of Agriculture, Tanzania

The nonlinear Fourier method of Callebaut consists in concentrating on the family of higher order terms of a single Fourier term of the linearized analysis [1-4]. Thus we have obtained the higher order terms of plasma perturbations, gravitational ones, etc. In the simplest case of cold plasma this resulted in obtaining an analytical expression for the higher order terms. This allowed to investigate the convergence of the series, which in this case is e^{-1} of the equilibrium density. For the cases without an analytical expression we developed a numerical-graphical method to obtain the convergence limit. Near this limit the total amplitude of the wave becomes very large. The convergence limit decreases with increasing pressure.

Thus a wave with moderate first order amplitude may carry a very large energy due to the higher orders. This may be relevant in many situations. E.g. in the case of ball lightning [5] a tremendous energy may be accumulated while the glowing is still restricted. The triggering of solar flares or CMEs (Coronal Mass Ejections) may thus be caused. Again, when these eruptions reach the Earth the influence of a first order term may be far too small to cause electric power plants to break down; however, the total of all terms may be much more powerful. Cf. March 1989 when the whole state of Quebec, Canada, was a day without electricity due to a solar storm. This is an alternative mechanism from the one proposed by Callebaut and Tsintsadze [6,7], based on soliton envelope formation, although there the accent was on the heating of the plasma.

REFERENCES

1. Callebaut D. K., *Lineaire en niet-lineaire perturbaties in hydro-, magneto- en gravitodynamica*, Vol. Simon Stevin 45, 1, 1972.
2. Callebaut D. K. and G. K. Karugila, "Nonlinear Fourier Analysis for Unmagnetized Plasma Waves", *Physica Scripta*, Vol. 68, No. 1, 7, 2003.
3. Callebaut D. K. and G. K. Karugila, "Nonlinear Fourier Analysis for Unmagnetized Multi-species Plasma Waves", *International Journal of Theoretical Physics*, Submitted.
4. Callebaut D. K., G. K. Karugila and H. Kikuchi, "Nonlinear Stability of a Gravitating Medium with Cosmological Constant", *Kuwait J. Sci. Eng.*, in press.
5. Callebaut D. K. and G. K. Karugila, "Nonlinear Fourier Approach yielding High Fields in Ball Lightning", *Eighth International symposium on Ball Lightning (ISBL04), National Central University, Taiwan*, 38, 2004.
6. Callebaut D. K. and N. L. Tsintsadze, "Linear and Nonlinear Interaction of Electromagnetic Waves with Weakly Ionized Magnetized Plasmas", *Physica Scripta*, Vol. 52, No. 5, 565, 1995.
7. Callebaut D. K. and N. L. Tsintsadze, "Heating of Plasma by Alfvén Waves Envelope", *Physica Scripta*, Vol. 50, No. 3, 283, 1994.

On Vladimirov's Approximation for Ideal Inhomogeneous MHD

D. K. Callebaut
University of Antwerp, Belgium

G. K. Karugila
Faculty of Science, SUA, Tanzania

A. H. Khater
University of Cairo, Egypt

Vladimirov[1] and Vladimirov and Moffat[2−4] have considered configurations in ideal magnetohydrodynamics (MHD), i.e. inviscid and perfectly conducting. The matter is considered as incompressible. However, the density is allowed to vary slowly, e.g. in view of the application to inhomogeneous gas clouds and protostars. The basic equations according to Vladimirov are, with usual notations,

$$\partial_t h = curl(u \times h), \tag{1}$$

$$Du = (\partial_t + u.\nabla)u = -\nabla p_{-j\times h} - \rho\nabla\varphi, \tag{2}$$

$$D\rho = 0, \tag{3}$$

$$\nabla.u = \nabla.h = 0 \tag{4}$$

Normally the density should appear in front of Du in eq. (2). In view of eq. (3) we may write

$$\rho Du = (\partial_t + u.\nabla)(\rho u) \tag{5}$$

and with $U = \rho u$, but keeping D as it is, Vladimirov obtains (2). However, this is a mixing up of u and U. Moreover, he uses the energy equation in which U^2 stands for the kinetic enrgy density, while it should be ρu^2 or U^2/ρ. Even in a kind of Boussinesq approximation the results may be expected to be only crude. However, in many applications[2−7] the results are OK, because crucial in the those papers is the vanishing of $\nabla\rho \times \nabla\varphi$. Often both gradients are parallel and the results obtained by Vladimirov' approximation are nevertheless valid. Moreover for small density gradients and/or nearly parallel gradients the approximation is fair. Hence for linear perturbations and stability the results may turn out to be acceptable. However, for nonlinear stability a more extended analysis is required.

REFERENCES

1. Vladimirov V. A., *J. PMM*, USSR 50, 559, 1986.
2. Vladimirov V. A. & H. K. Moffat, *J. Fluid Mech. 159*, 359, 1985.
3. Vladimirov V. A. & H. K. Moffat, *J. Fluid Mech. 283*, 125, 1995.
4. Vladimirov V. A. & H. K. Moffat, *J. Plasma Phys. 57*, 89, 1997.
5. Khater A. H., D. K. Callebaut & S. M. Moawad, *J. Plasma Phys.*, Vol. 66, 1, 2001.
6. Khater A. H., D. K. Callebaut & S. M. Moawad, *J. Plasma Phys.*, Vol. 66, 339, 2003.
7. Khater A. H., D. K. Callebaut & T. N. Abdelhameed, *Astroph. J.*, submitted.

The Basic Common Concept of Plasma Universe and Thunderclouds Symmetry and Symmetry Breakdown, Dipoles, Electric Reconnection, and Critical Ionization Velocities

Hiroshi Kikuchi
Institute for Environmental Electromagnetics, Japan

From a philosophical point of view, a concept of *symmetry* seems to be an acceptable idea of basic importance in general. This is also true especially for a wide range of scientific structures and phenomena. In fact, elementary particles of a matter are constructed on the basis of a symmetry of particles and anti-particles and/or a pair of positively and negatively charged particles. Such an idea has been applied to 'cosmology' as found in Klein-Alfvén's model of matter and antimatter universe [1]. Although a symmetry of elementary particles has been well recognized and established both theoretically and experimentally, for example as seen in electron-positron pairs, it may be so difficult to obtain directly convincing proof of a symmetry of universe. One can see, however, a tiny universe in separation of positive and negative charges of thunderclouds consisting of vertical and horizontal dipole cells corresponding to separation of matter and antimatter consisting of matter and antimatter cells. Then *lightning* phenomena are regarded as a manifestation of *symmetry breakdown*. An astronomical study based on such an idea of *symmetry* can also been found in a hereditary book of secrets on astronomy written in Japanese by Zenkichi Kikuchi (1794-1863), an ancestor of the author's lineage [2, 3].

It has been found that in many 'lightning strokes', both *electric reconnection* and *critical ionization* effects are involved in all discharge processes as proved by many natural and triggered lightning and laboratory discharges [4]. For instance, positive and negative streamer-leader velocities can be estimated to be ion and electron critical velocities, respectively. It is of particular interest that lightning strokes to vertical needles on the ground surface at electrical cusp points before placing them had a most high probability in statistical survey experiments in a costal region of the Sea of Japan though this was accidentally found [4].

REFERENCES

1. Alfvén, H., *Cosmic Plasma*, 1981.
2. Kikuchi, Z., *Tenmon Hiden in Japanese*, 1794-1863.
3. Kikuchi, H., "An Astronomical Study in Japan in Eighteen Century by Zenkichi Kikuchi", *Invited Lecture at the International Congress on Arts and Communications, New Orleans/Louisiana*, 1998.
4. Kikuchi, H., *Electrohydrodynamics in Dusty and Dirty Plasmas*, 2001.

Low Level Pulsed Radio Frequency Field and Its Remedial Effect on Osteoporosis and Bone Fracture

Jitendra Behari, **Jayanand**
Jawaharlal Nehru University, India

Speculation that bone growth and remodeling can be controlled by external stimulation has assumed an interesting dimension in recent years. The concept seems exciting, for it acts as forerunner to provide basic insight into the mechanism of charge transport and bone growth and that in any other biological tissue in general. Also, this has vast clinical potential. From a mechanical point of view bone subjected to any stress (internal or external), adjusts itself to the demands of the situation so as to neutralize the effect of the stimulus (negative feedback system). It is widely accepted that bone remodeling is dependent on load-induced voltages. In the present investigations applying same type of electrical stimulations on two pathological problems of continuing concern tests the hypotheses: osteoporosis and fracture healing. Pulsed electromagnetic field (PEMF carrier frequency, 14 MHz Modulated at 16 Hz of amplitude 10V peak to peak) is chosen to be capacitively coupled to the affected site.

For osteoporotic patients several prophylactic measures to prevent loss of bone are available. Although these regimens have been effective in the treatment of osteoporosis, limitations, cautions and dangers are inherent in their extended use. The clinical potential of treating osteoporosis by non-invasive means is therefore, substantial.

For laboratory investigations rats were subjected to sciatic neuroectomy and ovariectomy to induce osteoporosis and thereafter electrical stimulation given through capacitive coupling electrodes placed on one leg skin (noninvasive) and other kept as sham exposed. After exposure, treated, non-treated and controlled bones were examined by densitometric, histological, mineralogical and biochemical tests. Statistically significant increase in bone mineral density in treated bone was observed compared to their sham-exposed counterpart, although it was not up to normal level. MRI T2 weighted images showed that exposed bones having high bone density in treated bones. SEM study also showed compactness of cancellous bone and diaphysis cortical thickness is more in exposed bones. Bone mineral content of exposed bone is more than shamexposed bone. Calcium content in bone ash is more in treated bone samples. On the basis of these results we can conclude that exposure treatment enhances the possibility of better bone quality.

A similar treatment of electromagnetic energy on an induced fracture in rats (0.5 cm gap in tibia) is found to accelerate the healing process. For this both the sides of the tibia were subjected to fracture, where only one is provided electrical stimulation (experimental). By comparing the ultrasonic attenuation in control and experimental portion of the leg in the same rat, it is verified that healing is faster in the latter. This further confirms that stimulated side showed greater bone mass than the contralateral position.

Decelerating bone loss in osteoporosis and accelerating bone fracture technique is found to be successful including in case of delayed union. These results suggest that such an effective window of pulsed radio frequency fields may be used therapeutically for the treatment of human patients. The technique has no side effects and can be extrapolated to humans.

EHD Effects for Activation and Life Elongation of Plants-experiments by Cage-type Devices

Hiroshi Kikuchi
Institute for Environmental Electromagnetics, Japan

T. Igarashi
Study Group of Shimotsuke-Archeology, Japan

On the basis of EHD (Electrohydrodynamics), it has been shown that high electric field (DC or quasi-DC) applications are effective for activation and life elongation of biological matter and two types of high voltage apparatus, cage-type and belt-type have been designed for this purpose [1, 2]. The cage-type device has already been used for water electrification and the use of such electrified water in a base rather than normal water leads to significant life elongation of flowers and could be used for indoor experiments of cut flowers, plant cutting or rice-plants, based on an experimental discovery of the increase of yields of rice plant by electrifying rice-plant soil-water in the field experiments.

Along this line, this paper presents some of the results of plant-cutting and cut-flower experiments under chronic exposure of 3 kV DC applied to a pair of copper-plate electrodes in a cage-type apparatus with 430 mm high, 225 mm width, and 430 mm depth; the upper plate is a plain surface (a) or a inner surface with 20×30 projections (b), and the lower plate is always plane, consisting of 4 kinds of experiments (A, B, C, D), (A: use of (a), normal water, and 2 hours application to a pair of electrodes per day; B: use of (b), normal water; and 2 hours application to a pair of electrodes per day; C: use of (a) and electrified water (1 hour electrification); D: use of (a) and normal water.

Plant cutting experiments had been carried out from 13 May to 8 July, 2004. Although the cutting took root for all cases of (A) to (D) more or less, the cases (A) and (B) were found to be most effective.

Cut-flower experiments had been carried out during 16-21 August, 2004. It was found that the case (B) was particularly effective.

REFERENCES

1. Kikuchi, H. and Y. Nagai, "New Electric Devices Common for Both Cancer Treatment and Life Elongation" *Proc. PIERS, March 28-31, 2004, Pisa/Italy*, 795, 2004.
2. Kikuchi, H., *Electrohydrodynamics in Dusty and Dirty Plasmas, Kluwer Academic Publishers, Dordrecht/The Netherlands*, 2001.

Session 5P7

Computational Electromagnetics

Controlling the Accuracy of MoM Applied to Complex Shaped Dielectric Objects, while Minimizing Computation Time and Memory

Thierry Gilles[1], **Marc Piette**[1], **Christophe Craeye**[2]

[1]Royal Military Academy, Belgium
[2]Université Catholique de Louvain la Neuve, Belgium

When an integral equation method such as the MoM is applied to find a good approximation of the fictive electric and magnetic currents at the surface of a dielectric body, eventually to derive quantities such as impedance, absorbed energy or radiation pattern, soon the question arises as how to obtain a desired accuracy at the minimum cost. For problems where the meshing leads to more than 500 triangular patches, computer memory and computing time quickly become critical issues.

Multilevel fast multipole algorithm has been proposed to overcome this problem, but it requires fundamental modifications to existing codes based on a classical MoM formulation. Instead it is possible to manage the desired accuracy while greatly reducing the cost of it by making optimal choices.

In this paper we present a global study on this topic, based on the widely used formulation PMCHW with Rao-Wilton-Glisson triangular patches and Galerkin testing.

The classical rule of thumb recommending at least ten triangles per wavelength is reviewed and commented. Optimalized choices for numerical integration schemes on flat triangles are investigated, such as the type and degree of quadratures. The question as where and how to extract or not the 1/R and $1/\mathrm{R}^3$ singularities is also addressed.

Measuring the accuracy of approximated solutions requires exact solutions to be known. Very few are actually available. In this paper a new original reference solution is used to support the accuracy study for geometries less trivial than spheres and cubes.

Finally, an efficient iterative resolution scheme is investigated to further reduce the computing time for the largest problems.

Parallel MLFMA for Scattering by Large Conducting Bodies on the Beowulf Linux Clusters

Xiao-Min Pan[1,2], **Xin-Qing Sheng**[1]

[1]Institute of Electronics, Chinese Academy of Sciences, China
[2]Graduate School, Chinese Academy of Sciences, China

This work is focused on the parallelization of MLFMA for large electromagnetic scattering problems on the Beowulf Linux clusters using the message passing interface (MPI). The goal of our MLFMA parallelization is to significantly reduce the memory requirement by each processor and keep the load balance among processors to achieve high efficiency. Three techniques have been employed to reduce the memory requirement in this work. First, a two-stage scheme to calculate the translation operators has been developed. Second, the symmetries in the algorithm have been exploited. Third, a memory recycling technique has been used. A technique has been developed to keep the load balance, which is decomposing the domain and allocating sub domains to processors based on Morton ordering. It can be ensured that all processors have roughly equal load by estimating the work of each sub domain. Reverse communication mode has been chosen in our parallelization of MLFMA according to the memory reducing techniques and work loading strategy. Numerical experiments of our parallel MLFMA code have been done on the Linux cluster at our group and the SHENTENG 6800 at the Chinese Academy of Sciences.

RCS of Aircraft Using HPC/CEM Hybrid Codes

John Norgard, **Randall Musellman**
US Air Force Academy, USA

In this paper, hybridized Computational Electromagnetic (CEM) codes are developed to predict radiation from antennas mounted on aircraft and the Radar Cross Section (RCS) of the aircraft. Modeling and simulation (M&S) is performed with a combination of Moment Method (MM), Finite Difference Method (FDM), and Uniform Theory of Diffraction (UTD) to analyze large, complex structures including surface-mounted radiators and external sources.

The overall goal of this study is to develop and demonstrate techniques for predicting radiation, scattering, and coupling on aircraft platforms. An F16 aircraft was chosen as an example because measured probe data was available from experiments performed on an actual aircraft at the "Upside-Down" Experimental Tests Facility at AFRL/RRS (Rome, NY).

Simple RCS experiments were also conducted with a scale model F16 aircraft to validate the code. The experiments were performed in the anechoic chambers at the AFRL/RRS (Sensors Directorate) and at the AFRL/PRS (Directed Energy Directorate). The experiments were performed using a thermal imaging technique. This technique uses a minimally perturbing, thin, planar IR detection screen to produce a thermal image (e.g., an IR thermogram) of the intensity of the EM energy over the two-dimensional region of the screen.

Several examples are presented using this thermal technique to measured EM fields using electric field detector screens (carbon loaded foams). These examples illustrate the use of this thermal technique to correlate numerically predicted data with experimental observations. This technique can be used to experimentally validate hybrid codes which predict electric field distributions in areas where conventional hard-wired probes would significantly perturb the fields being measured, for example inside the cavities of the aircraft and near apertures in the fuselage. Surface current distributions (magnetic fields) on metallic surfaces also can be measured with this technique using magnetic field detector screens (ferrite loaded foams).

The overall goal of this work is to achieve improved aircraft models and simulation capabilities to predict radiation, scattering, and coupling of aircraft fields. This hybrid code will improve the CEM M&S process.

CST MWS in Practice: Full-wave Time-domain Simulation of Radiation and Scattering Problems on Electrically Large Objects

Xiaoxia Zhou[1], **Zhiyuan Yu**[2], **Min Zhang**[1]

[1]CST China, China
[2]University of Electronic Science and Technology of China, China

With the rapid development of modern science and technology, large and complex problems which were only designed qualitatively before can now be solved quantitatively. Thanks to the high speed and cheap memory of computer, problem size which can be simulated becomes larger and larger. But still it can't catch up with ever-increasing demands. To address this issue, choosing suitable algorithms is critical. Among various simulation methods, time domain solver is the best choice for simulation of electrically large objects. We have selected CST Microwave Studio® for our practical designs.

FIT (Finite Integration Technique) and its validation for the simulation of electrically large objects are presented in the paper. Some practical skills in using this code are described. Several designs are given together their measurement data, which show good agreement with each other. It clearly demonstrates that the time-domain solver is an effective and versatile tool for studying such problems.

Using Parallel Iterative Multilevel Fast Multipole Method Solve the Electromagnetic Scattering From PEC Plate

Yun Lin, **Jun Hu**, **Zaiping Nie**, **Yongpin Chen**
University of Electronic Science and Technology of China, China

As one of the fastest integral equation solver, MLFMA (Multilevel Fast Multipole Method) has been extensively applied into the scattering and the radiation field. The basis of the MLFMA is the addition theorem, the interaction of the source point and the filed observation point is evaluated by the centre of the groups which multilevel multistage process. Although MLFMA has been realized, and the storage complexity is $O(N \log N)$, it still requires very expansive costs for store when the unknowns N$\gg$1. So the parallel technique has been introduced into this filed. The parallel MLFMA has received much attention. However, due to the characteristics of the integral equation, a lot of data must storage on each compute node then the size of the memory of a single compute node is the bottle-neck of this method, it confines the computational ability of the MLFMA code. In order to solve this problem, PIMLFMA (Parallel iteration Multilevel Fast Multipole Method) has been presented. PIMLFMA is based on the separation of the contribution of the near groups and the far groups, then the iteration formulate can be constructed. With the assistance of MPI (Message Passing Interface) the MLFMA tree structure and the near group impedance elements can be stored on different compute node, and then the computational ability of the MLFMA can be enlarged. In this paper, PIMLFMA will be discussed in detail, and it will used to solve the scattering from the PEC plate. Several numerical results are given to show that with very little iteration steps the true result can be obtained.

Solving Scattering from 3D Conducting Object by Multilevel Fast Inhomogeneous Plane Wave Algorithm (MLFIPWA) with Partly Approximate Iteration Technique

Jun Hu, **Zaiping Nie**, **Lin Lei**
Liming Xu, **Yongpin Chen**
University of Electronic Science and Technology of China, China

Recently, an efficient algorithm called multilevel fast inhomogeneous plane wave algorithm (MLFIPWA), similar to multilevel fast multipole algorithm (MLFMA), has been proposed by prof. chew in UIUC and applied to solve electromagnetic scattering from the target in free space and planar stratified media. Different from conventional MLFMA, the MLFIPWA is based on the plane wave expansion of Green function in complex angle spectrum. A modified steepest descent path (MSDP) is chosen to avoid the divergence of integration. By use of local interpolation/exterpolation technique, the computation in complex angle spectrum can be transformed to real angle spectrum. Because the number of angle spectrums required is related to the relative positions between the observation group and the source group, an inhomogeneous aggregation, translation and disaggregation process is implemented.

The MLFIPWA has been applied by us to solve scattering from 2D electrically large conducting cylinder and dielectric cylinder successfully, it is implemented to solve 3D vector scattering in this paper. To further speed up the efficiency of the MLFIPWA, partly approximate iteration technique developed by us is used. When the iterative error is low than the critical iteration error (CIE), the matrix-vector multiplication can be computed approximately by the interactions from nearby region. The technique reduces total CPU time greatly. Numerical results including the radar cross section (RCS) of almond and plate are given to demonstrate the validity and efficiency of the present method.

A Fast Algorithm for Solving Scattering from Multiple Inhomogeneous Dielectric Cylinders

Yongpin Chen, **Jun Hu**, **Zaiping Nie**, **Yun Lin**
University of Electronic Science and Technology of China, China

Scattering of Multiple inhomogeneous dielectric cylinders with arbitrary shape of cross section plays important roles in many fields such as microwave remote sensing. In this paper, a fast algorithm, multilevel fast inhomogeneous plane wave algorithm(MLFIPWA) is implemented to solve this problem. In conventional iterative method a computational complexity of $O(N^2)$ is needed, while in MLFIPWA it is reduced to $O(N \log N)$. This fast algorithm is based on expansion of the Greens function in far region as plane wave integration along a modified steepest decent path(MSDP) in the complex angular spectrum plane. A Lagrange interpolation/extrapolation technique is applied to transform the complex angular spectrum integration into real integration, thus the process of aggregation, translation and disaggregation is implemented in a inhomogeneous way. A volume integral equation is applied in the problem of scattering from multiple inhomogeneous dielectric cylinders, and a pulse basis function and point matching procedure is chosen. Some numerical results shows the accuracy and efficiency of this algorithm.

A Numerical Study of the Localization Uncertainty for Enhancing the EM Source Localization Accuracy

Ruopeng Liu[1], **Yu Luo**[1], **Da Huang**[1]
Xi Chen[1], **Mengyu Wang**[1], **Haogang Wang**[1], **T. J. Cui**[1,2]

[1]Zhejiang University, China
[2]Southeast University, China

With the development of wireless communication, the localization of electromagnetic (EM) source becomes a hot topic in the monitoring the EM pollution and also in the wireless communication system. Many techniques of localization have been proposed recently such as the method using time delay, blind signal separation (BSS) using independence component analysis technique (ICA) and also ray tracing technique. However the localization is of uncertainty because of the error between calculation and measurement (model error). The uncertainty reflects the performance and accuracy of localization. Our work is to study the uncertainty and improve localization performance when there is model error. So a numerical model is developed to describe the uncertainty by possible localization region (PLR) and its area (PLRA). Based on the numerical model different receivers set at different positions may lead to different PLR. We use our model to study the PLR of multi-isotropic receivers by changing the receivers' positions. From the analysis we give a general idea of how to arrange the receivers' positions. The receiver should be set closed to the EM source as much as possible and the different receivers should be set perpendicularly related to the EM source as much as possible. Then we discuss the antenna array receiver situation. We obtain different received data at one position from antenna array by rotating it. During the analysis of cost function by antenna array, a very useful function is derived, that is, localization function (LF). LF is a function of direction determined by the initial condition of localization such as the pattern of antenna array, the position of EM source and receiver but not by the model error. Only if the region satisfies LF being less than model error there may be the PLR. Therefore LF reflects the nature of the mechanism of localization which influences the PLR. We give the LF in some occasions that will show the character of localization by antenna array, which is agreed with the simulation result. The antenna array receiver has some advantages to the isotropic one in the localization. Finally some numerical simulation using ray tracing and UTD are given to show the PLR by antenna array receivers and isotropic receivers in the urban environment.

Local Multilevel Fast Multipole Algorithm for 3D Electromagnetic Scattering

Jun Hu, **Zaiping Nie**, **Lin Lei**, **Jun Wang**
University of Electronic Science and Technology of China, China

As the fastest integral equation solver up to now, multilevel fast multipole algorithm (MLFMA) has been applied successfully to solve electromagnetic scattering from 3D electrically large object. But for very large scale problems, the storage and CPU time required in MLFMA are still expensive. In this paper, a local multilevel fast multipole algorithm (LMLFMA) is proposed to further speed up the efficiency of MLFMA in conjugate gradient (CG) iteration. In the LMLFMA, only the local interactions between the subscatters are taken into account. And, the interaction regions in iteration are varying adaptively with iterative current density. With decrease of iterative error, iterative current density tends to real one, the interaction regions required are diminishing. This is accomplished by choosing different coarsest level for a given iterative error. Different from fast far field approximation (FAFFA), the contributions due to far field regions at the coarsest level are omitted in LMLFMA. When the iterative error is less than a critical iteration error, only the interaction between nearby regions at the finest level is considered. Numerical results show that the LMLFMA has good accuracy, and the efficiency can achieve over four times of the efficiency of traditional MLFMA.

*This work was supported by NSFC (No. 60431010), Research Funding (No.51403010203DZ0212)

Exploring Independent Component Analysis for GPR Signal Processing

An-Xing Zhao, **Yan-Sheng Jiang**, **Wen-Bing Wang**
Xi'an Jiaotong University, China

Ground-penetrating radar (GPR) as a means for the detection of objects buried under the ground surface, as well as civil engineering such as highway and railroad construction quality inspection or routine maintenance, has been attracting considerable interest lately. Especially, techniques based on GPR have been proposed for the detection of abandoned land mines and unexploded ordnance (UXO), which is not only of both military and humanitary importance, but also a great technical challenge. In recent years the GPR techniques have reached a certain level of maturity. However, the signal processing technique in GPR has still been an immature problem. Although some signal processing methods such as wavelet transform have been discussed in the literatures, none of these methods perform satisfactorily when applied to GPR data, especially for shallow buried targets in nonuniform ground. So it is necessary that new signal processing techniques be introduced to GPR signal processing.

This paper explores the utility of the Independent Component Analysis (ICA) for GPR signal processing. ICA is a linear transformation, which seeks prominent features in high-dimensional data. It is applied to represent the measured data with a linear combination of dominant statistical independent components and the mixing matrix [A]. The ICA is a powerful signal processing method that extracts independent signal sources from a composite signal. It has been applied to a wide area of applications ranging from electroencephalography, for understanding brain activity, to feature extraction, for edge detection and face recognition. Our supposition is that the technique has utility for GPR data analysis.

We introduce ICA technique in a creative way to GPR signal processing. Though there have been a lot problems to overcome , a primary study on FDTD simulation and experimental data has indicated ICA technique in GPR signal processing will be promising. Our primary results have showed it can remove the ground-reflected clutter and additive noise simultaneously. ICA will become a powerful technique in GPR signal processing.

Signal-to-Noise Ratio Enhancement in Multichannel GPR Data via the Karhunen-Loéve Transform

Anxing Zhao, **Yansheng Jiang**, **Wenbing Wang**
Xi'an Jiaotong University, China

Ground penetrating radar (GPR) has been widely used in civil engineering, landmine detection and identification, unexploded ordnance, environmental engineering, and so forth. However, ground-reflected clutter is often a performance-limiting factor in GPR application, especially in detection of near-surface targets in practical engineering. When we scan across the surface using GPR, the strong background which obscures shallow buried targets generates. Imperfection in the system impulse response (e.g., antenna ringing and cable reflections) also have an effect on the GPR detection performance. So how to get rid of the strong clutter has all along been a much troublesome problem.

Several clutter reduction techniques, such as time gating, ensemble average subtraction, etc. have been discussed in the literature, but none of these methods perform satisfactorily when applied to GPR data collected over shallow buried targets in nonuniform ground. Here we present a novel technique using Karhunen-Loéve transform (KLT) to eliminate the strong GPR background to greatly enhance the signal-to-noise ratio of the original GPR data. The assumption of KLT is that the data (or signals) to process are mutually correlated, and there is thus some redundancy in the data. The redundancy in KLT is measured by correlations between data elements. So signal processing using KLT is only based on second-order statistics. Data processed by KLT can remove the correlations between them. From the point of the mean-square error, the results by KLT process is optimum.

Based on the study to the characteristic of real-world GPR data, we find that the background has much strong correlations from channel to channel. So we propose to use KLT to process GPR signal. Synthetic and practical experimental data examples are included to demonstrate the effectiveness of the method. Results indicate that KLT technique can really eliminate the strong GPR background mostly. The signal-to-noise ratio of the data processed by KLT technique can be enhanced greatly.

Research of 3 Dimensional FEM Simulation on MFL of Steel Pipe

Zhiye Du, **Jiangjun Ruan**, **Xianqin Wang**, **Shifeng Yu**
Wuhan University, China

The magnetic flux leakage (MFL) method is commonly used in steel pipe inspection. In this technique, the pipe which is moving axially at constant velocity is magnetized axially and a circumferential array of Hall sensors is used to detect any leakage flux caused by the presence of defects in the pipe wall [1]. A 3-D finite element model consisting of two coils, a Hall sensor and a steel pipe is constructed and the parameters of all elements are set in term of the inspection geometry. Many different cases are simulated in order to achieve the optimal signal-noise ratio of MFL. It is developed that the coils current of 1A and the distance of 200mm is the optimal operating condition, on which the steel pipe is magnetized to critical saturation and the magnetic flux leakage caused by the defect-free pipe is rather small. Based on the optimal working status, the MFL testing (MFLT) signals due to different shapes of defects are simulated respectively. For the defect of small size, such as the width of the crack less than 0.1mm, the mesh of the defect and adjacent area must be strictly controlled. In order to obtain good convergent solutions, an effective method is presented, that is, refine the meshing area step by step from the whole region to the defect. The calculating results are in good agreement with the experimental values. Weve constructed a database including a large number of MFL signals of different shapes and scales of defects. Based on the data-base, the characterization of defect shape is realized by developing decomposed components combining with the wavelet analysis approach. The research can be employed for characterizing defects in steel pipe, which are inspected using the MFL method of nondestructive testing.

REFERENCES

1. Ida, N. and W. Lord, "3-D Finite Element Predictions of Magnetostatic Leakage Fields," *IEEE Trans.Magn*, Vol. MAG-19, 2260, 1983.

Cylindrical Target Reconstruction Using RCS Values

Hiroshi Shirai
Chuo University, Japan

Target identification/reconstruction is one of the important research topics for various areas such as remote sensing and advanced radar technologies. Various methods, which are mainly based on the signal processing techniques or numerical methods, have been proposed previously for target imaging. Radar Cross Section (RCS) is one of the fundamental indexes to evaluate the equivalent size of the scatterer, and it is known that the RCS value changes according to the scatterer's shape and materials. Many authors have already been studied and shown that high frequency asymptotic techniques such as the Geometrical Theory of Diffraction (GTD) and the Equivalent Source Method (ESM) can be confidently used for analyzing the electromagnetic wave scattering, and for estimating the RCS of large polygonal scatterers.

In this paper, a simple target reconstruction algorithm is proposed for polygonal cylindrical scatterers using high frequency techniques. This reconstruction algorithm is mainly based on our previous finding that for polygonal objects, the main contribution to the backscattering arises from the edge diffracted waves at the facets at the specular reflection direction, and each facet size can be estimated by the local RCS maxima and its lobe width. We have already proposed a reconstruction algorithm for closed convex cylindrical objects by simply connecting these facets in order. While this algorithm works well for convex bodies, the order of specular reflection direction may be interchanged when the surface of the scattering body has concave portions. In this paper, another reconstruction algorithm is proposed using monostatic RCS data in the time domain as well as in the frequency domain. While we assume primarily that the targets are all polygonal and their constitutive facets are straight metal plates, we will also mention the case when the scattering objects have facets with smooth curved surfaces.

Author Index